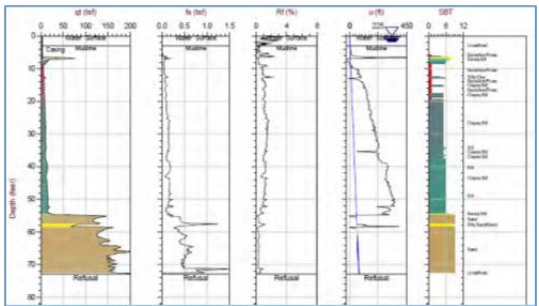
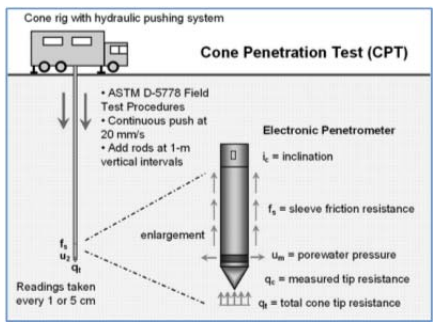




# Transportation Research Division



## Technical Report 15-12

### *CORRELATION OF ENGINEERING PARAMETERS OF THE PRESUMPCOT FORMATION TO THE SEISMIC CONE PENETRATION TEST (SCPTU)*

Technical Report Documentation Page

1. Report No. ME 15-12	2.	3. Recipient's Accession No.	
4. Title and Subtitle CORRELATION OF ENGINEERING PARAMETERS OF THE PRESUMPSCOT FORMATION TO THE SEISMIC CONE PENETRATION TEST (SCPTU)		5. Report Date August 2015	
		6.	
7. Author(s) Mathew A. Hardison, University of Maine Melissa L. Landon, Ph. D., Associate Professor of Civil Engineering, Advisor		8. Performing Organization Report No.	
9. Performing Organization Name and Address University of Maine – Advanced Structures and Composites Center		10. Project/Task/Work Unit No.	
		11. Contract © or Grant (G) No.	
12. Sponsoring Organization Name and Address Maine Department of Transportation State House Station 16 Augusta, Maine 04333		13. Type of Report and Period Covered	
		14. Sponsoring Agency Code	
15. Supplementary Notes			
16. Abstract (Limit 200 words)			
<p>The seismic cone penetration test with pore pressure measurement (SCPTu) is a geotechnical investigation technique which involves pushing a sensitized cone into the subsurface at a constant rate while continuously measuring tip resistance, sleeve friction, and pore pressure resulting from soil shearing. Additionally, shear wave velocity measurements can be collected at discrete intervals throughout the test. Empirical and theoretical correlations have been developed between these measurements and soil engineering properties such as preconsolidation pressure and undrained shear strength. Soil classification, location of silt/sand seams, seismic design parameters, and liquefaction potential can also be obtained from SCPTu results.</p> <p>The objective of this study is to evaluate the SCPTu as a tool to predict engineering properties of the Presumpscot Clay. When paired with conventional borings, the SCPTu can provide a more comprehensive understanding of the subsurface, help refine geotechnical analyses and give engineers access to continuous stratigraphy and engineering parameters throughout an entire deposit rather than at discrete sampling depths common for conventional field vane shear tests (FVT) and boring investigations for the deposit.</p> <p>Four locations where the Presumpscot Formation exist in Maine were selected for investigative and laboratory testing programs. At each location, SCPTu and conventional borings were conducted. During the conventional borings, field vane shear tests were performed and Shelby tube or Sherbrooke block samples were collected for laboratory testing at 5 foot depth intervals. High quality samples were analyzed in the laboratory to determine index properties, consolidation behavior, and undrained shear strength characteristics. With these results, published correlations of SCPTu results to engineering parameters were verified and refined for the Presumpscot Formation.</p> <p>Findings from the study indicate that predicting classification of the Presumpscot clay from CPTu classification charts is best performed using Robertson (1990) and Schneider <i>et al.</i>, (2008), both of which use the relationship between normalized tip resistance and normalized pore pressure. Applying a <i>k-value</i> of 0.33 to measurements of tip resistance provides a reasonable estimate of preconsolidation pressure and OCR at any depth. CPTu cone factors <math>N_{kt}</math> and <math>N_{cu}</math>, used to estimate undrained shear strength, were higher for the Presumpscot clay than most suggested values from similar studies in clay. Furthermore, <math>s_u</math> determined from triaxial compression versus direct simple shear caused a difference in both <math>N_{kt}</math> and <math>N_{cu}</math> of at least 5.0. Site-specific correlations resulted in the best CPTu correlation to engineering properties of the Presumpscot clay.</p>			
17. Document Analysis/Descriptors Seismic cone penetration test, Presumpscot clay		18. Availability Statement	
19. Security Class (this report)	20. Security Class (this page)	21. No. of Pages 392	22. Price

**CORRELATION OF ENGINEERING PARAMETERS OF THE PRESUMPCOT  
FORMATION TO THE SEISMIC CONE PENETRATION TEST (SCPTU)**

By

Mathew A. Hardison

B.S. University of Maine, 2013

A THESIS

Submitted in Partial Fulfillment of the

Requirements for the Degree of

Master of Science

(in Civil Engineering)

The Graduate School

The University of Maine

August 2015

Advisory Committee:

Melissa L. Landon, Ph. D., Associate Professor of Civil Engineering, Advisor

Thomas C. Sandford, Ph.D., P.E., Associate Professor of Civil Engineering

Edwin Nagy, Ph. D., P.E., S.E., Lecturer in Civil Engineering

## THESIS ACCEPTANCE STATEMENT

On the behalf of the Graduate Committee for Mathew A. Hardison, I affirm that this manuscript is the final accepted thesis. Signatures of all committee members are on file with the Graduate School at the University of Maine, 42 Stodder Hall, Orono, Maine.

---

Melissa Landon, Associate Professor of Civil Engineering

Date

## **LIBRARY RIGHTS STATEMENT**

In presenting this thesis in partial fulfillment of the requirements for an advanced degree at the University of Maine, I agree that the Library shall make it freely available for inspection. I further agree that permission for "fair use" copying of this thesis for scholarly purposes may be granted by the Librarian. It is understood that any copying or publication of this thesis for financial gain shall not be allowed without my written permission.

Signature:

Date:

**CORRELATION OF ENGINEERING PARAMETERS OF THE PRESUMPCOT  
FORMATION TO THE SEISMIC CONE PENETRATION TEST (SCPTU)**

By Mathew A. Hardison

Thesis Advisor: Dr. Melissa Landon

An Abstract of the Thesis Presented  
in Partial Fulfillment of the Requirements for the  
Degree of Master of Science  
(in Civil Engineering)  
August 2015

The seismic cone penetration test with pore pressure measurement (SCPTu) is a geotechnical investigation technique which involves pushing a sensitized cone into the subsurface at a constant rate while continuously measuring tip resistance, sleeve friction, and pore pressure resulting from soil shearing. Additionally, shear wave velocity measurements can be collected at discrete intervals throughout the test. Empirical and theoretical correlations have been developed between these measurements and soil engineering properties such as preconsolidation pressure and undrained shear strength. Soil classification, location of silt/sand seams, seismic design parameters, and liquefaction potential can also be obtained from SCPTu results.

The objective of this thesis is to evaluate the SCPTu as a tool to predict engineering properties of the Presumpscot Clay. When paired with conventional borings, the SCPTu can provide a more comprehensive understanding of the subsurface, help refine geotechnical analyses (i.e. settlement, slope stability), and give engineers access to continuous stratigraphy and engineering parameters throughout an entire deposit rather than at discrete sampling depths common for conventional field vane shear tests (FVT) and boring investigations for the deposit.

Four locations where the Presumpscot Formation exist in Maine were selected for investigative and laboratory testing programs. At each location, SCPTu and conventional borings were conducted. During the conventional borings, field vane shear tests were performed and Shelby tube or Sherbrooke block samples were collected for laboratory testing at 5 foot depth intervals. High quality samples were analyzed in the laboratory to determine index properties, consolidation behavior, and undrained shear strength characteristics. With these results, published correlations of SCPTu results to engineering parameters were verified and refined for the Presumpscot Formation.

Findings from the study indicate that predicting classification of the Presumpscot clay from CPTu classification charts is best performed using Robertson (1990) and Schneider *et al.*, (2008), both of which use the relationship between normalized tip resistance and normalized pore pressure. Applying a *k-value* of 0.33 to measurements of tip resistance provides a reasonable estimate of preconsolidation pressure and OCR at any depth. There appeared to be an increasing relationship between *k-value* and OCR which should be further investigated. CPTu cone factors  $N_{kt}$  and  $N_{\Delta u}$ , used to estimate undrained shear strength, were higher for the Presumpscot clay than most suggested values from similar studies in clay. Furthermore,  $s_u$  determined from triaxial compression versus direct simple shear caused a difference in both  $N_{kt}$  and  $N_{\Delta u}$  of at least 5.0. Site-specific correlations resulted in the best CPTu correlation to engineering properties of the Presumpscot clay.

## **DEDICATION**

To Mom and Dad: For your patience, love, and support.



## ACKNOWLEDGEMENTS

Firstly, I'd like to thank Dale Peabody, Laura Krusinski, and the Maine DOT for the interest and funding for this project.

A great deal of the site investigation and laboratory data results were obtained by others, or with the help of others, such as Adam Sampson, Chris Marchetti, Brad Hall, Nick Langlais, various personnel from UMass Amherst, Haley & Aldrich, and Golder Associates, Inc.

Dr. Melissa Landon, Academic Advisor and Committee Chair, for her expertise in laboratory procedures, data processing, data analysis, and Microsoft Word formatting. This thesis was much more enjoyable for me having a down to earth and enthusiastic advisor.

Dr. Thomas Sandford, Committee Member, the vast knowledge you've passed onto me in geotechnical engineering is invaluable, and I will carry it with me for my entire career. Go Sox.

The UMaine Civil & Environmental Engineering faculty members, I could not have chosen a more intelligent, generous, and genuinely considerate group of people to learn from over the past five and a half years.

Bill Peterlein and Craig Coolidge, for bringing me onto their consulting team and introducing me to the geotechnical engineering profession. The exposure to a variety of projects, especially those involving SCPTu testing, allowed me to integrate practical approaches to the analyses in this thesis. I look forward to working with and learning from you.

Devin Carrier, Patrick McKeown, and Dan Casey, because Fogler torture is best shared with good friends. Thanks for some of the best years of my life, I look forward to more.

## TABLE OF CONTENTS

ACKNOWLEDGEMENTS.....	iv
LIST OF TABLES.....	x
LIST OF FIGURES.....	xiii
LIST OF ABBREVIATIONS AND SYMBOLS.....	xxiv
1 INTRODUCTION.....	1
1.1 Objective and Approach.....	4
1.2 Organization.....	7
1.3 Exclusions from Research.....	8
2 LITERATURE REVIEW.....	9
2.1 Presumpscot Formation.....	9
2.1.1 Geotechnical Considerations.....	12
2.1.2 Index Properties.....	15
2.1.3 Stress History.....	16
2.1.4 Undrained Shear Strength.....	17
2.2 Cone Penetration Testing (CPTu).....	22
2.2.1 CPTu Use in Geotechnical Investigations in Soft Clay.....	25
2.2.2 Use of CPTu to Supplement Laboratory and Field Testing.....	25
2.2.3 Use of CPTu to Characterize Silty Clay.....	28
2.3 CPTu Correlation to Classification and Engineering Properties.....	29
2.3.1 Classification.....	29
2.3.2 Stress History.....	32
2.3.3 Undrained Shear Strength.....	39
2.3.4 Seismic Measurements in CPTu testing.....	48
3 METHODS.....	51
3.1 Seismic Cone Penetration Testing.....	52
3.1.1 Seismic Testing.....	56
3.1.2 CPTu Measurements.....	58
3.2 Field Vane Shear Testing.....	61
3.3 Soil Sampling.....	64
3.3.1 Tube Sampling.....	65

3.3.2	Sherbrooke Block Sampling.....	69
3.4	LABORATORY TESTING.....	70
3.4.1	Index Testing.....	70
3.4.2	Sample Preparation.....	72
3.4.3	Constant Rate of Strain (CRS) Consolidation Testing.....	73
3.4.4	Anisotropically Consolidated Undrained Triaxial (CAUC) Shear Testing.....	76
3.4.5	Direct Simple Shear Testing.....	79
3.4.6	SHANSEP Consolidated Undrained Triaxial Shear Testing.....	82
3.4.7	Sample Quality Assessment.....	82
3.4.8	Shear Strength and Remolded Shear Strength Discussion.....	83
3.5	SCPTu Correlations.....	84
4	ROUTE 26/100 FALMOUTH BRIDGE.....	85
4.1	Site Overview and Geology.....	85
4.1.1	Previous Geotechnical Investigations.....	87
4.1.2	Sherbrooke Block Sampling.....	88
4.2	Laboratory Characterization.....	89
4.2.1	Index Testing.....	90
4.2.2	One Dimensional Consolidation Results.....	97
4.2.3	Direct Simple Shear Undrained Strength Results.....	100
4.2.4	SHANSEP Direct Simple Shear Analysis.....	105
4.2.5	Summary and Interpretation of Laboratory Results.....	106
4.3	Seismic Cone Penetration Testing Results.....	108
4.3.1	Results.....	108
4.3.2	Correlations to Classification.....	112
4.3.3	Correlations to Stress History.....	117
4.3.4	Correlation to Undrained Shear Strength.....	120
4.3.5	Seismic Properties.....	127
5	MARTIN'S POINT BRIDGE.....	130
5.1	Site Overview.....	130
5.1.1	Previous Geotechnical Investigations.....	131
5.1.2	Site Geology.....	134

5.2	Laboratory Characterization.....	134
5.2.1	Index Test Results .....	136
5.2.2	One Dimensional Consolidation Results.....	141
5.2.3	Recompression Undrained Triaxial Shear.....	144
5.2.4	SHANSEP Consolidated Undrained Triaxial Shear Results.....	149
5.2.5	Summary and Interpretations of Laboratory Testing Results.....	153
5.3	Seismic Cone Penetration Testing.....	155
5.3.1	Results .....	156
5.3.2	Correlation to Classification.....	161
5.3.3	Correlations to Stress History .....	169
5.3.4	Correlations to Undrained Shear Strength .....	174
6	ROUTE 197 BRIDGE SITE .....	182
6.1	Site Overview .....	182
6.1.1	Geotechnical Investigation.....	183
6.1.2	Site Geology.....	185
6.2	Laboratory Characterization.....	185
6.2.1	Index Test Results .....	186
6.2.2	One Dimensional Consolidation Results.....	192
6.2.3	Recompression Undrained Triaxial Shear.....	195
6.2.4	SHANSEP Consolidated Undrained Triaxial Shear .....	201
6.2.5	Summary and Interpretations of Laboratory Testing Results.....	203
6.3	Seismic Cone Penetration Results.....	205
6.3.1	Results .....	206
6.3.2	Correlations to Classification .....	210
6.3.3	Correlations to Stress History .....	216
6.3.4	Correlations to Shear Strength .....	219
7	I-395 TERMINUS SITE .....	224
7.1	Site Overview .....	224
7.1.1	Geotechnical Investigation.....	224
7.1.2	Site Geology.....	226
7.2	Laboratory Characterization.....	228
7.2.1	Index Test Results .....	228

7.2.2	One Dimensional Consolidation Results.....	233
7.2.3	Recompression Undrained Triaxial Shear.....	237
7.2.4	SHANSEP Consolidated Undrained Triaxial Shear Results.....	241
7.2.5	Summary and Interpretations of Laboratory Testing Results.....	244
7.3	Seismic Cone Penetration Testing Results.....	246
7.3.1	Results.....	247
7.3.2	Correlations to Classification.....	251
7.3.3	Correlations to Stress History.....	257
7.3.4	Correlations to Shear Strength.....	259
8	COMPREHENSIVE COMPARATIVE ANALYSIS.....	265
8.1	Chapter Overview.....	265
8.1.1	The Route 26/100 Falmouth Bridge Site.....	265
8.1.2	Martin's Point Bridge Site.....	266
8.1.3	The Route 197 Richmond-Dresden Bridge Site.....	267
8.1.4	I-395 Terminus Site in Brewer.....	268
8.1.5	Comparison of the Measured Soil Properties.....	269
8.2	Benefits of Continuous Profiling.....	277
8.3	CPTu Classification Correlations.....	280
8.4	Stress History.....	297
8.4.1	Saye <i>et al.</i> (2013) Method.....	306
8.4.2	Stress History Sensitivity Analysis.....	308
8.4.3	Summary.....	312
8.5	Undrained Shear Strength.....	313
8.5.1	Correlations to $N_{kt}$ and $N_{du}$ .....	319
8.5.2	Been <i>et al.</i> , (2010) Method.....	325
8.5.3	Undrained Shear Strength Sensitivity Analysis.....	329
8.5.4	Shear Strength Summary.....	337
8.6	Seismic Characteristics.....	340
9	CONCLUSIONS AND RECOMMENDATIONS.....	343
9.1	Non-parametric CPTu Interpretations.....	344
9.2	Classification of Soil Type.....	345
9.3	CPTu Correlation to Stress History.....	346

9.4 CPTu Correlation to Undrained Shear Strength.....	348
9.5 Shear Stiffness.....	353
9.6 Future Work .....	354
REFERENCES .....	356
BIOGRAPHY OF THE AUTHOR.....	362

## LIST OF TABLES

Table 2.1: Holtz & Kovacs clay sensitivity scale (Holtz et al., 2011).	20
Table 2.2: Summary of SHANSEP parameters obtained from studies on Presumpscot clay and Boston Blue clay.	22
Table 2.3: Saye et al., (2013) $Q_{nc}$ and $m_{CPTu}$ equations for determining OCR of clays	39
Table 2.4: Suggested ranges and correlations of cone factor $N_{kt}$ for studies on different types of clays (reproduced from Remai, 2013).	42
Table 2.5: Summary of results from the Been et al. (2010) analysis on the estuarine clay. Each scenario represents a combination of selected $N_{kt}$ and $S$ value to achieve a $k$ -value output.	44
Table 3.1: Summary of field testing, sampling, and laboratory testing of the Presumpscot clay conducted at all four sites.	51
Table 4.1: Approximate distances between CPTu testing and borings conducted at the Falmouth Bridge Site.	88
Table 4.2: Summary of Atterberg Limits determined from Shelby tube and Sherbrook block samples collected at the Route 26/100 Falmouth Bridge site (reproduced from Langlais, 2011).	93
Table 4.3: Summary of grain size, unit weight, and USCS determined from Shelby tube and Sherbrook block samples collected at the Route 26/100 Falmouth Bridge site (after Langlais) 2011).	94
Table 4.4: Summary of fall cone undrained shear strength and sensitivity for recovered tube and block samples at the Route 26/100 Falmouth Bridge Site (after Langlais, 2011).	96
Table 4.5: Constant rate of strain (CRS) consolidation specimen properties and results from tube and Sherbrooke block samples collected at the Route 26/100 Falmouth Bridge Site (after Langlais, 2011).	98
Table 4.6: Summary of Direct Simple Shear Testing soil properties and pre-shear conditions of Presumpscot clay specimens from Route 26/100 Falmouth Bridge Site (after Langlais, 2011).	102
Table 4.7: Summary of Direct Simple Shear Testing results for the Presumpscot clay specimens from Route 26/100 Falmouth Bridge Site (after Langlais, 2011).	102
Table 4.8: Summary of $N_{kt(DSS)}$ and $N_{\Delta u(DSS)}$ values at the Route 26/100 Bridge site.	121
Table 4.9: Summary of $N_{kt(FVT)}$ and $N_{\Delta u(FVT)}$ values, averages, and coefficient of variations from the FVT results in the Presumpscot clay at the Route 26/100 Falmouth Bridge using SCPTu-P301 (data from Langlais, 2011).	126
Table 5.1: Summary of Atterberg Limits and plasticity data for Presumpscot clay collected from Boring BB-FPPR-317 at the Martin's Point Bridge site.	136
Table 5.2: Summary of grain size distribution, density, and USCS classification for Presumpscot clay collected from Boring BB-FPPR-317 at the Martin's Point Bridge site.	139

Table 5.3: Summary of fall cone undrained shear strength and sensitivity for Presumpscot clay collected from Boring BB-FPPR-317 at the Martin's Point Bridge site. ....	141
Table 5.4: Constant Rate of Strain (CRS) consolidation specimen properties and results for Presumpscot clay collected from Boring BB-FPPR-317 at the Martin's Point Bridge site. ....	142
Table 5.5: Summary of recompression consolidated undrained triaxial shear specimen and consolidation properties for Presumpscot clay collected from Boring BB-FPPR-317 at the Martin's Point Bridge site. ....	145
Table 5.6: Summary of recompression consolidated undrained triaxial shear results for Presumpscot clay collected from Boring BB-FPPR-317 at Martin's Point Bridge. ....	145
Table 5.7: Summary of specimen and consolidation properties for SHANSEP undrained triaxial tests conducted on specimens from Sample 8U of Presumpscot clay collected from Boring BB-FPPR-317 at the Martin's Point Bridge site. ....	150
Table 5.8: Summary of shear properties for SHANSEP undrained triaxial tests conducted on specimens from sample 8U of Presumpscot clay collected from Boring BB-FPPR-317 at the Martin's Point Bridge site. ....	150
Table 5.9: Location and profile depths of four CPT soundings at the Martin's Point Bridge site. ....	156
Table 5.10: Summary of CPTu classification chart effectiveness for SCPTu 101 and CPTu 104 conducted at the Martin's Point Bridge site. ....	167
Table 5.11: Comparison of OCR values between IL laboratory testing and a k-value of 0.38 applied to SCPTu101 and CPTu 10 of Presumpscot Clay at Martin's Point Bridge (some data from Golder Associates 2011a, b). ....	173
Table 5.12: Summary of $N_{kt(CAUC)}$ and $N_{Au(CAUC)}$ values at the Martin's Point Bridge site. ....	175
Table 5.13: Distances between SCPTu 101 and field vane shear test borings of the Presumpscot clay at the Martin's Point Bridge site. ....	179
Table 5.14: Summary of $N_{kt(FVT)}$ and $N_{Au(FVT)}$ values, averages, and coefficient of variations from the FVT results in the Presumpscot clay at Martin's Point Bridge using SCPTu 101. ....	180
Table 6.1: Summary of Atterberg Limit plasticity data for Presumpscot clay samples tested from BB-RDKR-206 conducted at the Route 197 Bridge site. ....	190
Table 6.2: Summary of grain size distribution, density, and USCS classification for Presumpscot clay samples tested from BB-RDKR-206 conducted at the Route 197 Bridge site. ....	190
Table 6.3: Summary of fall cone undrained shear strength and sensitivity results for tested samples of Presumpscot clay collected from Boring BB-RDKR-206 at the Route 197 Bridge site. ....	191
Table 6.4: Summary of Constant Rate of Strain (CRS) consolidation specimen properties and sample quality for tested samples of Presumpscot clay collected from Boring BB-RDKR-206 at the Route 197 Bridge site. ....	193
Table 6.5: Summary of pre-shear recompression anisotropically consolidated undrained triaxial shear specimen and consolidation properties from Presumpscot	



clay specimens collected from Boring BB-RDKR-206 at the Route 197 Bridge Site. ....	196
Table 6.6: Summary of recompression consolidated undrained triaxial shear results on tested samples of Presumpscot clay collected from Boring BB-RDKR-206 at the Route 197 Bridge. ....	197
Table 6.7: Summary of Specimen and consolidation properties for SHANSEP undrained triaxial tests conducted on specimens from BB-RDKR-206 Sample 8U at the Route 197 Bridge site. ....	201
Table 6.8: Summary of CPT classification chart effectiveness for SCPTu 109 at the Route 197 Bridge site. ....	214
Table 6.9: Summary of $N_{kt}$ and $N_{\Delta u}$ values at the Route 197 Bridge site. ....	219
Table 7.1: Summary of Atterberg Limits Plasticity Data for Presumpscot clay samples collected from Boring HB-BREW-102 at the I-395 Terminus site. ....	230
Table 7.2: Summary of grain size distribution, density, and USCS classification for Presumpscot clay samples collected from Boring HB-BREW-102 at the I-395 Terminus site. ....	230
Table 7.3: Summary of fall cone undrained shear strength and sensitivity for Presumpscot clay samples collected from Boring HB-BREW-102 at the I-395 Terminus site. ....	233
Table 7.4: Summary of Constant Rate of Strain (CRS) consolidation specimen properties and sample quality for Presumpscot clay samples collected from Boring HB-BREW-102 at the I-395 Terminus site. ....	234
Table 7.5: Summary of pre-shear recompression consolidated undrained triaxial shear specimen and consolidation properties for Presumpscot clay samples collected from Boring HB-BREW-102 at the I-395 Terminus site. ....	238
Table 7.6: Summary of recompression consolidated undrained triaxial shear results for Presumpscot clay samples collected from Boring HB-BREW-102 at the I-395 Terminus site. ....	238
Table 7.7: Summary of specimen and consolidation properties for SHANSEP undrained triaxial tests for Presumpscot clay samples collected from Boring HB-BREW-102 at the I-395 Terminus site. ....	242
Table 7.8: Summary of specimen and consolidation properties for SHANSEP undrained triaxial tests for Presumpscot clay samples collected from Boring HB-BREW-102 at the I-395 Terminus site. ....	242
Table 7.9: Location and depths of the six (S)CPTu soundings performed at the I-395 Terminus site (reproduced from ConeTec, 2013). ....	247
Table 7.10: Summary of CPT classification chart effectiveness for the Presumpscot clay using SBT based on results from SCPTu 101 and SCPTu 106 at the I-395 Terminus site. ....	256
Table 7.11: Summary of $N_{kt}$ and $N_{\Delta u}$ values at the I-395 Terminus site. ....	260
Table 8.1: Summary of the SCPTu sounding and the boring with sampling used at each for the correlations presented in this section. ....	270

Table 8.2: Summary of SCPTu classification chart effectiveness for each Presumpscot clay site based on comparison to Unified Soil Classification System determined classification. ....	281
Table 8.3: Stress history k-values back-calculated using discrete preconsolidation pressure measurements and depth corresponding CPTu results for Presumpscot clay. ....	299
Table 8.4: Summary of $R^2$ values for $\sigma'_p$ calculated versus $\sigma'_p$ measured using different CPTu stress history methods. ....	307
Table 8.5: Values used in CPTu settlement analysis, reference .....	309
Table 8.6: Magnitudes of predicted settlement of the Presumpscot clay at the I-395 Terminus site using stress history modeled from the laboratory testing and the k-value CPTu method. ....	310
Table 8.7: Summary of Presumpscot clay CPTu cone factor $N_{kt}$ . ....	314
Table 8.8: Summary of Presumpscot clay CPTu cone factor $N_{Au}$ . ....	315
Table 8.9: Summary of k-values and $N_{kt}$ values from Route 197 Bridge after the Been et al., (2010) method. ....	329
Table 8.10: Undrained shear strength ( $s_u$ ) values for the 12 modeled Presumpscot layer in the sensitivity analysis. ....	334
Table 8.11: Factors of safety of the Presumpscot clay slope model at the Route 26/100 Falmouth Bride modeled with different undrained shear strength methods. ....	335

## LIST OF FIGURES

Figure 1.1: Approximate location of the four research sites from this study relative to the mapped surficial geology of southern Maine. (reproduced from the Maine Geologic Survey, 2010). ....	6
Figure 2.1: Extent of the Presumpscot Formation, shown in blue, along the coast of Maine and inland along the Kennebec and Penobscot River valleys (Maine Geological Survey, 2005). ....	10
Figure 2.2: Idealized clay platelet structure for a) flocculated and b) dispersed clay (Lambe and Whitman, 1967). ....	14
Figure 2.3: SEM Photomicrograph of Boston Blue Clay (Terzaghi et al., 1996). ....	14
Figure 2.4: Slope failure modes replicated by laboratory shear strength testing of clays. (from Holtz et al., 2011). ....	19
Figure 2.5: Normalized undrained shear strength vs. plasticity index for triaxial compression (TC), direct simple shear (DSS), and triaxial extension (TE) testing on various silts and clays (such as Norwegian clay and Boston Blue clay, but excluding varved deposits) (from Ladd & DeGroot, 2003). ....	19
Figure 2.6: Theoretical soil behavior around the tip of an advancing cone (from Robertson, 2012). ....	24
Figure 2.7: Embankment cross section of Brazilian Sergipe clay redesigned after the initial failure (Ladd and DeGroot, 2003). ....	26

Figure 2.8: Interpreted stress history and undrained shear strength of the Boston Blue Clay site using CPTu correlations (Ladd and DeGroot, 2003).....	28
Figure 2.9: CPTu soil behavior type (SBT) classification charts developed by: a) Robertson (1990), b) Robertson, (1990), c) Robertson (2009), d) Schneider et al., (2008).....	31
Figure 2.10: Schneider et al., (2008) SCPTu classification chart (bold lines) overlaying the Robertson (1990) $B_q$ - $Q_t$ classification chart comparing predicted soil behavior type (from Schneider et al., 2008). .....	32
Figure 2.11: Relationship between normalized shear strength values and OCR of clay (note: $c_u$ = undrained shear strength) (Robertson and Campanella, 1983). .....	34
Figure 2.12: Yield stress (i.e. preconsolidation pressure) versus net cone resistance ( $q_{net}$ ) showing individual data points and the trendline of $k = 0.33$ (Mayne 2009).....	36
Figure 2.13: SHANSEP based approach for determining OCR of clays applied to the in situ data of Connecticut Valley Varved Clay (Saye et al., 2013). .....	37
Figure 2.14: CPTu factors $Q_{nc}$ and $m_{CPTu}$ for determining OCR of clays plotted with Atterberg Limits (Saye et al., 2013). .....	38
Figure 2.15: Computed cone factor $N_{kt}$ vs. Plasticity Index (from Aas et al., 1986). .....	41
Figure 2.16: Comparison of CPTu predicted undrained shear strength ( $N_{kt} = 12$ ) to laboratory undrained shear strength of a soft clay site in New Orleans (Wei et al., 2010).....	43
Figure 2.17: Plot of CPTu tip resistance term on the right hand side of Equation 2.13 with the median value shown as a bold line (Been et al. 2010).....	45
Figure 2.18: Computed cone factor $N_{Au}$ vs. $B_q$ (from Karlsrud et al., 1996). .....	46
Figure 2.19: Relationship between $N_{Du}$ , $S_t$ , and $I_p$ (Karlsrud et al., 2005). .....	47
Figure 3.1: Schematic of electric peizocones used at the research site (ASTM, 2012). .....	53
Figure 3.2: Image of a 1.4" diameter cone penetrometer showing the cone tip, pore pressure filter element, and friction sleeve (Vertek, 2014). .....	54
Figure 3.3: Schematic of Seismic Shear Wave Velocity testing during the CPT (from ConeTec, 2013). .....	57
Figure 3.4: Pore water pressure effects on cone penetrometer (Lunne et al, 1997). .....	59
Figure 3.5: Schematic of the seismic testing during a CPT sounding using the pseudo-interval method (from Butcher, et al. 2005). .....	61
Figure 3.6: Image of field vane (left) and theoretical failure plane used for the calculation of undrained shear strength (right) (www.gouda-geo.com and www.igeotest.com). .....	62
Figure 3.7: Modified Shelby tube fixed piston sampler with a $5^\circ$ machined cutting angle (from Landon, 2004). .....	66
Figure 3.8: Image of a tube sample of clay illustrating sample disturbance from drag along the inside of the tube (from Hvorslev, 1949).....	68
Figure 3.9: Sherbrooke block sampler (from Landon, 2007). .....	69

Figure 3.10: Geonor fall cone apparatus (from Geonor, 2010).....	72
Figure 3.11: Schematic of sample extraction method (from Ladd and DeGroot, 2003).....	73
Figure 3.12: Image of the CRS chamber cell setup used for all consolidation testing and the Trautwein GeoTAC Sigma-1 Automated Load Test Frame (from Langlais, 2011).....	74
Figure 4.1: Aerial image of the Route 26/100 Falmouth Bridge Site (Google Earth, 2014a).....	86
Figure 4.2: Laboratory determined results of a) natural water content, b) plasticity index, c) liquidity index, d) grain size distribution, e) index undrained and remolded shear strength from the fall cone apparatus, f) sensitivity from the fall cone results ,g) organic content, and h) unit weight (total, dry, and solids) of Presumpscot clay at the north approach of Route 26/100 Falmouth Bridge (data from Langlais, 2011).....	92
Figure 4.3: USCS Classification chart for fine content of tube and Sherbrook block samples from the Route 26/100 Falmouth Bridge Site (from Langlais, 2011).....	95
Figure 4.4: Plasticity Index versus clay fraction for tube and Sherbrook block samples recovered at the Route 26/100 Falmouth Bridge site (from Langlais, 2011).....	96
Figure 4.5: Subsurface profiles of a) $\sigma'_p$ , b) OCR, c) sample quality assessment from CRS consolidation testing on samples from the Route 26/100 Falmouth Bridge Site (after Langlais, 2011).....	99
Figure 4.6: Subsurface profile of a) undrained shear strength ( $s_u$ ), b) normalized shear strength and c) sample quality assessment obtained from DSS testing of samples from the Route 26/100 Falmouth Bridge Site reproduced from (from Langlais, 2011).....	104
Figure 4.7: Plot of normalized shear strength from recompression DSS tests vs. OCR for Presumpscot clay specimens collected from Route 26/100 Falmouth Bridge Site (from Langlais, 2011).....	106
Figure 4.8: Depth profile of (a) corrected tip resistance, (b) sleeve friction, (c) and pore pressure showing hydrostatic pore pressure from soil surface from CPT testing at Route 26/100 Bridge in Falmouth (reproduced from Langlais, 2011).....	109
Figure 4.9: Profile comparing remolded shear strength values ( $s_{u(r)}$ ) obtained from nearby field vane test results and fall cone tests with sleeve friction from SCPTu-P301 and -P305(data from Langlais 2011).....	111
Figure 4.10: Profile of a) normalized tip resistance ( $Q_t$ ), b) sleeve friction ratio ( $F_r$ ), and c) normalized pore pressure ratio ( $B_q$ ) with depth for SCPTu-P301, P302, and P305 at Route 26/100 Falmouth Bridge (data from Langlais, 2011).....	113
Figure 4.11 Soil classification results from SCPTuP301 comparing laboratory-determined USCS classification to classification charts using a) $Q_t$ vs. $F_r$ (Robertson 1990), b) $Q_t$ vs. $B_q$ (Robertson 1990), c) $Q_t$ vs. $F_r$ (Robertson 2009), d) $Q_t$ vs. $B_q$ (Schneider et al., 2008) at the Route 26/100 Falmouth Bridge (data from Langlais, 2011).....	115

Figure 4.12: Soil classification results from SCPTuP305 comparing laboratory-determined USCS classification to classification charts using a) $Q_t$ vs. $F_r$ (Robertson 1990), b) $Q_t$ vs. $B_q$ (Robertson 1990), c) $Q_t$ vs. $F_r$ (Robertson 2009), d) $Q_t$ vs. $B_q$ (Schneider et al., 2008) at the Route 26/100 Falmouth Bridge (data from Langlais, 2011).	116
Figure 4.13: Subsurface profiles of a) $k$ values determined from SCPTu-P301, SCPTu-P302, and SCPTu-P305, and b) preconsolidation pressure estimated using average, minimum, and maximum $k$ values from SCPTu-P301 compared to the laboratory-determine values at the Route 26/100 Falmouth Bridge site (after Langlais, 2011).	119
Figure 4.14: Subsurface profiles of $N_{kt(DSS)}$ , $N_{ke(DSS)}$ , and $N_{\Delta u(DSS)}$ correlated from SCPTu-P301, P302, and P305 with $s_u$ from DSS testing for Presumpscot clay at Route 26/100 Falmouth Bridge (data from Langlais, 2011).	122
Figure 4.15: Profile of undrained shear strength of Presumpscot clay at Route 26/100 Falmouth Bridge site using empirical cone factors a) $N_{kt(DSS)}$ and b) $N_{\Delta u(DSS)}$ applied to SCPTu-P301. Undrained shear strength determined from DSS testing is shown as the gray circles (data from Langlais, 2011).	124
Figure 4.16: Subsurface profiles of a) $N_{kt(FVT)}$ , b) $N_{\Delta u(FVT)}$ , and v) $N_{ke(FVT)}$ correlated from (S)CPTu-P301 and field vane shear testing (FVT) from borings within 200 feet of SCPTu-P301(data from Langlais, 2011).	126
Figure 4.17: a) Shear wave velocity ( $V_s$ ), b) small-strain shear modulus ( $G_o$ ), and c) rigidity index ( $I_r$ ) determined from SCPTu-P301, -P302, and -P305 conducted in Presumpscot clay at the Route 26/100 Falmouth Bridge (data from Langlais, 2011).	128
Figure 5.1: Location of Martin's Point Bridge between Portland and Falmouth, Maine at the mouth of the Preusmpcot River and Casco Bay (Google Earth 2013a).	130
Figure 5.2: Martin's Point Bridge between Portland and Falmouth, Maine at the mouth of the Presumpscot River and Casco Bay during low tide (from MaineDOT 2013).	131
Figure 5.3: Aerial view of boring and CPTu locations along the a) entire length of the bridge b) Falmouth side bridge approach for the newly constructed Martin's Point Bridge (Google Earth, 2015).	133
Figure 5.4: Interpreted subsurface profile from borings (Figure 5.3) conducted along the new Martin's Point Bridge alignment.	135
Figure 5.5: Aerial photograph of the Martin's Point Bridge site illustrating the effect of the Presumpscot River on the subsurface material (Googe Earth, 2014).	135
Figure 5.6 Laboratory test specimen use for BB-FPPR-317 3 in. Shelby tubes 1U - 6U from the Martin's Point Bridge site.	137
Figure 5.7: Laboratory test specimen use for BB-FPPR-317 3 in. Shelby tubes 7U - 13U from the Martin's Point Bridge site.	137
Figure 5.8: Laboratory determined results of a) Atterberg limits and natural water content, b) plasticity index, c) liquidity index, d) grain size distribution, e) index ( $s_u$ ) and remolded undrained shear strength ( $s_{u(r)}$ ) from the fall cone, f) sensitivity from the fall cone, g) organic content, and h) unit weight	

(total, dry, solids) of Presumpscot clay collected from the Martin's Point Bridge site.....	138
Figure 5.9: USCS Classification Charts using Atterberg Limits for Presumpscot clay collected from Boring BB-FPPR-317 at the Martin's Point Bridge site.....	140
Figure 5.10: Subsurface profiles of a) $\sigma'_p$ , b) OCR, c) initial void ratio, d) sample quality assessment from CRS consolidation testing for Presumpscot clay collected from Boring BB-FPPR-317 at the Martin's Point Bridge site. ....	143
Figure 5.11: Subsurface profile of a) undrained shear strength ( $s_u$ ), b) remolded undrained shear strength and c) and sensitivity from laboratory testing on undisturbed samples (BB-317) and field vane shear testing (other borings) at the Martin's Point Bridge site. ....	146
Figure 5.12: Recompression Consolidated Undrained Triaxial (CAUC) normalized effective stress paths for specimens from BB-FPPR-317 from the Martin's Point Bridge site. ....	148
Figure 5.13: Normalized effective stress paths for SHANSEP Triaxial tests conducted on specimens from Sample 8U of Presumpscot clay collected from Boring BB-FPPR-317 at the Martin's Point Bridge site. ....	151
Figure 5.14: Comparison of normalized undrained shear strength from recompression and SHANSEP triaxial compression tests of Presumpscot clay collected from Boring BB-FPPR-317 at the Martin's Point Bridge site. ....	152
Figure 5.15: Comparison of undrained shear strength and normalized undrained shear strength measured from triaxial recompression and SHANSEP compression ( $S = 0.28$ , $m = 0.83$ ) tests and best-fit SHANSEP estimates ( $S = 0.25$ , $m = 0.75$ ) for the Martin's Point Bridge Presumpscot clay. ....	153
Figure 5.16: Depth profile of (a) corrected tip resistance, (b) sleeve friction, (c) and pore pressure showing hydrostatic pore pressure from soil surface from CPT testing of Presumpscot clay at the Martin's Point Bridge site. ....	157
Figure 5.17: Profile comparing remolded shear strength values ( $s_{u(r)}$ ) obtained from Boring 311, 312, and 316 field vane test results and fall cone tests from BB-FPPR-317 with sleeve friction from SCPTu 101 from the Martin's Point Bridge site. ....	159
Figure 5.18: Depth profile of a) shear wave velocity ( $V_s$ ), b) small strain shear modulus ( $G_0$ ) and Rigidity index ( $I_r$ ) for SCPTu101 and 103 conducted at the Martin's Point Bridge site. ....	161
Figure 5.19: Profile of a) normalized tip resistance ( $Q_t$ ), b) sleeve friction ratio ( $F_r$ ), and c) normalized pore pressure ( $B_q$ ) collected from SCPTu 101, 103, and 104 at the Martin's Point Bridge site. ....	163
Figure 5.20: Soil classification results comparing laboratory-determined USCS classification to classification charts using a) $Q_t$ vs. $F_r$ (Robertson 1990), b) $Q_t$ vs. $B_q$ (Robertson 1990), c) $Q_t$ vs. $F_r$ (Robertson 2009), d) $Q_t$ vs. $B_q$ (Schneider et al., 2008) from SCPTu 101 conducted at the Martin's Point Bridge site.....	164
Figure 5.21: Soil classification results comparing laboratory-determined USCS classification to classification charts using a) $Q_t$ vs. $F_r$ (Robertson 1990), b)	

$Q_t$ vs. $B_q$ (Robertson 1990), c) $Q_t$ vs. $F_r$ (Robertson 2009), d) $Q_t$ vs. $B_q$ (Schneider et al., 2008) from CPTu 104 conducted at the Martin's Point Bridge site.....	165
Figure 5.22: Comparison of laboratory and field determined soil properties to plotted SBT trends for a) OCR (Robertson 1990), b) normalized remolded undrained shear strength (Robertson 2009), and c) Normalized remolded undrained shear strength with lower data range (Robertson 2009) from SCPTu 101 at the Martin's Point Bridge site.....	166
Figure 5.23: Subsurface profile showing (a) the CPTu correlated preconsolidation stress $k$ -value and (b) preconsolidation pressure correlated from SCPTu 101 based on the range of correlated values from the Martin's Point Bridge site. ....	170
Figure 5.24: Profile of a) overconsolidation ratio and b) sample quality for the consolidation samples collected and tested by Golder Associates in 2011 at Martin's Point Bridge.....	172
Figure 5.25 Subsurface profiles of $N_{kt(CAUC)}$ , $N_{ke(CAUC)}$ , and $N_{\Delta u(CAUC)}$ correlated from (S)CPTu 101,103, and 104 with $s_u$ from triaxial CAUC testing of Presumpscot clay at the Martin's Point Bridge site. ....	175
Figure 5.26: Profile of undrained shear strength of Presumpscot clay at Martin's Point Bridge using empirical cone factors $N_{kt(CAUC)}$ and $N_{\Delta u(CAUC)}$ applied to SCPTu 101. ....	177
Figure 5.27: Subsurface profiles of $N_{kt(FVT)}$ , $N_{\Delta u(FVT)}$ , and $N_{ke(FVT)}$ correlated from SCPTu-101 and field vane shear testing (FVT) from borings conducted in Presumpscot clay at Martin's Point Bridge.....	180
Figure 6.1: Aerial image of the Richmond Dresden Bridge site Route 197 Bridge site showing recent construction of the new bridge on the north side of the existing bridge structure (Google Earth, 2014).....	182
Figure 6.2: Image of the new bridge during construction in the foreground with the old bridge in the background (centralmaine.com, 2014).....	183
Figure 6.3: Interpretive subsurface profile at the Route 197 Bridge showing the approximate location of Boring BB-RDKR-206 and SCPTu 109 (after MaineDOT, 2011). Note: the elevation in feet is shown on the left of the figure and the station in feet is shown on the bottom.....	184
Figure 6.4: Sample usage for laboratory testing of the collected tube samples of Presumpscot clay at the Route 197 Bridge site. ....	187
Figure 6.5: Laboratory determined results of a) natural water content, b) plasticity index, c) liquidity index, d) grain size distribution, e) index undrained and remolded shear strength from the fall cone apparatus, f) sensitivity from fall cone results ,g) organic content, and h) unit weight (total, dry, and solids) of Presumpscot clay from BB-RDKR-206 performed at the Route 197 Bridge site.....	189
Figure 6.6: Plasticity data from laboratory testing of Presumpscot clay samples collected from Boring BB-RDKR-206 plotted on USCS Classification Charts at the Route 197 Bridge site. ....	191

Figure 6.7: Subsurface profiles of a) $\sigma'_p$ , b) OCR, c) initial void ratio, and d) sample quality assessment from CRS consolidation tests on samples of Presumpscot clay collected from Boring BB-RDKR-206 at the Route 197 Bridge site.....	194
Figure 6.8: Subsurface profile of a) undrained shear strength ( $s_u$ ), b) normalized shear strength and c) NGI sample quality assessment obtained from CAUC triaxial testing on samples of Presumpscot clay collected from Boring BB-RDKR-206 at the Route 197 Bridge. ....	197
Figure 6.9: Subsurface profile of a) undrained shear strength ( $s_u$ ), b) remolded undrained shear strength and c) and sensitivity from laboratory testing on specimens of Presumpscot clay collected from Boring BB-RDKR-206 at the Route 197 Bridge site.....	198
Figure 6.10: Recompression Consolidated Undrained Triaxial (CAUC) Normalized Effective Stress Paths for specimens from BB-RDKR-206 at the Route 197 Bride site.....	200
Figure 6.11: SHANSEP Recompression Consolidated Undrained Triaxial (CAUC) Normalized Effective Stress Paths for Presumpscot clay specimens from boring BB-RDKR-206 8U conducted at the Route 197 Bridge. ....	202
Figure 6.12: Comparison of normalized undrained shear strength from recompression and SHANSEP triaxial compression tests for Presumpscot clay specimens from boring BB-RDKR-206 8U conducted at the Route 197 Bridge site. ....	203
Figure 6.13: Depth profile of (a) corrected tip resistance, (b) sleeve friction, (c) and pore pressure showing hydrostatic pore pressure from SCPTu 109 conducted at the Route 197 Bridge.....	207
Figure 6.14: Profile comparing remolded shear strength values ( $s_{u(r)}$ ) obtained from Boring 104, 105B, and 207 field vane test results and fall cone tests from BB-RDKR-206 with sleeve friction from SCPTu 109 at the Route 197 Bridge site. ....	208
Figure 6.15: Profile of a) shear wave velocity ( $V_s$ ), b) small strain shear modulus ( $G_0$ ), and c) rigidity index ( $I_r$ ) for SCPTu 109 at the Route 197 Bridge site. ....	210
Figure 6.16: Profile of a) normalized tip resistance ( $Q_t$ ), b) sleeve friction ratio ( $F_r$ ), and c) Normalized Pore Pressure ( $B_q$ ) from SCPTu 109 conducted in Presumpscot clay at the Route 197 Bridge.....	212
Figure 6.17: Soil classification results from SCPTu109 comparing laboratory-determined USCS classification to classification charts using a) $Q_t$ vs. $F_r$ (Robertson 1990), b) $Q_t$ vs. $B_q$ (Robertson 1990), c) $Q_t$ vs. $F_r$ (Robertson 2009), d) $Q_t$ vs. $B_q$ (Schneider et al., 2008). ....	213
Figure 6.18 Soil trend results from SCPTu109 comparing laboratory and field determined soil properties to plotted trends on chart for a) OCR (Robertson 1990), b) Normalized remolded undrained shear strength (Robertson 2009). ....	215
Figure 6.19: Subsurface profile of a) k-value, b) estimated $\sigma'_p$ from applying min, max, and average k-values to the entire SCPTu 109 $q_{net}$ profile compared to laboratory-determine $\sigma'_p$ of Presumpscot clay at the Route 197 Bridge site.....	218



Figure 6.20 : Subsurface profiles of $N_{kt}$ , $N_{\Delta u}$ , and $N_{ke}$ correlated from SCPTu109 with $s_u$ from CAUC triaxial and field vane testing of Presumpscot clay at the Route 197 Bridge site. ....	220
Figure 6.21: Profiles of undrained shear strength using $N_{kt(CAUC)}$ and $N_{\Delta u(CAUC)}$ values as shown on the figure applied to SCPTu 109, compared to the laboratory-determined undrained shear strength of Presumpscot clay at the Route 197 Bridge site.....	222
Figure 7.1: Image of the I-395 Terminus site in Brewer, Maine (Google Earth, 2014b). ....	224
Figure 7.2: Boring and CPTu sounding locations at the 395 Terminus site (Google Earth, 2014b).....	226
Figure 7.3: Laboratory specimen use for HB-BREW-102 3" Shelby tubes 1U through 9U. ....	229
Figure 7.4: Laboratory determined results of a) natural water content, b) plasticity index, c) liquidity index, d) grain size distribution, e) index undrained and remolded shear strength from the fall cone, f) sensitivity from fall cone results ,g) organic content, and h) unit weight (total, dry, and solids) for Presumpscot clay samples collected from Boring HB-BREW-102 at the I-395 Terminus site. ....	231
Figure 7.5: USCS Classification Charts using Atterberg Limits for Presumpscot clay samples collected from Boring HB-BREW-102 at the I-395 Terminus site. ....	232
Figure 7.6: Subsurface profiles of a) $\sigma'_p$ , b) OCR, c) sample quality assessment from CRS consolidation testing for Presumpscot clay samples collected from Boring HB-BREW-102 at the I-395 Terminus site. ....	235
Figure 7.7: Subsurface profile of a) undrained shear strength ( $s_u$ ), b) normalized shear strength and c) NGI sample quality assessment obtained from CAUC triaxial testing for Presumpscot clay samples collected from Boring HB-BREW-102 at the I-395 Terminus site. ....	239
Figure 7.8: Recompression consolidated undrained triaxial (CAUC) normalized effective stress paths for Presumpscot clay samples collected from Boring HB-BREW-102 at the I-395 Terminus site. ....	241
Figure 7.9: SHANSEP recompression consolidated undrained triaxial (CAUC) normalized effective stress paths for Presumpscot clay sample 8U from Boring HB-BREW-102 conducted at the I-395 Terminus site.....	243
Figure 7.10: Comparison of normalized undrained shear strength from recompression and SHANSEP triaxial compression tests for Presumpscot clay specimens from boring HB-BREW-102 6U conducted at the I-395 Terminus site.....	244
Figure 7.11: Measured values of (a) corrected tip resistance, (b) sleeve friction, and (c) pore pressure from SCPTu 101, CPTu 102, and SCPTu 106 performed at the I-395 Terminus site.....	248
Figure 7.12: Profile comparing remolded shear strength values ( $s_{u(r)}$ ) obtained from HB-BREW-101 field vane tests and fall cone tests from HB-BREW-102 samples with sleeve friction from SCPTu 101 at the I-395 Terminus site.....	249
Figure 7.13: Depth profile of shear wave velocity ( $V_s$ ), shear modulus ( $G_0$ ), and rigidity index ( $I_r$ ) for SCPTu101 and -106 at the I-395 Terminus site.....	251

Figure 7.14: Measurements of a) normalized tip resistance ( $Q_t$ ), b) sleeve friction ratio ( $F_r$ ), and c) normalized pore pressure ( $B_q$ ) for SCPTu 101, 102, and 106 conducted at the I-395 Terminus site. ....	252
Figure 7.15: Soil classification results from SCPTu 101 at the I-395 Terminus site comparing laboratory-determined USCS classification to classification charts using a) $Q_t$ vs. $F_r$ (Robertson 1990), b) $Q_t$ vs. $B_q$ (Robertson 1990), c) $Q_t$ vs. $F_r$ (Robertson 2009), d) $Q_t$ vs. $B_q$ (Schneider et al., 2008) .....	254
Figure 7.16: Soil classification results from SCPTu 106 at the I-395 Terminus site comparing laboratory-determined USCS classification to classification charts using a) $Q_t$ vs. $F_r$ (Robertson 1990), b) $Q_t$ vs. $B_q$ (Robertson 1990), c) $Q_t$ vs. $F_r$ (Robertson 2009), d) $Q_t$ vs. $B_q$ (Schneider et al., 2008). ....	255
Figure 7.17: Subsurface profiles of a) stress history $k$ values determined from SCPTu 101, CPTu 102, and SCPTu 106, b) $\sigma'_p$ using minimum, maximum, and average $k$ -values from SCPTu 106 for (S)CPTu testing at the I-395 Terminus site. ....	258
Figure 7.18: Subsurface profiles of $N_{kt(\text{CAUC and FVT})}$ , $N_{ke(\text{CAUC and FVT})}$ , and $N_{\Delta u(\text{CAUC and FVT})}$ correlated from (S)CPTu 101, 102, and 106 with $s_u$ from triaxial CAUC testing and field vane shear testing (FVT) of Presumpscot clay at the I-395 Terminus site. ....	261
Figure 7.19: Subsurface profile of undrained shear strength ( $s_u$ ) with depth using the $N_{kt(\text{CAUC})}$ and $N_{\Delta u(\text{CAUC})}$ values from SCPTu 106 applied to measurements from SCPTu 106 and compared to the laboratory-determined $s_u$ of Presumpscot clay samples from the I-395 Terminus site. ....	263
Figure 8.1: Laboratory test results of overconsolidation ratio (OCR), undrained shear strength ( $s_u$ ) from triaxial shear, and sensitivity ( $S_t$ ) of Presumpscot clay collected at the four research sites. ....	270
Figure 8.2: Laboratory test results of overconsolidation ratio undrained shear strength ( $s_u$ ) shown as the gray circles compared to field vane shear test results (FVT) at a) Route 26/100 Bridge b) Martin's Point Bridge c) Route 197 Bride and d) I-395 Terminus site. ....	271
Figure 8.3: CPTu measurements of corrected a) tip resistance ( $q_t$ ), b) sleeve friction ( $f_s$ ), and c) pore water pressure ( $u_2$ ) collected in the Presumpscot clay deposits at the four research sites. ....	275
Figure 8.4: CPTu measurements of a) normalized tip resistance ( $Q_t$ ), b) sleeve friction ratio ( $F_r$ ), and c) normalized pore water pressure ( $B_q$ ) in the Presumpscot clay deposits at the four research sites. ....	276
Figure 8.5: CPTu measurements compared to measured values of undrained shear strength and OCR of Presumpscot clay. ....	277
Figure 8.6: Schematic illustrating discrete sampling locations at 2 foot and 5 foot intervals within the subsurface of the Route 197 Bridge alongside the CPTu profile of corrected tip resistance. ....	279
Figure 8.7: Comparison of CPTu profile collected at the Route 197 Bridge (modification of Figure 6.13, showing the soil layers by color) to the corresponding normalized measurement plotted on SBT classification charts. ....	283

Figure 8.8: CPTu normalized data from all four Presumpscot clay research sites plotted with corresponding USCS classification of undisturbed soil samples. Note: CH = fat clay, CL = lean clay, CL-ML = silty clay, and ML = silt.....	287
Figure 8.9: Comparison of Robertson (1990) a) $Q_t$ - $F_r$ and b) $Q_t$ - $B_q$ classification illustrating difference in predicted soil behavior type for CPTu data from the Route 197 Bridge site. ....	289
Figure 8.10: Comparison of CPTu data of Presumpscot clay from the four research sites plotted on SBT classification charts in accordance with silt content of the undisturbed soil samples. A and b show the data from all four sites and c and d show the results from only Route 26/100 Bridge and Route 197 sites (sensitive deposits). ....	291
Figure 8.11: Evaluation of the predicted engineering properties from the Robertson (1990) and Robertson (2009) SBT classification charts of the Presumpscot clay. Values of OCR, $S_t$ , and normalized remolded undrained shear strength ( $s_{u(r)}/\sigma'_{vo}$ ) were measured in the laboratory on high-quality samples. ....	295
Figure 8.12 Evaluation of the predicted engineering properties from the Robertson (1990) and Schneider et al., (2008) - $B_q$ SBT classification charts of the Presumpscot clay. Values of OCR, and $S_t$ , were measured in the laboratory on high-quality samples.....	296
Figure 8.13: Overconsolidation ratio (OCR) and preconsolidation pressure estimated using a k-value of 0.33 as suggested by Mayne (2014).....	301
Figure 8.14: CPTu k-value versus OCR for the Presumpscot clay.....	302
Figure 8.15: Estimates of $\sigma'_p$ versus depth for a) Route 26/100 Bridge b) Martin's Point Bridge c) Route 197 Bridge and d) I-395 Terminus using average and $\pm 1$ standard deviation for each site. ....	304
Figure 8.16: Analysis of OCR and $B_q$ relationship for the Presumpscot clay research sites. ....	306
Figure 8.17: Analysis of the Saye et al., (2013) method using Presumpscot clay data. ....	307
Figure 8.18: $N_{kt}$ and $N_{\Delta u}$ factors determined from laboratory testing and field vane shear testing (FVT) at all four Presumpscot clay research sites. ....	318
Figure 8.19: CPTu cone factor $N_{kt(CAUC \text{ or } DSS)}$ for the Presumpscot clay correlated to a) overconsolidation ratio (OCR), b) Plasticity Index (PI), c) undrained shear strength ( $s_u$ ) and d) normalized pore pressure ( $B_q$ ).....	322
Figure 8.20: CPTu cone factor $N_{\Delta u(CAUC \text{ or } DSS)}$ for the Presumpscot clay correlated to a) overconsolidation ratio (OCR), b) Plasticity Index (PI), c) undrained shear strength ( $s_u$ ) and d) normalized pore pressure ( $B_q$ ).....	323
Figure 8.21: Presumpscot clay CPTu data compared to ranges from a) Aas et al., (1986) b) Karlsrud et al., (1996), and c) Lunne et al., (1985) and Karlsrud (1996).....	324
Figure 8.22: Undrained shear strength coefficient $N_{\Delta u}$ vs. OCR, separating data points of high sensitivity and low sensitivity for Presumpscot clay.....	326
Figure 8.23: $N_{kt}$ and k-value estimated from the Been et al., (2013) method compared to actual values back-calculated from laboratory testing of Presumpscot clay .....	328

Figure 8.24: Profile of undraind shear strength ( $s_u$ ) using the site-specific CPTu $N_{kt}$ values compared to the laboratory determine $s_u$ for a) Route 26/100 Bridge, b) Martin's Point Bridge, c) Route 197 Bridge, and d) I-395 Terminus.....	332
Figure 8.25: Profile of undraind shear strength ( $s_u$ ) using the site-specific CPTu $N_{\Delta u}$ values compared to the laboratory determine $s_u$ for a) Route 26/100 Bridge, b) Martin's Point Bridge, c) Route 197 Bridge, and d) I-395 Terminus.....	333
Figure 8.26: Slope stability results of Presumpscot clay at the Route 26/100 Famlouth Bridge site using direct simple shear (DSS) and field vane shear testing (FVT) $s_u$ models. ....	336
Figure 8.27: Slope stability results of Presumpscot clay at the Route 26/100 Famlouth Bridge site using CPTu cone factors $N_{kt}$ and $N_{\Delta u}$ undraind shear strength models .....	336
Figure 8.28 Measurements of a) Shear wave velocity ( $V_s$ ) b) Small strain shear modulus ( $G_0$ ) and c) Rigidity index ( $I_r$ ) in the Presumpscot clay.....	341
Figure 8.29: a) $G_0$ vs. OCR and b) $G_0$ vs. void ratio ( $e_0$ ) for the Presumpscot clay research sites.....	342

## LIST OF ABBREVIATIONS AND SYMBOLS

### Symbols

$a$  = CPT cone calibration factor

$A_c$  = CPT cone cross sectional area of the cone ( $\text{ft}^2$ )

$A_s$  = cross sectional area of CPT sleeve ( $\text{ft}^2$ )

$B_q$  = CPT cone classification factor ( $\Delta u/q_{\text{net}}$ )

$e$  = void ratio

$e_{\text{vc}}$  = void ratio at final vertical consolidation stress

$e_{\text{vc-max}}$  = void ratio at maximum vertical consolidation stress [SHANSEP tests only]

$e_0$  = initial void ratio

$F_c$  = CPT cone total axial force applied to tip (lb-f)

$F_r$  = CPT cone sleeve friction over net tip resistance ( $f_s/q_{\text{net}} * 100$ ) (%)

$f_s$  = CPT cone sleeve friction (psf)

$F_s$  = CPT cone total axial force over sleeve (lb-f)

$G_0$  = small strain shear modulus (psf)

$I_r$  = rigidity index

$k$ -value = strength correlation factor with CPT results

$m$  = exponential factor in SHANSEP equation

$N_{kt}$  = empirical strength coefficient using tip resistance

$N_{\Delta u}$  = empirical strength coefficient using pore pressure

$N_{ke}$  = empirical strength coefficient using tip resistance and pore pressure

$q_c$  = CPT cone tip resistance (psf)

$q_{\text{net}}$  = CPT cone net tip resistance (psf)

$q_t$  = CPT cone tip resistance corrected for uneven pore pressures (psf)

$Q_t$  = CPT cone classification factor ( $q_{\text{net}}/\sigma'_{v0}$ )

$R_f$  = CPT cone classification factor

$S$  = normalized undrained shear strength at normally consolidated conditions

$S_t$  = sensitivity ( $s_u/s_{u-r}$ )

$s_u$  = undrained shear strength for intact soil (psf)  
 $s_{u-r}$  = undrained shear strength for remolded soil (psf)  
 $u_1$  = CPT cone penetrometer pore pressure measurement at apex of cone (psf)  
 $u_2$  = CPT cone penetrometer pore pressure measurement at shoulder of cone (psf)  
 $u_3$  = CPT cone penetrometer pore pressure measurement behind friction sleeve (psf)  
 $u_b$  = base pore pressure measured during CRS consolidation (psf)  
 $U$  = CPT cone classification factor  
 $V_s$  = shear wave velocity (ft/s)  
 $w_n$  = natural water content (%)  
 $\Delta L$  = horizontal displacement (in)  
 $\Delta u$  = difference in  $u_2$  measured and hydrostatic pore pressure (psf)  
 $\Delta u_f$  = change in pore pressure from the start of shear to failure (psf)  
 $\epsilon_{vc}$  = vertical consolidation strain (%)  
 $\gamma$  = shear strain (= horizontal displacement/specimen height) (%)  
 $\gamma_f$  = shear strain at failure (%)  
 $\gamma_t$  = total unit weight (pcf)  
 $\gamma_d$  = dry unit weight (pcf)  
 $\sigma_v$  = total vertical stress (psf)  
 $\sigma'_{vc}$  = vertical consolidation effective stress (psf)  
 $\sigma'_{vc-max}$  = maximum vertical consolidation effective stress (psf) [SHANSEP OCR >]  
 $\sigma'_{vf}$  = vertical effective stress at failure (psf)  
 $\sigma'_{v0}$  = estimated vertical consolidation stress (psf)  
 $q_f$  = shear stress (psf)

#### Acronyms

ASCE = American Society of Civil Engineers

bgs = below ground surface

BP = back pressure

CAUC = consolidated anisotropic undrained compression [laboratory strength method]

CIUC = consolidated isotropic undrained compression [laboratory strength method]

CPT = cone penetrometer testing

CPTu = cone penetrometer testing with pore pressure measurement

CRS = constant rate of strain [laboratory consolidation method]

MaineDOT = Maine Department of Transportation

DSS = direct simple shear [laboratory strength method]

FV = field vane shear test

IBC = International Building Code

IL = incremental load [laboratory consolidation method]

LI = liquidity index ( $= [w_n - LL] / PI$ )

LIR = load increment ratio ( $= [\sigma_{(i+1)} - \sigma_i] / \sigma_i$ )

LL = liquid limit

MSL = mean sea level

PI = plasticity index ( $= LL - PL$ )

PL = plastic limit

OCR = overconsolidation ratio ( $= \sigma'_{vc-max} / \sigma'_{vc}$ )

SCPTu = cone penetrometer testing with pore pressure measurement and seismic testing

SHANSEP = stress history and normalized soil engineering parameters [analysis]

SPT = standard penetration testing

TX = triaxial testing

ybp = years before presents

Units

feet = ft (')

inches = in (")

ksf = kips per square foot

pcf = pounds per cubic foot

psf = pounds per square foot

tsf = tons per square foot



## 1 INTRODUCTION

The Presumpscot Formation is a glacial marine sediment deposit located along the coast of Maine and inland along the Kennebec and Penobscot River valleys. The deposit consists of predominantly soft, silty clay with some interbedded silt and fine sand seams. Thickness of Presumpscot Formation (also known as "Presumpscot clay") deposits can vary from a couple of feet to over 200 feet (Thompson, 1987), generally increasing in depth closer to the coast. The Presumpscot clay is a challenging material with regards to characterization and design, as composition and engineering properties vary widely on both a local and regional scale.

Geotechnical investigations of the Presumpscot Formation traditionally involve the drilling of investigative borings, performing discrete disturbed sampling to obtain samples for index testing and classification, and conducting field vane shear tests (FVT) to identify *in situ* undrained shear strength at discrete depths. Additionally, when budget permits, undisturbed Shelby tube samples may be collected and tested in the laboratory to obtain compressibility, stress history, and strength. These tests are typically time-consuming and expensive, and the results from a few tests are assumed to apply over a broad portion of the deposit's lateral extent and depth. These methods have been used with success, however, assumptions (e.g., distance between drainage layers, approximate overconsolidation ratios) and empirical relationships (e.g., between index properties and compressibility) must sometimes be made to complete the design process. Thus routine, and often successful, geotechnical designs can rely heavily on past experience and the understanding of nearby conditions at similar Presumpscot clay sites.

The variability of the Presumpscot with depth and lateral extent creates a need for engineers to identify this variability quickly and use the information to interpret geotechnical properties as well. Seismic cone penetration testing with pore pressure measurements (SCPTu) can serve as a tool to fill in the gaps of discrete geotechnical testing and provide complete profiles

of soil behavior. There are many applications of the tool which can be employed throughout any stage of a geotechnical investigation. The SCPTu provides quick profiling of the subsurface which can be vital in identifying "depths of interest" (e.g. soft, compressible layers) for possible sampling and laboratory testing. Furthermore, the SCPTu can be used to confirm observations made during the drilling of traditional borings. CPTu results can also identify layering, supply engineering parameters based on appropriate correlations, and provide shear wave velocity used to directly determine stress-strain properties.

The CPTu is a geotechnical investigation technique which involves pushing a sensitized cone into the subsurface at a constant rate while continuously measuring tip resistance, sleeve friction, and pore pressure (hydrostatic in granular soils and excess from soil shearing of cohesive soils). Additionally, shear wave velocity measurements can be collected at discrete intervals throughout the test (this is denoted by the "S" in the SCPTu acronym). The "u" in the SCPTu or CPTu acronym indicates that dynamic pore pressure was measured during the cone penetration test. Empirical and theoretical correlations have been developed between these measurements and soil engineering properties such as preconsolidation pressure ( $\sigma'_p$ ) and undrained shear strength ( $s_u$ ). Soil classification, location of silt/sand seams, seismic design parameters, and liquefaction potential can also be obtained from CPTu results. Results from the CPTu test can be used to delineate the subsurface stratigraphy and correlate to engineering parameters which may otherwise be expensive and time consuming to obtain from laboratory testing.

As Maine's population grows, specifically in the southern and coastal region of the state, infrastructure will inevitably involve continuous interaction with the Presumpscot Formation. It will be worthwhile for geotechnical engineers to utilize the most effective tools in determining properties of the Presumpscot clay. This will improve engineering design, in turn increasing the reliability of infrastructure performance.

The advantage of the CPTu over other testing methods (such as the *in situ* field vane shear test and laboratory consolidation, index and classification, or laboratory shear strength testing) is that the results are continuous, rapid, and repeatable (DeGroot and Ladd, 2010). For classification purposes, the CPTu is widely used and especially useful for determining if deposits are homogeneous (DeGroot and Ladd, 2010) as well as locating discrete low strength horizons which may otherwise be missed in discrete testing (Rogers, 2006). The ability to determine the homogeneity of a Presumpscot clay deposit can help support or disprove the assumption of applying engineering properties determined from a discrete test to an entire deposit, which is common practice.

Correlations of SCPTu sounding results in the Presumpscot clay are valuable for estimating engineering properties for design. Preconsolidation pressure ( $\sigma'_p$ ) of clays refers to the maximum stress applied at that particular depth within the deposit, and is essential for geotechnical design for effective estimation of settlement or stress-strain behavior (Saye *et al.* 2013, DeGroot and Ladd, 2010). Continuous estimates of  $\sigma'_p$  can be interpreted from SCPTu results by applying an empirical factor to the measured tip resistance. Undrained shear strength ( $s_u$ ) is used to evaluate the stability of earth slopes, estimate deep foundation (e.g., pile) capacity, estimate pressure on retaining structures, and interpret bearing capacity of shallow foundations in clay. Undrained shear refers to the shearing process which occurs quickly enough to prevent water from flowing out of the sheared clay. This is representative of the most critical shear mode for soft Presumpscot clay. Similar to  $\sigma'_p$ , continuous estimates of  $s_u$  can be made available by applying empirical factors to CPTu measurements. However, unlike  $\sigma'_p$ ,  $s_u$  is not a unique clay property as  $s_u$  is dependent on the orientation of the principal stress causing the shear failure as well as the shear rate (Lambe and Whitman 1969, DeGroot and Ladd, 2010, Holtz *et al.* 2011).

Engineering properties (e.g.  $\sigma'_p$  and  $s_u$ ) of Presumpscot clay deposits are typically determined at discrete depths. If the desired  $\sigma'_p$  or  $s_u$  of a clay deposit is at a particular depth, this approach is valid and probably the most effective way to determine the properties for geotechnical analyses. However, in almost all geotechnical analyses of soft clay sites, it is preferable to have a complete profile of engineering properties since calculations such as total settlement, retaining structure pressures, and deep foundation capacity, depth (and therefore the potential change in properties with depth) is incorporated into the analysis. Geotechnical engineers have the opportunity to perform more accurate analyses with a complete profile of engineering properties and classification of Presumpscot clay, which the CPTu can provide with the right data interpretation methods, which this thesis aims to provide. They also have the ability to identify layers and other variation in the soil profile and correlated properties that may be critical to design, yet may have been missed when using discrete sampling alone.

The (S)CPTu is a powerful complimentary tool to other existing geotechnical investigation techniques. For site characterization (i.e. determining soil type, location and extent of the deposit, and groundwater condition), the (S)CPTu is the most suitable technique (DeGroot and Ladd, 2010). The results can also be used in conjunction with laboratory and field tests to refine and enhance geotechnical analyses based on the complete profile of measurements from the (S)CPTu. Practically all literature reviewed by the author about geotechnical design in soft clay suggested that a combination of in situ field testing (i.e. SPT, CPTu, sample collection, FVT, etc.) be used for the most effective design (Lunne *et al.* 1997, Rogers 2006, Long, 2008, Been and Sancio 2010, Ladd and DeGroot 2010, Saye *et al.* 2013, Ching and Phoon, 2013).

## 1.1 Objective and Approach

The objective of this research is to evaluate the SCPTu as a geotechnical investigation technique in the Presumpscot clay at several sites in Maine and to develop a suite of correlations to classification, preconsolidation pressure ( $\sigma'_p$ ), undrained shear strength ( $s_u$ ) that are both site

specific and universal. Since the measurements taken from a SCPTu sounding are continuous with depth with discrete shear wave velocity measurements, if the classification and engineering properties predicted prove to be reasonable, geotechnical engineers can use the results to refine and improve analyses of Presumpscot clay to allow for time and cost savings and reduced risk.

Four sites were selected in Maine by MaineDOT, for whom this research was conducted, with known deposits of Presumpscot clay from surficial geologic mapping, previous experience in area, and preliminary phase geotechnical investigations. Since the Presumpscot clay deposit varies from site to site, it was important to encompass sites with a wide range of properties. It is impossible to completely represent the Presumpscot clay as a "whole" since the deposit differs so widely, however some common characteristics were represented from these four sites. Some of the characteristics included previous construction, stress history, sensitivity, silt and sand seams, marine or freshwater environments, and fine grained soil content. Specific properties are discussed within each site's chapter. The four sites are listed below:

The four sites are listed below:

- 1) Route 26/100 Bridge Replacement – Falmouth, ME
- 2) Martin's Point Bridge Replacement – Portland and Falmouth, ME
- 3) Route 197 Bridge Replacement – Richmond and Dresden, ME
- 4) I-395 Terminus – I-395 Brewer, ME

Figure 1.1 shows the approximate location of each site relative to the mapped surficial geologic deposits of Maine.

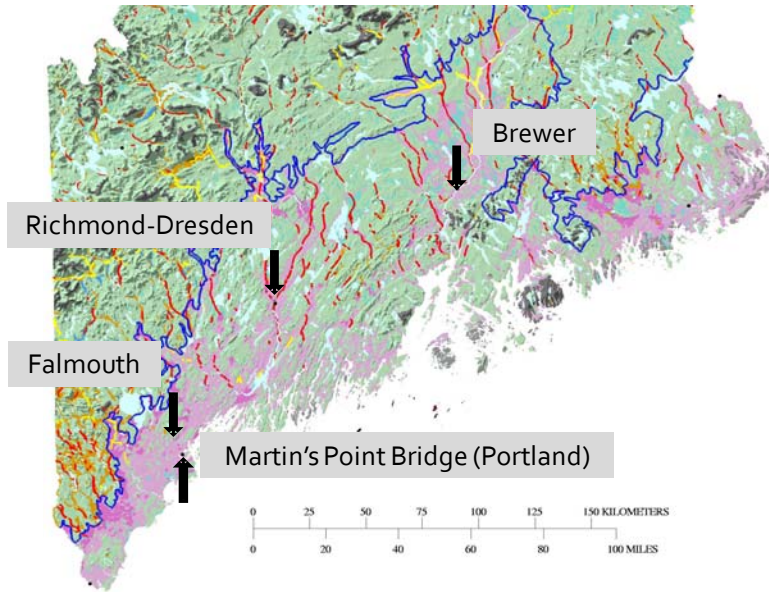


Figure 1.1: Approximate location of the four research sites from this study relative to the mapped surficial geology of southern Maine. (reproduced from the Maine Geologic Survey, 2010).

The following tasks were performed at each of the four sites:

- SCPTu testing within the Presumpscot layer to obtain continuous profiles of tip resistance, sleeve friction, and pore pressure. Additionally, perform discrete shear wave velocity during at least one SCPTu sounding per site.
- Traditional borings within the Presumpscot layer. During these borings, conduct field vane shear testing to obtain in situ undrained shear strength ( $s_u$ ) and collect undisturbed samples of Presumpscot clay for index and advanced laboratory testing.
- Typical index testing for each sample, which includes moisture contents, Atterberg limits, fall cone  $s_u$ , hydrometer, and organic content.
- One dimensional constant rate of strain (CRS) consolidation testing on samples from all undisturbed Shelby tube samples collected to determine stress history profiles.
- Direct simple shear (DSS) or undrained anisotropic consolidation triaxial (CAUC) testing on samples from all Shelby tubes collected from each site to determine  $s_u$  profiles.

- Comparison of consolidation and  $s_u$  obtained from laboratory testing to predicted values from empirical correlations from published CPTu literature
- Evaluation of the applicability and accuracy of published empirical correlations and provide range, minimum, maximum, and average resulting coefficients.

## 1.2 Organization

Chapter 2 presents a literature review on the Presumpscot Formation and the CPTu. Geologic history, composition and stratigraphy, and engineering properties are the focus of the Presumpscot Formation literature review.

Chapter 3 presents the field and laboratory testing methods used in the research. The chapter includes a description of the CPTu, soil sampling, field vane testing, and laboratory testing methods.

Chapter 4 through Chapter 7 provide a summary of research conducted at each site, including the layout of the site, summary of the previous geotechnical investigations conducted at the site, and the field testing performed for this study. The chapters present the laboratory results for index properties, stress histories, and undrained shear strengths determined from the undisturbed soil samples. The chapters conclude by presenting the SCPTu results from the site and the subsequent correlations for classification, stress history, and undrained shear strength. Chapter 4 focuses on the Route 26/100 Bridge Replacement Site in Falmouth. Chapter 5 focuses on the Martin's Point Bridge Replacement Site in Falmouth and Portland. Chapter 6 focuses on the Route 197 Bridge Replacement Site in Richmond and Dresden. Chapter 7 focuses on the I-395 Terminus Site in Brewer.

Chapter 8 presents correlations developed within the Presumpscot clay as a whole deposit in result of the four sites in this thesis. Chapter 9 summarizes the findings and provides recommendations for use of the SCPTu in Presumpscot clay and for future research.

### 1.3 Exclusions from Research

This thesis evaluates the use of SCPTu for predicting classification,  $\sigma'_p$ , and  $s_u$  in Presumpscot clay. There are many other geotechnical uses for the SCPTu which are excluded from this research. The first major exclusion is the interpretation of SCPTu results in granular soils. At all of our sites, the Presumpscot clay was either underlain or overlain by granular, non-cohesive material. SCPTu results can be used to estimate SPT-N blow counts, drained friction angle, liquefaction susceptibility, or other properties of these soils (Lunne *et al.*, 1997)

Other engineering properties of clay soils besides  $\sigma'_p$  and  $s_u$  estimated from SCPTu were not evaluated. This includes constrained modulus and compressibility. DeGroot and Ladd (2010) state that predicting these properties from SCPTu results are unreliable and are not recommended for geotechnical practitioners. Permeability estimates were not conducted in the Presumpscot clay from SCPTu dissipation tests. Liquefaction potential and seismic site class (in accordance with the International Building Code) can be predicted from shear wave velocity testing. This was not conducted at the sites in this thesis. If the reader is interested in learning more about the analyses excluded herein, please refer to Lunne *et al.*, (1997) and NCHRP (2007).



## 2 LITERATURE REVIEW

The cone penetration test with pore pressure measurements (CPTu) is a geotechnical investigation technique which provides near-continuous measurements of tip resistance, sleeve friction, and pore pressure that can be used to profile the subsurface and identify layering within the soil stratigraphy. When performed in clay deposits, the results from a CPTu can be interpreted to provide engineering parameters such as undrained shear strength ( $s_u$ ) and preconsolidation pressure ( $\sigma'_p$ ) with appropriate empirical correlations. The advantage to engineering properties obtained from a CPTu are that they are both continuous and determined from *in situ* behavior, eliminating the need to interpolate between discrete testing results as well as removing the influence of sample disturbance on testing results.

In Maine, the Presumpscot Formation (also known as Presumpscot clay) is a common surficial geologic deposit which presents major challenges to geotechnical engineers, mainly the characterization of  $s_u$  and  $\sigma'_p$ . The purpose of this thesis is to characterize four sites containing Presumpscot clay using current site investigation techniques (e.g., field vane shear testing and undisturbed sampling with subsequent laboratory testing) and correlate the results from this testing to CPTu results. This chapter summarizes Maine's Presumpscot clay deposit including its geologic history and range of engineering properties based on decades of geotechnical investigations performed throughout the deposit. Afterwards, the chapter will discuss the current use of CPTu to conduct investigations in similar soft clay deposits throughout the globe, its advantages and disadvantages, and the resulting empirical correlations used for determining classification,  $s_u$ , and  $\sigma'_p$  which will be evaluated in the Presumpscot clay.

### 2.1 Presumpscot Formation

The Presumpscot Formation is a glacial marine sediment deposit located along the coast of Maine and inland along the Kennebec and Penobscot River valleys (Figure 2.1). The deposit

consists of predominantly soft, silty clay with some interbedded silt and fine sand seams. The silty clay material ranges from homogeneous to stratified layers. Depending on bedrock elevation, deposit thicknesses can vary from two to 200 feet (Thompson, 1987).

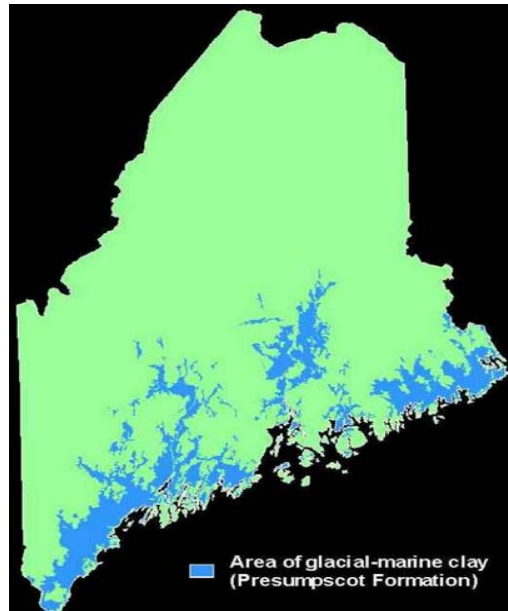


Figure 2.1: Extent of the Presumpscot Formation, shown in blue, along the coast of Maine and inland along the Kennebec and Penobscot River valleys (Maine Geological Survey, 2005).

The Presumpscot Formation has been studied for over a century. One of the first documented cases comes from an excavation in Lubec, Maine in 1837. Jackson describes a deposit which included many shells and barnacles close to bedrock elevation (Thompson, 1987). Some notable researchers of the Presumpscot Formation in the 19th century include Jackson, Hitchcock, and Stone (Thompson, 1987). It wasn't until 1960 that the Presumpscot Formation was formally named by Bloom for its good exposure in the Presumpscot river valley (Thompson, 1987). Since then, greater efforts have been taken to classify and predict behavior of the Presumpscot Formation. The reader is encouraged to explore references from the 1987 Presumpscot Formation Symposium (Andrews 1987, Morgan 1987, Sandford and Amos 1987, Thompson 1987, Weaver 1987) if additional information is required. Throughout this thesis,

"Presumpscot Formation," "Presumpscot clay," "Presumpscot," and "the deposit" all refer to the fine-grained geologic deposit described in this section.

During the Late Pleistocene era, approximately 17,000 years before present, an ice sheet covered Maine and New England (i.e. pre-Presumpscot clay deposition) and remained stagnant, resting against George's Bank in the Atlantic Ocean. Although the cause of the warming climactic change which initiated the retreat of the ice sheet is largely unknown, around 17,000 years before present (YBP) the ice sheet began melting and completely receded over the course of approximately 5,000 years (Kelley *et al.*, 2010). As the glacier retreated in a northern direction across the current landscape of Maine, a mixture of silt, sand, and clay flocculated out of suspension in the marine water either directly beneath or in front of the retreating glacier while the bedrock was depressed below sea level.

Subglacial and englacial meltwater stream systems within the Laurentide Ice Sheet carried a wide range of chemically and mechanically weathered material which was deposited at the front of the glacier. The resulting plume carried the fine grained material (i.e. materials that later formed the Presumpscot Formation) in suspension out away from the margin while the coarse grained material (i.e. glacial till, sand and gravel) settled out immediately. The depth of Presumpscot clay deposits are a function of how long (if at all) the glacier remained stagnant, as well as meltwater plume volume. The overall deposition of Presumpscot occurred from approximately 16,000 YBP to 11,000 YBP, a relatively rapid process in terms of geologic deposits.

After the Presumpscot Formation was deposited and the ice sheet melted, the weight relief of the removed glacier caused isostatic rebound of the bedrock and subsequent lowering of the relative mean sea level (MSL). In places, bedrock rebounded 200 feet over a 2,000 year period. This exposed the Presumpscot in some places to freshwater conditions. Since the

lowstand of the MSL (about 12,000 YBP), MSL has since risen approximately 200 feet and continues to rise slowly (Kelley *et al.*, 2010).

Material which underlies the Presumpscot clay generally consists of a combination of silty or clean sand, bedrock, or glacial till. If glacial till is the underlying material, the bottom of the Presumpscot layer may be interfingered or intermixed at the transitional zone, indicating an ice-pinning point during glacial retreat (Belknap, 1987). Abrupt transition from till to clay indicates that the glacier was retreating relatively quickly and the clay was sedimented in a low energy environment at the proximal zone of the glacier, where interfingering or intermixing indicates glacial stagnation and formation of the clay directly beneath the glacial contact zone. "Downward coarsening [of a Presumpscot Formation deposit] reflects the higher energy environment that prevailed when meltwater currents were still issuing from the nearby ice margin" (Thompson, 1987).

#### 2.1.1 Geotechnical Considerations

Presumpscot clay may cause difficulties for infrastructure design including major settlement, embankment shear failures, unpredictable time rate of consolidation, and reoccurring landslides. Properties of the deposit that can lead to these issues include high *in situ* water content, high sensitivity, interbedded silt and sand seams, varying deposit thicknesses, low undrained shear strength ( $s_u$ ), and high compressibility. The deposit has a reputation for characterization and design challenges. Often times the solution to the unpredictable behavior of the deposit results in over conservative designs and over engineered approaches, which can lead to major project expenses (Morgan, 1987). Examples of this may include the construction of deep foundations where shallow foundations are adequate, unnecessary pre-load magnitude and time periods to account for compressibility, oversized toe slope berms, or even abandoning a project due to the uncertainties of the clay properties.

Compositional characteristics of the Presumpscot Formation include the grain sizes and the material mineralogy. Sandford & Amos (1987) summarize grain sizes throughout the Presumpscot Formation as 0-35% fine sand, 20-55% silt, and 35-75% clay. The results of 43 grain size measurements performed by Goldthwait (1951) averaged values of 23.5% fine sand, 37.5% silt, and 39% clay. It is important to note that the presence of sand in the Presumpscot is typically due to sand seams or intermixing with overlying and underlying material. Quartz is the dominant material within Presumpscot clay, followed by feldspar and then muscovite mica (Schnitker & Borns, 1987). Thompson (1987) and Schnitker & Borns (1987) indicate the predominant clay mineral is illite with no traces of kaolinite or montmorillonite.

Due to the marine depositional environment, the clay particles, or "platelets," in the Presumpscot Formation have a mostly flocculated soil structure (Mitchell and Soga, 2005). This refers to the orientation of the particles being rather disorganized and having mostly edge-to-face contact (Figure 2.2a) with strong electrochemical bonds at the points of contact. As the Presumpscot clay platelets were originally deposited into the marine water by glacial streams at the glacier margin, they became individually suspended particles floating in suspension. The outside faces of the platelets were negatively charged while the ends of the platelets were positively charged. As they settled onto the sea floor, end-to-face contacts (flocculated structure) prevailed (Mitchell and Soga, 2005). Flocculated clay particles have  $s_u$ , higher permeability, and lower compressibility at stresses less than  $\sigma'_p$  compared to dispersed particle arrangement (Figure 2.2b) (Lambe & Whitman, 1967). The higher  $s_u$  and low compressibility can be attributed to the increased force required to break the electrochemical bonds, where the higher permeability is due to the channels formed by the random arrangement of flocculated particles. Figure 2.3 is an SEM photomicrograph of Boston Blue clay, showing the flocculated arrangement of clay particles similar to that found in Presumpscot clay. Pulverized rock flour is present in Presumpscot clay. Thompson (1987) even suggests that a majority of the clay-sized particles are rock flour. The

rock flour, very small and angular particles formed by mechanical weathering, exhibit no plasticity and can greatly affect the engineering behavior by occupying voids between the clay platelets (Terzaghi *et al.*, 1996).

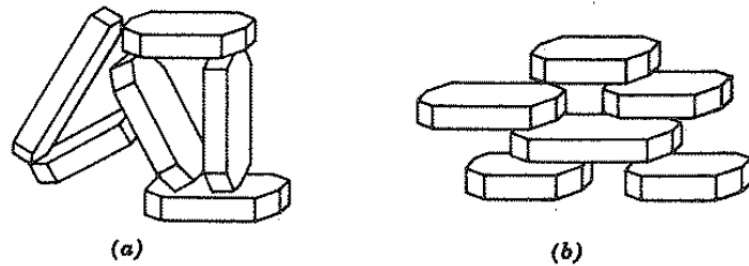


Figure 2.2: Idealized clay platelet structure for a) flocculated and b) dispersed clay (Lambe and Whitman, 1967).

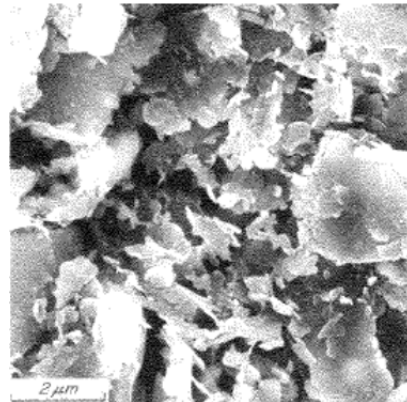


Figure 2.3: SEM Photomicrograph of Boston Blue Clay (Terzaghi *et al.*, 1996).

Engineering properties of the Presumpscot clay in this thesis refer to the preconsolidation pressure ( $\sigma'_p$ ) and undrained shear strength ( $s_u$ ). Engineering properties of the Presumpscot clay are influenced by depositional and post-depositional processes. The depositional environment controls the composition, layering and structure, which in turn influences plasticity, initial permeability, compressibility, undrained shear strength, and void ratio. Post-depositional

processes (including surface loading, surface unloading, groundwater fluctuations, cation exchange, etc.) controls water content, soil stresses, structure breakdown, and ion concentrations, which in turn influences  $\sigma'_p$ , compressibility,  $s_u$ , and the relative changes from the initial states. For example, shallow inland Presumpscot clay deposits are typically brown, oxidized stiff clay with a higher  $s_u$  than the soft, gray wet clay, which can be normally consolidated. The only differences between the crust and the lower, softer portion of these deposits are the water content and reorganized platelet structure, which is often due to desiccation from groundwater fluctuations.

### 2.1.2 Index Properties

Atterberg Limits represent water contents dividing where the clays act as a brittle, plastic, or liquid material. The plastic limit (PL) is the water content at which the clay transitions from brittle to plastic behavior (i.e. the clay can be deformed without volume change or cracking) (Mitchell and Soga, 2005). Plastic limit for Presumpscot clay ranges from 15-25 (Andrews, 1987) and averaged 22 for the sites in this thesis. Liquid limit (LL), defined as the water content at which the clay begins to exhibit liquid behavior (with an  $s_u$  of approximately 50 psf) (Mitchell and Soga, 2005) ranges from 25-41 (Andrew, 1987) and averaged 38 for the sites in this thesis. Plasticity index is the difference between liquid limit and plastic limit. Liquidity index (LI) relates the in situ water content to the plasticity behavior of the soil. LI below 0 indicates brittle behavior, LI between 0 and 1 indicates plastic behavior, and LI greater than 1 indicates liquid behavior. Based on the published LL and PL from Andrews (1987), Presumpscot clay PI typically ranges from 10-26. Based on published moisture content values from Andrews (1987), LI can range from 0 to 4.0.

Due to the low to moderate plasticity of the Presumpscot clay, it is almost always classified as lean clay CL in accordance to *ASTM D2487 Standard Practice for Classification of*

*Soils for Engineering Purposes (Unified Soil Classification System)*. Other possible classifications of Presumpscot include silty clay CL-ML with fine sand, silt ML, and clayey silty sand SC-SM. These are alternatives to lean clay that result from sand seams or material transition zones into overlying or underlying material.

### 2.1.3 Stress History

Stress history refers to the changes in stress (mechanical, pore pressure, physiochemical, and biochemical) which a soil deposit experiences after deposition. Preconsolidation pressure ( $\sigma'_p$ ) is defined as the apparent maximum past pressure and overconsolidation ratio (OCR) is the ratio of  $\sigma'_p$  to the current *in situ* vertical effective stress ( $\sigma'_{v0}$ ). If the current estimated *in situ* vertical effective stress,  $\sigma'_{v0}$  is equivalent to the measured  $\sigma'_p$ , that soil is normally consolidated. If the soil's existing  $\sigma'_{v0}$  is lower than  $\sigma'_p$ , the soil is overconsolidated. Very few, if any, deposits are truly normally consolidated due to the action of secondary compression (Holtz *et al.*, 2011) and aging. Mechanisms which contribute to  $\sigma'_p$  include the application of mechanical pressure to the ground surface (soil, construction activities, buildings, etc.), pore pressure changes from groundwater flow, desiccation from groundwater fluctuations, long-term drained creep (secondary compression), and other less common physiochemical and biochemical processes (Mitchell and Soga, 2005).

Stress history of Presumpscot clay deposits is a site-specific, complex phenomenon which typically requires laboratory consolidation testing and inferring of the geologic history at a site. Quantification of the stress history and overconsolidation ratio of a deposit at specific depths is critical for determining settlement and stress-strain behavior expected from applied loads. Volume change characteristics are directly related to the OCR of deposits, where samples which remain in stress states below  $\sigma'_p$  (i.e. analogous to the recompression portion of the consolidation curve from 1D consolidation testing) will experience less settlement than those soils loaded



beyond a stress state of the  $\sigma'_p$  (i.e. analogous to loading into the virgin compression portion of the consolidation curve from 1D consolidation testing).

The OCR of Presumpscot clay depends on site-specific characteristics such as clay depth, overlying soil (if any) overburden stresses, geologic and anthropomorphic loading at the site, and groundwater movement through the clay. Andrews (1987) presents the OCR results from a "well documented" Presumpscot clay deposit in Portland, Maine to range from 4.4 at 5 foot depth to 1.12 at 60 foot depth. A deep deposit of Presumpscot clay in Westbrook, Maine studied by Devin & Sandford (2000) was found to have an OCR of 1.44 at 15 foot depth and an OCR of 1.03 at 72 foot depth. The higher OCR value in the shallower portion of the deposit at Westbrook is attributed to groundwater movement, chemical weathering, and desiccation.

The compression index ( $C_c$ ) of clay is determined from the slope of the void ratio vs. effective stress plot in the virgin compression portion of the consolidation curve. The higher the value, the more deformation is expected upon application of loading.  $C_c$  has been found to range from 0.33 to 0.60 for Presumpscot clay throughout the state (Andrews, 1987). Cole (1987) documented a Presumpscot clay site at Warren Avenue in Portland, Maine to have  $C_c$  values ranging from 0.52 to 0.89 with an average of 0.73. This was determined on oedometer tests on undisturbed Shelby tube specimens.

#### 2.1.4 Undrained Shear Strength

Shear strength of soil is the resistance to differential loading. It is not a specific soil property but rather a behavior based on stress history, type of loading, drainage conditions, and confining pressure (Terzaghi *et al.*, 1996, Mitchell and Soga 2005, Holtz *et al.*, 2011). For fine grained cohesive materials such as Presumpscot clay, permeability is low and pore water pressures generated during shear failure cannot dissipate, thus undrained conditions are used to represent the lower bound shear strength (Lambe and Whitman, 1967).

Undrained shear strength ( $s_u$ ) of Presumpscot clay is typically estimated using either *in situ* field vane shear testing (FVT) (Figure 3.6) or advanced laboratory testing on undisturbed samples collected from the subsurface (Andrew 1987, Morgan 1987, Devin and Sandford, 2000, Langlais 2011). For both FVT and laboratory testing,  $s_u$  will vary depending on mode and rate of shear and testing method. For laboratory testing, three types of undrained shear tests have been developed to estimate  $s_u$  based on three common expected failure mechanisms. These are triaxial compression (TC), direct simple shear (DSS), and triaxial extension (TE). The three types of  $s_u$  are illustrated using a theoretical slope failure in Figure 2.4. The difference in  $s_u$  from these three methods is due to the variation in the angle of the applied load during the test, also known as the deviator stress. In TC testing, the deviator stress is directly vertical ( $0^\circ$ ), where the deviator stress for DSS testing is somewhere between  $30^\circ$  and  $60^\circ$  (DeGroot and Ladd 2010), and the deviator stress for TE is  $90^\circ$ . Laboratory testing on an identical specimen of clay would result in  $s_u$  magnitudes from highest to lowest from TC, DSS, and TE, respectively. Figure 2.5 illustrates the difference in  $s_u$  measured from triaxial CAUC (anisotropically consolidated undrained compression; or named "triaxial compression" in Figure 2.5) and DSS. It should be noted that the plasticity index (PI, seen as the x-axis in Figure 2.5) of Presumpscot clay is generally around 20, and the expected ratio of  $s_u/\sigma'_{v0}$  for TC testing to range from approximately 0.28 to 0.35 and of  $s_u/\sigma'_{v0}$  for DSS testing to range from 0.18 to 0.28.  $s_u$  can also be measured *in situ* using the field vane shear test (FVT). Typical values of  $s_u$  in soft, normally to lightly overconsolidated Presumpscot clay were observed to range from 215 to 750 psf (Weaver 1984, Sandford and Amos 1987, Morgan 1987, Andrews 1987, Devin 1990). This includes values from FVT, anisotropic consolidated triaxial compression, and isotropic consolidated triaxial compression testing.

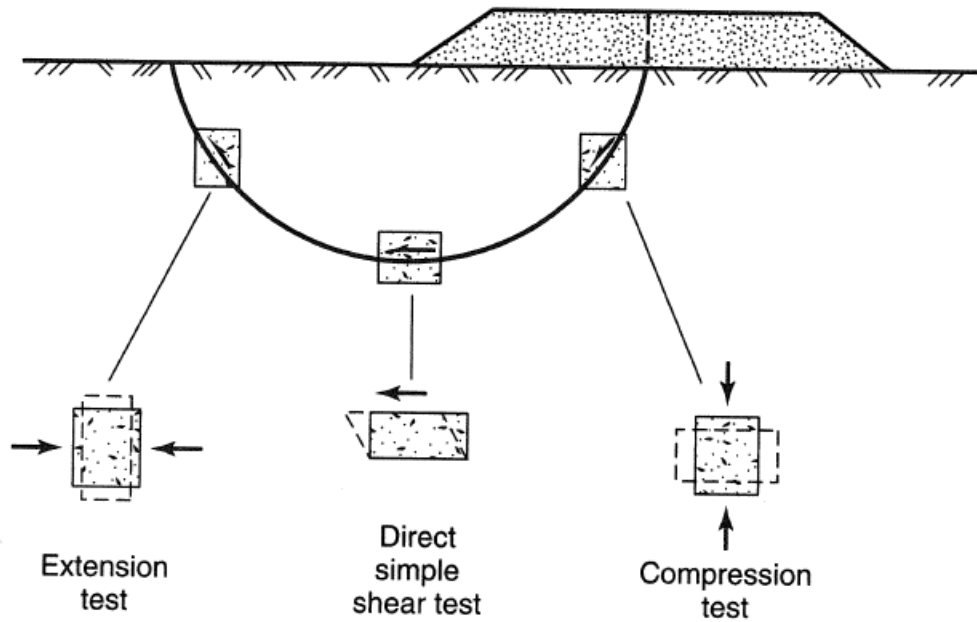


Figure 2.4: Slope failure modes replicated by laboratory shear strength testing of clays. (from Holtz *et al.*, 2011).

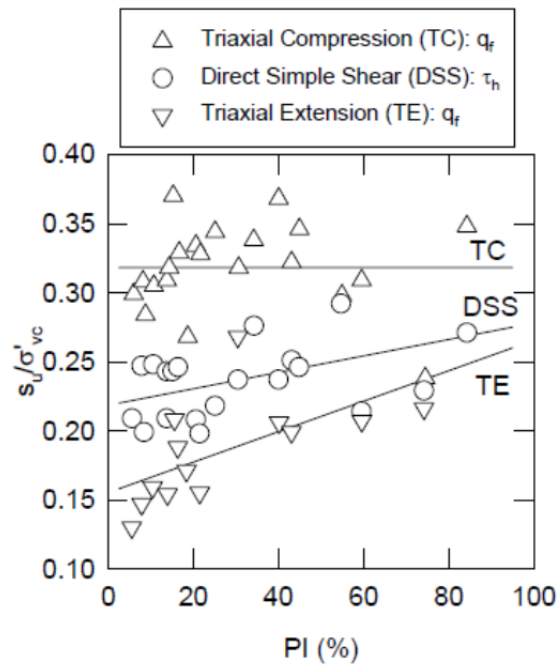


Figure 2.5: Normalized undrained shear strength vs. plasticity index for triaxial compression (TC), direct simple shear (DSS), and triaxial extension (TE) testing on various silts and clays (such as Norwegian clay and Boston Blue clay, but excluding varved deposits) (from Ladd & DeGroot, 2003).

Remolded undrained shear strength ( $s_{u(r)}$ ) is the measurement of remaining undrained shear strength at the in situ water content upon complete destructuring of the soil along the failure plane. Likewise with  $s_u$ ,  $s_{u(r)}$  is not a distinct property of clay, rather a measurement dependent on the condition of the tested clay. Specifically for  $s_{u(r)}$ , the determined value is highly depended on the extent of remolding. During the FVT, the vane is completely rotated 5 to 10 times in an attempt to completely remold the clay (ASTM, 2008), however, this may not be enough rotations to cause complete remolding along the failure plane (DeGroot and Ladd, 2010). In the laboratory, it is easier to cause complete remolding by kneading of the soil sample. In result, the  $s_{u(r)}$  measured from the FVT and the fall cone apparatus are not strictly comparable (Terzaghi *et al.*, 1996), and in general the  $s_{u(r)}$  from FVT will be higher than  $s_{u(r)}$  from fall cone testing.

Sensitivity ( $S_t$ ), defined as the ratio of measured  $s_u$  to  $s_{u(r)}$ , indicates how much strength loss occurs during the remolding of clay structure at the natural water content. Table 2.1 presents sensitivity classification defined by Holts & Kovacs (1981). Presumpscot clay has a low to moderate to high sensitivity due to its flocculated structure from glacial marine deposition and clay content (Devin and Sandford, 1990). Glacially deposited clay, such as the Presumpscot, will have be made more sensitive following deposition as it is expected that sodium ions that attached to the clay platelets during deposition are leached out over time in freshwater environments (Lambe & Whitman, 1969).

Table 2.1: Holtz & Kovacs clay sensitivity scale (Holtz et al., 2011).

Sensitivity ( $S_t$ )	Classification
2 - 4	<i>Low Sensitivity</i>
4 - 8	<i>Medium Sensitivity</i>
8 - 16	<i>Highly Sensitive</i>
> 16	<i>Quick</i>

Stress history of a deposit can have an effect on the undrained shear strength. Some portions of deposits of Presumpscot clay have been subjected, and continue to be subjected to, mechanical stress changes from the unloading of surficial material or fluctuations in groundwater

table elevation that result in total stress changes. Changes in total and effective stress (due to pore pressure fluctuation or dissipation following loading) re-orient the clay platelet structure and reduces the water content, effectively densifying the material and decreasing voids. This is common in the upper few feet of Presumpscot clay deposits, called the "crust," which produce samples of clay with a brown, oxidized, and/or mottled appearance which is stiffer than the softer clay below. OCR in this crust can range from 2 to 37 (Devin and Sandford, 1995). Andrews (1987) found the  $s_u$  in this layer to range from 2,000 psf to 3,500 psf.

Ladd and Foott (1974) observed a relationship between the stress history and the  $s_u$  of clay deposits. They determine that the stress-strain behavior and undrained shear strength of clays is directly controlled by the amount of overconsolidation of a deposit. For clay under normally consolidated conditions (i.e., OCR=1), the undrained shear strength normalized by effective overburden stress ( $s_u/\sigma'_{v0}$ ) was found to be more or less constant (Ladd and DeGroot, 2003). As OCR increases,  $s_u$  increases exponentially. This relationship is called the Stress History and Normalized Soil Engineering Parameter (SHANSEP) relationship and is shown in Equation 2.1:

$$(s_u/\sigma'_{v0})_{(OC)} = S*OCR^m \quad 2.1$$

where  $s_u$  = undrained shear strength,  $\sigma'_{v0}$  = *in situ* vertical effective stress, OC notates overconsolidated state,  $S = (s_u/\sigma'_{v0})$  for normally consolidated conditions, OCR = overconsolidation ratio, and  $m$  = exponential coefficient found to range from approximately 0.5 to 1.0 (Karlsrud and Hernandez-Martinez, 2013).

A relationship exists between the effective overburden stress and  $s_u$ . For normally consolidated clays,  $s_u/\sigma'_{v0}$  or  $S$ , is assumed constant for a deposit and generally ranges from 0.19 to 0.25 (Ladd & DeGroot, 2003). This results in a linearly increasing profile of  $s_u$  with increasing confining pressure, which is often the assumed condition in geotechnical design. However, in overconsolidated portions of the clays, including Presumpscot clay,  $s_u/\sigma'_{v0}$  will increase

exponentially with increasing overconsolidation (DeGroot & Ladd 2010), hence the exponential term on the OCR.  $s_u/\sigma'_{v,0}$  values of normally consolidated Presumpscot clay can vary between 0.13 and 0.40 (Andrews, 1987). Andrews (1987) does not specify the mode of undrained shear from which this range derives, but the article does discuss the different expected  $s_u$  from different testing methods, so it is likely that this range represents different types of undrained shear strength testing (both field and laboratory).

Karlsruud and Hernandez-Martinez (2013) performed CAUC SHANSEP testing on high quality block samples of Norwegian clay and found the  $S$  parameter to range from 0.25 to 0.35 with an average of 0.30 and the  $m$  coefficient to range from 0.65 to 0.75 with an average of 0.70 when using triaxial compression as the reference shear strength. Review literature for Presumpscot clay and Boston Blue Clay, a nearby glacially deposited soil located in the greater Boston, MA area, produced SHANSEP relationship parameters shown in Table 2.2.

Table 2.2: Summary of SHANSEP parameters obtained from studies on Presumpscot clay and Boston Blue clay.

<b>Soil Deposit</b>	<b>S</b>	<b>m</b>	<b>Reference</b>
Presumpscot Clay	0.34	0.55	Devin (1990)
Boston Blue Clay	0.28	0.60	Landon (2007)
Boston Blue Clay	0.19	0.75	DeGroot (2003)
Boston Blue Clay	0.28	0.68	Ladd et al., (1999)

## 2.2 Cone Penetration Testing (CPTu)

Cone penetration testing with pore pressure measurement (CPTu) has been in use by the geotechnical community for both terrestrial and offshore projects since the 1980's. It remains one of the most useful *in situ* devices for projects worldwide, and has surpassed the Standard Penetration Test (SPT) in use in Europe and parts of Asia. Cone penetration testing (CPT) generally refers to any manner of *in situ* testing using an electric cone that measures tip resistance and friction along the friction sleeve behind the cone tip during penetration into subsurface soils. Variations in cone penetration equipment that allow for pore pressure measurement in soft to

medium clays at different positions (e.g.,  $u_1$  on the face of the cone tip,  $u_2$  behind the cone tip) are referred to as piezocone tests with the acronym CPTu (cone penetration testing with pore pressure measurement). Variations that allow for shear wave velocity,  $V_s$ , measurement are given the acronym SCPTu (seismic cone penetration testing with pore pressure measurement).

A 2007 report of the National Cooperative Highway Research Program (NCHRP) provides a comprehensive review of current practices followed by US and Canada Departments of Transportation (DOTs). NCHRP (2007) states:

*"In its simplest application, the cone penetrometer offers a quick, expedient, and economical way to profile the subsurface soil layering at a particular site. No drilling, soil samples, or spoils are generated; therefore, CPT is less disruptive from an environmental standpoint. The continuous nature of CPT readings permit clear delineations of various soil strata, their depths, thicknesses, and extent, perhaps better than conventional rotary drilling operations that use a standard drive sampler at 5-ft vertical intervals. Therefore, if it is expected that the subsurface conditions contain critical layers or soft zones that need detection and identification, CPT can locate and highlight these particular features. In the case of piles that must bear in established lower foundation formation soils, CPT is ideal for locating the pile tip elevations for installation operations."*

The seismic piezocone penetrometer provides near continuous profiles of tip resistance ( $q_c$ ) and corrected tip resistance, which is corrected for pore pressures behind the cone tip ( $q_t$ ), sleeve friction ( $f_s$ ), and penetration induced pore pressure water ( $u_2$ ) which are used to indicate layering and stratigraphy, lateral site heterogeneity between multiple soundings, and relative soil composition (e.g., from "soft" clays to "stiff" sands). As the cone penetrates the subsurface, the tip resistance measured on the penetrometer is essentially a cumulative resistance of the soil within a zone of influence around the tip of the cone, not just the resistance of the soil directly in front of the cone. Figure 2.6 illustrates a theoretical zone of influence around an advancing cone with the corresponding stress-strain response of the soil at different points beyond the tip of the cone. Soil that is directly in front of the cone is strained well beyond the point of failure, and for clay, reaches the state of remolding. However, as the distance from the tip of the cone increases, the resulting stress on the soil reduces to pre-shear magnitudes and the strain is theoretically

elastic. Hence, the tip resistance measurement is a cumulative measurement of clay within the plastic and elastic zone. Sleeve friction and pore pressure measurements only measure the post-sheared soil in contact with the cone (Robertson, 2012). The relationship between remolded shear strength and sleeve friction values will be discussed later in Chapter 3.

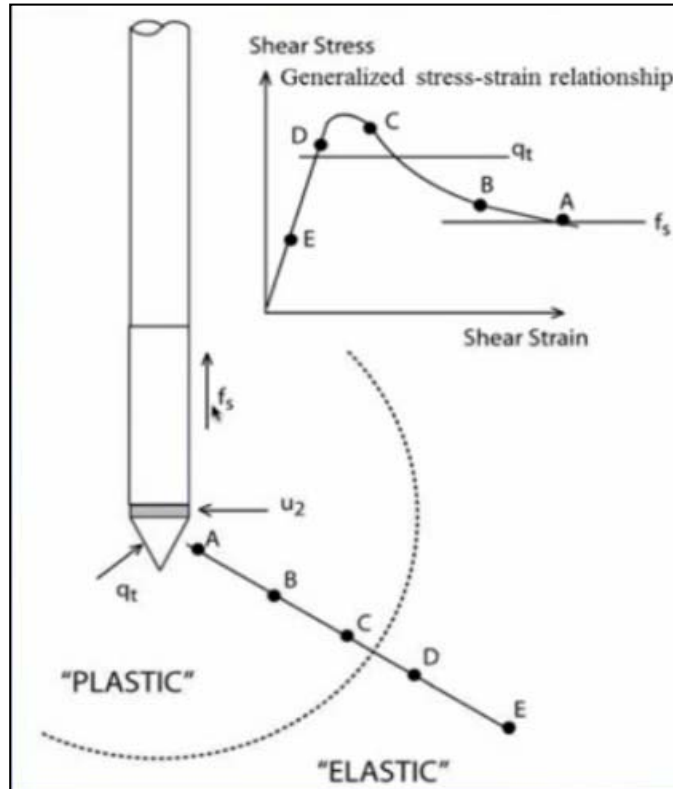


Figure 2.6: Theoretical soil behavior around the tip of an advancing cone (from Robertson, 2012).

Seismic shear wave velocity measurements are not continuous, but are made at discrete intervals within the subsurface, usually at each rod break. Shear waves are generated at the soil-water interface by striking a source (discussed in Section 3.1) and shear wave traces are received to be processed using the pseudo-interval method. The distance between the shear wave tests is used as the shear wave travel distance ( $\Delta l$ ), and the difference in the time of arrival of the shear waves determined for each trace at the different test depths is used as the travel time ( $\Delta t$ ). Shear wave velocity,  $V_s$ , can then be calculated using Equation 3.5.



### 2.2.1 CPTu Use in Geotechnical Investigations in Soft Clay

Successful applications of CPTu in embankment stability and structure foundation designs of soft clays have been well-documented. Ladd and DeGroot (2003) highlight the importance of site-specific correlations when interpreting CPTu results for geotechnical design. Empirical cone factors used to determine  $s_u$  have a wide range based on published data, and have been found to vary based on clay sensitivity, plasticity, overconsolidation ratio (OCR), as well as types of piezocones used and test operators (Robertson 2009, Rogers 2006, Ladd and DeGroot 2003). Two sites of Boston Blue Clay (BBC, a marine clay deposited in the greater Boston area during the same time period of the Presumpscot clay) were examined for their correlated  $s_u$  values to the CPTu. The BBC at both sites is covered by 30 feet of fill and contains an overconsolidated crust overlying low OCR clay. Both sites have been studied extensively at the Massachusetts Institute of Technology (MIT) which includes high quality laboratory tested specimens. Cone factor  $N_{kt}$  was determined at each site by back-calculating to laboratory determined values of  $s_u$  from direct simple shear (DSS) testing.  $N_{kt}$  varied from approximately 8 to 13 for one site and 17 to 22 for the other. Ladd and DeGroot (2003) state that the difference in strength correlations is not soil plasticity and is from unknown reasons.

### 2.2.2 Use of CPTu to Supplement Laboratory and Field Testing

Wei *et al.*, (2010) performed a geotechnical investigation that included CPTu soundings at the crown of a levee in New Orleans which consists of silty and sandy clay fill over a deep deposit of high plasticity clay to characterize the undrained shear strength and determine the stability of the clay-supported levee. Adjacent to CPTu sounding, high quality tube samples were collected and tested in unconsolidated unconfined compression and triaxial unconsolidated undrained compression tests (the consolidation conditions were not specified) to determine  $s_u$  with depth. Analysis of the laboratory results and correlation to the CPTu measurements provided

an optimum cone factor  $N_{kt}$  12.0 and Wei *et al.*, (2010) concluded that the CPTu correlation derived  $s_u$  profile correlated well with the laboratory undrained shear testing results, even when the measured strengths were scattered.

Another geotechnical investigation described by Ladd and DeGroot (2003) involved the use of SCPTu in a failing earth embankment in Brazil. The project consisted of the construction of an approximately 25 foot earth embankment over 13 feet of sand over 25 feet of soft, plastic Sergipe clay (Figure 2.7).

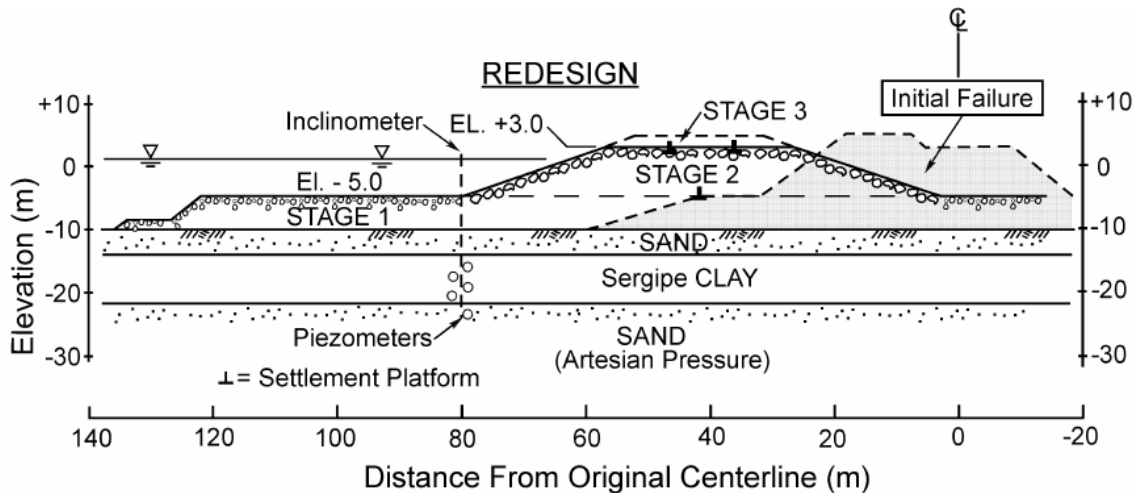


Figure 2.7: Embankment cross section of Brazilian Sergipe clay redesigned after the initial failure (Ladd and DeGroot, 2003).

When the embankment failed, the contractor hired MIT to perform testing of the clay samples to help redesign the slope and ensure failure would not occur. 18 one dimensional (1D) consolidation tests and 10 automated SHANSEP  $CK_0U$  and DSS undrained shear tests were performed in the laboratory, which resulted in considerable scatter in measured the preconsolidation pressure ( $\sigma'_p$ ) from consolidation testing. The scatter caused uncertainty in the stress history across the site and made settlement calculations difficult. In result, MIT performed

CPTu testing at four locations throughout the site, which provided laterally consistent profiles of  $q_{net}$ , which could be correlated to measured  $\sigma'_p$ . This led to more accurate predictions of  $\sigma'_p$  and settlement of the earth embankment, which may not have been possible without the use of CPTu testing.

Ladd and DeGroot (2003) present an additional case history which illustrates the ability of the CPTu to provide acceptable estimates of  $s_u$  and  $\sigma'_p$  profiles even with insufficient results from other testing methods, including Standard Penetration Testing (SPT) blow counts of "weight of rod," scattered field vane shear test (FVT) results, and poor quality laboratory testing results from undisturbed tube samples. This situation is particularly applicable to the Presumpscot clay, since these aforementioned testing procedures are common practice for geotechnical investigations in Maine and furthermore since the case history is in BBC, a deposit very similar to the Presumpscot clay. The case history covers the design of a bridge replacement for a soil profile consisting of thin sand deposits overlying a 130 foot thick deposit of soft, silty BBC. Poor quality laboratory samples improperly characterized the deposit to be underconsolidated (i.e.  $OCR < 1.0$ ), which is impossible due to the known geologic history of the site. Furthermore, the FVT results were scattered throughout the entire profile, likely the result of no drilling mud used during the boring. However, a CPTu sounding performed at the site proved to be the most useful testing method in terms of determining  $s_u$  and  $\sigma'_p$  of the clay. Using a conservative stress history  $k$ -value of 0.30 (by matching the  $\sigma'_p$  profile to the in situ vertical effective stress profile assuming the clay is normally consolidated, which is a conservative approach) and an  $N_{kt}$  of 18.0, complete profiles of  $\sigma'_p$  and  $s_u$  values were available at the site. The resulting profiles compared to the poor laboratory and FVT results are shown in Figure 2.8.

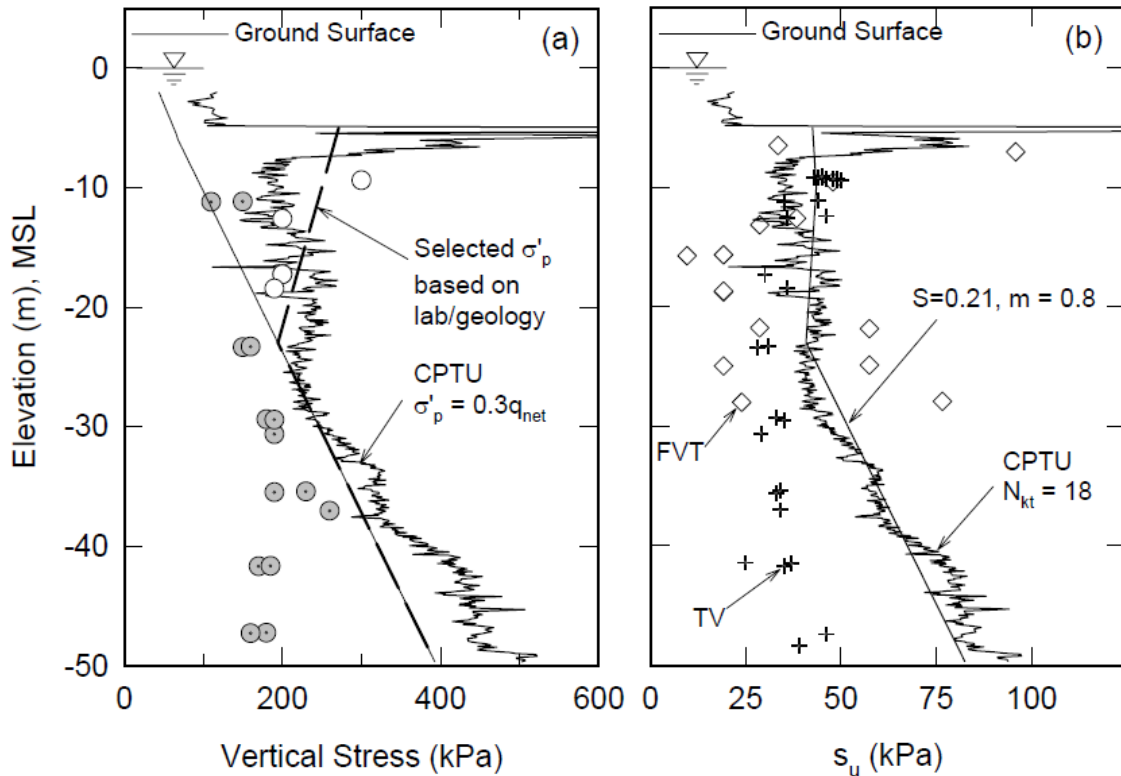


Figure 2.8: Interpreted stress history and undrained shear strength of the Boston Blue Clay site using CPTu correlations (Ladd and DeGroot, 2003).

By using the CPTu to obtain engineering parameters, the negative effects of sample disturbance and operator error were avoided altogether. When appropriate correlations are determined, the CPTu can serve as a powerful tool to supplement or even replace laboratory testing and other field testing methods when performing analysis and design in clay soils.

### 2.2.3 Use of CPTu to Characterize Silty Clay

Long (2008) describes the use of SCPTu at the Os Norwegian research site intended to develop the behavior of silty soils. The soil profile of one of the tested deposit is a silty, stiffer clay overlying a softer, more clayey layer – similar stratigraphy to inland deposits of Presumpscot clay. Results indicate that classification charts using pore pressure measurements are particularly useful for classifying the silty clay, whereas the classification charts using sleeve friction are

much less suitable (Long, 2008). Karlsrud (2005) performed anisotropically consolidated triaxial compression (CAUC) testing on the same Norwegian clay alongside SCPTu testing and found that  $s_u$  predicted using cone factor  $N_{Au}$  (Section 3.1, which uses pore pressure measurements) provided a much more reliable and narrower range of  $s_u$  than other empirical cone factors, mainly  $N_{kt}$ . Boylan et al., (2007) completed similar testing on the Bothkennar Norwegian test site using high quality Sherbrooke block sampling, and concluded that  $N_{Au}$  predicted shear strength most accurately, reinforcing Karlsrud (2005) findings.

### 2.3 CPTu Correlation to Classification and Engineering Properties

Classification and engineering properties of soils can be estimated from CPTu measurements through simple empirical methods. Classification is estimated based on normalized measurements of tip resistance, sleeve friction, and pore pressure, which, when plotted with one another on two-dimensional charts, form zones designated for specific soil types.

#### 2.3.1 Classification

More than 25 different empirical classification charts have been developed by researchers for use with CPTu results (NCHRP, 2007). In current geotechnical practice, charts created by Robertson (1990) have emerged as some of the most useful and applicable charts for general classification of soils with CPTu results (NCHRP, 2007). The two charts published by Robertson (1990) plot normalized tip resistance ( $Q_t$ ) versus both sleeve friction ratio ( $F_r$ ; Figure 2.9a) and normalized pore pressure ( $B_q$ ; Figure 2.9b). Robertson (2009) acknowledges the convenience of normalizing the parameters by *in situ* vertical effective and total stresses in attempt to eliminate the influence of depth increasing overburden stresses on CPTu measurements (Equations 2.2 through 2.4).

$$Q_t = (q_t - \sigma_{v0}) / \sigma'_{v0} = q_{net} / \sigma'_{v0} \quad 2.2$$

$$F_r = f_s / (q_t - \sigma_{v0}) = f_s / q_{net} \quad 2.3$$

$$B_q = (u_2 - u_0) / (q_t - \sigma_{v0}) = \Delta u / q_{net} \quad 2.4$$

where  $q_t$  = measured corrected tip resistance (psf),  $\sigma_{v0}$  = estimated *in situ* total vertical effective stress (psf),  $\sigma'_{v0}$  = estimated *in situ* vertical effective stress (psf),  $f_s$  = measured sleeve friction (psf),  $u_2$  = measured pore pressure (psf), and  $u_0$  = hydrostatic water pressure (psf).

Normalization using overbearing pressures is not a "perfect" solution since they are not the only factor altering CPTu measurements; however it is the most practical and easiest normalization method (Schneider *et al.*, 2008). Normalizing by overburden stresses also allows for the plotted CPTu data to be classified based on other soil properties. The regions within the two charts by Robertson (1990) represent a large spectrum of soil types, ranging from sensitive fine grained soil to gravelly sand. The regions were empirically created based on a wealth of worldwide published and unpublished test data. Robertson (2009) provided an updated version of the Robertson (1990)  $Q_t$  vs.  $F_r$  plot to include trends in the values of OCR, soil sensitivity, and normalized remolded shear strength based on additional data collected (Figure 2.9c). Schneider *et al.* (2008) developed a new classification chart (Figure 2.9d) using  $Q_t$  and  $B_q$  with refined regions based more on deposits of soft clay and silty clay with varying degrees of clay sensitivity. Essentially, the data plot at the same  $Q_t$ - $B_q$  space at Figure 2.9b, but the classification regions differ from Robertson (1990). Figure 2.10 illustrates the two charts together for comparison. The curvature of the region separation lines within Figure 2.9d is due to the theory of increasing  $Q_t$  with decreasing  $B_q$  from partial drainage and consolidation that occurs in stiffer soils, which is supported by data presented by Schneider *et al.* (2008). In addition, the sensitive clay region for the updated chart encompasses a wider range of measured values of  $B_q$ . Schneider *et al.* (2008) states that this region isn't necessarily intended to capture all sensitive clay deposits, but is more for the purpose of identifying clays with highly collapsible structure.

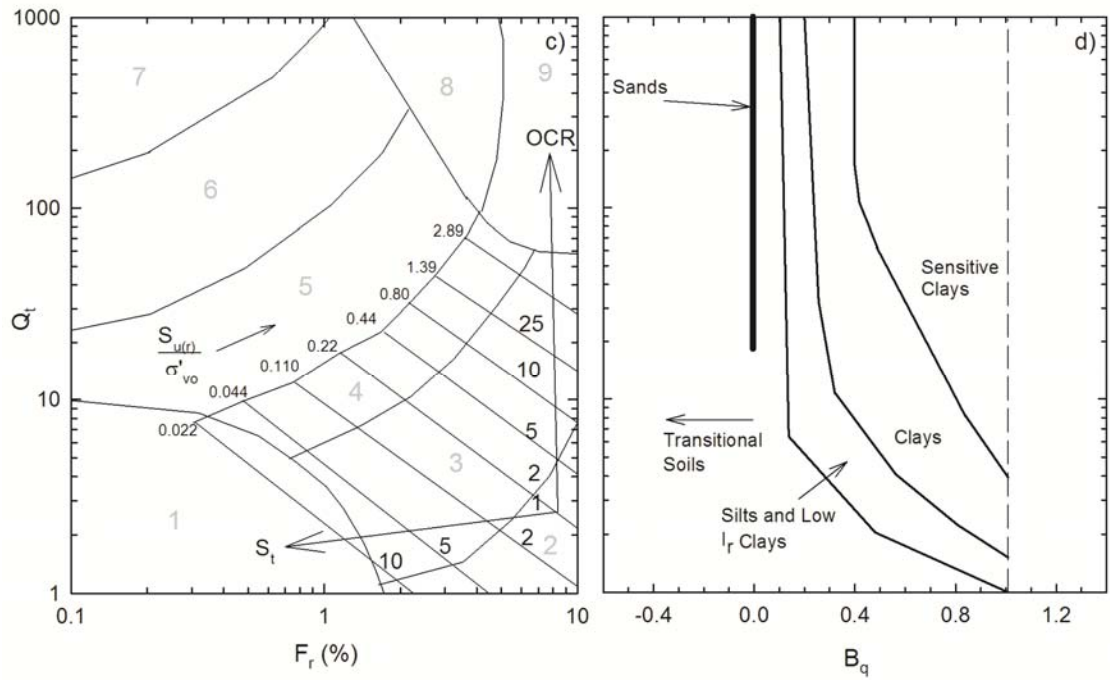
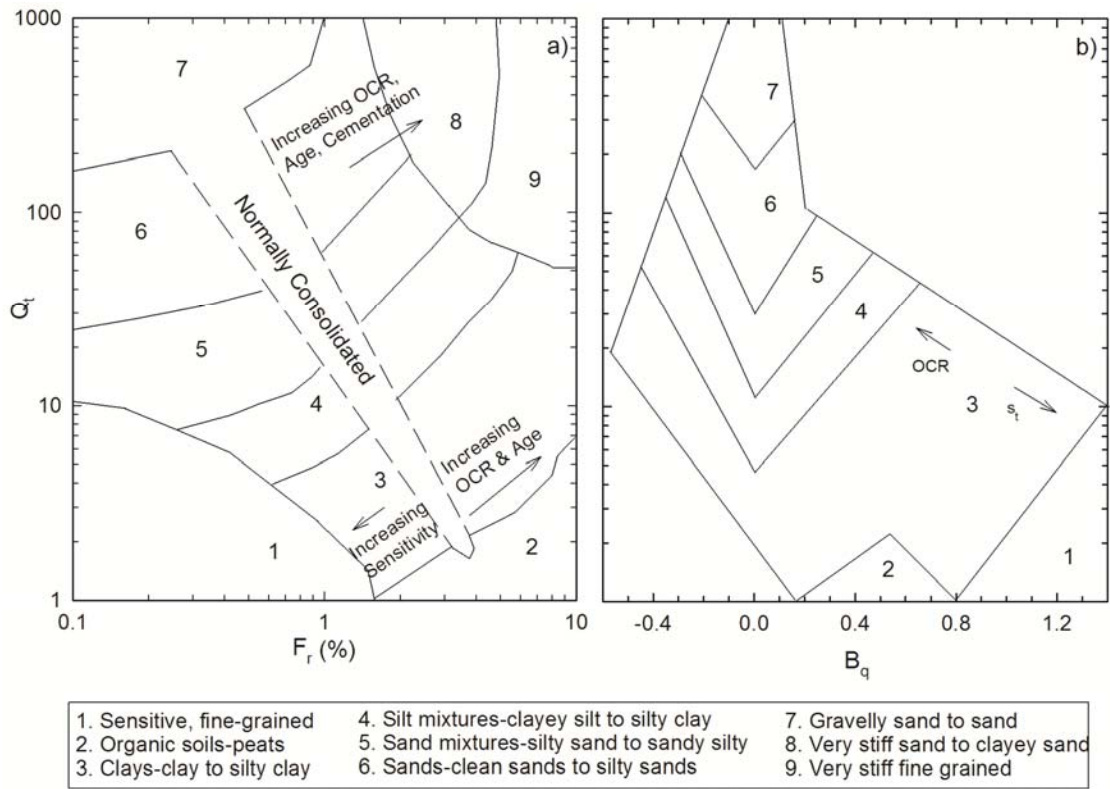
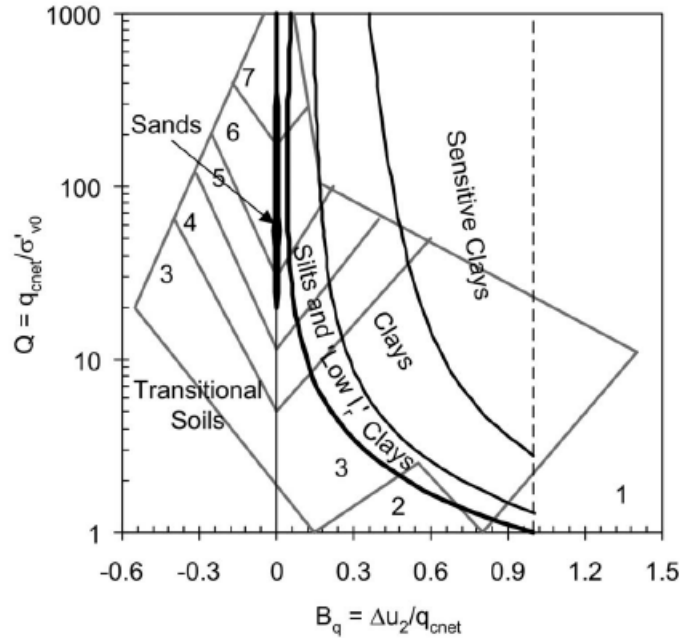


Figure 2.9: CPTu soil behavior type (SBT) classification charts developed by: a) Robertson (1990), b) Robertson, (1990), c) Robertson (2009), d) Schneider *et al.*, (2008).



Soil behavior type zones (Robertson 1991):

1. Sensitive, fine grained
2. Organic soils-peats
3. Clays - clay to silty clay
4. Silt mixtures - clayey silt to silty clay
5. Sand mixtures – silty sand to sandy silt
6. Sands – clean sands to silty sands
7. Gravelly sand to sand

Figure 2.10: Schneider et al., (2008) SCPTu classification chart (bold lines) overlaying the Robertson (1990)  $B_q$ - $Q_t$  classification chart comparing predicted soil behavior type (from Schneider *et al.*, 2008).

### 2.3.2 Stress History

The stress history of clay (i.e. preconsolidation pressure, or  $\sigma'_p$ ) has been theoretically and empirically correlated with the measurements of tip resistance and pore pressure from a CPTu sounding. Over 15 methods are discussed in Lunne *et al.*, (1997) which use varying interpretation processes to obtain values of  $\sigma'_p$  and overconsolidation ratio (OCR) from CPTu results.



Robertson and Campanella (1983) suggest the normalized undrained shear strength parameter  $S$  from the Stress History and Normalized Engineering Parameter (SHANSEP, further discussed below) method to estimate OCR from CPTu results. In their approach, undrained shear strength ( $s_u$ ) is estimated from  $q_t$  measurements,  $s_u$  is normalized to in situ effective stress, and then this normalized strength is compared to the normalized strength at normally consolidated conditions using Figure 2.11. This method is meant to be a general approach to give reasonable estimates of OCR since the method uses both FVT and DSS undrained shear strength values to derive the relationship, and the  $s_u$  from these two shear modes will not always be consistent. Saye *et al.*, (2013) highlights the disadvantages with this approach, which include the discrepancy between the shearing mode modeled by both FVT and DSS testing methods.

Mayne (1991) acknowledged that the majority of current suggested correlations between CPTu measurements and OCR are empirical and based merely on observations from a limited number of sites without theoretical support. He presented Equation 2.5 for obtaining the OCR of clays from CPTu measurements using a combination of cavity expansion theory and critical state soil mechanics. The cavity expansion theory used in his derivation includes the undrained shear strength modeled from triaxial compression tests. An additional assumption made in Equation 2.5 includes a plastic volumetric strain ratio (equal to 1 minus the ratio of isotropic swelling index and the isotropic compression index) of 0.75 (typical for triaxial compression of clays).

$$OCR = 2 * ((1/1.95 * M) * ((q_t - u_2) / \sigma'_{v0})^{1.33}) \quad 2.5$$

where  $M$  = slope of the critical state line ( $6 * \sin\phi' / 3 - \sin\phi'$ )  $q_t$  = corrected tip resistance,  $u_2$  = measured pore pressure, and  $\sigma'_{v0}$  = in situ effective vertical stress,  $\phi'$  = effective friction angle

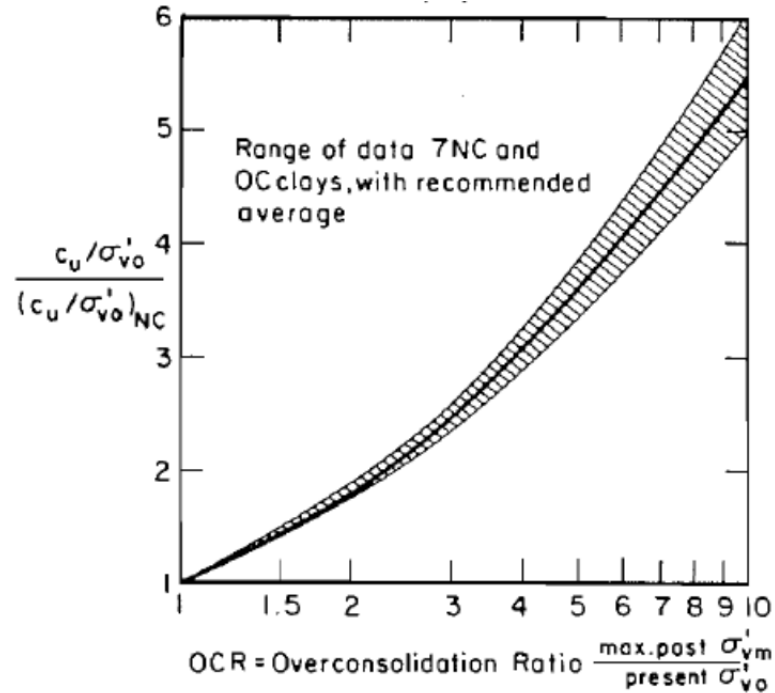


Figure 2.11: Relationship between normalized shear strength values and OCR of clay (note:  $c_u$  = undrained shear strength) (Robertson and Campanella, 1983).

Other CPTu to OCR correlations include measurements of pore pressures at the cone tip, behind the cone tip, and the difference between the two (Lunne *et al.*, 1997). However, there does not appear to be theoretical support for this correlation. Furthermore, Robertson and Campanella (1988) reviewed published correlations between CPTu measured pore pressure and OCR and concluded there to be no unique relationship between the two parameters.

The first-order *k-value* method using tip resistance values has emerged as the most popular and effective way of obtaining values of  $\sigma'_p$  and OCR of clays (Mayne 2014, Lunne *et al.*, 1997, Long 2008). Equations 2.6 and 2.7 present the *k-value* method for obtaining  $\sigma'_p$  and OCR from CPTu results.

$$OCR = k * Q_t \tag{2.6}$$

$$\sigma'_p = k * q_{net} \tag{2.7}$$

where  $OCR$  = overconsolidation ratio ( $\sigma'_p/\sigma'_{v0}$ ),  $k$  = empirical constant,  $Q_t$  = normalized tip resistance (Equation 2.2),  $\sigma'_p$  = preconsolidation pressure (psf), and  $q_{net}$  = net tip resistance (psf, Equation 3.3).

From a theoretical standpoint, the  $k$ -value method can be assessed by drawing a comparison to the SHANSEP  $S$  parameter. The  $S$  parameter, or  $s_u/\sigma'_{v0}$  for the normally consolidated condition, is constant for a normally consolidated deposit. Additionally, cavity expansion theory of a spherical cavity can relate the tip resistance measured during a CPTu sounding to undrained shear strength, shear modulus, and rigidity index of clay (Mayne 1991). Therefore, if the latter two properties are assumed to be constant, the undrained shear strength can be assumed to be directly related to measurements of tip resistance. In effect, if tip resistance is proportional to undrained shear strength, then normalized tip resistance ( $Q_t$ ) is directly proportional to normalized undrained shear strength. Finally, from the SHANSEP equation, we know that the  $S$  parameter is related to the OCR (Equation 2.1). Therefore, we would expect  $Q_t$  (i.e. the measured tip resistance relative to the in situ stress) to be related to the level of overconsolidation of the clay.

$k$ -value has been found to typically range from 0.20 to 0.50 for clays with an increase in  $k$ -value with increasing overconsolidation (Lunne *et al.*, 1997). Mayne (2014) suggests using a constant  $k$ -value of 0.33 for clay deposits which have no previously correlated value. A  $k$ -value of 0.33 has been shown to reasonably predict the  $\sigma'_p$  (and OCR) of at least 20 clay deposits from investigations using the CPTu (Figure 2.12, note  $\sigma'_p$  is also referred to as yield stress).

Preconsolidation pressure was obtained using one of three laboratory testing methods: 1) incremental load oedometers 2) constant rate of strain consolidometers and 3) restricted flow tests on undisturbed samples using a variety of sampling methods (NCHRP, 2007). A  $k$ -value of 0.33 underpredicted  $\sigma'_p$  for fissured clays (Mayne 2014), which may be due to the blocks of clay being

pushed away from the axis of penetration during the CPTu, effectively reducing the tip resistance value (NCHRP, 2007).

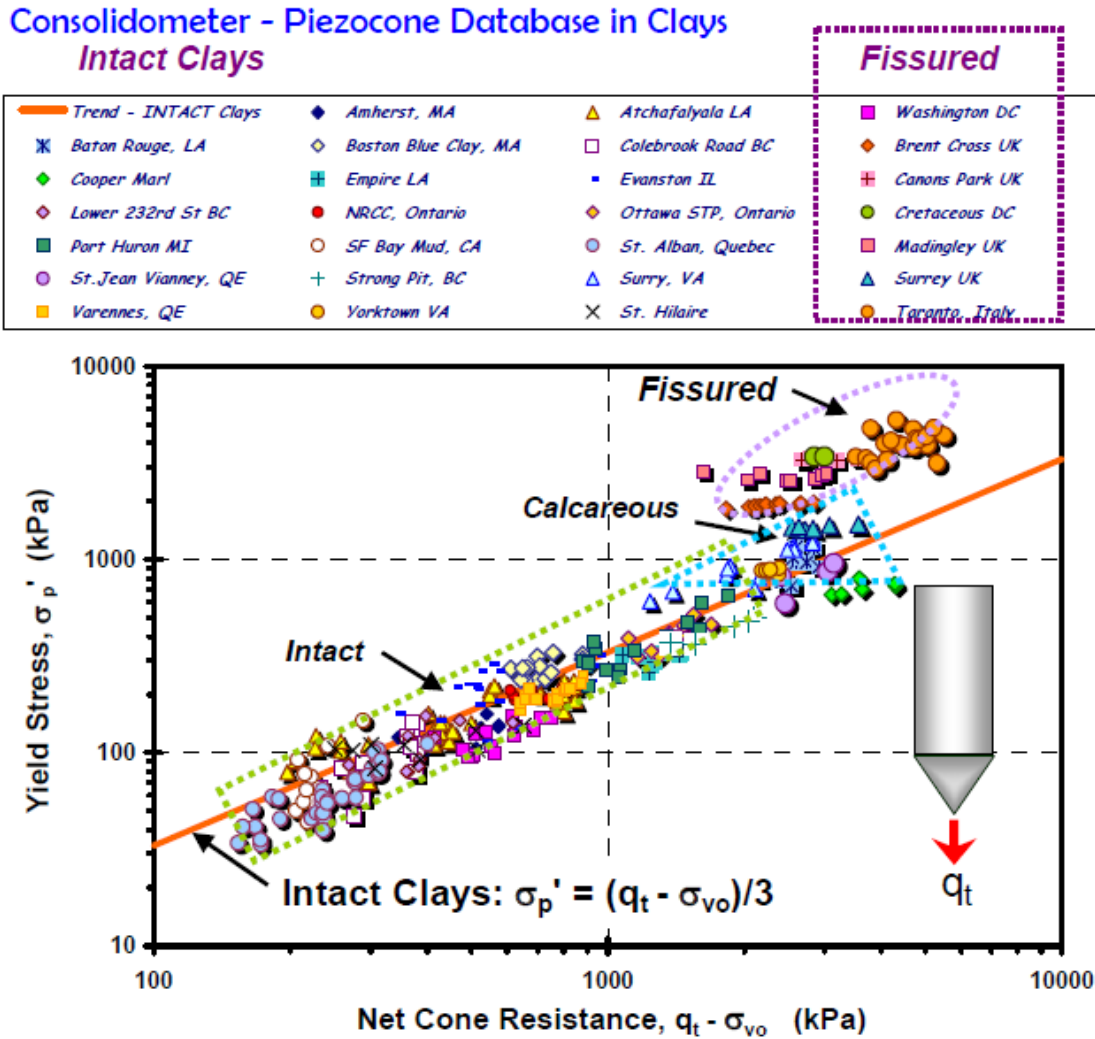


Figure 2.12: Yield stress (i.e. preconsolidation pressure) versus net cone resistance ( $q_{net}$ ) showing individual data points and the trendline of  $k = 0.33$  (Mayne 2009).

Saye *et al.*, (2013) recommend a Stress History and Normalized Soil Engineering Parameter (SHANSEP) based relationship for determining OCR based on index behavior (Equation 2.8)

$$OCR = (Q_t/Q_{nc})^{(1/m_{CPTu})} \tag{2.8}$$

where  $OCR$  = overconsolidation ratio ( $\sigma'_p/\sigma'_{v0}$ ),  $Q_t$  = normalized tip resistance (Equation 2.2),  $Q_{nc}$  = empirical coefficient dependent on Liquid Limit (LL) or Plastic Limit (PL), and  $mCPTu$  = empirical coefficient dependent on LL or PL.

Saye *et al.*, (2013) observed a linear relationship between the log-log plot of OCR versus  $Q_t$ , OCR versus normalized field vane strength, and OCR versus the flat dilatometer horizontal stress index (Figure 2.13) for Connecticut Valley Varved Clay, a glacially deposited layered lake deposit. The empirically observed relationship between  $Q_t$  and OCR (an  $R^2$  value of 0.99, with a  $Q_{nc}$  value of 3.59 and an  $mCPTu$  of 0.92) was applied to other tested clay sites to evaluate the resulting coefficients. This included clay deposits in Norway, United States, Canada, and others. OCR was obtained at the sites using laboratory oedometer tests on undisturbed soil samples (Saye *et al.*, 2013). The resulting  $Q_{nc}$  and  $mCPTu$  values were compared to Atterberg limits of the tested samples in order to evaluate a relationship between index testing and the CPTu coefficients.

Figure 2.14 illustrates the resulting comparisons.

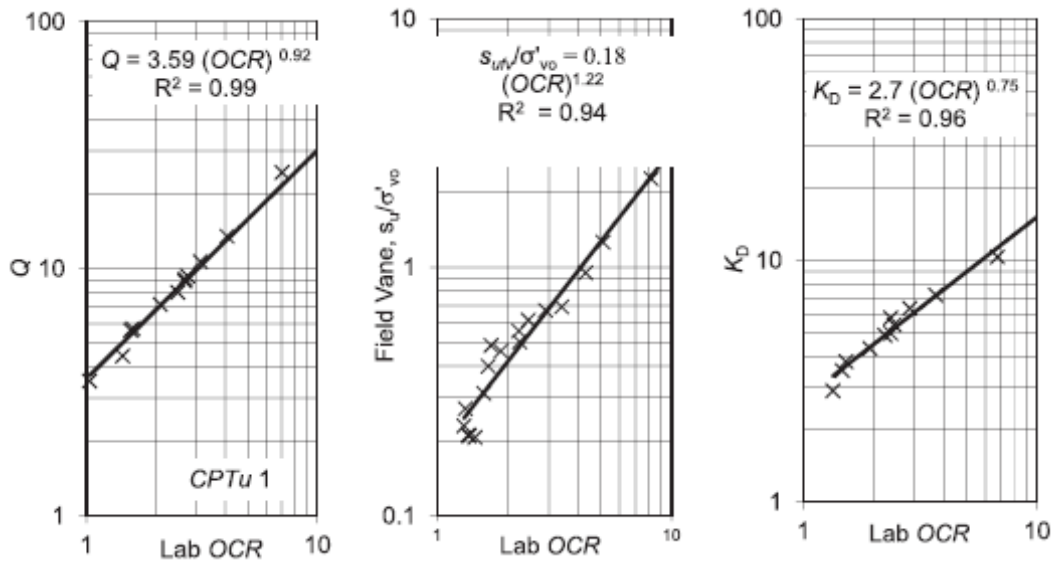


Figure 2.13: SHANSEP based approach for determining OCR of clays applied to the in situ data of Connecticut Valley Varved Clay (Saye *et al.*, 2013).

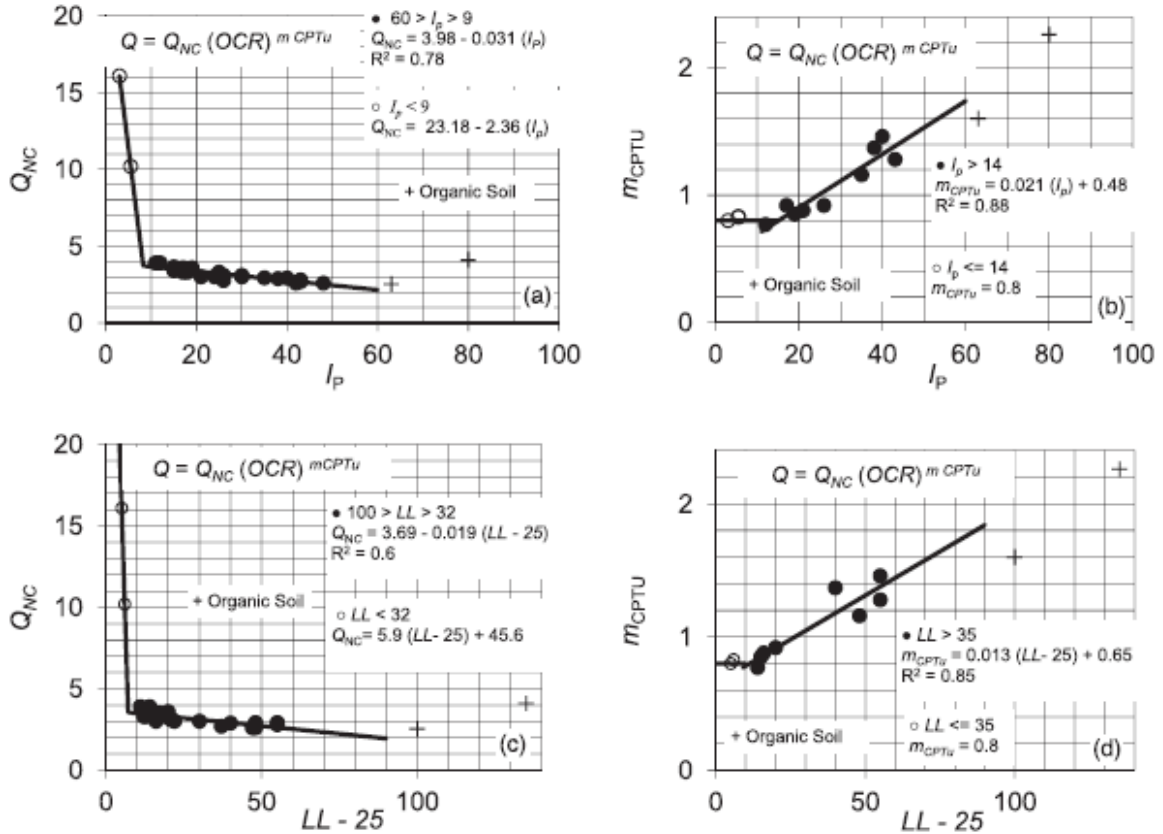


Figure 2.14: CPTu factors  $Q_{nc}$  and  $m_{CPTu}$  for determining OCR of clays plotted with Atterberg Limits (Saye *et al.*, 2013).

A transition between the  $Q_{nc}$  and  $m_{CPTu}$  values was observed at specific measurement of index properties. A plasticity index (PI) of 9 and a liquid limit (LL) of 32 appeared to cause a significant change in measured  $Q_{nc}$ , while a PI of 14 and a LL of 35 yielded the same behavioral difference for  $m_{CPTu}$ . Based on the relationship observed between the index values,  $Q_{nc}$ , and  $m_{CPTu}$ , Saye *et al.* (2013) proposed the equations relating  $Q_{nc}$  and  $m_{CPTu}$  index properties shown in Table 2.3. The Saye *et al.*, (2013) method selects the  $Q_{nc}$  and  $m_{CPTu}$  coefficients to use in the OCR equation based on index testing results, and for different clay deposits around the world with varying index properties, the method appears to be an improvement upon the simple *k-value* method.

Table 2.3: Saye et al., (2013)  $Q_{nc}$  and  $m_{CPTu}$  equations for determining OCR of clays

Condition	Equation
PI < 9	$Q_{nc} = 23.18 - 2.36*PI$
65 > PI > 9	$Q_{nc} = 3.98 - 0.031*PI$
PI > 14	$m_{CPTu} = 0.021*PI - 0.48$
PI ≤ 14	$m_{CPTu} = 0.80$
LL < 32	$Q_{nc} = 5.9*(LL-25) - 45.6$
100 > LL > 32	$Q_{nc} = 3.69 - 0.019*(LL-25)$
LL > 35	$m_{CPTu} = 0.013*(LL-25) + 0.65$
LL ≤ 35	$m_{CPTu} = 0.80$

Note: PI = Plasticity Index, LL = Liquid Limit

### 2.3.3 Undrained Shear Strength

Undrained shear strength,  $s_u$ , can be predicted from CPTu results using empirical correlations developed based on in-situ effective stress, cone tip resistance, and in situ and cone-measured pore pressures. Although theoretical methods have been developed to predict undrained shear strength from (S)CPTu results, Lunne et al., (1997) state that since CPTs are elaborate tests, the simplifying assumptions made in theoretical methods are ineffective in determining accurate  $s_u$  values, and empirical methods should be used. Thus,  $s_u$  correlations used herein are empirically based.

Three primary methods exist for determining undrained shear strength ( $s_u$ ) from CPTu results. These include empirical correlations developed based on in-situ effective stress, tip resistance, and pore pressure (Lunne *et al.*, 1997, Remai 2013). Equations 2.9 through 2.11 are used to obtain  $s_u$  from CPTu measurements.

$$N_{kt} = q_{net}/s_u \quad 2.9$$

$$N_{ke} = ([q_t - u_2]/s_u) \quad 2.10$$

$$N_{\Delta u} = \Delta u/s_u \quad 2.11$$

where  $q_{net}$  = net tip resistance (psf, Equation 3.3),  $s_u$  = undrained shear strength,  $q_t$  = corrected tip resistance (psf, Equation 3.2),  $u_2$  = measured pore pressure (psf),  $\Delta u$  = difference between measured pore pressure and hydrostatic pore pressure (psf,  $u_2$  and  $u_0$ ).

Strength coefficient  $N_{kt}$  is considered the classical approach and is most commonly used for correlating CPTu and  $s_u$  for clays and clayey silts (NCHRP, 2007).  $N_{kt}$  incorporates tip resistance and  $\sigma'_{v0}$  to correlate to  $s_u$ , and is derived assuming an undrained bearing capacity failure at the cone tip during penetration for a soil with undrained friction angle,  $\phi = 0^\circ$  (Wei *et al.*, 2010). A wide range of  $N_{kt}$  values exist depending on the type of clay, type of laboratory testing used for correlation to CPTu results (i.e., mode of shear), and quality of samples tested in the laboratory.  $N_{kt}$  has been found to typically range from 10 to 20, and average 15, when CPTu results are correlated to triaxial compression or field vane shear testing (FVT) reference  $s_u$  (Lunne *et al.*, 1997).

Aas *et al.* (1986) calculated  $N_{kt}$  cone factors of onshore Norwegian clays and North Sea clays using direct simple shear (DSS), triaxial compression (TC), and triaxial extension (TE) measured laboratory  $s_u$ . When the resulting  $N_{kt}$  cone factors were compared to plasticity index of the same undisturbed soil samples, PI, an increasing trend was observed between the two parameters (Figure 2.15). Note that the  $N_{kt}$  cone factors displayed in the top plot in Figure 2.15 are calculated using the average  $s_u$  value from DSS, TC, and TE, while the  $N_{kt}$  in the bottom plot of Figure 2.15 are calculated using only TC.  $N_{kt}$  values using the average  $s_u$  ranged from 8 to 16.

Wei *et al.* (2010) calculated the  $N_{kt}$  cone factor for a clay deposit underlying an existing levee in New Orleans using a single CPTu sounding and an adjacent boring from which 5 Shelby tube samples were collected at various depths and unconsolidated unconfined compression and triaxial unconsolidated undrained compression tests (the consolidation conditions were not specified) was performed to determine  $s_u$  with depth. The resulting  $N_{kt}$  values ranged from 10 to 15, with a best-fit value of 12. The resulting undrained shear strength profile estimated from the



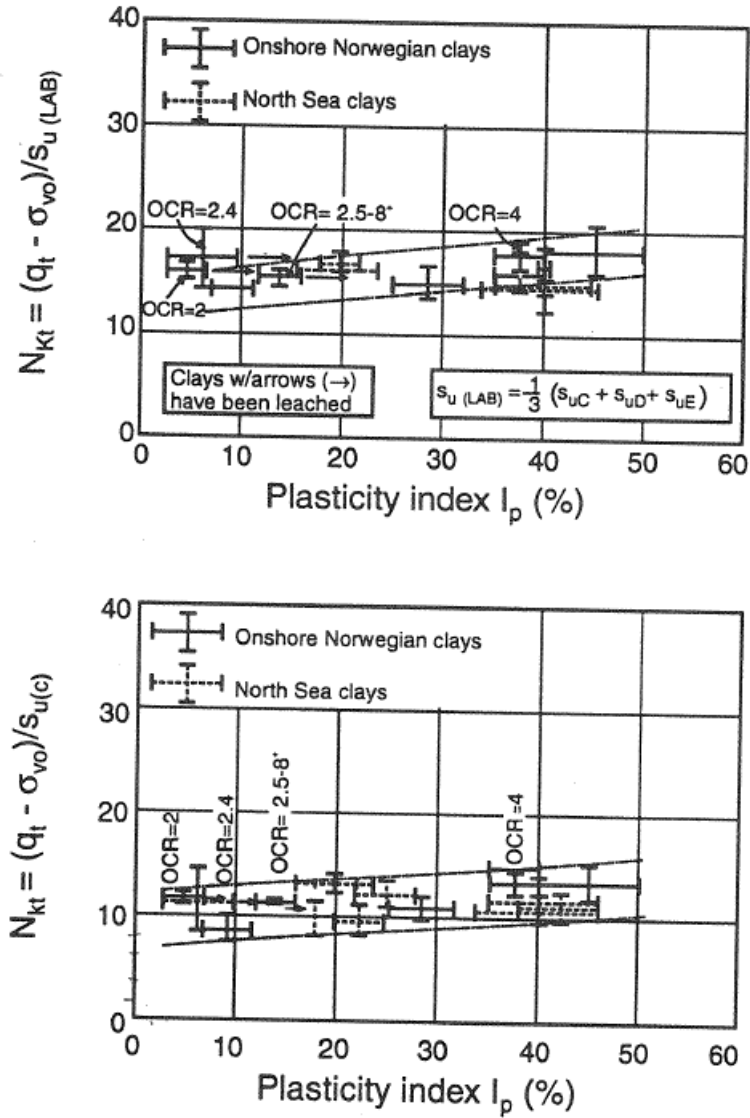


Figure 2.15: Computed cone factor  $N_{kt}$  vs. Plasticity Index (from Aas *et al.*, 1986).

CPTu with an  $N_{kt}$  of 12 is presented in Figure 2.16 alongside the individual specimen results from the laboratory tests.

Remai (2013) performed consolidated undrained triaxial compression testing and unconfined compression testing of samples of soft, Holocene-era clays from 8 different sites in Hungary to back calculate cone factor  $N_{kt}$  from nearby CPTu results. Results showed that  $N_{kt}$  ranged from 11.9 to 32.1 with an average value of 23.3. Upon comparison of the resulting values

to other clay properties and the CPTu measurement of  $B_q$ , Remai (2013) found that  $N_{kt}$  decreased with increasing plasticity index, which opposes the findings from Aas *et al.* (1986).

Table 2.4: Suggested ranges and correlations of cone factor  $N_{kt}$  for studies on different types of clays (reproduced from Remai, 2013).

$N_{kt}$ Range	Reference $s_u$	Proposed Correlation	Reference
8 - 16	TC, TE, DSS	Increase with PI	Aas <i>et al.</i> (1986)
11 - 18		None	La Rochelle <i>et al.</i> (1988)
8 - 29	TC	Varies with OCR	Rad and Lunne (1988)
10 - 20	TC	None	Powell and Quarterman (1988)
6 - 15	TC	Decreases with $B_q$	Karlsrud (1996)
7 - 20	TC	None	Hong <i>et al.</i> (2010)
4 - 16	VST	None	Almeida <i>et al.</i> (2010)
10 - 15	TC	None	Wei <i>et al.</i> (2013)

Note:  $s_u$  = undrained shear strength, TC = triaxial compression, TE = triaxial extension, DSS = direct simple shear, PI = plasticity index, OCR = overconsolidation ratio,  $B_q$  = normalized pore pressure ratio

Been *et al.* (2010) proposed a SHANSEP-based approach for determining  $N_{kt}$  and stress history  $k$ -value (Section 2.3.3) directly from CPTu measurements. They do not propose that this method can be used to replace laboratory or field testing to obtain  $s_u$  or stress history (which they explicitly state is the most effective method and is universally supported in the literature), but they do suggest using the method when testing data is unavailable and reasonable estimates of SHANSEP parameters are known. The method was developed by manipulating the SHANSEP equation (Equation 2.1; Ladd and Foott, 1974) to accommodate CPTu measurements.  $N_{kt}$  and the  $k$ -value are substituted for  $s_u$  and OCR, respectively, where SHANSEP  $S$  and  $m$  parameters remain, and are assumed to be constant for an entire deposit (Ladd and Foott, 1974). The resulting relationship between stress history and strength is shown as Equation 2.13:

$$(s_u/\sigma'_{v0})_{OC} = S \cdot OCR^m \quad 2.12$$

$$N_{kt} \cdot S \cdot k^m = [(q_t - \sigma'_{v0})/(\sigma_{v0})]^{(1-m)} \quad 2.13$$

where  $s_u$  = undrained shear strength,  $\sigma'_{v0}$  = *in situ* vertical effective stress,  $\sigma_{v0}$  = *in situ* total stress, OC notates overconsolidated state,  $S = (s_u/\sigma'_{v0})$  for normally consolidated conditions, OCR = overconsolidation ratio,  $m$  = exponential coefficient found to range from approximately 0.5 to 1.0, and  $q_t$  = corrected tip resistance measured from the CPTu sounding. Table 2.2 summarizes some  $S$  and  $m$  parameters determined from studies in Presumpscot clay and Boston Blue clay.

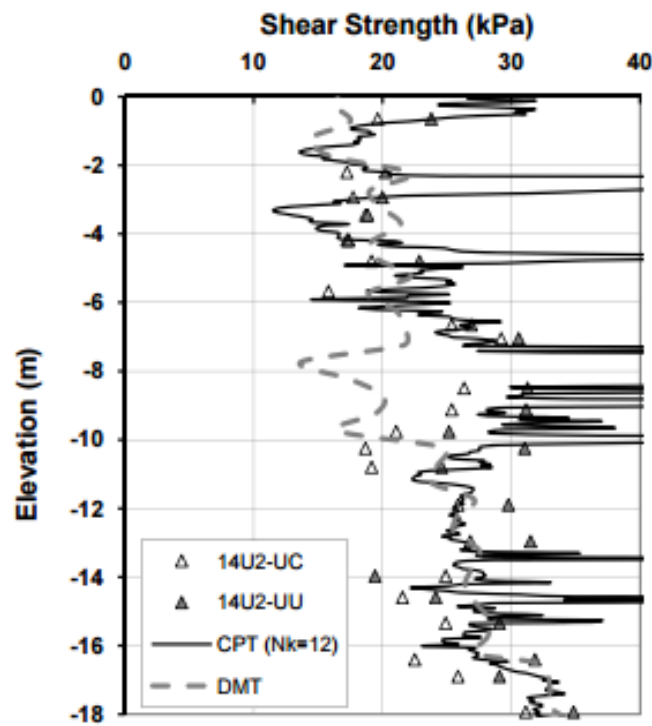


Figure 2.16: Comparison of CPTu predicted undrained shear strength ( $N_{kt} = 12$ ) to laboratory undrained shear strength of a soft clay site in New Orleans (Wei *et al.*, 2010).

The Been *et al.* (2010) method assumes that the left side of Equation 2.13 is constant for a deposit as a necessary simplifying assumption. The authors propose re-arranging Equation 2.13 to solve for  $N_{kt}$  using an assumed reasonable  $k$ -value and then identifying the trend of  $N_{kt}$  with

depth. The authors suggest this be performed assuming multiple, and a range of,  $k$ -values to identify the corresponding range of  $N_{kt}$ . Thereafter, the authors suggest the same process to identify an appropriate  $k$ -value using multiple reasonable estimates of  $N_{kt}$ . At the end of the process, the result is an expected range of both the  $k$ -value and  $N_{kt}$ , which can provide guidance for the selection of each variable. Been *et al.* (2010) applied their developed method to an estuarine nearshore organic clay classified as CH in accordance with ASTM D4318 and having a PI from 60 to 101 and water content ranging from approximately 20% to 200%. For their analysis, the left hand side of Equation 2.13 was kept constant with a selected  $N_{kt}$ ,  $m$ , and  $S$ , with the resulting  $k$ -value being the desired output. The resulting plot is illustrated in Figure 2.17. The results from the analysis are summarized in Table 2.5. In each of the four scenarios, the  $m$  is kept constant and the  $N_{kt}$  and  $S$  value are adjusted within reasonable limits (from typical ranges), and the resulting average  $k$ -value from each scenario is presented. From the resulting  $k$ -value from each scenario, the scenario which provided the most reasonable  $k$ -value (from typical ranges) with accompanying assumed  $S$  and  $N_{kt}$  values is selected as the appropriate parameters. In result, the  $N_{kt}$  and  $k$ -value associated with that scenario are used to predict the  $s_u$  and OCR profiles from the CPTu results or the resulting  $N_{kt}$  and  $k$ -value from each scenario can be used as expected ranges of OCR and  $s_u$ .

Table 2.5: Summary of results from the Been et al. (2010) analysis on the estuarine clay. Each scenario represents a combination of selected  $N_{kt}$  and  $S$  value to achieve a  $k$ -value output.

Parameter	Scenario A	Scenario B	Scenario C	Scenario D
$N_{kt}$	20	14	20	14
$S$	0.25	0.30	0.30	0.36
$m$	0.85	0.85	0.85	0.85
$k$ (median)	0.246	0.302	0.198	0.244

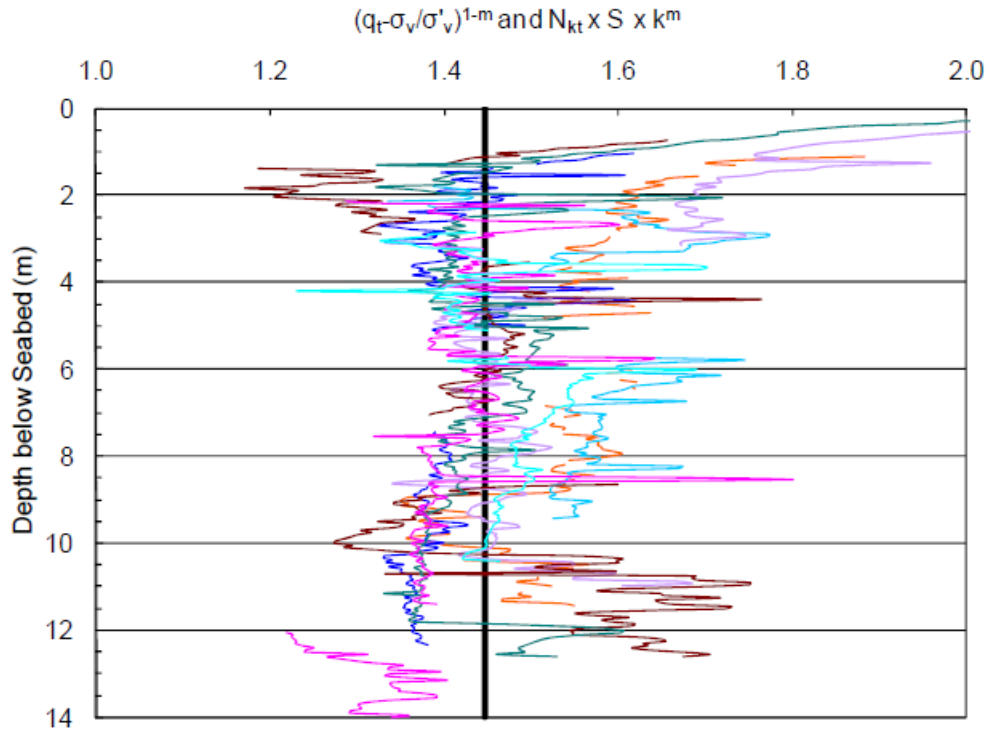


Figure 2.17: Plot of CPTu tip resistance term on the right hand side of Equation 2.13 with the median value shown as a bold line (Been *et al.*, 2010).

The strength coefficient  $N_{\Delta u}$  is an alternative correlation method for  $s_u$ , which used pore pressure measured behind the shoulder of the cone ( $u_2$ ) during cone penetration, and which has been shown in the literature to be effective if accurate  $u_2$  values are measured. Fine-grained soils below the water table typically provide reliable measurements of pore pressure provided the filters are fully saturated with an incompressible fluid at the start of testing, as required by *ASTM D5778* (ASTM 2007).  $N_{\Delta u}$  typically ranges from 4 to 10 for soft clays (Lunne *et al.*, 1997). Figure 2.18 illustrates a range of  $N_{\Delta u}$  obtained from CAUC testing on normally consolidated to lightly overconsolidated Norwegian clays from Karlsrud *et al.*, (1996). It is not directly described in the reference how the pore pressure parameter  $B_q$  was corresponded to the cone factor  $N_{\Delta u}$ , however it is assumed that the CPTu tests were performed within a reasonable lateral distance to the

undisturbed soil samples and the measured  $B_q$  at the sample depth was used to back-calculate  $N_{\Delta u}$  from CAUC testing.

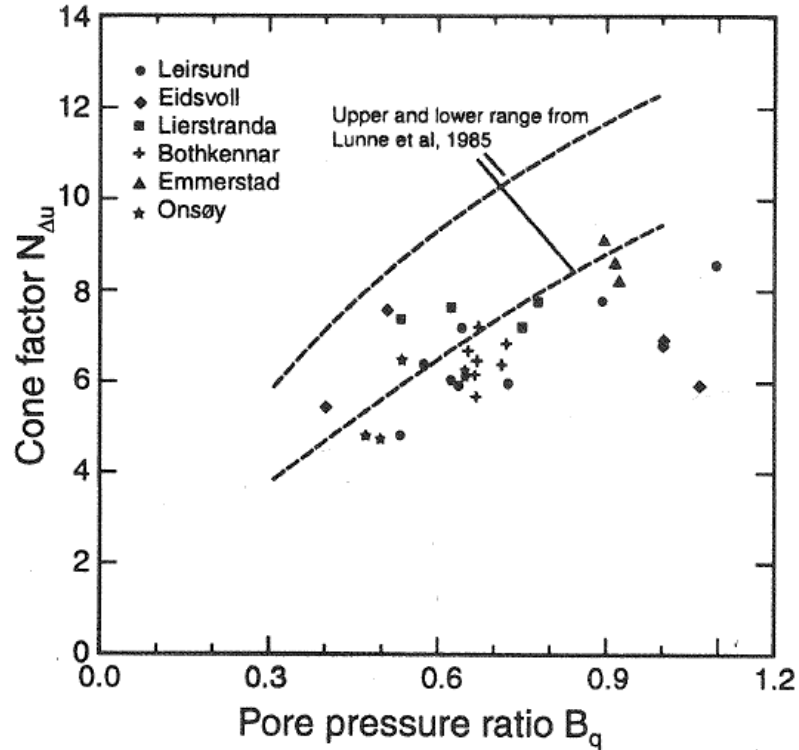


Figure 2.18: Computed cone factor  $N_{\Delta u}$  vs.  $B_q$  (from Karlsrud *et al.*, 1996).

Remai (2013) performed consolidated undrained triaxial compression testing and unconfined compression testing of samples of soft, Holocene-era clays from 8 different sites in Hungary to back calculate cone factor  $N_{\Delta u}$  from nearby CPTu results. Results showed that  $N_{\Delta u}$  ranged from 1.8 to 13.1 with an average value of 6.3. Remai (2013) suggested an increasing trend between  $B_q$  and  $N_{\Delta u}$ , with the resulting equation:

$$N_{\Delta u} = (24.3 * B_q) \pm 2 \quad 2.14$$

Karlsrud *et al.* (2005) performed high quality Sherbrook block sampling of Norwegian clay and subsequent CAUC  $s_u$  testing to determine  $N_{\Delta u}$  values. The resulting  $N_{\Delta u}$  values were plotted with respect to OCR, sensitivity ( $S$ ) and plasticity index as shown in Figure 2.19. The

resulting equations were as for deposits with sensitivity less than 15 and greater than 15, respectively:

$$N_{\Delta u(CAUC)} = 6.9 - 4.0 \cdot \log(OCR) + 0.07 \cdot PI \quad 2.15$$

$$N_{\Delta uAUC} = 9.8 - 4.5 \cdot \log(OCR) \quad 2.16$$

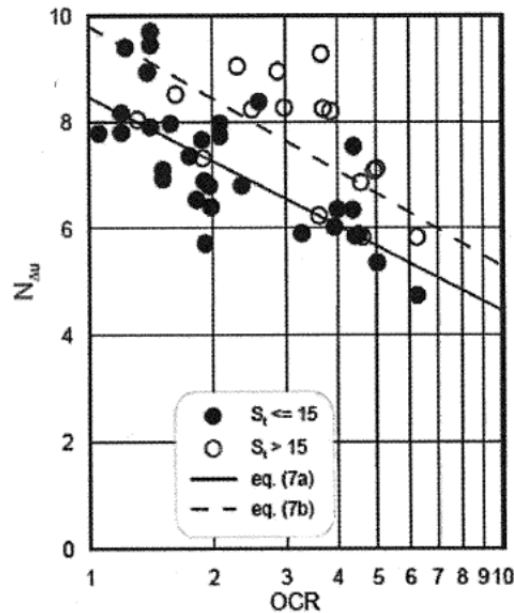


Figure 2.19: Relationship between  $N_{Du}$ ,  $S_t$ , and  $I_p$  (Karlsrud *et al.*, 2005).

Aside from cone factors  $N_{kt}$  and  $N_{\Delta u}$ , the cone factor  $N_{ke}$  has been proposed.  $N_{ke}$  uses a combination of corrected tip resistance and pore pressure measured behind the sleeve of the cone to estimate  $s_u$ . Strength coefficient  $N_{ke}$  correlates both measured CPTu tip resistance and pore pressure to  $s_u$ , which can therefore capture the range of behavior and works well in soft clays (practically normally consolidated). However, as pore pressure measurements are often close in magnitude to tip resistance, small changes in either of the measurements can greatly affect the correlated  $s_u$  and can be unreliable (Lunne *et al.*, 1997). Therefore, it has been found to be more appropriate to use either tip resistance or pore pressure alone ( $N_{kt}$  or  $N_{\Delta u}$ ) instead of combining the

two parameters (Remai 2013) Typical values of  $N_{ke}$  range between 6 and 12 and average of 9 (Lunne *et al.*, 1997).

#### 2.3.4 Seismic Measurements in CPTu testing

During seismic CPTu testing, seismic shear wave velocity measurements can be conducted at discrete intervals throughout the subsurface profile. The generated shear waves cause low, non-destructive shear strains in the clay which can be correlated to elastic stress-strain behavior of clay (Mayne, 2000). The measurement of shear wave velocity during a CPTu test is described subsequently in methods Section 3.1.2.

Small strain shear modulus,  $G_0$ , is soil property used to determine soil response to dynamic loading from earthquakes, construction activity, or pile installations. It is an important measure of soil stiffness and is an essential input parameter for the analysis and design of foundations on clay (Nguyen *et al.*, 2014). Shear wave velocity measured during seismic cone penetration testing can be related to the  $G_0$  through Equation 2.17. Shear straining during the seismic testing imparts strains less than 0.001%, which is non-destructive and well within the linear portion of the stress-strain curve (Kim and Stokoe, 1995).

$$G_0 = \gamma * V_s^2 \quad 2.17$$

where  $\gamma$  is total unit weight (pcf) and  $V_s$  is measured shear wave velocity (ft/s)

Additionally, the small strain shear modulus can be relation to the rigidity index ( $I_r$ ) of the soil (Equation 2.18), which can be used in foundation design to estimate displacement response to surface loading. This relationship requires the undrained shear strength of the material.

$$I_r = G_0/s_u \quad 2.18$$

where  $G_0$  = the small strain shear modulus (psf) and  $s_u$  = undrained shear strength (psf)



A study by Long and Donohue (2008) examined 11 Norwegian clay sites using both surface waves and CPTu to obtain  $V_s$  values. The studied clay ranged from 17% to 60% clay, had OCR of 1.0 to 6.0, and sensitivities ranging from 2 to 1000. Values of  $V_s$  in the study ranged from 131 ft/s to 1,148 ft/s and  $G_0$  values ranged from 56 ksf to 5,140 ksf. The study suggested that  $G_0$  is related to in situ applied stress, void ratio, and OCR.

Landon (2007) conducted SCPTu testing on Boston Blue clay, a silty clay deposit in Massachusetts which has similar silt content to the Presumpscot clay and was deposited from the same geologic process and period as the Presumpscot clay. At the Newbury, Massachusetts site Landon (2007) measured the  $V_s$  of the BBC to range from 410 ft/s to 525 ft/s on a clay deposit which ranged on OCR from 4.6 to 2.1.

Review of published literature has identified that geotechnical analyses and design in the silty Presumpscot clay has posed considerable challenges when it comes to settlement and slope stability. The challenges are mainly due to the highly variable properties of the Presumpscot clay and the inevitable sample disturbance from conventional sampling methods and inconsistency of current in situ techniques (i.e. field vane shear testing, FVT) effecting test results. While both sampling and FVT can be performed with skilled operators and proper procedures, there still remains a gap between the test results and their reliability of in situ behavior due to inevitable effects of sample disturbance.

Review of published literature on the CPTu method has shown that the CPTu can be used to properly characterize deposits of clay based on measurement of tip resistance, pore pressure, sleeve friction, and shear wave velocity. Where current sampling techniques rely on discrete sampling and test results, the CPTu provides nearly continuous measurements over the entire deposit. The resulting measurements can be used to classify the clay based on empirical "soil behavior type" classification chart and can also be correlated to engineering properties of

undrained shear strength and OCR. Correlations to these parameters have been proposed between index properties and CPTu measurements, however most (if not all) literature suggests that the development of engineering properties using CPTu results should be performed on a site-specific basis using other forms of testing. Conclusively, the CPTu appears to contain great potential for helping to solve geotechnical challenges for the Presumpscot clay.

### 3 METHODS

This chapter presents the procedures used for field testing, sample collection, laboratory testing, and analysis of the testing results. Field testing includes standard penetration testing (SPT), Seismic cone penetration testing with pore pressure (SCPTu), cone penetration testing with pore pressure (CPTu), and field vane shear testing (FVT). It should be noted that the SCPTu is the same process as the CPTu with the addition of seismic shear wave velocity measurements. Sample collection includes Shelby tube samples, modified Shelby tube samples, and Sherbrook block samples. Laboratory testing includes constant rate of strain (CRS) consolidation testing, anisotropically consolidated undrained triaxial shear (CAUC) testing, direct simple undrained shear (DSS) testing, and index testing.

In general, the same field testing and laboratory testing program was implemented at each site. This included at least one CPT, one SCPTu, field vane shear testing, modified Shelby tube samples, CRS consolidation testing, either CAUC or DSS undrained shear strength testing, and index testing. However, there were variations in sample and testing quantities at each site. Table 3.1 summarizes the field testing, sampling, and laboratory testing (excluding index testing) conducted at each site.

Table 3.1: Summary of field testing, sampling, and laboratory testing of the Presumpscot clay conducted at all four sites.

		<b>Falmouth</b>	<b>MPB</b>	<b>R-D</b>	<b>Brewer</b>
<i>Field Testing</i>	SCPTu	3	2	1	4
	CPTu	-	1	-	2
	FVT	44	53	15	6
<i>Sampling</i>	Shelby	2	-	-	-
	Mod. Shelby	9	13	9	9
	Block	12	-	-	-
<i>Laboratory Testing</i>	CRS	14	13	10	8
	CAUC	-	13	9	5
	DSS	13	-	-	-

Note: SCPTu denotes a cone penetration test with seismic shear wave ( $V_s$ ) measurements

### 3.1 Seismic Cone Penetration Testing

Seismic cone penetration testing (SCPTu) was performed in general accordance with *ASTM D5778 (ASTM 1995 or 2007) Standard Test Method for Electronic Friction Cone and Piezocone Penetration Testing for Soils*. SCPTu at Route 26/100 Falmouth Bridge was performed by geotechnical engineering faculty and students at the University of Maine and University of Massachusetts, Amherst (Langlais, 2011). SCPTu testing at Martin's Point Bridge, Route 197 Bridge Replacement Site, and the I-395 Terminus Investigation in Brewer was performed by the independent geotechnical investigation contractors, ConeTec Inc. of West Berlin, NJ. This section will summarize the SCPTu procedures at the sites, however Route 26/100 Falmouth Bridge testing methods are presented in more detail in Langlais (2011) and the Martin's Point Bridge, Route 197 Bridge Site, and I-395 Terminus Investigation Site in Brewer are presented in more detail in ConeTec (2011), ConeTec (2012), and ConeTec (2013), respectively. In this section, a brief overview of the testing equipment and procedure is discussed where site-specific details provided in each subsequent site chapter. Metric units are included in brackets after the provided English units.

All piezocone equipment and data acquisition system used Route 26/100 Falmouth Bridge was supplied by the University of Massachusetts, Amherst. This equipment included a VERTEK cone penetrometer and DataPack 2000 acquisition system manufactured by Applied Research Associates, Inc. (Langlais, 2011). Equipment used at Martin's Point Bridge, Route 197 Bridge, and I-395 Terminus Investigation in Brewer was manufactured and supplied by ConeTec.

Electric seismic piezocone penetration testing was conducted at each site using a 1.4 inch diameter [35.7 cm] or 1.72 inch diameter [43.7 cm] piezocone with a projected area of 1.55 in<sup>2</sup> [10 cm<sup>2</sup>] or 2.33 in<sup>2</sup> [15 cm<sup>2</sup>], respectively. All piezocones used had an apex angle of 60°. Located directly behind the cone tip (at the  $u_2$  position) was a 0.24 inch [6 mm] thick high density polyethylene (HDPE) porous element used to collect dynamic pore pressure measurements during

penetration. Located directly behind the porous element was the friction sleeve with a length of 5.28 inches [134 mm] or [164 mm], dependent on the size of the cone tip (larger cone tip with larger friction sleeve). Projected friction sleeve areas are 23.25 in<sup>2</sup> [150 cm<sup>2</sup>] and 34.88 in<sup>2</sup> [225 cm<sup>2</sup>], respectively. The diameter of the bottom of the friction sleeve matched the diameter of the cone base. The electric piezocone used at Route 26/100 Falmouth Bridge gradually increased in diameter from 1.42 inch [36 mm] at the bottom to 1.60 inch [40.5 mm] over a distance of 1.46 inches [37 mm] to allow for easier pushing at greater depths (Langlais, 2011). The diameter of the friction sleeve remained constant for the piezocones used at the other three sites. Figure 3.1 provides a schematic with dimensions of the two types of piezocones used at the research sites. Figure 3.2 presents a picture of a typical cone penetrometer.

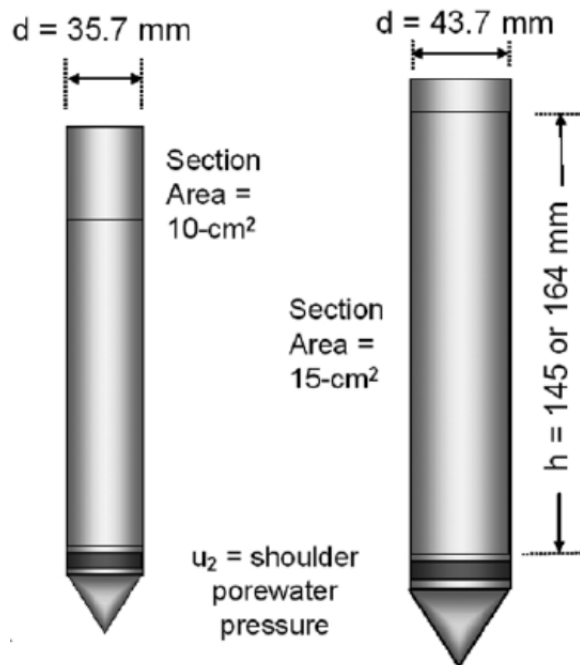


Figure 3.1: Schematic of electric piezocones used at the research site (ASTM, 2012).



Figure 3.2: Image of a 1.4" diameter cone penetrometer showing the cone tip, pore pressure filter element, and friction sleeve (Vertek, 2014).

On the interior of the cones, two separate compression load cells measure the force applied to the cone tip and the friction sleeve independently. A pressure transducer, which is hydraulically connected to the porous filter element located at the  $u_2$  position, measured dynamic pore pressure on the cone during advancement. Operational capacity of the tip resistance load cell, sleeve friction load cell, and pore pressure transducers for the cone used at the Route 26/100 Falmouth Bridge Site was 6,440 psi [44,400 kPa], 189 psi [1300 kPa], and 250 psi [1724 kPa], respectively (Langlais, 2011). Operational capacity of the cones used at the remaining three sites was not provided, however, it is expected that they are relatively similar to the ones mentioned above and that the readings at all three sites never surpassed the capacity of the load cells or transducers.

All piezocones used were also equipped with inclinometers used to determine inclination during the advancement of the cone, thermistor to determine temperature during penetration, analog geophones positioned  $90^\circ$  from each other in the horizontal plane to determine the horizontal and vertical components of the arriving shear wave, and up-hole oscilloscope. Since geophones were only positioned at one location inside of the piezocones, the pseudo-interval

method was used to determine shear wave velocity. Seismic measurements were collected during the test at the addition of every new rod (3.28 feet).

Prior to the SCPTu procedures, the HDPE porous filter elements were saturated in high viscosity silicone oil. The viscosity of the silicone oil for Route 26/100 Falmouth Bridge SCPTu was 10,000 centistokes, and was unspecified for the SCPTu conducted at the other three sites. Cables which collect the data during the test were pre-strung through the 3.28 foot [1 m] rod lengths before the test began. One end of the cable connects to the back of the penetrometer and the other end connects to the data acquisition system. With the cone tip separated from the cone body, the silicone oil is either poured or injected into the pore pressure transducer (where the cone tip threads into the body) to make a hydraulic connection with the porous filter and the transducer. Water is not used due to the difficulties with removing air from the liquid, and since the air is compressible, incorrect pore pressures can be measured during the test or de-saturation can occur. Once the cone tip is tightly threaded onto the body of the cone, the excess silicone oil squeezed out from the insertion of the cone tip is wiped clean from the outside of the cone. One end of the cable was attached to the back of the cone and the other attached to the data acquisition system. The cone is held stationary vertically and the readings are zeroed. Langlais (2011) discusses the zeroing procedure for the SCPTu conducted at Route 26/100 Bridge in more detail. For the remaining three sites, before each sounding, the analog to digital conversion is checked using a multi-meter to ensure the readings being collected (or "digitized") on the screen are accurate. After each test, baseline readings are collected to observe any baseline drift which may have occurred during the test. ASTM (2012) states that SCPTu measurements collected with a baseline drift smaller than 2% of the cone's full scale output (FSO) is acceptable. Baseline drift at all four sites did not exceed 0.1% of FSO. The push rig used at each site differed between the sites and will be covered in the specific site chapters.

Data was acquired from soundings at all four sites using a DataPack 2000 manufactured by Applied Research Associates (ARA). During advancement, the cone was pushed vertically at a standard constant rate of 0.79 in/s [2 cm/s] while the acquisition system collects the analog readings of tip resistance, sleeve friction, and pore pressure and converts them to digital readings displayed in real-time on a computer screen. Readings were taken every three seconds for the testing at the Route 26/100 Falmouth Bridge Site and taken at 1.97 in [5 cm] depth intervals at the other three sites. Penetration depth is recorded by an external string pot system which records the exact depth of the cone tip and is matched with the measurements for that depth. Once a full rod length (3.28 feet) has been pushed, the advancing is stopped; a seismic test is conducted (see below), another rod is attached to the top of the previously advanced rod, and the test is continued.

### 3.1.1 Seismic Testing

Seismic testing was conducted for 3 CPTu soundings at Route 26/100 Falmouth Bridge, 2 CPTu soundings at Martin's Point Bridge, 1 CPTu sounding at the Route 197 Bridge, and 4 CPTu soundings at the I-395 Terminus Investigation in Brewer. Seismic testing yielded shear wave velocity measurements at discrete, 3.28 foot [1 m] intervals throughout the entire sounding profile.

A typical set-up for the seismic testing performed at all four research sites is illustrated in Figure 3.3. Each site used a different type of beam source (shown as the I-Beam in Figure 3.3). Since the measurements of shear wave velocity rely on the times of shear wave arrival, the difference in the beam source (which changes the magnitude of the shear wave, not the speed) should not affect the determined shear wave velocity. The specific devices used for producing the shear waves including the source, hammer, and normal force on the source are specified in each



chapter. The normal force is applied to the source to increase energy transmission into the subsurface.

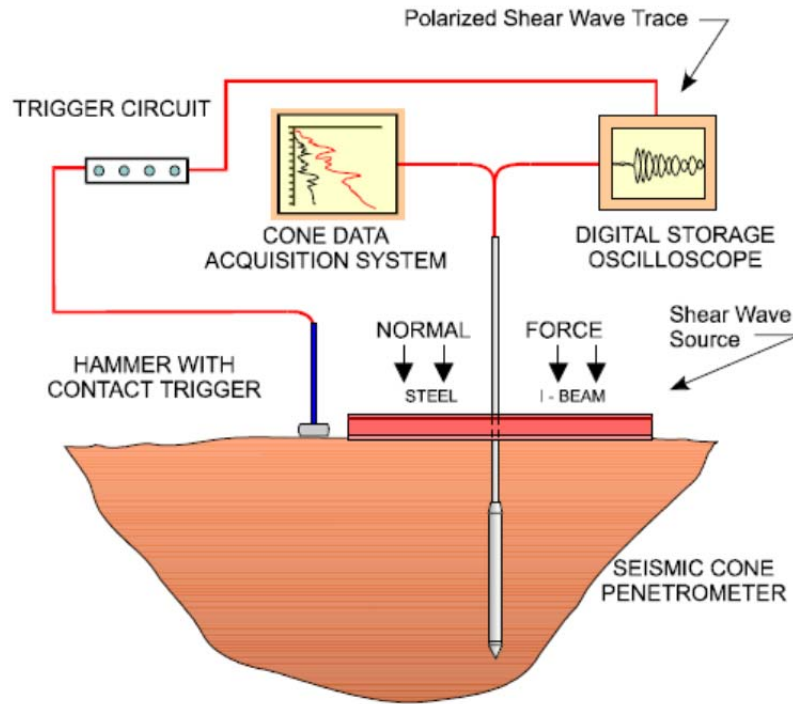


Figure 3.3: Schematic of Seismic Shear Wave Velocity testing during the CPT (from ConeTec, 2013).

The body of the cone used for the Route 26/100 Falmouth Bridge SCPTu soundings contained analog geophones positioned  $90^\circ$  from each other in the horizontal plane to determine the horizontal and vertical components of the arriving shear waves. The cones used for the remaining three research sites used only one geophone mounted horizontally. Two geophones allow for the effect of cone inclination to be accounted for when calculating shear wave velocity. Inclination of the cone penetration tests for the Martin's Point Bridge, Route 197 Richmond-Dresden Bridge, and I-395 Terminus Investigation Brewer sites were not reported.

Before any CPTu was started, the shear beam source was placed on a flat portion of ground, which was cleared of all topsoil and debris to ensure sufficient contact between the base of the source and the ground surface. The distance between the source and the CPT bore hole was measured. The normal force was then applied to the source by driving the drill rig on top or extending the out rigging to contact the top of the source.

Once the SCPTu began, seismic testing was conducted at each rod break (3.28 feet), when the penetration was paused. The beam source was struck with a hammer, which initiates the recording equipment, and the shear wave measured from the geophone is displayed on the computer screen in real time. If the shear waves appeared on the screen within the defined gain and time intervals, the test results were saved and the CPT was continued. Otherwise, the gain and/or time interval display options were adjusted to ensure an adequate shear wave was produced before the results were saved. This procedure was performed at every rod break for the entirety of the test.

### 3.1.2 CPTu Measurements

CPTu testing yielded near-continuous measurements of force at the tip of the cone,  $F_c$ , force along the cone sleeve,  $F_s$ , and pore water pressure behind the cone tip at the  $u_2$  position. The forces at the cone tip and along the cone sleeve are applied over the respective cone and sleeve areas to obtain equivalent pressures,  $q_c$ , and sleeve friction,  $f_s$ .  $q_c$  is calculated using Equation 3.1 using the measured force and the projected area or cross-sectional area of the cone,  $A_c$ . Corrected tip resistance,  $q_t$  (Equation 3.2), accounts for measured pore pressures acting downwards above the cone tip at the shoulder location, which reduce the measured force at the cone tip (Figure 3.4). According to NCHRP (2007),  $q_t$  can be 70% greater than the original  $q_c$  value for clay soils due to the high pore pressure caused when penetrating clays. The net area ratio,  $a$ , is the cross sectional area of the cone shaft ( $A_n$ ) divided by the cross sectional area of cone ( $A_c$ ) (Figure 3.4). The cone

penetrometers used at the sites in this study had a net area ratio of 0.80. Lastly, the effect of geostatic stresses can be removed from tip resistance measurements to obtain  $q_{net}$ , which is helpful for soil behavior classification (discussed subsequently), and is calculated using Equation 3.3.

$$q_c = F_c / A_c \quad 3.1$$

$$q_t = q_c + u_2 (1 - a) \quad 3.2$$

$$q_{net} = q_t - \sigma_{v0} \quad 3.3$$

where,  $F_c$  is total axial force measured at tip (lb-f),  $A_c$  is cross sectional area of the cone tip ( $\text{ft}^2$ ),  $u_2$  is measured pore pressure measured behind the cone tip (psf),  $\sigma_{v0}$  is in situ total vertical stress (psf), and  $a$  is net area ratio, or the area of the cone shaft divided by the area of the cone (typically provided by the cone manufacturer from calibration)

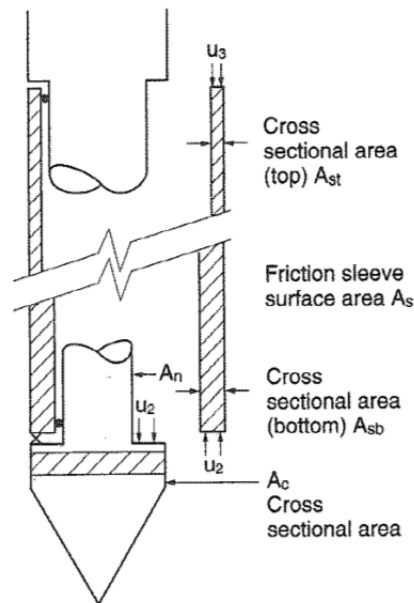


Figure 3.4: Pore water pressure effects on cone penetrometer (Lunne et al, 1997).

Sleeve friction,  $f_s$ , (Equation 3.4) is a measurement of the frictional forces along the cone sleeve. As the cone penetrates the clay, shearing occurs, and the measured friction along the cone

sleeve provides the residual resistance remaining post-shear. In general, sleeve friction is a measurement of remolded shear strength of soft clay soils at the natural water content and a measure of post-peak resistance for granular soils.

$$f_s = F_s/A_s \quad 3.4$$

where,  $F_s$  is total axial force over sleeve (lb-f) and  $A_s$  is cross sectional area of sleeve (ft<sup>2</sup>)

Pore pressure  $u_2$  is a measurement of the pore pressures induced from the shearing of fine grained soils during cone penetration. The "shoulder," or  $u_2$  position, pore water measurement is the most commonly used to provide reliable pore water measurements and was the method used for the soundings performed at the research sites in this thesis.

Lastly, shear wave velocities were measured at every 1 m or 3.28 feet rod break. Shear waves were generated at the soil-water interface by striking a source (discussed in Section 3.1) and shear wave traces were received to be processed using the pseudo-interval method. The distance between the shear wave tests was used as the shear wave travel distance ( $\Delta l$ ), and the difference in the time of arrival of the shear waves determined for each trace at the different test depths was used as the travel time ( $\Delta t$ ). Shear wave velocity,  $V_s$ , was then calculated using Equation 3.5

$$V_s = \Delta l/\Delta t \quad 3.5$$

where  $\Delta l$  is the difference in straight travel path distance from the source to the geophone between two tests (see L1 and L2 in Figure 3.5) and  $\Delta t$  is the difference between arrivals times of the shear wave to the geophone between two tests.

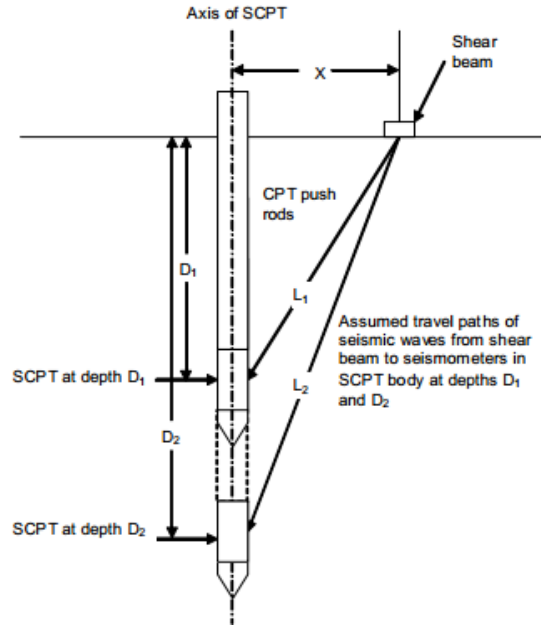


Figure 3.5: Schematic of the seismic testing during a CPT sounding using the pseudo-interval method (from Butcher *et al.*, 2005).

### 3.2 Field Vane Shear Testing

Field vane shear testing (FVT) was conducted at all four research sites to estimate the in situ undrained shear strength ( $s_u$ ) of Presumpscot clay. FVT testing at the four sites was conducted in general accordance with ASTM D2573 (2008) *Standard Test Method for Field Vane Shear Test in Cohesive Soil*. The procedure involves penetrating a four-finned steel vane into saturated clay, applying a torque to the rod to rotate the vane and cause a shear failure in the clay. An undrained shear strength value is estimated from the applied torque and vane size (which controls the assumed rupture plane).

At all four sites, the FVT was conducted during the drilling of traditional borings throughout the deposit at each site. Locations, quantity, and depths of FVT were determined by either the Maine Department of Transportation (MeDOT) for preliminary explorations or by consultants conducting the geotechnical investigations and/or designs. University of Maine personnel were not present for all of the conducted FVT. This section will describe the method as

presented by ASTM (2008) and assume that these processes were followed throughout all of the tests.

Once the borings were advanced to the desired testing depths, the boring was stopped and the rods were retrieved from the bore hole, the drill head was removed from the end of the rods, a steel vane was attached in its place, and the rod assembly was lowered back to the bottom of the bore hole. Dimensions of the vanes ranged from 1.5 inches to 4.0 inches in diameter, ranged in a height-to-diameter ratio from 1.0 to 2.5, were made of steel, and had four fins. Figure 3.6 illustrates a typical field vane and resulting theoretical failure surface used to calculate  $s_u$ . When penetrating the clay, vanes were advanced in a single thrust by self-weight of rods, weight of a person, or direct hydraulic push (and not vibration) to eliminate the amount of disturbance in the clay (ASTM, 2008).



Figure 3.6: Image of field vane (left) and theoretical failure plane used for the calculation of undrained shear strength (right) ([www.gouda-geo.com](http://www.gouda-geo.com) and [www.igeotest.com](http://www.igeotest.com)).

Once the vane was penetrated to the desired depth, a torque wrench was attached to the top of the rods. The torque wrench is a hand tool which measures applied torque using a dial gauge on the face of the tool which presents the maximum torque applied during a test. After the

torque wrench is attached (and within 5 minutes of the vane penetrating the clay), the torque wrench is rotated at 0.1 deg/s until failure occurs in the soil. Once this occurs, the maximum torque is recorded and the undrained shear strength can be determined. To determine the remolded undrained shear strength ( $s_{u(r)}$ ), the field vane is rotated another five to ten times after the initial failure to completely remold the soil. The test is then re-conducted at the same rate, the maximum torque reported, and the  $s_{u(r)}$  evaluated.

The FVT is one of the most widely used in situ tests for estimating  $s_u$  of clay (Terzaghi *et al.*, 1996, DeGroot and Ladd, 2010, Holtz *et al.*, 2011). The reason it is so popular is because the test can be performed quickly and consistently during standard rotary drilling or cased wash borings investigations, which saves time and money associated with additional sampling and subsequent testing required for laboratory tests.

However, the FVT has flaws inherent in the test methods. Before a FVT is performed, the weight relief of the extracted material overlying the tested portion can allow the clay to expand, which results in stress applied to the sample due to the Terminus, as well as unrepresentative in situ anisotropic conditions. Also, once the vane is penetrated into the clay, there is a "disturbed" zone around the blades (Holtz *et al.* 2011) which reduces the undrained shear strength. For soft clays such as the Presumpscot clay, bigger vanes must often be used to increase the size of the rupture plane to allow for better torque resolution to properly determine  $s_u$  (ASTM 2008). The use of bigger vanes results in larger zones of disturbance.

Additional sources of inaccurate FVT results can include ((Terzaghi *et al.*, 1996, DeGroot and Ladd, 2010, Holtz *et al.*, 2011, ASTM 2008):

- Increased strain rate
- Non-verticality of applied torque
- Loose rod connections being tightened during test

- Inclusions of silt and sand seams
- Rod friction
- Damaged vane

If the test procedure is conducted correctly, the resulting  $s_u$  can be reliable. However, there is currently no method to estimate sample quality of a conducted FVT so the engineer must rely heavily on the operators' competency and adjust the predicted values of  $s_u$  accordingly.

### 3.3 Soil Sampling

Samples of the Presumpscot clay were collected at each site for laboratory testing of engineering properties and index properties. Three methods were employed to collect these samples: Shelby tube, modified Shelby tube, and Sherbrooke block sampling. All three methods, described in the sections below, are sampling procedures for cohesive soils which aim to reduce the amount of disturbance caused by the sampling process. This is important because clay samples for laboratory tests of engineering properties should be as close to in situ state as possible, including the water content, stress history, structure, and density (Holtz *et. al.*, 2011, Karlsrud and Hernandez-Martinez 2013, Landon, 2007). Increasing amounts of disturbance increases the difference between in situ state and tested state, which subsequently decreases the representation of the test results of the in situ state. Karlsrud and Hernandez-Martinez (2013) states that undisturbed samples from Norwegian silty-type, sensitive, low plasticity clays are particularly difficult to obtain. The Presumpscot clay is similar to the Norwegian silty clay.

Sample disturbance affects the properties determined from laboratory consolidation and undrained shear strength ( $s_u$ ) testing. For consolidation testing on a disturbed clay specimen, recompression slope ( $C_r$ ) will be steeper, reduced definition (lack of a distinct "break" between recompression and virgin compression zones) for determining the preconsolidation pressure ( $\sigma'_p$ ) will occur, and virgin compression slope ( $C_c$ ) will be shallower (Hvorslev, 1949). For  $s_u$  testing,



increased sample disturbance decreases the effective stress on a soil sample, and in turn decreases the resulting  $s_u$  and increase the strain to failure (Ladd and DeGroot, 2003). So with a disturbed sample of clay tested in the laboratory, one can expect an under prediction of  $C_c$ ,  $\sigma'_p$ ,  $s_u$  and an over prediction of  $C_r$  and strain rate at shear failure. It was important that the undisturbed soil samples of Presumpscot clay at all of the research sites be obtained with minimal disturbance so that the engineering properties determined from laboratory testing, and subsequently the correlation of those properties to the CPTu measurements, be as representative of in situ properties as possible.

During the process of clay sampling for laboratory testing, disturbance can occur at stages other than just the sampling of the clay. Transportation, storage, extraction, trimming, and test setup are all sources of potential sample disturbance in addition to the sampling process (Landon 2007, Ladd and DeGroot 2003). These issues are addressed later in this chapter. All processes of sampling, transportation, storage, extraction, trimming, and test setup were all completed in an effort to minimize sample disturbance throughout this research.

Index properties of clay do not change with the amount of disturbance. Therefore, index test were performed on the bottom 3" of the collected tube samples (which is considered to be disturbed by DeGroot and Ladd (2010)), as well as trimmed portions of the tested clay specimens for consolidation and shear strength testing.

### 3.3.1 Tube Sampling

Tube sampling, also called Shelby Tube sampling, of Presumpscot clay was performed at all four research sites. Figure 3.7 presents an image of a fixed piston modified Shelby Tube similar to the one used at the research sites. All undisturbed soil samples of Presumpscot clay at Martin's Point Bridge, Route 197 Bridge, and the I-395 Terminus Investigation in Brewer were collected via tube sampling. Presumpscot clay samples collected at the Route 26/100 Falmouth

Bridge were collected using a combination of tube sampling and Sherbrooke block sampling (discussed in the next section). All Shelby tube sampling was conducted in general accordance with ASTM D1587, *Standard Practice for Thin-Walled Tube Sampling for Geotechnical Purposes*. This section will present the general method for tube sampling used at each site, and the individual site chapters will summarize the specific equipment and sample depths.

To minimize disturbance to the undisturbed soil samples, piston tube sampling was used instead of push sampling. Ladd and DeGroot (2003) and Terzaghi et al. (1996) highlight the advantage of both higher quality and more recovery of piston tube sampling over push tube sampling. The sampling tubes were 3 inch diameter, 24 inch long stainless steel or brass tubes modified with an ICR (inside clearance ratio) of 0 and a cutting angle of  $5^{\circ}$ . To achieve this modification, the bottom 0.5 inches of the Shelby tubes were removed and machined to match the desired diameter



Figure 3.7: Modified Shelby tube fixed piston sampler with a  $5^{\circ}$  machined cutting angle (from Landon, 2004).

and cutting angle. ICR is the percent difference between the diameter of the cutting edge and the inside diameter of the tube. When these diameters match (i.e.,  $ICR = 0$ ), the sample will not expand or contract after entering the sampling tube in theory and therefore avoid shear distortions which cause sample disturbance.

Cased wash borings were used as the drilling method at all of the sites for obtaining tube samples. Drilling mud, which consisted of Bentonite slurry, was used during the borings to counteract the weight relief of the removed material during the drilling at all sites except for the I-395 Terminus Investigation Brewer site. Borings were advanced using a rotary cone with recirculated drilling mud. Drilling mud was weighed at regular intervals and the resulting densities were reported on the boring logs. The density of the drilling mud increased with increasing boring depth to account for more soil removal.

Once the desired sampling depth was encountered, the rotary cone was stopped and retracted from the bore hole, a tube sampler was attached to the end of the rods in place of the rotary cone, and it was hydraulically lowered back to the sampling depth. The tube was slowly advanced into the soil while the piston controlled the amount of sample entering the tube. Once the tube was fully advanced into the clay, it was allowed to rest for 5 to 15 minutes so bonding between inside of the tube and the remolded clay interface occurred. After the 5 to 15 minute resting period, the tube was completely rotated twice to shear the clay at the bottom of the tube and the sampler was slowly retracted from the bore hole. With the tube sample recovered from the bore hole, both ends were wax sealed and capped, and the recovery amount (along with any visual damage to the sampler) was recorded.

Tube sampling methods were performed in order to obtain the highest quality sample possible by minimizing disturbance; however, some disturbance always occurs during any tube sampling process (Terzaghi et al, 1996). When the theoretically empty sampler (which has

hopefully not picked up any additional material during the advancement to the bottom of the bore hole) begins penetration into the intact clay, the friction and adhesion on the outside of the sampler combined with instability of the bottom of the drill hole may cause the clay to enter the sampler at a quicker rate than the sampler is advanced, which causes extension distortion of the clay. Additionally, friction between the inside of the sampler and the entering clay sample, especially any silt or sand seams which are commonly present in Presumpscot clay, can cause distortion of the sample collected inside the tube (Hvorslev, 1949). An example of a visually disturbed sample due to silt or sand seams in a tube is presented in Figure 3.8. Disturbance from tube sampling was determined by assessing sample quality of all tested specimens. Some of the disturbance identified by the sample quality assessment may also come from transportation of the sample, extracting the sample from the tube, and the trimming process for the test set up. All of these disturbances were minimized as much as possible, which is discussed in following sections.

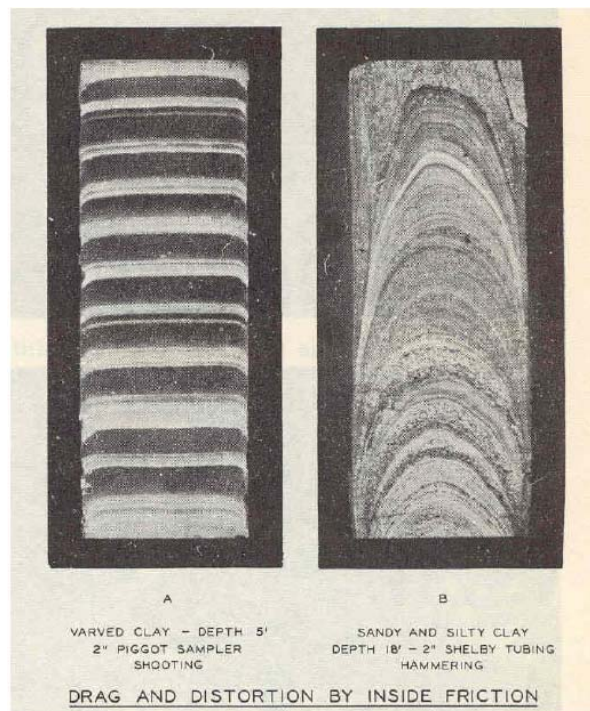


Figure 3.8: Image of a tube sample of clay illustrating sample disturbance from drag along the inside of the tube (from Hvorslev, 1949)

### 3.3.2 Sherbrooke Block Sampling

Sherbrooke block sampling represents the state-of-the-art method to obtain the highest quality samples of soft clays (Ladd and DeGroot 2010, Karlsrud and Hernandez-Martinez 2013). Laboratory testing of clays for undrained shear strength and consolidation properties provides unanimously higher quality results from block samples over any type of tube samples. Due to budget and time constraints, block sampling was only performed at the Route 26/100 Falmouth Bridge.

Block sampling has typically been performed by creating a large diameter open excavation in the subsurface and "carving" out a block of the clay (Terzaghi et al., 1996). This method was limited by the ability or access of cutting an open excavation as well as the stability of an open cut. Lefebvre and Poulin (1979) developed the Sherbrooke Block sampler which allows for the recovery of a block sample in a bore hole. Figure 3.9 presents an image of the Sherbrook Block Sampler.



Figure 3.9: Sherbrooke block sampler (from Landon, 2007)

### 3.4 LABORATORY TESTING

Presumpscot clay samples collected at all four sites were tested at the University of Maine Advanced Geotechnics Laboratory. Laboratory testing of the undisturbed soil samples included index, consolidation, and shear strength testing. All consolidation testing was performed using the constant rate of strain (CRS) method and shear strength testing was performed using the direct simple shear (DSS) method on samples collected at the Route 26/100 Falmouth Bridge and the recompression undrained triaxial shear (CAUC) method on samples collected at Martin's Point Bridge, Route 197 Bridge, and I-395 Terminus Investigation in Brewer. All collected Presumpscot clay samples were stored in a temperature and humidity controlled room.

#### 3.4.1 Index Testing

Index testing was conducted on the bottom 3 to 4 inches of soil from each tube or block sample and included water content, organic content, Atterberg limits, grain size analysis, classification, and specific gravity in general accordance with the following American Society of Testing and Materials (ASTM) standards.

- Water content: ASTM D2216 (2010) *Standard Test Method for Laboratory Determination of Water (Moisture) Content of Soil and Rock*
- Organic content: ASTM D2974 (2007) *Standard Test Methods for Moisture, Ash, and Organic Matter of Peat and Other Organic Soils*
- Atterberg Limits: ASTM D4318 (2010) *Standard Test Method for Liquid Limit, Plastic Limit and Plasticity Index of Soils* using the wet method
- Grain size analysis: ASTM D442 (2007) *Standard Test Method for Particle-Size Analysis of Soils*

- Unified Soil Classification System (USCS) classification: ASTM D2487 (2011) *Standard Classification of Soils for Engineering Purposes (Unified Soil Classification System)*
- Specific gravity: ASTM D854 (2010) *Standard Test Methods for Specific Gravity of Soil Solids by Water Pycnometer.*

Fall cone testing was performed in accordance to Hansbo (1957) on both intact and remolded specimens at the natural water content for each of the collected tube samples. Figure 3.10 is an image of a fall cone apparatus. Fall cone testing provides an estimate of intact shear strength and remolded shear strength of clay. This is achieved by correlating the penetration depth of a small metal cone into the clay sample to shear strength values on an empirical chart provided by Geonor. There are four metal cones, differentiated by mass and apex angle (400g/30°, 100g/30°, 60g/60°, 10g/60°). The cone is selected based on preliminary estimated shear strength of clay specimens. Intact shear strength is measured on samples which remain confined in the tube.

For all tubes collected at each of the research site, a 3 inch to 4 inch section of tube was cut and placed under the fall cone apparatus. One of the four metal cones was selected and placed into the apparatus and held in place by a magnet. The cone was lowered so the tip was slightly above the clay sample. The magnet was then released, the cone penetrated the clay, and the penetration depth was measured. This depth correlated to an undrained shear strength according to the selected cone. The clay sample was then removed from the tube, completely remolded, and the test was repeated to measure the remolded shear strength.



Figure 3.10: Geonor fall cone apparatus (from Geonor, 2010).

The total unit weight of all specimens was determined by using the measured volume and total mass of the prepared intact specimens for one dimensional consolidation and triaxial specimens. Measured water content and total unit weight values were used to compute the dry unit weight.

#### 3.4.2 Sample Preparation

Intact specimens from each of the tube samples were obtained by cutting sections of a desired length from the tube using a four-wheel hinged cutter followed by a single wheel, three point tube cutter. These specimen sections were then debonded from the tube wall by rotating a thin wire along the soil-wall interface (Figure 3.11). Traditional hydraulic extrusion can cause sample disturbance from the shear distortions resulting from the clay and tube wall interface (Ladd and DeGroot, 2003). Thereafter, specimens were hand-extruded from the tube section with minimal pressure using wood or plastic cut blocks. No specimens were hydraulically extruded or cut from the tube using vibration devices.



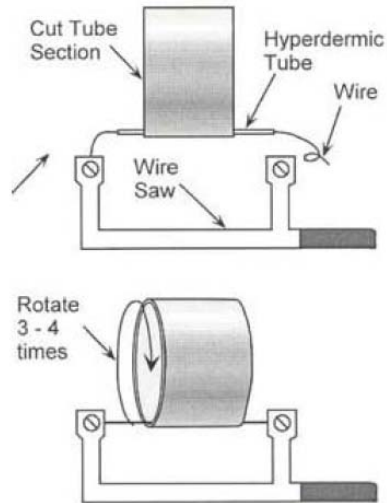


Figure 3.11: Schematic of sample extraction method (from Ladd and DeGroot, 2003).

### 3.4.3 Constant Rate of Strain (CRS) Consolidation Testing

Constant rate of strain (CRS) consolidation testing was performed on intact specimens at the natural water content in general accordance with ASTM D4186 *Standard Test Method for One-Dimensional Consolidation Properties of Soils Using Controlled-Strain Loading* (2006) and Sandbækken et al., (1986). The CRS has advantages over the more traditional incremental load (IL) consolidation test. These advantages include continuous measurements of deformation, vertical load, and pore pressure for direct calculation of coefficient of consolidation and permeability. In addition, the continuous data points result in an improved consolidation curve and more clear definition of the preconsolidation pressure ( $\sigma'_p$ ) (DeGroot and Ladd, 2010).

Figure 3.12 presents the CRS chamber cell setup used for all consolidation testing of the Presumpscot clay samples. The load frames used for all consolidation testing is similar to the one shown in Figure 3.12

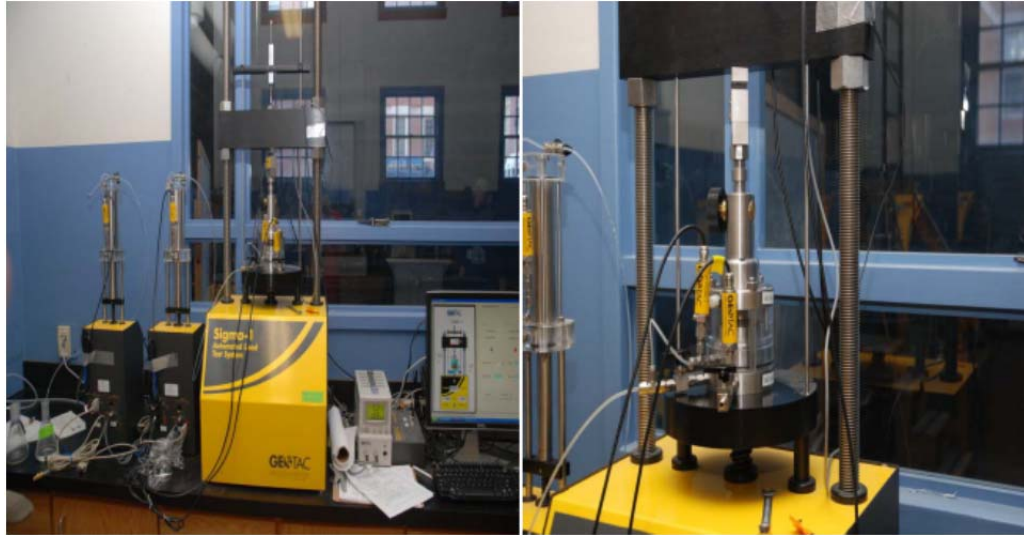


Figure 3.12: Image of the CRS chamber cell setup used for all consolidation testing and the Trautwein GeoTAC Sigma-1 Automated Load Test Frame (from Langlais, 2011).

A Trautwein GeoTac Sigma-1™ automated load test system with computer control and sensor data acquisition (including axial load cell, axial displacement sensor, cell and pore pressure sensors, and a temperature sensor) was used. Prior to testing, the specimen chamber was calibrated to determine system deflection under load and uplift forces.

Specimens were trimmed into a rigid ring with a sharp cutting edge using a wire saw and lathe to finished dimensions of 2.5 inch diameter by 0.75 inch tall. Clean, moist porous stones were fitted at the top and bottom of the specimen for drainage. The top porous stone matched the diameter of the specimen, and the bottom porous stone was 1 inch diameter, fit into the base of the CRS cell. The specimen was installed into a sealed chamber that allows for back pressure saturation using deaired water. CRS testing included three test phases: seating and incremental loading, saturation with back pressure, and constant rate of strain loading. Back pressure saturation was used to eliminate air pockets and achieve more reliable water flow data.

A 104 psf seating load was applied for all specimens. This was followed by incremental loading to  $\frac{1}{8}$  in situ vertical effective stress ( $\sigma'_{v0}$ ) and  $\frac{1}{4}$   $\sigma'_{v0}$  using a load increment ratio (LIR) of

one. Axial strain was monitored during each increment to ensure primary consolidation was complete before addition of the next increment. Upon full primary consolidation at  $\frac{1}{4} \sigma'_{v0}$ , the specimen chamber was filled with deionized, deaired water and specimens were back pressure saturated under constant height conditions in increments of 150 psf to a final back pressure of 607 psf. The final increment was applied for 12-18 hours to achieve 100% saturation before constant rate of strain consolidation was initiated.

Constant rate of strain loading was performed at a rate of 2% axial strain per hour to a maximum strain of 20 to 25%. As recommended by ASTM D4186 (2006), the base excess pore pressure ratio ( $\Delta u_b/\sigma_v$ ) was monitored to ensure it remained between 3% and 30%. It has been found that a strain rate of 2% per hour typically results in a  $\Delta u_b/\sigma_v$  ratio of less than 20% for the majority of the test duration. During CRS loading, the data acquisition system recorded all transducers at an axial strain interval of about 0.08%. After the test was complete, the specimen was retained and dried to determine density and water content, and the data processed according to ASTM D4186 and Sandbækken et al., (1986).

$\sigma'_p$  was determined using the strain energy method of Becker *et al.*, (1987). The method identifies the intersection of tangent strain lines for the initial shallow slope recompression region and higher stress steeper slope virgin compression regions of a strain energy vs. vertical effective stress plot as  $\sigma'_p$ . The overconsolidation ratio (OCR, or  $\sigma'_p/\sigma'_{v0}$ ) is taken as the ratio of  $\sigma'_p$  determined using the strain energy method to  $\sigma'_{v0}$ , the latter of which is determined using the unit weights measured from undisturbed, intact CRS specimens.

Coefficient of consolidation was determined using the following equation:

$$c_v = M^*k/\gamma_w$$

**3.6**

where,  $M$  = compressive modulus,  $k$  is hydraulic conductivity measured during the test at a specific load increment, and  $\gamma_w$  is the unit weight of water.

#### 3.4.4 Anisotropically Consolidated Undrained Triaxial (CAUC) Shear Testing

Anisotropic Consolidation Undrained Triaxial Shear in Compression (CAUC) testing was performed on intact, undisturbed specimens at the natural water content in general accordance with ASTM D4767 (2011) *Standard Test Method for Consolidated Undrained Triaxial Compression Test for Cohesive Soils*. A Trautwein GeoTac TruePath™ automated load test system with computer control and sensor data acquisition (including vertical displacement, internal and external axial loads, cell pump and witness pressures, pore pump and witness pore water pressures, and temperature) was used. Sensor voltages were recorded at regular intervals (time for seating and back-pressure phases and strain for consolidation and shear) and post-processed to determine engineering units. Prior to testing, the triaxial pedestal, top cap, and stones were calibrated to determine system deflection under vertical loading to correct test data for system compliance and isolate specimen behavior.

Specimens were trimmed using a soil lathe, wire saw, and finally a knife edge to finished dimensions of 1.4 inch diameter by 2.8 inches tall. Clean, moist porous stones and filter paper were used at the top and bottom of each specimen for drainage. No filter paper was used around the outside diameter of the specimens. The specimens were carefully placed on the bottom platen and fitted with two thin (0.003 in. each) rubber membranes secured to the platens with O-rings to prevent contact between the specimen and the confining fluid. Drainage lines were fitted to the top and bottom platens, the cell wall and top cap were secured using three tie rods, and the cell was placed into the load frame.

The cell was then filled with confining fluid, silicone oil in this case, to allow use of a load cell inside the chamber between the piston and top cap for greater accuracy, and an initial

confining pressure of 104 psf (5 kPa) applied. Drainage lines and porous stones were then flushed using deaired and deionized water, after which specimens were back pressure saturated at a constant effective stress of 317 psf (15 kPa) up to a maximum cell pressure of 7310 psf (350 kPa) at this final constant effective stress. Backpressure was maintained for 18 hours or longer. A check of saturation was made using the Skempton B parameter, which is the ratio of the measured change in pore pressure to change in cell pressure under undrained conditions. B parameters in excess of 0.90 to 0.95 were accepted as 100% saturation, allowing for greater stiffness of the silty clay. If an appropriate B parameter was measured, the specimen stress was returned to pre- B parameter test conditions, drainage reinitiated, and consolidation phase was initiated. If the B parameter was too low, the cell pressure was increased at constant effective stress by an additional 2090 psf (100 kPa) and maintained for another 24 hours. The B parameter was then checked again to ensure an appropriate level of saturation was achieved.

Specimens were then reconsolidated to the estimated anisotropic in situ effective stress state, where in situ vertical effective stress,  $\sigma'_{v0}$ , was estimated based on the saturated density values determined from intact CRS consolidation specimens. The coefficient of lateral earth pressure at rest,  $K_0$ , was estimated based on the stress history and overconsolidation results from CRS consolidation and published correlations between OCR, PI, and  $K_0$  (Equation 3.7; Mayne and Kulhawy, 1982).

$$K_0(OC) = K_0(NC) \cdot OCR^h = (1 - \sin\phi) OCR^{\sin\phi} \quad 3.7$$

where OC indicates overconsolidated and NC indicates normally consolidated states,  $\phi$  is drained friction angle, and  $h$  is an empirical coefficient generally equal to 0.5.

A  $K_0(NC)$  value of 0.5 and OCR exponent  $h$  of 0.5 were assumed, which are generally accepted assumptions made for clay soils. When specimens had an overconsolidation ratio that lead to an estimate of  $K_0$  greater than 1, specimens were anisotropically consolidated to  $K_0 = 0.95$

(nearly isotropically consolidated) prior to shear. Laboratory capabilities did not allow  $K_0 > 1$  consolidation.

Specimens were consolidated in drained conditions up to the estimated in situ effective stress at a constant  $K_0$  value using an axial strain rate of 0.1%/hour under constant cell pressure. Thereafter, specimens were allowed to creep for 24 hours to allow for equilibration of internal pore pressures, as pore pressure was measured only at the drainage boundaries. Following creep, specimens were sheared in an undrained condition by application of a constant axial strain rate of 0.5%/hour to a maximum axial strain of 20%. The data acquisition system recorded all transducers at an axial strain interval of 0.02%. After the test was complete, the specimen was retained and dried to determine density and water content, and data processed according to ASTM D4767 (2011).

The failure mode represented by anisotropically consolidated undrained triaxial compression (CAUC) testing can be observed visually in Figure 2.4. The test simulates a specimen of clay confined laterally by a constant stress with an increasing vertical load (deviator stress angle of  $0^\circ$ ) to failure. Undrained shear strength obtained from CAUC testing ( $s_{u(TC)}$ ), where the "TC" denotes triaxial compression, is the highest value of  $s_u$  obtained from the three laboratory testing methods consisting of triaxial compression, triaxial extension, and direct simple shear. CAUC testing was selected for the Martin's Point Bridge, Route 197 Bridge, and the I-395 Terminus Investigation in Brewer because the testing equipment allows for precise control of the applied stresses throughout the entirety of the test, which permits boundary condition control and provides in high quality test results.

An ideal CAUC testing procedure includes consolidation of the specimen, prior to shear, under the same estimated in situ stresses in order to best re-create in situ  $s_u$ . However, due to test equipment limitations, the vertical effective consolidation stress during recompression ( $\sigma'_{vc}$ ) will

inevitably be different from the estimated  $\sigma'_{v0}$  and will affect the resulting  $s_u$  values. The horizontal effective stress may also differ, resulting in a lateral earth pressure coefficient during recompression ( $K_c$ ) to differ from the estimated  $K_0$ .  $K_c$  and  $\sigma'_{vc}$  values are presented on all the test result summary tables to compare to estimated in situ values.

The effect of the inevitable  $\sigma'_{vc} \neq \sigma'_{v0}$  condition can cause the  $s_u$  to increase and/or decrease. While  $\sigma'_{vc} > \sigma'_{v0}$  may increase the  $s_u$  since the clay is sheared under greater confining pressure, the same condition may also weaken the specimen by breaking down soil structure and pre-straining it. In general, the destructing of the clay from the  $\sigma'_{vc} > \sigma'_{v0}$  condition likely dominates and leads to lower  $s_u$  values, where the  $\sigma'_{vc} < \sigma'_{v0}$  condition likely leads to higher  $s_u$  values.

#### 3.4.5 Direct Simple Shear Testing

Langlais (2011) describes the method for DSS testing: "*Direct simple shear (DSS) testing was performed on block and tube samples, using Recompression procedures, in general accordance with ASTM D6528 (2007) Standard Test Method for Consolidated Undrained Direct Simple Shear Testing of Cohesive Soils. Tests were conducted using a Trautwein GeoTAC DigiShear® apparatus. The system consists of top and bottom caps, 14 steel confining rings, horizontal and vertical motors and load cells, horizontal linear variable differential transducer (LVDT), a vertical direct current digital transducer (DCDT), and burette. The testing procedure consisted of specimen setup, recompression consolidation, and shear. All data acquisition occurred through a computer using DigiShear computer software.*

*Porous stones and o-rings were cleaned in an ultrasonic cleaner, and the o-rings were vacuum greased prior to use. The specimens were extruded and placed in the DSS trimming jig on plastic wrap and trimmed with the lubricated DSS cutting ring and small spatula. Cuttings were used to confirm the natural water content of the test specimen. The final cutting ring*

*position was approximately in the middle of the sample, and the top and bottom faces were trimmed and smoothed with a wire saw. The soil in the cutting ring had an initial height of 0.75 inches [1.91 cm] and diameter of 2.62 inches [6.68 cm]. The trimmed specimen was extruded from the cutting ring onto the bottom cap, and a latex membrane was installed around the bottom cap and sample using a stretcher and vacuum pressure. Three o-rings were placed around the membrane and bottom cap. The outside of the membrane and the steel rings were coated with silicon oil, and the steel rings were stacked and lowered around the sample for lateral confinement (Baxter et al., 2002). The top of the membrane was stretched down over the confining rings, and the top cap was set on top of the sample. The top cap weight resulted in a 31.3 psf [1.5 kPa] seating load to engage lateral confinement. The membrane was stretched over the top cap and secured with an o-ring. The confining pins were then tightened simultaneously to prevent lateral displacement during consolidation, and the setup was transferred to the load frame.*

*The positions of the base and top connector of the apparatus were manually adjusted (horizontally and vertically, respectively), and the top and bottom caps were secured when in the necessary position. The burette was attached to the bottom cap, a tube connecting the caps was attached, and a drainage tube with an open/close valve was connected to the top cap. The positions and readings on the load cells, LVDT, and DCDT were zeroed, and the consolidation and shear phases were set up in the DigiShear software. The burette was filled with deionized water to a height approximately level with the midpoint of the test specimen in the load frame.*

*For the recompression consolidation, the specimens were loaded to their approximate in situ vertical effective stress,  $\sigma'_{v0}$  with a load increment ratio (LIR) of roughly 1. Loads of 1/8, 1/4, and 1/2 of  $\sigma'_{v0}$  were applied until primary consolidation was approximately complete. The final consolidation load of  $\sigma'_{v0}$  was applied for 12 to 18 hours to ensure consolidation to the final stress was complete. The burette and drainage valves were opened just prior to the application of*



*the 1/8  $\sigma'_{v0}$  load. The burette was kept open for the first few minutes of consolidation or until all air was flushed from the system, while the water level in the burette was maintained. The drain valve was closed when no air was noticeable, but the burette was kept open throughout the test to prevent drying and facilitate drainage.*

*At the end of consolidation, the confining pins were removed, the horizontal load cell was rezeroed, and shear was initiated. The vertical load during shear automatically adjusted itself to maintain constant sample height (constant volume) during shear. The specimen was sheared at approximately 4.8% per hour to a final shear strain of approximately 20%. Data was recorded by the transducers at a shear strain interval of about 0.02% during shear. The setup was dismantled, specimen retained and dried, and data reduced using a spreadsheet template. The data reduction template was calibrated to account for confining ring friction and system deflection under horizontal and vertical loading."*

The failure mode represented by direct simple shear (DSS) testing can be observed visually in Figure 2.4. The test simulates shearing along a horizontal plane, similar to conditions at the deepest portion of any slope failure. Unlike triaxial compression or extension testing, DSS has indeterminate and non-uniform states of stress and indeterminate deviator stress angle. DeGroot and Ladd (2010) suggest that the deviator stress angle probably lies somewhere in between 30° and 60°. The undrained shear strength obtained from DSS testing ( $s_{u(DSS)}$ ) is generally larger than triaxial extension and smaller than triaxial compression (i.e.  $s_{u(TC)} < s_{u(DSS)} < s_{u(TE)}$ ). Langlais (2011) states that DSS testing was selected for the Presumpscot clay at Falmouth because of its applicability to slope stability determination as well as it's generally used to estimate  $s_{u(avg)}$ .

### 3.4.6 SHANSEP Consolidated Undrained Triaxial Shear Testing

Consolidated undrained triaxial compression tests were performed on specimens from Martin's Point Bridge, Richmond Dresden Bridge, and I-395 Terminus site employing the Stress History and Normalized Soil Engineering Parameter (SHANSEP) method in general accordance with ASTM D4767 and Ladd (1991). Specimens were anisotropically consolidated to the in situ  $\sigma'_{v0}$  and then  $K_0$  consolidated past  $\sigma'_{v0}$  to a value representing either 10% axial strain or twice the maximum past pressure,  $\sigma'_p$ , as determined from CRS consolidation tests.  $K_0$  consolidation by definition is when axial strain and volumetric strain are continually equal. In our testing it was maintained by active computer control. Two specimens from the same tube sample were consolidated in this way. The first specimen was sheared at an OCR of 1 following a 24 hour period of drained creep (e.g., secondary compression). The second specimen was first unloaded at a rate of 0.02% axial strain to an OCR of 2 followed by a 24 hour period of drained creep prior to shearing. The results of these tests were used to determine the relationship between undrained shear strength and stress history using Equation 2.1 (Ladd and Foott 1974), where  $s_u$  is undrained shear strength at either the normally consolidated ( $_{NC}$ ) or overconsolidated ( $_{OC}$ ) state and  $m$  is the SHANSEP OCR exponent.

### 3.4.7 Sample Quality Assessment

Sample quality was evaluated using the Norwegian Geotechnical Institute (NGI) method of Lunne *et al.* (2006). This method uses normalized change in void ratio upon recompression to the estimated in situ effective stress state,  $\Delta e/e_0$  at  $\sigma'_{v0}$ , to determine sample quality, where  $\Delta e$  is the change in void ratio,  $e_0$  is the initial void ratio of the specimen, and  $\sigma'_{v0}$  is estimated in situ vertical effective stress. Specimens experiencing low deformations upon reapplication to  $\sigma'_{v0}$  are of higher quality than those having greater deformations resulting from disturbance during the sampling, transportation, storage, or specimen preparation. This method was developed for low

overconsolidation ratio ( $OCR < 4$ ) soft clays having low to moderate sensitivity. It should be noted that the Presumpscot clay that is the focus of this study occasionally has a higher OCR and most often higher silt content than the soils used for development of the  $\Delta e/e_0$  sample quality method. Soils with increasing silt content experience more rounded stress-strain curves than are observed for predominately clayey soils, possibly leading to under predictions of sample quality of Presumpscot clay.

#### 3.4.8 Shear Strength and Remolded Shear Strength Discussion

Undrained shear strength ( $s_u$ ) of the Presumpscot clay was estimated throughout this research using the following methods:

- Anisotropically Consolidated Undrained Compression (CAUC) [Laboratory]
- Direct Simple Shear (DSS) [Laboratory]
- Field Vane Shear Test (FVT) [Field]
- Geonor fall cone apparatus [Laboratory]

Remolded undrained shear strength ( $s_{u(r)}$ ) of the Presumpscot clay was estimated throughout this research using the following methods:

- Field Vane Shear Test (FVT) [Test]
- Geonor fall cone apparatus [Laboratory]

The goal of the  $s_u$  correlations of Presumpscot clay to the CPTu is to accurately predict  $s_u$  values directly from CPTu measurements. To achieve this, a "reference"  $s_u$  has to be selected to back-calculate the empirical coefficients for the CPTu result ( $N_{kt}$ ,  $N_{\Delta u}$ ,  $N_{ke}$ , Section 2.3.3). Since  $s_u$  was estimated using multiple testing methods,  $N_{kt}$ ,  $N_{\Delta u}$ , and  $N_{ke}$  will always have a subscript associated with it to denote which test was used as the "reference" strength. For instance,  $N_{kt(CAUC)}$  denotes that the  $N_{kt}$  coefficient was calculated using triaxial compression as the reference  $s_u$ .

Laboratory determined  $s_u$  (i.e. CAUC and DSS testing) is the most reliable reference shear strength because the sample quality of the tested specimens can be determined. In addition, the boundary conditions and testing procedures of laboratory tests can be well controlled, whereas the FVT can have some unexpected influences of testing error or unforeseen site conditions (such as a silt or sand seam within the tested sample, which can easily be observed before testing is conducted on laboratory samples). In no case should the fall cone apparatus be used to estimate  $s_u$  values for design purposes.  $s_u$  determined from the fall cone is only used in conjunction with the  $s_{u(r)}$  from the fall cone to estimate sensitivity. See Section 2.1.4 for a discussion between  $s_u$  determined from CAUC and DSS testing methods.

### 3.5 SCPTu Correlations

Empirical correlations of SCPTu measurements to engineering properties and classification were performed in the Presumpscot clay at each site. Methods were selected based on two criteria: prevalence in current geotechnical practice as well as applicability to the properties of Presumpscot clay. All of the selected methods are supported by tens, if not hundreds, of empirical studies conducted in soft clays and in some cases sensitive and/or silty clays which closely replicate the geologic deposition of the Presumpscot clay (Lunne *et al.*, 1997; NCHRP 2007; Mayne 2014; Schneider *et al.*, 2008, Long 2008, Karlsrud 2005). Correlations to classification, stress history, and undrained shear strength are outlined in Section 2.3.1 to 2.3.3.

## **4 ROUTE 26/100 FALMOUTH BRIDGE**

The Route 26/100 Bridge in Falmouth, Maine was the first of four Presumpscot clay deposits investigated for this thesis. This chapter provides an overview of the site, a summary of the geotechnical investigations conducted, results from the laboratory testing on high quality samples of the clay, and the correlation of those results to the cone penetration testing (CPTu) performed at the site.

### **4.1 Site Overview and Geology**

The Route 26/100 Falmouth Bridge crosses the Presumpscot River in Falmouth, ME. The bridge is approximately one-half mile east of Interstate 95 near Exit 53 (Figure 4.1) oriented in a north-south direction. The new bridge, completed in 2012, consists of a 720 ft deck span supported by three two-column concrete pier bents (H&A, 2009).

Presumpscot clay samples were collected and CPTu soundings were performed at the northern approach of the Route 26/100 Falmouth Bridge. At this approach, Presumpscot clay was the thickest throughout the entire site, at some locations up to 80 feet thick and approximately 63 feet at the location of the geotechnical investigation discussed herein. Two geotechnical investigations were conducted by Haley & Aldrich (H&A) for the design of the new bridge. In addition to this, Nick Langlais collected Presumpscot clay samples and conducted SCPTu testing for his M.S. thesis, completed in 2011. This paper includes the results from Langlais' 2011 M.S. thesis as well as field vane shear testing (FVT) results from the two H&A geotechnical investigations.

The subsurface conditions at the site consist of sand overlying stiff Presumpscot clay, overlying soft Presumpscot clay, overlying silty sand, overlying glacial till, overlying bedrock (Langlais 2011 and H&A 2009). All but the topmost layer of sand were deposited in the marine environment during the last glacial retreat of the Laurentide ice sheet.



Figure 4.1: Aerial image of the Route 26/100 Falmouth Bridge Site (Google Earth, 2014a).

The glacial till was deposited directly where the ice sheet made contact with the bedrock, which was pushed below sea level due to the weight of the ice. As the ice sheet retreated, the marine sand was deposited on top of the glacial till. Eventually, as the ice sheet retreated further, the Presumpscot clay was deposited on top of the marine sand. All of these deposits were submerged in marine water when formed.

The sand layer at the surface of the north bridge approach is a more recent stream alluvium deposit. As glacial meltwater likely formed after deglaciation and the alluvial material was deposited on top of the Presumpscot clay. Eventually, some of these streams dried up and other formed permanent rivers. The Presumpscot River formed as a post-glacial river and carved out what was likely once a similar deposit of glacial marine clay, marine sand, and glacial till into the exiting river valley.

#### 4.1.1 Previous Geotechnical Investigations

The Maine Department of Transportation (MaineDOT) subcontracted a preliminary geotechnical investigation of the Falmouth Bridge Site in 2008, during which 6 test borings were drilled along the proposed bridge alignment. Borings were drilled using a track-mounted B-50 rig, a CME 45 skid-mounted rig on a barge, or a CME550X ATV mounted rig. All drilling and in situ testing was performed in accordance with Maine Department of Transportation (MaineDOT) standards (H&A, 2009). In each boring, disturbed split spoon samples were collected at 5 foot intervals through the Presumpscot clay for visual classification and laboratory index testing. Field vane shear testing (FVT) was conducted at various depths. A second geotechnical investigation at the Falmouth Bridge Site was completed in 2009 in addition to the preliminary investigation. A total of twelve new borings were conducted along the proposed bridge and approach alignments (H&A, 2009). Similar drilling and in situ testing procedures were deployed in the design phase investigation as in the preliminary investigation described above.

A separate investigation was performed at the site by University of Maine and University of Massachusetts Amherst personnel in 2010 for this research. This investigation included three seismic cone penetration tests (SCPTu), one boring with twelve Sherbrook block samples, and one boring with ten modified Shelby tube samples and two traditional Shelby tube samples. The samples were transported to the University of Maine Advanced Geotechnics Laboratory for subsequent testing. Table 4.1 summarizes the location of the FVT borings in respect to the approximate location of the CPTu soundings.

Seismic cone penetration testing (SCPTu) was performed in general accordance with ASTM D5778 (2007) *Standard Test Method for Electronic Friction Cone and Piezocone Penetration Testing for Soils* and the methodology outlined in Section 3.1. Samples of the Presumpscot clay were collected using Sherbrook block sampling, Shelby tube sampling using

piston sampler and tubes modified to provide higher quality samples, and traditional tube sampling. All Shelby tube sampling was conducted in general accordance with ASTM D1587 (2000) *Standard Practice for Thin-Walled Tube Sampling for Geotechnical Purposes*. Sherbrooke block sampling was performed in accordance to the methodology presented in Section 3.3.2.

Table 4.1: Approximate distances between CPTu testing and borings conducted at the Falmouth Bridge Site.

Boring	Approx. Distance from CPT testing (ft)	Reference
BB-FRR-BT303/BB304	10	Langlais, 2011
BB-FRR-101	45	H&A, 2009
BB-FRR-102	155	H&A, 2009
BB-FPR-208	315	H&A, 2009
BB-FPR-101	270	H&A, 2009
BB-FPR-102	400	H&A, 2009
BB-FRR-201	150	H&A, 2009
BB-FRR-202	80	H&A, 2009
BB-FRR-203	190	H&A, 2009

#### 4.1.2 Sherbrooke Block Sampling

Langlais (2011) describes the Sherbrook block sampling performed at the Route 26/100

Falmouth Bridge:

*Sherbrooke block sampling was performed according to methods discussed by Lefebvre and Poulin (1979) and Degroot et al. (2003), using a Cummins B-47 drill rig in borehole BB-FRR-BB 304. The procedure employed at the Falmouth site is outlined below.*

*The borehole was prepared by drilling to approximately 3.9 feet [1.2 meters] depth using a large diameter auger. Large diameter plastic pipe (1.74 feet) was used as block sample borehole casing to a depth of about 2.7 feet [0.84 m] to keep drilling fluid in the borehole from escaping into the fill material. Bentonite powder was used to fill around the outside of the casing to prevent entry of cobbles, gravel, or sand. Bentonite and recirculated cuttings were used as drilling fluid to prevent bottom heave and facilitate cuttings removal. Drilling mud weight increased from 64.9 pcf to 73.0 pcf [1.04 to 1.17 g/cm<sup>3</sup>] from 3.9 feet to 17.7 feet [1.2 m to 5.4 m] depth due to the increase in soil cuttings added to the mud. Ladd and Degroot (2003) provide mud weight recommendations. A flat bottom auger was used to clean the bottom of the borehole of cuttings and debris. The block sampler was prepared by locking the cutting blades in the open position, attaching it to the drill string, and lowering it into the borehole until it was just above the bottom. The drilling mud was pumped through the drill string to the fluid jets at the base of*



*the sampler at 1462 psf to 4386 psf [70 to 210 kPa], depending on the sample, and rotation was started at approximately 25 to 60 revolutions per minute. The sampler was then lowered to the bottom of the borehole to begin sampling, with penetration rates ranging from approximately 0.6 inches to 6.0 inches [15 to 150 mm] per minute for 11.8 inches to 13.8 inches [300 to 350 mm] of penetration. The rotation of the sampler and water jets carved the soil from the subsurface. The rate of advance and rotation was determined by analyzing the recovery of the previous samples. Generally, faster rotation rates and slower penetration rates were used on shallower samples, while slower rotation rates and faster penetration rates were used on deeper samples. It was found that the fastest rotation rates with slower penetration rates resulted in the least amount of sample recovery (diameter), as the drilling mud in the jets had more time to erode the soil.*

*After sampler penetration reached the desired depth, rotation and advance of the sampler was paused, and a donut drop hammer was lowered down the drill string and dropped 2 to 3 times on the sampler to release the cutting blades at the bottom of the sampler (locked in with cams). After the blades were activated, rotation was continued without advance for approximately 5 minutes while the fluid jets were active. This process allowed the cutting blades to shear the bottom of the sample from the underlying soil, and the blades in the closed position provide basal support for the block sample. Rotation and fluid circulation was stopped, and the block sample was lifted slowly out of the borehole. The sample was cleaned of cuttings and drilling mud, and the blades were opened to release the soil from the sampler. The samples were transported and the bottoms were trimmed, approximately 1.97 inches to 2.95 inches [50 to 75 mm], using one side of a 0.82 foot [0.25 m] diameter aluminum split mold. The sampler was then cleaned with a pressure washer and reset for reuse.*

*After the block sample was trimmed, the bottom was first painted with a wax/petroleum jelly mixture (approximately 50:50 by volume) and secured to a plywood base that was also covered with several layers of wax/petroleum and plastic cling film dipped in the mixture. The block was lifted upright, and the remainder of the sample was coated in several alternating layers of dipped plastic wrap and wax/petroleum jelly. Several of the finished blocks were also wrapped in a layer of cheese cloth. The samples were well sealed to minimize contact with air and prevent drying. When the samples were sealed, they were placed in wooden transportation boxes filled with packing peanuts (ASTM D4220, and Degroot et al. 2003) to mitigate sample disturbance. Some block samples could not be covered in several layers of the wax and plastic wrap in the field due to time constraints, so they were finished in the University of Maine laboratory and placed in a humid room. In all, 12 successful block samples were obtained to a depth of approximately 19.7 feet [6 m] in two days.*

## 4.2 Laboratory Characterization

A total of 12 Sherbrooke block samples and 12 modified standard Shelby tube samples were collected at the Route 26/100 Falmouth Bridge Site and tested at the University of Maine Advanced Geotechnics Laboratory. Each collected sample was tested for index properties (moisture content, Atterberg Limits, hydrometer, organics, specific gravity, and fall cone

strength), consolidation properties, and shear strength properties. All testing methods were in general accordance with ASTM standards and are outlined in Chapter 3.

#### 4.2.1 Index Testing

Figure 4.2 illustrates the depth trends of natural water content, Atterberg limits, grain size distribution, index undrained shear strength ( $s_u$ ) and sensitivity ( $S_t$ ) measured using the fall cone apparatus, organic content, and unit weight (total, dry, and solids) of Presumpscot clay from the Route 26/100 Falmouth Bridge. Total and dry unit weights of the Presumpscot clay were determined in accordance with *ASTM D4186 (2006)* using the tested specimen for each consolidation test. Unit weight of solids was determined from the specific gravity index test using *ASTM D854 (2010) Standard Test Methods for Specific Gravity of Soil Solids by Water Pycnometer*.

Natural water content, Atterberg Limits (liquid limit, LL, plastic limit, PL, plasticity index, PI, and liquidity index, LI), and Activity (the ratio of plasticity index to the percent grain size finer than 0.002 mm, or clay fraction) values are summarized in Table 4.2. Grain size, organic content, total, dry, and solids unit weights, and Unified Soil Classification System (USCS) designations are tabulated in Table 4.3.

Natural water content ranged from 37% to 54% over the entire profile of Presumpscot clay at the north approach, generally remaining constant in the top 25 feet of the layer around 47% and decreasing with depth below 25 feet. Plastic limit (PL) over the entire profile ranged from 19 to 29 with no distinct trend with depth. The bottom three specimens resulted in PL from 19 to 21, indicating the reduction in plasticity as the clay transitions into the underlying outwash sand. Liquid limit (LL) of the clay ranged from 29 to 54 and showed a distinct decreasing trend below 25 feet depth, matching the trend of water content.

Plasticity index (PI), defined as the difference of LL and PL, ranged from 9 to 27 over the entire deposit. In general, there was a minor decreasing trend in PI with depth. The three deepest samples, collected from 52.0 to 62.0 feet below ground surface, resulted in low PI values ranging from 10 to 13. The reduced plasticity with depth is consistent with an increase in silt and sand content in the samples.

Fine-grained soils (those which contain greater than 50% of its material by weight passing the #200 sieve) are classified in accordance to their plasticity behavior. Figure 4.3 plots the PI vs. LL (*ASTM D4318, 2010*), which is the Unified Soil Classification System (USCS) method for classifying fine grained soils. The resulting classification can be observed in Table 4.3

Sensitivity ( $S_r$ ), defined as the ratio of undrained shear strength ( $s_u$ ) to remolded shear strength ( $s_{u(r)}$ ) at the natural water content measured using the fall cone apparatus, ranged from 9 to 58 with one value greater than 100 (Table 4.4). This classifies the deposit as highly sensitive to highly quick (Holtz *et al.*, 2011). This may indicate a high degree of platelet flocculation, which is supported by high void ratios measured on intact consolidation specimens. The open structure of the Presumpscot clay at the Route 26/100 Falmouth Bridge suggests that the depositional environment had a high salt ion concentration.

Increased salt ions present in sea water encourage end-to-end clay platelet bonding, which results in flocculated clay with high void ratios and high degree of structure (Mitchell and Soga, 2005). Since deposition, the subsequent replacement of sea water with fresh water has caused the salt ion concentration to decrease, leading to very low shear strength when the structure is eliminated during remolding. The measured sensitivity values provide an expected resistance to shear when soil is fully disturbed along the shear failure plane. In addition, it can provide insight on the in situ clay structure and potential response during cone penetration testing.

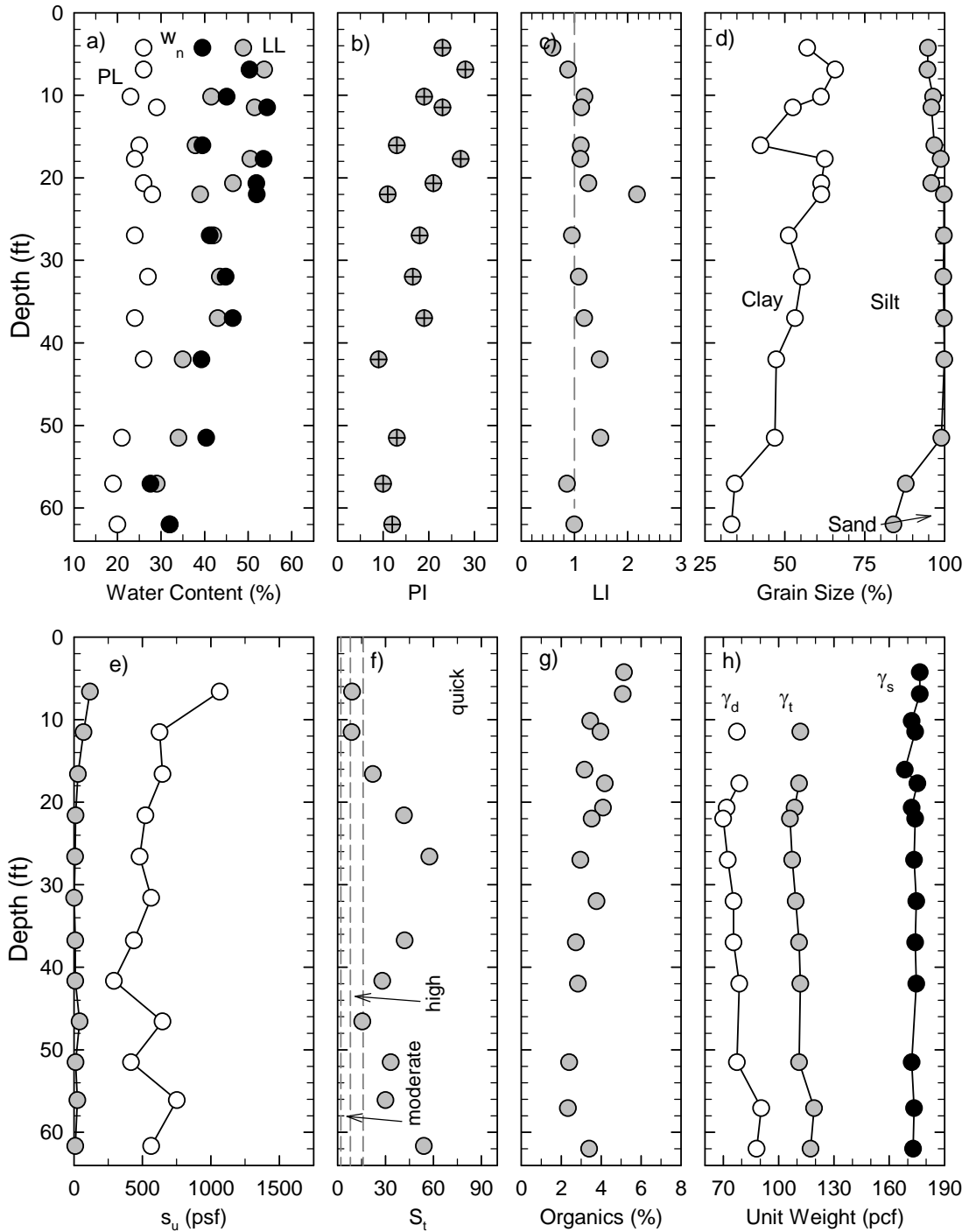


Figure 4.2: Laboratory determined results of a) natural water content, b) plasticity index, c) liquidity index, d) grain size distribution, e) index undrained and remolded shear strength from the fall cone apparatus, f) sensitivity from the fall cone results, g) organic content, and h) unit weight (total, dry, and solids) of Presumpscot clay at the north approach of Route 26/100 Falmouth Bridge (data from Langlais, 2011).

Table 4.2: Summary of Atterberg Limits determined from Shelby tube and Sherbrook block samples collected at the Route 26/100 Falmouth Bridge site (reproduced from Langlais, 2011).

Sample Type	Sample No.	Depth (ft)	w <sub>n</sub> (%)	LL (%)	PL (%)	PI (%)	LI (%)	Activity
SB	BB-1	4.3	39.5	49	26	23	0.6	0.40
SB	BB-2	7.0	50.3	54	26	28	0.9	0.42
MST	BT-1	7.0	38.8	39	25	14	1.0	0.31
SB	BB-4	10.0	45.1	42	23	19	1.2	0.30
SB	BB-5	11.4	54.3	52	29	23	1.1	0.43
MST	BT-2	12.0	48.0	48	25	23	1.0	0.49
SB	BB-9	16.1	39.5	38	25	13	1.1	0.30
SB	BB-10	17.2	53.5	51	24	27	1.1	0.42
MST	BT-3	17.0	46.9	41	25	16	1.4	0.31
SB	BB-13	20.5	51.9	47	26	21	1.3	0.33
MST	BT-4	22.0	52.0	39	28	11	2.2	0.18
MST	BT-5	27.0	41.2	42	24	18	1.0	0.35
MST	BT-6	32.0	44.8	44	27	17	1.1	0.30
MST	BT-7	37.0	46.5	43	24	19	1.2	0.36
MST	BT-8	42.0	39.3	35	26	9	1.5	0.19
SST	BT-9	47.0	37.0	40	23	17	0.8	0.36
MST	BT-10	52.0	40.4	34	21	13	1.5	0.28
SST	BT-11	57.0	27.6	29	19	10	0.9	0.29
MST	BT-12	62.0	32.0	32	20	12	1.0	0.36

SB = Sherbrooke Block Sample, MST = Modified Shelby Tube, SST = Standard Shelby Tube.

Table 4.3: Summary of grain size, unit weight, and USCS determined from Shelby tube and Sherbrook block samples collected at the Route 26/100 Falmouth Bridge site (after Langlais 2011).

Sample Type	Sample No.	Depth (ft)	Sand (%)	Silt (%)	Clay (%)	Organics (%)	$\gamma_t$ (pcf)	$\gamma_d$ (pcf)	$\gamma_s$ (pcf)	USCS
SB	BB-1	4.3	5.2	37.8	57.0	5.2	-	-	177	CL
SB	BB-2	7.0	5.3	28.9	65.8	5.1	-	-	177	CH
MST	BT-1	7.0	0.1	55.3	44.6	2.3	113	82	172	CL
SB	BB-4	10.0	3.6	35.1	61.3	3.5	-	-	172	CL
SB	BB-5	11.4	4.1	43.4	52.5	4.0	112	77	174	CH
MST	BT-2	12.0	0.1	52.5	47.4	2.5	110	75	173	CL
SB	BB-9	16.1	3.2	54.4	42.4	3.2	-	-	169	CL
SB	BB-10	17.2	4.2	33.3	62.5	4.2	111	79	175	CH
MST	BT-3	17.0	0.1	48.0	51.9	3.2	107	75	174	CL
SB	BB-13	20.5	4.1	34.4	61.4	4.1	109	72	172	CL
MST	BT-4	22.0	0.2	38.4	61.4	3.5	106	70	174	ML
MST	BT-5	27.0	0.2	48.6	51.2	3.0	107	72	174	CL
MST	BT-6	32.0	0.4	44.3	55.3	3.8	109	76	175	ML
MST	BT-7	37.0	0.2	46.6	53.2	2.7	111	76	174	CL
MST	BT-8	42.0	0.1	52.6	47.3	2.8	112	79	175	ML
SST	BT-9	47.0	3.7	49.0	47.3	2.7	112	79	176	CL
MST	BT-10	52.0	1.0	52.1	46.9	2.4	111	77	172	CL
SST	BT-11	57.0	12.2	53.5	34.4	2.3	119	91	174	CL
MST	BT-12	62.0	16.0	50.7	33.3	3.4	117	88	173	CL

SB = Sherbrooke Block Sample, MST = Modified Shelby Tube, SST = Standard Shelby Tube, USCS = Unified Soil Classification System *ASTM D2487 (2011)*,  $\gamma_t$  = total unit weight,  $\gamma_d$  = dry unit weight,  $\gamma_s$  = unit weight of solids

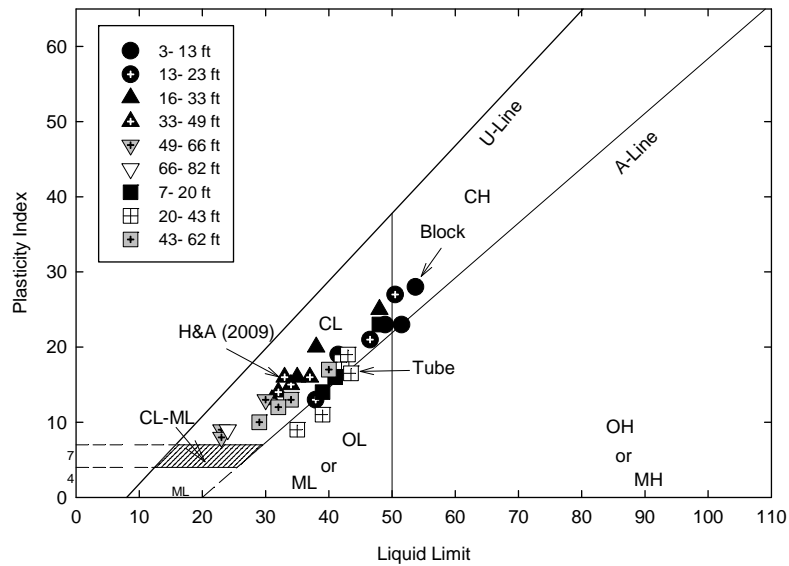


Figure 4.3: USCS Classification chart for fine content of tube and Sherbrook block samples from the Route 26/100 Falmouth Bridge Site (from Langlais, 2011).

Figure 4.4 presents the PI versus the clay fraction of the tested Presumpscot clay at the Route 26/100 Falmouth Bridge. This chart is commonly used to predict the mineralogy of tested clay samples. Two lines are shown on the plot,  $A = 0.90$  and  $A = 0.38$ . These correspond to illite and kaolinite clay minerals, respectively. Kaolinite appears to be the dominant clay material in Presumpscot clay; however, x-ray diffraction of Presumpscot clay indicates that kaolinite is not present in Presumpscot clay (Schnitker & Borns, 1987). The discrepancy is likely due to the determination of clay fraction, which is defined as any particle smaller than 0.002 mm in diameter. The pulverized rock flour portion of Presumpscot clay is incorporated into the “clay fraction” portion. Therefore, the actual clay fraction of the Presumpscot clay is lower than determined by the hydrometer test.

Table 4.4: Summary of fall cone undrained shear strength and sensitivity for recovered tube and block samples at the Route 26/100 Falmouth Bridge Site (after Langlais, 2011).

Sample	Depth (ft)	w <sub>n</sub> (%)	<sup>1</sup> Intact s <sub>u(FC)</sub> (psf)	Intact Cone	<sup>2</sup> s <sub>ur</sub> (psf)	Remolded Cone	<sup>3</sup> s <sub>t</sub>
BT-1	6.6	35.7	1065	400g/30°	116.9	100g/30°	9
BT-2	11.5	33.7	626	100g/30°	71.0	60g/60°	9
BT-3	16.6	36.6	647	100g/30°	29.2	60g/60°	22
BT-4	21.6	39.8	522	100g/30°	12.5	10g/60°	42
BT-5	26.6	37.3	480	100g/30°	8.4	10g/60°	58
BT-6	31.6	40.6	564	100g/30°	2.1	10g/60°	> 100
BT-7	36.7	42.2	438	100g/30°	10.4	10g/60°	42
BT-8	41.7	41.2	292	100g/30°	10.4	10g/60°	28
BT-9	46.6	38.4	647	400g/30°	41.8	60g/60°	16
BT-10	51.5	41.0	418	100g/30°	12.5	10g/60°	33
BT-11	56.1	30.2	752	100g/30°	25.1	60g/60°	30
BT-12	61.7	24.9	564	100g/30°	10.4	10g/60°	54

Note: <sup>1</sup>intact undrained shear strength; <sup>2</sup>remolded; <sup>3</sup>Sensitivity (s<sub>u</sub>/s<sub>ur</sub>)

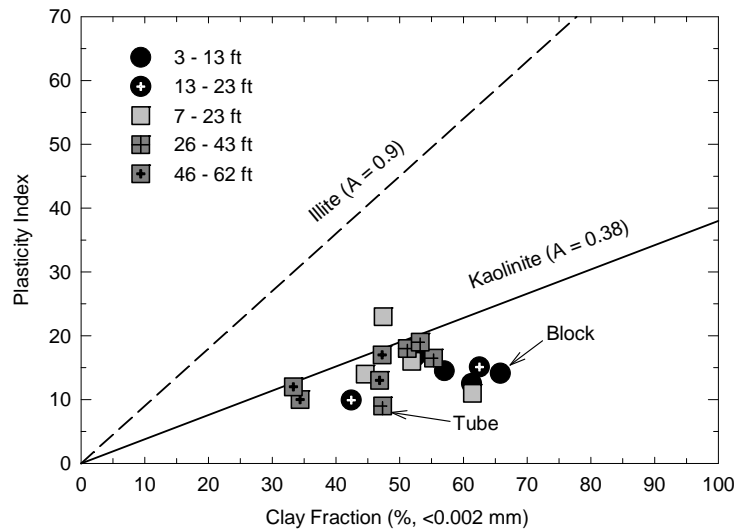


Figure 4.4: Plasticity Index versus clay fraction for tube and Sherbrook block samples recovered at the Route 26/100 Falmouth Bridge site (from Langlais, 2011).



#### 4.2.2 One Dimensional Consolidation Results

Constant rate of strain (CRS) consolidation testing was conducted on fourteen samples collected at the Route 26/100 Falmouth Bridge Site. Preconsolidation pressure ( $\sigma'_p$ ) was determined using the Becker *et al.*, (1987) strain energy method. Table 4.5 presents specimen and test parameters for the CRS consolidation tests, as well as stress-strain and flow parameters for the loading phase of the tests and calculated  $\sigma'_p$  and compression indices. Specimens were generally of very good to excellent quality with the exception of five specimens having good to fair quality and one poor quality specimen based on the Lunne (2006) sample quality assessment method. Specimens of poor quality may be less reliable in predicting  $\sigma'_p$  and other consolidation parameters due to sample disturbance misrepresenting in situ conditions. In situ effective stress ( $\sigma'_{vo}$ ) for the determination of overconsolidation ratio (OCR) was estimated from unit weights calculated from the tested consolidation samples and the groundwater levels observed in the cone penetration tests.

$\sigma'_p$  at the Route 26/100 Falmouth Bridge Site ranged from 2,297 psf at the top of the deposit to 4,573 psf near the bottom, decreasing from the shallow samples to a depth of approximately 21 feet, after which it begins a nearly linearly increasing trend with depth. OCR, defined as the ratio of  $\sigma'_p$  to the in situ effective stress ( $\sigma'_{vo}$ ) is highest at the shallowest depth of the Presumpscot clay, starting at 3.4, and decreases to a value of 1.8 at 21.3 feet depth. Refer to Figure 4.5 for the profile of laboratory determined  $\sigma'_p$ , OCR, and the associated sample quality of the tested Presumpscot clay samples.

The resulting profile of  $\sigma'_p$  and OCR of the tested samples indicate a lightly overconsolidated crust overlying a practically normally consolidated (i.e. OCR = 1) deposit. Overconsolidation of the upper crust is likely due to the fluctuation of groundwater through this sample depth and the resulting wetting and drying cycle altering the interparticle stresses. This

mechanism is apparent in the tested samples from the shallowest sample at 11.3 feet to approximately 21 feet (approximately elevation 36 feet to 26 feet, compared to a “normal water” elevation of 18.4 feet of the Presumpscot River from H&A 2009). Below this depth, OCR generally remains consistent with depth while  $\sigma'_p$  increases linearly to match the slope of the estimated  $\sigma'_{v0}$  depth profile. Stress conditions at the site may be due in part to loading from the old bridge structure. Although the superstructure is pile supported, the contact of the abutment and roadway approach with the ground surface imparts some surficial loading which translates to stress applied to the subsurface (potentially increasing the  $\sigma'_p$ ).

Table 4.5: Constant rate of strain (CRS) consolidation specimen properties and results from tube and Sherbrooke block samples collected at the Route 26/100 Falmouth Bridge Site (after Langlais, 2011).

<sup>1</sup> Sample Type	Sample No.	Specimen Information					<sup>2</sup> Sample Quality				Consolidation Properties			
		Depth (ft)	$\sigma'_{v0}$ (psf)	$w_n$ (%)	$e_0$	$\gamma_t$ (pcf)	$\Delta e/e_0$ at $s'_{v0}$	NGI Rating	$c_v$ @ $\sigma'_{v0}$ (ft <sup>2</sup> /yr)	<sup>3</sup> $\sigma'_p$ (psf)	OCR	$C_c$	$C_r$	
SB	BB-5	11.2	912	44.7	1.25	112	0.012	VG/E	326	3132	3.4	0.46	0.075	
MST	BT-2	11.5	929	47.1	1.32	110	0.017	VG/E	187	2339	2.5	0.46	0.071	
MST	BT-3	16.4	1159	46.3	1.37	107	0.012	VG/E	190	2443	2.1	0.48	0.082	
SB	BB-10	16.7	1173	41.9	1.24	111	0.030	VG/E	115	2297	2.0	0.38	0.075	
SB	BB-13	20.0	1328	51.3	1.40	109	0.014	VG/E	340	3758	2.8	0.59	0.072	
MST	BT-4	21.3	1389	51.4	1.49	106	0.036	VG/E	115	2506	1.8	0.53	0.085	
MST	BT-5	26.2	1620	48.3	1.39	107	0.047	G/F	51	2506	1.5	0.38	0.004	
MST	BT-6	31.2	1850	45.1	1.32	109	0.070	G/F	68	2610	1.4	0.43	0.078	
MST	BT-7	36.4	2096	47.5	1.31	111	0.054	G/F	88	2819	1.3	0.44	0.080	
MST	BT-8	41.3	2326	42.3	1.22	112	0.069	G/F	12	2380	1.0	0.33	0.067	
SST	BT-9	46.2	2558	42.2	1.24	112	0.029	VG/E	61	4573	1.8	0.39	0.014	
MST	BT-10	51.5	2802	44.1	1.22	111	0.048	G/F	95	3863	1.4	0.45	0.078	
SST	BT-11	56.1	3017	31.9	0.92	119	0.019	VG/E	54	4218	1.4	0.30	0.047	
MST	BT-12	61.3	3264	33.9	0.97	117	0.085	P	29	3800	1.2	0.28	0.005	

<sup>1</sup>SB = Sherbrooke Block, MST = Modified Shelby Tube, SST = Standard Shelby Tube, <sup>2</sup>From Lunne et al. (2006), where VG/E: very good to excellent quality, G/F: good to fair, P: poor; <sup>3</sup>Using the Strain Energy Method of Becker et al. (1987)

Recompression index ( $C_r$ ) and virgin compression index ( $C_c$ ) (Section 3.4.3) predict the expected volume change from applied stresses prior to and beyond  $\sigma'_p$ , respectively.  $C_r$  ranges from 0.004 and 0.085 and  $C_c$  ranges from 0.28 and 0.59 for the 14 tested specimens. These compression indices fell within the ranges of values provided by Andrews (1987) for “typical”

Presumpscot clay values. Consolidation testing results presented in H&A (2009) had  $C_r$  and  $C_c$  values from 0.002 to 0.031 and 0.23 to 0.32, respectively.

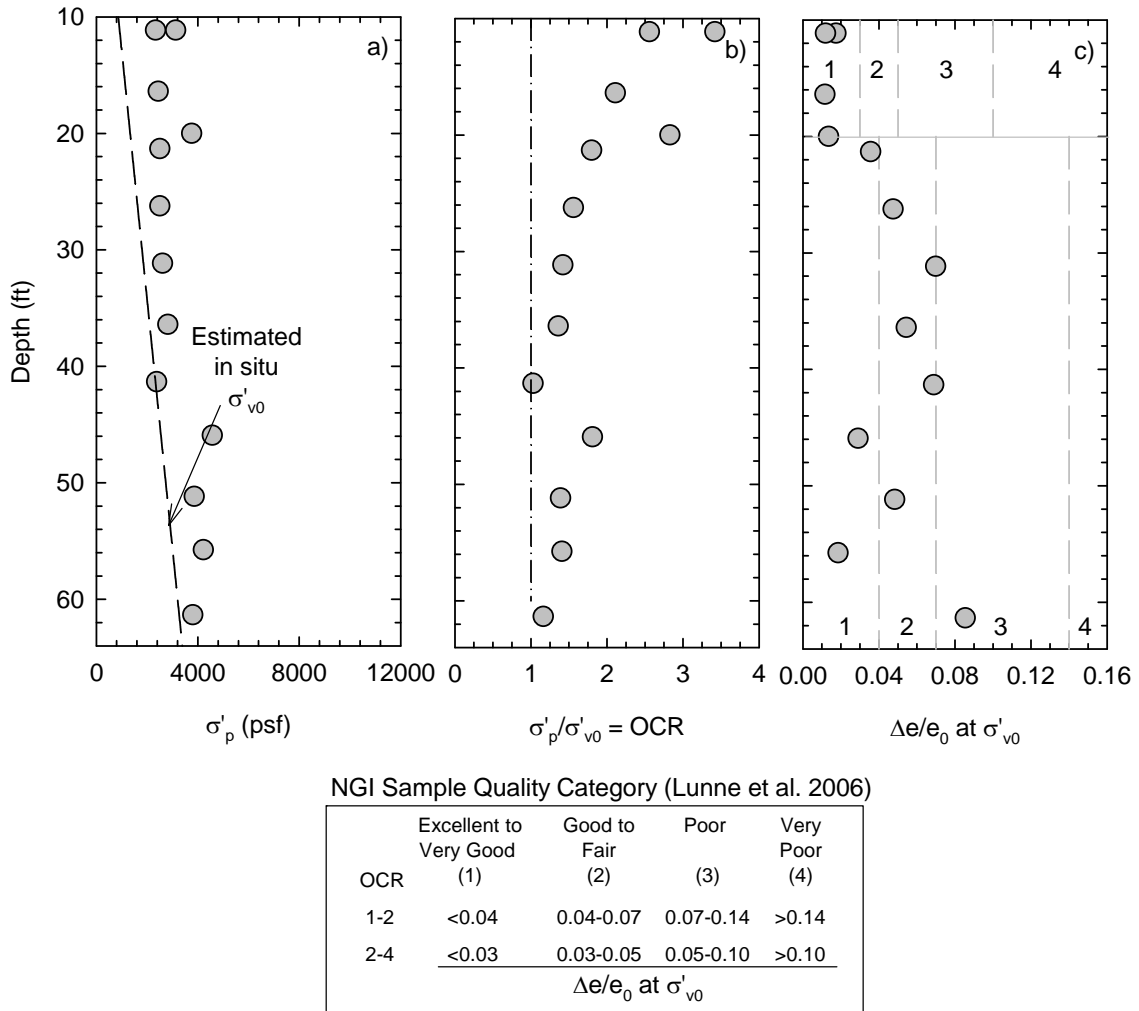


Figure 4.5: Subsurface profiles of a)  $\sigma'_p$ , b) OCR, c) sample quality assessment from CRS consolidation testing on samples from the Route 26/100 Falmouth Bridge Site (after Langlais, 2011).

Vertical coefficient of consolidation at  $\sigma'_{v0}$  ( $c_v @ \sigma'_{v0}$ ), ranged from 12 ft<sup>2</sup>/yr to 340 ft<sup>2</sup>/yr.

This shows an order of magnitude range of values for the tested samples. Consistent with the index testing results and initial void ratio measurements, the upper 25 feet of the deposit exhibited

a more open structure with  $c_v$  values averaging 212 ft<sup>2</sup>/yr while the lower portion of the deposit resulted in a  $c_v$  average of 57 ft<sup>2</sup>/yr. The sand content average in the upper 25 feet is 2.7% while it is 4.0% in the lower portion, showing a potential relationship between increased  $c_v$  with increasing sand content. Andrews (1987) reported the  $c_v$  of Presumpscot clay in the Portland, Maine region to range from 18 ft<sup>2</sup>/yr to 54 ft<sup>2</sup>/yr, indicating that the samples recovered at the Route 26/100 Bridge resulted in higher than expected  $c_v$  values.

#### 4.2.3 Direct Simple Shear Undrained Strength Results

Direct simple shear (DSS) testing was performed on 13 undisturbed tube and Sherbrooke block samples to determine undrained shear strength ( $s_u$ ) values of the Presumpscot clay at the Route 26/100 Falmouth Bridge. Table 4.6 presents specimen properties, conditions following recompressions to the estimated in situ effective stress state, sample quality, and pre-shear parameters of the tested DSS samples.

Table 4.7 presents the results of the DSS testing for all 13 specimens including strength, pore pressure and strain. Sample quality (using the Norwegian Geotechnical Institute (NGI) method of Lunne *et al.* 2006) is typically very good to excellent or good to fair for DSS specimens from shallow depths and decreases with depth as stress relief from removal of overburden increases.  $s_u$  is taken as the maximum measured shear stress during the test. For soils with significant natural structure, sample disturbance can lead to structural break down (i.e. breaking bonds). This diminishes its ability to withstand stress during shear compression. For soils without significant natural structure, disturbance leads to densification (e.g., lower void ratio) following reapplication of in situ stresses which subsequently leads to an increase in strength compared to the higher void ratio in situ soil. For significantly structured soil, the effects of structural damage and subsequent strength loss likely surpass increases in strength from

densification, and measured strength is less than in situ strength. Sensitivity, an indirect measurement of the amount of is high for the sire soils, indicating a structured soil deposit. For samples with low sample quality (see Table 4.6), it is likely that the resulting  $s_u$  is lower than the in situ value.

$s_u$  of the Presumpscot clay at the Route 26/100 Falmouth Bridge Site from DSS testing ranged from 305 psf at 11.2 feet to 766 psf at 61.3 feet (Figure 4.6). In general, the  $s_u$  varied little within the overconsolidated portion of the deposit from 11.2 feet to 26.2 feet ranging from 305 psf to 426 psf, where after, a nearly linearly increasing trend in  $s_u$  was apparent from 26.2 feet to the bottom of the deposit at 61.3 feet (increasing from 401 psf to 766 psf). These values agree well with the ranges of in situ  $s_u$  estimated from FVT testing by H&A (2009), which ranged from 200 psf to 1,100 psf. It is important to note that the failure mode imparted by the FVT method is similar to the failure mode replicated by the direct simple shear (DSS) testing method (i.e. horizontal failure plane) (Terzaghi *et al.*, 1996). Therefore, the resulting  $s_u$  from both of the methods can be expected to be reasonably similar. Based on the work of Karlsrud and Hernandez-Martinez (2013),  $s_u$  from DSS is in the order of 0.74 times the anisotropically consolidated undrained compression (CAUC) strength for high quality samples. Based on this, the equivalent triaxial compression  $s_u$  of the Presumpscot clay at the Route 26/100 Bridge is estimated to range from 411 psf to 969 psf. Analysis of the resulting equivalent CAUC  $s_u$  is presented in Chapter 8. The summary and analysis provided in this chapter use only the DSS  $s_u$ .

Pore pressure at failure, calculated as the effective normal stress applied at the start of shear minus the effective normal stress at failure, for specimens at Falmouth ranged from 173 psf to 1,305 psf, generally increasing linearly with depth over the entire deposit. Sensitive clays are especially subject to large positive pore pressures generated during shear failure as the metastable skeleton collapses (Lambe & Whitman, 1969). In all but three tested specimens (BT-2, BB-5, and BB-13), the pore pressure at failure was higher than the shear strength.

Table 4.6: Summary of Direct Simple Shear Testing soil properties and pre-shear conditions of Presumpscot clay specimens from Route 26/100 Falmouth Bridge Site (after Langlais, 2011).

<sup>1</sup> Sample Type	Depth (ft)	w <sub>n</sub> (%)	e <sub>0</sub>	σ' <sub>v0</sub> (psf)	<sup>2</sup> OCR	σ' <sub>vc</sub> (psf)	Δe at σ' <sub>v0</sub>	Δe/e <sub>0</sub> at σ' <sub>v0</sub>	<sup>3</sup> NGI Rating
MST	11.2	51.2	1.58	912	2.5	917	0.043	0.027	VG/E
SB	11.2	56.5	1.75	912	3.4	910	0.015	0.009	VG/E
MST	16.4	43.3	1.37	1159	2.1	1155	0.072	0.053	P
SB	20.0	51.4	1.57	1328	2.8	1326	0.025	0.016	VG/E
MST	21.3	50.9	1.59	1389	1.8	1399	0.078	0.049	G/F
MST	26.2	49.0	1.52	1620	1.5	1616	0.085	0.056	G/F
MST	31.2	45.4	1.43	1850	1.4	1846	0.119	0.083	P
MST	36.4	47.0	1.47	2096	1.3	2088	0.106	0.072	P
MST	41.3	43.2	1.34	2326	1.0	2324	0.182	0.136	P
SST	45.9	41.2	1.31	2541	1.8	2539	0.066	0.050	G/F
MST	51.2	43.9	1.33	2787	1.4	2781	0.120	0.090	P
SST	55.8	33.6	1.06	3003	1.4	2998	0.073	0.069	G/F
MST	61.3	35.4	1.11	3264	1.2	3261	0.104	0.094	P

ISB = Sherbrooke Block, MST = Modified Shelby Tube, SST = Standard Shelby Tube, <sup>2</sup>Using the Strain Energy Method of Becker et al. (1987), <sup>3</sup>From Lunne et al. (2006), where VG/E: very good to excellent quality, G/F: good to fair, P: poor;

Table 4.7: Summary of Direct Simple Shear Testing results for the Presumpscot clay specimens from Route 26/100 Falmouth Bridge Site (after Langlais, 2011).

<sup>1</sup> Sample Type	Depth (ft)	s <sub>u</sub> (psf)	ε <sub>f</sub> (%)	Δu <sub>f</sub> (psf)	σ <sub>u</sub> /σ' <sub>v0</sub>	Δu <sub>f</sub> /σ' <sub>vc</sub>
MST	11.2	305	3.3	276	0.33	0.30
SB	11.2	416	1.7	173	0.46	0.19
MST	16.4	305	5.0	484	0.26	0.42
SB	20.0	426	1.3	261	0.32	0.20
MST	21.3	390	3.9	551	0.28	0.39
MST	26.2	401	3.9	603	0.25	0.37
MST	31.2	451	3.9	758	0.24	0.41
MST	36.4	555	3.9	871	0.26	0.42
MST	41.3	505	3.9	975	0.22	0.42
SST	45.9	718	3.6	933	0.28	0.37
MST	51.2	697	4.9	1276	0.25	0.46
SST	55.8	710	2.7	1194	0.24	0.40
MST	61.3	766	3.3	1305	0.23	0.40

Notes: <sup>1</sup>SB=Sherbrooke block, MST=modified Shelby tube, SST=standard Shelby tube, ε<sub>f</sub>= strain at failure

$s_u$  normalized by the in situ vertical effective stress ( $s_u/\sigma'_{v0}$ ) for tested specimens ranged from 0.46 to 0.23 throughout the entire profile. When using the CAUC equivalent  $s_{us}$ ,  $s_u/\sigma'_{v0}$  ranged from 0.61 to 0.29. Typically,  $s_u/\sigma'_{v0}$  increases with increasing OCR for clays. This is consistent with the DSS results at the Route 26/100 Falmouth Bridge site, where  $s_u/\sigma'_{v0}$  averaged 0.34 for the overconsolidated region of the deposit and 0.25 for the nearly normally consolidated region of the deposit. For naturally structured clays (like the Presumpscot clay at this site)  $s_u/\sigma'_{v0}$  typically ranges from 0.2 to 0.3 (Ladd and DeGroot, 2003). This is similar to the range of DSS testing on Norwegian clays by Karlsrud and Hernandez-Martinez (2013), who found the  $s_u/\sigma'_{v0}$  to range from 0.18 to 0.26 with an average of 0.22 for normally consolidated clay, as compared to values ranging from 0.25 to 0.35 for triaxial compression testing.

Figure 4.6 also illustrates the  $s_{u(FVT)}$  from FVT performed in nearby borings. Within the top 28 feet of the Presumpscot clay deposit, the  $s_{u(DSS)}$  and  $s_{u(FVT)}$  matched fairly well, but as depth increases beyond 28 feet, the  $s_{u(FVT)}$  is consistently lower than the  $s_{u(DSS)}$  for the remainder of the deposit.

Langlais (2011) describes the rationale of the general under prediction of  $s_u$  using the FVT at the Route 26/100 Falmouth Bridge:

*Both  $s_u$  profiles increase linearly with depth, however the  $s_{u(DSS)}$  increases more. At 65 foot depth,  $s_{u(DSS)}$  is approximately 230 psf greater than  $s_{u(FVT)}$ . The  $s_{u(DSS)}/\sigma'_{v0}$  at 65 feet is approximately 0.24 and  $s_{u(FVT)}/\sigma'_{v0}$  is 0.17 at the same depth.*

*The field vane appears to underestimate  $s_u$  in this study. The estimated in situ  $s_{u(DSS)}$  and design  $s_{u(FVT)}$  profile differ as a result of differences in test procedure and shear mode/rate. In general, the vane device is pushed into the soil, disturbing natural soil structure, at the desired depth and rotated at a rate of  $0.1^\circ$  per second and the torque is measured.*

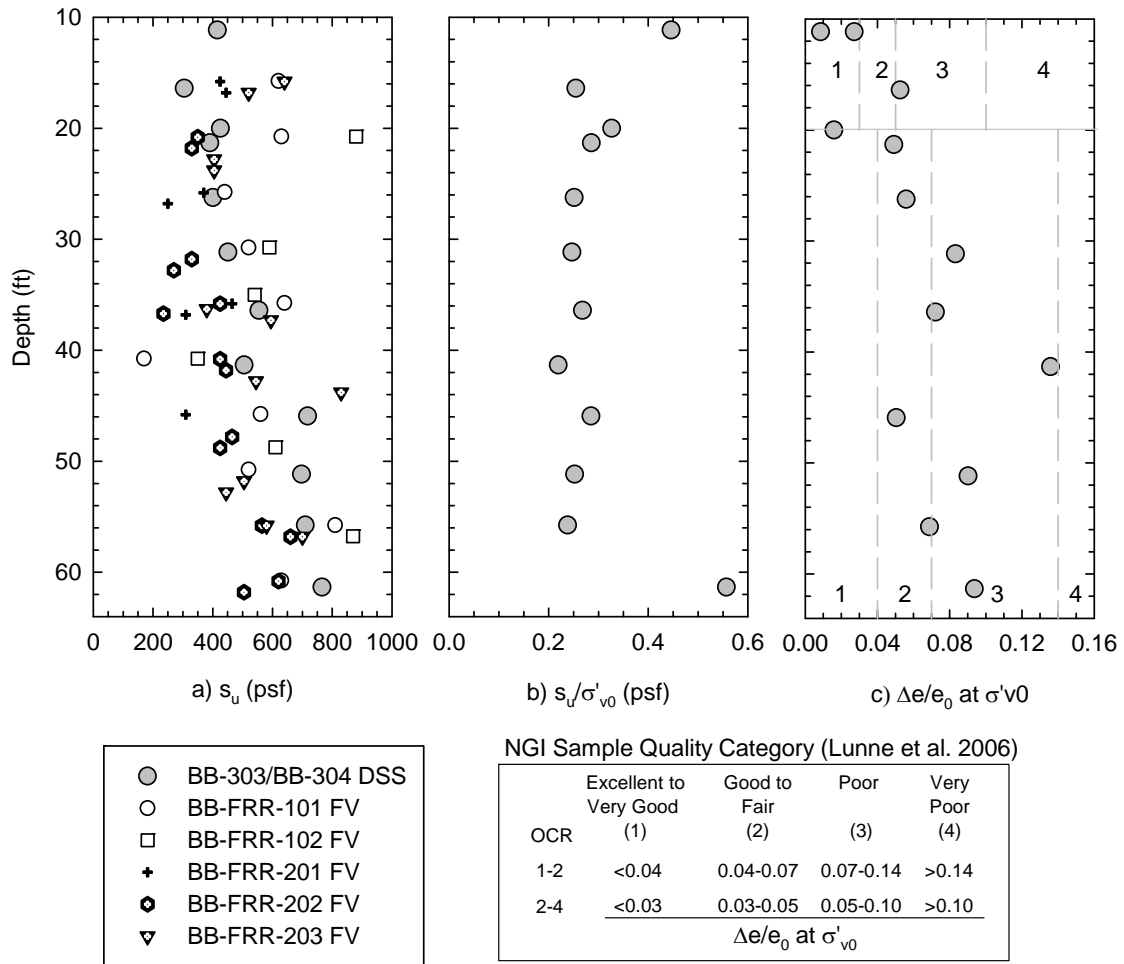


Figure 4.6: Subsurface profile of a) undrained shear strength ( $s_u$ ), b) normalized shear strength and c) sample quality assessment obtained from DSS testing of samples from the Route 26/100 Falmouth Bridge Site reproduced from (from Langlais, 2011).

*The conventional interpretation of the vane test is based on the assumption that the clay shears along the side and ends of the cylinder circumscribing the rectangular vane; the vane strength is derived from shearing in the top and bottom horizontal planes and from shearing horizontally in the vertical surface (Terzaghi et al., 1996). This failure mode does not correspond to any actual failure condition in the field, however Terzaghi et al., (1996) state that this mode of shear approximates the direct simple shear of a horizontal specimen subjected to an axial consolidation pressure equal to  $\sigma'_{v0}$ . If the soil contains layers of sand or dense silt, the torque may be greater than that required if the layers were not present; when these conditions exist, results of vane tests may be misleading (Terzaghi et al., 1996).*



#### 4.2.4 SHANSEP Direct Simple Shear Analysis

Ladd and Foott (1974) empirically observed that the  $s_u$  of clay is directly related to the stress history of the clay (i.e. OCR). They developed the Stress History and Normalized Soil Engineering Parameter (SHANSEP) relationship which estimates  $s_u/\sigma'_{v0}$  at a selected OCR using  $s_u/\sigma'_{v0}$  at normal consolidation (OCR = 1) and an empirical constant, both of which are constant for any specific deposit (Equation 2.1).  $s_u/\sigma'_{v0}$  at normal consolidation is labeled as “ $S$ ” and the empirical constant is labeled as “ $m$ .” These two parameters were determined from the DSS testing of Presumpscot clay at the Route 26/100 Falmouth Bridge.

SHANSEP testing is conducted using on specimens brought to a specific OCR after compression into the normally consolidated zone. This method requires two or more tested samples, and results in  $s_u/\sigma'_{v0}$  at normal consolidation ( $S$ ) and  $s_u/\sigma'_{v0}$  at other defined OCRs. A best-fit line can be fit through the data to provide the  $m$  coefficient.

A different analyses was used for the DSS results of the Presumpscot clay from Route 26/100 Falmouth Bridge using  $s_u/\sigma'_{v0}$  versus OCR, where OCR was determined from the consolidation testing and  $S$  and the  $m$  from the best-fit line (Figure 4.7). The resulting relationship for the Presumpscot clay collected from Route 26/100 Falmouth Bridge site is as follows:

$$s_{u(OCR)} = 0.21 \cdot OCR^{0.50} \quad 4.1$$

The resulting  $S$  ( $s_u/\sigma'_{v0}$  at OCR =1) is 0.21 and the resulting  $m$  is 0.50. Karlsrud and Hernandez-Martinez (2013) provides a range of  $S$  values from 0.18 to 0.26, with an average of 0.22. The range of values for  $m$  was 0.75 to 0.90 with an average of 0.80. This testing was conducted on Norwegian marine clay. The  $S$  value matches well with Karlsrud and Hernandez-Martinez (2013) results; however, the  $m$  is much lower for the Presumpscot clay than the Norwegian clay. If the  $s_u$

is converted from DSS to CAUC strength using the conversion stated above, the resulting  $S$  and  $m$  coefficients are 0.28 and 0.51, respectively.

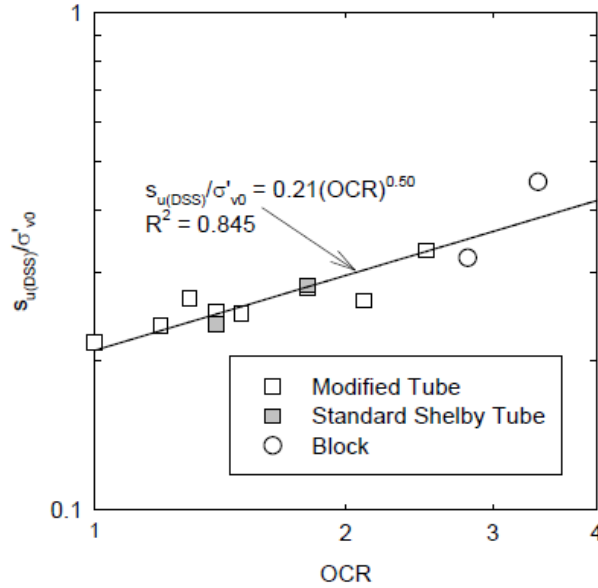


Figure 4.7: Plot of normalized shear strength from recompression DSS tests vs. OCR for Presumpscot clay specimens collected from Route 26/100 Falmouth Bridge Site (from Langlais, 2011)

#### 4.2.5 Summary and Interpretation of Laboratory Results

The Presumpscot clay at the north approach of the Route 26/100 Falmouth Bridge is soft, sensitive, and structured. Analysis of the index, CRS, and DSS test results indicates a distinct boundary within the deposit at a depth of 25 feet below ground surface, at which the deposit transitions from a mildly overconsolidated, highly sensitive to highly quick flocculated structure to a practically normally consolidated, mildly flocculated structure with moderate to high sensitivity and lower void ratio. The surface water elevation of the Presumpscot river at the site is approximately 18.3 feet (H&A, 2009), corresponding to a sample depth of approximately 30 feet.

Laboratory results in the upper portion of the deposit, which ranges from 4.3 feet to 25.0 feet, yielded higher sensitivity, moisture content, initial void ratio, OCR, clay content, plasticity,

organic content, recompression and compression indices, and  $s_u$  when compared to the bottom portion of the deposit (25.0 feet to 63 feet). However, the differences in these properties between the upper and lower portions of the deposit are not severe.

The following trends are apparent from the laboratory results of index, consolidation, and shear strength testing of the Presumpscot clay samples tested from Route 26/100 Bridge:

- A boundary was observed at 25 feet, above which the clay is more structured (higher voids), and below which the influence of granular materials (e.g. silt and sand) become more prominent with depth;
- An overconsolidated crust lies above the soft clay which ranges from approximately ground to surface to 4.0 feet;
- Water content and void ratio decrease with depth. Water contents are generally at or above the liquid limit (LI values range from 0.9 to 2.2); meaning that the clay will act as a liquid, rather than a solid;
- Silt content of the Presumpscot clay samples recovered below 25 feet increased with depth. The increase of silt content with depth was accompanied by reductions in void ratio, water content, organic content, and compression indices;
- Sensitivity of the clay at the site ranged from 9 to greater than 100. The high sensitivity causes the low remolded shear strength and the high virgin compression index ( $C_c$  from the CRS testing was as high as 0.59);
- Test results from Sherbrooke block sample specimens have sample quality that is typically higher than tube samples, as shear strains are eliminated in this method of sampling;
- The deposit is mildly overconsolidated (OCR between 1.8 and 2.5) from 11.0 feet to 25.0 feet and nearly normally consolidated (OCR between 1.0 and 1.8) from 25.0 to 62.0 feet.

### 4.3 Seismic Cone Penetration Testing Results

Three Seismic Cone Penetration Tests with pore pressure measurement (SCPTu) were conducted at the Route 26/100 Falmouth Bridge. SCPTu-P301 and SCPTu-P302 were completed on August 24, 2010 and SCPTu-P305 was completed on September 2, 2010. All tests were conducted in accordance with *ASTM D5778* and method outlined in Section 3.1 by a crew from University of Maine and University of Massachusetts Amherst. Pseudo-interval shear wave velocity testing was performed during each sounding at every rod break.

#### 4.3.1 Results

Figure 4.8 presents measurements of corrected tip resistance ( $q_t$ , Equation 3.2), sleeve friction ( $f_s$ ), and pore pressure ( $u_2$ ) with depth below ground surface from (S)CPTu-P301, -P302, and -P305. Ground surface elevation for the three tests is approximately 47.5 feet above mean sea level (MSL) Tests were conducted from 2 feet below ground surface through the Presumpscot deposit, approximately 70 feet below ground surface.

$q_t$  measured from SCPTu-P301 and SCPTu-P302 in the first 5 feet of penetration start at 55,000 psf and decreases rapidly to 8,000 psf. Once below 5 feet,  $q_t$  measured in all three soundings starts around 8,000 psf and increases generally linearly with depth to approximately 18,000 psf at 58 foot depth. The high tip resistance values measured from 2 to 5 feet in SCPTu-P301 and -P302 are due to penetration through the stiff, overconsolidated crust overlying the soft clay. In the crust layer, groundwater fluctuations have stiffened the clay material from desiccation and re-wetting processes over time (which increases the apparent preconsolidation pressure) as soil desiccates, causing increased resistance to penetration, as observed in the tip resistance and sleeve friction measurements. Furthermore, the crust is a relatively free-draining material which can be observed in the low to no pore pressure measurements in SCPTu-P301 and -302 in the top 5 feet of the deposit.

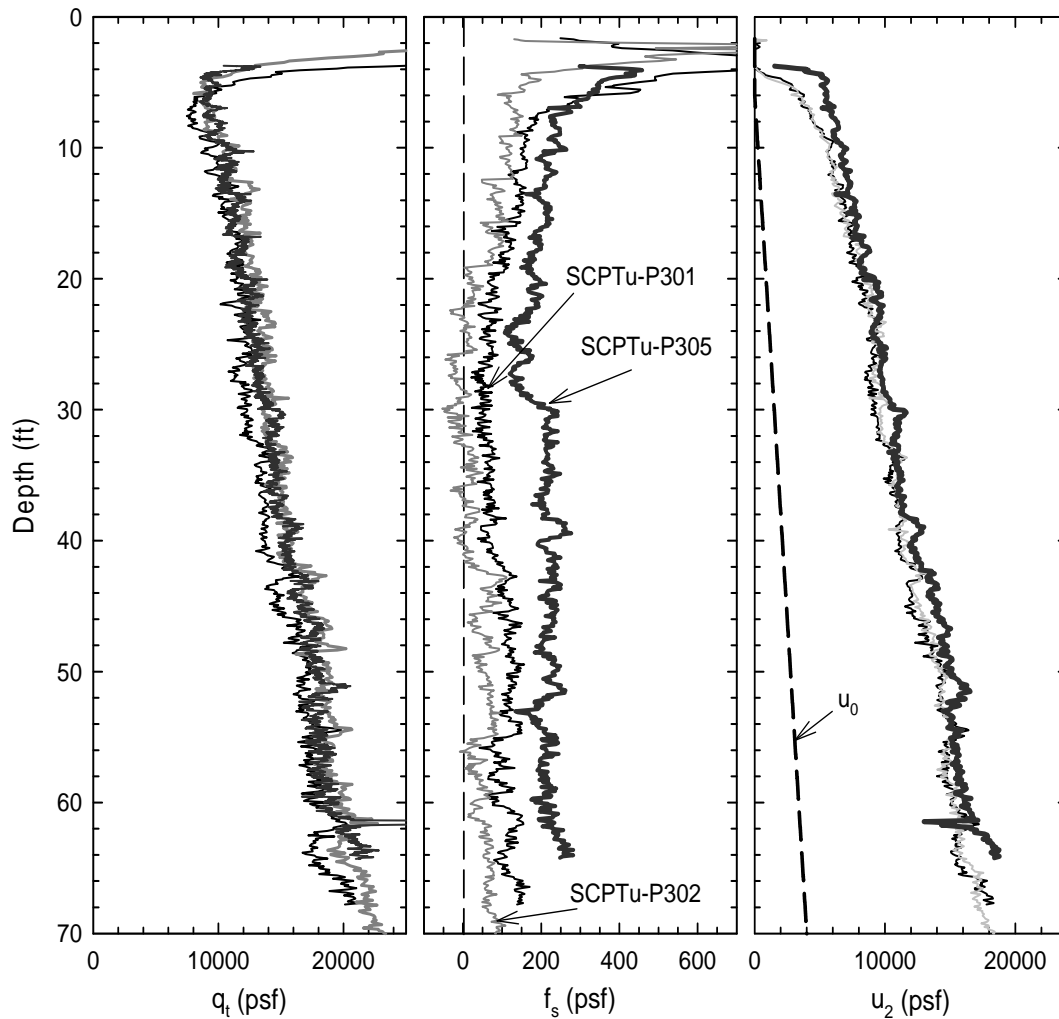


Figure 4.8: Depth profile of (a) corrected tip resistance, (b) sleeve friction, (c) and pore pressure showing hydrostatic pore pressure from soil surface from CPT testing at Route 26/100 Bridge in Falmouth (reproduced from Langlais, 2011).

In the soft, nearly normally consolidated Presumpscot layer from 5 feet to 58 feet,  $q_t$  measurements and trends show a linear increase from 8,000 psf at 5 feet to 14,000 psf at 45 feet, where an abrupt increase in  $q_t$  by 2,000 to 2,500 psf occurs in all three soundings. This rapid increase  $q_t$  is due to the presence of fine to medium sand starting at this depth. The three closets borings (BB-FRR-101, -201, and -202) all noted increasing fine to medium sand in split spoon samples taken at and below this depth. Additionally, grain size testing conducted on collected samples at this depth (Table 4.3) indicates an increase in sand content starting at 47 feet. From 47

feet to the bottom each sounding,  $q_t$  increases consistently, with some increasing and decreasing fluctuations from small silt and sand seams (also observed in the split spoon samples collected).

Measurements of  $f_s$  in the Presumpscot clay ranged from -20 psf to 229 psf.  $f_s$  values measured from SCPTu-P301 and P302 decrease linearly from 200 psf to 0 psf from 5 feet to 20 feet depth, remain at 0 psf to 43 feet, where  $f_s$  abruptly increases to and remains around 60 psf for the remainder of penetration. SCPTu-P305 illustrated a different trend of measured values from SCPTu-P301 and P305.  $f_s$  measured from SCPTu-P305 decreased linearly from 200 psf to 100 psf from 5 feet to 20 feet depth. Once at 20 feet,  $f_s$  abruptly increases to approximately 200 psf and remains at this value until the end of penetration. Difference in measured  $f_s$  between SCPTu-P305 and the other two soundings may be due to zero readings shifts on the load cell or other environmental effects. SCPTu-P301 and P302 were conducted on August 24 and SCPTu-P305 was conducted on September 2.

Mayne (2014) hypothesizes that measured  $f_s$  is analogous to remolded undrained shear strength ( $s_{u(r)}$ ) of clay. This is consistent with the assumption of complete shearing of penetrated clay occurring at the tip. Once this penetrated clay is sheared, it passes by the sleeve of the cone as penetration continues and the measured resistance ( $f_s$ ) would indicate the remolded shear strength at the natural water content since shearing is undrained. However,  $s_{u(r)}$  measurements can change dependent on the method of testing (i.e. field vane shear test (FVT) versus the fall cone apparatus) and the level of remolding. To determine the accuracy of using  $f_s$  to predict  $s_{u(r)}$ , the  $f_s$  measured from SCPTu-P301 and SCPTu-P305 were compared to  $s_{u(r)}$  estimated from FVT and fall cone apparatus testing (Figure 4.9). SCPTu-P302 was not included because it is practically identical to SCPTu-P301.

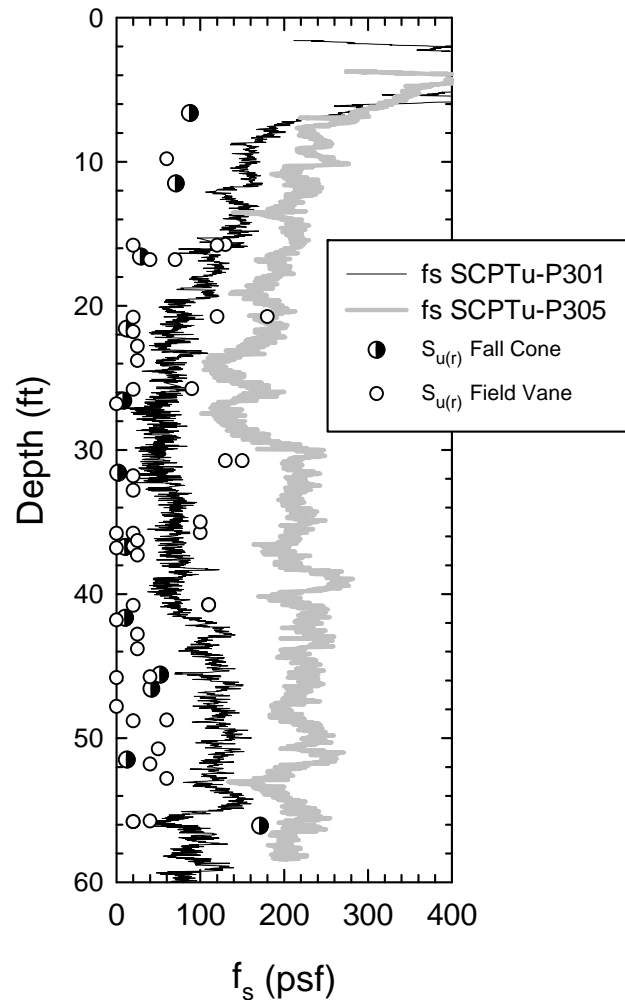


Figure 4.9: Profile comparing remolded shear strength values ( $s_{u(r)}$ ) obtained from nearby field vane test results and fall cone tests with sleeve friction from SCPTu-P301 and -P305 (data from Langlais 2011).

In general,  $f_s$  values from SCPTu-P301 matched closest with the  $s_{u(r)}$  estimated from FVT. In most cases the  $f_s$  values were a little higher than the  $s_{u(r)}$ , but for a few FVT conducted between 20 feet and 43 feet depth the  $s_{u(r)}$  resulted in a lower value than the  $f_s$ . All  $s_{u(r)}$  measurements from the fall cone apparatus gave values lower than the measured  $f_s$  from both SCPTu-P301 and P305, except for the deepest sample at 56 feet which fell above  $f_s$  from SCPTu-P301 and remained lower than  $f_s$  from SCPTu-P305. Throughout the entire profile  $f_s$  values from SCPTu-P305 were

larger (in most cases more than double) than the  $s_{u(r)}$  from both the fall cone apparatus and FVT results.

Karlsrud and Hernandez-Martinez (2013) states that the  $s_{u(r)}$  from FVT will generally be higher than the  $s_{u(r)}$  from fall cone apparatus. They state that the two reasons for this are the inability of the FVT to accurately read low  $s_{u(r)}$  as well as the effect of rod friction increasing the measured  $s_{u(r)}$ . It is also likely that specimens remolded in the laboratory for fall cone testing are “truly” remolded, where only partial remolding may be taking place during the FVT and CPTu process. It appears that  $f_s$  measured from CPTu soundings for Presumpscot clay at Route 26/100 Falmouth Bridge match closer with FVT results.

Measurements of  $u_2$  in the Presumpscot clay range from 3,000 psf to 15,000 psf, increasing nearly linearly with depth. The slope of  $u_2$  is shallower than the hydrostatic water pressure line, which indicates that these two pressures are independent.  $u_2$  measured in the crust is either negative in magnitude or zero. This is consistent with the theory of negative pore pressures which develop in overconsolidated clays subject to shearing.

#### 4.3.2 Correlations to Classification

Empirical charts have been proposed by Robertson (1990), Schneider *et al.* (2008), and Robertson (2009) to classify soils based on CPTu measurements (Section 2.3). These charts plot normalized tip resistance ( $Q_t$ ) versus normalized sleeve friction ( $F_r$ ) or normalized pore pressure ( $B_q$ ) and the resulting data fall into a region which has a corresponding soil type deemed the “Soil Behavior Type” or SBT. The SBT regions were developed based on observed  $Q_b$ ,  $F_r$ , and  $B_q$  measurements taken in specific types of soils. Normalized CPTu parameters are used to eliminate the influence of depth increase in soil properties due to overburden stress on measurements. Figure 4.10 displays the profiles of the three normalized parameters  $Q_b$ ,  $F_r$ , and  $B_q$  collected from SCPTu-P301, P302, and P305.



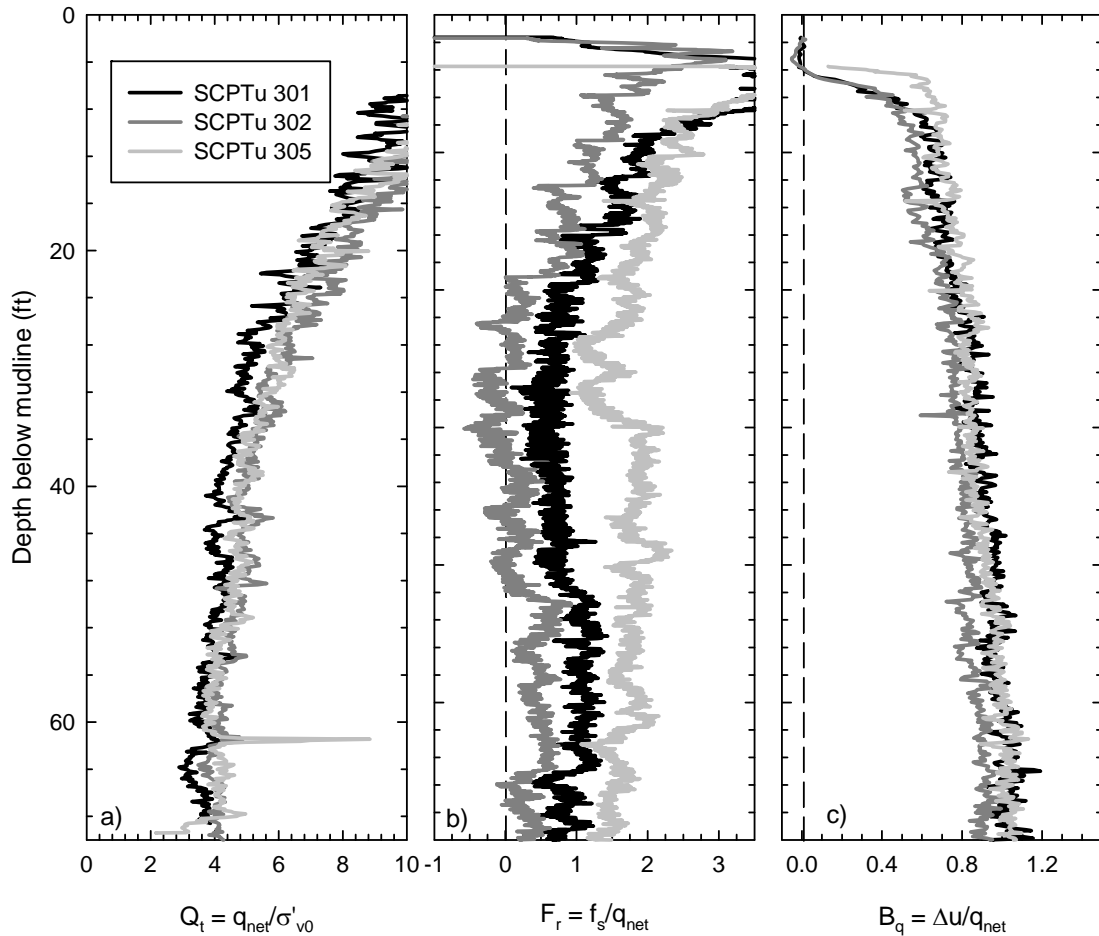


Figure 4.10: Profile of a) normalized tip resistance ( $Q_t$ ), b) sleeve friction ratio ( $F_r$ ), and c) normalized pore pressure ratio ( $B_q$ ) with depth for SCPTu-P301, P302, and P305 at Route 26/100 Falmouth Bridge (data from Langlais, 2011).

Each of the four classification charts were evaluated for their correlation to the Presumpscot clay classification at the Route 26/100 Falmouth Bridge. To do this, samples from each of the undisturbed Shelby tube or Sherbrooke blocks were classified using laboratory results of grain size analyses and plasticity in accordance with the Unified Soil Classification System (USCS). In general, samples classified as CL “Lean Clay,” which is typical for Presumpscot clay. Additionally, values of  $Q_t$ ,  $F_r$ , and  $B_q$  collected from SCPTu-P301 and P305 from depths corresponding to the tested samples were plotted. SCPTu-P302 was not used because it is

practically identical to SCPTu-P301. For three of the charts (Robertson 1990 and Robertson 2009), there are 9 regions corresponding to soil types. Of these regions, region 1 “sensitive fine grained,” region 3 “clay to silty clay,” and region 4 “clayey silt to silty clay” were considered to be correct classifications of the Presumpscot clay. For the fourth chart (Schneider *et al.* 2008), a different classification system is used, of which the “clays” and “sensitive clays” regions were considered to be correct classifications of the Presumpscot clay. The plotted data points from SCPTu-P301 and P305 are presented in Figure 4.11 and Figure 4.12, respectively.

All four charts resulted in 100 percent classification effectiveness for both SCPTu-P301 and P305. For SCPTu-P301, data plots in Regions 1 (sensitive clay) and Region 4 (clayey silt to silty clay) when plotted on the  $F_r$  vs  $Q_t$  charts and in Region 3 (clay to silty clay) and the “clays” region when plotted  $B_q$  vs  $Q_t$ . This illustrates the difference between the classifications using  $F_r$  and  $B_q$ . For SCPTu-P305, the data plotted entirely in region 3 (clay to silty clay) in the Robertson (1990) and Robertson (2009) charts and entirely in the “sensitive clay” region in the Schneider *et al.* (2008) chart. Unlike SCPTu-P301, the classification results between the Robertson  $F_r$  (1990) and Robertson  $B_q$  (1990) for SCPTu-P305 are consistent. Furthermore, the classification from Schneider *et al.* (2008) did not agree with Robertson  $B_q$  (1990), and both charts use the relationship between  $Q_t$  and  $B_q$ . Zero reading shift of the friction sleeve from one CPTu test to the other could be the cause of different classification using the  $F_r$  vs  $Q_t$  charts. The difference in plotted region for the Presumpscot clay between the two types of SBT chart is explored in depth in Section 8.3 using data points from all four sites. Essentially, the variation of the plotted regions between the two types of charts is not unexpected (as Robertson 1990 states) when using CPTu charts, since the classification is behavioral based as opposed to grain-size or mineralogy-based.

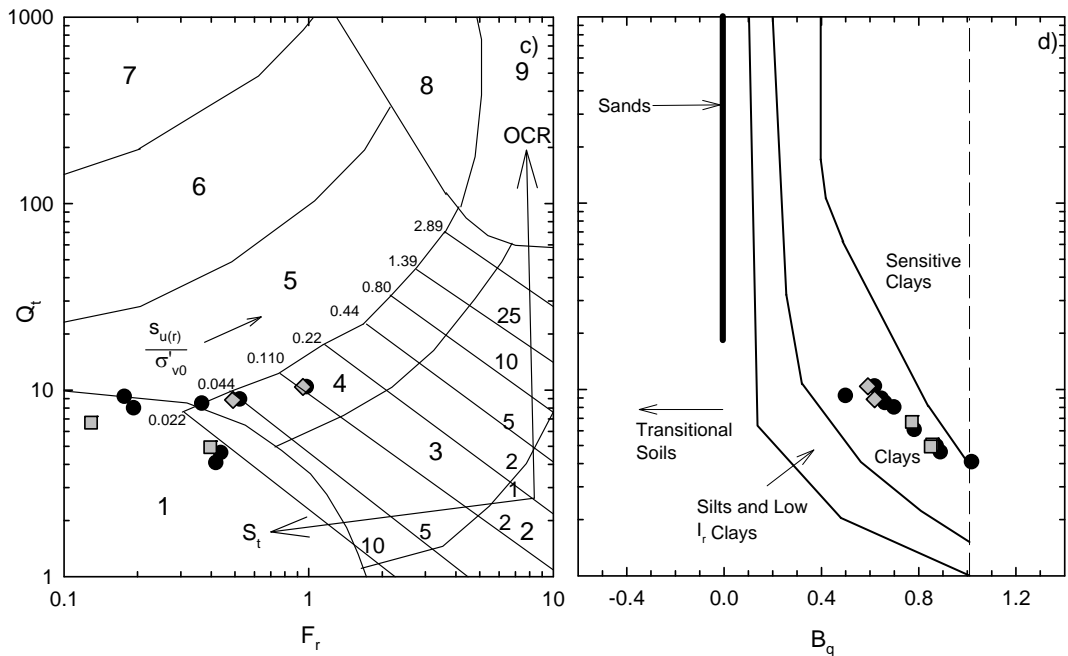
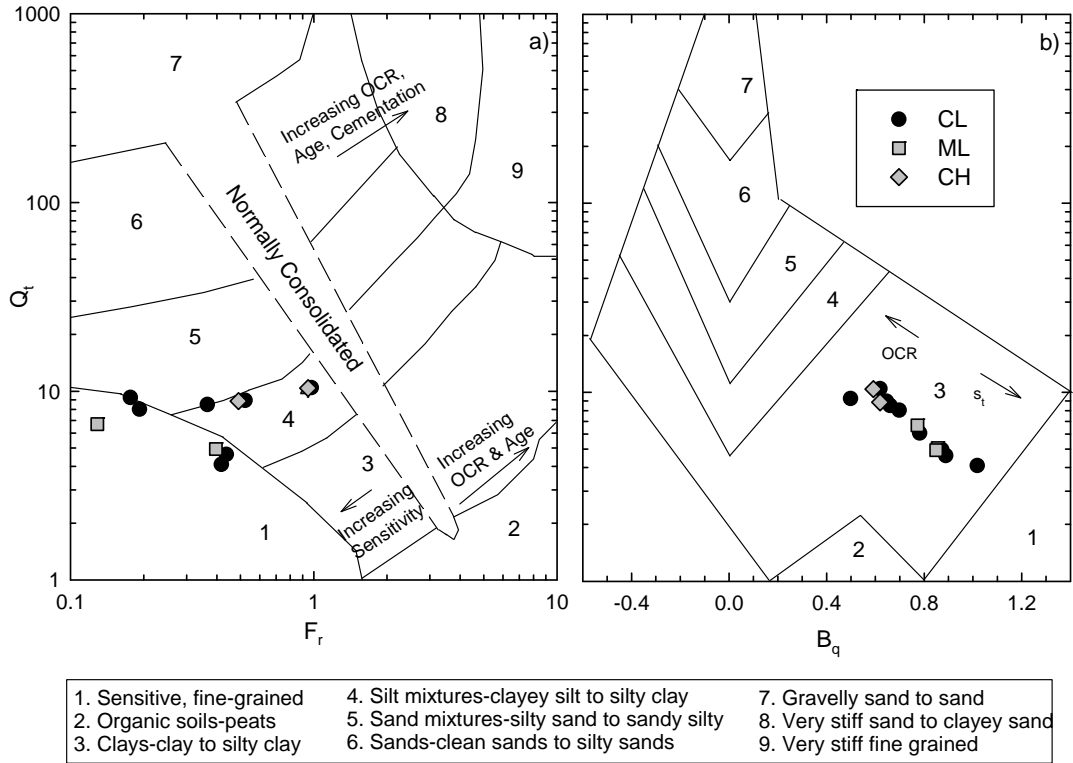
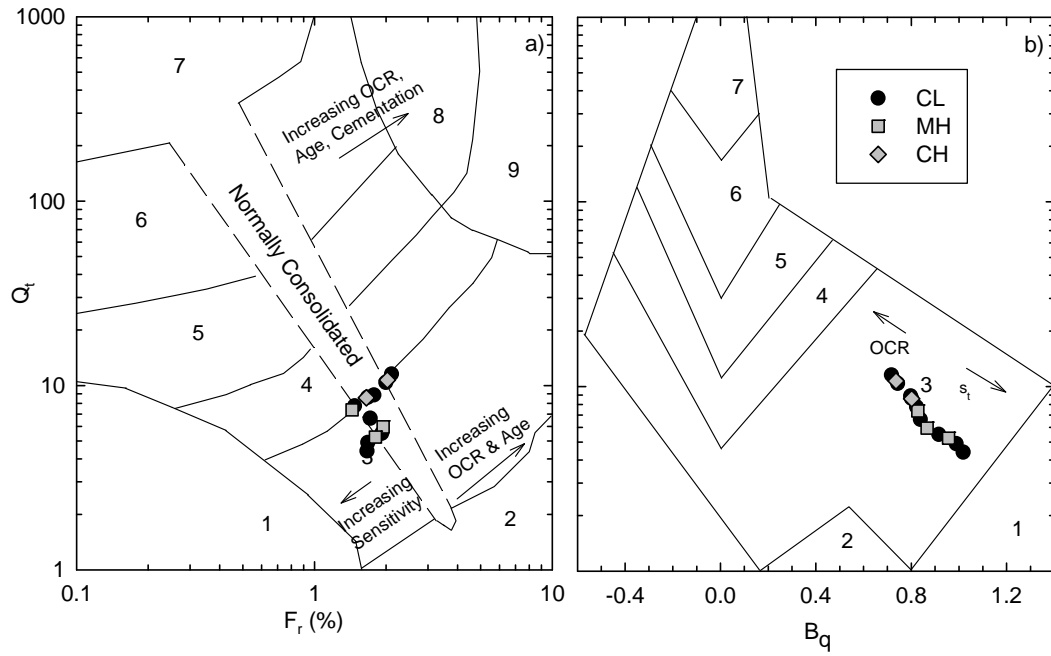


Figure 4.11 Soil classification results from SCPTuP301 comparing laboratory-determined USCS classification to classification charts using a)  $Q_t$  vs.  $F_r$  (Robertson 1990), b)  $Q_t$  vs.  $B_q$  (Robertson 1990), c)  $Q_t$  vs.  $F_r$  (Robertson 2009), d)  $Q_t$  vs.  $B_q$  (Schneider *et al.*, 2008) at the Route 26/100 Falmouth Bridge (data from Langlais, 2011).



- |                             |  |                                   |
|-----------------------------|--|-----------------------------------|
| 1. Sensitive, fine-grained  | 4. Silt mixtures-clayey silt to silty clay | 7. Gravelly sand to sand          |
| 2. Organic soils-peats      | 5. Sand mixtures-silty sand to sandy silty | 8. Very stiff sand to clayey sand |
| 3. Clays-clay to silty clay | 6. Sands-clean sands to silty sands        | 9. Very stiff fine grained        |

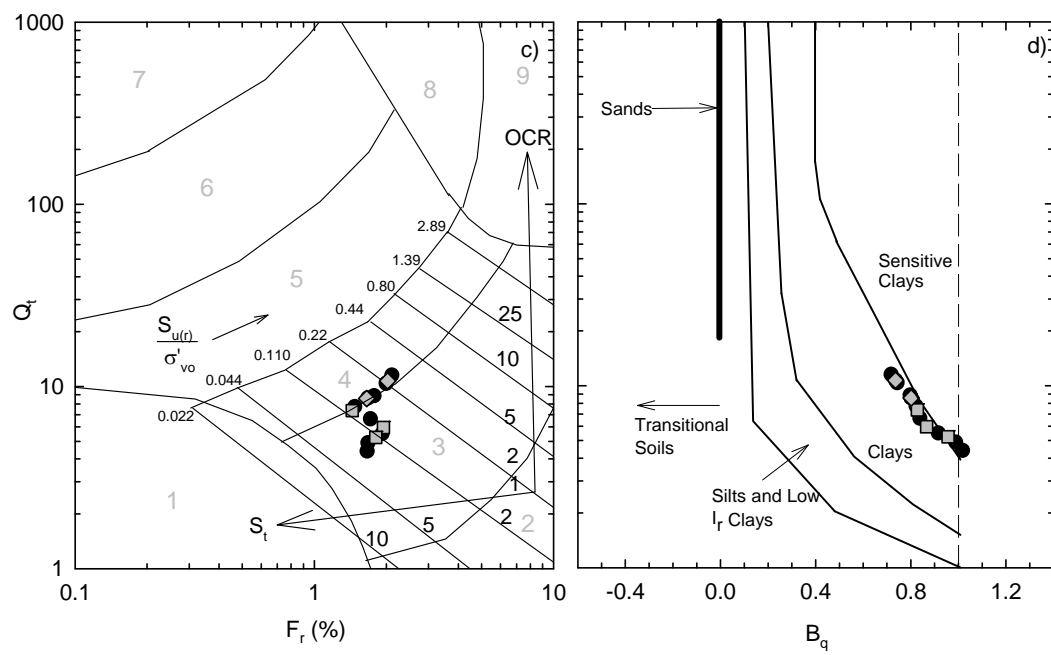


Figure 4.12: Soil classification results from SCPTuP305 comparing laboratory-determined USCS classification to classification charts using a)  $Q_t$  vs.  $F_r$  (Robertson 1990), b)  $Q_t$  vs.  $B_q$  (Robertson 1990), c)  $Q_t$  vs.  $F_r$  (Robertson 2009), d)  $Q_t$  vs.  $B_q$  (Schneider *et al.*, 2008) at the Route 26/100 Falmouth Bridge (data from Langlais, 2011).

When CPTu data is collected in a clay deposit and plotted on the SBT charts, one might expect the classification based on sleeve friction (i.e.  $F_r$  vs  $Q_t$ ) to not be entirely consistent with the pore pressure classification (i.e.  $B_q$  vs  $Q_t$ ), which is the pattern observed at the Route 26/100 Bridge.

The Presumpscot clay at the Route 26/100 Falmouth Bridge site is sensitive clay, apparent from the FVT and fall cone testing (Table 4.4). It is classified as sensitive clay using Robertson  $F_r$  (1990) Robertson (2009) charts for SCPTu-P301 and using Schneider *et al.* (2008) chart for SCPTu-P305.  $F_r$  values were lower (corresponding to a low remolded undrained shear strength and hence a sensitive clay) for SCPTu-P301 and  $B_q$  values were higher (corresponding to a higher pore pressure at shear failure hence a sensitive clay) for SCPTu-P305.

#### 4.3.3 Correlations to Stress History

Stress history of the Presumpscot clay was estimated from the CPTu soundings conducted at the Route 26/100 Falmouth Bridge site using the *k-value* method. Using Equation 2.7, *k-value* was back-calculated using preconsolidation pressure ( $\sigma'_p$ ) determined from constant rate of strain (CRS) consolidation testing (Table 4.5) and  $q_{net}$  measured from the CPTu soundings (Section 4.3.1) at the corresponding sample depths.  $\sigma'_p$  was estimated from CRS testing using the Becker *et al.*, (1987) method and in situ vertical effective stress ( $\sigma'_{v0}$ ) was estimated using unit weights from the tested CRS specimens. Figure 4.13 presents the *k-values* determined for the Presumpscot clay at the Route 26/100 Falmouth Bridge site along with the estimated  $\sigma'_p$  profile using determined *k-values* applied to SCPTu-P301 (the closest sounding to the collected samples).

In Figure 4.13a, each symbol represent a *k-value* back calculated from one of the CPTu soundings. Each “set” of symbols (i.e. the multiple symbols shown at one specific depth) correspond to a single  $\sigma'_p$ , with a  $q_{net}$  value taken from one of the CPTu soundings and applied to

that  $\sigma'_p$  to solve for  $k$ . The range of values between the symbols represents the difference in  $q_{net}$  from the soundings. The soundings were conducted within approximately 20 feet of each other; however, SCPTu-P301 was closest to the samples collected for the consolidation testing. The dotted lines at values of 0.20 and 0.50 represent the “typical” range of values for clays (Lunne *et al.*, 1997). In Figure 4.13b, the average, minimum, and maximum  $k$ -values from SCPTu-P301 were applied to the entire profile of  $q_{net}$  from SCPTu-P301 and compared to the laboratory-determined  $\sigma'_p$ .

$k$ -values ranged from 0.20 to 0.43, which agrees with the published range from Lunne *et al.* (1997) of 0.20 to 0.50. Between 10 feet and 42 feet depth,  $k$ -values are generally consistent around 0.25 except for values deeper than 20 feet, which are approximately 0.40. This increase at 20 feet is due to the higher  $\sigma'_p$  value estimated at that depth. Sample quality of that specimen was “very good to excellent,” so the higher  $\sigma'_p$  is unlikely to be from sample disturbance. Index testing results from that depth do not indicate a significant change in composition, however, sensitivity is significantly higher than the surrounding samples. Furthermore, the virgin compression index ( $C_c$ ) is highest for this sample of all of the tested samples (0.59), which is indicative of greater structure and stiffness (DeGroot and Ladd, 2010).

Below 43 feet, there is a sustained increase in the  $k$ -value, which is directly due to greater  $\sigma'_p$  (refer to Figure 4.5). The  $k$ -value from SCPTu-P301 below 43 feet ranges from 0.35 to 0.43. Typically, sample quality decreases with depth due to removal of larger amounts of overburden stress during sampling, i.e. stress relief, often leading to lower estimates of  $\sigma'_p$  due to destructuration. However, at the Route 26/100 Bride site, sample quality remained good with depth and data from deeper depths are considered reliable. Samples collected and tested within the middle depths of the profile (from 20 feet to 43 feet) were of slightly lower quality and provided lower  $\sigma'_p$  estimates due to sample disturbance and subsequently caused  $k$ -values to be

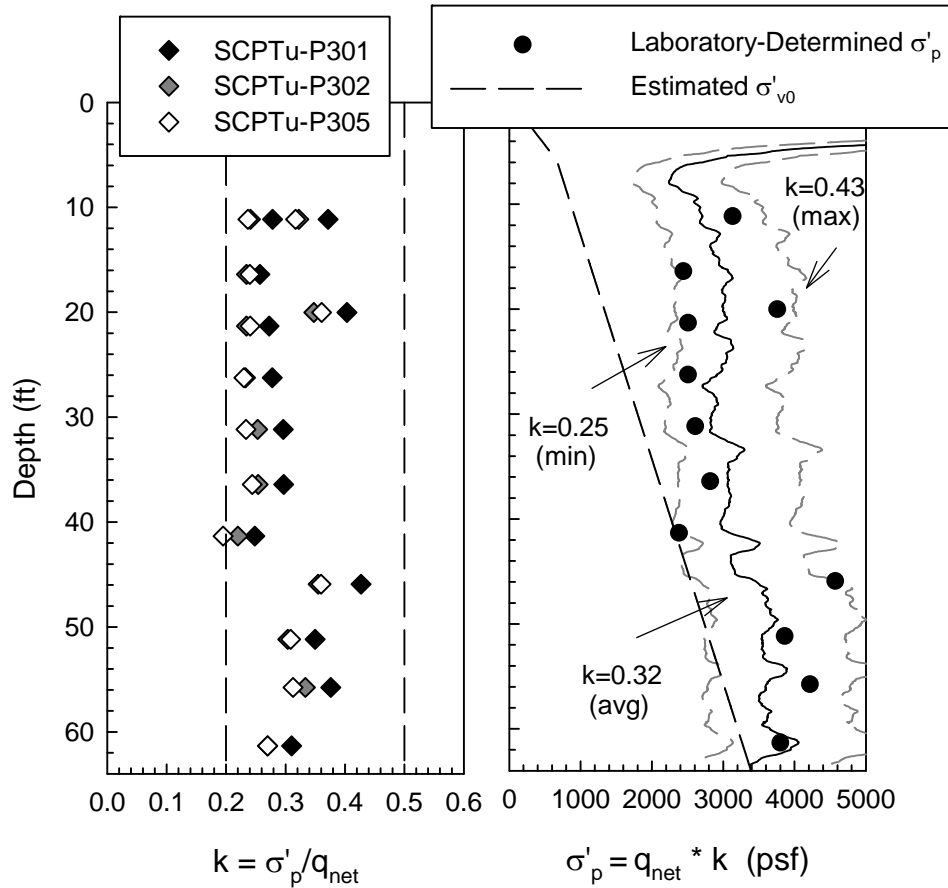


Figure 4.13: Subsurface profiles of a)  $k$  values determined from SCPTu-P301, SCPTu-P302, and SCPTu-P305, and b) preconsolidation pressure estimated using average, minimum, and maximum  $k$  values from SCPTu-P301 compared to the laboratory-determine values at the Route 26/100 Falmouth Bridge site (after Langlais, 2011).

lower than expected. Inspection of the consolidation curve for the sample at 41 feet showed a more rounded curve compared to the other samples and the sample quality was lower, both of these factors contributing to a lower estimate of  $\sigma'_p$  and hence a lower  $k$ -value, as shown in Figure 4.13.

Trends in  $k$ -value with measured clay properties were explored. Saye *et al.*, (2013) suggests that  $k$ -value may be related to plasticity index and liquid limit, however no such correlation was found for the Presumpscot clay at the Route 26/100 Bridge site. There were no

apparent trends between *k-value* and plasticity, clay content, sand content, sensitivity, or any other investigated property. This is analyzed further in Section 8.4.

#### 4.3.4 Correlation to Undrained Shear Strength

Undrained shear strength ( $s_u$ ) of clays can be estimated from CPTu results using empirical cone factors  $N_{kt}$ ,  $N_{ke}$ , and  $N_{\Delta u}$  (Equations 2.9 through 2.11).  $N_{kt}$  is derived from tip resistance ( $q_t$ ),  $N_{ke}$  is derived from  $q_t$  and pore pressure measurements ( $u_2$ ), and  $N_{\Delta u}$  is derived from  $u_2$ . These empirical coefficients were determined for the Presumpscot clay at the Route 26/100 Falmouth Bridge using  $s_u$  from laboratory direct simple shear (DSS) testing and field vane shear testing (FVT) results conducted within a lateral distance of 200 feet of the CPTu soundings. This 200 feet distance was chosen as an arbitrary limiting distance.

Throughout this section, the empirical cone factors will have a subscript of either or DSS, FVT, indicating the reference undrained shear strength used to determine that cone factor. It is important to note the reference  $s_u$ , because the  $s_u$  is not a distinct soil property, rather a measurement dependent on many factors including rate of shear, anisotropy, and deviator stress angle. The resulting  $s_u$  will differ when using the different test methods.

Figure 4.14 displays  $N_{kt(DSS)}$ ,  $N_{ke(DSS)}$ , and  $N_{\Delta u(DSS)}$  with depth calculated using each of the three CPTu soundings. In Figure 4.14, each symbol represents one empirical cone factor back calculated from one of the CPTu soundings. Each “set” of symbols (i.e. multiple symbols shown at one specific depth) correspond to a single  $s_{u(DSS)}$  with a  $q_t$  or  $u_2$  (or both for  $N_{ke(DSS)}$ ) value taken from one of the CPTu soundings and applied to that  $s_{u(DSS)}$  to solve for the cone factor. The soundings were conducted within close proximity of each other; however, SCPTu-P301 was closest to the samples collected for the DSS testing. Note that the empirical cone factors are inversely proportional to  $s_u$ , so that a higher cone factor predicts a lower  $s_u$ . Table 4.8 summarizes the  $N_{kt(DSS)}$  and  $N_{\Delta u(DSS)}$  determined from the three CPTu soundings at the site.



Table 4.8: Summary of  $N_{kt(DSS)}$  and  $N_{\Delta u(DSS)}$  values at the Route 26/100 Bridge site.

		Minimum	Average	Maximum	S.D.	C.O.V.
SCPTu-P301	$N_{kt(DSS)}$	15.0	20.5	31.4	4.9	0.24
	$N_{\Delta u(DSS)}$	13.6	17.3	22.1	2.3	0.13
SCPTu-P302	$N_{kt(DSS)}$	18.0	24.1	34.3	5.4	0.22
	$N_{\Delta u(DSS)}$	13.6	17.8	21.3	2.4	0.30
SCPTu-P305	$N_{kt(DSS)}$	17.8	24.5	33.5	5.1	0.21
	$N_{\Delta u(DSS)}$	17.4	21.0	26.7	2.9	0.14

Note: S.D. = standard deviation; C.O.V. = coefficient of variation

$N_{kt(DSS)}$  ranged from 15.0 to 34.3 with average values of values of 20.9 (SCPTu-P301), 24.1 (SCPTu-P302) and 24.5 (SCPTu-P305). Coefficients of variations for  $N_{kt(DSS)}$  of the three soundings are 0.24, 0.22, and 0.21 for SCPTu-P301, -302, and, -305 respectively.  $N_{ke(DSS)}$  ranged from 3.5 to 16.9 with average values of values of 7.2 (SCPTu-P301), 10.0 (SCPTu-P302) and 7.3 (SCPTu-P305). Coefficients of variations for  $N_{ke(DSS)}$  of the three soundings are 0.44, 0.37, and 0.35 for SCPTu-P301, 302, and, 305 respectively.  $N_{\Delta u(DSS)}$  ranged from 13.6 to 26.7 with average values of 17.4 (SCPTu-P301), 17.8 (SCPTu-P302) and 21.0 (SCPTu-P305). Coefficients of variations for  $N_{\Delta u(DSS)}$  of the three soundings are 0.14, 0.13, and 0.14 for SCPTu-P301, 302, and, 305 respectively.

$N_{kt(DSS)}$ ,  $N_{ke(DSS)}$ , and  $N_{\Delta u(DSS)}$  values for the shallowest four samples (from 11.2 feet to 21.3 feet) fluctuate, likely because of sample quality. The Sherbrooke block samples at 11.2 and 20.0 resulted in higher sample quality, higher  $s_u(DSS)$  and subsequently lower  $N_{kt(DSS)}$ ,  $N_{ke(DSS)}$ , and  $N_{\Delta u(DSS)}$  values. From 21.3 feet to 36.4 feet, all three DSS cone factors decreased with depth. Below 36.4 feet,  $N_{ke(DSS)}$  continued to decrease with depth where  $N_{kt(DSS)}$  and  $N_{\Delta u(DSS)}$  increased at 41.3 feet, and then decreased and remained constant from 45.9 to 55.8 feet.

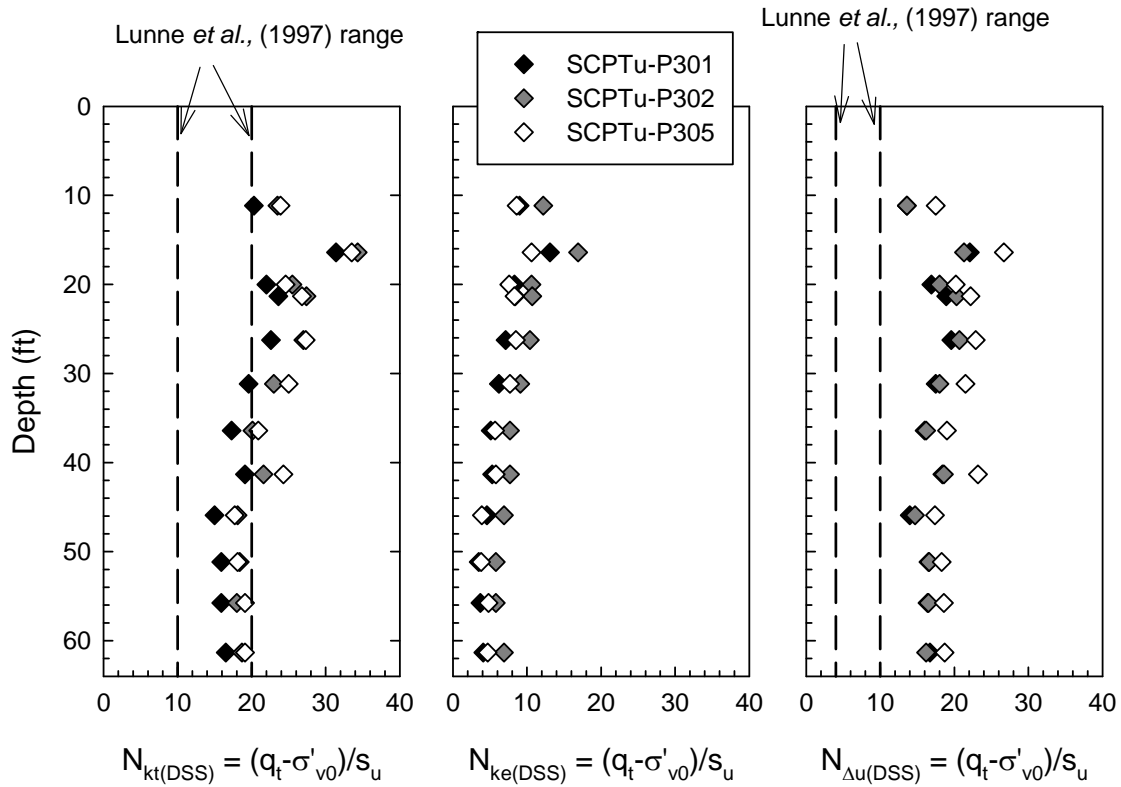


Figure 4.14: Subsurface profiles of  $N_{kt(DSS)}$ ,  $N_{ke(DSS)}$ , and  $N_{\Delta u(DSS)}$  correlated from SCPTu-P301, P302, and P305 with  $s_u$  from DSS testing for Presumpscot clay at Route 26/100 Falmouth Bridge (data from Langlais, 2011).

The sudden increase in  $N_{kt(DSS)}$  and  $N_{\Delta u(DSS)}$  at 41.3 feet is likely due to the low sample quality and subsequent low measured  $s_u$  of the tested specimen at that depth. It was the lowest sample quality of all tested DSS specimens at the Route 26/100 Falmouth Bridge Site.

The general trend of decreasing values of  $N_{kt(DSS)}$  with depth results from the relationship between normalized undrained shear strength and normalized tip resistance. Firstly, rearranging Equation 2.9 equates  $s_u/\sigma'_{v0}$  to  $q_{net}/\sigma'_{v0}$  ( $Q_t$ , Figure 4.10), both of which decrease with depth as OCR decreases (Figure 4.6 and Figure 4.10). If the rate of decrease with depth of these two factors remained constant, the resulting  $N_{kt(DSS)}$  would also remain constant. However, since

$N_{kt(DSS)}$  decreases with depth, either the  $s_u/\sigma'_{v0}$  is disproportionately higher than the  $q_{net}/\sigma'_{v0}$ , or vice versa. Conclusively, the  $q_{net}/\sigma'_{v0}$  appears to decrease at a faster rate than the measured  $s_u/\sigma'_{v0}$ . In addition, Lunne *et al.*, (1985) and Karlsrud (1996) suggest that  $N_{kt(DSS)}$  decreases with increasing  $B_q$ , which is consistent with the results observed at the Route 26/100 Bridge since  $B_q$  increases with depth.

$N_{\Delta u(DSS)}$  remains relatively constant with depth, indicating the pore pressure measured during the SCPTu soundings at the Route 26/100 Bridge provided a good estimation of  $s_u$  behavior. Lunne *et al.*, (1985) and Karlsrud (1996) suggest that  $N_{\Delta u}$  may increase slightly with increasing  $B_q$  values (increasing depth), however their correlation is loose and the magnitude of  $B_q$  at the Route 26/100 Bridge may not be severe enough to result in an  $N_{\Delta u}$  increase.

Cone factor  $N_{ke}$  is an inconsistent method for determining  $s_u$  of clay (Lunne *et al.*, 1997). The factor is derived from the difference in measured tip resistance and pore pressure. In the Presumpscot clay, the pore pressure measured during penetration can approach (and possibly exceed) measured tip resistance, indicated by a high normalized pore pressure parameter  $B_q$ . The resulting difference in measurements is small in magnitude, and in result, predicted  $s_u$  is sensitive to small variations in this value. For instance, an increase in  $N_{ke}$  from 10 to 11 might decrease the predicted  $s_u$  by 200 psf where an increase in  $N_{kt}$  or  $N_{\Delta u}$  from 10 to 11 might decrease the predicted  $s_u$  by 50 psf. In effect, the  $N_{ke}$  factor has less “forgiveness” than the other two strength N factors.

Figure 4.15 illustrates  $s_u$  of the Presumpscot clay with depth at the Route 26/100 Falmouth Bridge site using  $N_{kt}$  and  $N_{\Delta u}$  cone factors applied to SCPTu-P301, which was conducted closest to the undisturbed sampling.

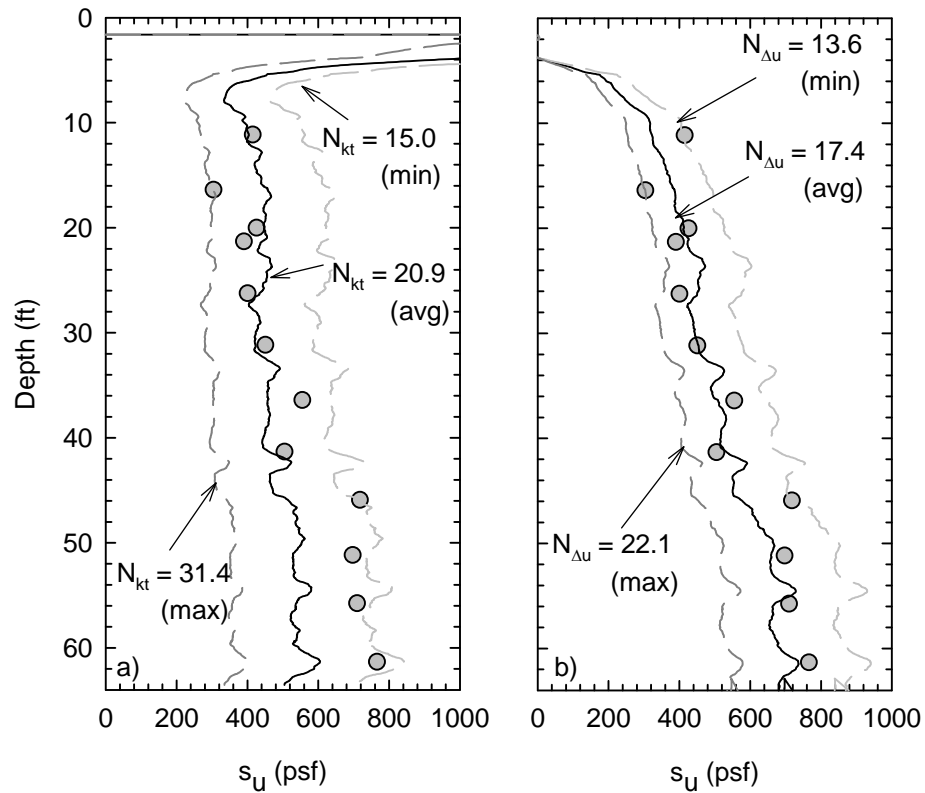


Figure 4.15: Profile of undrained shear strength of Presumpscot clay at Route 26/100 Falmouth Bridge site using empirical cone factors a)  $N_{kt(DSS)}$  and b)  $N_{\Delta u(DSS)}$  applied to SCPTu-P301. Undrained shear strength determined from DSS testing is shown as the gray circles (data from Langlais, 2011).

Review of Figure 4.15 illustrates that from the top of the deposit to a depth of approximately 40 feet, there does not appear to be a major difference between  $s_u$  predicted from the average  $N_{kt(DSS)}$  or the  $N_{\Delta u(DSS)}$ , and within this depth range, the  $s_u$  predicted from both of the methods matched closely with the laboratory test results. However, once below 40 feet, the  $N_{\Delta u(DSS)}$  continued to follow the laboratory data but the  $N_{kt(DSS)}$ -predicted  $s_u$  profile remained well below laboratory data results. Decreasing  $N_{kt(DSS)}$  with depth (Figure 4.14) is responsible for this under-prediction.  $N_{\Delta u(DSS)}$  also resulted in a tighter range of minimum and maximum  $s_u$  estimates whereas the  $N_{kt(DSS)}$  range was much wider throughout the entire profile.

In addition to the analysis of laboratory data,  $s_u$  measured from FVT was also correlated to the CPTu cone factors. Figure 4.16 presents values of  $N_{kt(FVT)}$ ,  $N_{ke(FVT)}$ , and  $N_{\Delta u(FVT)}$  with depth using field vane shear testing (FVT)  $s_u$  results paired with measurements from SCPTu-P301. SCPTu-P301 was chosen for simplicity of showing only one set of  $N_{kt(DSS)}$ ,  $N_{ke(DSS)}$ , and  $N_{\Delta u(DSS)}$  values. Values from SCPTu-P302 and SCPTu-P305 would show similar results if plotted.  $N_{kt(FVT)}$  show a lot of variation and ranged from 10.8 to 54.6 with an average of 21.8.  $N_{\Delta u(FVT)}$  also showed a lot of variation and ranged from 8.4 to 52.8 with an average value of 19.3. Coefficient of variation (COV) ranged from 0.19 to 0.60 for  $N_{kt(FVT)}$  and from 0.20 to 0.66 for  $N_{\Delta u(FVT)}$ . A summary of these values is presented in Table 4.9.

Both  $N_{kt(FVT)}$  and  $N_{\Delta u(FVT)}$  were in the lower range of values in the upper portion of the deposit from 10 feet to 18 feet depth, and then become scattered from 18 feet to the bottom of the deposit. The lower values in the upper portion of the deposit are consistent with the higher  $s_u$  of the Presumpscot clay due to the higher overconsolidation ratio (OCR) at those depths. The higher OCR stiffens the clay resulting in a higher  $s_u$  as seen in the lab testing result in Figure 4.6. However, the trend of lower values of  $N_{kt(FVT)}$  and  $N_{\Delta u(FVT)}$  in this overconsolidated shallow soil is opposite the trend of  $N_{kt(DSS)}$  and  $N_{\Delta u(DSS)}$ , which were greater at shallow depths. This could be explained by localized differences due to large distances of these borings from the sample borings, or the  $s_u$  measured from the FVT may be higher than the  $s_u$  measured from DSS testing due to increased strain rate, encountering a sand layer or differences in the orientation of the deviator stress which is inherent in the testing procedures.

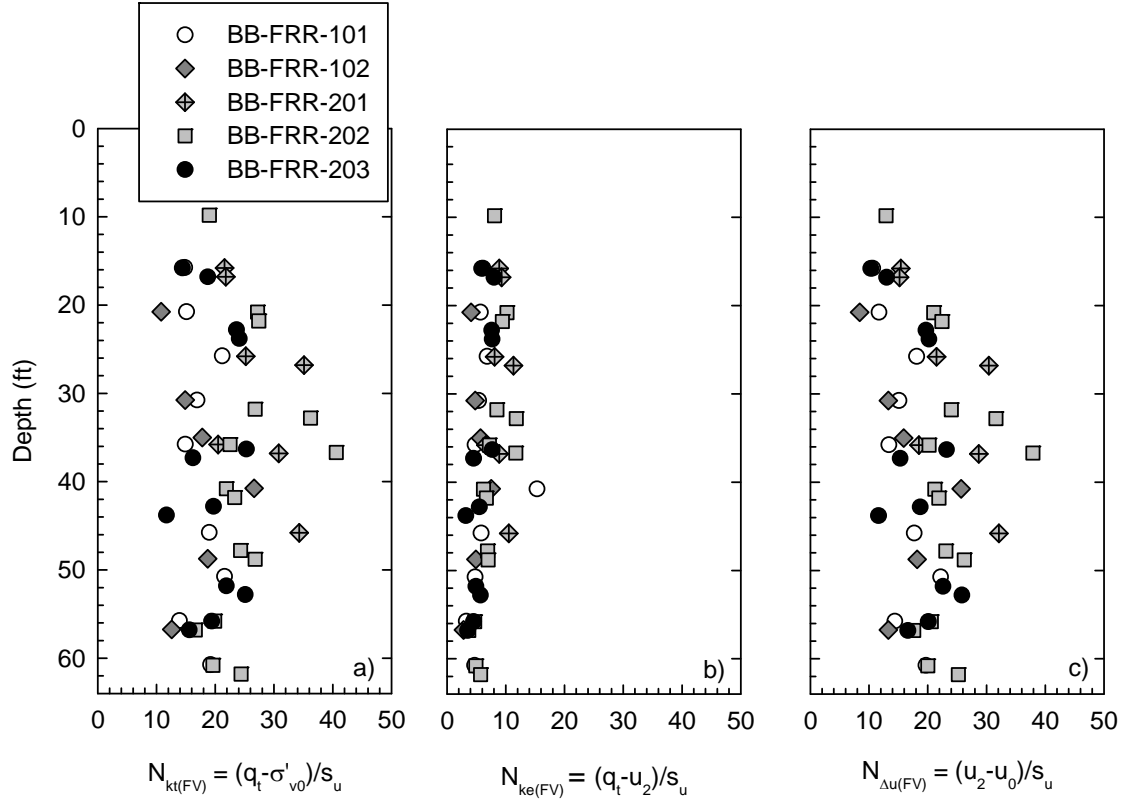


Figure 4.16: Subsurface profiles of a)  $N_{kt(FVT)}$ , b)  $N_{\Delta u(FVT)}$ , and v)  $N_{ke(FVT)}$  correlated from (S)CPTu-P301 and field vane shear testing (FVT) from borings within 200 feet of SCPTu-P301 (data from Langlais, 2011).

Table 4.9: Summary of  $N_{kt(FVT)}$  and  $N_{\Delta u(FVT)}$  values, averages, and coefficient of variations from the FVT results in the Presumpscot clay at the Route 26/100 Falmouth Bridge using SCPTu-P301 (data from Langlais, 2011).

FVT Boring	Distance from SCPTu-P301 (ft)	No. of tests	Strength Factor $N_{kt}$			Strength Factor $N_{\Delta u}$		
			Range	Average	COV	Range	Average	COV
BB-FRR-101	45	9	13.9-54.6	21.3	0.60	10.6-52.8	19.6	0.66
BB-FRR-102	155	5	10.8-26.6	17.8	0.33	8.4-25.7	16.3	0.39
BB-FRR-201	150	7	20.5-35.1	27.0	0.23	15.2-32.1	23.1	0.31
BB-FRR-202	80	12	19-36.2	25.0	0.19	12.9-31.6	22.3	0.20
BB-FRR-203	190	11	11.7-25.3	20.0	0.23	10.3-25.8	18.2	0.28

Average  $N_{kt(FVT)}$  and  $N_{\Delta u(FVT)}$  ranged from 17.8 to 27.0 and 16.3 to 23.1, respectively.

Average  $N_{kt(DSS)}$  and  $N_{\Delta u(DSS)}$  ranged from 20.9 to 24.5 and 17.4 to 21.0, respectively. The range of averages for the FVT was larger than the DSS as expected, however they were relatively similar

between testing methods. Furthermore, the maximum and minimum average  $N_{kt(FVT)}$  and  $N_{\Delta u(FVT)}$  values came from borings which included no more than seven FVT conducted in that borings, whereas the remaining borings which has increased number of FVT resulted in average values closer to the DSS averages (Table 4.9).

Below 18 feet, neither  $N_{kt(FVT)}$  nor  $N_{\Delta u(FVT)}$  provided any overall trend with depth (i.e., increasing or decreasing). Taken together, correlated values are highly variable, however less scatter occurs when isolating individual FVT borings. For both  $N_{kt(FVT)}$  and  $N_{\Delta u(FVT)}$ , BB-FRR-201 and BB-FRR-202 are consistently in the upper range of values throughout the profile, where BB-FRR-101 and BB-FRR-102 are consistently in the lower range, with BB-FRR-203 in the middle.

In summary,  $N_{\Delta u(DSS)}$  cone factor appeared to provide the best estimate of the  $s_u$  profile as compared to the laboratory data at the Route 26/100 Bridge. In particular, an average value of 21.0 followed the  $s_{u(DSS)}$  closely throughout the entire profile when applied to SCPTu-P301.  $N_{kt(DSS)}$  resulted in reasonable estimates of  $s_u$  from the surface of the deposit down to approximately 40 feet, where after  $s_u$  was under predicted when using the average  $N_{kt(FVT)}$  of 24.5. Scatter between minimum and maximum predicted  $s_u$  from  $N_{kt(DSS)}$  and  $N_{\Delta u(DSS)}$  values was larger with  $N_{kt(DSS)}$ .  $N_{kt(FVT)}$  and  $N_{\Delta u(FVT)}$  showed more scatter throughout the site than  $N_{kt(DSS)}$  and  $N_{\Delta u(DSS)}$  values, however FVT borings which included greater number of FVT increased the similarity to average  $N_{kt(DSS)}$  and  $N_{\Delta u(DSS)}$  values.

#### 4.3.5 Seismic Properties

Shear wave velocity measurements were collected at 3.28 foot depth intervals for all three CPTu soundings performed at Route 26/100 Falmouth Bridge. From these measurements, small strain modulus and rigidity index can be obtained from Equations 2.17 and 2.18. Unit weight in Equation 2.17 was assumed to be 109 pcf for all Presumpscot clay (an approximate average from the laboratory testing results) and undrained shear strength ( $s_u$ ) in Equation 2.18

was estimated using  $s_u$  estimated from a best-fit profile determined from DSS laboratory testing at the depth that  $V_s$  was measured as shown in Langlais (2011). Shear wave velocity ( $V_s$ ) was not measured in the upper 45 feet of SCPTu-P305 due to malfunctioning data collection equipment. The seismic properties are displayed with depth Figure 4.17.

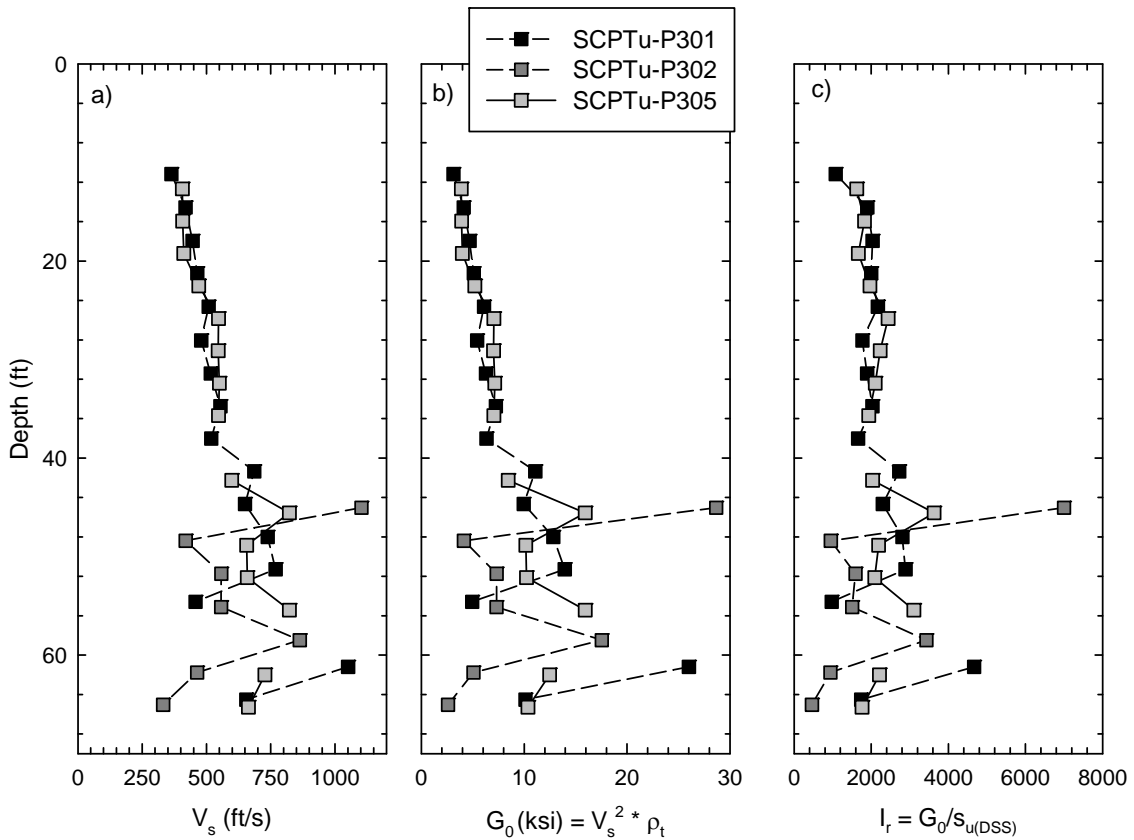


Figure 4.17: a) Shear wave velocity ( $V_s$ ), b) small-strain shear modulus ( $G_0$ ), and c) rigidity index ( $I_r$ ) determined from SCPTu-P301, -P302, and -P305 conducted in Presumpscot clay at the Route 26/100 Falmouth Bridge (data from Langlais, 2011).

Measurements of  $V_s$  were consistent between SCPTu-P301 and P302 in the upper 38 feet of the Presumpscot clay increasing linearly from 320 ft/s to 580 ft/s. Below 38 feet,  $V_s$  measurements became more variable, without an apparent trend with depth. Between 38 feet and



60 feet,  $V_s$  from all three soundings ranged from 400 ft/s to 870 ft/s with one outlier of 1,200 ft/s at a depth of 45 feet measured in SCPTu-P305 which was likely due to a silt or sand seam.

$G_o$  ranged from 3 to 8 ksi in the upper 38 feet of the deposit and ranged from 4 to 18 ksi from 38 feet to 60 feet depth, excluding the outlier of 29 ksi at 45 feet.  $I_p$  ranged from 800 to 2,400 in the upper 38 feet of the deposit and ranged from 900 to 3,600 from 38 feet to 60 feet depth, excluding the outlier of 7,400 at 45 feet.

## 5 MARTIN'S POINT BRIDGE

### 5.1 Site Overview

Martin's Point Bridge spans from the southern tip of Falmouth along Route 1 to Martin's Point in Portland, Maine. It connects Route 1 over the outlet of the Presumpscot River into the Portland Harbor. Figure 5.1 is an aerial imagine showing the location of the site.



Figure 5.1: Location of Martin's Point Bridge between Portland and Falmouth, Maine at the mouth of the Preusmpcot River and Casco Bay (Googe Earth 2013a).

The previous Martin's Point Bridge structure (Figure 5.2) was constructed in 1943. The bridge connects the city of Portland at its southern end to the Town of Falmouth at its northern end over the Presumpscot River on U.S. Route 1. The old bridge superstructure consisted of a 47-span painted steel girder system supported on timber pile bents extending to bedrock. The southern (Portland) abutment was timber pile supported while the northern end (Falmouth) sat atop bedrock. The substructure consisted entirely of timber piles. Both the superstructure and substructure received a "Poor" rating by the 2010 Maine Department of Transportation (MaineDOT) Bridge Maintenance Inspection Report (Maine DOT, 2010).



Figure 5.2: Martin's Point Bridge between Portland and Falmouth, Maine at the mouth of the Presumpscot River and Casco Bay during low tide (from MaineDOT 2013).

#### 5.1.1 Previous Geotechnical Investigations

Three geotechnical investigations were conducted at the Martin's Point Bridge site for the design of the replacement bridge. These included a preliminary geotechnical investigation in 2010 (MaineDOT, 2010), an additional preliminary geotechnical investigation conducted in 2011 (Golder Associates, 2011a), and a final supplemental geotechnical investigation in 2011 (Golder Associates, 2011b). The results of all three investigations are summarized in Golder Associates (2011b) Supplemental Geotechnical Data Report. The location of all pertinent borings, CPTu soundings, and sampling locations from the geotechnical investigations are shown in Figure 5.3.

The preliminary geotechnical investigation included 11 test borings (BB-FPPR-101 through BB-FPPR-110) taken from the old bridge deck along US Route 1 that were spaced approximately 250 ft apart. All borings were driven cased and wash drilled with solid stem auger techniques. Standard Penetration Testing (SPT; ASTM D1586) was conducted at 5-ft intervals using an automatic hammer calibrated within two months of testing. 2-in diameter split spoon

samples were collected and SPT N-values were recorded where applicable. In borings BB-FPPR-105 through BB-FPPR-110, field vane shear testing (FVT) was performed at discrete intervals throughout the Presumpscot clay to measure undrained shear strength ( $s_u$ ) and remolded undrained shear strength ( $s_{u(r)}$ ) of the clay. FVT was performed at various intervals ranging in depth spacing from 1 ft to greater than 10 ft.

A secondary geotechnical investigation was conducted east of the existing bridge along the proposed new bridge alignment. (Golder Associates Inc., 2011a). Seven additional borings (BB-FPPR-201 through -203 and BB-FPPR-205 through -208) were drilled in the tidal zone using a skid rig on a spud barge. Boring BB-FPPR-204 was eliminated from the schedule due to time constraints. Boring depths ranged from 60 ft to 134 ft below ground surface (bgs). Boring BB-FPPR-201 and -203 were advanced with an HW steel casing using the drill and wash method until refusal. The other five borings were started with HW casing driven 20 to 35 ft bgs and completed with the open hole method. All drilling mud used for the borings had unit weights between 75 and 85 pcf. Field vane shear tests were completed in accordance with ASTM D2573 using 55 x 100 mm and 65 x 130 mm vanes (specified in boring logs). Three inch diameter undisturbed modified Shelby tube samples for laboratory testing were collected using a hydraulic Gregory Undisturbed Sampler (GUS) in accordance with ASTM D6519.

The final supplemental geotechnical investigation including 15 borings (BB-FPPR-301 through BB-FPPR-316) was completed in 2011 (Golder Associates Inc., 2011b). In addition, a sixteenth boring (BB-FPPR-317) was drilled to collect 3 inch diameter, modified Shelby tube samples throughout the Presumpscot clay to test for this research. Three barge-mounted rigs were used for over-water borings and a track-mounted rig was used for the land borings. Two of the barges were spud barges with CME 45 drill rigs and the third was a jack-up barge with a Dietrich D-50 drill rig. The track-mounted barge used a Mobile B-53 drill rig. Borings ranged in depth from 13 to 145 ft bgs using wash boring methods. The borings were started with HW casing

driven 20 to 35 ft bgs, continued using open hole to the Lower Marine Sand Layer, and completed using NW casing and drive and wash methods until refusal. Drilling mud used for the borings had unit weights between 75 and 85 pcf except for borings BB-FPPR-303, -304, and -305, where water alone was used. Field vane shear tests were completed in general accordance with ASTM D2573 using 16 x 32 mm, 55 x 100 mm and 65 x 130 mm vanes (specified in boring logs) at five ft intervals where cohesive material was discovered. Undisturbed samples for laboratory testing were collected using a hydraulic GUS in accordance with ASTM D6519 as outlined in Section 3.3.1. As part of this final geotechnical investigation, four cone penetration tests (CPT) were performed by ConeTec (ConeTec 2011) for use by the design build teams for both the bridge design and this research. Figure 5.3 presents the locations of the borings and CPTu soundings performed at Martin's Point Bridge. SCPTu 101, 103, and 104 were performed approximately 32 ft, 692 ft, and 205 ft away from Boring BB-FPPR-317, respectively.



Figure 5.3: Aerial view of boring and CPTu locations along the a) entire length of the bridge b) Falmouth side bridge approach for the newly constructed Martin's Point Bridge (Google Earth, 2015).

The borings shown in Figure 5.3 only include those in which FVT was performed in the Presumpscot clay (seen as the small white circles) as well as boring BB-FPPR-317 which included the collected tube samples of Presumpscot clay tested at the University of Maine for this research (seen at the white square). Locations of the four CPTu soundings are shown as the large white circles. CPTu-102 is excluded from this research since Presumpscot clay was not present at that location. Figure 5.3b is an enlarged view for clarity of the Falmouth side of the bridge approach where a cluster of testing was performed.

### 5.1.2 Site Geology

The general stratification of the site consists of organic silt overlying soft marine clay (Presumpscot clay), overlying glacial outwash sand, overlying bedrock. Depths of each layer vary along the bridge alignment. The southern (Portland) end of the site contains thick deposits of the organic silt layer with little to no Presumpscot clay, whereas the northern (Falmouth) end of the site has little to no organic silt and a thick deposit of Presumpscot clay (Figure 5.4). Figure 5.5 is an aerial photograph illustrating the distinct boundary between the two deposits at the site. The absence of the Presumpscot clay at the southern end of the site is due to Presumpscot River washing away the clay material since its deposition. Bedrock elevation is approximately 120 ft below mean sea level (MSL) at the northern end of the site and 21 ft above MSL at the southern end. Figure 5.4 is an interpreted profile of the soil subsurface along the new bridge alignment. Since the focus of this study is to characterize the Presumpscot clay, field vane testing, sampling, and CPTu soundings were focused on the northern end of the site where the Presumpscot deposit is present.

## 5.2 Laboratory Characterization

Thirteen modified Shelby tube samples of Presumpscot clay were collected from Boring BB-FPPR-317 at the Martin's Point Bridge site for testing at the UMaine Advanced Geotechnics Laboratory. Shelby tube samples were modified to improve sample quality, see Section 3.3.1 for

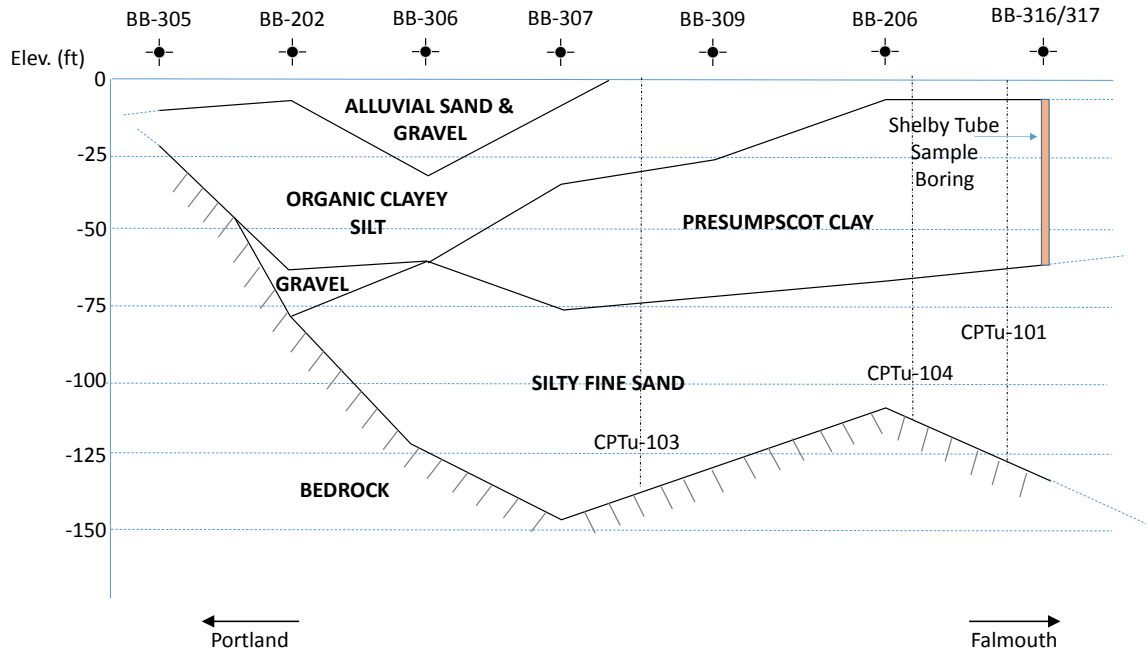


Figure 5.4: Interpreted subsurface profile from borings (Figure 5.3) conducted along the new Martin's Point Bridge alignment.



Figure 5.5: Aerial photograph of the Martin's Point Bridge site illustrating the effect of the Presumpscot River on the subsurface material (Google Earth, 2014).

more details. Samples were collected from depths 7.0 ft to 45.9 ft at 2 to 3 ft intervals. Samples of Presumpscot clay from each tube were tested for index properties (moisture content, Atterberg Limits, hydrometer, organics, specific gravity, and fall cone index undrained strength (index  $s_u$ )), consolidation properties, and undrained shear strength properties. All testing methods were in accordance with ASTM standards and are outlined in Chapter 3. Figure 5.6 and Figure 5.7 illustrate the portion of each tube sample used for testing.

### 5.2.1 Index Test Results

Figure 5.8 illustrates the depth trends of natural water content, Atterberg limits, grain size distribution, index  $s_u$ , and sensitivity measured using the fall cone apparatus, organic content, and unit weight (total, dry, and solids) of Presumpscot clay from Boring BB-FPPR-317. Natural water content, Atterberg Limits (liquid limit, LL, plastic limit, PL, plasticity index, PI, and liquidity index, LI), and Activity (the ratio of plasticity index to the % grain size finer than 0.002 mm) values are summarized in Table 5.1. Grain size, organic content, total, dry, and solids unit weights, and Unified Soil Classification System (USCS) designations are tabulated in Table 5.2.

Table 5.1: Summary of Atterberg Limits and plasticity data for Presumpscot clay collected from Boring BB-FPPR-317 at the Martin's Point Bridge site.

Sample	Depth (ft)	$w_n$ (%)	LL	PL	PI	LI	Activity
1U	8.9	37.3	38	22	16	0.97	0.35
2U	11.4	42.7	41	24	17	1.13	0.34
3U	16.9	44.1	47	25	21	0.89	0.37
4U	18.9	39.5	43	24	19	0.80	0.41
5U	20.8	38.5	45	26	18	0.66	0.33
6U	24.5	41.5	44	24	19	0.88	0.33
7U	27.3	38.7	40	21	19	0.92	0.43
8U	30.5	37.8	41	23	18	0.83	0.35
9U	34.3	39.9	44	24	20	0.78	0.36
10U	37.4	38.9	43	25	18	0.79	0.32
11U	40.7	31.6	34	20	14	0.84	0.38
12U	43.5	31.1	25	17	8	1.72	0.23
13U	45.8	23.4	24	17	7	0.90	0.30



	1U 22"	2U 24"	3U 24"	4U 23"	5U 16"	6U 24"
Shelby Tube = 24" of Soil						
		3.5" CAUC TX 18				
			3.5" CAUC TX 20			
				3.5" CAUC TX 21	3.5" CAUC TX 14	
	3.5" CAUC TX 7	2.5" CRS 57				3.5" CAUC TX 3
	2.5" CRS 54		2" CRS 49	2" CRS 50	2" CRS 55	2" CRS 47
	3" Index Testing	3" Index Testing	3" Index Testing	3" Index Testing	3" Index Testing	3" Index Testing

Figure 5.6 Laboratory test specimen use for BB-FPPR-317 3 in. Shelby tubes 1U - 6U from the Martin's Point Bridge site.

	7U 22"	8U 23"	9U 21"	10U 13"	11U 22"	12U 24"	13U 21"
Shelby Tube = 24" of Soil							
		3.25" SHANSEP TX 37					
	3.5" CAUC TX 22	3.25" SHANSEP TX 36					
	2" CRS 76	3.5" CAUC TX 23				3.5" CAUC TX 17	
	2.5" DS 11				2" CRS 88		
				2" CRS 56			
		2" CRS 46	3.5" CAUC TX 15	3.5" CAUC TX 16	3.5" CAUC TX 5		3.5" CAUC TX 6
	4" Index Testing	2" CRS 45	2" CRS 52	2" CRS 53	2" CRS 51	2" CRS 48	2" CRS 53
	3" Index Testing	3" Index Testing	3" Index Testing	3" Index Testing	3" Index Testing	3" Index Testing	

Figure 5.7: Laboratory test specimen use for BB-FPPR-317 3 in. Shelby tubes 7U - 13U from the Martin's Point Bridge site.

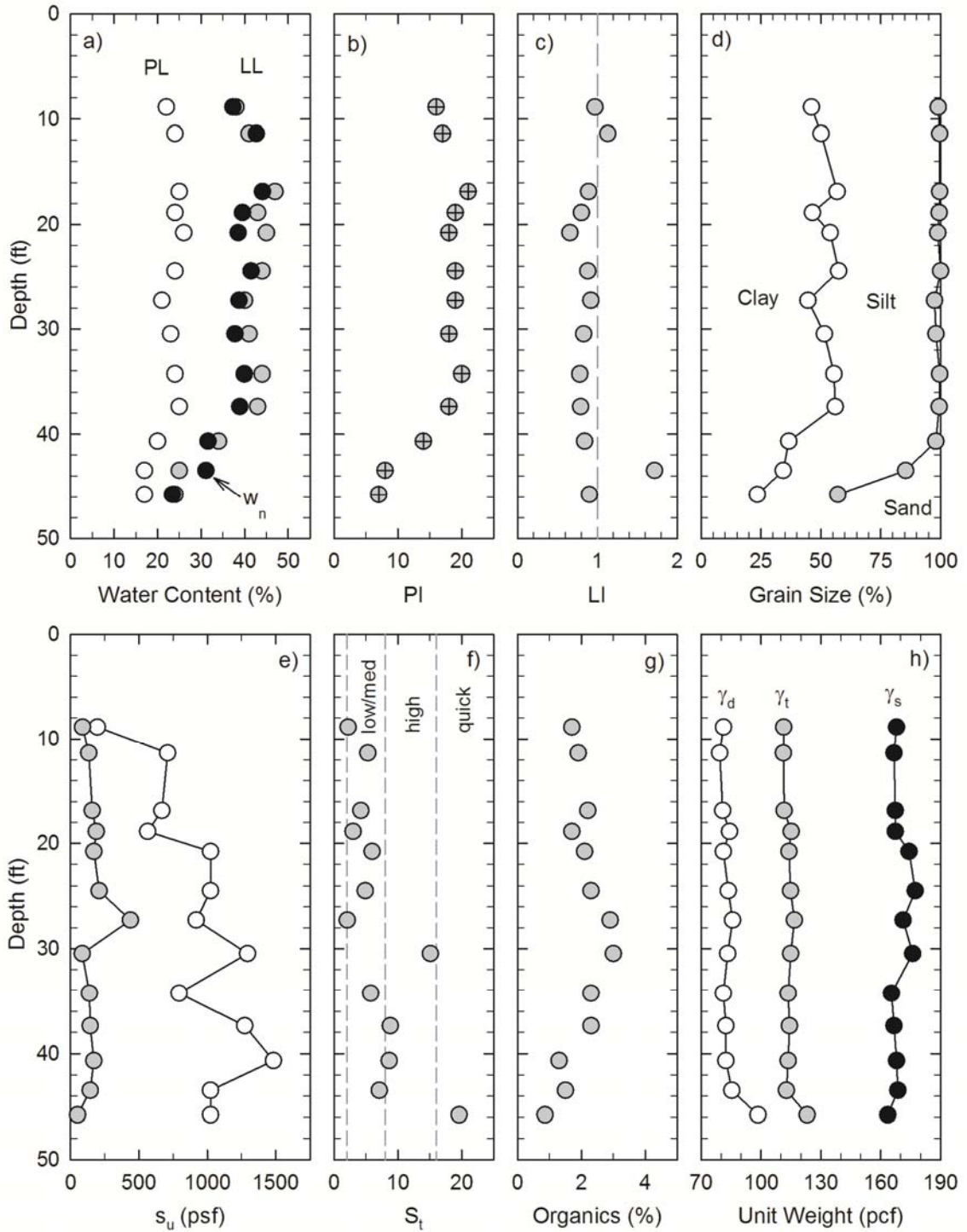


Figure 5.8: Laboratory determined results of a) Atterberg limits and natural water content, b) plasticity index, c) liquidity index, d) grain size distribution, e) index ( $s_u$ ) and remolded undrained shear strength ( $s_{u(r)}$ ) from the fall cone, f) sensitivity from the fall cone, g) organic content, and h) unit weight (total, dry, solids) of Presumpscot clay collected from the Martin's Point Bridge site.

Table 5.2: Summary of grain size distribution, density, and USCS classification for Presumpscot clay collected from Boring BB-FPPR-317 at the Martin's Point Bridge site.

Sample	Depth (ft)	Sand (%)	Fines (%)	Silt (%)	Clay (%)	Organics (%)	$\gamma_t$ (pcf)	$\gamma_d$ (pcf)	$\gamma_s$ (pcf)	USCS
1U	8.9	1.1	99.0	52.9	46.1	1.7	111	81.2	167.9	Lean Clay (CL)
2U	11.4	0.4	99.6	49.5	50.1	1.9	111	79.3	166.7	Lean Clay (CL)
3U	16.9	0.4	99.6	42.8	56.8	2.2	112	80.9	167.3	Lean Clay (CL)
4U	18.9	0.6	99.4	52.9	46.5	1.7	115	84.3	167.3	Lean Clay (CL)
5U	20.8	1.2	98.8	44.9	53.9	2.1	114	81.2	174.2	Lean Clay (CL)
6U	24.5	0.0	100.0	42.5	57.5	2.3	115	83.7	177.3	Lean Clay (CL)
7U	27.3	2.5	97.5	52.9	44.6	2.9	117	85.8	171.3	Lean Clay (CL)
8U	30.5	1.9	98.1	46.6	51.5	3.0	115	83.3	176.1	Lean Clay (CL)
9U	34.3	0.4	99.6	44.1	55.5	2.3	114	81.2	165.4	Lean Clay (CL)
10U	37.4	0.6	99.4	43.4	56.0	2.3	114	82.4	166.7	Lean Clay (CL)
11U	40.7	2.0	98.0	61.4	36.6	1.3	114	82.4	167.9	Lean Clay (CL)
12U	43.5	14.7	85.4	51.1	34.3	1.5	113	85.4	168.6	Lean Clay w/
13U	45.8	42.9	57.1	33.6	23.5	0.9	123	98.5	163.6	Fine Sandy Silty

Grain size data show that the Presumpscot clay at the Martin's Point Bridge site consists of approximately 0.4% to 2.5% sand, 42% to 61% silt, and 37% to 58% clay in the upper 41 ft of the profile. Sand content increases between 41 and 46 ft depth from 15% to 43% and decreases in both silt and clay content occur. This is consistent with the observed transition into the underlying marine sand layer from the boring logs and CPTu soundings. Throughout the profile, the organic content ranges from 1% to 3%. The soil is classified using USCS (Figure 5.9a) as either low plasticity (i.e., lean) clay (CL) and low plasticity silty clay (CL-ML) based on Atterberg Limits and grain size. Table 5.1, Table 5.2 and Figure 5.8 present the ranges of total and dry unit weight and unit weight of solids for the Presumpscot clay profile at the site. Total unit weight,  $\gamma_t$ , ranges from 111 to 123 pcf.

Plasticity data indicate similar soils between 11 and 40 ft, where liquid limit (LL) ranges between 40 and 47, plastic limit (PL) between 21 and 26, plasticity index (PI) between 17 to 21, and liquidity index (LI) between 0.66 to 0.92 (with extremes at 20.8 and 27.3 ft). Between 40 and

46 ft, LL decreases with depth (from 34 to 24), PL decreases from 20 to 17, PI decreases from 14 to 7, and LI varies between 0.84 and 1.72. Increasing sand composition influences these results.

Index  $s_u$  values for the intact and remolded soil and strength sensitivity determined using the fall cone apparatus are illustrated in Figure 5.8 and Table 5.3. Intact undrained shear strength,  $s_u$ , generally increases with depth without a clear trend and ranges from 196 psf to 1,483 psf. Soil remolded at the natural water content ( $s_{u(r)}$ ) showed no depth increase trends in  $s_u$ , where values range from 52 psf to 439 psf. The resulting sensitivity of the soil (where sensitivity,  $S_s$ , is the ratio of the intact to remolded  $s_u$ ) ranges from 2 to 9 over most of the profile, with outliers of 15.1 and 19.6 at depths 30.5 and 45.8 ft, respectively. Soils having sensitivity between 2 and 8 are considered low to medium sensitivity, 8 to 16 are highly sensitive, and greater than 16 are quick clays (Holtz *et al.*, 2011; Table 2.1).

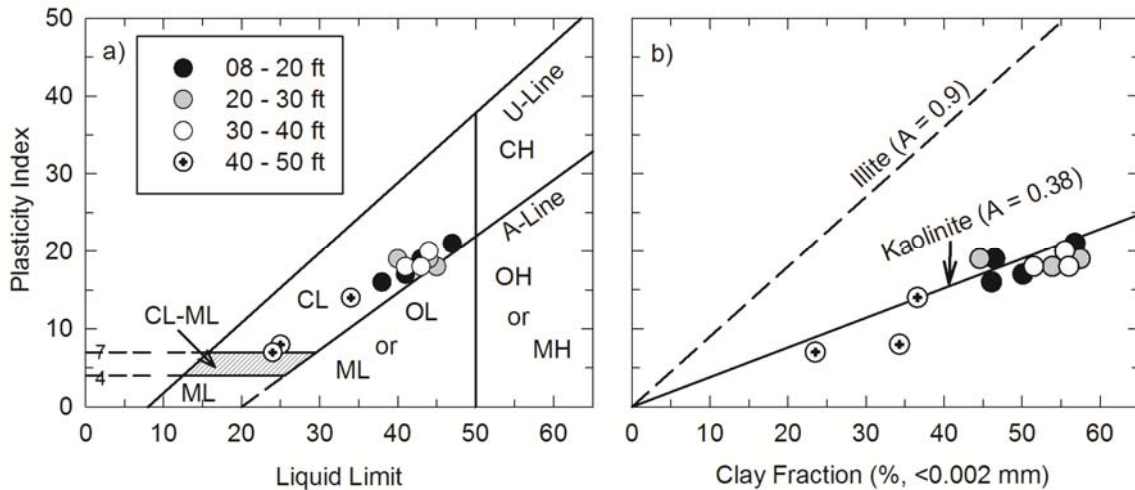


Figure 5.9: USCS Classification Charts using Atterberg Limits for Presumpscot clay collected from Boring BB-FPPR-317 at the Martin's Point Bridge site.

Table 5.3: Summary of fall cone undrained shear strength and sensitivity for Presumpscot clay collected from Boring BB-FPPR-317 at the Martin's Point Bridge site.

Sample	Depth (ft)	$\sigma'_{v0}$ (psf)	Intact $s_u$ <sup>1</sup> (psf)	$s_u/\sigma'_{v0}$ (-)	Intact Cone	$s_{u(r)}$ <sup>2</sup> (psf)	$s_{u(r)}/\sigma'_{v0}$ (-)	Remolded Cone	$S_t$ <sup>3</sup>
1U	8.9	432.3	196	0.45	100g 30°	88	0.20	60g 60°	2.2
2U	11.4	554.1	710	1.28	400g 30°	134	0.24	100g 30°	5.3
3U	16.9	822.0	668	0.81	400g 30°	159	0.19	100g 30°	4.2
4U	18.9	926.2	564	0.61	400g 30°	188	0.20	100g 30°	3.0
5U	20.8	1025.9	1023	1.00	400g 30°	171	0.17	100g 30°	6.0
6U	24.5	1219.9	1023	0.84	400g 30°	209	0.17	100g 30°	4.9
7U	27.3	1366.8	919	0.67	400g 30°	439	0.32	100g 30°	2.1
8U	30.5	1534.7	1295	0.84	100g 30°	86	0.06	60g 60°	15.1
9U	34.3	1734.0	794	0.46	400g 30°	138	0.08	100g 30°	5.8
10U	37.4	1896.6	1274	0.67	400g 30°	144	0.08	100g 30°	8.8
11U	40.7	2082.0	1483	0.71	400g 30°	171	0.08	100g 30°	8.7
12U	43.5	2249.8	1023	0.45	400g 30°	144	0.06	100g 30°	7.1
13U	45.8	2387.7	1023	0.43	400g 30°	52	0.02	60g 60°	19.6

Note: <sup>1</sup>intact undrained shear strength; <sup>2</sup>remolded; <sup>3</sup>Sensitivity ( $s_u/s_{ur}$ )

### 5.2.2 One Dimensional Consolidation Results

Constant rate of strain (CRS) consolidation testing was performed on specimens from each of the 13 Presumpscot clay samples at Martin's Point Bride in accordance with the procedures outlined in Section 3.3.1. Seven Specimens were of very good to excellent quality, two specimens were of good to fair quality, and four were of poor quality. Table 5.4 presents the specimen information, change in void ratio upon recompression for sample quality designation, and results of the consolidation testing including preconsolidation pressure (determined using the Becker *et al.*, 1987 method), overconsolidation ratio (OCR), and coefficients of consolidation. Preconsolidation pressure ( $\sigma'_p$ ), initial void ratio ( $e_0$ ), and sample quality designation are illustrated with depth in Figure 5.10.

Table 5.4: Constant Rate of Strain (CRS) consolidation specimen properties and results for Presumpscot clay collected from Boring BB-FPPR-317 at the Martin's Point Bridge site.

Sample	Specimen Information					<sup>1</sup> Sample Quality		Strain	Consolidation Properties				
	Depth (-) (ft)	$\sigma'_{v0}$ (psf)	$w_n$ (%)	$e_0$ (-)	$\rho_t$ (pcf)	$\Delta e/e_0$ at $\sigma'_{v0}$	NGI Rating	Rate (%)	<sup>2</sup> $\sigma'_p$ (psf)	$c_v$ @ $\sigma'_{v0}$ (ft <sup>2</sup> /yr)	OCR (-)	$C_r$ (-)	$C_c$ (-)
1U	8.5	414	37.1	1.06	111	0.011	VG/E	2.0	4290	27.1	10.4	0.04	0.41
2U	11.0	536	40.5	1.10	111	0.012	VG/E	2.0	3660	8.8	6.8	0.06	0.37
3U	16.7	812	42.0	1.12	112	0.044	G/F	1.9	5020	25.3	6.2	0.05	0.41
4U	18.7	915	36.6	0.98	115	0.024	VG/E	1.9	5020	15.4	5.5	0.05	0.37
5U	20.6	1015	40.4	1.14	114	0.024	VG/E	1.9	5540	22.2	5.5	0.05	0.42
6U	24.0	1195	37.2	1.11	115	0.094	P	1.9	6580	17.8	5.5	0.05	0.43
7U	27.0	1352	36.1	0.97	115	0.025	VG/E	2.0	6270	20.3	4.6	0.04	0.40
8U	30.4	1528	38.0	1.11	115	0.069	P	2.0	7210	18.8	4.7	0.09	0.47
9U	34.1	1725	39.8	1.03	114	0.027	VG/E	1.9	8250	22.2	4.8	0.05	0.45
10U	36.4	1845	38.8	1.02	114	0.025	VG/E	2.0	8990	17.6	4.9	0.05	0.46
11U	40.0	2042	38.3	1.04	114	0.049	G/F	2.0	8210	26.1	4.0	0.08	0.44
12U	43.3	2239	32.1	0.97	113	0.054	P	2.0	9190	27.1	4.1	0.07	0.43
13U	45.6	2375	25.0	0.66	123	0.080	P	1.9	7420	56.4	3.1	0.06	0.23

<sup>1</sup>From Lunne et al. (2006), where VG/E: very good to excellent quality, G/F: good to fair, P: poor; <sup>2</sup>Using the Strain Energy Method of Becker et al., (1987)

$\sigma'_p$  of the Presumpscot clay at Martins Point Bridge ranges from 3,660 psf at 11 ft depth to 8,990 psf at 43.3 ft depth, displaying a general linear increase with depth from 8.5 ft to 36.4 ft. There is an initial decrease in  $\sigma'_p$  at shallow depths indicating high overconsolidation in the upper deposit (shallower than 11 feet). The linear increase with depth is consistent with an increased overburden stress as overlying material increases with depth. The deepest three samples tested, which are of comparatively lower quality and clay content, illustrate more rounded compression curves (i.e., effective stress vs. strain) and thus lower  $\sigma'_p$ . OCR ( $\sigma'_p/\sigma'_{v0}$ ) ranges from 10.4 at 8.5 ft to 3.1 at 45.6 ft. A decrease in OCR from 6.8 to 5.5 is observed between 11 and 24 ft. Between 24 and 36 ft, OCR is nearly constant, which is likely the result of stress history, but could also be related to decreases in sample quality and clay content.

Coefficient of consolidation at  $\sigma'_{v0}$  ranges from 9 ft<sup>2</sup>/year to 27 ft<sup>2</sup>/year with the exception of the deepest specimen, which had a high value of 56.4 ft<sup>2</sup>/year. This is due to the more abundant drainage paths from the increasing sand content. Recompression index ( $C_r$ ) and virgin

compression index ( $C_c$ ) ranged from 0.04 to 0.09 and 0.23 to 0.47, respectively. In general,  $C_r$  values are assumed to be approximately 10% of the  $C_c$  values which appears to overestimate  $C_r$  at the Martin's Point Bridge site. Andrews (1987) presents a typical range of values for  $C_c$  of Presumpscot clay in Portland to range from 0.40 to 0.60.  $C_c$  values from Martin's Point Bridge are in the lower portion of this range and even fall below the minimum of 0.40, indicating that the Presumpscot clay at the site is less compressible than other Portland deposits in the virgin compression stress range.

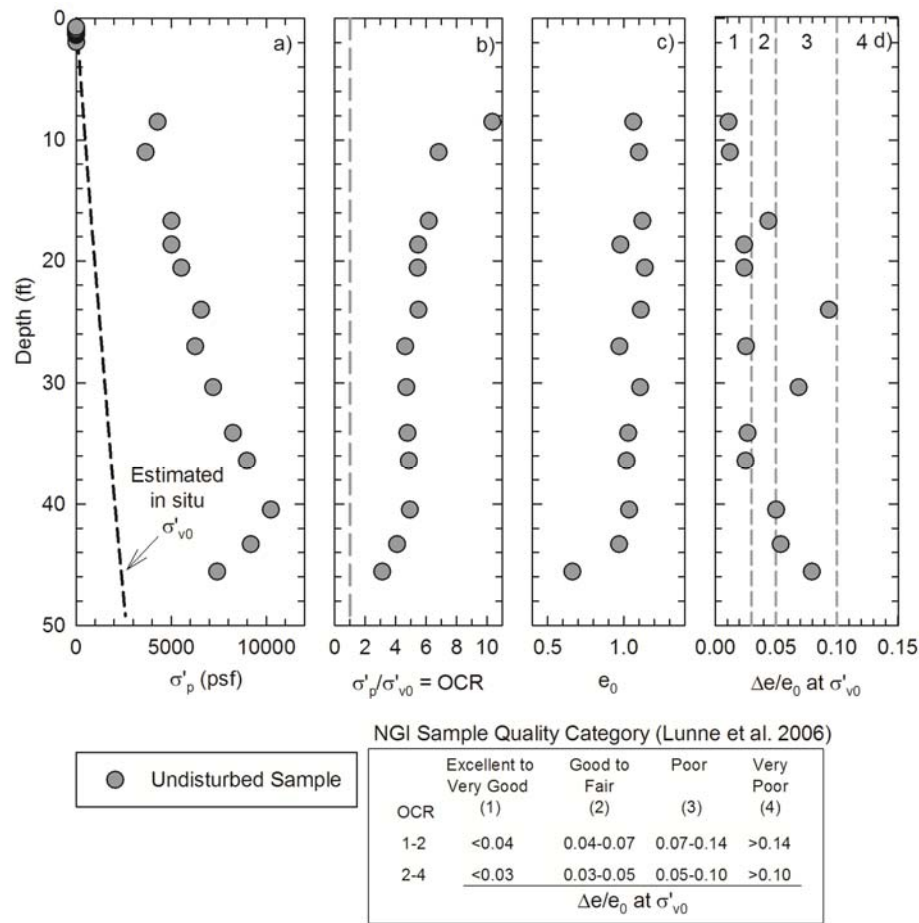


Figure 5.10: Subsurface profiles of a)  $\sigma'_p$ , b) OCR, c) initial void ratio, d) sample quality assessment from CRS consolidation testing for Presumpscot clay collected from Boring BB-FPPR-317 at the Martin's Point Bridge site.

Void ratio ( $e$ ) remained relatively constant from 0.97 to 1.12 without a trend with depth. The sample collected at the bottom of the deposit had an  $e$  of 0.66 due to the increased sand content.

### 5.2.3 Recompression Undrained Triaxial Shear

Recompression consolidated undrained triaxial shear testing was performed on specimens from each of the 13 Presumpscot clay samples at the Martin's Point Bridge site in accordance with the procedures outlined in Section 3.4.4. Table 5.5 presents specimen properties, conditions following recompression to the estimated  $\sigma'_{v0}$ , sample quality, and pre-shear parameters for the triaxial specimens. Table 5.6 presents results from the shear phase of the triaxial tests, including peak shear stress, strain at failure, pore pressure at failure, and undrained shear strength normalized to vertical effective stress (note:  $s_u = q_f =$  undrained shear strength). Specimens were mainly of very good to excellent quality (10 total) with the exception of one specimen each having good to fair quality, poor quality specimens, and very poor quality.

Undrained shear strength ( $s_u = q_f$ ) ranged from 661 psf at 10.2 ft depth to 1,557 psf at 42.5 ft depth.  $s_u$  normalized by the preshear vertical consolidation stress ( $\sigma'_{vc}$ ) ranges from 1.59 to 0.52 while  $s_u/\sigma'_{v0}$  ranges from 1.83 to 0.57. Normalized  $s_u$  typically ranges from 0.2 to 0.3 for normally consolidated clays and increases with OCR, as expressed in Equation 2.1. The difference in  $\sigma'_{vc}$  values and  $\sigma'_{v0}$  is due to limitations of the test procedure. The effect of the  $\sigma'_{vc} \neq \sigma'_{v0}$  condition on measured  $s_u$  is discussed in Section 3.4.4. In summary, the effect of the different  $\sigma'_{v0}$  is not quantifiable; however, the  $\sigma'_{vc} > \sigma'_{v0}$  condition likely results in a lower measured  $s_u$  value than in situ conditions due to destructuring of the clay specimen, where  $\sigma'_{vc} < \sigma'_{v0}$  condition results in a higher  $s_u$ . Table 5.6 shows that all but three specimens were consolidated to approximately  $\sigma'_{vc} < \sigma'_{v0}$  or  $\sigma'_{vc} = \sigma'_{v0}$  conditions.



Table 5.5: Summary of recompression consolidated undrained triaxial shear specimen and consolidation properties for Presumpscot clay collected from Boring BB-FPPR-317 at the Martin's Point Bridge site.

In Situ							Laboratory Stress History									
Sample	Depth (ft)	$w_n$ (%)	$e_0$ (-)	$\sigma'_{v0}$ (psf)	$\sigma'_p$ <sup>1</sup> (psf)	OCR	In situ		$\sigma'_{vc}$ (psf)	$\sigma'_{hc}$ (psf)	$K_c$ <sup>3</sup> (-)	OCR <sub>c</sub> <sup>4</sup> (-)	$e_c$ (-)	$\epsilon_{vol}$ at		<sup>5</sup> NGI Qual. (-)
							$K_0$ <sup>2</sup> (-)	$\Delta e/e_0$ (-)						$\sigma'_{v0}$ (%)	$\Delta e/e_0$ (-)	
1U	8.5	36.0	1.03	416	4290	10.4	1.55	550	375	0.68	8.0	1.03	0.15	0.003	VG/E	
2U	10.2	39.8	1.08	497	3660	6.8	1.25	416	403	0.97	9.3	1.08	0.10	0.002	VG/E	
3U	15.9	38.8	1.02	773	5020	6.2	1.16	780	769	0.98	6.2	1.01	0.49	0.010	VG/E	
4U	18.4	35.3	0.96	890	5020	5.5	1.14	754	640	0.85	6.9	0.95	0.52	0.010	VG/E	
5U	20.0	40.1	1.19	988	5540	5.5	1.12	1043	961	0.92	5.5	1.17	0.87	0.016	VG/E	
6U	23.9	38.5	1.18	1187	6580	5.5	1.10	911	893	0.98	7.2	1.16	1.27	0.023	VG/E	
7U	26.7	36.3	1.00	1306	6270	4.6	1.08	1169	1055	0.90	6.2	0.98	0.97	0.019	VG/E	
8U	30.0	41.6	1.24	1497	7210	4.7	1.07	1537	1478	0.96	5.2	1.20	1.42	0.026	VG/E	
9U	34.0	39.9	1.05	1719	8250	4.8	1.06	1457	1424	0.98	6.0	1.03	0.65	0.013	VG/E	
10U	37.0	38.6	1.03	1876	8990	4.9	1.05	1908	1775	0.93	4.9	1.00	1.21	0.024	VG/E	
11U	40.2	36.4	0.91	2055	8210	4.0	1.03	2009	1985	0.99	5.2	0.86	3.01	0.063	P	
12U	42.5	31.6	0.81	2189	9190	4.1	0.97	2080	1613	0.78	4.6	0.78	1.49	0.033	G/F	
13U	45.3	23.8	0.66	2358	7420	3.1	0.86	2525	1876	0.74	3.3	0.59	4.05	0.102	VP	

Notes: <sup>1</sup>From the best fit profile; <sup>2</sup> $K_0(OC) = 0.46(OCR)^{0.52}$  based on CAUC NC  $\phi'$  and estimated parameters; <sup>3</sup> $K_c = \sigma'_{hc}/\sigma'_{vc}$ ; <sup>4</sup>OCR<sub>c</sub> =  $\sigma'_p/\sigma'_{vc}$ ; <sup>5</sup>From Lunne et al. (2006), where VG/E: very good to excellent quality, G/F: good to fair, P: poor, VP: very poor.

Table 5.6: Summary of recompression consolidated undrained triaxial shear results for Presumpscot clay collected from Boring BB-FPPR-317 at Martin's Point Bridge.

In Situ		Laboratory Stress History							At Failure						
Sample	Depth (ft)	$\sigma'_{vc}$ (psf)	$\sigma'_{hc}$ (psf)	OCR <sub>c</sub> <sup>4</sup> (-)	$\epsilon_{vol}$ at		$\epsilon_a$ at		<sup>5</sup> NGI Qual. (-)	$q_f$ (psf)	$\epsilon_{a-f}$ (%)	$\Delta u_f$ (psf)	$q_f/\sigma'_{vc}$ (-)	$p_f/\sigma'_{vc}$ (-)	$q_f/\sigma'_{v0}$ (-)
					$\sigma'_{v0}$ (%)	$\sigma'_{v0}$ (%)	$\Delta e/e_0$ (-)	$q_f$ (psf)							
1U	8.5	550	375	8.0	0.15	0.08	0.003	VG/E	757	2.3	-5	1.38	2.00	1.83	
2U	10.2	416	403	9.3	0.10	0.06	0.002	VG/E	661	3.6	0	1.59	2.46	1.34	
3U	15.9	780	769	6.2	0.49	0.26	0.010	VG/E	941	3.0	369	1.21	1.91	1.22	
4U	18.4	754	640	6.9	0.52	0.25	0.010	VG/E	850	5.5	117	1.13	1.90	0.96	
5U	20.0	1043	961	5.5	0.87	0.38	0.016	VG/E	900	3.3	255	0.86	1.54	0.92	
6U	23.9	911	893	7.2	1.27	0.003	0.023	VG/E	1274	2.1	495	1.40	1.92	1.08	
7U	26.7	1169	1055	6.2	0.97	0.41	0.019	VG/E	1013	3.4	420	0.87	1.47	0.78	
8U	30.0	1537	1478	5.2	1.42	0.64	0.026	VG/E	1067	2.6	788	0.69	1.17	0.72	
9U	34.0	1457	1424	6.0	0.65	0.65	0.013	VG/E	1194	1.8	631	0.82	1.35	0.70	
10U	37.0	1908	1775	4.9	1.21	0.72	0.024	VG/E	1377	2.2	744	0.72	1.24	0.74	
11U	40.2	2009	1985	5.2	3.01	0.90	0.063	P	1549	2.2	1001	0.77	1.16	0.76	
12U	42.5	2080	1613	4.6	1.49	0.97	0.033	G/F	1557	4.2	490	0.75	1.28	0.72	
13U	45.3	2525	1876	3.3	4.05	4.95	0.102	VP	1322	4.1	1018	0.52	0.81	0.57	

Notes: <sup>1</sup>From the best fit profile; <sup>2</sup> $K_0(OC) = 0.46(OCR)^{0.52}$  based on CAUC NC  $\phi'$  and estimated parameters; <sup>3</sup> $K_c = \sigma'_{hc}/\sigma'_{vc}$ ; <sup>4</sup>OCR<sub>c</sub> =  $\sigma'_p/\sigma'_{vc}$ ; <sup>5</sup>From Lunne et al. (2006), where VG/E: very good to excellent quality, G/F: good to fair, P: poor, VP: very poor.

*In situ*  $K_0$  was estimated using Equation 3.7 and a  $\phi'$  of  $32^\circ$ .  $K_c$ , the lateral earth pressure coefficient during the recompression phase of the CAUC test, ranged from 4% to 78% difference between the estimated *in situ* values, generally decreasing with depth. Figure 5.11 illustrates  $s_u$  from intact and remolded *in situ* field vane shear tests (FVT) from twelve other borings at the Martin's Point Bridge site, fall cone tests conducted on tube sample ends from BB-FPPR-317, and CAUC  $s_u$  from Table 5.6. The gray dotted line shown in Figure 5.11a is the approximated *in situ*  $s_u$  profile. These data indicate the variability of the  $s_u$  across the site and with depth, as well as variability inherent in measurement tools and states (e.g., field vane shear and triaxial tests were near *in situ* effective stresses, fall cone tests were at the residual effective stress state (zero total stress)) and FVT were conducted on soil from other locations/depths different than BB-FPPR-317.

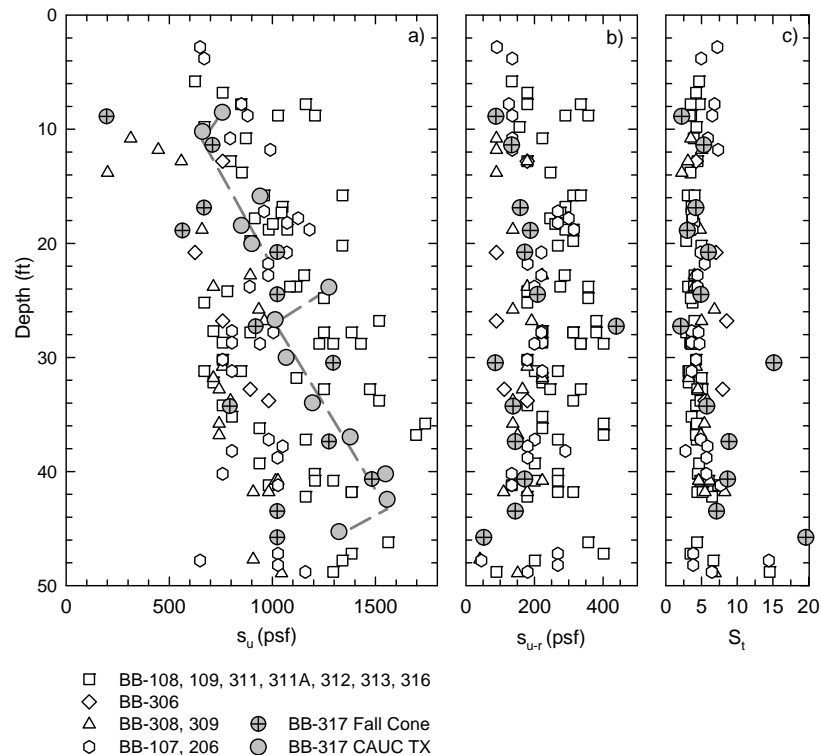


Figure 5.11: Subsurface profile of a) undrained shear strength ( $s_u$ ), b) remolded undrained shear strength and c) and sensitivity from laboratory testing on undisturbed samples (BB-317) and field vane shear testing (other borings) at the Martin's Point Bridge site.

Review of Figure 5.11 illustrates that, in general,  $s_u$  from the fall cone tests is less than the  $s_u$  from the CAUC tests throughout the profile and FVT  $s_u$  is more scattered than the other two methods. The under prediction of  $s_u$  from the fall cone may be a result of sample disturbance (the test is performed on the bottom of the recovered Shelby tube) and also from the fact that there is no confining stress on the sample. FVT  $s_u$  yielded greater scatter likely because the testing was performed at multiple locations throughout the deposit, hence clay in varying stress states was encompassed in the test results. FVT from Boring BB-FPPR-316 was closest to the collected laboratory samples. Remolded  $s_u$  ( $s_{u(r)}$ ) values are higher for the FVT than the fall cone test, however, the same is true for  $s_u$ , therefore the sensitivity ( $S_s; s_u/s_{u(r)}$ ) is similar for both testing procedures.

Review of test data and normalized stress paths from the recompression triaxial tests (illustrated in Figure 5.12) indicated that the highly overconsolidated specimens generated negative or no pore water pressures during undrained shear. Lower overconsolidation ratio specimens produced consistently greater positive pore pressures during undrained shear. It is interesting to note that normalized effective stress paths illustrated in Figure 5.12 increase to the left and overshoot the failure line with slope  $\psi'$  before looping downward to the failure line ( $\psi'$ ). This is consistent with overconsolidated and structured soils presented in the literature that experience rapid shifts in pore pressure from low to negative values prior to shear (Lambe and Whitman, 1967; Holtz *et al.*, 2011). The  $\psi'$  failure angle ranges from 28.2° to 34.7° for the Presumpscot at the test site assuming a zero  $q = s_u$  intercept (i.e.,  $a = 0$ ). Equation 5.1 can be used to convert  $p'$ - $q$  failure characteristics ( $\psi$  and  $a$ ) to Mohr Coulomb failure characteristics ( $\phi$  and  $c$ ). Assuming cohesion  $c = 0$ , effective friction angle  $\phi'$  ranges from 32.4° to 43.8°. Amos and Sandford (1987) determined the  $\phi'$  of a collected Presumpscot clay specimen from Gorham,

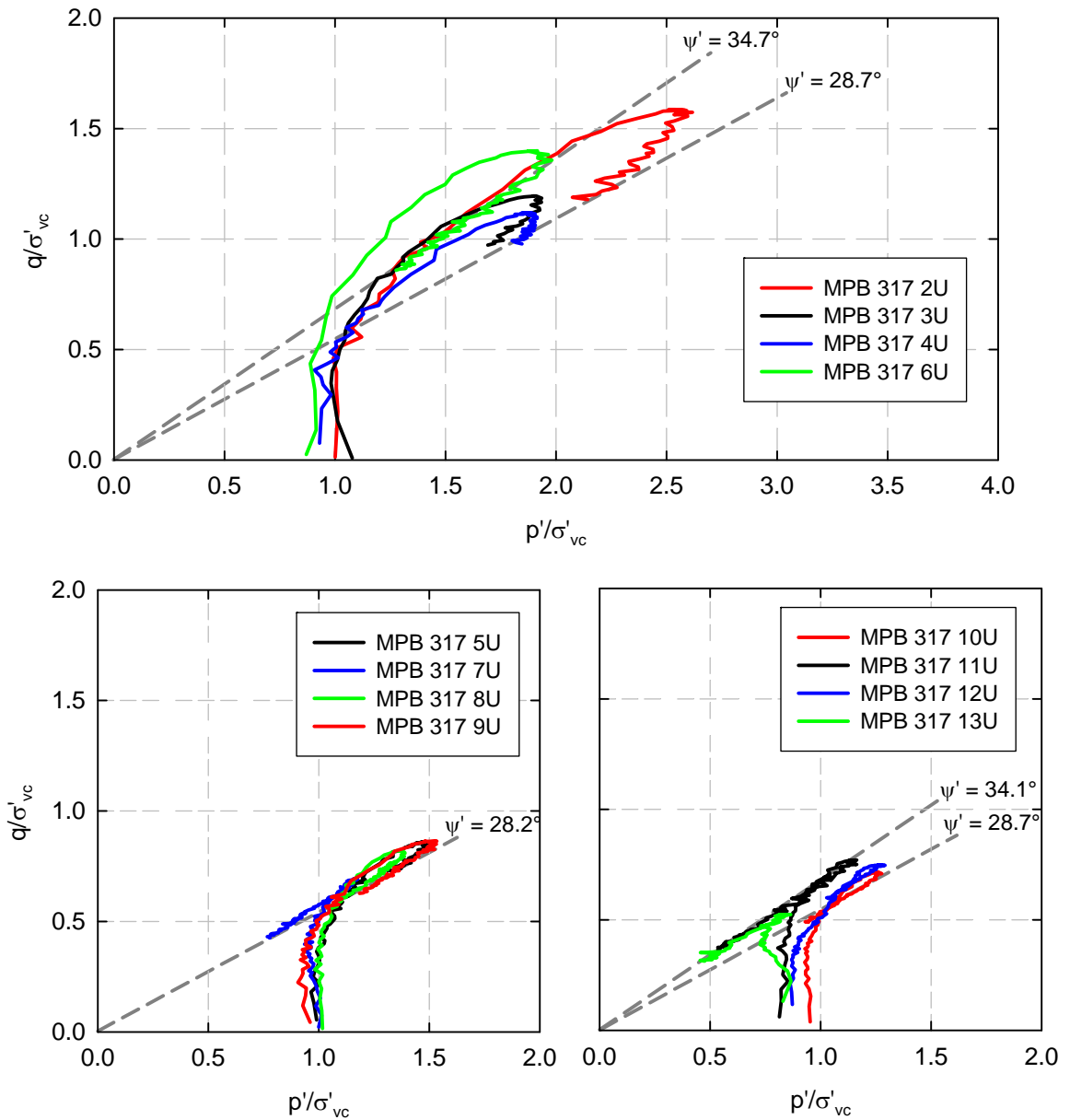


Figure 5.12: Recompression Consolidated Undrained Triaxial (CAUC) normalized effective stress paths for specimens from BB-FPPR-317 from the Martin's Point Bridge site.

Maine to have a drained friction angle of  $35.6^\circ$ , which is a relatively high  $\phi'$  as compared to other clays (Devin and Sandford, 1990). The  $\phi'$  range from  $32.4^\circ$  to  $43.8^\circ$  is a moderate to high value for clay.

$$\sin \phi = \tan \psi$$

5.1

(where  $c = 0$  and  $a = 0$ )

The total stress path of sheared clay in  $p'$ - $q$  space can be drawn as a  $45^\circ$  line measured counterclockwise from the x-axis, starting at the initial stress point. The effective stress paths (the lines shown on Figure 5.12) which remain to the left side of the total stress path line indicate a soil which is exerting positive excess pore pressure (i.e. effective stress is less than total stress). This is the behavior exhibited by all of the tested specimens displayed in Figure 5.12. However, one thing to note is that the deeper that sample, the lower the OCR (Table 5.4) and the further away the effective stress path from the total stress path, indicating higher excess pore pressure (as shown in Table 5.6)

#### 5.2.4 SHANSEP Consolidated Undrained Triaxial Shear Results

SHANSEP testing (Section 2.1.4) was conducted on the Presumpscot clay at the Martin's Point Bridge test site to determine if this type of testing is appropriate for the overconsolidated clay. Table 5.7 and Table 5.8 present results from SHANSEP triaxial compression tests including peak shear stress, strain at failure, pore pressure at failure, and shear stress normalized to vertical effective compressive stress and the predicted relationship between overconsolidation and normalized shear strength. Figure 5.13 illustrates the normalized effective stress paths for the 8U, 29 ft depth, SHANSEP specimens.

The OCR = 1 specimen exhibited normally consolidated behavior as indicated in Figure 5.13. During undrained shear, positive pore water pressures were generated, causing the effective stress path to curve to the left. The OCR = 2 specimen showed low positive pore pressure generation during early shear (the effective stress path moving more vertical before transitioning left in  $p'$ - $q$  space). Following peak shear strength, the normalized effective stress path decreased to the left and approached the failure line. The failure line was the same for both specimens,

having a slope  $\psi' = 30.5^\circ$ , which is equivalent to  $\phi' = 36.0^\circ$  (Equation 5.1). This SHANSEP  $\phi'$  value is larger than  $\phi' = 28.2^\circ$  obtained from recompression test on soil from the same tube, indicating that the densification of specimens during consolidation to the normally consolidated stress region leads to an over prediction of strength. Both the lateral earth pressure ( $K$ ) values and normalized undrained shear strength ( $s_u/\sigma'_{vc}$  or  $q_f/\sigma'_{vc}$ ) values are similar to low OCR clays. The void ratios at the end of compression ( $e_c$ ) for the tested specimens were 1.12 and 1.02, respectively. The *in situ* estimated void ratio for the CAUC tested specimen was 1.24, indicating that the specimens may have been densified and is therefore stronger in compression.

Table 5.7: Summary of specimen and consolidation properties for SHANSEP undrained triaxial tests conducted on specimens from Sample 8U of Presumpscot clay collected from Boring BB-FPPR-317 at the Martin's Point Bridge site.

In Situ			Laboratory Stress History									
Depth (ft)	$w_c$ (%)	$e_0$ (-)	$\sigma'_{v \max}$ (psf)	$\sigma'_{vc}$ (psf)	OCR	K	$\varepsilon_{vol-max}$ (%)	$e_c$ (-)	$\varepsilon_{vol}$ at	$\varepsilon_a$ at	$\Delta e/e_0$ at	NGI Qual.
					$(\sigma'_p/\sigma'_{vc})$ (-)	$(\sigma'_3/\sigma'_1)$ (-)			$\sigma'_{v0}$ (%)	$\sigma'_{v0}$ (%)	$\sigma'_{v0}$ (-)	
29.5	41.7	1.24	402.6	386.7	1.04	0.60	5.25	1.12	0.47	0.50	0.008	VG/E
28.9	40.6	1.21	393.9	199.9	1.97	0.72	8.87	1.02	0.98	0.98	0.018	VG/E

Table 5.8: Summary of shear properties for SHANSEP undrained triaxial tests conducted on specimens from sample 8U of Presumpscot clay collected from Boring BB-FPPR-317 at the Martin's Point Bridge site.

In Situ			At Failure						Prediction	
Depth (ft)	$w_c$ (%)	$e_0$ (-)	$q_f$ (psf)	$\varepsilon_a$ (%)	A	$\Delta u_f$ (psf)	$q_f/\sigma'_{vc}$ (-)	$p'_f/\sigma'_{vc}$ (-)	S	m
									(-)	(-)
29.5	41.7	1.24	2235	0.38	0.90	1089	0.28	0.73	0.28	0.83
28.9	40.6	1.21	2049	0.89	0.07	214	0.49	1.02		

Using the  $s_u$  at failure (defined as the peak) normalized by the consolidation along with the consolidation OCR from the tests, a best-fit curve was applied to the resulting normalized shear strength and overconsolidation ratios to determine the two SHANSEP coefficients, S and m

for Equation 2.1 (see Figure 5.14). The resulting normalized  $s_u$  for the normally consolidated soil is 0.28 and the resulting OCR exponent is 0.83, resulting in the following SHANSEP relationship.

$$s_{u(OCR)} = 0.28 \cdot OCR^{0.83} \quad 5.2$$

The SHANSEP  $S$  parameter from this study is similar to values obtained for Boston blue clay by Ladd et al., (1999) and Landon (2007), while the  $m$  overconsolidation exponent from this study is greater than those listed, but more similar to the Boston blue clay study by DeGroot (2003) (Table 2.2). Overall, the SHANSEP parameters from this study are higher than expected.

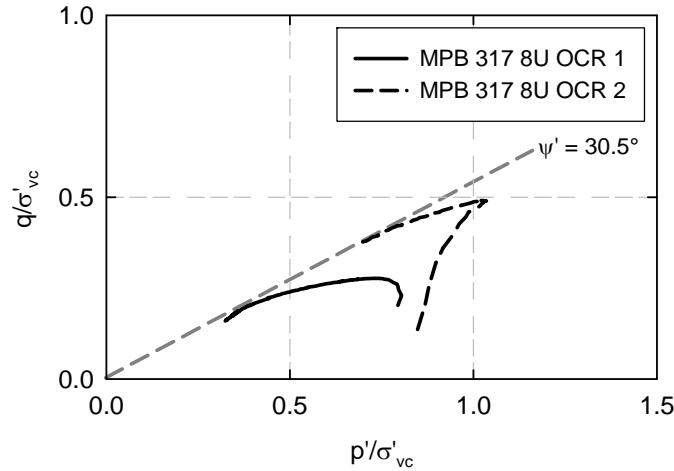


Figure 5.13: Normalized effective stress paths for SHANSEP Triaxial tests conducted on specimens from Sample 8U of Presumpscot clay collected from Boring BB-FPPR-317 at the Martin's Point Bridge site.

Comparison of measured recompression strengths (from CAUC triaxial compression tests) and SHANSEP predicted strengths normalized by the effective overburden stress with overconsolidation is illustrated in Figure 5.14. The SHANSEP equation developed from lower OCR (1 and 2) specimens over predicts strength over the range of OCR values plotted, particularly for higher OCR soils. However, a best fit line under predicts a reasonable  $S$  value and

over predicts a reasonable  $m$ . This is additionally illustrated in Figure 5.15, which plots non-normalized and normalized  $s_u$  with depth. The plotted data illustrate that the SHANSEP parameters from this study ( $S = 0.28$ ,  $m = 0.83$ ) are similar to measured  $s_u$  for high OCR and shallow depths (less than 24 feet), but significantly over predict  $s_u$  at greater depths and lower OCR values. Figure 5.15 additionally shows a modified SHANSEP profile that uses lower  $S$  and  $m$  parameters (0.25 and 0.75, respectively) to better match  $s_u$  measured from recompression triaxial tests. These values were based on a close-match analysis by back-calculating the  $S$  and  $m$  parameter for each tested sample and obtaining the resulting average values. They show under predictions of strength for shallower, higher OCR soil, but good agreement with lower OCR soils at depth. These modified parameters are still greater than those found at Route 26/100 Bridge (Chapter 4) located approximately 4.5 miles up the Presumpscot River from Martin's Point Bridge, indicating the variability of the Presumpscot clay.

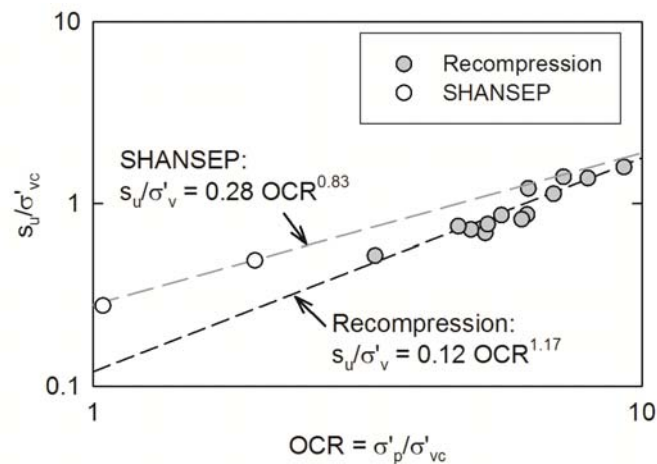


Figure 5.14: Comparison of normalized undrained shear strength from recompression and SHANSEP triaxial compression tests of Presumpscot clay collected from Boring BB-FPPR-317 at the Martin's Point Bridge site.



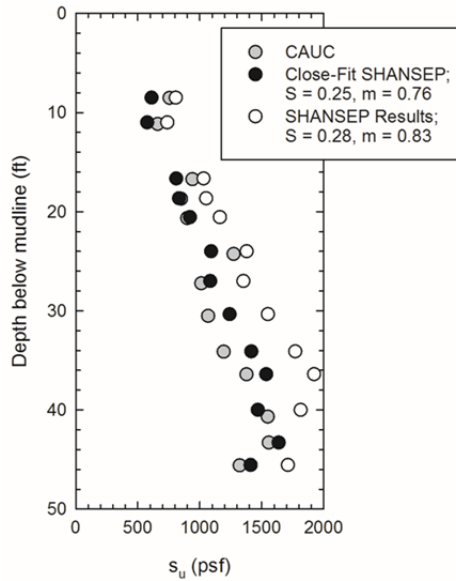


Figure 5.15: Comparison of undrained shear strength and normalized undrained shear strength measured from triaxial recompression and SHANSEP compression ( $S = 0.28$ ,  $m = 0.83$ ) tests and best-fit SHANSEP estimates ( $S = 0.25$ ,  $m = 0.75$ ) for the Martin's Point Bridge Presumpscot clay.

### 5.2.5 Summary and Interpretations of Laboratory Testing Results

This section provides a synthesis of the laboratory testing results in order to characterize the deposit of the Presumpscot clay at the Martin's Point Bridge site using the index results, consolidation properties, and undrained shear strength properties. In general, the Presumpscot clay at the Martin's Point Bridge site appears to be a mechanically overconsolidated deposit with relatively high undrained shear strength ( $s_u$ ) when compared to the nearby Falmouth deposit of soft Presumpscot clay. Index properties of the clay are consistent with depth. The two deepest Shelby Tube samples collected at Martin's Point Bridge (samples 12U and 13U at depths 41 ft and 46 ft respectively) include increasing percentages of sand content. This depth may be considered a transition zone from the Presumpscot clay into the underlying fine sand. This affected index, consolidation, and undrained shear properties of the sandy samples.

Sample 6U at 26 ft depth resulted in a noticeably higher shear strength and OCR than the surrounding samples and the overall trend in the deposit. Two hypotheses were formulated for the

cause of this. The first is the possibility of this behavior signifying a geologic or depositional change which occurred during formation of the deposit. Index and consolidation properties of the overlying and underlying clay material are very similar to that of 6U, and perhaps this depth was formerly deposited in a looser configuration and altered from the weight above. The second possibility is that the increase in  $s_u$  and OCR is due to increased granular composition from either a sand or silt seam. Sand or silt grains can increase frictional resistance to shearing and decrease the compressibility of clay (increasing OCR). Seams were encountered during borings and CPT testing. Although the hydrometer performed on sample 6U did not show an irregular increase in silt or sand, it is likely that the seam was not located within the portion of the sample used for index testing.

Overall index test data (Figure 5.8) show the following trends for the Presumpscot clay at the Martin's Point Bridge site:

- Water content is generally near the liquid limit, with liquidity index ranging between 0.66 and 1.13. There is no apparent relationship between clay content, depth, sensitivity, or other measured parameters and Atterberg limits.
- Sensitivity and clay content are generally well correlated in the upper 38 ft of the deposit, but not correlated for depths greater than this, where fall cone  $s_u$  remains high while clay content decreases and silt and sand content increase.
- In situ void ratio (Figure 5.10) generally follows the trend of clay content, where soils with higher void ratios typically have higher clay content.

Overall stress history (Figure 5.10) and undrained shear strength (Figure 5.11) show the following trends for the Presumpscot clay at the Martin's Point Bridge site:

- Between 11 and 40 ft (sample 2U to 11U),  $\sigma'_p$  increases with depth, which is consistent with mechanical overconsolidation. OCR generally decreases from 6 to 3 for the deposit.

- The cause of the significantly higher  $\sigma'_p$  of sample 1U is likely pore pressure induced from tidal action extending to the sample depth.
- Overconsolidation is likely caused by mechanical unloading (e.g., removal of previously deposited sediment or ice), cycles of wetting or drying, cementation, aging, secondary compression, or other biogeochemical processes.
- The  $\sigma'_p$  of samples 12U and 13U are not representative of the Presumpscot clay deposit due to the high sand content.
- $s_u$  from triaxial testing of the Presumpscot clay at the site ranged from 661 psf to 1557 psf and showed a general increase with depth
- The high  $s_u$  of sample 6U may represent a sand/silt seam inclusions in the sample
- Shear strain at failure ranged from 1.8% to 5.5% with no observed trends with depth or index properties.

### 5.3 Seismic Cone Penetration Testing

Four piezocone penetrometer tests were performed at the Martin's Point Bridge on October 18 and 19, 2012 (Conetec, 2012) in general accordance ASTM D-5778 *Standard Test Method for Electronic Friction Cone and Piezocone Penetration Testing of Soils* and the methods outlined in Section 3.1. These included two piezocone penetrometer tests, CPTu 102 and CPTu 104, and two seismic piezocone penetrometer tests SCPTu 101 and SCPTu 103. Table 5.9 provides location information and test depths for the three profiles. Figure 5.3 indicates the locations of these soundings. CPTu 102 was conducted in a location with no Presumpscot clay and was therefore omitted from the analysis. The penetrometer used for CPTu testing at Martin's Point Bridge contained a cone tip diameter of 1.4 inches. A Dietrich D-50 drill rig mounted on a jack-up barge operated by Maine Test Borings was used to push the cones. Seismic waves were created by striking an anvil on top of metal rods extending down to a wedge placed at the mudline (Section 3.1.1).

Table 5.9: Location and profile depths of four CPT soundings at the Martin's Point Bridge site.

Sounding	Total Depth (ft)	Northing (m)	Easting (m)	# $V_s$ Readings	Depth Extent of Presumpcot Clay (ft)
SCPTu 101	72.8	4838577.697	399790.400	20	6.3 - 52.0
SCPTu 103	81.4	4838410.743	399688.482	24	21.8 - 62.5
CPTu 104	96.1	4838526.331	399758.731	-	3.0 - 64.2

### 5.3.1 Results

Figure 5.16 presents measurements of tip resistance ( $q_t$ ), sleeve friction ( $f_s$ ), and pore pressure ( $u_2$ ) with depth below mudline for (S)CPTu 101, 103, and 104.  $q_t$  from the three tests shows good correlation across the site. Each profile starts close to 2,500 psf at the top of the Presumpcot layer and increases generally linearly with depth. The small, high frequency fluctuations observed in the tip resistance profiles are attributed to the influence of the silt and sand that provide more non-uniform frictional resistance.

The dramatic increase in  $q_t$  at shallow depths from profile SCPTu 101 is from penetration through stiffer marine alluvium. For SCPTu 103 and CPT 104, casing was installed through this alluvium layer, eliminating the penetration record through this material. Data show that  $q_t$  in the top 18 ft of SCPTu 103 is lower than  $q_t$  from the other two profiles. Sediment information from boring BB-FPPR-308, closest boring to SCPTu103, identifies an 18 ft thick layer of soft, silty river bottom deposits overlying the Presumpcot clay. This is consistent with the drained behavior observed in pore pressure measurements. The magnitude of tip resistance measured from all three (S)CPTu soundings at Martin's Point Bridge is higher than “typical” soft clay.

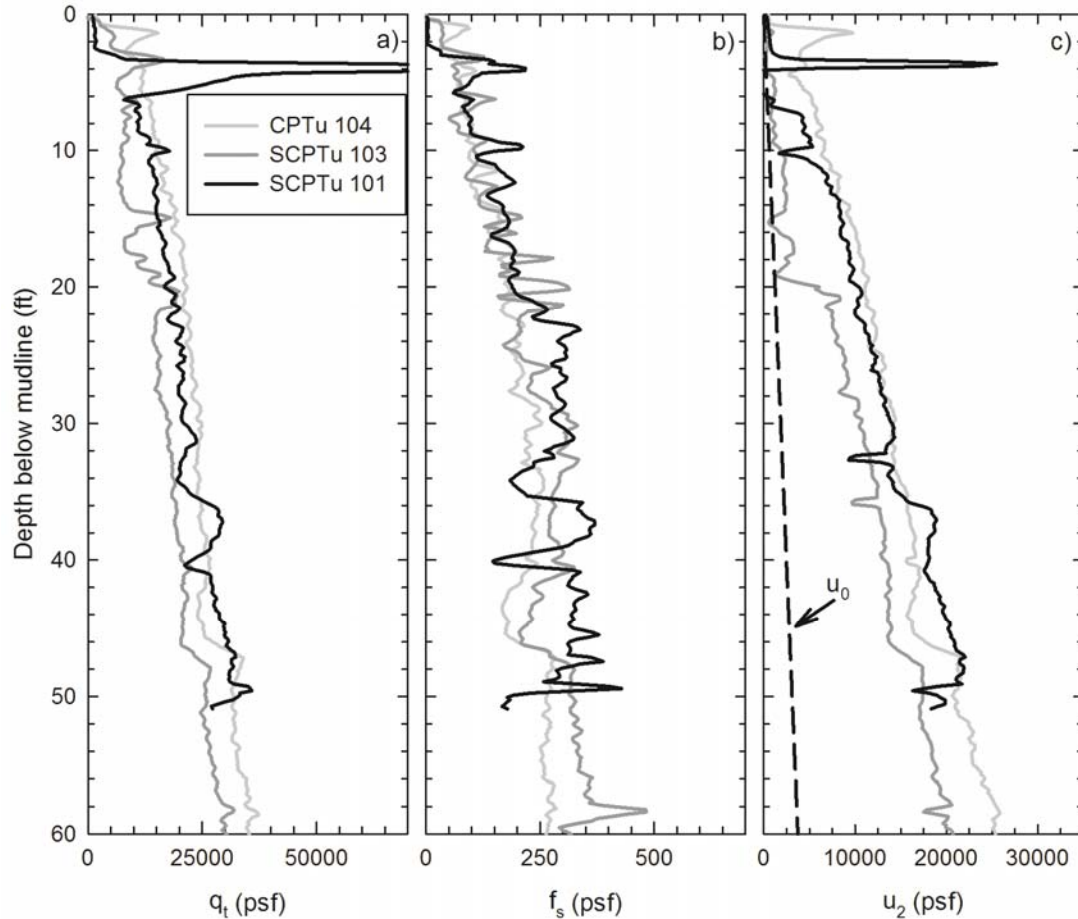


Figure 5.16: Depth profile of (a) corrected tip resistance, (b) sleeve friction, (c) and pore pressure showing hydrostatic pore pressure from soil surface from CPT testing of Presumpscot clay at the Martin's Point Bridge site.

In similar deposits of soft normally consolidated or lightly overconsolidated marine clays, tip resistance reaches a maximum of approximately 20,000 psf (Landon 2007, Lunne *et al.*, 1997, Long 2008). Presumpscot clay at Martin's Point Bridge reaches 40,000 psf, twice the typical magnitude. This is a direct result of the deposit's overconsolidation.

Values of  $f_s$  are similar among the three profiles. A general increase in  $f_s$  is observed with depth to about 22 ft, after which  $f_s$  values remain near constant with continued depth. The variation in  $f_s$  indicated thin layering within the silty clay and possibly thin sand layers where  $f_s$  is

greatest. SCPTu 103 shows more variation with depth at shallow layers (less than 20 ft), while SCPTu 101 indicates more variation at deeper depths.

$f_s$  measurements provide information about the post-shear behavior of the soil, and can approximate the remolded undrained shear strength of soft soils.  $f_s$  measured within the subsurface at the Martin's Point Bridge site are relatively high compared to other studied Presumpscot clay deposits (Figure 8.3). Figure 5.17 compares  $f_s$  from SCPTu101 with remolded shear strength values,  $s_{u(r)}$ , obtained from in situ field vane shear tests from nearby borings and fall cone tests from BB-FPPR-317 (see Figure 5.8 for these data).

Generally,  $s_{u(r)}$  from field vane tests represent the upper bound remolded strength in the top 22 ft of the subsurface and the  $f_s$  profile is more closely matched to  $s_{u(r)}$  from the fall cone measurements. Between 22 ft and 32 ft,  $f_s$  is more similar to field vane shear measured  $s_{u(r)}$ . At greater depths,  $s_{u(r)}$  from both field vane shear and fall cone measurements are less than  $f_s$  values from piezocone measurements. Analysis of soil classification and index parameters yields no conclusive correlation between changing  $f_s$  compared to  $s_{u(r)}$ . However, the strong correlation with remolded  $s_u$  at shallow depths, but poor correlation with continued depth is likely the result of stress two affects: 1) increased stress relief disturbance in field vane shear tests as the effects of overburden removal increases resulting in lower  $s_{u(r)}$  compared to  $f_s$ ; and 2) decreased level of remolding occurring at higher geostatic stresses that results in higher measured  $s_{u(r)}$  for both field vane shear and piezocone profiling compared to  $s_{u(r)}$  from completely remolded fall cone specimens.

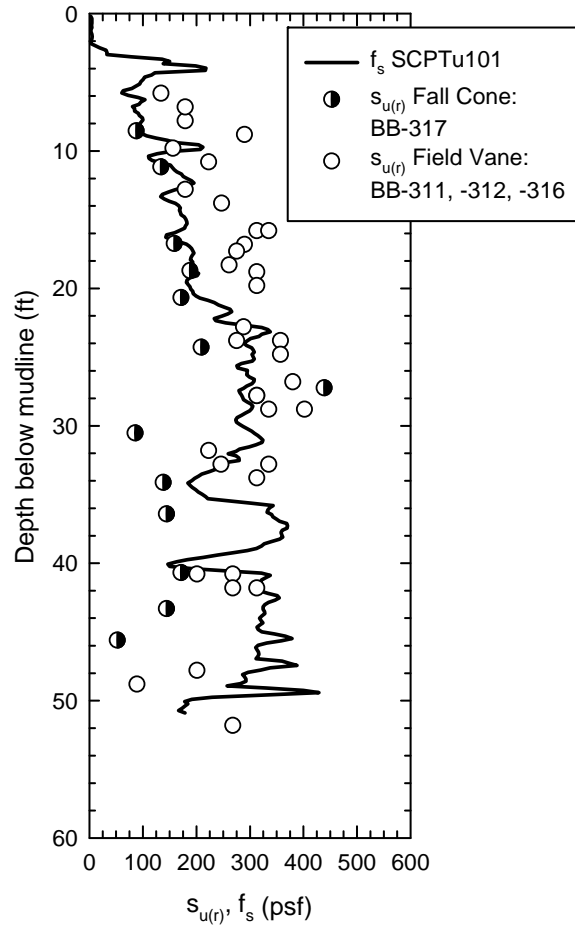


Figure 5.17: Profile comparing remolded shear strength values ( $s_{u(r)}$ ) obtained from Boring 311, 312, and 316 field vane test results and fall cone tests from BB-FPPR-317 with sleeve friction from SCPTu 101 from the Martin's Point Bridge site.

Positive pore pressure measured during penetration of the clay exhibited undrained behavior, as expected. Magnitudes and rate of change with depth of  $u_2$  was consistent between all three (S)CPTu soundings. Small, high frequency fluctuations in  $u_2$  in each profile are due to the influence of silt and sand, which are more permeable and serve to reduce measured pore pressure during penetration. There is a distinct silt seam encountered in the deposit apparent from the  $u_2$  profiles, at depths 32 ft, 36 ft, and 40 ft at SCPTu 101, CPTu 103, and SCPTu 104 respectively. At these depths, there is a localized decrease in pore pressures, which indicate more drained behavior than occurs in clay-dominated soil. It is likely a silt seam exists at these depths; because

only partial drainage was obtained (pore pressures measured in sand seams will generally approach hydrostatic pressures unless it is too small or penetration is too fast).

Shear wave velocity ( $V_s$ ) profiles for SCPTu 101 and SCPTu 103 are illustrated in Figure 5.18.  $V_s$  values are represented at the mid-point between the tests (see Section 3.1.1).  $V_s$  values increase with depth with some variation between 200 ft/s and 550 ft/s shallower than 22 ft below mudline and from 500 ft/s to 750 ft/s from 22 ft to 54 ft depth below mudline. The two profiles generally have similar values, however  $V_s$  is lower for SCPTu 103 between 30 and 44 ft below mudline. This is consistent with variations in  $q_t$  (Figure 5.16) between the two profiles, as sediment in SCPTu 101 profile is stiffer and offers more penetration resistance over this approximate depth range.

Figure 5.18 additionally shows small-strain (e.g., elastic) shear modulus ( $G_0$ ) over the range where undisturbed samples were available from BB-FPPR-317 and measures of in situ measures bulk density ( $\rho_t$ ) were available.  $G_0$  is calculated using Equation 2.17. It should be noted that bulk density values from BB-FPPR-317 were used for both profiles, as this was the boring with consistent collection of undisturbed samples.  $G_0$  ranges from approximately 5 to 12 ksi over the depth range shown, with a general trend of increasing with depth. Lastly, the rigidity index,  $I_r$ , often used for foundation design applications and numerical simulations, was determined using interpreted  $G_0$  and  $s_u$  determined from CAUC triaxial compression tests on undisturbed samples from BB-FPPR-317.  $I_r$  ranges from 910 to 1,120 in the location of SCPTu 101. A report by Long and Donohue (2008) studied 11 Norwegian clay sites using both surface waves and CPTu to obtain  $V_s$  values. The studied clay ranged from 17% to 60% clay, had OCR of 1.0 to 6.0, and sensitivities ranging from 2 to 1000. Values of  $V_s$  in the study ranged from 131 ft/s to 1,148 ft/s



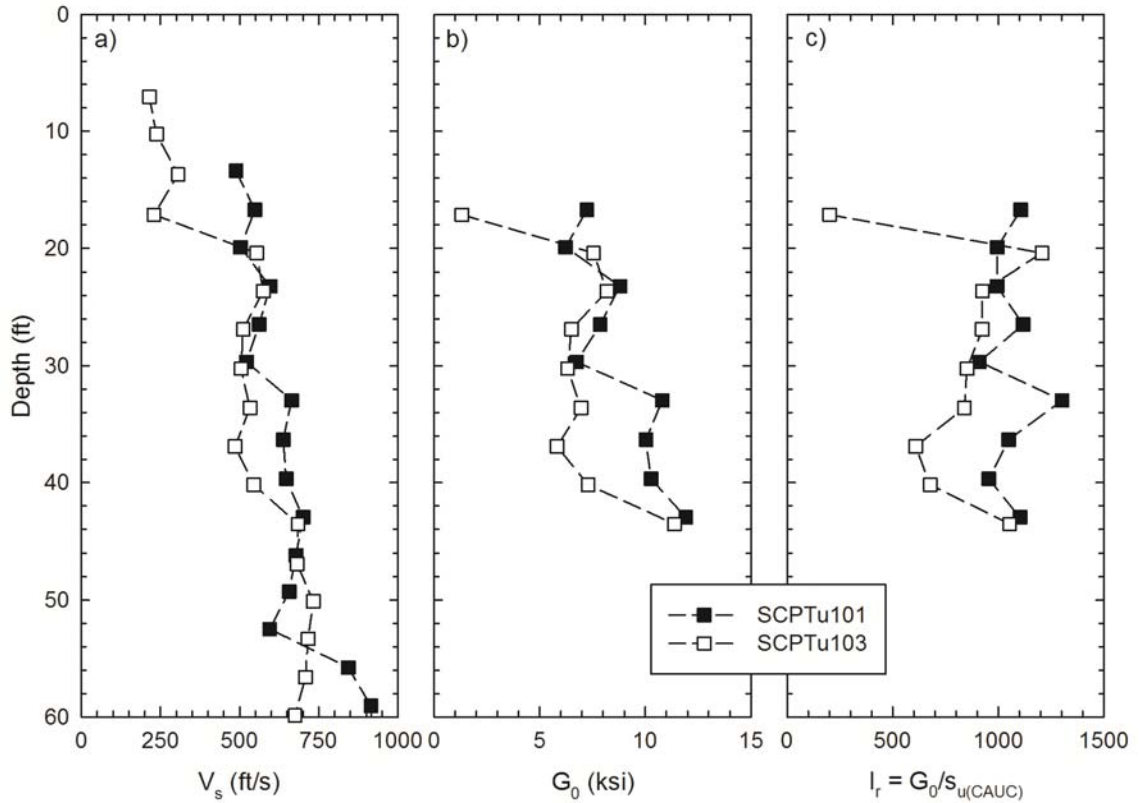


Figure 5.18: Depth profile of a) shear wave velocity ( $V_s$ ), b) small strain shear modulus ( $G_0$ ) and Rigidity index ( $I_r$ ) for SCPTu101 and 103 conducted at the Martin's Point Bridge site.

### 5.3.2 Correlation to Classification

Empirical charts have been proposed by Robertson (1990), Schneider *et al.* (2008), and Robertson (2009) to classify soils based on CPTu measurements (Section 2.3.1). The proposed charts plot normalized tip resistance ( $Q_t$ ) versus sleeve friction ratio ( $F_r$ ) or normalized pore pressure ( $B_q$ ) and place the resulting data point into a region which has a corresponding soil type deemed the “Soil Behavior Type” or SBT. The SBT regions were developed based on observed  $Q_t$ ,  $F_r$ , and  $B_q$  measurements taken in specific types of soils. Normalized values are used to eliminate the influence of depth on measurements. Figure 5.19 displays the profiles of the three normalized parameters  $Q_t$ ,  $F_r$ , and  $B_q$  collected from SCPTu 101, 103, and 104 with depth.

Each of the four classification charts were evaluated for their applicability to the Presumpscot clay at Martin's Point Bridge using Unified Soil Classification System (USCS) results from laboratory analyses of collected soil samples and values of  $Q_t$ ,  $F_r$ , and  $B_q$  collected from SCPTu 101 and CPTu 104 at corresponding depths. SCPTu 104 was not used because it is practically identical to SCPTu 101. For three of the charts (Robertson 1990 and Robertson 2009; Figure 5.20a, b, and c), there are 9 regions corresponding to Soil Behavior Types (SBT). SBT 1 “sensitive fine grained,” SBT 3 “clay to silty clay,” and SBT 4 “clayey silt to silty clay” were considered correct classifications of the Presumpscot clay at this site based on lab data. For the fourth chart (Schneider *et al.*, 2008; Figure 5.20d), a different classification system is used, of which the “clays” and “sensitive clays” regions were considered to be correct classifications of the Presumpscot clay. Plotted data from SCPTu 101 and 104 are presented in Figure 5.20 and Figure 5.21, respectively. Table 5.10 presents a summary of this analysis including the number of laboratory samples tested, number of USCS classifications matching the SBT classification, and the resulting percent effectiveness (USCS-SBT matches divided by the number of samples).

In general, the Presumpscot clay at the Martin's Point Bridge site plotted within SBT regions 4 and 5 using the  $Q_t$ - $F_r$  plots of Robertson (1990) and Robertson (2009), while most data plotted in SBT region 3 (with a minor amount in SBT region 4) when using the  $B_q$ - $Q_t$  plot of Robertson (1990). Practically all data points plotted in the “clay” region of the Schneider *et al.*, (2008) plot.

Comparison of SBT and USCS classification is tabulated in Table 5.10. Soil Behavior Type (SBT) and Unified Soil Classification System (USCS) classifications match for 100% of the samples when SBT is determined using  $Q_t$  and  $B_q$  for both the Robertson (1990) and Schneider *et al.*, (2008). SBT and USCS classifications based on  $Q_t$  and  $F_r$  have a lower prediction correlation, which were 90% and 79% for SCPTu 101 and CPTu 104, respectively.  $B_q$  better predicts

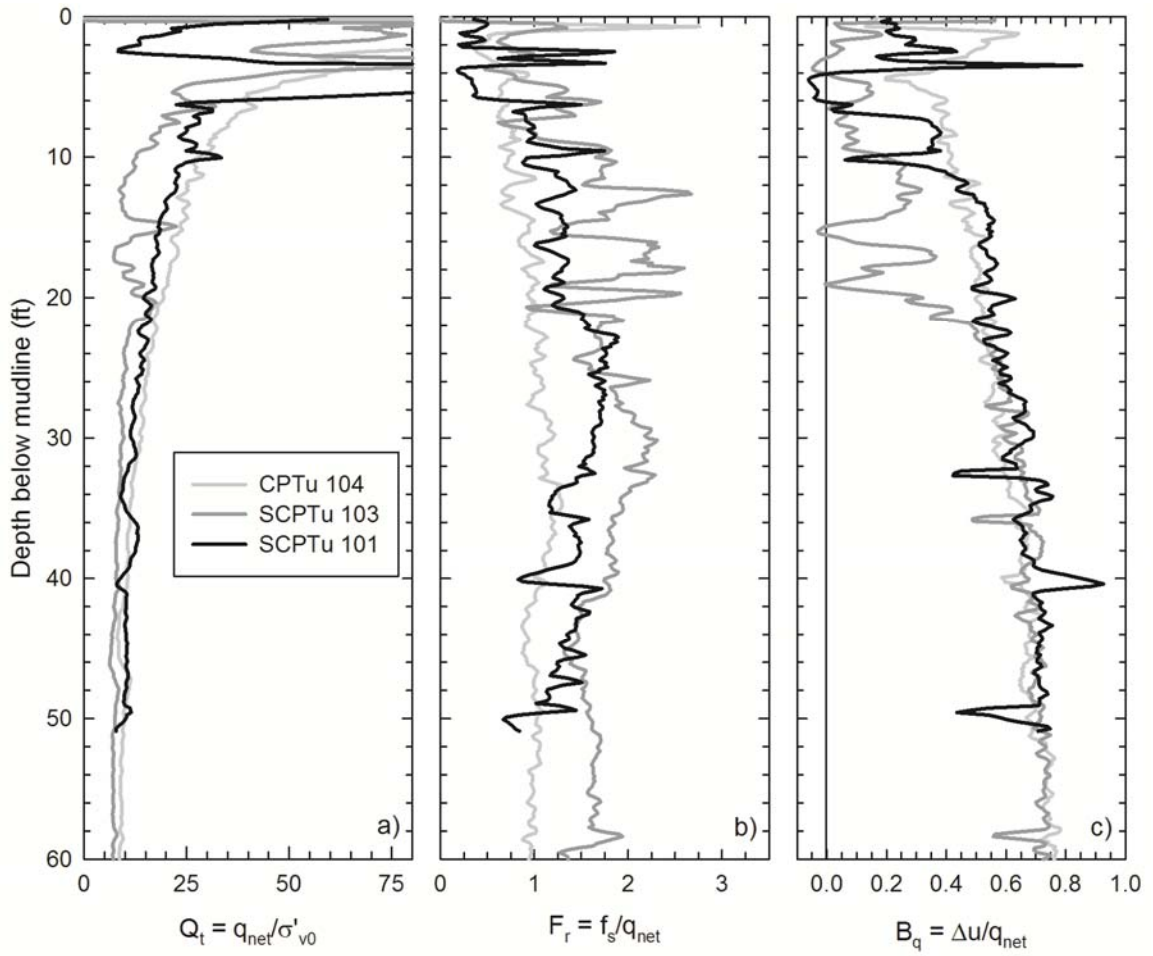


Figure 5.19: Profile of a) normalized tip resistance ( $Q_t$ ), b) sleeve friction ratio ( $F_r$ ), and c) normalized pore pressure ( $B_q$ ) collected from SCPTu 101, 103, and 104 at the Martin's Point Bridge site.

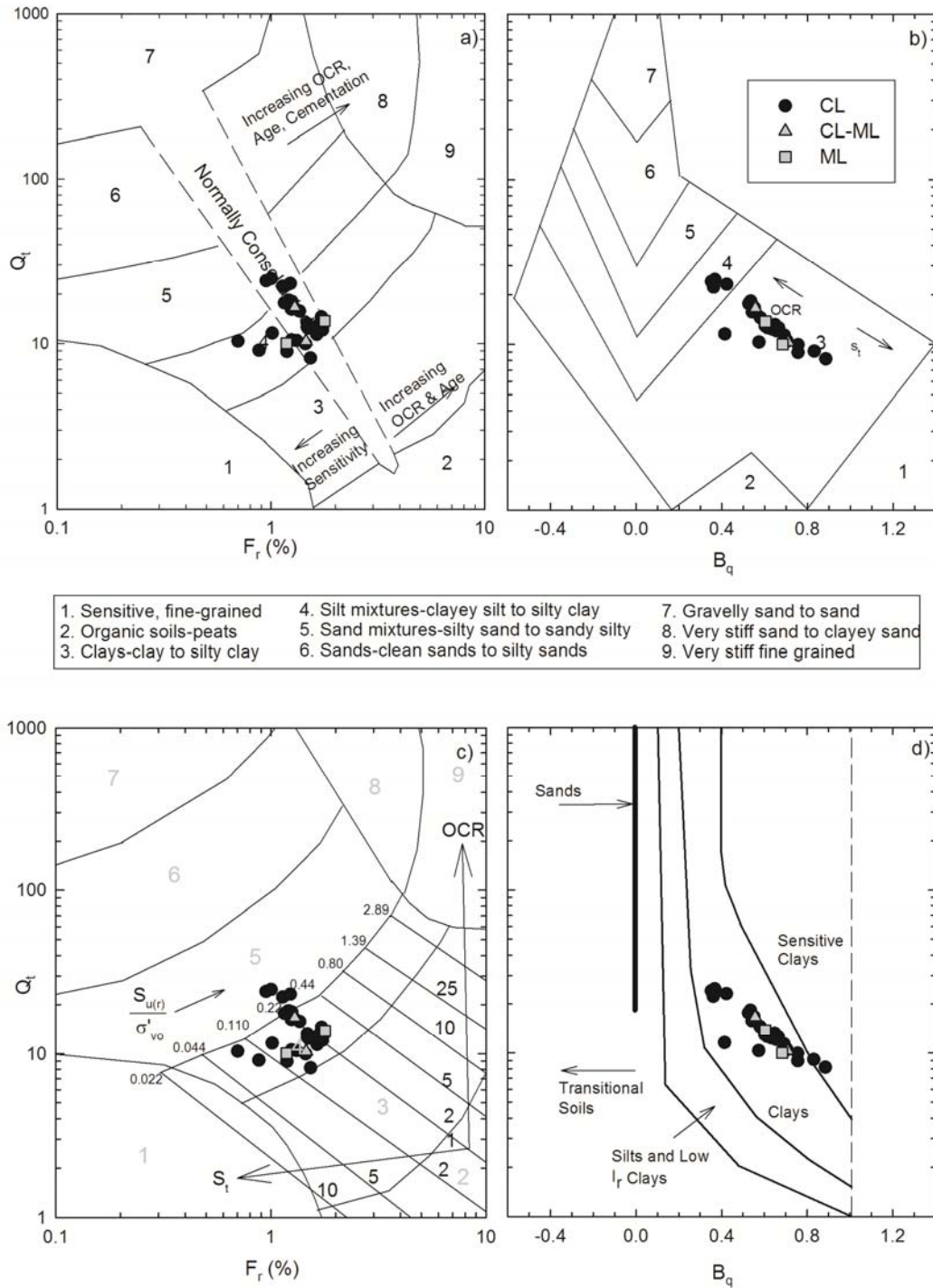


Figure 5.20: Soil classification results comparing laboratory-determined USCS classification to classification charts using a)  $Q_t$  vs.  $F_r$  (Robertson 1990), b)  $Q_t$  vs.  $B_q$  (Robertson 1990), c)  $Q_t$  vs.  $F_r$  (Robertson 2009), d)  $Q_t$  vs.  $B_q$  (Schneider *et al.*, 2008) from SCPTu 101 conducted at the Martin's Point Bridge site.

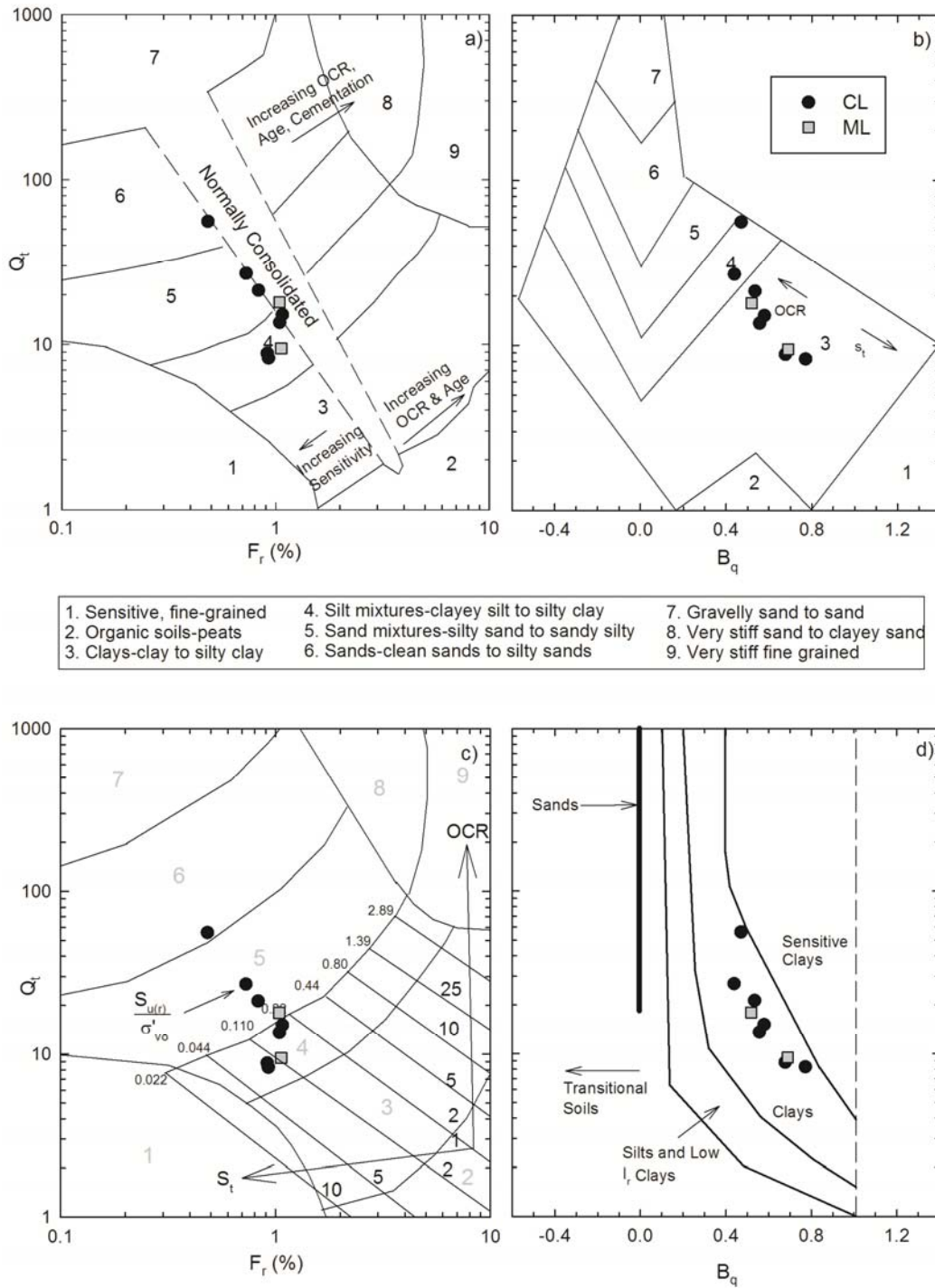


Figure 5.21: Soil classification results comparing laboratory-determined USCS classification to classification charts using a)  $Q_t$  vs.  $F_r$  (Robertson 1990), b)  $Q_t$  vs.  $B_q$  (Robertson 1990), c)  $Q_t$  vs.  $F_r$  (Robertson 2009), d)  $Q_t$  vs.  $B_q$  (Schneider *et al.*, 2008) from CPTu 104 conducted at the Martin's Point Bridge site.

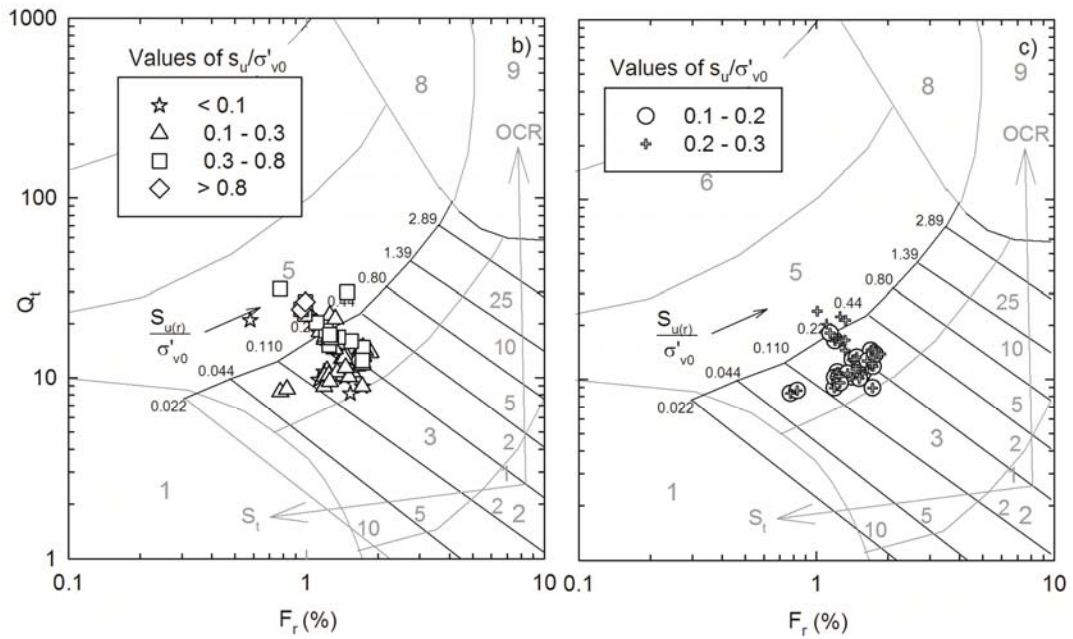
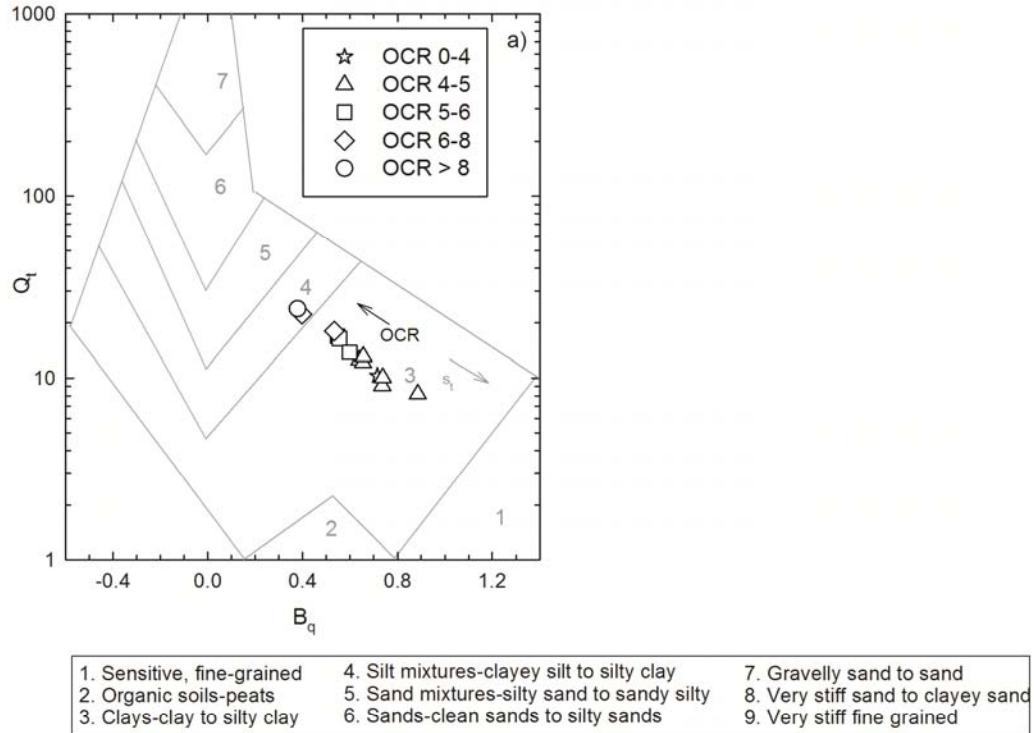


Figure 5.22: Comparison of laboratory and field determined soil properties to plotted SBT trends for a) OCR (Robertson 1990), b) normalized remolded undrained shear strength (Robertson 2009), and c) Normalized remolded undrained shear strength with lower data range (Robertson 2009) from SCPTu 101 at the Martin's Point Bridge site.

Table 5.10: Summary of CPTu classification chart effectiveness for SCPTu 101 and CPTu 104 conducted at the Martin's Point Bridge site.

Reference	# samples	SCPTu101		# samples	CPTu104	
		SBT-USCS Correlation	% Effective		SBT-USCS Correlation	% Effective
<i>Robertson 1990 (<math>F_r</math>)</i>	40	36	90	14	11	79
<i>Robertson 1990 (<math>B_q</math>)</i>	40	40	100	14	14	100
<i>Robertson (2009)</i>	40	36	90	14	11	79
<i>Schneider et al., (2008)</i>	40	40	100	14	14	100

Notes: SBT: soil behavior type from CPT correlations; USCS: Unified Soil Classification System (ASTM D2487).

classification than  $F_r$  when using the charts from this study. This is similar to results published by Long (2008), who used Robertson (1990)  $B_q$  and Schneider *et al.*, (2008) to classify a transitional silt/clay deposit and found that using pore pressure parameter  $B_q$  was much more efficient than  $F_r$  for classification.

Regarding  $F_r$ ,  $f_s$  is low compared to  $q_t$  and  $F_r$  is greatly affected by small changes in  $q_{net}$  (i.e.,  $q_t - \sigma_{v0}$ ).  $B_q$  is a better predictor because pore pressures generated during shear are distinct properties of clays/silts and low permeability prevents dissipation when penetration is undrained (which is the case in Presumpscot clay). Soils with sufficiently low hydraulic conductivity (e.g., clays) will be completely undrained during cone penetration, soils with sufficiently high hydraulic conductivity (e.g., sands) will be completely drained during cone penetration, and soils between, will be partially drained, producing lower values of penetration induced pore pressure. It should be noted that effective use of  $B_q$  for classification purposes is reliant on complete saturation of the pore pressure filter element. Should improper saturation occur, lower pore pressures than those actually induced during penetration will be measured, resulting in prediction of higher hydraulic conductivity or partially drained soils than may be present. This is not the case for these soils. It should be additionally noted that  $Q_t$ - $B_q$  SBT classification may be more reliable than  $Q_t$ - $F_r$  classification as sleeve friction is generally a less reliable measurement than pore pressure due to the following factors: pore pressure effects on the end of the sleeve;

tolerance in dimensions between the cone and the sleeve; surface roughness of the sleeve; load cell design and calibration (Lunne *et al.*, 2006).

SBT charts from Robertson (1990, 2009) additionally provide information for using  $Q_t$ ,  $F_r$ , and  $B_q$  to predict changes in overconsolidation (OCR), values of remolded  $s_u$  normalized by in situ effective stress ( $s_{u(r)}/\sigma'_{v0}$ ), and sensitivity ( $S_t$ ). Review of SCPTu 101 data plotted in Figure 5.22 shows a significant number of data points plotting in the central normally consolidated region; however laboratory data from Boring BB-FPPR-317 indicate the Presumpscot is overconsolidated with OCR values ranging from 10.4 to 3.1 within the layer. Thus, this aspect of SBT chart is not reliable for the Presumpscot at this site. Figure 5.22a indicated that  $Q_t$  vs.  $B_q$  may be used to indicate the relative level of overconsolidation over the depth of a deposit. Data are plotted by OCR grouping. Higher OCR soils have higher  $Q_t$  and lower  $B_q$  values. Figure 5.22a was additionally used to analyze for trends in sensitivity,  $S_t$ , for the Presumpscot (data not shown), however a trend was not found for the soils at this site.

Figure 5.22b and Figure 5.22c show  $Q_t$  vs.  $F_r$  data for SCPTu 101 categorically separated by  $s_{u(r)}/\sigma'_{v0}$  measured from field vane shear testing (FVT) and fall cone testing on samples from Shelby tubes. While SCPTu 101 data predicts  $s_{u(r)}/\sigma'_{v0}$  values ranging from 0.11 to 0.35, measured  $s_{u(r)}/\sigma'_{v0}$  values from in situ and laboratory testing ranges from less than 0.1 to greater than 0.8. Larger values are from in situ testing where complete remolding of specimens was likely incomplete (the standard is 10 rotations of the shear vane between tests to disturb the sheared zone). Review of fall cone data (Figure 5.12) indicates completely remolded specimens yield  $s_{u(r)}/\sigma'_{v0}$  values of 0.02 to 0.06 for deeper soil and 0.17 and 0.32 for shallower soil. Completely remolded  $s_{u(r)}/\sigma'_{v0}$  values are generally less than those predicted by Figure 5.22c by SCPTu101  $Q_t$  and  $F_r$  data. In summary, it appears as though  $s_{u(r)}/\sigma'_{v0}$  can be loosely estimated using plots of  $Q_t$  vs.  $F_r$ , and these values may potentially more clustered than  $s_{u(r)}/\sigma'_{v0}$  derived



from field vane shear tests. Remolded undrained shear strength of the Presumpscot clay measured by SCPTu 101 and field vane tests are higher than fall cone data due to the in situ horizontal and vertical confining pressure on the specimen during the in situ tests.

### 5.3.3 Correlations to Stress History

CPTu sounding data of the Presumpscot clay data were correlated to measured stress history of the site using the *k-value* correlation method outlined in Section 2.3.2. Using Equation 2.7, *k-value* was back-calculated using preconsolidation pressure ( $\sigma'_p$ ) determined from CRS testing (Section 3.4.3) of laboratory specimens and  $q_{net}$  assessed from the CPTu soundings at the corresponding sample depths. Figure 5.23 presents the *k-values* determined for the Presumpscot clay at Martin's Point Bridge along with the estimated  $\sigma'_p$  profile using determined *k-values* applied to SCPTu 101 (the closest sounding to the collected samples).

In Figure 5.23, each symbol represents a *k-value* back calculated from one of the CPTu soundings. Each grouping of symbols at a common depth correspond to a single  $\sigma'_p$ , with a  $q_{net}$  value taken from one of the CPTu soundings to solve for the *k-value*. The range of values in the grouping represents the difference in  $q_{net}$  between the soundings. Presumpscot clay was not encountered in SCPTu 103 until 22 ft depth, therefore the *k-value* was not calculated above 22 ft.

The vertical dotted lines at values of 0.20 and 0.50 represent the “typical” range of values for clays (Lunne *et al.*, 1997). In Figure 5.23b, the average, minimum, and maximum *k-values* from SCPTu 101 were applied to the entire profile of  $q_{net}$  from SCPTu 101 and compared to the laboratory-determined  $\sigma'_p$ .

The resulting *k-values* from the three soundings at Martin's Point Bridge ranged from 0.25 to 0.59 with average values of 0.38, 0.53, and 0.35 for SCPTu 101, 103 and 104, respectively. With the exception of the *k-value* of 0.53 for SCPTu 101 calculated at 34 ft, all *k-values* for SCPTu 101 and 104 remained within the proposed range of 0.20 to 0.50 given by

Lunne *et al.* (1997) for soft to mildly overconsolidated clays. SCPTu 103, however, resulted in  $k$ -values from 0.49 to 0.59, exceeding the proposed range, which discussed below.

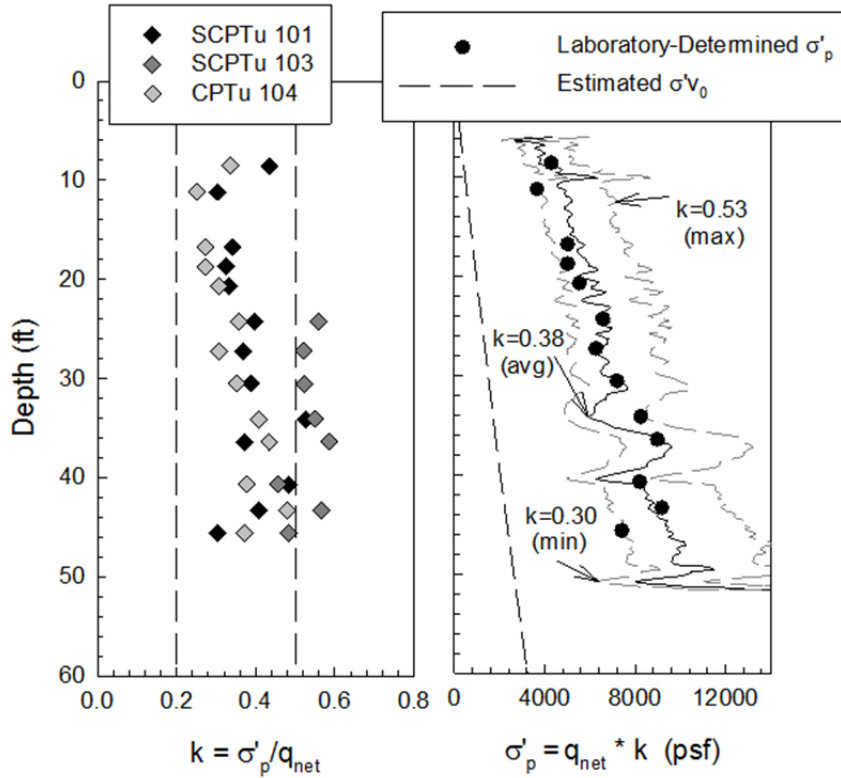


Figure 5.23: Subsurface profile showing (a) the CPTu correlated preconsolidation stress  $k$ -value and (b) preconsolidation pressure correlated from SCPTu 101 based on the range of correlated values from the Martin's Point Bridge site.

For SCPTu 101 and 104, the  $k$ -value was initially high at the shallowest samples (OCR = 10.4), and dropped sharply in magnitude as OCR decreased to 6.8 at 11.1 ft. From 11.1 ft to 30.5 ft, the  $k$ -value remained within a narrow range of values as OCR steadily decreased from 6.8 to 4.7. Below 30.5 ft, the  $k$ -value are more scattered with depth for both soundings. The deepest three samples yielded low sample quality specimens from CRS consolidation testing and subsequently caused the  $\sigma'_p$  (and  $k$ -value) to vary widely. Inspection of Figure 5.23 reveals good consistency between the  $\sigma'_p$  estimated using a  $k$ -value average of 0.38 compared to the laboratory results of  $\sigma'_p$  throughout the entire deposit.  $\sigma'_p$  profiles estimated from the minimum and

maximum *k-values* create an upper and lower-bound range of  $\sigma'_p$  and the laboratory  $\sigma'_p$  at this site tend to remain closer to the minimum profile. Percent difference of  $\sigma'_p$  from the laboratory and  $\sigma'_p$  estimated from an average *k-value* of 0.38 ranges from -32% to 22% with an average (of the absolute value) percent difference of 13%.

*k-values* correlated from SCPTu 103 were consistently higher than *k-values* correlated from the other two CPTu soundings. It should be noted that the OCR and  $\sigma'_p$  used to back-calculate the *k-values* from SCPTu 103 came from Boring BB-FPPR-317, located approximately 700 feet laterally from SCPTu 103, therefore the stress history conditions at both of the locations may not match precisely. Results from the field vane shear tests (FVT) at the site indicate lower undrained shear strength ( $s_u$ ) closer to SCPTu 103 and higher  $s_u$  closer to BB-FPPR-317. It can be inferred that lower  $s_u$  clay is at a lower in situ OCR state (explicit from the SHANSEP equation, Section 2.3.3), therefore the  $\sigma'_p$  used to back-calculate the *k-values* from SCPTu 103 may exceed in situ conditions. According to the *k-value* equation (Equation 2.7), the result of a higher  $\sigma'_p$  is a higher *k-value*, and this caused the observed increase in *k-value* from SCPTu 103 in Figure 5.23.

The same *k-value* used to estimate  $\sigma'_p$  can be used to predict OCR using Equation 2.6. The resulting OCR profile from the Martin's Point Bridge site using the average *k-value* from SCPTu 101 was compared to incremental load (IL) consolidation test data reported in Golder Associates, Inc. (2011a, b) for samples collected at the site. Table 5.11 summarizes the comparison of OCR predicted using the average  $k = 0.38$  from SCPTu101 with the OCR measured from consolidation tests from various borings throughout the site. Generally, SCPTu estimates based on a *k-value* of 0.38 are greater than OCR from IL consolidation tests, by 6% to 100%. However, the IL consolidation samples (Golder, 2011a, b) were collected throughout the entire site and may not represent the same stress history conditions as the clay at the CPTu soundings. Figure 5.24 illustrates the OCR between IL consolidation tests (Golder, 2011a, b),

CRS consolidation tests from this study, and the OCR profile estimated using a  $k$ -value of 0.38 applied to SCPTu 101.

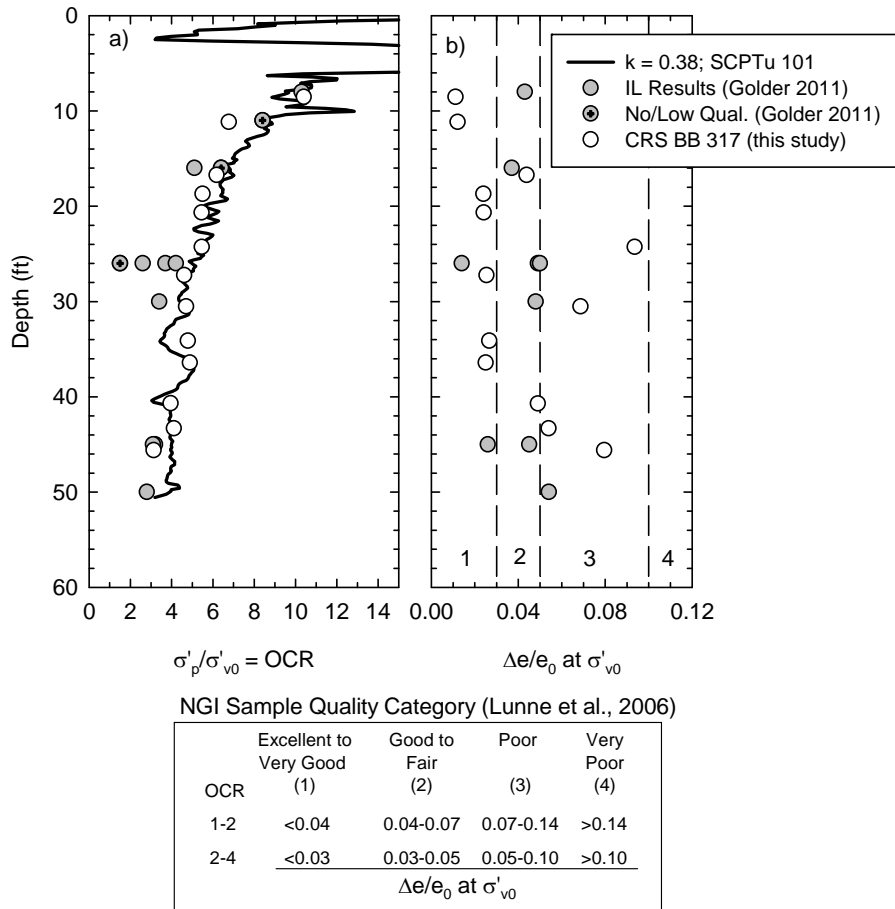


Figure 5.24: Profile of a) overconsolidation ratio and b) sample quality for the consolidation samples collected and tested by Golder Associates in 2011 at Martin's Point Bridge.

One observation made from the comparison between IL consolidation tests and the CPTu values is the tendency for OCR estimated from the CPTu to be greater than OCR from IL test results. Specimens tested in the IL method are subject to sample disturbance from the collection, storage, trimming, and testing of the sample, all of which contribute to the decrease of  $\sigma'_p$  estimates (and therefore lower OCR). The  $k$ -value of 0.38 was developed from high quality samples with minimal disturbance and applied to an in situ test, therefore mitigating the effects of

sample disturbance from the OCR estimates and potentially providing higher values that comparable IL test results.

Table 5.11: Comparison of OCR values between IL laboratory testing and a k-value of 0.38 applied to SCPTu101 and CPTu 10 of Presumpscot Clay at Martin's Point Bridge (some data from Golder Associates 2011a, b).

Depth (ft)	Boring	(S)CPTu	IL Consol . OCR <sup>1</sup>	Sample Quality <sup>2</sup>	Q <sub>t</sub>	estimated OCR using k = 0.38	% diff.
8	BB-FPPR-311A	SCPTu	10.3	G/F	25.2	9.9	-4
11	BB-FPPR-208	101	8.4	<i>unknown</i>	22.3	9.7	15
16	BB-FPPR-312		6.4	<i>VP</i>	17.8	6.9	8
26	BB-FPPR-108		2.6	G/F	13.2	5.2	100
26	BB-FPPR-311A		3.7	VG/E	13.2	5.1	38
26	BB-FPPR-313		4.2	<i>P</i>	13.2	5.1	21
30	BB-FPPR-109		3.4	G/F	11.6	4.6	35
45	BB-FPPR-108		3.2	G/F	10.4	4.1	28
45	BB-FPPR-107	CPTu	3.1	G/F	6.7	3.3	6
16	BB-FPPR-107	104	5.1	VG/E	11.4	8.4	64
26	<i>BB-FPPR-206</i>		1.5	<i>unknown</i>	9.4	5.9	293

Notes: <sup>1</sup>Data from Golder Associates, Inc. (2011a,b); <sup>2</sup>Sample quality based on Lunne et al., (2006), where italic text indicates poorer quality data.

In summary of the CPTu stress history correlations, the *k-value* at Martin's Point Bridge ranged from 0.25 to 0.59 with average values of 0.38, 0.53, and 0.35 for SCPTu 101, 103 and 104, respectively. These values fit reasonably well within the published range of 0.20 to 0.50 from Lunne *et al.*, (1997). Correlations to SCPTu 101 and SCPTu 104 matched well with the laboratory data, particularly when using the average *k-value* of 0.38 from SCPTu 101 (the closest sounding to the collected samples). Correlations to SCPTu 103 resulted in consistently higher *k-values* than the previously mentioned soundings due to the softer and less consolidated condition of the Presumpscot clay in this part of the site. Overall, using an average *k-value* of 0.38 gave an average difference of ±13% from the laboratory values of  $\sigma'_p$ .

### 5.3.4 Correlations to Undrained Shear Strength

Undrained shear strength ( $s_u$ ) of clay can be estimated from CPTu results using empirical cone factors  $N_{kt}$ ,  $N_{ke}$ , and  $N_{\Delta u}$  (Equations 2.9 through 2.11). Section 2.3.3 outlines the methodology used to obtain the three empirical coefficients.  $N_{kt}$  is derived from tip resistance ( $q_t$ ),  $N_{ke}$  is derived from  $q_t$  and pore pressure measurements ( $u_2$ ), and  $N_{\Delta u}$  is derived from  $u_2$ . These empirical coefficients were determined for the Presumpscot clay at the Martin's Point Bridge site using  $s_u$  from laboratory CAUC triaxial shear testing and field vane shear testing (FVT) results.

Figure 5.25 presents the CPTu undrained shear strength factors  $N_{kt(CAUC)}$ ,  $N_{ke(CAUC)}$ , and  $N_{\Delta u(CAUC)}$  calculated from SCPTu 101, 103, and 104 data where each symbol represents an  $N_{kt(CAUC)}$ ,  $N_{ke(CAUC)}$ , or  $N_{\Delta u(CAUC)}$  value back-calculated from one of the CPTu soundings using the  $s_u$  measured from the CAUC triaxial testing from BB-FPPR-317 at the corresponding depth. SCPTu 101 was the closest sounding to Boring BB-FPPR-317. CPTu 103 and SCPTu 104 were conducted 692 ft and 205 ft away from Boring BB-FPPR-317, respectively.  $N_{kt(CAUC)}$ ,  $N_{ke(CAUC)}$ , and  $N_{\Delta u(CAUC)}$  values are not reported for SCPTu 103 above 22 ft because Presumpscot clay was not encountered during the sounding until this depth. Table 5.12 presents the  $N_{kt(CAUC)}$  and  $N_{\Delta u(CAUC)}$  values correlated at the Martin's Point Bridge site from all three soundings.

$N_{kt(CAUC)}$  for the three profiles ranged from 9.3 to 22.1 with average values of values of 15.9 (SCPTu 101), 11.5 (SCPTu 103) and 17.6 (CPTu 104). Lunne *et al.*, provides a general range of values for  $N_{kt}$  between 10 and 20, illustrating that the ranges from Martin's Point Bridge fit in well with published data. Coefficients of variations for  $N_{kt(CAUC)}$  of the three soundings are 0.16, 0.10, and 0.18 for SCPTu 101, 103, and, 104 respectively.  $N_{ke(CAUC)}$  ranged from 2.6 to 13.3 with average values of values of 7.4 (SCPTu 101), 5.5 (SCPTu 103) and 9.08 (CPTu 104). Typical values of  $N_{ke}$  range between 6 and 12 and average of 9 (Lunne *et al.*, 1997). Coefficients of variations for  $N_{ke(CAUC)}$  of the three soundings are 0.31, 0.09, and 0.26 for SCPTu-101, 103,

and, 104 respectively.  $N_{\Delta u(CAUC)}$  ranged from 5.0 to 13.3 with average values of 9.7 (SCPTu 101), 7.4 (SCPTu 103) and 9.7 (CPTu 104). Coefficients of variations for  $N_{\Delta u(CAUC)}$  of the three soundings are 0.22, 0.14, and 0.13 for SCPTu 101, 103, and, 104 respectively.  $N_{\Delta u}$  typically ranges from 4 to 10 for soft clays (Lunne *et al.*, 1997), illustrating that Martin's Point Bridge is in the upper portion of this published range. As mentioned in Section 2.3.3, the cone factor  $N_{ke}$  has been found to be unreliable for clay deposits and will be omitted from the correlation analysis.

Table 5.12: Summary of  $N_{kt(CAUC)}$  and  $N_{\Delta u(CAUC)}$  values at the Martin's Point Bridge site.

		Minimum	Average	Maximum	S.D.	C.O.V.
SCPTu 101	$N_{kt(CAUC)}$	11.0	15.9	18.6	2.6	0.16
	$N_{\Delta u(CAUC)}$	5.0	9.7	13.3	2.1	0.22
SCPTu 103	$N_{kt(CAUC)}$	9.3	11.5	13.0	1.2	0.10
	$N_{\Delta u(CAUC)}$	5.2	7.4	8.4	1.0	0.14
CPTu 104	$N_{kt(CAUC)}$	12.4	17.6	22.1	3.1	0.18
	$N_{\Delta u(CAUC)}$	7.4	9.7	11.2	1.2	0.13

Note: S.D. = standard deviation; C.O.V. = coefficient of variation

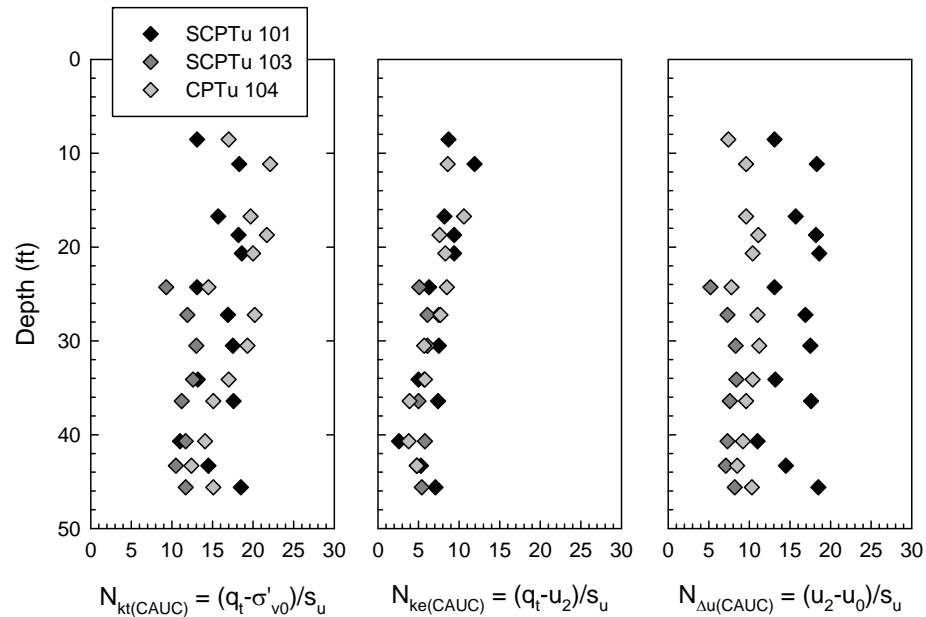


Figure 5.25 Subsurface profiles of  $N_{kt(CAUC)}$ ,  $N_{ke(CAUC)}$ , and  $N_{\Delta u(CAUC)}$  correlated from (S)CPTu 101, 103, and 104 with  $s_u$  from triaxial CAUC testing of Presumpscot clay at the Martin's Point Bridge site.

$N_{kt(CAUC)}$  values from SCPTu 101 ranged between 11.0 and 18.6 throughout the entire profile.  $N_{kt(CAUC)}$  values from SCPTu 101 vary around a consistent value of approximately 18.0 with depth with occasional decreases in magnitude. These localized decreases were compared to the laboratory testing results of index, consolidation properties, and undrained shear strength properties of samples at these depths, along with the entire profile of the sounding in attempt to identify the cause (or causes) of the decreases. The following factors were identified to cause the decreases in magnitude of  $N_{kt(CAUC)}$  from SCPTu 101 seen throughout the profile at localized depths:

- $N_{kt(CAUC)}$  of 13.1 at 24 ft depth is due to the unusually high  $s_u$  determined from laboratory CAUC testing (see Figure 5.11). It is unclear what caused the high  $s_u$ , however it is possible that the Presumpscot clay at this depth experienced a change in geologic depositional setting and may have been exposed to stresses which stiffened and strengthened the clay, which is consistent with the higher preconsolidation pressure determined at this depth.
- $N_{kt(CAUC)}$  of 13.2 and 11.0 at depths 34.1 and 40.7 ft, respectively, were both caused by localized decreases in corrected tip resistance ( $q_t$ ) at these depths evident in Figure 5.16. The decreases in  $q_t$  indicate a softer seam of clay (less resistance to penetration), and would intuitively be accompanied by a decrease in  $s_u$ , which does not occur in the CAUC results, therefore the  $N_{kt(CAUC)}$  values decrease.

Further analysis of the  $N_{kt(CAUC)}$  and  $N_{\Delta u(CAUC)}$  factors from all three soundings yielded a pattern of consistent values between SCPTu 101 and 104, where  $N_{kt(CAUC)}$  and  $N_{\Delta u(CAUC)}$  values from SCPTu 103 are generally lower than both of the other soundings throughout the entire profile, with the exception of  $N_{kt(CAUC)}$  at 40.7 ft being 11.7 for SCPTu 104 and 11.0 for SCPTu 101. The lower calculated values for SCPTu 103, which subsequently estimates a higher  $s_u$ ,



matches the conclusion presented in the previous stress history analysis (Section 5.3.3) where the Presumpscot clay at the location of SCPTu 103 is less consolidated and weaker in undrained shear than the clay at the location of the other soundings. In result, the  $s_u$  used to correlated the  $N_{kt(CAUC)}$  and  $N_{\Delta u(CAUC)}$  factors is high compared to the in situ strength, and therefore causes the ratio of tip resistance or pore pressure to  $s_u$  (i.e.  $N_{kt(CAUC)}$  and  $N_{\Delta u(CAUC)}$ ) to be reduced, hence lower values.

Figure 5.26 presents estimated  $s_u$  profiles using the resulting average, minimum, and maximum  $N_{kt(CAUC)}$  and  $N_{\Delta u(CAUC)}$  values from SCPTu 101 compared to the laboratory-determined  $s_u$ .

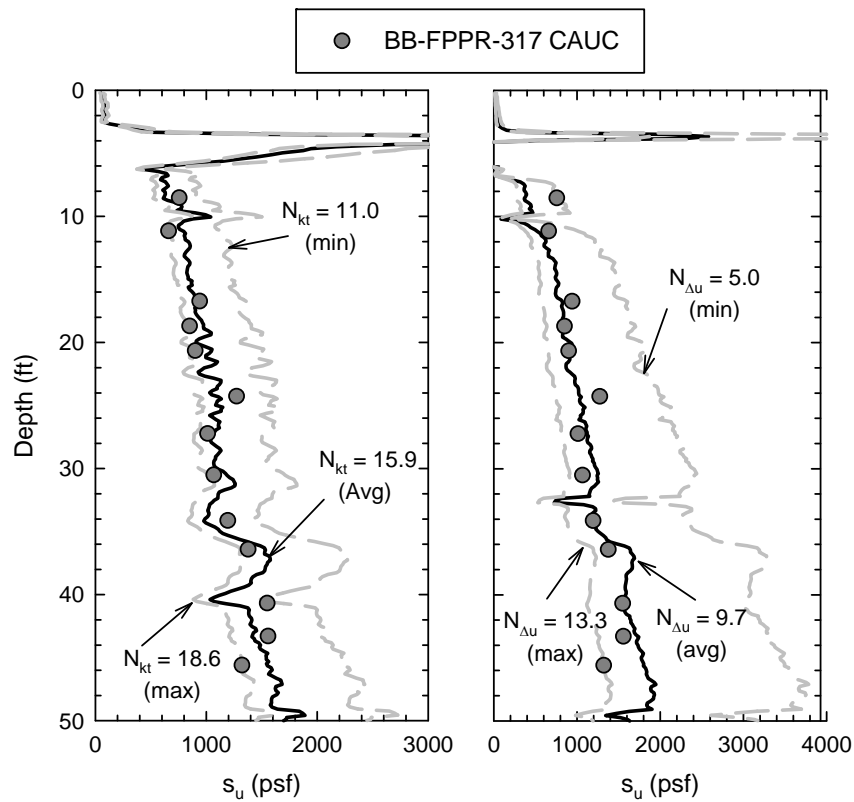


Figure 5.26: Profile of undrained shear strength of Presumpscot clay at Martin's Point Bridge using empirical cone factors  $N_{kt(CAUC)}$  and  $N_{\Delta u(CAUC)}$  applied to SCPTu 101.

For both profiles, the average  $N_{kt(CAUC)}$  or  $N_{\Delta u(CAUC)}$  predicted slightly higher  $s_u$  than the maximum value. Conversely, the minimum  $N_{kt(CAUC)}$  or  $N_{\Delta u(CAUC)}$  values overestimated  $s_u$  profiles using CPTu data. This illustrates the importance of selecting an appropriate  $N_{kt(CAUC)}$  and  $N_{\Delta u(CAUC)}$  to apply to a particular sounding.

Figure 5.27 presents values of  $N_{kt(FVT)}$ ,  $N_{ke(FVT)}$ , and  $N_{\Delta u(FVT)}$  with depth using field vane shear testing (FVT)  $s_u$  results paired with measurements from SCPTu 101. SCPTu 101 was chosen because it was the closest SCPTu sounding to the conducted FVT. Refer to Table 5.13 for distances between the FVT borings and SCPTu 101. FVT borings BB-FPPR-108 and BB-FPPR-109 were excluded from the analysis as both of the borings were conducted from the old bridge deck and required extra lengths of rod, which in turn may have increased rod friction and decreased  $s_u$ .  $N_{kt(FVT)}$  ranged from 8.6 to 41.0 with an average of 15.4.  $N_{\Delta u(FVT)}$  ranged from 0.4 to 18.0 with an average value of 8.3. Coefficient of variation (COV) ranged from 0.16 to 0.50 for  $N_{kt(FVT)}$  and from 0.22 to 0.48 for  $N_{\Delta u(FVT)}$ . A summary of these values is presented in Table 5.14. Above 12 ft depth,  $N_{kt(FVT)}$  is variable, ranging from 8.3 to 21.6, whereas  $N_{\Delta u(FVT)}$  remained within a narrow range of values between approximately 7.0 and 13.0. From 12 ft to approximately 30 ft, both  $N_{kt(FVT)}$  and  $N_{\Delta u(FVT)}$  remained within a narrow range of values and appeared to be constant with depth. Below 30 ft depth,  $N_{kt(FVT)}$  and  $N_{\Delta u(FVT)}$  both became scattered with depth but illustrated an increasing trend with depth.

As expected, cone factors  $N_{kt(FVT)}$  and  $N_{\Delta u(FVT)}$  illustrated more scatter than  $N_{kt(CAUC)}$  and  $N_{\Delta u(CAUC)}$  due to the wider range of  $s_u$  values from the FVT as compared to the CAUC laboratory test (Figure 5.11). However, even with a wider range of values, the average  $N_{kt(FVT)}$  and  $N_{\Delta u(FVT)}$  yielded values similar to  $N_{kt(CAUC)}$  and  $N_{\Delta u(CAUC)}$  average values.  $N_{kt(FVT)}$  and  $N_{kt(CAUC)}$  average values from SCPTu 101 are 15.4 and 15.9 respectively, where  $N_{\Delta u(FVT)}$  and  $N_{\Delta u(CAUC)}$  average values are 8.3 and 7.4 respectively. It appears from the comparison of both cone factors, that utilizing the

average value from FVT and CAUC testing results at the Martin’s Point Bridge provides similar estimates of  $s_u$  profiles when applied to the SCPTu soundings. As the number of FVT increases, the influence of outlier values and/or erroneous results from poor testing methods become less pronounced, and the averaged  $s_u$  profile approaches that of the laboratory tested conditions. It appears that the number of FVT performed at the Martin’s Point Bridge site was adequate enough to properly correlate to  $N_{kt}$  and  $N_{\Delta u}$  values for  $s_u$  profiling.

Table 5.13: Distances between SCPTu 101 and field vane shear test borings of the Presumpscot clay at the Martin's Point Bridge site.

(S)CPTu Sounding	Corresponding Boring	Sounding to Boring Distance (ft)
SCPTu 101	BB-FPPR-108	107.2
	BB-FPPR-109	218.9
	BB-FPPR-208	205.3
	BB-FPPR-311	53.1
	BB-FPPR-311A	60.2
	BB-FPPR-312	34.7
	BB-FPPR-313	38.8
	BB-FPPR-316	11.9

Inspection of Figure 5.26 illustrates the applicability of average  $N_{kt}$  and  $N_{\Delta u}$  to appropriately represent  $s_u$  profiles at the Martin’s Point Bridge. The  $s_u$  profile predicted from both the average  $N_{kt}$  and  $N_{\Delta u}$  follows the laboratory profile closely with the exception of the bottom three tested samples in the  $N_{\Delta u}$  profile. Excluding these bottom three samples,  $s_u$  predicted from the laboratory and the  $N_{kt(CAUC)}$  CPTu profiles ranges in percent difference from -16% to 20%. On the

Table 5.14: Summary of  $N_{kt(FVT)}$  and  $N_{\Delta u(FVT)}$  values, averages, and coefficient of variations from the FVT results in the Presumpscot clay at Martin's Point Bridge using SCPTu 101.

FVT Boring	Distance from SCPTu 101 (ft)	No. of tests	Strength Factor $N_{kt}$			Strength Factor $N_{\Delta u}$		
			Range	Average	COV	Range	Average	COV
BB-FPPR-208	205	11	14.2-25.9	18.2	0.22	0.5-18	10.5	0.48
BB-FPPR-311	53	9	13.4-41	17.7	0.50	5.7-11.5	9.1	0.22
BB-FPPR-311A	60	4	12.4-21.3	16.5	0.25	4.7-12.3	8.0	0.40
BB-FPPR-312	35	6	10.1-16.6	12.5	0.21	3.6-9.5	6.3	0.36
BB-FPPR-313	39	8	8.6-15.8	12.6	0.23	3.1-9.6	7.2	0.36
BB-FPPR-316	12	15	10.8-19.6	15.0	0.16	0.4-14	8.8	0.39

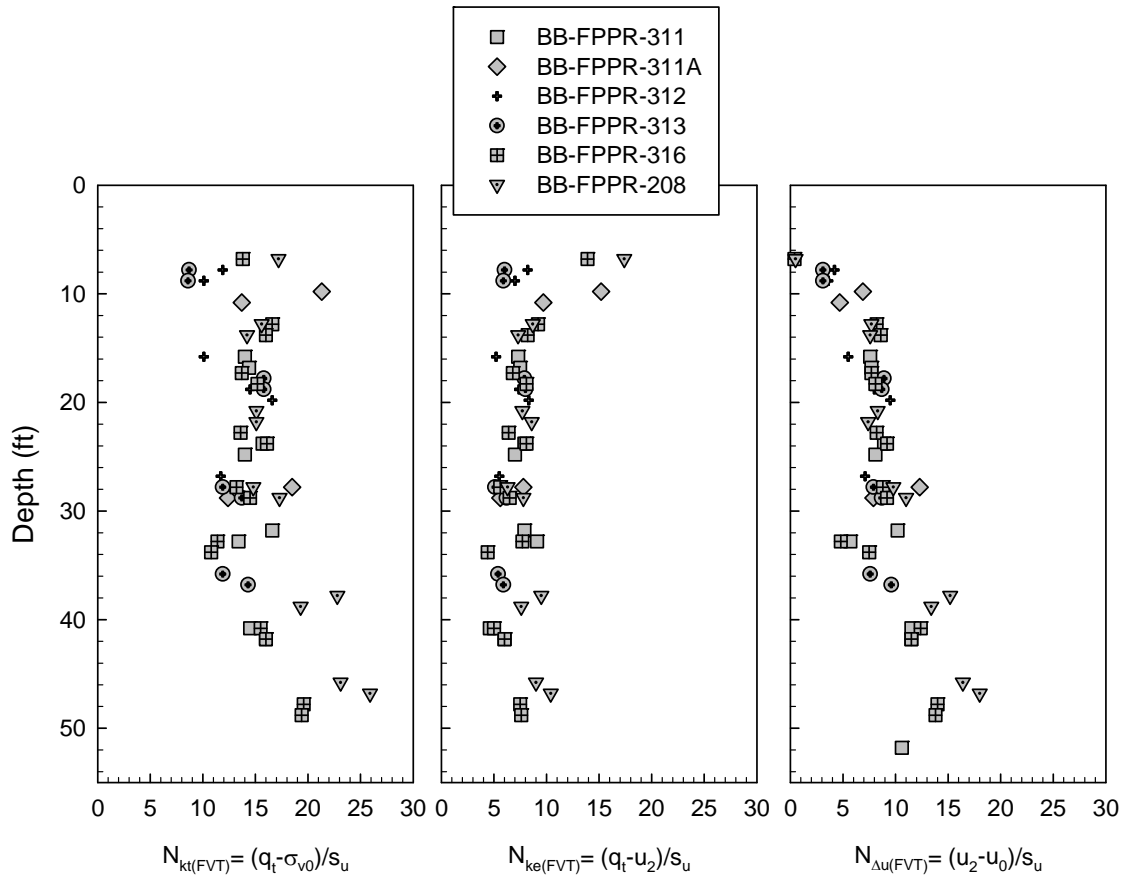


Figure 5.27: Subsurface profiles of  $N_{kt(FVT)}$ ,  $N_{\Delta u(FVT)}$ , and  $N_{ke(FVT)}$  correlated from SCPTu-101 and field vane shear testing (FVT) from borings conducted in Presumpscot clay at Martin's Point Bridge.

other hand,  $N_{\Delta u(CAUC)}$  ranged from -17% to 65% (still excluding the bottom three samples) when compared to laboratory results, generally over predicting  $s_u$  more than the  $N_{kt(CAUC)}$  cone factor. It appears that  $N_{kt(CAUC)}$  value of 15.9 is the most appropriate correlation to use for  $s_u$  profiles estimates using CPTu data at the Martin's Point Bridge.

In summary,  $N_{kt(CAUC)}$  ranged from 9.3 to 22.1 with an average value of 15.9 (SCPTu 101) and  $N_{\Delta u(CAUC)}$  ranged from 5.0 to 13.3 with an average value of 7.4 (SCPTu 101). Both cone factors remained within published averages of values for similar testing of clays.  $N_{kt(FVT)}$  and  $N_{\Delta u(FVT)}$  yielded a much larger scatter of values, but ultimately averaged at 15.4 and 8.3, respectively, agreeing well with the CAUC cone factors.  $N_{kt}$  provided more consistent  $s_u$  predictions compared to laboratory data than  $N_{\Delta u}$  when using the average values, therefore it appears that utilizing an  $N_{kt}$  of 15.9 applied to the SCPTu profile at Martin's Point Bridge yielded the most effective prediction of  $s_u$  of the Presumpscot clay.

## 6 ROUTE 197 BRIDGE SITE

### 6.1 Site Overview

The Route 197 Bridge (Figure 6.1 and Figure 6.2) carries Route 197 between the towns of Richmond and Dresden over the Kennebec River in Maine. The bridge was completed in November of 2014, replacing the 1931 bridge. The newly constructed bridge is located approximately 75 feet north (upstream) of the old bridge alignment. Instead of a pivoting section to allow for watercraft passage, which is the system the old bridge used, the new bridge is built to provide a permanent 75 foot clearance. The new bridge is supported by 6 piers spaced 240 feet apart.



Figure 6.1: Aerial image of the Richmond Dresden Bridge site Route 197 Bridge site showing recent construction of the new bridge on the north side of the existing bridge structure (Google Earth, 2014)



Figure 6.2: Image of the new bridge during construction in the foreground with the old bridge in the background (centralmaine.com, 2014)

### 6.1.1 Geotechnical Investigation

Two geotechnical investigations were conducted at the Route 197 Bridge for the design and construction of the new bridge. The first investigation was performed in November and December of 2011 (MaineDOT, 2011). This investigation included nine test borings drilled within the approximate proposed bridge alignment, using cased wash boring and solid stem auger techniques. For over-water borings, a CME 45 skid rig on an anchor barge was used. During this investigation, Presumpscot clay was encountered in Borings BB-RDKR-103, -104, and -105 near the middle of the Kennebec River channel at the location of a proposed pier. A total of 12 Field vane shear tests (FVT) were performed in BB-RDKR-104 at various depths within the Presumpscot layer. Split spoon samples were also collected throughout the layer for visual classification and index testing of the Presumpscot clay at alternating depths of the FVT.

The second geotechnical investigation was performed in June of 2012 as part of the final phase investigation for the new bridge (Golder, 2011). Nine additional test borings were drilled and nine cone penetration tests with seismic measurements (SCPTu) were conducted along the proposed bridge alignment. Two of the borings (BB-RDKR-206 and -207) and one of the SCPTu profiles (SCPTu 109) were performed within a deeper portion of the Presumpscot clay deposit in the river channel. A CME 45 drill rig on an anchor barge with cased wash borings was used for the drilling of borings BB-RDKR-206 and -207. Continuous Shelby tube samples were collected during BB-RDKR-206 using modified Shelby tubes and a Gregory Undisturbed Sampler (GUS) with drilling mud ranging in density from 70 to 73 pcf. Field vane shear testing (FVT) was performed at 5 different depths within the Presumpscot clay during the drilling of BB-RDKR-207. SCPTu 109 was conducted using a B-53 drill rig on a spud barge. Refer to Section 6.3 for the SCPTu testing procedure. Figure 6.3 shows the interpretive subsurface profile created by the MaineDOT (2011) with the approximate location of Boring BB-RDKR-206 and SCPTu 109 added.

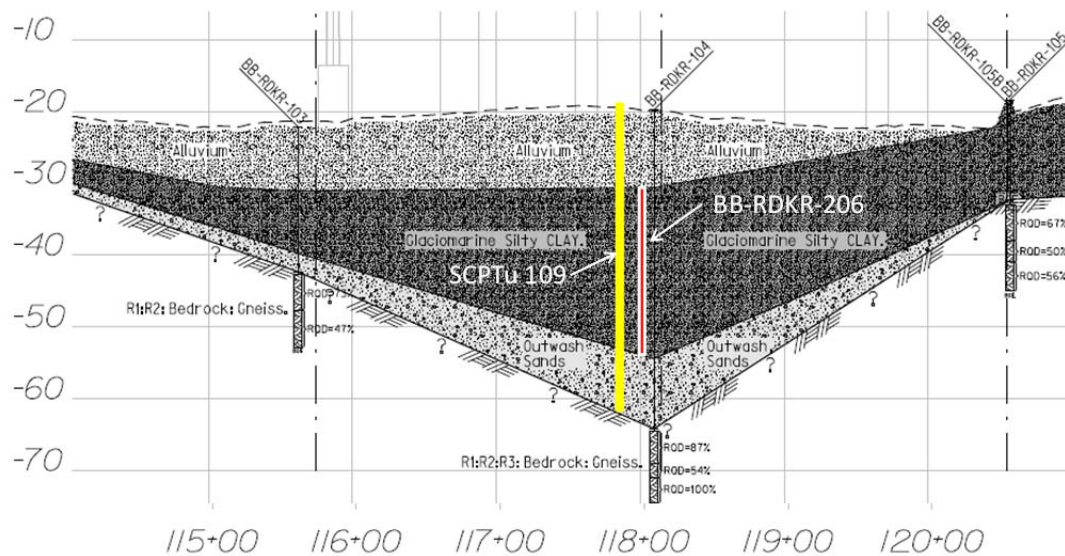


Figure 6.3: Interpretive subsurface profile at the Route 197 Bridge showing the approximate location of Boring BB-RDKR-206 and SCPTu 109 (after MaineDOT, 2011). Note: the elevation in feet is shown on the left of the figure and the station in feet is shown on the bottom.



The field testing and sample collection of the Presumpscot clay at Route 197 Bridge used in this study include the FVT results from Borings BB-RDKR-104 and -207, the modified Shelby tubes collected during BB-RDKR-206, and SCPTu 109. The tube samples were all transported to the UMaine Advanced Geotechnics Laboratory for the purpose of conducting testing for this research.

### 6.1.2 Site Geology

The Presumpscot clay deposit at the Route 197 Bridge site is thickest in the middle of the river channel and thins out towards each shoreline. Directly below the Presumpscot clay is a layer of outwash sand which is atop bedrock. Overlying the Presumpscot clay is a layer of alluvial sand.

The outwash sand and Presumpscot clay at the site was deposited on the ocean floor during the last deglaciation of the Laurentide ice sheet as it retreated. The underlying outwash sands were deposited before the Presumpscot clay. As the meltwater from the ice sheet discharged into the ocean, it caused turbulence in the marine water, pushing fine-grained soils (silt and clay) further away from the glacier margin, while the sand settled. Once the glacier retreated further northward, the turbulence of the ocean at the location of the current Route 197 Bridge site decreased and the fine grained sediments (Presumpscot clay) were able to settle out. The alluvial sand deposit overlying the Presumpscot clay is a postglacial deposit resulting from soil transported by the Kennebec River.

## 6.2 Laboratory Characterization

Ten modified Shelby tube samples of Presumpscot clay were collected at the Route 197 Bridge site for testing at the UMaine Advanced Geotechnics Laboratory. Each tube sample was tested for index properties (moisture content, Atterberg Limits, grain size, organic content, specific gravity, and index undrained shear strength), consolidation properties, and undrained

shear strength properties. Testing methods used were in general accordance with ASTM standards and are discussed in Chapter 3.

### 6.2.1 Index Test Results

Ten Shelby tube samples of Presumpscot clay were collected at the Route 197 Bridge for testing at the UMaine Advanced Geotechnics Laboratory. Samples were collected during Boring BB-RDKR-207 from depth 12.0 feet to 33.0 feet continuously. A sand seam was encountered during the sampling of tube 6U which caused the samples to become disturbed, therefore the tube sample was discarded. All collected tubes were sealed and transported back to the University of Maine in temperature and moisture controlled storage. Figure 6.4 illustrates the portion of each tube sample used for testing. Blank spaces in the figure indicate specimens which became disturbed upon extraction and were not tested or specimens which were tested but later superseded by a higher quality specimen from the same tube.

Natural water content, Atterberg Limits (liquid limit, LL; plastic limit, PL; plasticity index, PI; and liquidity index, LI), and Activity (the ratio of plasticity index to the % grain size finer than 0.002 mm, or clay fraction) values are summarized in Table 6.1. Grain size, organic content, total, dry, and solids unit weights, and Unified Soil Classification System (USCS) designations are tabulated in Table 6.2. All index testing results are presented with depth in Figure 6.5.

Water content ranges from 42.3% at 14 ft to 26.7% at 33 ft and generally decreases with depth. Plastic limit is consistent with depth throughout the deposit, ranging between 17 and 22 above 30 feet. Below 30 ft, increasing sand content (particularly the sand seams, which are identified by the CPTu results in Figure 4.10) results in decreases in plasticity. The deepest sample, 11U, could not be tested for Atterberg Limits because the sand content was too high and

		1U 19"	2U 23"	3U 24"	4U 23"	5U 22"
Shelby Tube = 24" of Soil						
	3.5" CAUC TX 19	3.5" CAUC TX 24	3.5" CAUC TX 25	3.5" CAUC TX 26	3.5" CAUC TX 27	
	2" CRS 61	2" CRS 59	2" CRS 62	2" CRS 63	2" CRS 64	
	3" Index Testing	3" Index Testing	3" Index Testing	3" Index Testing	3" Index Testing	
		7U 24"	8U 24"	9U 22"	10U 24"	11U 21"
Shelby Tube = 24" of Soil						
			3.5" TX 35 SHAN OCR5			4.25" CAUC TX32
			3.5" TX 34 SHAN OCR2	4.25" CAUC TX 30	3.5" CAUC TX 31	2.5" CRS 73
		2" CRS 83	3.5" TX 33 SHAN OCR1			
		3.75" CAUC TX 28	3.5" CAUC TX 29		2.5" CRS 72	
			2" CRS 68	2" CRS 69		
	3" Index Testing	3" Index Testing	3" Index Testing	3" Index Testing	3" Index Testing	

Figure 6.4: Sample usage for laboratory testing of the collected tube samples of Presumpscot clay at the Route 197 Bridge site.

was categorized as non-plastic (NP). Liquid limit ranged from 40 at 14 ft to 33 at 29 ft, generally decreasing with depth. Sample 7U had an outlier liquid limit value of 44.

Figure 6.6 presents the plasticity index test results plotted with clay fraction (Figure 6.6a) and liquid limit (Figure 6.6b). As discussed in Section 2.1.2, the Kaolinite is not present in the Presumpscot clay; rather the dominant clay mineral found is illite. The cause of this misclassification in Figure 6.6b derives from the false clay fraction estimated from the hydrometer results as the rock flour is smaller than 0.002 mm and is therefore incorporated into the clay fraction.

Clay and rock flour content decreases with depth and sand content increases with depth. Silt content remains generally constant with depth except for sample 7U, which had a value of 63.2%. Clay and rock flour content ranges from 56.5% at 14 feet to 25.6% at 33 feet. Silt content ranges from 43.4% at 14 feet to 50.3% at 26.9 feet (excluding 7U). Sand content ranges from 0.2% at 14 feet to 26.4% at 32.9 feet. Organic content of the Presumpscot clay remains between 1% and 3%. Properties of the clay are not significantly affected by the organic content at this low of a concentration (Mitchell and Soga, 2005). Sample 11U did not have enough clay content to perform Atterberg Limit testing,

Sensitivity of the Presumpscot clay at Route 197 Bridge site (Figure 6.5) measured using the fall cone apparatus ranges from 7.5 to 45.0 with no apparent trend with depth. Soils having sensitivity between 2 and 8 are considered low to medium sensitivity, 8 to 16 are highly sensitive, and greater than 16 are quick clays (Holtz *et al.*, 2011). The deposit is considered highly sensitive to quick. Table 6.3 presents the fall cone results for BB-RDKR-206 samples. The deepest sample which classified as “quick” may have resulted in a high initial  $s_u$  due to the high sand content increasing the frictional resistance and a subsequent low  $s_{u(r)}$  when the sample was remolded, ultimately causing a high sensitivity.

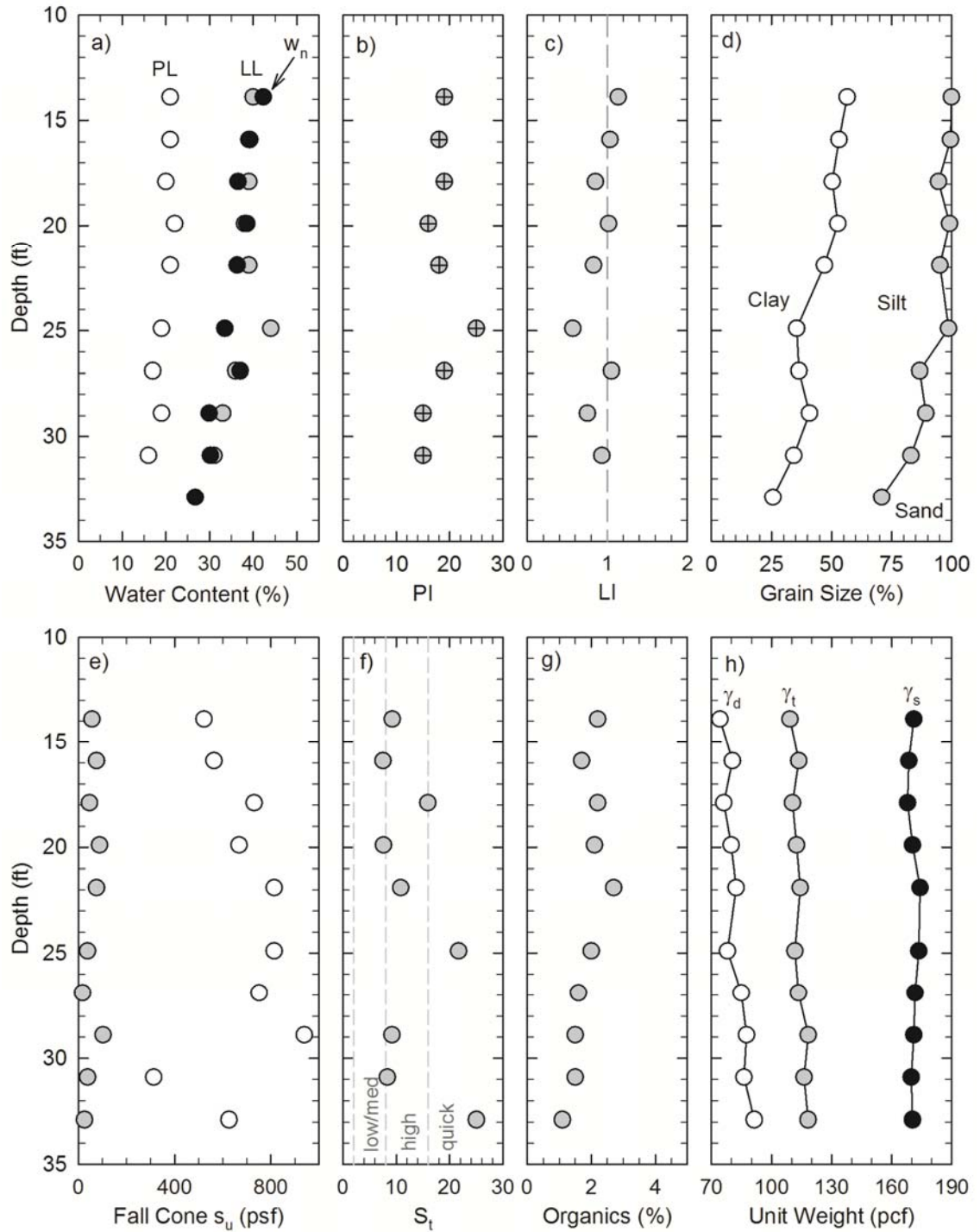


Figure 6.5: Laboratory determined results of a) natural water content, b) plasticity index, c) liquidity index, d) grain size distribution, e) index undrained and remolded shear strength from the fall cone apparatus, f) sensitivity from fall cone results, g) organic content, and h) unit weight (total, dry, and solids) of Presumpscot clay from BB-RDKR-206 performed at the Route 197 Bridge site.

Table 6.1: Summary of Atterberg Limit plasticity data for Presumpscot clay samples tested from BB-RDKR-206 conducted at the Route 197 Bridge site.

Sample	Depth (ft)	w <sub>n</sub> (%)	LL	PL	PI	LI
1U	13.9	42.3	40	21	19	1.14
2U	15.9	39.2	39	21	18	1.03
3U	17.9	36.5	39	20	19	0.85
4U	19.9	38.5	38	22	16	1.02
5U	21.9	36.3	39	21	18	0.83
7U	24.9	33.5	44	19	25	0.57
8U	26.9	37	36	17	19	1.05
9U	28.9	29.9	33	19	15	0.75
10U	30.9	30.2	31	16	15	0.93
11U	32.9	26.7	NP	NP	NP	NP

Note: NP = non-plastic

Table 6.2: Summary of grain size distribution, density, and USCS classification for Presumpscot clay samples tested from BB-RDKR-206 conducted at the Route 197 Bridge site.

Sample	Depth (ft)	Gravel (%)	Sand (%)	Silt (%)	Clay (%)	Organics (%)	$\gamma_t$ (pcf)	$\gamma_d$ (pcf)	$\gamma_s$ (pcf)	USCS (ASTM D2487)
1U	13.9	0.0	0.2	43.4	56.5	2.2	109	74	171	Lean Clay (CL)
2U	15.9	0.0	0.5	46.4	53.1	1.7	114	81	169	Lean Clay (CL)
3U	17.9	0.0	5.5	44.2	50.3	2.2	111	76	168	Lean Clay (CL)
4U	19.9	0.0	0.9	46.5	52.6	2.1	113	80	170	Lean Clay (CL)
5U	21.9	0.0	4.9	48.1	47.0	2.7	114	82	174	Lean Clay (CL)
7U	24.9	0.0	1.4	63.2	35.5	2.0	112	78	174	Lean Clay (CL)
8U	26.9	0.4	12.8	50.3	36.4	1.6	113	85	172	Lean Clay (CL)
9U	28.9	0.0	10.7	48.4	40.8	1.5	118	88	171	Lean Clay (CL)
10U	30.9	0.0	17.0	48.7	34.3	1.5	116	86	170	Lean Clay (CL) w/ Fine Sand
11U	32.9	2.7	26.4	45.3	25.6	1.1	118	91	170	Silty Clay (CL) w/ Sand & Gravel

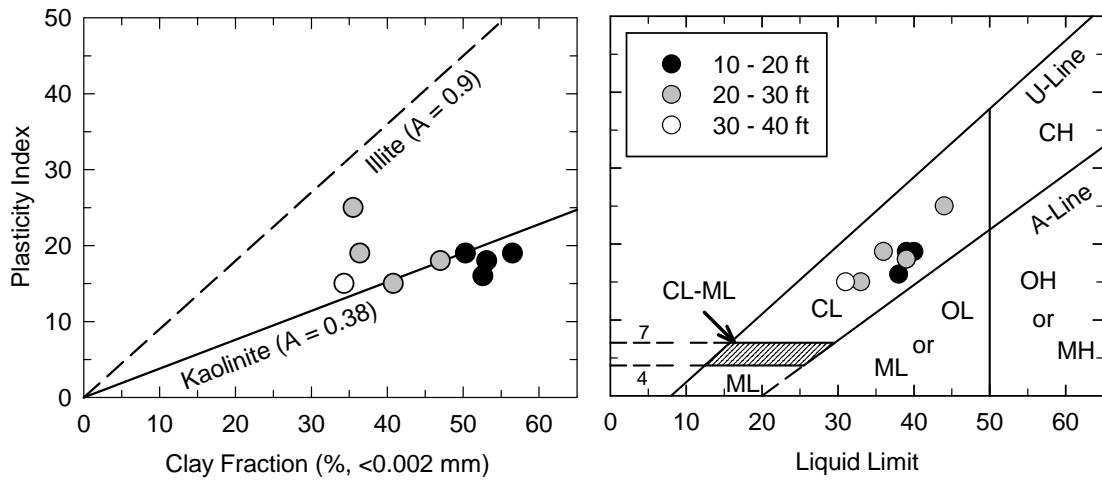


Figure 6.6: Plasticity data from laboratory testing of Presumpscot clay samples collected from Boring BB-RDKR-206 plotted on USCS Classification Charts at the Route 197 Bridge site.

Table 6.3: Summary of fall cone undrained shear strength and sensitivity results for tested samples of Presumpscot clay collected from Boring BB-RDKR-206 at the Route 197 Bridge site.

Sample	Depth (ft)	Intact $s_u$ <sup>1</sup> (psf)	Intact Cone	$s_{ur}$ <sup>2</sup> (psf)	Remolded Cone	$S_t$ <sup>3</sup>
1U	13.9	522	100g 30°	56	60g 60°	9.3
2U	15.9	564	100g 30°	75	60g 60°	7.5
3U	17.9	731	100g 30°	46	60g 60°	15.9
4U	19.9	668	100g 30°	88	60g 60°	7.6
5U	21.9	815	100g 30°	75	60g 60°	10.8
7U	24.9	815	100g 30°	38	60g 60°	21.7
8U	26.9	752	100g 30°	17	10g 60°	45.0
9U	28.9	940	100g 30°	102	60g 60°	9.2
10U	30.9	313	100g 30°	38	60g 60°	8.3
11U	32.9	627	400g 30°	25	60g 60°	25.0

Note: <sup>1</sup>intact undrained shear strength; <sup>2</sup>remolded; <sup>3</sup>Sensitivity ( $s_u/s_{ur}$ )

Overall index test data show the following trends for the Presumpscot clay at the Route 197 Bridge:

- There is a general decrease in plastic limit, PL, liquid limit, LL, and plasticity index, PI, with depth that correlates well with a decrease in clay content and possibly organic content (although the latter is low and likely has little effect on soil properties and behavior).
- Sensitivity correlates loosely with water content, where low water content soils are less sensitive. This is because the remolded undrained shear strength and undisturbed undrained shear strength both increase with decreasing water content.
- Void ratio generally follows the trend of clay content, where soils with higher void ratios typically have higher clay content.
- The soil at the lower depths of the deposit has sand seams

## 6.2.2 One Dimensional Consolidation Results

Constant rate of strain (CRS) consolidation testing was performed on Presumpscot clay specimens trimmed from the 10 Shelby tube samples at the Route 197 Bridge site in general accordance with the procedures described in Section 3.4.3. Specimens were mainly of very good to excellent quality with the exception of two good to fair quality specimens and two poor quality specimens. Table 6.4 presents specimen information of each tested specimen, change in void ratio upon recompression for sample quality designation, and results of the consolidation testing including preconsolidation pressure (determined using the Becker *et al.*, 1987 method), overconsolidation ratio (OCR), coefficient of consolidation and coefficients of compressibility.



Preconsolidation pressure ( $\sigma'_p$ ), initial void ratio ( $e_0$ ), and sample quality designation are illustrated with depth in Figure 6.7.

$\sigma'_p$  generally increases with depth within the deposit from 3,970 psf at 13.7 feet to 5,640 psf at 26.7 feet and then generally decreases with depth to 3,560 psf at 31.9 feet. The increase in  $\sigma'_p$  with depth observed in the upper portion of the soil is consistent with increased overburden stress as overlying material increases. The decreasing trend following 27 ft is likely the result of lower clay content and the rounding of the compression curve that makes delineation of  $\sigma'_p$  less precise. The soil is overconsolidated and overconsolidation ratio decreases with depth from 5.8 to 2.2 over the profile. The overconsolidation at the site is likely from the removal of overburden soils and does not have an anthropomorphic origin. At the Route 197 Bridge site, the only bridge elements close enough to stress the Presumpscot clay deposit are the piers near the middle of the span, which are pile supported (Maine DOT, 2012). Since pile-supported elements transfer the load directly to the bedrock without loading the clay, the bridge piers likely did not cause increased OCR values at the site. Thus, the OCR likely derives from geologic deposition at the site which has since been scoured from the riverbed.

Table 6.4: Summary of Constant Rate of Strain (CRS) consolidation specimen properties and sample quality for tested samples of Presumpscot clay collected from Boring BB-RDKR-206 at the Route 197 Bridge site.

Sample (-)	Specimen Information					<sup>1</sup> Sample Quality		Strain	Consolidation Properties					
	Depth (ft)	$\sigma'_{v0}$ (psf)	$w_n$ (%)	$e_0$ (-)	$\gamma_t$ (pcf)	$\Delta e/e_0$ at $\sigma'_{v0}$	NGI Rating	Rate (%/hr)	<sup>2</sup> $\sigma'_p$ (psf)	$k$ (in/s)	$c_v$ @ $\sigma'_{v0}$ (ft <sup>2</sup> /yr)	OCR (-)	$C_r$ (-)	$C_c$ (-)
1U	13.7	683	46.8	1.30	109.3	0.016	VG/E	2.1	3970	$3.9 \times 10^{-8}$	12	5.8	0.07	0.45
2U	15.7	783	40.7	1.12	113.6	0.036	VG/E	1.0	4330	$4.8 \times 10^{-8}$	15	5.8	0.06	0.67
3U	17.8	887	44.7	1.19	110.5	0.012	VG/E	2.1	4520	$3.7 \times 10^{-8}$	18	4.9	0.04	0.43
4U	19.7	983	40.7	1.12	112.5	0.026	VG/E	2.1	5020	$2.6 \times 10^{-8}$	13	4.9	0.04	0.43
5U	21.6	1079	38.8	1.11	114.3	0.030	VG/E	2.0	5140	$4.5 \times 10^{-8}$	22	4.6	0.05	0.40
7U	24.7	1232	43.3	1.22	111.8	0.041	G/F	2.0	4350	$2.1 \times 10^{-8}$	5	3.6	0.09	0.43
8U	26.7	1332	33.6	1.02	113.5	0.019	VG/E	2.0	5640	$5.7 \times 10^{-8}$	35	4.2	0.04	0.38
9U	28.7	1432	35.2	0.95	118.3	0.020	VG/E	2.0	4700	$1.8 \times 10^{-8}$	11	3.4	0.05	0.36
10U	30.7	1532	34.8	0.96	116.3	0.065	P	2.0	3910	$4.2 \times 10^{-8}$	16	2.7	0.07	0.32
11U	31.9	1595	29.5	0.86	118.3	0.069	P	2.0	3560	$3.2 \times 10^{-8}$	47	2.2	0.07	0.25

<sup>1</sup>From Lunne et al., (2006), where VG/E: very good to excellent quality, G/F: good to fair, P: poor; <sup>2</sup>Using the Strain Energy Method of Becker et al., (1987)

In general, initial void ratio decreases with depth from 1.30 at the shallowest sample to 0.86 at the deepest sample. Void ratio in the upper 25 feet of the deposit ranged from 1.11 to 1.30 and between 0.86 and 1.02 in the lower portion of the deposit. The decrease of void ratio with depth can be attributed to both increases in overburden stress and increasing sand content. Recompression index ( $C_r$ ) ranges from 0.04 to 0.09. Virgin compression index ( $C_c$ ) ranges between 0.36 and 0.45 and decreases with decreasing clay content with one outlier of 0.67. Soil from deeper within the soil profile has a shallower virgin compression slope due to higher silt and sand content and  $C_c$  was measured as 0.25 and 0.32.

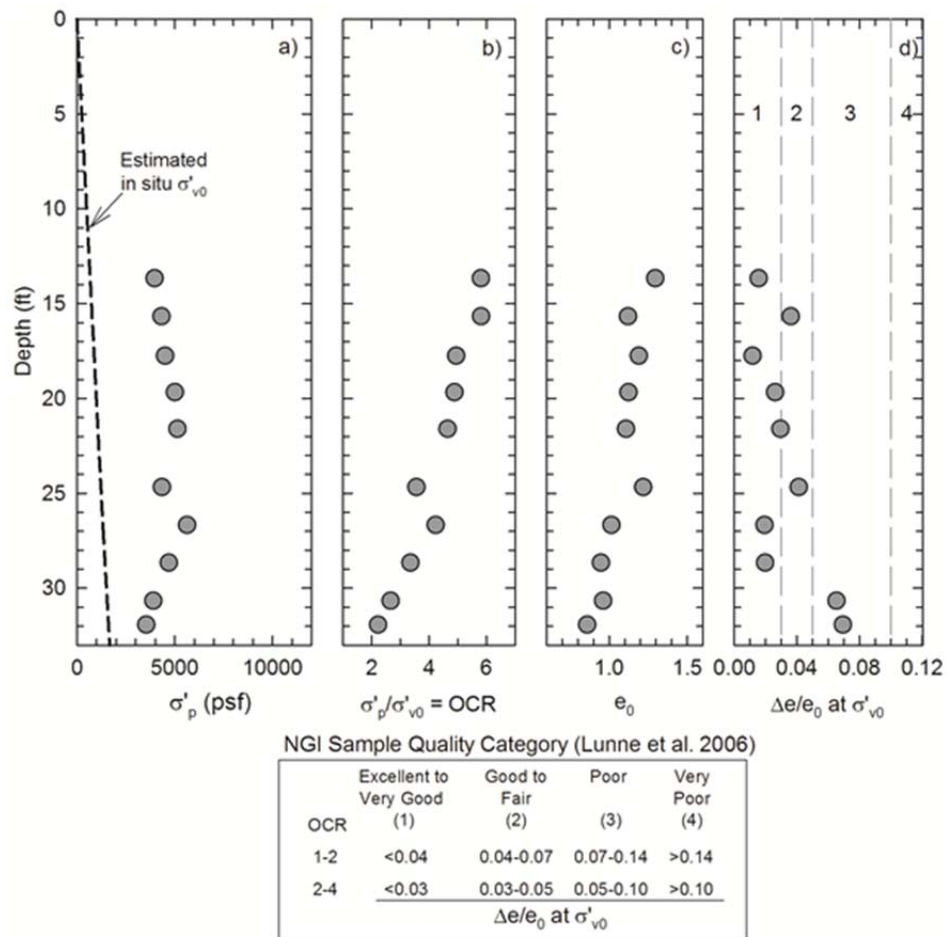


Figure 6.7: Subsurface profiles of a)  $\sigma'_p$ , b) OCR, c) initial void ratio, and d) sample quality assessment from CRS consolidation tests on samples of Presumpscot clay collected from Boring BB-RDKR-206 at the Route 197 Bridge site.

Lastly, coefficient of consolidation determined at the  $\sigma'_{v0}$  for the Presumpscot clay (Section 3.4.3) ranged from 5 ft<sup>2</sup>/year to 47 ft<sup>2</sup>/year, however the most common values measured are between 11 and 22 ft<sup>2</sup>/year. Increased coefficient of consolidation values nearer to the bottom of the deposit are likely due to increased sand and silt content. Permeability values ranged from 1.8 x 10<sup>-8</sup> in/s to 5.7 x 10<sup>-8</sup> in/s with no trend in depth. Considering the increase in sand content with depth, permeability should theoretically increase with depth, but this did not occur in the tested specimens.

Review of Figure 6.7 confirms the expected trends of decreasing OCR and void ratio with depth (as discussed above). Sample quality had a general decrease in quality with depth, indicating that the  $\sigma'_p$  and OCR estimates in the upper portion of the deposit are more reliable than the lower specimens. Lower sample quality represents more disturbance of the natural soil structure, in turn flattening the consolidation curve from the CRS test and a generally lower  $\sigma'_p$  estimate.

### 6.2.3 Recompression Undrained Triaxial Shear

Anisotropically consolidated undrained compression (CAUC) triaxial shear testing was performed on Presumpscot clay specimens from the 10 collected Shelby tube samples from the Route 197 Bridge site in general accordance with the procedures described in Section 3.4.4. Table 6.5 presents specimen properties, conditions following recompression to the estimated  $\sigma'_{v0}$ , sample quality, and pre-shear parameters for the triaxial specimens. Table 6.6 presents results from the shear phase of the testing, including peak shear stress, strain at failure, pore pressure at failure, and shear stress normalized to vertical effective compressive stress. Specimens were mainly of very good to excellent quality, with the exception of one good to fair quality specimen.

Table 6.5: Summary of pre-shear recompression anisotropically consolidated undrained triaxial shear specimen and consolidation properties from Presumpscot clay specimens collected from Boring BB-RDKR-206 at the Route 197 Bridge Site.

In Situ							Laboratory Stress History & Quality									
Sample (-)	Depth (ft)	$w_n$ (%)	$e_0$ (-)	$\sigma'_{v0}$ (psf)	$\sigma'_p$ <sup>1</sup> (psf)	OCR (-)	Est.		$\sigma'_{vc}$ (psf)	$\sigma'_{hc}$ (psf)	$K_c$ <sup>3</sup> (-)	OCR <sub>c</sub> <sup>4</sup> (-)	$\varepsilon_{vol}$ at $\sigma'_{v0}$ (%)	$\varepsilon_a$ at $\sigma'_{v0}$ (%)	$\Delta e/e_0$ (-)	<sup>5</sup> NGI Qual. (-)
							$K_0$ <sup>2</sup> (-)	$e_c$ (-)								
1U	13.5	37.2	1.00	672	3970	5.8	1.21	0.99	500	496	0.99	7.9	0.50	0.14	0.010	VG/E
2U	15.5	38.0	1.02	772	4330	5.8	1.21	1.01	538	465	0.86	8.0	0.47	0.23	0.009	VG/E
3U	17.5	41.3	1.09	872	4520	4.9	1.14	1.08	705	683	0.97	6.4	0.63	0.24	0.012	VG/E
4U	19.4	39.6	1.10	970	5020	4.9	1.13	1.08	1019	982	0.96	4.9	0.77	0.30	0.015	VG/E
5U	21.4	39.2	1.12	1070	5140	4.6	1.11	1.10	840	822	0.98	6.1	0.74	0.32	0.014	VG/E
7U	24.4	43.3	1.26	1219	4350	3.6	1.00	1.23	1074	976	0.91	4.0	1.15	0.59	0.021	VG/E
8U	26.4	36.2	1.02	1321	5640	4.2	1.07	0.98	1339	1315	0.98	4.2	1.23	0.45	0.024	VG/E
9U	27.7	34.7	0.98	1382	4700	3.4	0.97	0.95	1296	1166	0.90	3.6	1.12	0.43	0.023	VG/E
10U	30.1	27.5	0.78	1501	3910	2.7	0.89	0.71	1389	1090	0.78	2.8	2.08	0.57	0.047	G/F

Notes: <sup>1</sup>Best fit profile; <sup>2</sup>Estimated  $K_{0(OC)} = 0.6(OCR)^{0.4}$  (from Ladd et al. 1999); <sup>3</sup> $K_c = \sigma'_{hc}/\sigma'_{vc}$ ; <sup>4</sup>OCR<sub>c</sub> =  $\sigma'_p/\sigma'_{vc}$ ; <sup>5</sup>From Lunne et al., (2006), where VG/E: very good to excellent quality, G/F: good to fair, P: poor, and VP: very poor;

Figure 6.8 presents undrained shear strength ( $s_u$  or  $q_f$ ), undrained shear strength normalized to estimated in situ vertical effective stress ( $s_u/\sigma'_{v0}$ ), and sample quality of the tested specimens. Included in the figure is  $s_u/\sigma'_{v0}$  determined using the fall cone apparatus on unconfined specimens and the natural water content and from nearby FVT for comparison to the CAUC testing results. Figure 6.8 illustrates that  $s_u$  increases with depth up to 26.4 ft. depth, likely due to increasing overburden pressures.  $s_u$  then decreases with depth, likely the result of decreasing OCR. Values of  $s_u/\sigma'_{vc}$  ( $s_u$  normalized by the preshear vertical consolidation stress) ranges from 1.08 to 0.53 (Table 6.6), and shows a general decrease with depth, related to the reduction in OCR with depth. Note that in the tables  $q_f = s_u =$  undrained shear strength.

In situ lateral earth pressure ( $K_0$ ) was estimated using the Ladd *et al.*, (1999) equation with the OCR determined from the CRS testing and a  $K_{0(NC)}$  of 0.60. Table 6.5 shows that there are some differences between the estimated in situ stress history conditions of the Presumpscot clay and those under which the specimens were tested during the CAUC procedure. The cause of the difference in these stresses (i.e.  $\sigma'_{vc} \neq \sigma'_{v0}$  condition) is due to the limitations of the test equipment and is discussed further in Section 3.4.4.

Table 6.6: Summary of recompression consolidated undrained triaxial shear results on tested samples of Presumpscot clay collected from Boring BB-RDKR-206 at the Route 197 Bridge.

In Situ		Laboratory Stress History & Quality					At Failure					
Sample (-)	Depth (ft)	$\sigma'_{vc}$ (psf)	$\sigma'_{hc}$ (psf)	$K_c^3$ (-)	$OCR_c^4$ (-)	$^5NGI$ Qual. (-)	$q_f$ (psf)	$\varepsilon_{a-f}$ (%)	$\Delta u_f$ (psf)	$q_f/\sigma'_{vc}$ (-)	$p_f'/\sigma'_{vc}$ (-)	$q_f/\sigma'_{v0}$ (-)
1U	13.5	500	496	0.99	7.9	VG/E	527	3.1	202	1.05	1.74	0.78
2U	15.5	538	465	0.86	8.0	VG/E	582	2.3	205	1.08	1.54	0.75
3U	17.5	705	683	0.97	6.4	VG/E	683	2.6	377	0.97	1.48	0.78
4U	19.4	1019	982	0.96	4.9	VG/E	780	2.1	510	0.77	1.27	0.80
5U	21.4	840	822	0.98	6.1	VG/E	765	2.4	357	0.91	1.44	0.71
7U	24.4	1074	976	0.91	4.0	VG/E	803	2.5	425	0.75	1.23	0.66
8U	26.4	1339	1315	0.98	4.2	VG/E	877	2.9	713	0.65	1.07	0.66
9U	27.7	1296	1166	0.90	3.6	VG/E	825	3.3	733	0.64	1.02	0.60
10U	30.1	1389	1090	0.78	2.8	G/F	718	3.8	767	0.53	0.84	0.48

Notes: <sup>1</sup>Best fit profile; <sup>2</sup>Estimated  $K_{0(OCR)} = 0.6(OCR)^{0.4}$  (from Ladd et al. 1999); <sup>3</sup> $K_c = \sigma'_{hc}/\sigma'_{vc}$ ; <sup>4</sup> $OCR_c = \sigma'_p/\sigma'_{vc}$ ; <sup>5</sup>From Lunne et al., (2006), where VG/E: very good to excellent quality, G/F: good to fair, P: poor, and VP: very poor;

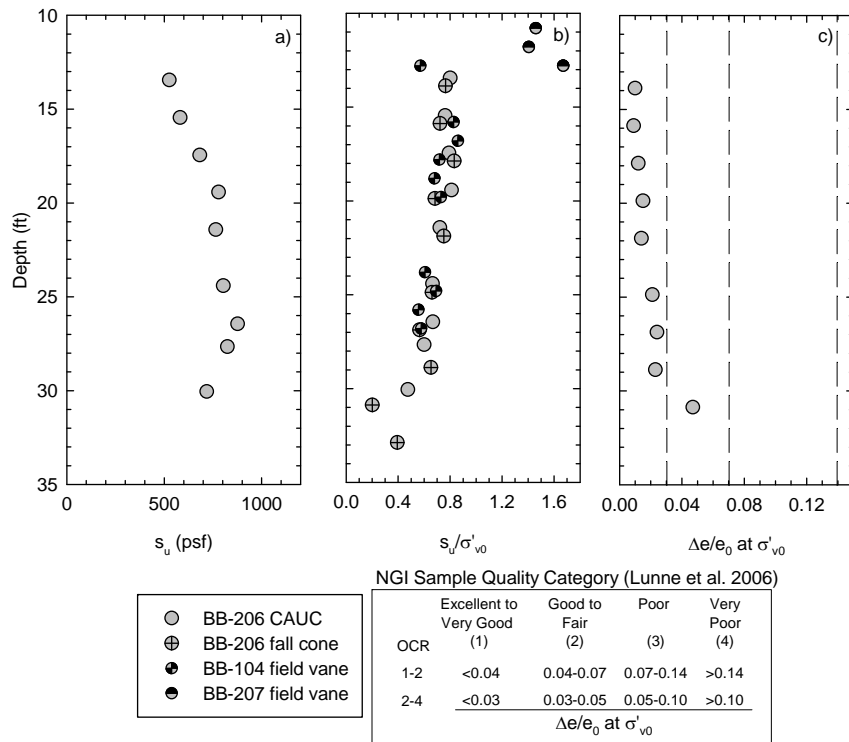


Figure 6.8: Subsurface profile of a) undrained shear strength ( $s_u$ ), b) normalized shear strength and c) NGI sample quality assessment obtained from CAUC triaxial testing on samples of Presumpscot clay collected from Boring BB-RDKR-206 at the Route 197 Bridge.

For almost all of the tested samples, the vertical effective consolidation stress was less than the in situ vertical effective stress leading to OCR of the tested samples to remain lower than in situ conditions. While the effect of these differing conditions are not strictly quantifiable, it is generally assumed that lower  $\sigma'_{vc}$  than  $\sigma'_{v0}$  generates higher measured  $s_u$  (since more of the natural clay structure has been kept intact), therefore, the  $s_u$  measured from the CAUC testing at the Route 197 Bridge site may represent slightly higher values than in situ conditions. As expected, the resulting normalized  $s_u$  is higher when normalized by  $\sigma'_{vc}$  rather than  $\sigma'_{v0}$ .

Typical values of  $s_u/\sigma'_{v0}$  range from 0.2 to 0.3 for normally consolidated clays and increase with OCR, and since the Presumpscot clay at the Route 197 Bridge site is overconsolidated, it is expected to be higher than 0.30. Undrained shear strength normalized by  $\sigma'_{vc}$  ranges from 0.53 to 1.08 while  $s_u/\sigma'_{v0}$  values range from 0.48 to 0.80.

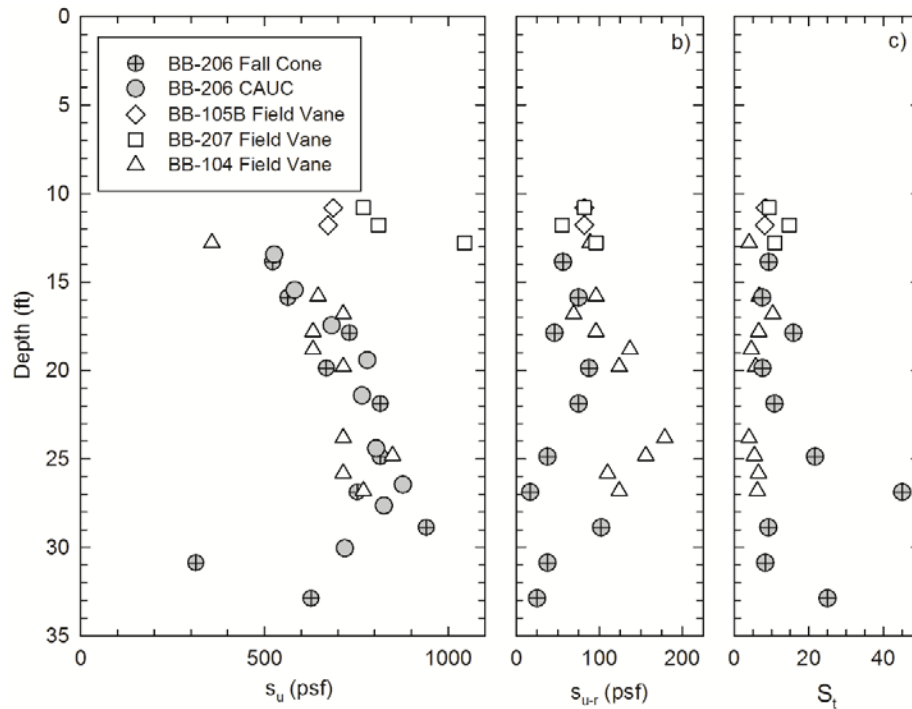


Figure 6.9: Subsurface profile of a) undrained shear strength ( $s_u$ ), b) remolded undrained shear strength and c) and sensitivity from laboratory testing on specimens of Presumpscot clay collected from Boring BB-RDKR-206 at the Route 197 Bridge site.

Review of Figure 6.9 indicated a relatively small scatter between  $s_u$  values measured over the Presumpscot clay profile from CAUC, fall cone (Table 6.3), and field vane shear testing (FVT). FVT during borings BB-RDKR-207 and BB-RDKR-105B was conducted in the top, more overconsolidated region of the deposit, thus the higher  $s_u$  values which may be due to the influence of intermixed alluvium material in the upper portion of the clay. Furthermore, the sensitivity ( $s_u/s_{u(r)}$ ) measured with the fall cone tests indicate the soil a higher sensitivity (values between 7 and 45) compared with field vane shear sensitivities (values between 4 and 10) because of the lower  $s_{u(r)}$  values from fall cone testing. The higher measured  $s_{u(r)}$  values (and subsequently lower sensitivity) from the FVT likely comes from the inability of the FVT procedure to completely remold the clay. Rotating the vane 5 to 10 times (which is typical practice) may leave some of the clay structure intact, and the measured  $s_{u(r)}$  may be higher than that measured from the fall cone test. The complete remolding process is easier in the laboratory during the fall cone procedure. Percent difference of the  $s_{u(r)}$  values between the tests range from approximately 0% to greater than 150%.

Review of test data and normalized stress paths from the recompression triaxial tests (i.e., Figure 6.10) indicated the lightly to moderately overconsolidated specimens generated positive pore pressures during undrained shear (Table 6.6). The normalized effective stress paths illustrated in Figure 6.10 increase to the left and overshoot the failure line with slope before looping downward to the failure line ( $\psi'$ ). This is consistent with overconsolidated and structured soils presented in the literature that experience rapid shifts in pore pressure from low to negative values prior to shear. The  $\psi'$  failure angle ranges from  $32^\circ$  to  $38^\circ$  for the Presumpscot at the test site, assuming a zero  $q = s_u$  intercept (i.e.,  $a = 0$ ). Equation 6.1 can be used to convert p'-q failure characteristics ( $\psi$  and  $a$ ) to Mohr Coulomb failure characteristics ( $\phi$  and  $c$ ). Note that  $p' = (\sigma'_1 + \sigma'_3)/2$  and that  $q = (\sigma'_1 - \sigma'_3)/2$ . Assuming cohesion  $c = 0$ , effective friction angle  $\phi'$  ranges from

38.6° to 51.5°. These values are high compared to many clay soils, but the combination of silt content and overconsolidation likely explains this.

$$\sin \phi = \tan \psi$$

(where  $c = 0$  and  $a = 0$ )

6.1

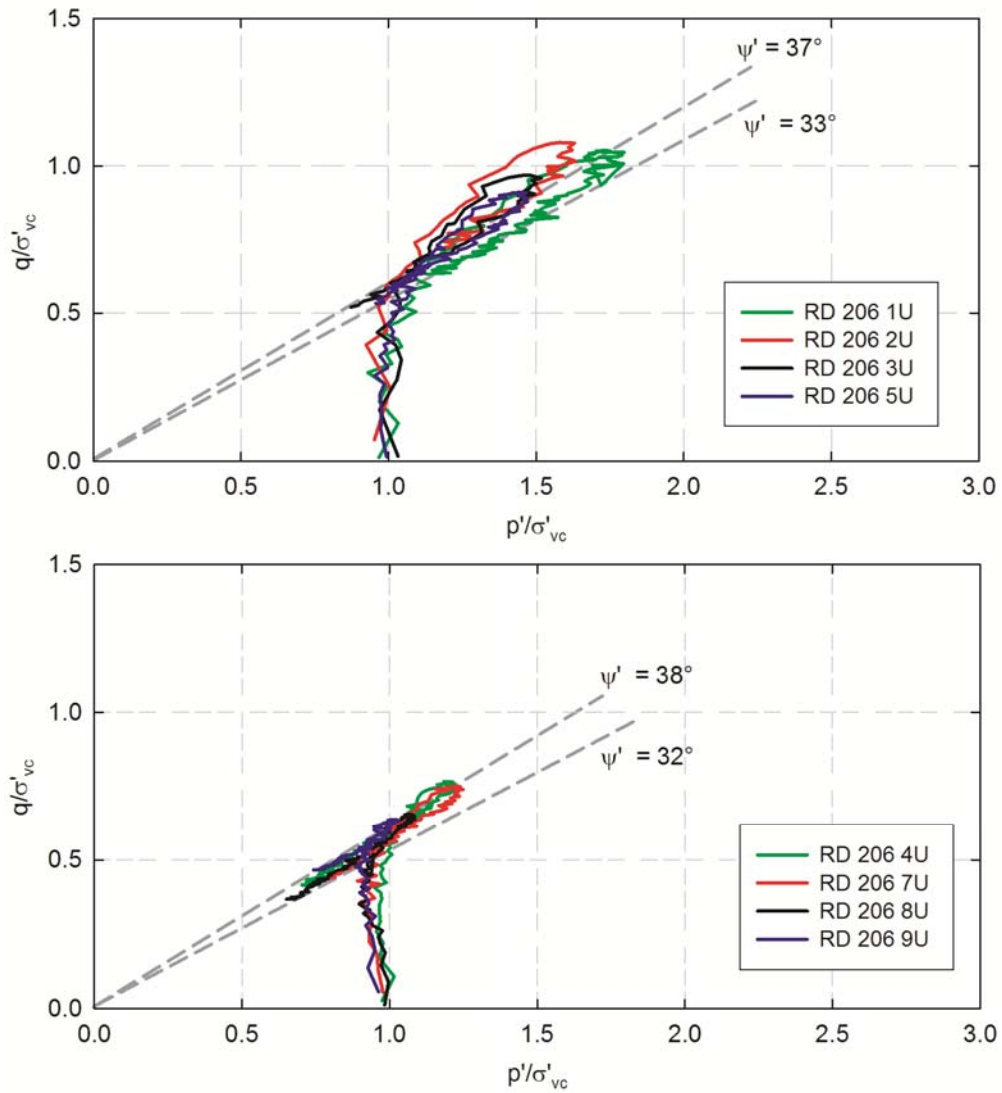


Figure 6.10: Recompression Consolidated Undrained Triaxial (CAUC) Normalized Effective Stress Paths for specimens from BB-RDKR-206 at the Route 197 Bride site.



## 6.2.4 SHANSEP Consolidated Undrained Triaxial Shear

SHANSEP (Stress History and Normalized Engineering Parameters) testing was conducted on Presumpscot clay specimens collected at the Route 197 Bridge site to determine if this type of testing is appropriate for the overconsolidated clay. The testing was performed in accordance with procedures described in Section 3.4.6. SHANSEP testing results provide two empirical coefficients which can then estimate the  $s_u$  at varying values of OCR and  $\sigma'_{v0}$  using Equation 2.1. Table 6.7 presents specimen information and stresses applied to the tested specimens during the consolidation phase, and measurements of pore pressure, shear strength, and normalized shear strength collected at failure during shear. The resulting  $S$  and  $m$  parameters of the OCR  $s_u/\sigma'_{v0}$  analyses are included in the table.

Table 6.7: Summary of Specimen and consolidation properties for SHANSEP undrained triaxial tests conducted on specimens from BB-RDKR-206 Sample 8U at the Route 197 Bridge site.

Depth (ft)	In Situ		Laboratory Stress History					At Failure					Prediction	
	$e_0$ (-)	$\sigma'_{v0}$ (psf)	$\sigma'_{v \max}$ (psf)	$\sigma'_{vc}$ (psf)	OCR ( $\sigma'_p/\sigma'_{vc}$ )	K ( $\sigma'_3/\sigma'_1$ )	$e_c$ (-)	$q_f$ (psf)	$\epsilon_a$ (%)	$\Delta u_f$ (psf)	$q_f/\sigma'_{vc}$ (-)	$p'_f/\sigma'_{vc}$ (-)	S	m
26.1	0.93	1303	10286	10070	1.02	0.59	0.75	2785.1	0.003	1114.2	0.28	0.76	0.27	0.77
25.9	1.08	1291	10044	4936	2.03	0.63	0.85	2416.9	0.01	355.2	0.47	1.00		

Figure 6.11 illustrates the normalized effective stress paths for the BB-206 8U SHANSEP specimens. Using the  $s_u$  at failure (defined as the peak) normalized by the consolidation OCR from the tests, a best-fit trend-line was applied to the resulting normalized shear strength and overconsolidation ratios to determine the two SHANSEP coefficients,  $S$  and  $m$  for Equation 2.1. The specimens were tested as OCRs of 1.02 and 2.03 and resulted in  $s_{u(OCR)}/\sigma'_{vc}$  values of 0.28 and 0.47, respectively. The resulting normalized  $s_u$  for the normally consolidated soil ( $S$ ;  $s_{u(OCR)}/\sigma'_{v0}$  at OCR=1) is 0.27 and the resulting OCR exponent ( $m$ ) is 0.77. The resulting SHANSEP relationship is illustrated in Equation 6.2.

$$s_{u(OCR)}/\sigma'_{v0} = 0.27 \cdot OCR^{0.77}$$

6.2

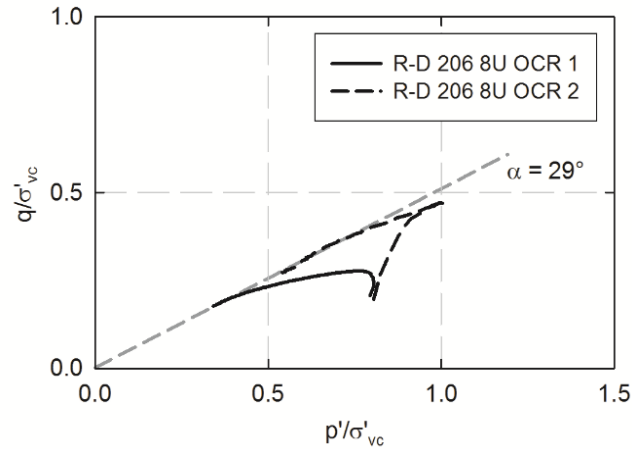


Figure 6.11: SHANSEP Recompression Consolidated Undrained Triaxial (CAUC) Normalized Effective Stress Paths for Presumpscot clay specimens from boring BB-RDKR-206 8U conducted at the Route 197 Bridge.

The SHANSEP  $S$  parameter from this study is more similar to values obtained for Boston blue clay by Ladd et al., (1999) and Landon (2007), (Table 2.2) while the  $m$  overconsolidation exponent from this study is greater than those listed, but more similar to the Boston blue clay study by DeGroot (2003). Overall, the SHANSEP parameters from this study are on the high end of values reported in the literature for similar soils. As discussed previously, the difference between  $\sigma'_{vc}$  and  $\sigma'_{v0}$  will translate to effects on the measured  $s_u$ . Since the SHANSEP testing method increases the  $\sigma'_{vc}$  well beyond  $\sigma'_{v0}$  and the specimen is strained to normally consolidated conditions, none of the clay structure is preserved in the tested specimen. Essentially, the testing procedure attempts to isolate the  $s_u$  in respect only to consolidation stresses (in order to define the  $S$  parameter). However, the specimen which is unloaded to the OCR = 2 conditions develops structure, and the strength increase measured in the sheared specimen is a combination of consolidation stress and clay structure, which is quantitatively encompassed in the SHANSEP equation.

Comparison of measured recompression strengths (from CAUC triaxial compression tests) and SHANSEP predicted strengths normalized by the effective overburden stress with overconsolidation is illustrated in Figure 6.12. The SHANSEP equation developed from lower OCR (1 and 2) specimens over predicts strength over the range of OCR values determined for in situ soil, particularly for the higher OCR soil, when compared with the recompression triaxial shear data.

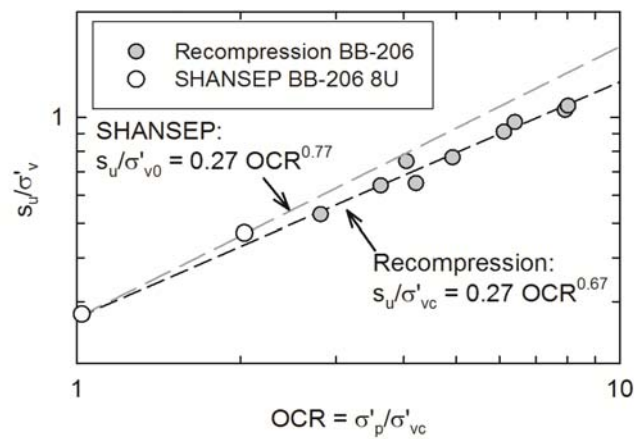


Figure 6.12: Comparison of normalized undrained shear strength from recompression and SHANSEP triaxial compression tests for Presumpscot clay specimens from boring BB-RDKR-206 8U conducted at the Route 197 Bridge site.

### 6.2.5 Summary and Interpretations of Laboratory Testing Results

This section provides a combined analysis of index (Figure 6.5), consolidation stress history (Figure 6.7), and undrained shear strength (Figure 6.8) laboratory testing and a geotechnical synthesis of engineering behavior of the Presumpscot clay at the Route 197 Bridge site. Measured results indicate important trends in the soil deposit, as well as transitions in characteristics and behavior at several locations. Additionally, previous studies and an understanding of regional geologic and glacial activity are important in characterizing the site.

Overall index test data show the following trends for the Presumpscot clay at the Route 197 Bridge:

- There is a general decrease in plastic limit, PL, liquid limit, LL, and plasticity index, PI, with depth that correlates well with a decrease in clay content and possibly organic content (although the latter is low and likely has little effect on soil properties and behavior).
- Sensitivity correlates loosely with water content, where low water content soils are less sensitive. This is because the remolded undrained shear strength and undisturbed undrained shear strength both increase with decreasing water content.
- Void ratio generally follows the trend of clay content, where soils with higher void ratios typically have higher clay content.
- The soil at the deeper depths of the deposit has sand seams

1D CRS consolidation testing yielded the following compressibility parameters:

- Recompression ratio values range from 0.04 to 0.09, and normally consolidated virgin compression ratios range from 0.25 to 0.67, with more typical values ranging from 0.32 to 0.45.
- Coefficient of consolidation,  $c_v$ , values ranging from 5 to 47 ft<sup>2</sup>/year, with most values ranging from 11 to 22 ft<sup>2</sup>/year. Permeability values ranged from  $1.8 \times 10^{-8}$  in/s to  $5.7 \times 10^{-8}$  in/s with no trend in depth.

Overall stress history and undrained shear strength ( $\sigma'_p$ , OCR, and  $s_u$ ) show the following trends for the Presumpscot clay at the Richmond-Dresden Bridge site:

- $\sigma'_p$  generally increases with depth to 27 ft. and then decreases to 33 ft. The decrease in  $\sigma'_p$  within the deeper portion of the layer is likely the result of increasing sand and decreasing clay content and a flattening of stress-strain curves that obscures determination of  $\sigma'_p$ .
- OCR decreases from about 5.8 to 2.2 over the deposit as  $\sigma'_{v0}$  increases with depth and  $\sigma'_p$  changes. This soil can be classified as low or moderately overconsolidated.
- Overconsolidation is likely caused by mechanical unloading (e.g., removal of previously deposited sediment or ice), aging, secondary compression, and/or other biogeochemical processes.
- $s_u$  increases with depth from 527 to 877 psf from 13.5 feet to 27.7 feet respectively, before decreasing to 767 psf at 30.1 feet.
- Most specimens were sheared at a lower  $\sigma'_{v0}$  state than estimated in situ, and it is anticipated that measured  $s_u$  under predicts in situ  $s_u$  to an unknown degree.
- Normalized  $s_u$  decreases consistently with depth.  $s_u$  normalized by the preshear stress state,  $s_u/\sigma'_{vc}$ , decreases from 1.05 to 0.53 with depth within the profile, while  $s_u$  normalized by the in situ estimated stress state,  $s_u/\sigma'_{v0}$ , decreases from 0.78 to 0.48, which is similar to expected values using the SHANSEP  $S$  and  $m$  parameters of testing on similar Presumpscot clay deposits (Table 2.2). Higher OCR soil has greater normalized  $s_u$ , as expected.

### 6.3 Seismic Cone Penetration Results

One seismic cone penetration test SCPTu 109 was performed in the Presumpscot clay at the Route 197 Bridge site. The test was conducted on June 28, 2012 in general accordance ASTM D-5778-95 *Standard Test Method for Electronic Friction Cone and Piezocone Penetration Testing of Soils* and the methods outline in Section 3.1 (ConeTec, 2012). Pseudo-interval seismic

testing was conducted at every rod break (1 meter or 3.28 ft) during penetration. The total depth of the test was 32 ft, approximately 20 feet (from 10 feet to 30 feet below ground surface) consisting of penetration through Presumpscot clay.

### 6.3.1 Results

Figure 6.13 presents measurements of tip resistance ( $q_t$ ), sleeve friction ( $f_s$ ), and pore pressure ( $u_2$ ) with depth below mudline from SCPTu109. The figure illustrates stratification of the subsurface at the Route 197 Bridge site. The upper ten feet of stream alluvium is identifiable from high  $q_t$  and  $f_s$  values and hydrostatic (drained) water pressure to approximately 10 feet in depth. Below this, the transition into Presumpscot clay is made clear by the decrease in  $q_t$  and  $f_s$  with a subsequent increase in  $u_2$ . Sand seams and the eventual transition into the underlying outwash sand appear in the bottom of the clay deposit (starting at 23 feet), where localized increases in  $q_t$  and  $f_s$  and decreases in  $u_2$  occur. Refusal was encountered at 32 feet below mudline likely due to dense outwash sand or bedrock.

Alluvium material overlying the Presumpscot layer resulted in higher magnitude  $q_t$  values observed from 0 to 10 foot depth. Variation in  $q_t$  and  $f_s$  in the alluvium layer indicate a stratified layer of alternating dense and soft layers. Once in the Presumpscot clay,  $q_t$  values ranged from 10,000 psf at the top of the layer to 34,800 psf at the “spike” near 27 foot depth. Excluding the three sharp increases in the deep transitional zone,  $q_t$  increased slightly, and nearly linearly, with depth through the Presumpscot clay layer because of increasing effective stress from overlying material. Localized  $q_t$  increases at 23, 27, and 29 foot depths are a result of silt or sand seams in the bottom of the Presumpscot deposit. These seams were also encountered in the borings in the Presumpscot clay at the same depths.

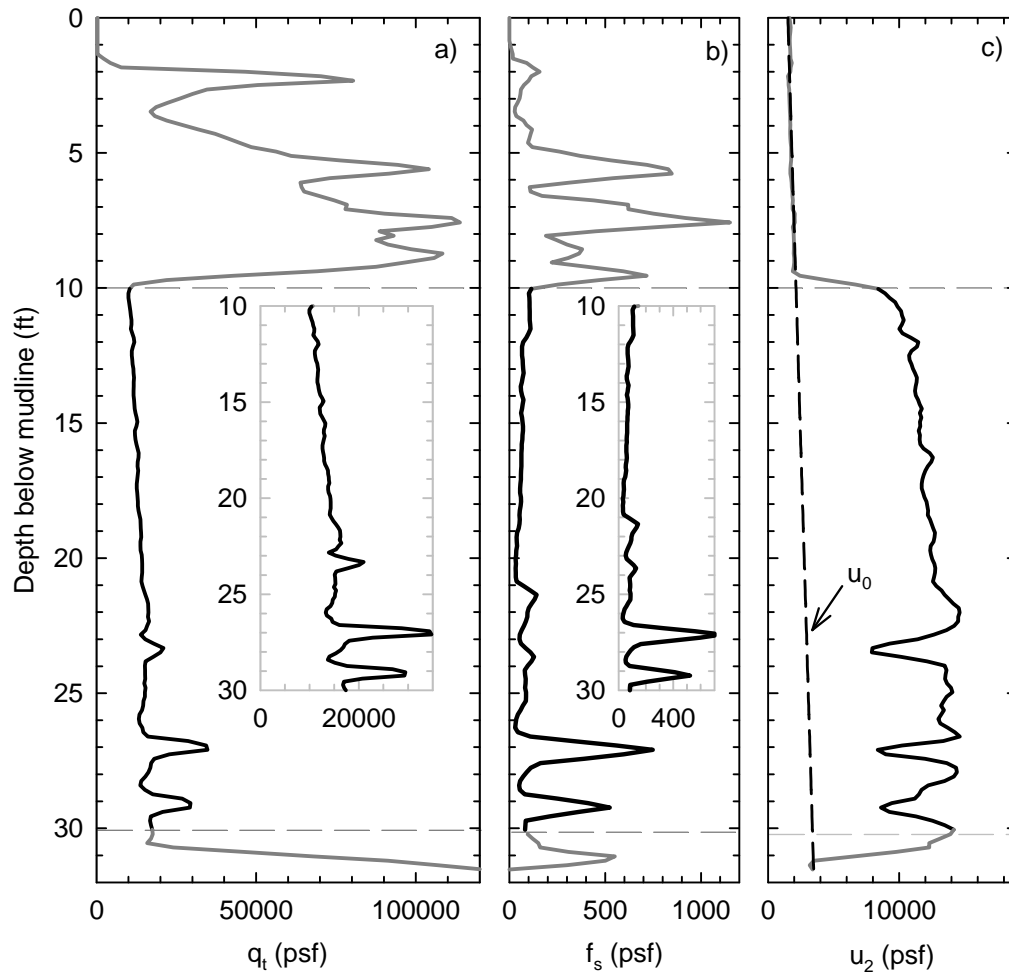


Figure 6.13: Depth profile of (a) corrected tip resistance, (b) sleeve friction, (c) and pore pressure showing hydrostatic pore pressure from SCPTu 109 conducted at the Route 197 Bridge.

$f_s$  values essentially follow the trend of tip resistance. High and variable  $f_s$  values occur in the overlying 10 feet of layered stream alluvium, low values in the Presumpscot clay, and high values in the silt/sand seams and transition into the underlying outwash sand. Excluding the seams at the bottom of the clay deposit, values in the Presumpscot clay range from 32 psf at 20 feet to 142 psf at 21.5 feet with a general decrease with depth. Values spike as high as 749 psf at the location of the seams. Since the  $f_s$  measurement is suggested to estimate remolded undrained

shear strength ( $s_{u(r)}$ ; discussed below), the slight decrease with depth is due to the decreasing  $s_{u(r)}$  values, which is matched by laboratory and field data.

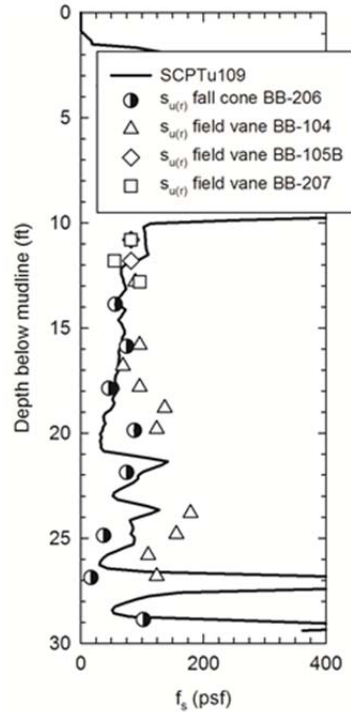


Figure 6.14: Profile comparing remolded shear strength values ( $s_{u(r)}$ ) obtained from Boring 104, 105B, and 207 field vane test results and fall cone tests from BB-RDKR-206 with sleeve friction from SCPTu 109 at the Route 197 Bridge site.

$f_s$  measurements provide information about the post-shear behavior of the penetrated soil.  $f_s$  is essentially the  $s_{u(r)}$  of the soil. Figure 6.14 compares remolded shear strength values ( $s_{u(r)}$ ) obtained from field vane and fall cone tests (Figure 6.9) with sleeve friction from SCPTu 109. Generally,  $s_{u(r)}$  from field vane shear tests represents the upper bound, as values are greater than both  $f_s$  from SCPTu109 and fall cone measurements. SCPTu109  $f_s$  and fall cone  $s_{u(r)}$  correlated well at depths less than 18 feet for deeper soils that are known to be variable,  $f_s$  and fall cone  $s_{u(r)}$  are less correlated. Slight over-prediction from field vane remolded tests can be attributed to incomplete remolding specimen during in-situ testing. Overall, SCPTu  $f_s$  appears to be an



effective method for estimating  $s_{u(r)}$  within the Presumpscot deposit, however where layering and variability exist in the soil, caution should be taken.

Pore pressure  $u_2$  measurements in the upper 10 feet of stream alluvium were at the hydrostatic level, indicating free-draining material. Once the Presumpscot clay deposit was penetrated, pore pressure jumped to 8,400 psf and increased approximately linearly with depth to the bottom of the deposit. From depth 10 feet to 20 feet, the  $u_2$  profile indicates some sub-layering that is not highlighted by  $q_t$  and  $f_s$  measurements. The small, localized increases in  $u_2$  within these depths suggest small decreases in permeability and coefficient of consolidation. Localized decreases in pore pressure can be seen at the sand/silt seams at 23, 27, and 29 foot depths. The sudden increase to 8,400 psf at the start of the Presumpscot clay deposit is consistent with the high sensitivity clay. In a study of glaciated clays (Landon, 2007), similar trends appeared during cone penetration testing where sensitive clay resulted in much larger pore pressures occurring at the start of penetration through the layer.

Shear wave velocity,  $V_s$ , measurements from SCPTu 109 is illustrated in Figure 6.15.  $V_s$  values are represented at the mid-point between the tests (Section 3.1.1).  $V_s$  values are consistent with depth with some variation between 550 and 650 ft/s. Figure 6.15 additionally shows small-strain (e.g., elastic) shear modulus ( $G_0$ ) over the range where undisturbed samples were available and measures of in situ bulk density ( $\rho_t$ ) were available from BB-RDKR-206.  $G_0$  is calculated using Equation 2.10 and ranges from approximately 7.5 to 9.5 ksi over the depth range shown, without a strong trend. Lastly, the rigidity index,  $I_r$ , often used for foundation design applications, was determined using interpreted  $G_0$  and  $s_u$  determined from CAUC triaxial compression tests on undisturbed samples from BB-RDKR-206. Landon (2007) conducted SCPTu testing on Boston Blue clay (BBC), a silty clay deposit in Massachusetts which has similar silt content to the Presumpscot clay and was deposited from the same geologic process and period as the Presumpscot clay. At the Newbury, Massachusetts site Landon (2007) measured the  $V_s$  of the

BBC to range from 410 ft/s to 525 ft/s which ranges in OCR from 4.6 to 2.1 (similar to the Presumpscot clay at the Route 197 Bridge site). Thus,  $V_s$  measurements are relatively similar between the BBC and the Presumpscot clay at the Route 197 Bridge site. Long and Donohue (2008) suggest that  $G_0$  is related to both the OCR and void ratio of clay samples. Section 8.6 presents an analysis of OCR, void ratio and  $G_0$  from all four sites and found the relationship to be inconclusive.

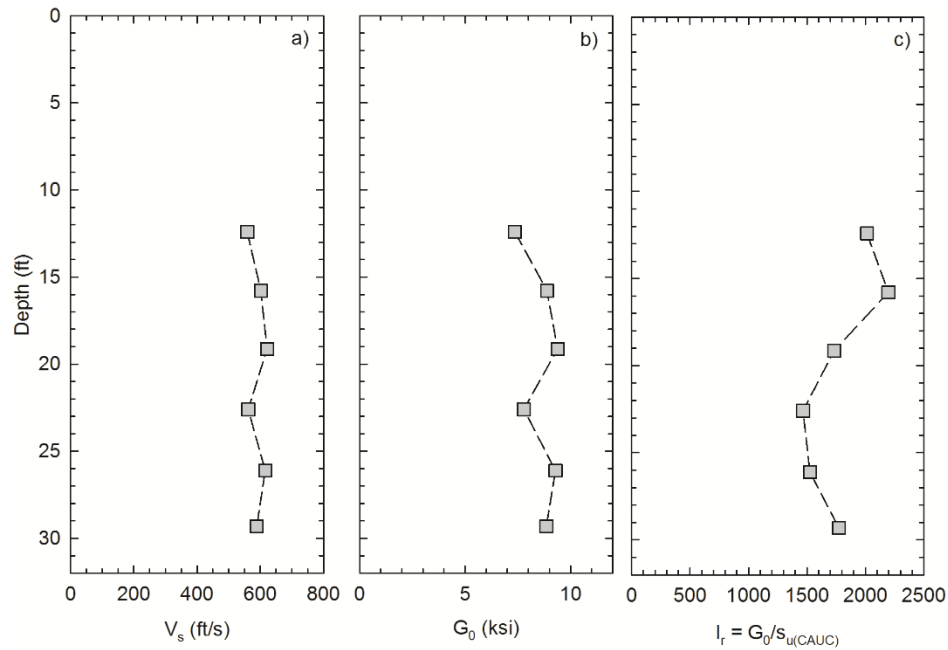


Figure 6.15: Profile of a) shear wave velocity ( $V_s$ ), b) small strain shear modulus ( $G_0$ ), and c) rigidity index ( $I_r$ ) for SCPTu 109 at the Route 197 Bridge site.

### 6.3.2 Correlations to Classification

Empirical charts have been proposed by Robertson (1990), Schneider *et al.* (2008), and Robertson (2009) to classify soils based on CPTu measurements (Section 2.3.1). The proposed charts plot normalized tip resistance ( $Q_t$ ) versus sleeve friction ratio ( $F_r$ ) or normalized pore pressure ( $B_q$ ) and place the resulting data point into a region which has a corresponding soil type deemed the “Soil Behavior Type” or SBT. The SBT regions were developed based on observed

$Q_b$ ,  $F_r$ , and  $B_q$  measurements taken in specific types of soils. Normalized values are used to eliminate the influence of depth on measurements. Figure 6.16 displays the profiles of the three normalized parameters  $Q_b$ ,  $F_r$ , and  $B_q$  collected from SCPTu 109.

Each of the four classification charts were evaluated for their applicability to the Presumpscot clay at the Route 197 Bridge site using Unified Soil Classification System (USCS) results from laboratory analyses of collected soil samples and values of  $Q_b$ ,  $F_r$ , and  $B_q$  collected from SCPTu 109 at corresponding depths. For three of the charts (Robertson 1990 and Robertson 2009; Figure 6.17a, b, and c), there are 9 regions corresponding to Soil Behavior Types (SBT). SBT 1 “sensitive fine grained,” SBT 3 “clay to silty clay,” and SBT 4 “clayey silt to silty clay” were considered correct classifications of the Presumpscot clay at this site based on lab data. For the fourth chart (Schneider *et al.*, 2008; Figure 6.17d), a different classification system is used, of which the “clays” and “sensitive clays” regions were considered to be correct classifications of the Presumpscot clay. Table 6.8 presents a summary of this analysis including the number of samples laboratory samples tested, number of USCS classifications matching the SBT classification, and the resulting percent effectiveness (USCS-SBT matches divided by the number of samples). It should be noted that the vertical dotted line in Figure 6.17d is used as a match line to compare to another classification plot not used in this study, and that the “sensitive clay” region still applies to data plotted on the right side of the line.

Normalizing by overburden stresses also allows for the plotted CPTu data to be classified based on other soil properties. By doing this for the Presumpscot clay at the Route 197 Bridge (Figure 6.16), layering within the deposit becomes more pronounced than the raw measurements alone. One noticeable trend on Figure 6.16 is the steadily decreasing  $Q_t$  with depth from 10 feet down to the bottom of the deposit. This is an example of the normalization process highlighting soil behavior, and in this case, it is OCR. The  $Q_t$  has been found to relate to the overconsolidation of the clay, and the values will be used to estimate OCR in Section 6.3.3. Another noticeable

trend in Figure 6.16 is the consistency of  $B_q$  when normalized by overburden stress. Except for the confined layers within the deposit,  $B_q$  values are practically constant with depth suggesting that the  $B_q$  parameter may be an effective method for soil classification (since in terms of material classification based on USCS, the Presumpscot clay at the site is relatively uniform).

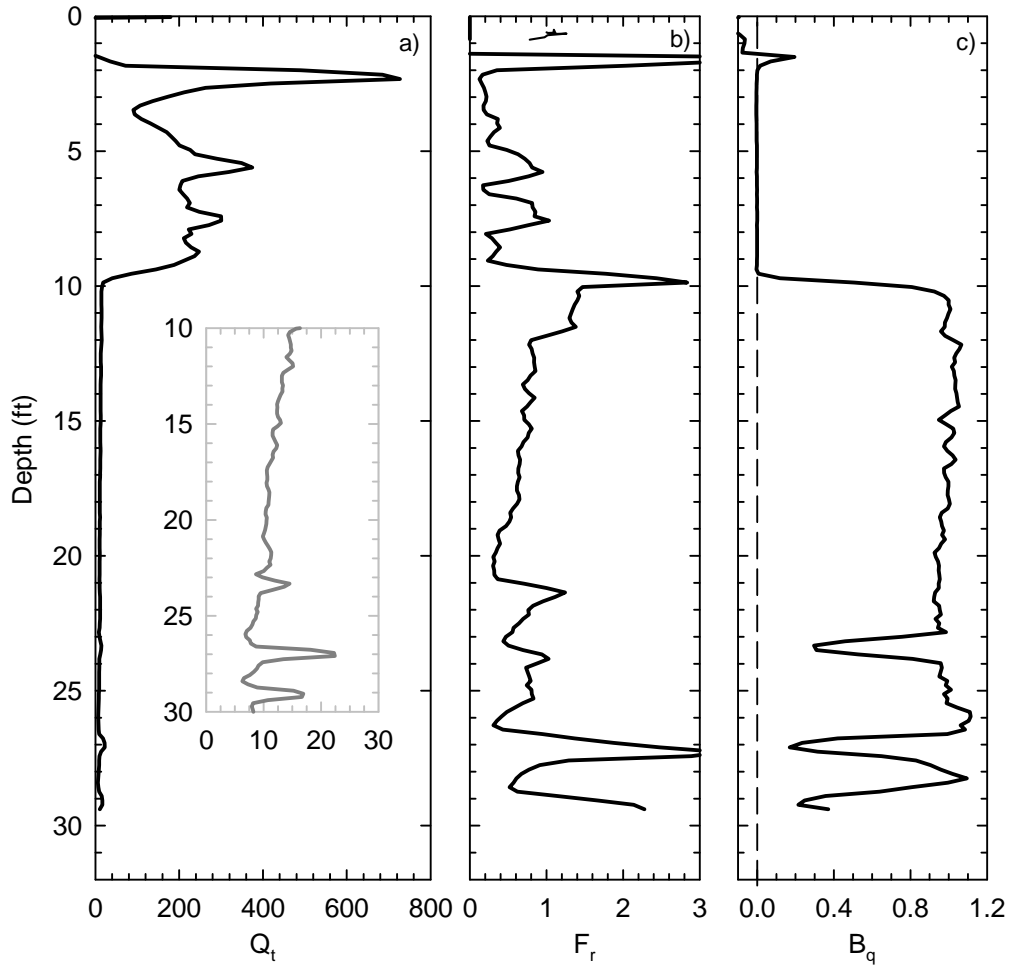


Figure 6.16: Profile of a) normalized tip resistance ( $Q_t$ ), b) sleeve friction ratio ( $F_r$ ), and c) Normalized Pore Pressure ( $B_q$ ) from SCPTu 109 conducted in Presumpscot clay at the Route 197 Bridge.

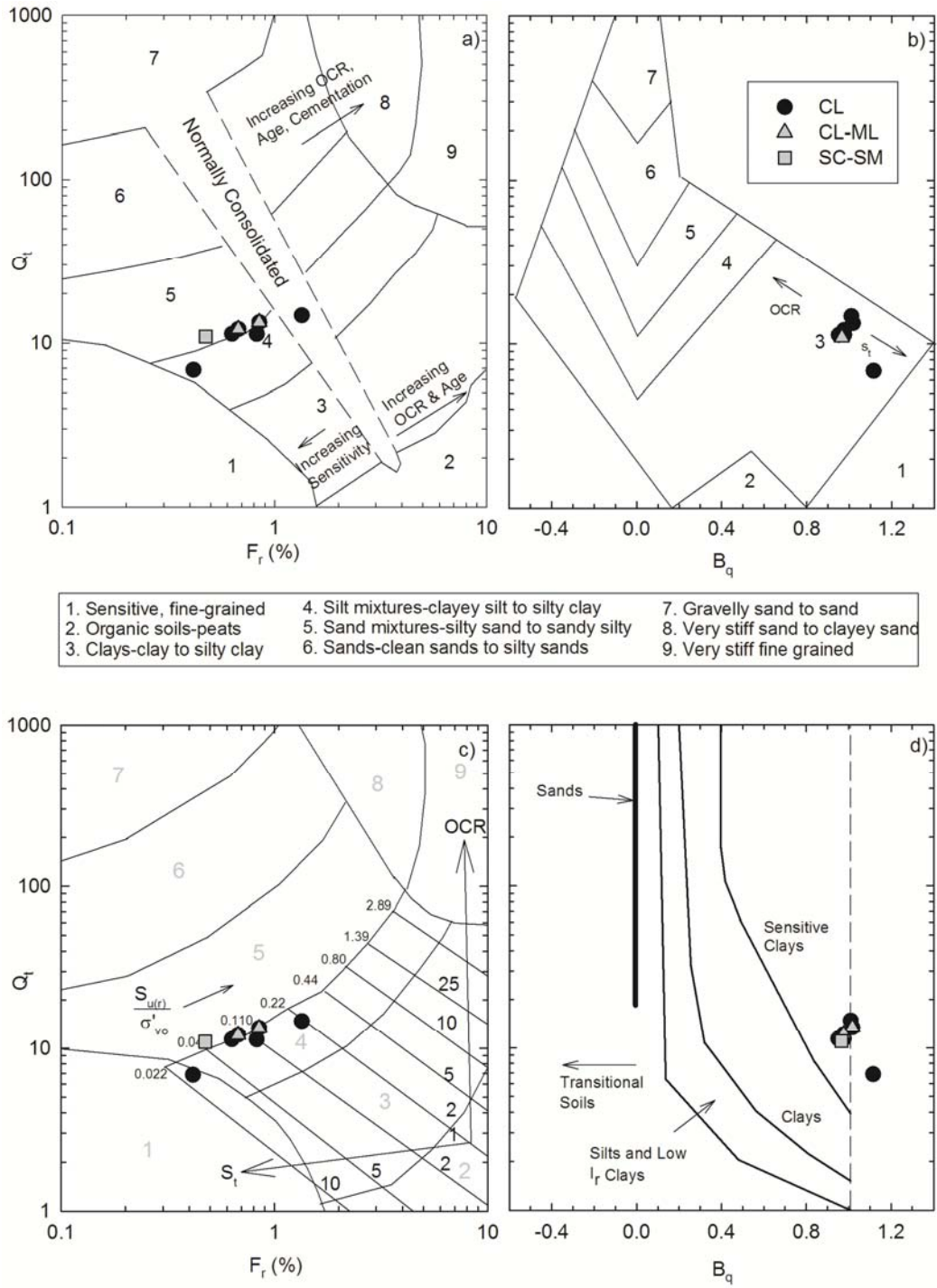


Figure 6.17: Soil classification results from SCPTu109 comparing laboratory-determined USCS classification to classification charts using a)  $Q_t$  vs.  $F_r$  (Robertson 1990), b)  $Q_t$  vs.  $B_q$  (Robertson 1990), c)  $Q_t$  vs.  $F_r$  (Robertson 2009), d)  $Q_t$  vs.  $B_q$  (Schneider *et al.*, 2008).

Table 6.8: Summary of CPT classification chart effectiveness for SCPTu 109 at the Route 197 Bridge site.

Reference	# samples	SBT-USCS Correlation	% Effective
<i>Robertson 1990 (<math>F_r</math>)</i>	11	5	45.5
<i>Robertson 1990 (<math>B_q</math>)</i>	11	11	100
<i>Schneider et al. 2008</i>	11	5	45.5
<i>Robertson 2009</i>	11	11	100

Notes: SBT: soil behavior type from CPT correlations; USCS: Unified Soil Classification System (ASTM D2487).

When using the  $F_r$  and  $Q_t$  SBT charts (Figure 6.17a and c), the SCPTu 109 data plotted within the SBT regions 4 and 5, “silt mixtures” and “sand mixtures,” respectively. All of the plotted data remained close to the threshold between these two regions and one of the data points fell in the “normally consolidated” zone of Figure 6.17a. All samples that plotted in SBT region 5 were considered to be misclassified since the Presumpscot clay is not a sand mixture. When using the  $B_q$  and  $Q_t$  SBT charts (Figure 6.17b and d), all data plotted within the SBT region 3 “clays” for Robertson (1990) and within the “sensitive clays” region of Schneider *et al.*, (2008) plot. Data plotted on these two charts were considered to be classified 100% effectively. Delineating the plotted data by the USCS classification did not appear to make a difference on any of the plots. One might expect those samples classified as CL-ML or SC-SM, which have higher composition of granular material than CL alone (silt and sand), to have higher tip resistance, sleeve friction, and lower pore pressure measurements; however, this trend did not appear on the plots. This may be due to the inconsistency of the USCS data depth matched to the SCPTu 109. The exact depth of the SCPTu 109 measurement at the collected sample depth was used on the plots, but since there was some lateral distance between Boring BB-RDKR- 206 and SCPTu 109, the stratigraphy (e.g., sand or silt seam) may change between these locations.

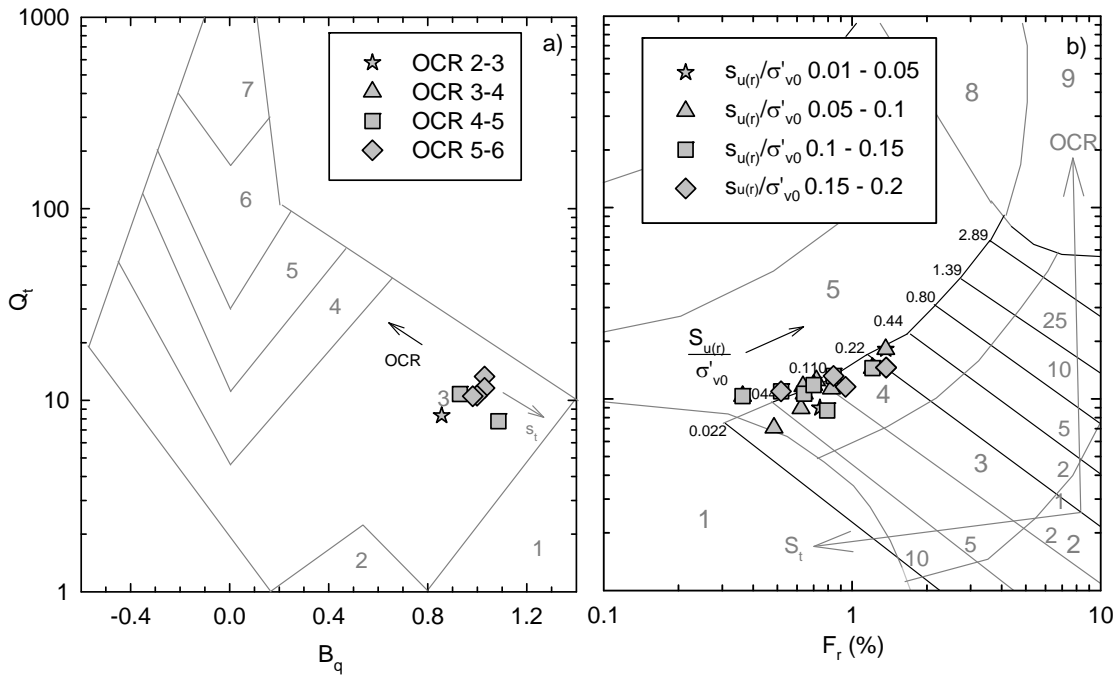


Figure 6.18 Soil trend results from SCPTu109 comparing laboratory and field determined soil properties to plotted trends on chart for a) OCR (Robertson 1990), b) Normalized remolded undrained shear strength (Robertson 2009).

SBT from CPTu measurements match 100% of the sample USCS values from the same depth when SBT is determined using  $Q_t$  and  $B_q$ . for both the Robertson  $B_q$  (1990) and Schneider *et al.*, (2008) methods. SBT and USCS classifications based on  $Q_t$  and  $F_r$  (Robertson, 1990; Robertson, 2009) have a lower prediction correlation of 45%.  $B_q$ - $Q_t$  relationship better predicts the soil classification than  $F_r$ - $Q_t$ . An initial indicator of this result was inspection of Figure 6.16, when it was presented that  $B_q$  showed more consistency with depth when compared to  $F_r$ . Behaviorally, the misclassification using the  $F_r$ - $Q_t$  plots for the Route 197 Bridge SBT classification is likely a result of the high sensitivity of the clay in conjunction with a moderate OCR. Sandy soils have been found to have higher  $Q_t$  and lower  $F_r$  as compared to clay soils (Lunne *et al.*, 1997). Coincidentally, all of the "misclassified" data points from the Route 197 Bridge plotted in Region 5 (sand mixtures), a region defined by comparably higher  $Q_t$  and lower

$F_r$  (Figure 8.8). Higher OCR will cause tip resistance (and hence  $Q_t$ ) to increase, while high sensitivity will cause sleeve friction (and hence  $F_r$ ) to decrease. The combination of these two behaviors imitates the behavior of a weak sand, which is exactly where the "misclassified" data points plot (i.e., in the sand mixture region, but close to the border of silt mixtures).

SBT charts in Figure 6.18 additionally provide information for using  $Q_t$ ,  $F_r$ , and  $B_q$  to predict changes in OCR, values of  $s_{u(r)}$  normalized by  $\sigma'_{v0}$  ( $s_{u(r)}/\sigma'_{v0}$ ), and sensitivity,  $S_t$ . Figure 6.18a illustrates that  $Q_t$  vs.  $B_q$  is not useful in estimating the relative OCR difference for soil over the depth of the deposit at the site. The data are clustered even though OCR ranges between 2 and 6 at the site. Figure 6.18a does not appear to be particularly useful for estimating changes in sensitivity. Sensitivity values were found to vary significantly with depth between 7.5 and 45.0 using the fall cone test (Table 6.3), and on Figure 6.18a the plotted data remained clustered within a small portion of the plot, suggesting a constant sensitivity. Figure 6.18b illustrates  $Q_t$  vs.  $F_r$  data for SCPTu 109 categorically separated by a range of  $s_{u(r)}/\sigma'_{v0}$  measured from field vane shear tests and laboratory fall cone index tests on samples from BB-RDKR-206. In situ and laboratory measured  $s_{u(r)}/\sigma'_{v0}$  values are less than 0.2, and generally plot within the appropriate range shown in Figure 6.18b, however the data are clustered and interspersed and show no real trend of increasing  $s_{u(r)}/\sigma'_{v0}$  up and to the right. Also, a few data plot in regions that predict  $s_{u(r)}/\sigma'_{v0}$  values greater than have been measured. Overall, Figure 6.18b does not significantly over predict the range of  $s_{u(r)}/\sigma'_{v0}$  within the deposit and may only be useful for preliminary site assessment before FVT or other testing can be completed.

### 6.3.3 Correlations to Stress History

CPTu soundings data were correlated to measured stress history of the site using the  $k$ -value correlation method outlined in Section 2.3.2. Using Equation 2.7,  $k$ -values were back-calculated using preconsolidation pressure ( $\sigma'_p$ ) determined from CRS testing of laboratory



specimens and  $q_{net}$  assessed from the CPTu sounding at the corresponding sample depths. Figure 6.19 presents the  $k$ -values determined for the Presumpscot clay at the Route 197 Bridge site along with the estimated  $\sigma'_p$  profile using determined  $k$ -values applied to SCPTu 109.

In Figure 6.19a, each symbol represents a  $k$ -value back calculated from the CPTu soundings data at that depth. The vertical dotted lines at values of 0.20 and 0.50 represent the “typical” range of values for clays (Lunne *et al.*, 1997). In Figure 6.19b, the average, minimum, and maximum  $k$ -values from SCPTu 109 were applied to the entire profile of  $q_{net}$  and compared to the laboratory-determined  $\sigma'_p$ .  $k$ -value at Route 197 Bridge site ranged from 0.55 at 26.4 ft to 0.31 at the bottom of the deposit (30 ft) with an average value over the entire deposit of 0.45. Between 13.5 ft to 21.4 ft,  $k$ -value ranges from 0.45 and 0.5 (OCR decreased from 6.0 to 4.8). These values are in the upper limits of Lunne *et al.*, (1997) recommended range of 0.2 to 0.5, which agrees with the observed trend of increased  $k$ -value for overconsolidated soils. Below 21.4 ft, OCR and  $k$ -value generally decreased, although a  $k$ -value of 0.55 was found for 26.4 ft, likely the result of increased tip resistance from a silt/sand seam.

$k$ -values in Figure 6.19 appear to be separated into two groups:  $k$ -values from 13 feet to 22 feet which yield constant values with depth and  $k$ -values below 22 feet which are more scattered and decreasing. OCR of the tested specimens in the upper portion of the deposit are nearly constant and are matched by nearly constant  $k$ -values (average of 0.49) in the upper range of published values from 0.20 to 0.50 from Lunne *et al.*, (1997). Lunne *et al.*, (1997) also suggest that higher  $k$ -values are expected for overconsolidated clays, similar to the specimens collected in this portion of the Route 197 Bridge deposit which range in OCR from 4.9 to 5.8. In the lower portion of the deposit, aside from the one high  $k$ -value at 26 feet (from sample 8U, Table 6.4), the  $k$ -value generally decreases with depth below 22 feet. OCR of the specimens in the lower portion decrease from 4.6 to 2.7. A Presumpscot clay samples was collected and tested for  $\sigma'_p$  below the

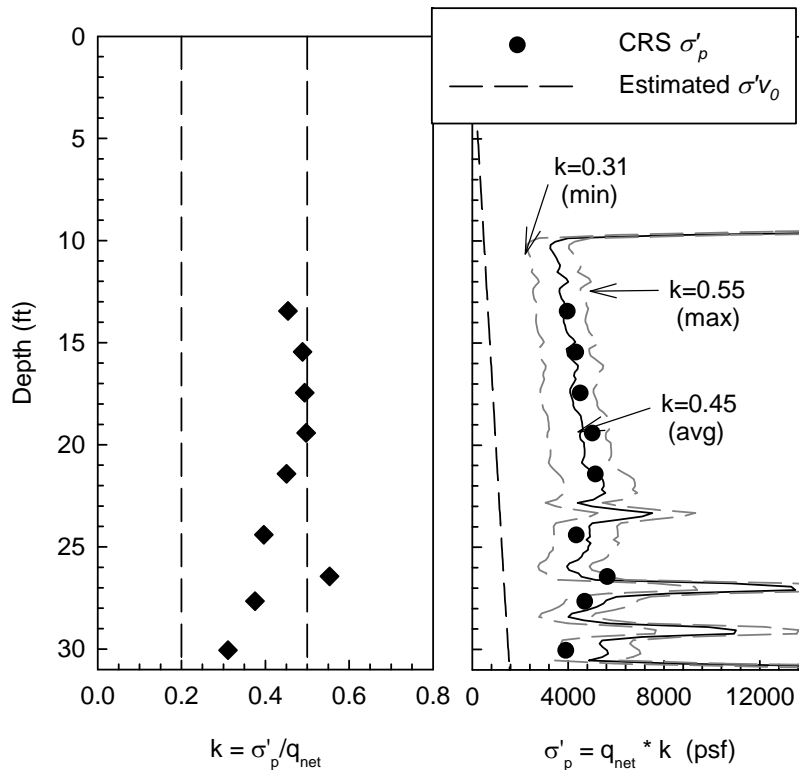


Figure 6.19: Subsurface profile of a)  $k$ -value, b) estimated  $\sigma'_p$  from applying min, max, and average  $k$ -values to the entire SCPTu 109  $q_{net}$  profile compared to laboratory-determine  $\sigma'_p$  of Presumpscot clay at the Route 197 Bridge site.

depths shown in Figure 6.19. Since SCPTu 109 encountered free draining material at this depth (shallower sand than the location of Boring BB-RDKR-206), these testing results are not shown.

It would appear from Figure 6.19 that dividing the deposit into two sections and applying individual  $k$ -values to each of the two sections might be the most appropriate method for predicting  $\sigma'_p$  at the Route 197 Bridge site. However, even when applying the average  $k$ -value (0.45) for all of the Presumpscot clay at the Route 197 Bridge site, estimates of  $\sigma'_p$  for the upper portion of the deposit were adequate and only slightly over predicted  $\sigma'_p$  for the lower portion. If the top and the bottom of the deposit were to be separated, the average  $k$ -values for the two portions would be 0.49 and 0.42, respectively. At the Route 197 Bridge  $k$ -value begins to

decrease at an OCR of approximately 4.5. The percent difference of  $\sigma'_p$  estimates in the lower portion of the deposit using a  $k$ -value of 0.42 versus 0.45 results in a percent difference of 7%, translating to  $\sigma'_p$  value differences from 306 psf to 378 psf. When considering the assumptions of soil unit weight and the potential error in  $\sigma'_p$  determination from consolidation curves, this appears to be a relatively inconsequential difference.

#### 6.3.4 Correlations to Shear Strength

Undrained shear strength ( $s_u$ ) of clay can be estimated from CPTu results using empirical cone factors  $N_{kt}$ ,  $N_{ke}$ , and  $N_{\Delta u}$  (Equations 2.9 through 2.11). Section 2.3.3 outlines the methodology used to obtain the three empirical coefficients.  $N_{kt}$  is determined from tip resistance ( $q_t$ ),  $N_{ke}$  is determined from  $q_t$  and pore pressure measurements ( $u_2$ ), and  $N_{\Delta u}$  is determined from  $u_2$ . These empirical coefficients were determined for the Route 197 Bridge site using  $s_u$  from laboratory CAUC triaxial shear testing and field vane shear testing (FVT) results.

Figure 6.20 presents the CPTu undrained shear strength factors  $N_{kt(CAUC\ or\ FVT)}$ ,  $N_{ke(CAUC\ or\ FVT)}$ , and  $N_{\Delta u(CAUC\ or\ FVT)}$  calculated using laboratory-determined  $s_u$  from CAUC and FVT testing. Undisturbed samples were collected from Boring BB-RDKR-206 and FVT was performed during Borings BB-RDKR-207, BB-RDKR-105B, and BB-RDKR-104. The vertical dotted lines in Figure 6.20 are typical ranges provided by Lunne *et al.*, (1997). The summary of  $N_{kt}$  and  $N_{\Delta u}$  values are presented in Table 6.9. As mentioned in Section 2.3.3, the cone factor  $N_{ke}$  has been found to be unreliable for clay deposits and will be omitted from the correlation analysis.

Table 6.9: Summary of  $N_{kt}$  and  $N_{\Delta u}$  values at the Route 197 Bridge site.

	Minimum	Average	Maximum	S.D.	C.O.V.
$N_{kt(CAUC)}$	11.7	14.6	17.6	1.9	0.13
$N_{\Delta u(CAUC)}$	12.7	14.1	17.2	1.6	0.11
$N_{kt(FVT)}$	7.9	15.0	31.5	5.9	0.19
$N_{\Delta u(FVT)}$	8.2	13.1	23.8	3.6	0.15

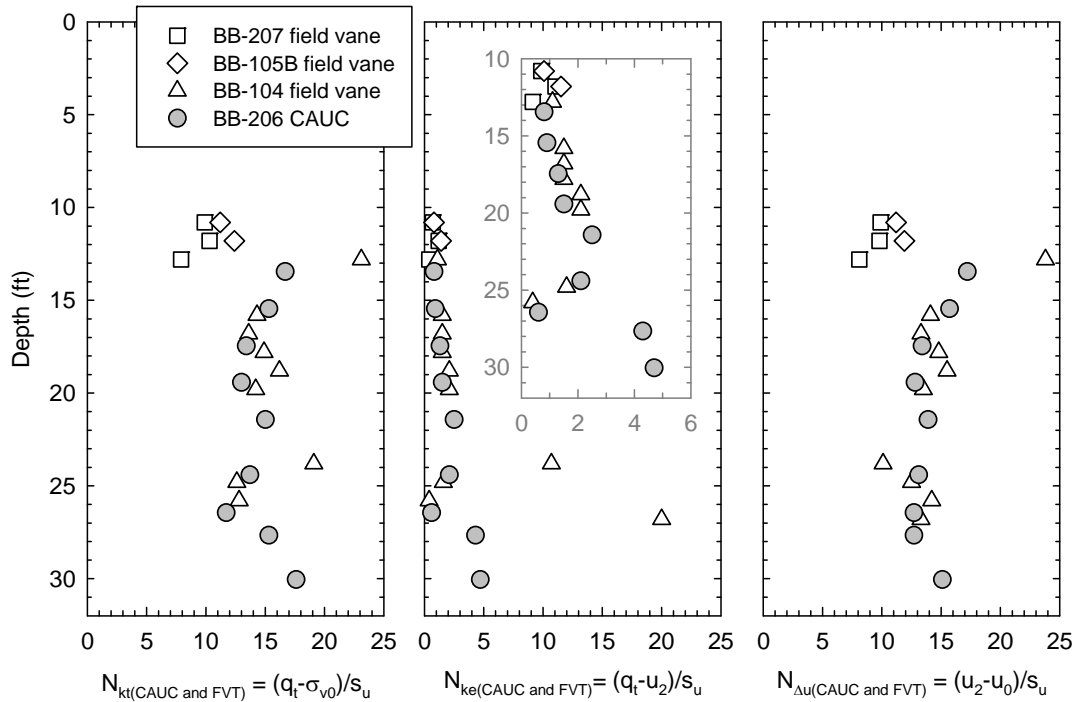


Figure 6.20 : Subsurface profiles of  $N_{kt}$ ,  $N_{\Delta u}$ , and  $N_{ke}$  correlated from SCPTu109 with  $s_u$  from CAUC triaxial and field vane testing of Presumpscot clay at the Route 197 Bridge site.

Correlating to tip resistance,  $N_{kt(CAUC)}$  at the Route 197 Bridge site ranged from 11.7 to 17.6, with an average value 14.6.  $N_{kt(CAUC)}$  decreases from 16.7 to 13.0 from depth 13.5 feet to 19.4 feet. Below 19.4 feet,  $N_{kt(CAUC)}$  values become more variable with depth, ranging between 11.7 and 17.6 without an apparent trend with  $\sigma'_{v0}$  increase or clay properties. The coefficient of variation for  $N_{kt(CAUC)}$  at the Route 197 Bridge site is 0.13.  $N_{kt(FVT)}$  at the site showed good agreement with  $N_{kt(CAUC)}$ , indicating consistent undrained shear strength ( $s_u$ ) from both the CAUC and FVT throughout the Presumpscot clay.  $N_{kt(FVT)}$  at the site ranged from 7.9 to 31.5 with an average of 15.0 and a coefficient of variation of 0.19.

Calibrating to pore pressure and tip resistance,  $N_{\Delta u(CAUC)}$  ranged from 12.7 to 17.2 with an average of 14.1 and a coefficient of variation of 0.11 at the Route 197 Bridge site. Similarly with  $N_{kt(CAUC)}$ ,  $N_{\Delta u(CAUC)}$  values decreased in magnitude from depth 13.5 feet to 19.4 feet. However,

from 19.4 feet to 27.7 feet,  $N_{\Delta u(CAUC)}$  remained within a narrow range, indicating the consistency of using pore water pressure ( $u_2$ ) to predict the  $s_u$  of Presumpscot clay at this site. Upon further analysis, the laboratory testing of Presumpscot clay samples at these depths showed relatively similar results within these depths of undrained shear strength ( $s_u$ ) and overconsolidation ratio (OCR) (Figure 6.8 and Figure 6.7, respectively). This indicates that the  $N_{\Delta u(CAUC)}$  factor may be a more consistent predictor of  $s_u$  than  $N_{kt(CAUC)}$  if the stress history and strength properties of the clay remain similar.  $N_{\Delta u(FVT)}$  yielded values ranging from 8.2 to 23.8, with an average of 13.1 and a coefficient of variation of 0.15.

Inspection of Figure 6.20 illustrates narrow ranges of both  $N_{kt(CAUC \text{ and } FVT)}$  and  $N_{\Delta u(CAUC \text{ and } FVT)}$  with depth throughout the entire profile showing that both of the cone factors can provide good estimates of  $s_u$ . Furthermore, the consistency of both factors with depth also shows that choosing a single value (the average) is an effective method for estimating entire  $s_u$  profiles. The few depths at which  $N_{kt(FVT)}$  and  $N_{\Delta u(FVT)}$  fall outside of the narrow range (at depths 13 feet and 23 feet) can be attributed to two different causes. The lower  $N_{kt}$  and  $N_{\Delta u}$  at 13 feet are due to the stiffness of the Presumpscot clay at this depth (the upper crust) increasing  $s_u$  measured from the FVT (Figure 6.9) and subsequently higher  $N_{kt}$  and  $N_{\Delta u}$  values. The high  $N_{kt}$  and low  $N_{\Delta u}$  at 23 feet are due to a sand seam increasing measured  $q_t$  and decreasing  $u_2$ , subsequently increasing and decreasing  $N_{kt}$  and  $N_{\Delta u}$  respectively.

$N_{kt}$  fell within the published range of 10 to 20 from Lunne *et al.*, (1997).  $N_{\Delta u}$  is consistently higher than the upper published range of 4 to 10. This may be due to the sensitivity of the Presumpscot clay; however this is speculative. The generally higher  $N_{\Delta u}$  values for the Presumpscot clay are consistent throughout the other three sites in this study and are analyzed further in Section 8.5.1.

Figure 6.21 presents profiles of  $s_u$  determined from applying the average, minimum, and maximum  $N_{kt(CAUC)}$  and  $N_{\Delta u(CAUC)}$  values to SCPTu 109. These resulting  $s_u$  profiles are compared to the laboratory-determined  $s_u$  to evaluate the accuracy of these two methods. At most, the difference between  $s_u$  determined from CAUC and  $N_{kt(CAUC)}$  or  $N_{\Delta u(CAUC)}$  is approximately 200 psf, and this occurs at either the top of the deposit where the clay is very overconsolidated and stiff, or at the deepest depth, which resulted in the lowest sample quality of all CAUC triaxial tested samples and subsequently lower resulting  $s_u$ , both of which effect the  $N_{kt(CAUC)}$  and  $N_{\Delta u(CAUC)}$  values.

Also apparent from Figure 6.21 is the advantage of using  $N_{\Delta u(CAUC)}$  over  $N_{kt(CAUC)}$ . Where  $s_u$  estimated from  $N_{kt(CAUC)}$  values can differ up to 40% at any given depth,  $s_u$  estimated from  $N_{\Delta u(CAUC)}$  only differs by 34%.

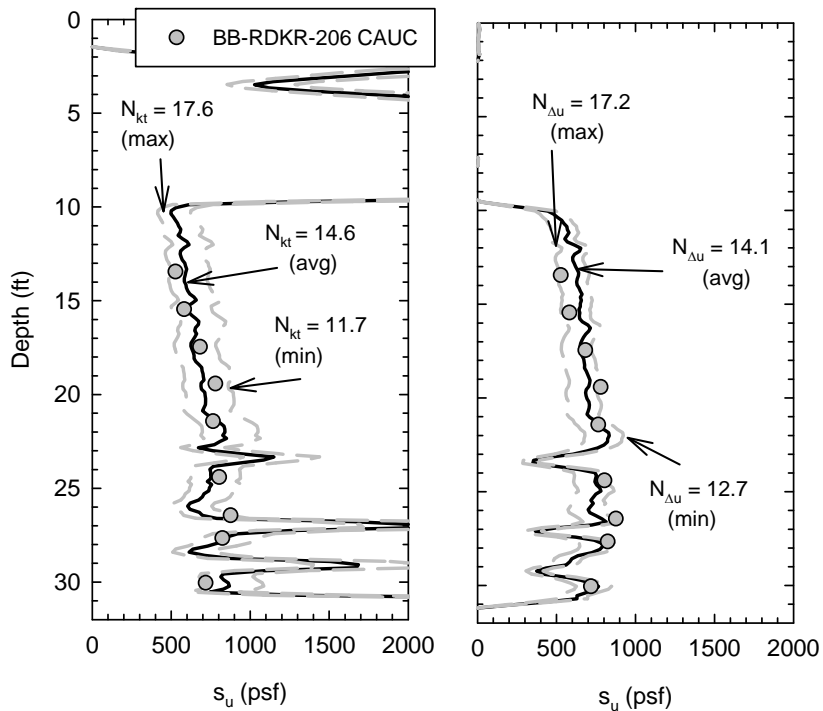


Figure 6.21: Profiles of undrained shear strength using  $N_{kt(CAUC)}$  and  $N_{\Delta u(CAUC)}$  values as shown on the figure applied to SCPTu 109, compared to the laboratory-determined undrained shear strength of Presumpscot clay at the Route 197 Bridge site.

When classifying the Presumpscot clay at the Route 197 Bridge site, SBT charts based on  $B_q$ - $Q_t$  relationship should be used. Due to the slight overconsolidation of the clay combined with its sensitivity, the  $F_r$ - $Q_t$  relationship resulted in the clay classifying as a silt or sand mixture. When using the Robertson (199)  $B_q$ - $Q_t$  chart, the sensitivity of the clay was not identified, however; the Schneider *et al.*, (2008) plot did correctly classify the deposit as sensitive clay. Stress history of the Presumpscot clay at the site can be reasonably predicted using a  $k$ -value of 0.45 applied to the entire deposit. If desired, using a  $k$ -value of 0.42 for the deposit where OCR falls below 4.5 provided a 7% increase in  $\sigma'_p$  estimates.

The  $s_u$  profile of the Presumpscot clay at the Route 197 Bridge was most effectively estimated from CPTu results using an  $N_{\Delta u}$  of 14.1 applied to the entire profile. Using an  $N_{kt(CAUC)}$  value of 14.6 also provided good estimates. Overall,  $N_{kt}$  and  $N_{\Delta u}$  values ranged from 11.7 to 17.6 and 12.7 to 17.2, respectively and remained relatively constant with depth. While  $N_{kt}$  values agree well with published ranges,  $N_{\Delta u}$  is higher than similar CPTu studies in other clays. As expected,  $N_{kt(FVT)}$  and  $N_{\Delta u(FVT)}$  values were a little more scattered, however, in general they followed the laboratory correlated values well.

## 7 I-395 TERMINUS SITE

### 7.1 Site Overview

The I-395 Terminus site is located in Brewer, Maine adjacent to the US Route 1A on ramp connector for I-395 West (Figure 7.1). Felt Brook runs along the eastern boundary of the project site and eventually drains into the Penobscot River. Groundwater table elevation at the site are typically close to the ground surface resulting in saturated conditions during periods of high rainfall or snowmelt. A 40 ft high, 70 ft wide berm runs parallel along the eastern edge on-ramp a distance of approximately 200 ft west of the project site. Drainage from this man-made berm contributes to the surface saturated conditions of the site. Using a Boussinesq elastic stress distribution, the weight of the berm does not affect the site



Figure 7.1: Image of the I-395 Terminus site in Brewer, Maine (Google Earth, 2014b).

#### 7.1.1 Geotechnical Investigation

One geotechnical investigation was performed at the site by the Maine Department of Transportation (Maine DOT) from March 6 through 11, 2013. The investigation included the drilling of two borings (HB-BREW-101 & -102) and six CPTu soundings (SCPTu101 to -106).



HB-BREW-101 & -102 were drilled by Maine Test Borings under Maine DOT supervision on March 6<sup>th</sup> and 8<sup>th</sup>, 2013. The borings were drilled with a Mobile B53 Track rig using cased wash boring techniques advanced with a rotary cone. To penetrate the frozen topsoil, solid stem augers were advanced to 2 feet below ground surface. These were extracted and where after casing was used. HB-BREW-101 was advanced in increments consistent with testing and sampling to refusal at 35.5 feet. Field vane shear testing (FVT) was conducted in accordance with Section 3.2 throughout the Presumpscot clay layer (approximately 5 feet to 27 feet depth) at a rate of 2 per each five-foot interval. A split spoon sampler was deployed through the field vane tested clay to collect disturbed samples for interpretation of field vane testing data and for index testing at the University of Maine Advanced Geotechnics Laboratory. HB-BREW-102 was advanced to the bottom of the Presumpscot clay layer at 29 feet below ground surface in increments consistent with testing and sampling. Shelby tubes modified to improve sample quality were collected in accordance with Section 3.3.1 at 3-foot intervals throughout the Presumpscot deposit. The tubes were capped and sealed on site and transported back to the University of Maine Advanced Geotechnics Laboratory for testing.

Seismic cone penetration testing with pore pressure measurements (SCPTu) was conducted by ConeTec of West Berlin, NJ using a CME55 drill rig mounted on a Morooka carrier. Six cone penetration tests with pore pressure readings (CPTu) were conducted at various locations throughout the I-395 Brewer Site, four of which included seismic measurements. Locations of the soundings were selected in an attempt to best represent the entire deposit at the site. SCPTu 101 is closest to HB-BREW-101 (which included FVT and split spoon sampling) and SCPTu 106 is closest to HB-BREW-102 (which included the undisturbed tube sampling). The remainder of the tests were placed throughout the site to identify variability should it exist. Four of the CPTu tests (SCPTu101, -104, -105, and -106) included the measurement of shear wave velocity at 3.28 feet (1 meter) intervals. Tests were conducted using the methodology presented in

Section 3.1. Figure 7.2 shows the location of the borings and cone penetration tests at the I-395 Terminus. Borings HB-BREW-101 and 102 were performed approximately 80 feet apart. The driller remarks from the HB-BREW-102 boring logs indicated that artesian pressures lifted water from the borehole 2.1 feet above the ground surface.

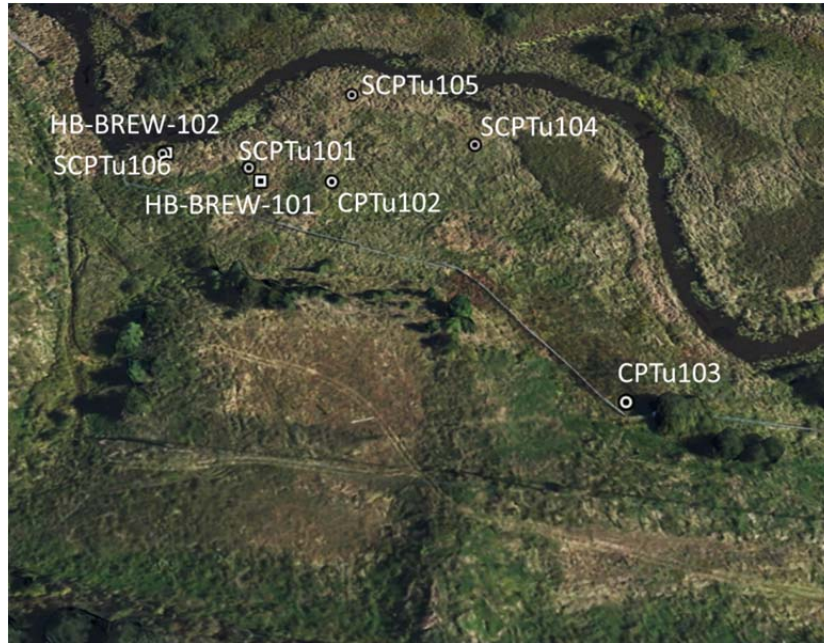


Figure 7.2: Boring and CPTu sounding locations at the 395 Terminus site (Google Earth, 2014b).

#### 7.1.2 Site Geology

In general, the soil at the site consists of sandy silt overlying stiff, silty clay (Presumpscot), overlying soft silty clay (Presumpscot), overlying fine to coarse sand, and finally overlying bedrock. The upper stiff silt and silty clay extends from the ground surface to approximately 13 feet below ground surface. In this layer, Standard Penetration Test (SPT)  $N$  values ranged from 5 to 12 and the two FVT tests attempted could not be relied on due to the material's stiffness. One FVT test at a depth of 5 feet yielded an undrained shear strength ( $s_u$ ) of 236 psf, which is significantly lower than expected. Samples collected in this layer are stiff,

blocky and mottled, indicating significant overconsolidation possible due to groundwater table fluctuations through this layer.

The soft, silty clay extends from 13 feet below ground surface to approximately 28 feet below ground surface. A total of six field vanes were performed in this layer, resulting in  $s_u$  values ranging from 228 psf to 446 psf. The material below the Presumpscot clay is a gray, wet fine to coarse sand with some gravel and trace silt. This layer extends from approximately 28 feet below ground surface to bedrock at 35.5 feet.

The deposition of the Presumpscot clay at the I-395 Terminus site differs from the coastal settings of the deposits investigated at the other three research sites in this study. The site is located at an approximate elevation of 83 feet above current mean sea level (MSL). Therefore sea level rise during deglaciation, which caused the deposition of the Presumpscot, did not reach much higher than this site. In fact, the site is approaching the inland boundary of the Presumpscot clay illustrated in Figure 1.1. Beyond this boundary, the topography was too high to be submerged by the rising sea level therefore resulting in no marine water, and no Presumpscot clay. Refer back to Section 2.1 for further discussion of the Presumpscot clay's geologic deposition.

The shallow marine environment of the I-395 Terminus site at the time of the Presumpscot clay deposition effected the composition of the clay. Shallow waters create a higher energy environment as compared to deep marine waters. Inflow of glacial meltwater streams or tidal changes likely encouraged the finer-grained particles (clay) to be washed out further to sea to a lower energy environment where they could settle to the seabed. The coarser grained (silt) particles remained within the shallow marine environment since they are more resistant to the turbulence, creating sediment which would be higher in silt content than clay content.

## 7.2 Laboratory Characterization

Nine modified Shelby tube samples of Presumpscot clay were collected from Boring HB-BREW-102 at the I-395 Terminus site for laboratory testing of index, consolidation, and shear strength properties at the University of Maine Advanced Geotechnics Laboratory. All testing methods were performed in general accordance with applicable ASTM standards and methods outlined in Chapter 3. Figure 7.3 illustrates the portion of each tube sample used for testing. The clay in sample tube 3U contained a large lateral crack running continuously through the entire sample, so undisturbed consolidation and triaxial testing was not possible. This may be attributed to the artesian pressures present at this depth (Section 7.3.1).

### 7.2.1 Index Test Results

Figure 7.4 illustrates the results of natural water content, Atterberg limits, grain size distribution, index undrained shear strength ( $s_u$ ) and index remolded undrained shear strength ( $s_{u(r)}$ ) measured using the fall cone apparatus, organic content, and unit weight (total, dry, and solids) of Presumpscot clay from the tube samples. Table 7.1 and 7.2 summarize these results.

Water content of the clay ranged from 22.6% to 40.2% over the entire deposit. In the top 13 feet, water content increased gradually with depth from 22.6% to 28.4%, generally following the increase of clay content. Within this upper zone, samples in the laboratory were visibly mottled and stiffer, indicating groundwater fluctuations through the clay played a role in the decreasing the water content. Below 13 feet, water content increased from 28.4% to 40.2% at 19.8 feet (where clay content was the highest), and subsequently decreased with depth to 28.7% at 28.5 feet. Plastic limit remained within a narrow range of 19 to 22 for the entire deposit and liquid limit showed a similar increase to approximately 20 feet, then decreases with depth, ranging from 31 to 37. Similar to water content, liquid limit trends also appeared to be directly

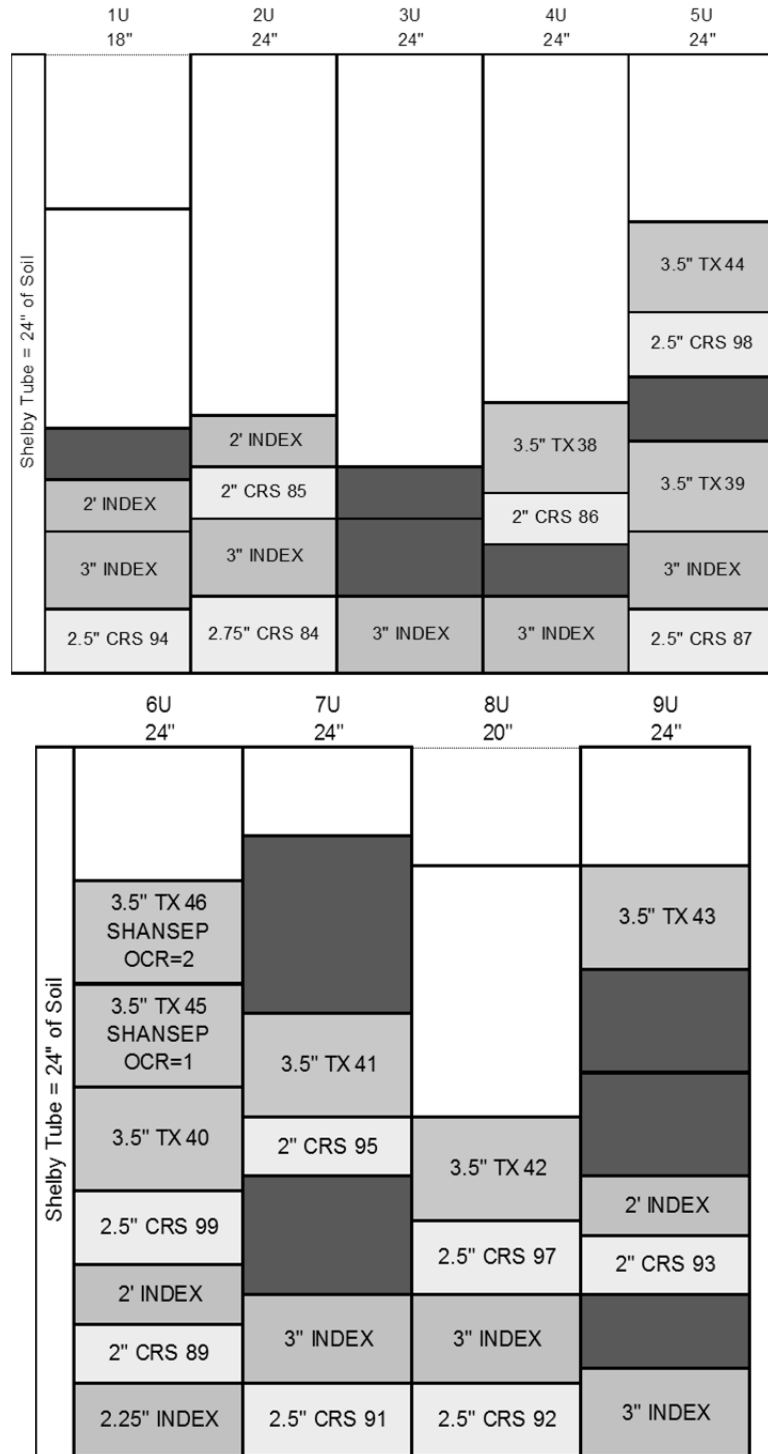


Figure 7.3: Laboratory specimen use for HB-BREW-102 3" Shelby tubes 1U through 9U.

proportional to the clay content. Liquidity Index (an indication of brittle solid, plastic or liquid behavior) was less than 1.0 in the upper zone affected by groundwater fluctuations and below 25

feet where silt content began to increase. Liquidity index was 1.0 or greater from depth 13.5 to 22.4 feet.

Composition of the Presumpscot at the I-395 Terminus site is dominated by silt. The highest percentage (74.7%) of silt came from the top sample at 4.8 feet depth. There is no trend with depth for clay or silt composition. Sand content within the deepest sample was 0.4%, demonstrating a likely abrupt transition from the Presumpscot clay to the underlying sand. The Presumpscot clay at the I-395 Terminus site is of moderate plasticity ( $LL < 50$ ) and plots in the “CL” (lean clay) region of the Casagrande Plasticity chart (Figure 7.5a).

Table 7.1: Summary of Atterberg Limits Plasticity Data for Presumpscot clay samples collected from Boring HB-BREW-102 at the I-395 Terminus site.

Sample	Depth (ft)	$w_n$ (%)	LL	PL	PI	LI	Activity
1U	4.8	22.6	32	20	12	0.22	0.48
2U	7.4	28.1	35	22	13	0.47	0.28
3U	11.7	28.4	33	20	13	0.65	0.28
4U	13.5	32.0	32	20	12	1.00	0.30
5U	16.1	37.8	37	20	17	1.05	0.68
6U	19.8	40.2	36	21	15	1.28	0.41
7U	22.4	37.3	35	20	15	1.15	0.44
8U	25.3	35.4	36	20	16	0.96	0.45
9D	28.5	28.7	31	19	12	0.81	0.36

Table 7.2: Summary of grain size distribution, density, and USCS classification for Presumpscot clay samples collected from Boring HB-BREW-102 at the I-395 Terminus site.

Sample	Depth (ft)	Sand (%)	Silt (%)	Clay (%)	Organics (%)	$\gamma_t$ (pcf)	$\gamma_d$ (pcf)	$\gamma_s$ (pcf)	USCS (ASTM D2487)
1U	4.8	0.2	74.7	25.1	2.1	127	104	172	Lean Clay (CL)
2U	7.5	2.0	52.1	45.9	2.6	119	92	172	Lean Clay (CL)
3U	11.7	0.2	53.0	46.8	2.3	*	*	172	Lean Clay (CL)
4U	13.8	0.9	58.7	40.4	3.5	116	91	169	Lean Clay (CL)
5U	16.6	1.4	63.7	34.9	2.6	114	83	169	Lean Clay (CL)
6U	19.8	0.4	62.8	36.8	2.5	112	79	167	Lean Clay (CL)
7U	22.8	0.6	65.6	33.8	3.2	114	82	167	Lean Clay (CL)
8U	25.8	0.2	64.2	35.6	3.3	116	86	169	Lean Clay (CL)
9D	28.8	0.4	66.5	33.1	2.4	122	94	169	Lean Clay (CL)

\*Unable to determine density from sample 3U due to disturbed sample

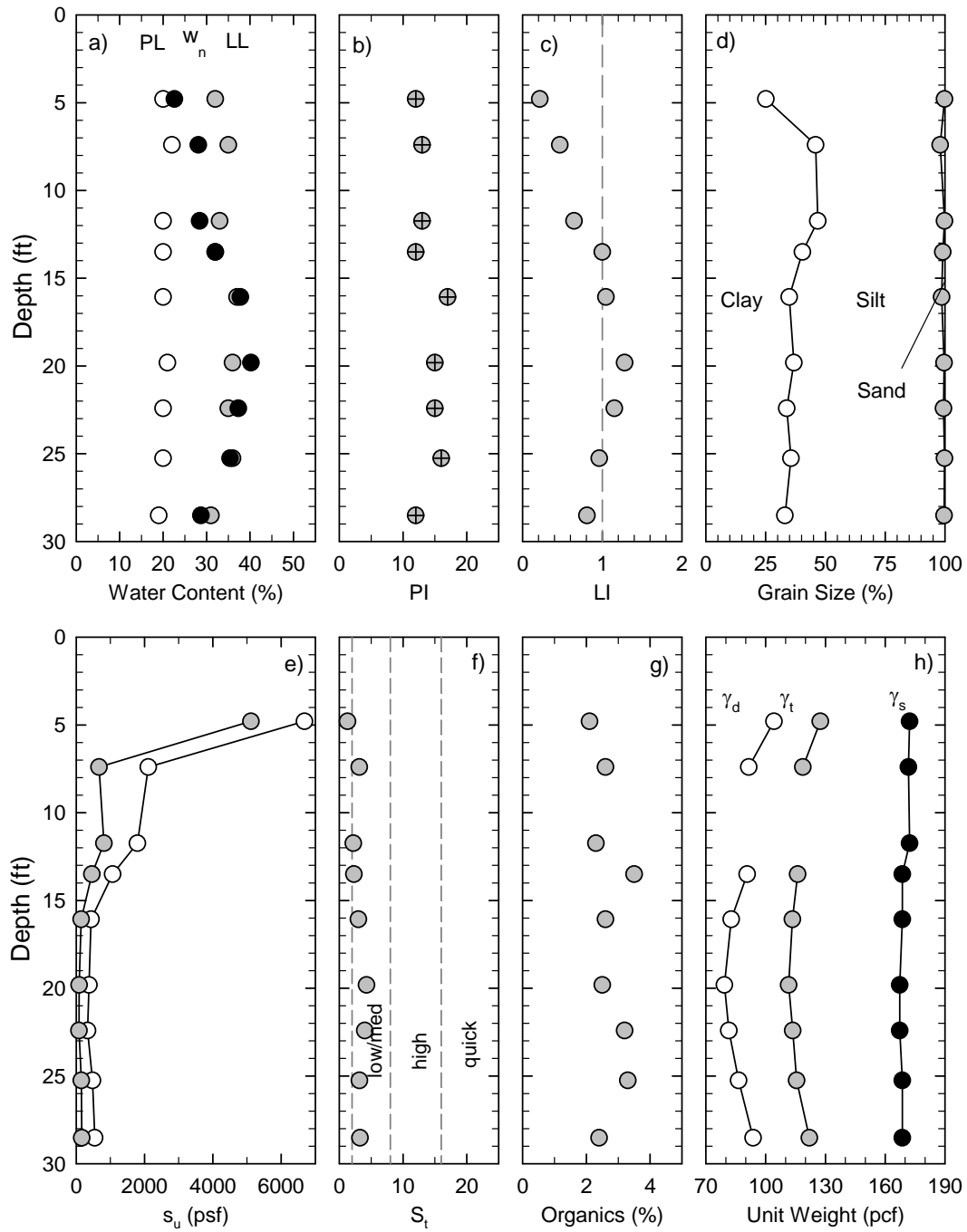


Figure 7.4: Laboratory determined results of a) natural water content, b) plasticity index, c) liquidity index, d) grain size distribution, e) index undrained and remolded shear strength from the fall cone, f) sensitivity from fall cone results, g) organic content, and h) unit weight (total, dry, and solids) for Presumpscot clay samples collected from Boring HB-BREW-102 at the I-395 Terminus site.

Sand content ranged from 0.2 to 2.0%. Some fine to coarse sand and gravel was removed from the bottom of tube sample 9U before index tests were completed. Organic content of the clay ranged from 2.1% to 3.5%, which is below the range that affects index behavior (Mitchell & Soga, 2005). Activity, defined as the ratio of plastic limit to clay fraction (Figure 7.5b) ranged from 0.28 to 0.68 and plots near the “Kaolinite” mineralogy line. As discussed in Section 2.1.2, the clay fraction is likely overestimated from the hydrometer test due to the presence of rock flour and the actual mineralogy of the samples is dominated by illite (although no X-ray diffraction tests were performed to determine this).

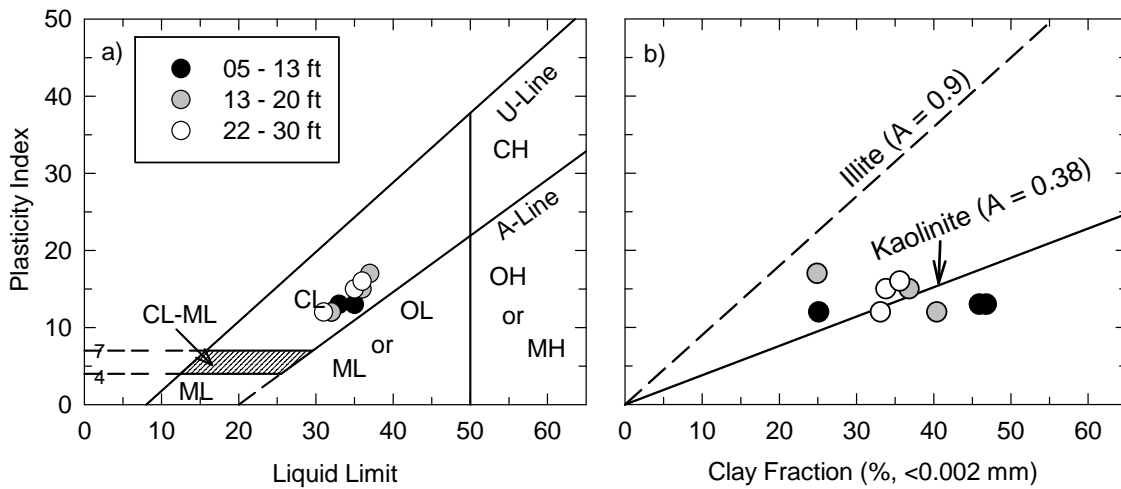


Figure 7.5: USCS Classification Charts using Atterberg Limits for Presumpscot clay samples collected from Boring HB-BREW-102 at the I-395 Terminus site.

Sensitivity, defined as the ratio of undrained shear strength ( $s_u$ ) to remolded shear strength ( $s_{u(r)}$ ), was performed in the laboratory on unconfined portions of tube samples at the natural water content using the fall cone apparatus. Remolded state of the soil was obtained by removing the clay from the tube and mechanically mixing until complete structure breakdown. Sensitivity of a material provides insight of the structuring of the clay platelets and post-shear behavior. Sensitivity from fall cone measurements ranged from 1.3 to 4.3, characterizing the soil as “low to medium” sensitivity (Holtz *et al.*, 2011; Table 2.1). FVT sensitivity measured in



Boring HB-BREW-101 ranged from 2.5 to 6.3, generally agreeing with the fall cone sensitivity measurements. Table 7.3 presents the fall cone sensitivity results.

Table 7.3: Summary of fall cone undrained shear strength and sensitivity for Presumpscot clay samples collected from Boring HB-BREW-102 at the I-395 Terminus site.

Sample	Depth (ft)	Intact $s_u^1$ (psf)	Intact Cone	$s_{ur}^2$ (psf)	Remolded Cone	$S_t^3$
1U	4.8	6683	400g 30°	5117	400g 30°	1.3
2U	7.5	2109	400g 30°	668	100g 30°	3.2
3U	11.7	1796	400g 30°	815	400g 30°	2.2
4U	13.8	1065	100g 30°	459	100g 30°	2.3
5U	16.6	439	100g 30°	146	100g 30°	3.0
6U	19.8	376	100g 30°	88	60g 60°	4.3
7U	22.8	334	100g 30°	84	60g 60°	4.0
8U	25.8	480	400g 30°	150	100g 30°	3.2
9D	28.8	543	100g 30°	167	100g 30°	3.3

#### 7.2.2 One Dimensional Consolidation Results

Constant rate of strain (CRS) consolidation testing was performed on Presumpscot clay samples from 8 of the 9 modified Shelby tubes at the I-395 Terminus site in accordance with the procedures outlined in Section 3.4.3. Sample 3U was not tested as a crack was found along the length of the sample. In situ vertical effective stress ( $\sigma'_{v0}$ ) was estimated using cumulative unit weights values from tested samples and a groundwater elevation at the ground surface. Specimens were mainly of very good to excellent or good to fair sample quality, with the exception of one poor quality specimen

Table 7.4 presents the specimen information, change in void ratio upon recompression for sample quality designation and results of the consolidation testing, including: preconsolidation pressure (determined using the Becker *et al.*, 1987 method), overconsolidation ratio (OCR), coefficient of consolidation and compressibility characteristics. Preconsolidation pressure ( $\sigma'_p$ ), initial void ratio ( $e_0$ ), and sample quality designation are illustrated with depth in Figure 7.6.

Table 7.4: Summary of Constant Rate of Strain (CRS) consolidation specimen properties and sample quality for Presumpscot clay samples collected from Boring HB-BREW-102 at the I-395 Terminus site.

Sample	Specimen Information				Sample Quality				Strain Consolidation Properties					
	Depth (ft)	$\gamma_t$ (pcf)	$\gamma_d$ (pcf)	$e_o$	$w_n$ (%)	$\sigma'_{vo}$ (psf)	$\Delta e/e_o$ at $\sigma'_{vo}$	$^1$ NGI Rating	Rate (%/hr)	$^2\sigma'_p$ (psf)	$c_v @ \sigma'_{vo}$ (ft <sup>2</sup> /yr)	OCR (-)	$C_r$ (-)	$C_c$ (-)
1U	4.79	127.5	104.2	0.69	22.6	249	0.033	G to F	1.87	3007	188	12.1	0.10	0.22
2U	7.4	118.7	91.6	0.87	28.1	408	0.034	G to F	1.89	4804	98	11.8	0.06	0.33
4U	13.5	116.1	90.7	0.93	32.0	701	0.016	VG to E	1.89	6057	96	8.6	0.06	0.29
5U	16.79	113.5	82.8	0.99	37.8	829	0.025	VG to E	2.04	2819	30	3.4	0.10	0.35
6U	19.8	111.6	79.3	1.21	40.2	1007	0.049	VG to E	2.05	1462	108	1.5	0.06	0.35
7U	22.4	113.6	81.5	1.05	37.3	1159	0.037	G to F	1.93	2130	51	1.8	0.08	0.34
8U	25.8	115.5	86.4	0.95	35.4	1307	0.048	G to F	1.92	2026	26	1.5	0.06	0.30
9D	28.5	121.9	93.8	0.79	28.7	1479	0.060	Poor	2.02	3133	135	2.1	0.07	0.21

<sup>1</sup>From Lunne et al. (2006), where VG/E: very good to excellent quality, G/F: good to fair, P: poor; <sup>2</sup>Using the Strain Energy Method of Becker et al. (1987)

In the shallow portion of the deposit,  $\sigma'_p$  increases from 3,007 psf to 6,057 psf, from 4.8 feet to 13.5 feet, and overconsolidation ratio (OCR or  $\sigma'_p/\sigma'_{v0}$ ) ranges from 12.1 to 8.6. OCR of the shallow soil is likely due to structure and density changes stemming from the groundwater fluctuations. As the groundwater level decreases,  $\sigma'_{v0}$  throughout the entire deposit increases (due to the dissipation of pore pressure). If and when the groundwater rises again, the  $\sigma'_{v0}$  decreases to match the increase in pore pressure, but the previous maximum vertical stress from the overburden at low groundwater conditions are “locked in,” and result in an increase in  $\sigma'_p$ , and subsequently OCR. Furthermore, drying due to evaporation, transpiration, and freezing cycles can change the structure of the clay and cause erratic stress history profiles within the zone of drying (Mitchell & Soga, 2005). The upper overconsolidated zone is referred to as a “crust” and is common in Presumpscot clay deposits (Langlais, 2011). Index properties of water content and fall cone shear strength are consistent with these findings.

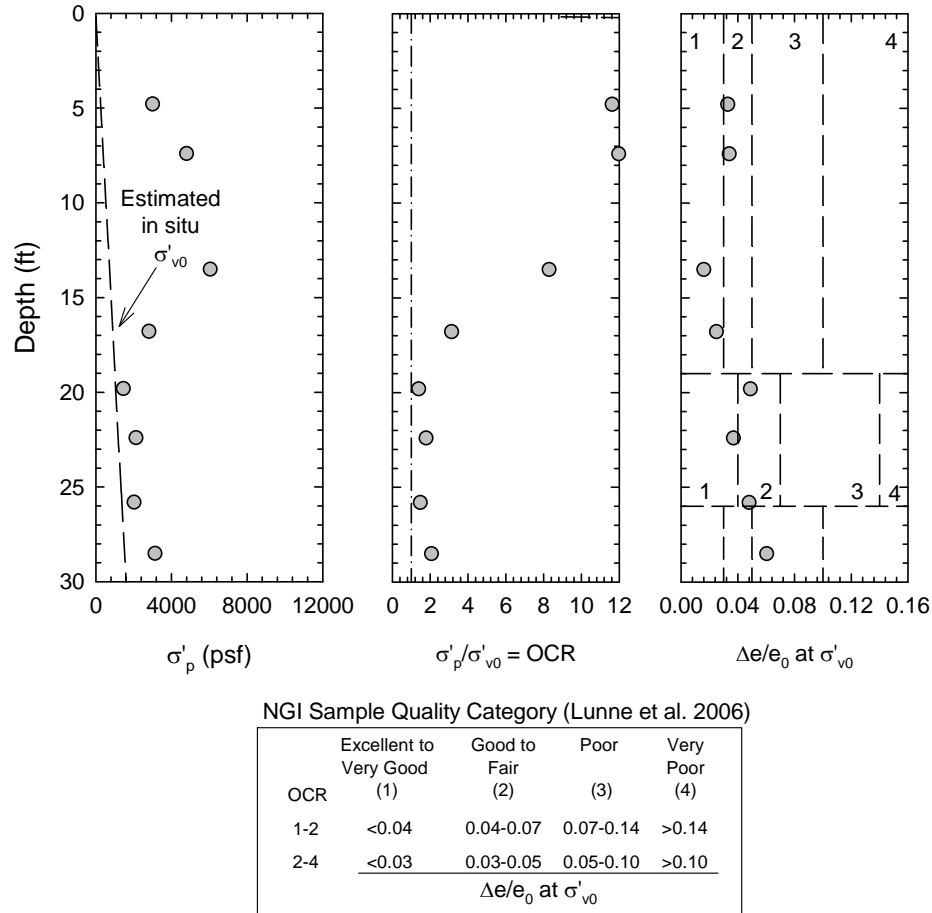


Figure 7.6: Subsurface profiles of a)  $\sigma'_p$ , b) OCR, c) sample quality assessment from CRS consolidation testing for Presumpscot clay samples collected from Boring HB-BREW-102 at the I-395 Terminus site.

Below 13.5 feet,  $\sigma'_p$  decreases and approaches the estimated  $\sigma'_{v0}$ . Laboratory testing of index properties and observations made from split spoon samples recovered from Boring BB-BREW-101 align with the consolidation testing results. There is a distinct boundary at 14 feet between overlying, stiffer material and underlying soft clayey soil which may demonstrate the extent of groundwater fluctuations at the site.

Coefficient of consolidation at  $\sigma'_{v0}$  ranges from 30 ft<sup>2</sup>/year to 188 ft<sup>2</sup>/year without an apparent trend with depth or other soil properties. Recompression index ( $C_r$ ) and virgin

compression index ( $C_c$ ) ranged from 0.06 to 0.10 and 0.21 to 0.35, respectively. In general,  $C_r$  values are assumed to be approximately 10% of the  $C_c$  values which appears to overestimate  $C_r$  at the I-395 Terminus site. Andrews (1987) presents a typical range of values for  $C_c$  of Presumpscot clay in Maine to range from approximately 0.33 to 0.60 showing that  $C_c$  values from the site are in and below the lower portion of this presented range. The lowest values of  $C_c$  came from both the shallowest and deepest specimens, both of which correspond to a lower composition of clay as compared to the middle of the deposit.

In terms of stress history, the deposit can be divided into two sections. The upper portion, which is subject to groundwater fluctuations, frost action, drainage, and drying ranges in OCR from 3.4 to 12.1. Within this portion, the higher OCR is due to a combination of the aforementioned factors and decreases abruptly with depth. Secondary compression and sample quality likely has little effect on the OCR determined from specimen in this portion. In the lower portion of the deposit (below 15 feet), OCR ranges from 1.5 to 2.1 and has minor fluctuations with depth. The overconsolidation of the clay at these depths is likely due to two independent sources; secondary compression and sample disturbance. The clay particles have re-arranged under constant  $\sigma'_{v0}$  once primary consolidation is complete. Over time, this results in stiffening, which appears as an increase in  $\sigma'_p$  on the consolidation curve. Secondly, the OCR values within these depths are likely affected by decreasing sample quality with depth. A decrease in sample quality results as an increase in estimated  $\sigma'_p$  from the flattening of the “break” in the consolidation curve. Furthermore, a decrease in sample quality also indicates that part of the structure of the clay has been destroyed and leads to more deformations prior to  $\sigma'_p$  (higher  $C_r$  values).

### 7.2.3 Recompression Undrained Triaxial Shear

Anisotropically consolidated undrained compression (CAUC) triaxial shear testing was performed on 5 of the 9 tube samples of Presumpscot clay for the I-395 Terminus site in accordance with the procedures outlined in Section 3.4.4. Table 7.5 presents specimen properties, conditions following recompression to the estimated  $\sigma'_{v0}$ , sample quality, and pre-shear parameters for the triaxial specimens. Table 7.6 presents results from the shear phase of the triaxial tests, including peak shear stress, strain at failure, pore pressure at failure, and shear stress normalized to vertical effective compressive stress. All tested specimens were of very good to excellent quality. Note that  $s_u = q_f =$  undrained shear strength.

Shallow samples 1U and 2U were not tested because they were highly overconsolidated and could hardly be trimmed with a wire saw during specimen preparation. Since these samples were so heavily overconsolidated, undrained shear testing does not properly characterize the critical shear strength properties of the clay, which in this case would be drained shear strength. Samples 3U and 7U were not tested due to disturbance of the extracted samples. Resulting profiles of  $s_u$  and Resulting profiles of  $s_u$  and  $s_u$  normalized by  $\sigma'_{v0}$  ( $s_u/\sigma'_{v0}$ ) are presented in Figure 7.7.

$s_u$  of the tested specimens ranged from 1,196 psf at 13.2 feet depth to 404 psf at 19.3 feet depth. Aside from the specimen from 13.2 feet, which was collected in the upper, overconsolidated portion of the deposit, all of the  $s_u$  values fell within  $\pm 80$ psf of 464 psf showing strong consistency with depth. Within these same depths of the deposit,  $s_u$  from the field vane shear testing (FVT) agreed well with these CAUC values.

Table 7.5: Summary of pre-shear recompression consolidated undrained triaxial shear specimen and consolidation properties for Presumpscot clay samples collected from Boring HB-BREW-102 at the I-395 Terminus site.

In Situ		Laboratory Stress History & Quality															
Sample	Depth (ft)	$w_n$ (%)	$e_0$ (-)	$\sigma'_{v0}$ (psf)	$\sigma'_p$ <sup>1</sup> (psf)	OCR (-)	In situ					OCR <sub>c</sub> <sup>4</sup> (-)	$\epsilon_{vol}$ at		$\epsilon_a$ at		<sup>5</sup> NGI Qual. (-)
							$K_0$ <sup>2</sup> (-)	$e_c$ (-)	$\sigma'_{vc}$ (psf)	$\sigma'_{hc}$ (psf)	$K_c$ <sup>3</sup> (-)		$\sigma'_{v0}$ (%)	$\sigma'_{v0}$ (%)	$\Delta e/e_0$ (-)		
4U	13.2	28.3	0.83	712	6426	8.6	1.44	0.83	879	850	0.97	7.3	0.10	0.02	0.002	VG/E	
5U	15.8	37.1	1.02	849	5060	3.4	1.16	1.01	754	610	0.81	6.7	0.44	0.23	0.009	VG/E	
6U	19.3	39.2	1.06	1036	1976	1.5	0.64	1.06	1002	821	0.82	2.0	0.18	0.39	0.004	VG/E	
8U	25.3	35.4	0.97	1349	2564	1.5	0.64	0.96	1294	956	0.74	2.0	0.76	0.39	0.015	VG/E	
9U	27.4	35.8	0.93	1464	2781	2.1	0.64	0.90	1361	1204	0.88	2.0	1.54	0.50	0.032	VG/E	

Notes: <sup>1</sup>Best fit profile; <sup>2</sup> $K_{0(OC)} = 0.46(OCR)^{0.52}$  (from Ladd et al. 1999); <sup>3</sup> $K_c = \sigma'_{hc}/\sigma'_{vc}$ ; <sup>4</sup> $OCR_c = \sigma'_p/\sigma'_{vc}$ ; <sup>5</sup>From Lunne et al., (2006), where VG/E: very good to excellent quality, G/F: good to fair, P: poor, and VP: very poor;

Table 7.6: Summary of recompression consolidated undrained triaxial shear results for Presumpscot clay samples collected from Boring HB-BREW-102 at the I-395 Terminus site.

In Situ		Laboratory Stress History & Quality					At Failure								
Sample	Depth (ft)	OCR (-)	$\sigma'_{vc}$ (psf)	$\sigma'_{hc}$ (psf)	$K_c$ <sup>3</sup> (-)	OCR <sub>c</sub> <sup>4</sup> (-)	<sup>5</sup> NGI		$q_f$ (psf)	$A_f$	$\epsilon_{a-f}$ (%)	$\Delta u_f$ (psf)	$q_f/\sigma'_{vc}$ (-)	$p'_f/\sigma'_{vc}$ (-)	$q_f/\sigma'_{v0}$ (-)
							Qual. (-)	$q_f$ (psf)							
4U	13.2	8.6	879	850	0.97	7.3	VG/E	1196	-0.12	8.2	-287	1.36	2.82	1.68	
5U	15.8	3.4	754	610	0.81	6.7	VG/E	535	0.26	2.4	241	0.71	1.19	0.63	
6U	19.3	1.5	1002	821	0.82	2.0	VG/E	404	0.97	1.5	603	0.40	0.67	0.39	
8U	25.3	1.5	1294	956	0.74	2.0	VG/E	564	0.50	1.2	401	0.44	0.86	0.42	
9U	27.4	2.1	1361	1204	0.88	2.0	VG/E	560	0.66	1.3	632	0.41	0.81	0.38	

Notes: <sup>1</sup>Best fit profile; <sup>2</sup> $K_{0(OC)} = 0.46(OCR)^{0.52}$  (from Ladd et al. 1999); <sup>3</sup> $K_c = \sigma'_{hc}/\sigma'_{vc}$ ; <sup>4</sup> $OCR_c = \sigma'_p/\sigma'_{vc}$ ; <sup>5</sup>From Lunne et al., (2006), where VG/E: very good to excellent quality, G/F: good to fair, P: poor, and VP: very poor;

In situ lateral earth pressure ( $K_0$ ) was estimated using the Ladd *et al.*, (1999) equation with the OCR determined from the CRS testing and a  $K_{0(NC)}$  of 0.46. Table 7.6 shows that there are some differences between the estimated in situ stress history conditions of the Presumpscot clay and those under which the specimens were tested during the CAUC procedure. The cause of the difference in these stresses (i.e.  $\sigma'_{vc} \neq \sigma'_{v0}$  condition) is due to the limitations of the test equipment and is discussed further in Section 3.4.4. While the effect of these differing conditions are not strictly quantifiable, it is generally assumed that lower  $\sigma'_{vc}$  than  $\sigma'_{v0}$  generates higher measured  $s_u$  (since more of the natural clay structure has been kept intact).

For the most part,  $\sigma'_{vc}$  and  $\sigma'_{v0}$  were relatively similar with the exception of specimen 4U, which was consolidated more than 150 psf more than the estimated  $\sigma'_{v0}$ . However, since the

specimen was highly overconsolidated, this likely did not have a large effect on the resulting  $s_u$ . From the remaining samples, percent difference in the OCR preshear versus in situ values ranged from 5% to 65%. Also presented in Figure 7.7 are  $s_u$  measurements from FVT from Boring HB-BREW-101.  $s_u$  values from FVT are generally slightly lower than  $s_u$  testing CAUC but agree reasonably well.  $s_u$  determined from the FVT at 5 feet resulted in a low value, likely from the use of a very small vane and a resulting small shear plane.

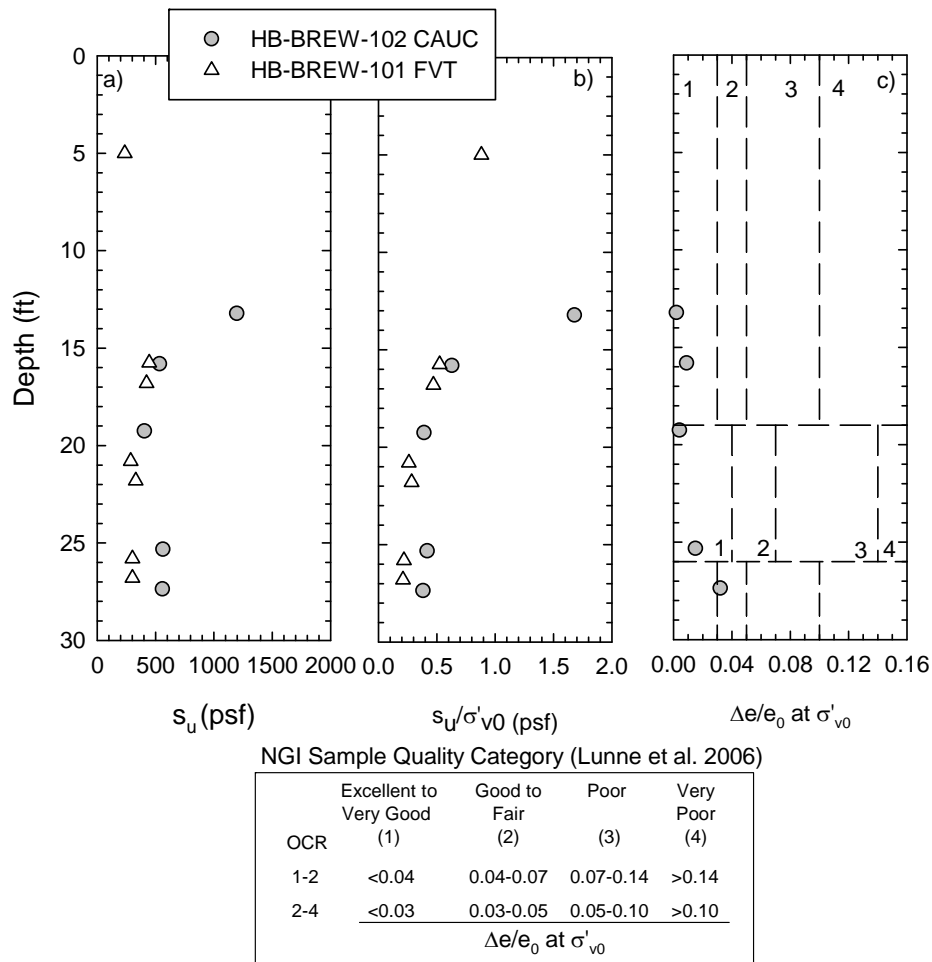


Figure 7.7: Subsurface profile of a) undrained shear strength ( $s_u$ ), b) normalized shear strength and c) NGI sample quality assessment obtained from CAUC triaxial testing for Presumpscot clay samples collected from Boring HB-BREW-102 at the I-395 Terminus site.

$s_u/\sigma'_{v0}$  ranged from 0.38 to 0.42 in the low OCR specimens (OCR from 1.5 to 2.1).

Normalized  $s_u$  in similar soft clays typically ranges from 0.2 to 0.3 and will increase with increasing overconsolidation. When using SHANSEP  $S$  and  $m$  parameters (discussed below) from SHANSEP testing in similar clays (Table 2.2), the normalized values obtained at the I-395 Terminus site match well with these past studies. Since the  $\sigma'_{vc}$  values in the CAUC testing were slightly lower than  $\sigma'_{v0}$ , the resulting  $s_u/\sigma'_{vc}$  values were slightly higher (0.40 to 0.44) than when normalized with  $s_u/\sigma'_{v0}$ .

Figure 7.8 presents the stress paths from CAUC testing normalized by consolidation effective stress. The high overconsolidation ratio specimen (sample 4U) generated negative pore water pressures during undrained shear. For the moderately overconsolidated specimen 5U, shear induced pore pressures were initially negative, generated as the sample dilated, but eventually pore pressure became positive during undrained shear. Lightly overconsolidated samples (6U, 8U, and 9U) produced positive pore water pressures during the shearing process ranging from 401 to 632 psf at failure. The tendency of the leftward curvature from the start of the test is consistent with the lightly overconsolidated behavior determined from the consolidation testing. The  $\psi'$  failure angle ranges from 27° to 32° for the Presumpscot at the test site, assuming a zero  $q = s_u$  intercept (i.e.,  $a = 0$ ). Equation 7.2 can be used to convert p'-q failure characteristics ( $\psi$  and  $a$ ) to Mohr Coulomb failure characteristics ( $\phi$  and  $c$ ). Note that  $p' = (\sigma'_1 + \sigma'_3)/2$  and that  $q = (\sigma'_1 - \sigma'_3)/2$ . Assuming cohesion  $c = 0$ , effective friction angle  $\phi'$  ranges from 30.6° to 38.7°, which fits well with drained shear testing for Presumpscot clay (Devin & Sandford, 1990)

$$\sin \phi = \tan \psi \quad 7.1$$

(where  $c = 0$  and  $a = 0$ )



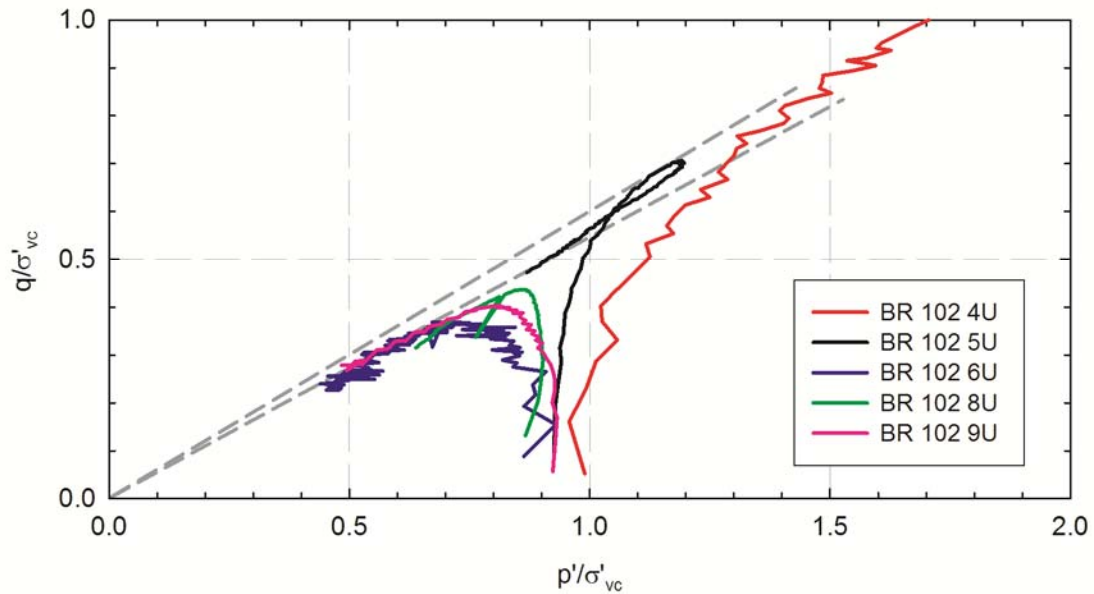


Figure 7.8: Recompression consolidated undrained triaxial (CAUC) normalized effective stress paths for Presumpscot clay samples collected from Boring HB-BREW-102 at the I-395 Terminus site.

#### 7.2.4 SHANSEP Consolidated Undrained Triaxial Shear Results

SHANSEP testing (Section 2.1.4) was conducted on the Presumpscot clay at the I-395 Terminus site to determine if this type of testing is appropriate for the silty clay. Table 7.7 presents specimen properties, reconsolidation conditions, sample quality, and pre-shear parameters for SHANSEP triaxial tests conducted on two specimens from sample 6U. Table 7.8 presents results from the shear phase of the same SHANSEP triaxial tests including peak shear stress, strain at failure, pore pressure at failure, and shear stress normalized to vertical effective compressive stress and the predicted relationship between overconsolidation and normalized shear strength. SHANSEP undrained triaxial tests conducted on two specimens from sample 6U.

Table 7.7: Summary of specimen and consolidation properties for SHANSEP undrained triaxial tests for Presumpscot clay samples collected from Boring HB-BREW-102 at the I-395 Terminus site.

In Situ			Laboratory Stress History												
Depth (ft)	$w_c$ (%)	$e_0$ (-)	$\sigma'_{v0}$ (psf)	$\sigma_p^{-1}$ (psf)	$\sigma'_{v\ max}$ (psf)	$\sigma'_{vc}$ (psf)	OCR ( $\sigma'_p/\sigma'_{vc}$ )	$K_c$ ( $\sigma'_3/\sigma'_1$ )	$\varepsilon_{vol-max}$ (%)	$e_c$ (-)	$\varepsilon_{vol}$ at $\sigma'_{v0}$ (%)	$\varepsilon_a$ at $\sigma'_{v0}$ (%)	$\Delta e/e_0$ at $\sigma'_{v0}$	NGI Qual.	
19.0	40.5	1.1	1015	1462	3388	2736	1.24	0.45	4.40	1.04	4.40	2.36	0.01	VG to E	
18.7	40.0	1.1	999	1462	2978	1487	2.00	0.87	0.66	1.07	0.42	4.52	0.01	VG to E	

Table 7.8: Summary of specimen and consolidation properties for SHANSEP undrained triaxial tests for Presumpscot clay samples collected from Boring HB-BREW-102 at the I-395 Terminus site.

In Situ		Laboratory Stress History						At Failure					Prediction	
Depth (ft)	$\sigma'_{v\ max}$ (psf)	$\sigma'_{vc}$ (psf)	OCR ( $\sigma'_p/\sigma'_{vc}$ )	$K_c$ ( $\sigma'_3/\sigma'_1$ )	$e_c$ (-)	$\Delta e/e_0$ at $\sigma'_{v0}$	NGI Qual.	$q_f$ (psf)	$\varepsilon_a$ (%)	$\Delta u_f$ (psf)	$q_f/\sigma'_{vc}$ (-)	$p'_f/\sigma'_{vc}$ (-)	S	m
19.0	3388	2736	1.24	0.45	1.04	0.01	VG to E	971.6	0.151	114.9	0.35	0.75		
18.7	2978	1487	2.00	0.87	1.07	0.01	VG to E	762.7	0.721	430.9	0.51	1.1	0.30	0.78

A best-fit curve was applied to the resulting normalized shear strength and overconsolidation ratios to determine the two SHANSEP coefficients,  $S$  and  $m$  for Equation 2.1. The resulting normalized  $s_u$  for the normally consolidated soil is 0.30 and the resulting OCR exponent is 0.78. The resulting SHANSEP relationship is illustrated in Equation 7.2. Figure 7.9 illustrates the resulting stress path for each tested specimen. SHANSEP  $S$  coefficient, representing of  $s_u/\sigma'_{v0}$  at normally consolidated conditions of the clay, and  $m$  coefficient at the I-395 Terminus site are very similar to the values reported Ladd *et al.*, (1999) for Boston blue clay (BBC), which resulted in  $S$  and  $m$  parameters of 0.28 and 0.68, respectively. When compared to other SHANSEP studies of Presumpscot clay and BBC, the  $S$  parameter is similar but the  $m$  parameter determined at this site is higher than other clay deposits.

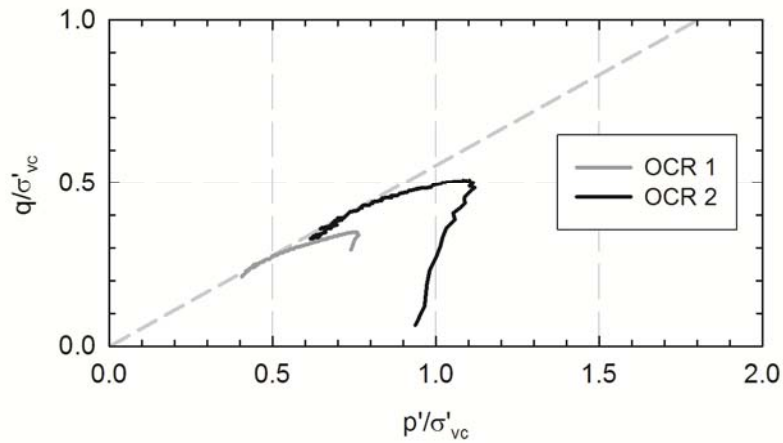


Figure 7.9: SHANSEP recompression consolidated undrained triaxial (CAUC) normalized effective stress paths for Presumpscot clay sample 8U from Boring HB-BREW-102 conducted at the I-395 Terminus site.

The sample with an OCR of 1 exhibited strictly normally consolidated behavior. As compression occurred after the consolidation phase, positive pore pressures were generated since the specimen had a tendency to reduce in volume (outward pressure of pore water). This reduced the effective stress of the sample, behavior which is shown as the sharp leftward curvature of the stress path.

The sample with an OCR of 2 had initial dilative behavior accompanied by negative pore pressures (as the sample swelled) during compression. Once the normalized effective stress during compression reached unity, the sample no longer increased in volume and returned to normally consolidated behavior. Ultimate stress paths for both samples resulted in the same slope.

$$s_{u(OCR)} = 0.30 \cdot OCR^{0.78} \quad 7.2$$

Comparison of measured recompression strengths (from CAUC triaxial compression tests) and SHANSEP predicted strengths normalized by the effective overburden stress with

overconsolidation is illustrated in Figure 7.10. The SHANSEP equation developed from lower OCR (1 and 2) specimens over predicts strength over the range of OCR values determined for in situ soil, particularly for the higher OCR soil, when compared with the recompression triaxial shear data. For the lightly overconsolidated soil, the SHANSEP equation is similar to the CAUC undrained shear strength results, but as OCR of the tested specimens increases, the scatter of normalized  $s_u$  becomes too scattered to evaluate if the SHANSEP properly matches in situ data.

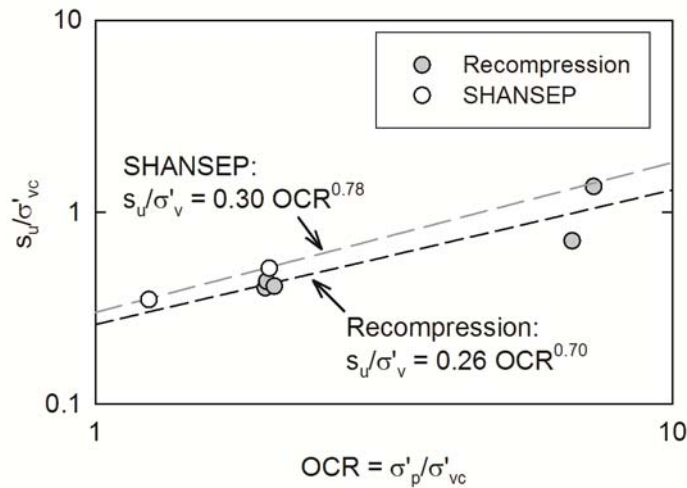


Figure 7.10: Comparison of normalized undrained shear strength from recompression and SHANSEP triaxial compression tests for Presumpscot clay specimens from boring HB-BREW-102 6U conducted at the I-395 Terminus site.

### 7.2.5 Summary and Interpretations of Laboratory Testing Results

This section provides a synthesis of the laboratory testing results in order to characterize the deposit of the Presumpscot clay at the I-395 Terminus site using the index results, consolidation properties, and shear strength properties. The following trends can be established from the laboratory results of index, consolidation, and shear strength testing of the Presumpscot clay samples tested from the site:

- Water content in the overconsolidated crust ranged from 22% to 28% and ranged from 29% to 40% in the softer, mildly overconsolidated soil at depth 15 feet to 28 feet.
- Atterberg Limits are consistent throughout the entire deposit. Plastic limit ranged from 19 to 22 while liquid limit ranged from 31 to 37. Liquidity index is well below 1.0 in the overconsolidated crust, but ranges from 0.81 to 1.28 in the deeper soil.
- The sensitivity of the Presumpscot at the site is low. It is likely that this derives from two factors: a high remolded shear strength from the silt content since the granular particles can still actively resist shearing forces after remolding, and a low concentration of salt ions within the marine environment in which the clay was deposited. Lower salt ion concentration reduces the amount of potential ion leaching, which leads to higher sensitivity.
- OCR in the crust ranged from 12.1 to 8.6, and generally decreased with depth. The preconsolidation pressure ( $\sigma'_p$ ) determined from one dimensional consolidation testing within this layer is an “apparent” preconsolidation, which is caused by  $\sigma'_{v0}$  changes due to groundwater fluctuations. Shallow, crustal samples were mottled, blocky, and relatively dry compared to the deeper, less overconsolidated samples.
- OCR in the deeper, softer portion of the deposit ranged from 3.4 to 1.5. The source of the mild overconsolidation of clay within this depth is due to a combination of secondary compression and frost penetration.
- Recompression Index ( $C_r$ ) ranged from 0.06 to 0.10 and virgin compression index ( $C_c$ ) ranged from 0.21 to 0.35. Often,  $C_r$  is assumed to be about 0.05- 0.10 of  $C_c$  (Holtz *et al.*, 2011), however,  $C_r$  ranges from 0.17- 0.43 of  $C_c$  for this site.

- $s_u$  measured in the laboratory is likely similar to in situ value because OCR and  $K_0$  values were similar to test conditions.  $s_u$  of the overconsolidated sample 4U (OCR = 8.6) resulted in 1,196 psf. All tested specimens at a depth of 15 feet and fell within  $\pm 80$ psf of 464 psf.  $s_u/\sigma'_{v0}$  ranged from 0.38 to 0.42 in the low OCR specimens.
- SHANSEP  $S$  and  $m$  values are 0.30 and 0.78, respectively and are similar to the recompression  $S$  and  $m$  values of 0.26 and 0.70. However, the similarity may be somewhat fortuitous since most of the CAUC tested samples were lightly overconsolidated and the other two plotted well off of the best-fit recompression trend line.

### 7.3 Seismic Cone Penetration Testing Results

Six piezocone penetrometer tests were performed at the I-395 Brewer site on March 7th, 2013 by ConeTec of West Berlin, New Jersey in general accordance ASTM D-5778 *Standard Test Method for Electronic Friction Cone and Piezocone Penetration Testing of Soils*. These included two piezocone penetrometer tests, CPTu 102 and CPTu 103, and four seismic piezocone penetrometer tests where seismic testing was conducted at 1 m or 3.28 feet intervals, SCPTu101, 104, 105, and 106. Figure 7.2 illustrates the locations of these profiles. Table 7.9 summarizes the depths of each sounding and the lateral distance between the soundings and the two drilled borings HB-BREW-101 and -102, which included field vane shear testing (FVT) and undisturbed Shelby tube sampling, respectively. All six soundings were advanced to refusal using a 1.7 inch diameter cone advanced with a CME 55 rig mounted on a Morooka carrier. The seismic source was a steel I-Beam placed directly on the ground struck with a hammer. Normal force was applied to the beam via the dead weight of the rig.

Table 7.9: Location and depths of the six (S)CPTu soundings performed at the I-395 Terminus site (reproduced from ConeTec, 2013).

Sounding	Total Depth (ft)	Dist. To HB-BREW-101 (ft)	Dist. To HB-BREW-102 (ft)
SCPTu 101	26.7	18.8	58.2
CPTu 102	25.3	46.4	119.5
CPTu 103	31.7	286.3	352.8
SCPTu 104	27.1	152.6	218.2
SCPTu 105	29.9	102.4	145.8
SCPTu 106	29.5	74.8	8.0

HB-BREW-101 included field vane shear testing (FVT), HB-BREW-102 included undisturbed sampling

### 7.3.1 Results

Figure 7.11 presents measurements of corrected tip resistance ( $q_t$ ), sleeve friction ( $f_s$ ), and pore pressure ( $u_2$ ) with depth measured from SCPTu 101, -102, and -106, the three closest soundings to the sampling location (HB-BREW-102). The remaining three soundings were excluded from the analysis for simplicity. Visual inspection of the results from the other three soundings indicated similar stratigraphy encountered from the three soundings presented in Figure 7.11.

Corrected tip resistance ( $q_t$ ) in the top foot of the deposit was high for all three soundings due to the presence of frozen soil. From 1 ft to 8 ft depth, there was large fluctuations in  $q_t$  between (S)CPTu 101, 102, and 106.  $q_t$  within these depths ranged from 20,000 psf to 85,000 psf in magnitude without any particular layering or trend with depth. At a depth of 8 feet, the three  $q_t$  profiles converge at a value of approximately 40,000 psf and begin to decrease steadily with depth to 19 feet. Below 19 feet, the three  $q_t$  profiles increase practically linearly with depth (due to greater overburden) until refusal is encountered. A depth of 19 feet coincides with the practically normally consolidated conditions encountered from the tested specimens.

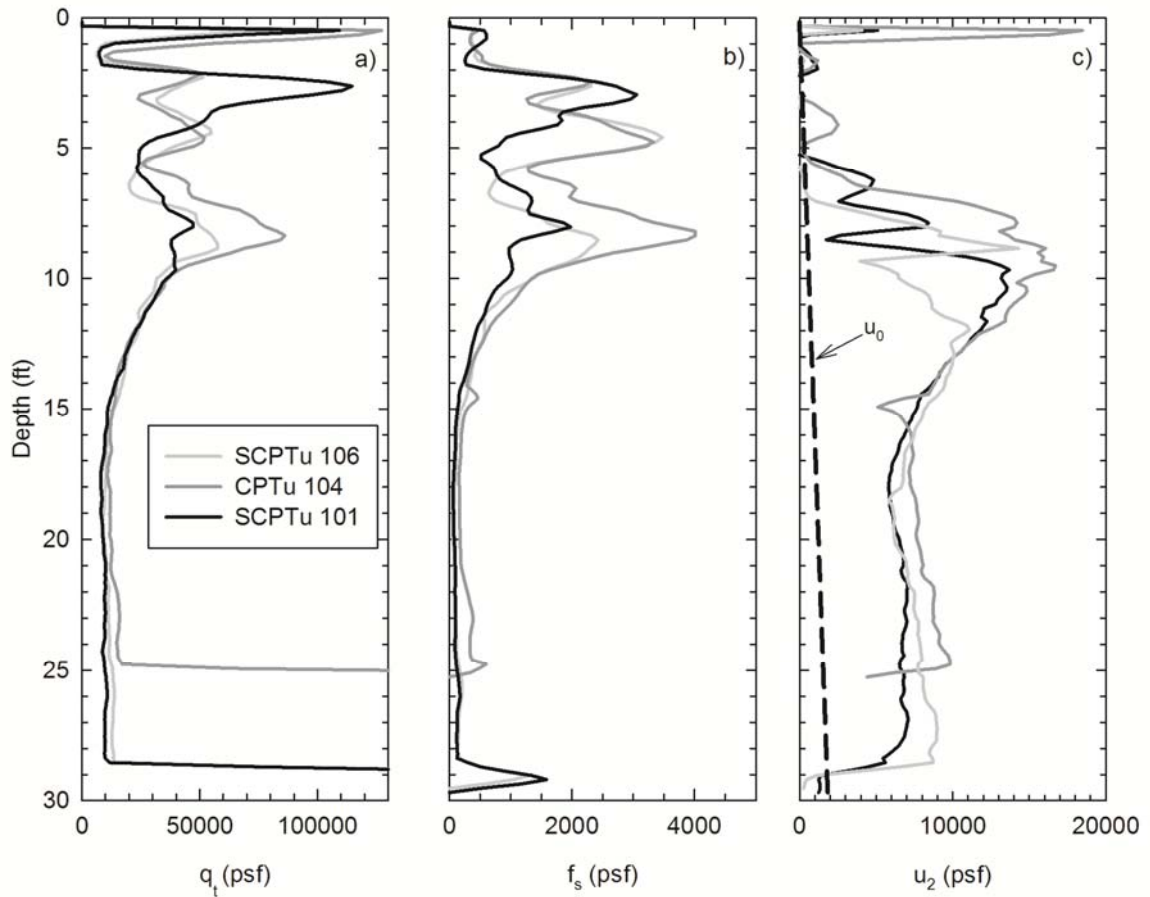


Figure 7.11: Measured values of (a) corrected tip resistance, (b) sleeve friction, and (c) pore pressure from SCPTu 101, CPTu 102, and SCPTu 106 performed at the I-395 Terminus site.

$f_s$  exhibited a similar trend to  $q_t$  for both the shallow stiff and deeper soft clay deposits of the Presumpscot clay. Values fluctuated from 1 feet to 12 feet, showing a reduction from 8 feet to 14 feet with a peak at approximately 9 feet. Below the stiff clay,  $f_s$  from all three soundings showed a similar and consistent decrease with depth. Values of  $f_s$  in the stiff Presumpscot clay ranged from 200 psf to 4,000 psf and values in the soft Presumpscot clay ranged from approximately 100 psf to 200 psf.

$f_s$  measurements are theorized to be analogous to remolded shear strength ( $s_{u(r)}$ ) of clay (Mayne, 2014). To test this theory for the Presumpscot clay at the I-395 Terminus site,  $f_s$



measurements from SCPTu 101 was compared to  $s_{u(r)}$  values collected from field vane shear testing (FVT) and laboratory fall cone testing (FVT) and laboratory fall cone testing (Figure 7.12). SCPTu 101 was selected for comparison because it was closest to Boring HB-BREW-101, where FVT was conducted.

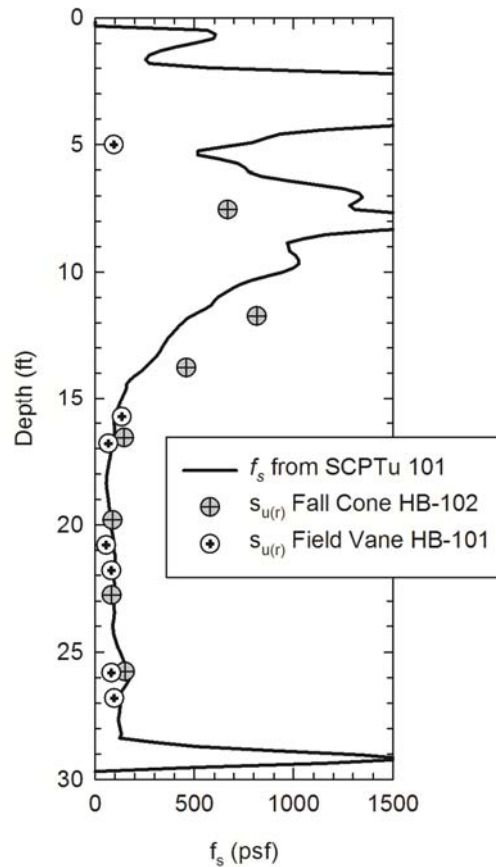


Figure 7.12: Profile comparing remolded shear strength values ( $s_{u(r)}$ ) obtained from HB-BREW-101 field vane tests and fall cone tests from HB-BREW-102 samples with sleeve friction from SCPTu 101 at the I-395 Terminus site.

Figure 7.12 shows a strong correlation between measured  $f_s$  and measured  $s_{u(r)}$  in the soft clay below 14 feet depth. Conversely, for the stiff clay above 14 feet, correlation between  $f_s$  and  $s_{u(r)}$  was poor, which is influenced by the fact that the CPTu soundings indicated large variation in the properties of the stiff clay layer. Therefore the  $f_s$  and  $s_{u(r)}$  values may not be strictly comparable since they were all performed at different locations.

$u_2$  in the stiff clay ranged from -1,400 psf to 18,500 psf. Since the clay in this zone is overconsolidated, the soil has a tendency to dilate during shear causing a reduction in pore pressure and subsequent negative values of  $u_2$  are measured. When a CPTu is advanced into free-draining soils such as gravels and sands, the  $u_2$  measurement is equivalent to the hydrostatic pore water pressure ( $u_0$ ). In soft, cohesive soils such as the lower portion of the Presumpscot clay at the site, since the shearing of the soil induces pore pressures from the undrained shear process, the  $u_2$  measurements is a cumulative value of the  $u_0$  and pore pressure generated during the shear of the soil. Inspection of the  $u_2$  collected in the lower portions of the deposit corresponds to the expected behavior (i.e. excess pore pressures which steadily increase with depth); however,  $u_2$  measurements from 7 feet to 13 feet are higher than expected.

Clay specimens collected from this portion of the deposit indicate overconsolidated clay that would theoretically generate less (or negative) pore pressure during shear as compared to the deeper, more normally consolidated clay. Therefore, the elevated  $u_2$  measurements from depths 7 to 13 feet can be inferred to be caused by artesian pressure occurring within the clay at these depths. Driller remarks from the HB-BREW-102 indicated “Artesian Water Pressure, lifted water 2.1 ft above ground level” even though the groundwater elevation was noted to be at the current ground surface. In the soft, lightly overconsolidated layer, pore pressures started around 5,800 psf and increased to 8,700 psf at the bottom of the layer due to increasing overburden stress with increasing overburden soil.

Shear wave velocity,  $V_s$ , measurements from SCPTu 101 and SCPTu 106 are illustrated in Figure 7.13.  $V_s$  values are represented at the mid-point between the tests conducted at each rod break during penetration (3.28 feet).  $V_s$  values vary between 343 and 691 ft/s with depth and show fairly good agreement between soundings and a narrow range. Figure 7.13 additionally shows small-strain (e.g., elastic) shear modulus ( $G_0$ ) over the range where undisturbed samples were available from HB-BREW-102 and measures of in situ measures bulk density ( $\rho_t$ ;  $\gamma_t$  in

summary tables) were available.  $G_0$ , calculated using Equation 2.10, ranges from approximately 2.9 to 12.0 ksi over the depth range shown. Lastly, the rigidity index,  $I_r$ , often used for foundation design applications, was determined using Equation 2.18 interpreted  $G_0$  and  $s_u$  determined from CAUC triaxial compression tests on undisturbed samples from HB-BREW-102.  $I_r$  values range from 624 to 3092. Lower values near the ground surface indicate a stiffer soil resulting from the higher OCR and  $s_u$  values.

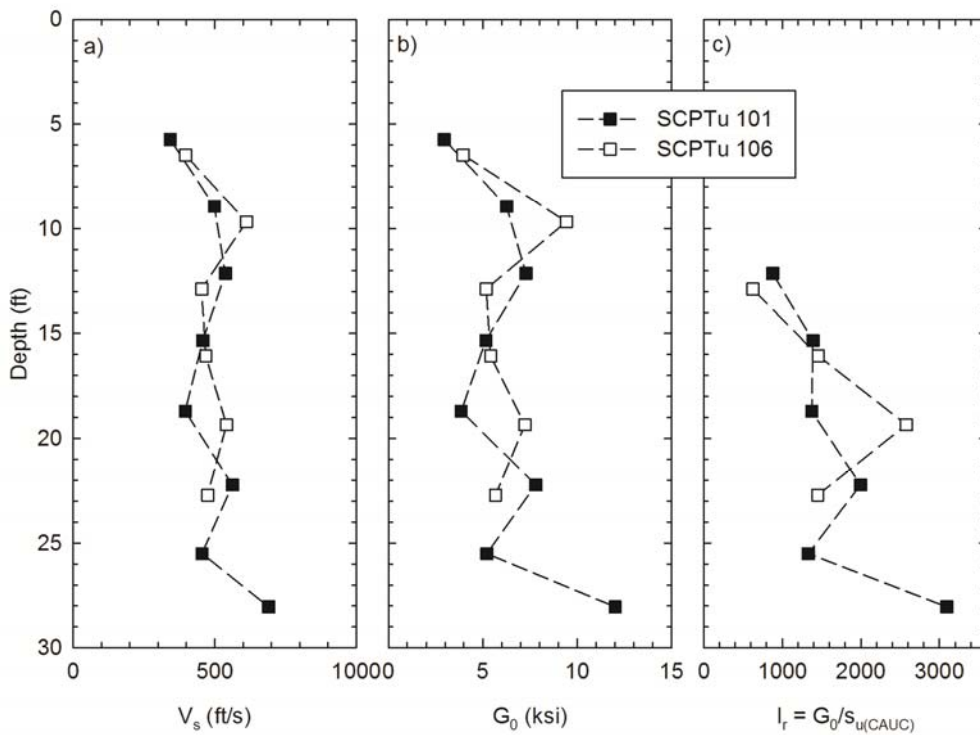


Figure 7.13: Depth profile of shear wave velocity ( $V_s$ ), shear modulus ( $G_0$ ), and rigidity index ( $I_r$ ) for SCPTu101 and -106 at the I-395 Terminus site.

### 7.3.2 Correlations to Classification

Empirical charts proposed by Robertson (1990), Schneider *et al.* (2008), and Robertson (2009) to classify soils based on CPTu measurements (Section 2.3.1) plot normalized tip resistance ( $Q_t$ ) versus sleeve friction ratio ( $F_r$ ) or normalized pore pressure ( $B_q$ ). Measured data

plots in a region which has a corresponding “Soil Behavior Type” or SBT. SBT regions were developed based on observed  $Q_b$ ,  $F_r$ , and  $B_q$  measurements from specific types of soils and correlated with laboratory measured soil behavior. Normalized CPTu measurements are used to eliminate the influence of depth related to increases in overburden pressure. Figure 7.14 displays the profiles of the three normalized parameters  $Q_b$ ,  $F_r$ , and  $B_q$  collected from SCPTu 101, 102, and 106.

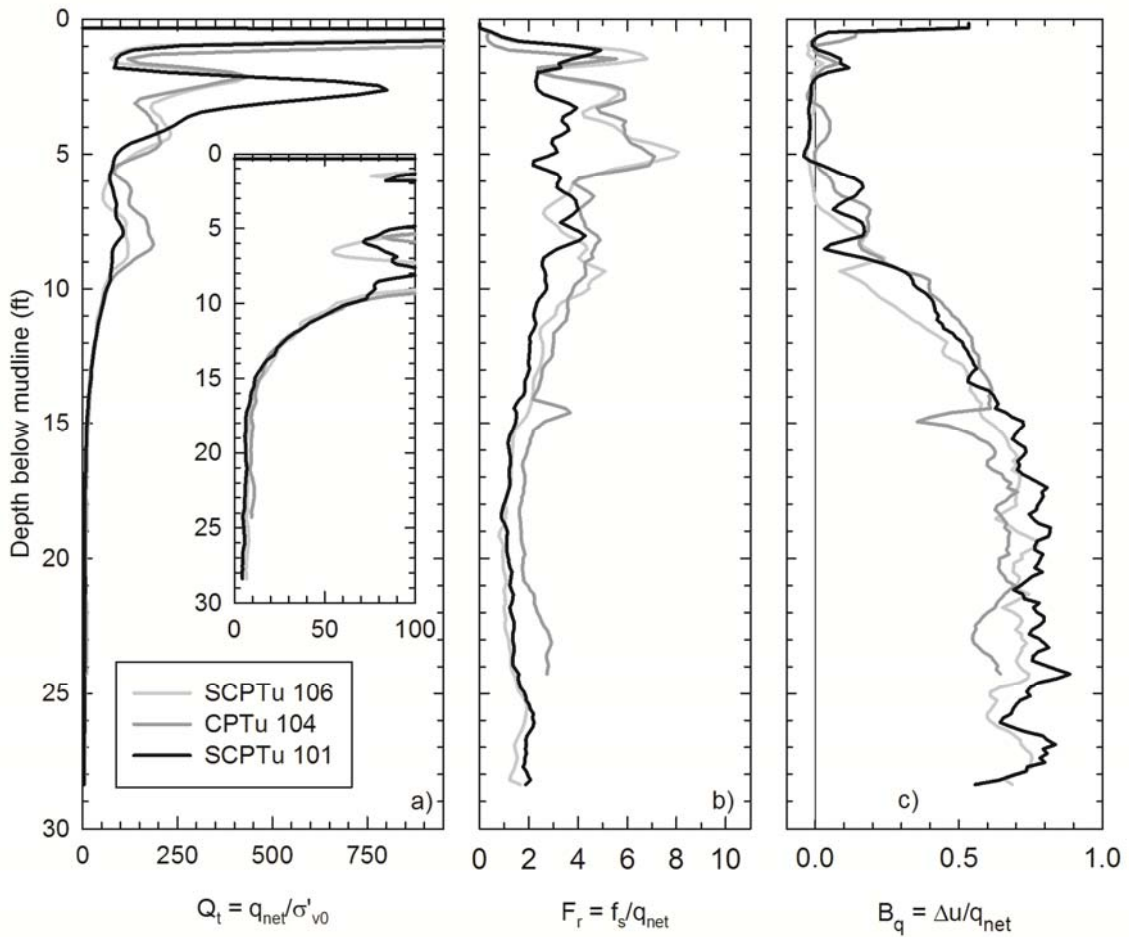


Figure 7.14: Measurements of a) normalized tip resistance ( $Q_t$ ), b) sleeve friction ratio ( $F_r$ ), and c) normalized pore pressure ( $B_q$ ) for SCPTu 101, 102, and 106 conducted at the I-395 Terminus site.

Each of the four classification charts were evaluated for their applicability to the Presumpscot clay at the I-395 Terminus site using Unified Soil Classification System (USCS) results from laboratory analysis of Boring HB-BREW-102 soil samples and values of  $Q_b$ ,  $F_r$ , and  $B_q$  collected from SCPTu 101 and CPTu 106 at corresponding depths. SCPTu 102 was not used because it was the furthest away from HB-BREW-102. For three of the charts (Robertson 1990 and Robertson 2009; Figure 7.15a, b and c), there are 9 regions corresponding to SBT. SBT 3 “clay to silty clay” and SBT 4 “clayey silt to silty clay” were considered correct classifications of the Presumpscot clay based on laboratory data. SBT 9 “very stiff fine grained” was also considered an adequate classification of the stiff clay in the upper portion of the deposit. For the fourth chart (Schneider *et al.* 2008; Figure 7.15d), a different classification system is used, of which the “clays” region was considered to be correct classification of the Presumpscot clay. Plotted data points from SCPTu 101 and 106 are presented in Figure 7.15 and Figure 7.16, respectively. CPTu data for the Presumpscot clay at the site plotted in SBT 3 “clays,” SBT 4 “silt mixtures,” SBT 5 “sand mixtures,” SBT 6 “sands,” and SBT 9 “very stiff fine grained” classifications from the Robertson (1990 and 2009) plots and “clays,” “silts and low rigidity index clays,” and “sand” for the Schneider *et al.*, (2008) plot. All of the tested specimens classified as CL, lean clay in accordance with USCS. Clearly, the SBT-based classification results in a variety of classes as opposed to the USCS method.

In general, the upper, highly overconsolidated portion of the deposit (from 1 ft to approximately 10 ft) resulted in SBT 5, 6, and 9 and the lower, softer portion of the deposit classified in SBT 3 and 4. Similarly, all of the data points classified as non-clay come from the upper part of the deposit. Table 7.10 presents the results of this analysis including the number of samples laboratory samples tested, number of USCS classifications matching the SBT classification, and the resulting percent effectiveness (USCS-SBT matches divided by the number of samples). The  $F_r$  and  $B_q$  shown in front of the Robertson (1990) in Table 7.10 is notation for

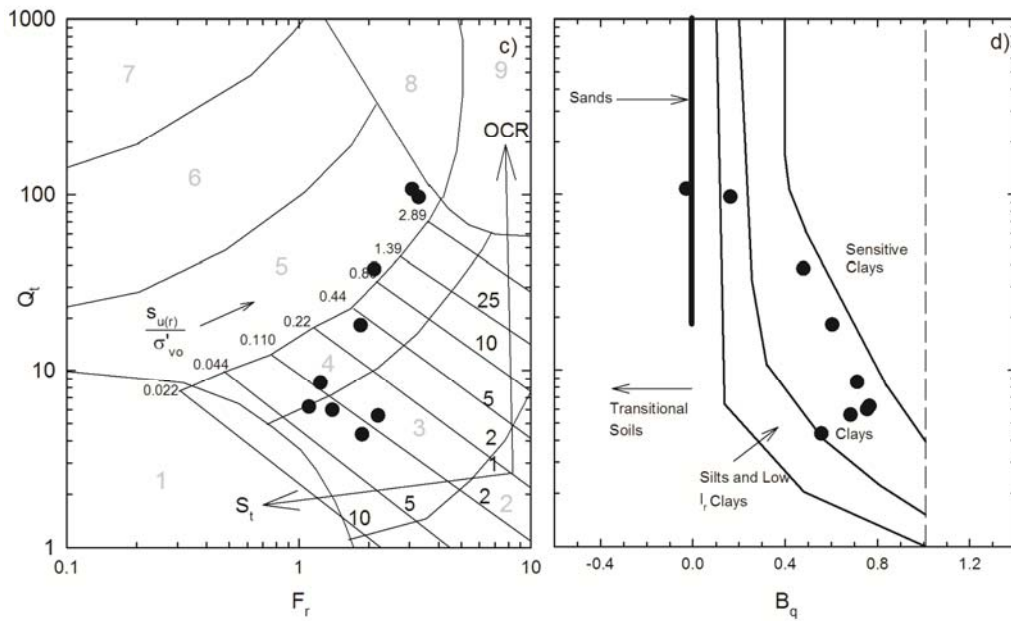
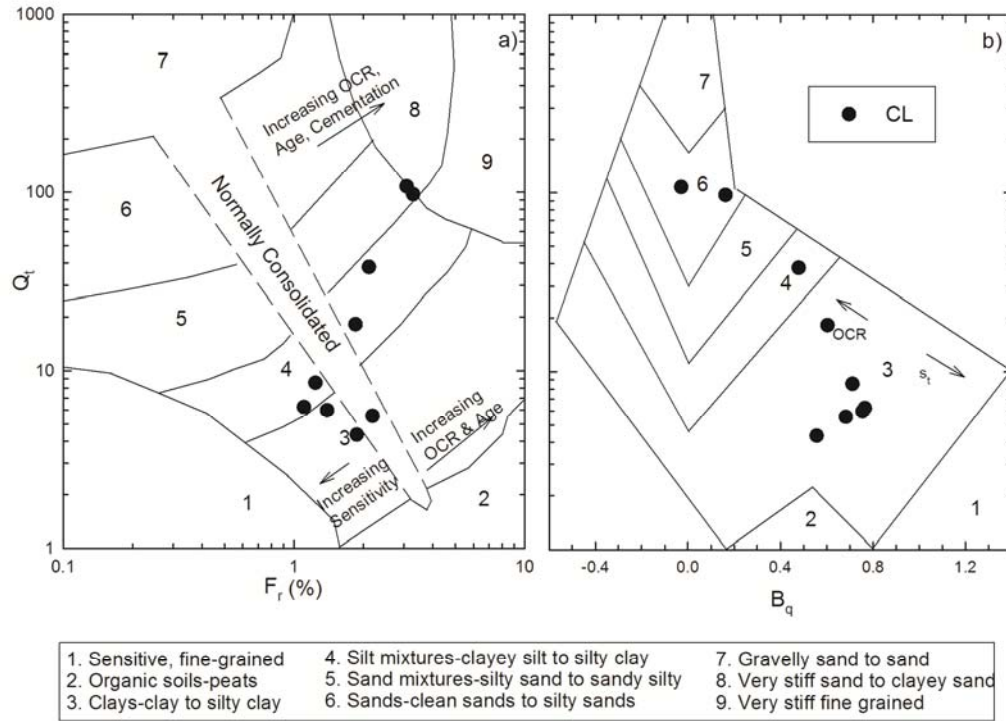


Figure 7.15: Soil classification results from SCPTu 101 at the I-395 Terminus site comparing laboratory-determined USCS classification to classification charts using a)  $Q_t$  vs.  $F_r$  (Robertson 1990), b)  $Q_t$  vs.  $B_q$  (Robertson 1990), c)  $Q_t$  vs.  $F_r$  (Robertson 2009), d)  $Q_t$  vs.  $B_q$  (Schneider *et al.*, 2008)

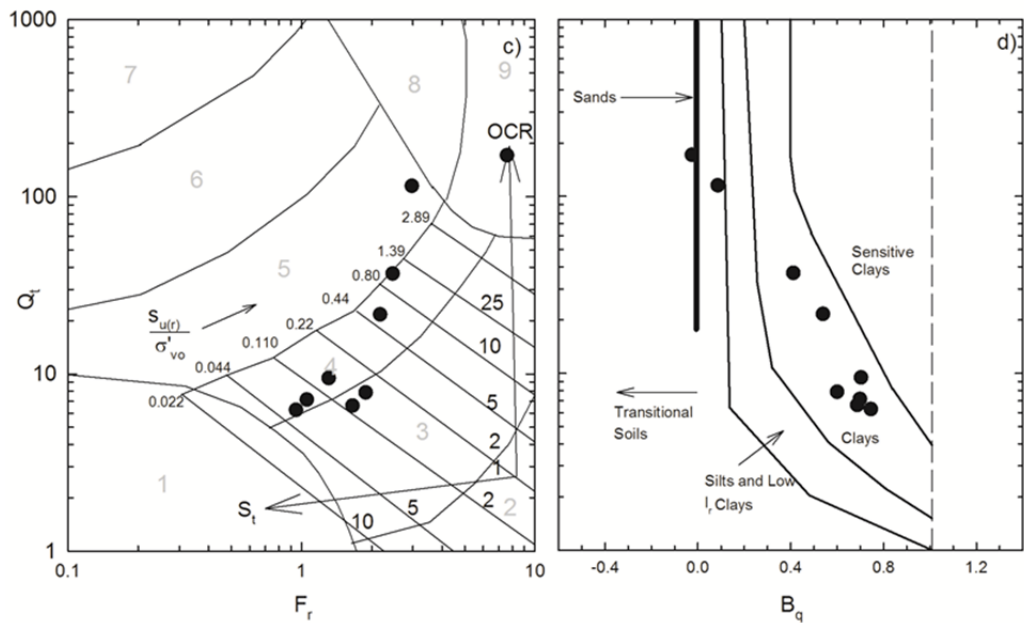
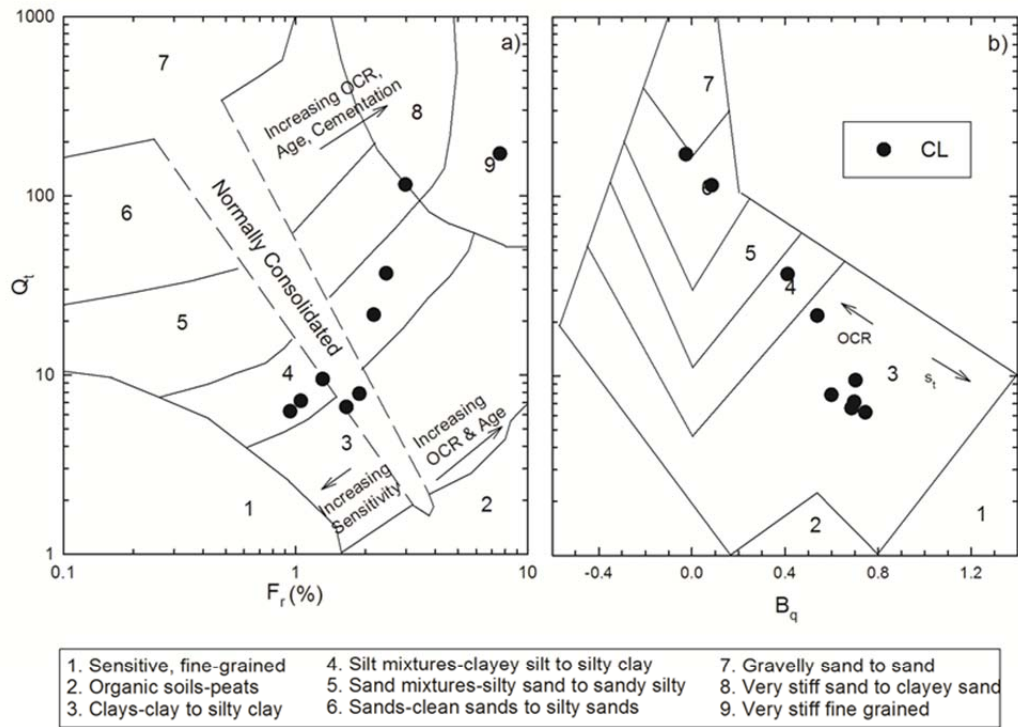


Figure 7.16: Soil classification results from SCPTu 106 at the I-395 Terminus site comparing laboratory-determined USCS classification to classification charts using a)  $Q_t$  vs.  $F_r$  (Robertson 1990), b)  $Q_t$  vs.  $B_q$  (Robertson 1990), c)  $Q_t$  vs.  $F_r$  (Robertson 2009), d)  $Q_t$  vs.  $B_q$  (Schneider *et al.*, 2008).

distinguishing between the classification charts using sleeve friction ratio and normalized pore pressure, respectively.

Table 7.10: Summary of CPT classification chart effectiveness for the Presumpscot clay using SBT based on results from SCPTu 101 and SCPTu 106 at the I-395 Terminus site.

Reference	# samples	SCPTu101		SCPTu106		
		SBT-USCS Correlation	% Effective	# samples	SBT-USCS Correlation	% Effective
<i>Robertson 1990 (<math>F_r</math>)</i>	9	7	78	9	8	89
<i>Robertson 1990 (<math>B_q</math>)</i>	9	7	78	9	7	78
<i>Robertson 2009</i>	9	7	78	9	8	89
<i>Schneider et al. 2008</i>	9	7	78	9	7	78

Notes: SBT: soil behavior type from CPT correlations; USCS: Unified Soil Classification System (ASTM D2487).

Correlation between CPTu SBT classification and USCS classification was generally 78% (i.e. 7 of the 9 tested samples were correctly classified). Robertson  $F_r$  (1990) and Robertson (2009) for SCPTu 106 resulted in 89% (8 of the 9 tested samples were correctly classified). Review of the plotted data points on Figure 7.15 and Figure 7.16 illustrate two distinct patterns of the plotted data for both SCPTu 101 and SCPTu 106. Data where  $Q_t$  exceeds 10 have greater scatter whereas data for which  $Q_t$  is less than 10 cluster around a common location on the charts. In general, the data where  $Q_t$  exceeds 10 correspond to the stiff, silt-dominated clay in the upper portion of the deposit and data where  $Q_t$  is less than 10 correspond to the softer clay in the lower deposit.  $Q_t = 10$  corresponds to an approximate OCR of 3.3 which is consistent with the stress history analysis (i.e. Equation 2.6, and assumed  $k$ -value = 0.33 such as discussed in Section 2.3.2).

Robertson  $F_r$  (1990) and Robertson (2009) performed the best for classification of the Presumpscot clay deposit at the site. Considering only the soft portion of the clay (OCR less than 3.3), Robertson  $B_q$  (1990) and Schneider *et al.*, (2008) were the most effective classification charts. In the upper stiff clay region, the most shallow data points which were highly



overconsolidated (OCR around 12.0) plotted in or near the SBT 9 “very stiff fine grained” using the Robertson  $F_r$  (1990) and Robertson (2009) charts and is considered to be correctly classified. However, the transitional zone from highly overconsolidated to practically normally consolidated (OCR from approximately 3.0 to 12.0) the data become scattered throughout various granular-based SBT (i.e. sands, sand mixtures, and silts) when using all of the classification charts. Once in the softer, practically normally consolidated depths (OCR from 1.5 to 3.0) the CPTu data is scattered between SBT 3 and 4 for the Robertson  $F_r$  (1990) and Robertson (2009) charts where as they plot more consistently within SBT 3 (clays) or the “clays” region for Robertson  $B_q$  (1990) and Schneider *et al.*, (2008), respectively.

### 7.3.3 Correlations to Stress History

CPTu soundings data were correlated to measured stress history of the site using the  $k$ -value correlation method outlined in Section 2.3.2. Using Equation 2.7,  $k$ -values were back-calculated using preconsolidation pressure ( $\sigma'_p$ ) determined from CRS testing of laboratory specimens and  $q_{net}$  assessed from the CPTu sounding at the corresponding sample depths. Figure 7.17 presents the  $k$ -values determined for the Presumpscot clay at the I-395 Terminus site along with the estimated  $\sigma'_p$  profile using determined  $k$ -values applied to SCPTu 106.

In Figure 7.17a, each symbol represents a  $k$ -value back calculated from one of the CPTu soundings. Each grouping of symbols at a common depth correspond to a single  $\sigma'_p$ , with a  $q_{net}$  value taken from one of the CPTu soundings to solve for the  $k$ -value. The range of values in the grouping represents the difference in  $q_{net}$  between the soundings. The vertical dotted lines at values of 0.20 and 0.50 represent the “typical” range of values for clays (Lunne *et al.*, 1997). In Figure 7.17b, the average, minimum, and maximum  $k$ -values from SCPTu 106 were applied to the entire profile of  $q_{net}$  from SCPTu 106 and compared to the laboratory-determined  $\sigma'_p$ .

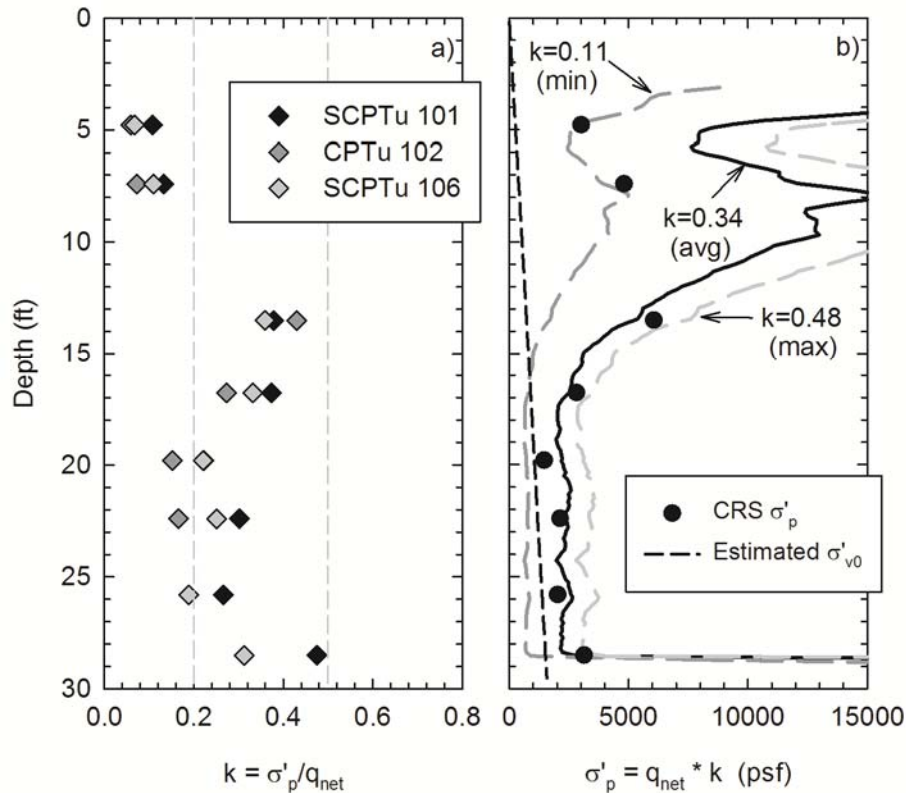


Figure 7.17: Subsurface profiles of a) stress history  $k$  values determined from SCPTu 101, CPTu 102, and SCPTu 106, b)  $\sigma'_p$  using minimum, maximum, and average  $k$ -values from SCPTu 106 for (S)CPTu testing at the I-395 Terminus site.

Review of the Figure 7.17 shows that  $k$ -values for the Presumpscot clay at this site remained within the typical range (of 0.20 to 0.50) for the clay in the lower, softer portion of the deposit (OCR from 8.6 to 1.5), where  $k$ -values in the stiff clay (OCR 11.8 to 12.1) were lower (0.06 to 0.13). A low  $k$ -value derives from a lower  $\sigma'_p$ ,  $q_{net}$  measurement, or both. It is likely that both of these factors result in the low  $k$ -value in the shallowest two samples. The extracted specimens from the shallowest two samples were extremely stiff and difficult to trim for the CRS testing procedure and exhibited rounded compression curves indicating low clay structure. Firstly, the low  $\sigma'_p$  may be attributed to lower (“good to fair”) sample quality for these shallow samples (Table 7.4) and a rounded compression curve. Secondly, measurements of  $q_{net}$  in the stiff

clay are likely higher (relative to the OCR of the clay) in comparison to the soft clay. This can be due to suction pressure in the stiff clay occurring during shear (i.e. cone penetration) further increasing the strength of the clay beyond just the stiffening from the increased  $\sigma'_p$ , which directly affects the  $q_{net}$  measurement. At the depth of the CRS tested specimen 1U, the measured pore pressure ( $u_2$ ) is negative (Figure 7.11) indicating dilative behavior.

In the soft clay portion of the deposit, the *k-value* method provides good estimates of stress history. Values ranged 0.15 to 0.48 from the three soundings. In general, a decrease in *k-value* occurred with depth as interpreted OCR and sample quality also decreased. This is consistent with the observation of Lunne *et al.*, (1997), who suggest that the *k-value* decreases with decreasing OCR. At the deepest sample, the *k-value* increases to 0.31 for SCPTu 106 and to 0.48 for SCPTu 101, likely due to the difference of the clay properties between locations.

For highly overconsolidated clay at the I-395 Terminus site, the *k-value* was well below the recommended range of Lunne *et al.*,(1997) and under predicted OCR and  $\sigma'_p$  when applied to the rest of the deposit. As OCR decreased from 8.6 down to 1.5, the *k-value* also decreases from 0.36 to 0.19. The deepest specimen, which resulted in “poor” sample quality from the CRS test, resulted in an OCR of 2.1 and the *k-value* also increased to 0.32. In the lower portion of the deposit below the highly overconsolidated layer, averaging the *k-values* in this region provided a *k-value* of 0.34, and when applied to SCPTu, gave reasonable predictions of  $\sigma'_p$  throughout the profile.

#### 7.3.4 Correlations to Shear Strength

Undrained shear strength ( $s_u$ ) of clay can be estimated from CPTu results using empirical cone factors  $N_{kt}$ ,  $N_{ke}$ , and  $N_{\Delta u}$  (Equations 2.9 through 2.11). Section 2.3.3 outlines the methodology used to obtain the three empirical coefficients.  $N_{kt}$  is determined from tip resistance ( $q_t$ ),  $N_{ke}$  is determined from  $q_t$  and pore pressure measurements ( $u_2$ ), and  $N_{\Delta u}$  is determined from

$u_2$ . These empirical coefficients were determined at the I-395 Terminus site using  $s_u$  from laboratory CAUC triaxial shear testing and field vane shear testing (FVT) results.

Figure 7.18 presents the CPTu shear strength factors  $N_{kt}$ ,  $N_{ke}$ , and  $N_{\Delta u}$  calculated from SCPTu 101, 102, and 106 using laboratory-determined  $s_u$  from CAUC testing and field vane shear testing (FVT) on Presumpscot clay samples. A subscript of CAUC or FVT indicates the testing method from which the  $s_u$  was measured.  $N_{kt(CAUC)}$ ,  $N_{ke(CAUC)}$ , or  $N_{\Delta u(CAUC)}$  values were back-calculated from each of the CPTu soundings using the  $s_u$  measured from CAUC test results from HB-BREW-102 at the corresponding depth.  $N_{kt(FVT)}$ ,  $N_{ke(FVT)}$ , or  $N_{\Delta u(FVT)}$  values were back-calculated from SCPTu 101 (as it was the closest sounding to FVT from Boring HB-BREW-101). SCPTu 101 and CPTu 102 were conducted 58.2 feet and 119.5 feet away from Boring HB-BREW-102, respectively. CPTu encountered refusal at 25 feet, so values were not obtained below this depth. The summary of  $N_{kt}$  and  $N_{\Delta u}$  values are presented in Table 7.11. As mentioned in Section 2.3.3, the cone factor  $N_{ke}$  has been found to be unreliable for clay deposits and will be omitted from the correlation analysis.

Table 7.11: Summary of  $N_{kt}$  and  $N_{\Delta u}$  values at the I-395 Terminus site.

		Minimum	Average	Maximum	S.D.	C.O.V.
SCPTu 101	$N_{kt(CAUC)}$	11.9	13.9	16.3	1.6	0.11
	$N_{\Delta u(CAUC)}$	6.6	9.1	12.5	2.4	0.26
CPTu 102	$N_{kt(CAUC)}$	11.8	18.4	23.9	6.1	0.33
	$N_{\Delta u(CAUC)}$	7.2	11.7	15.9	4.4	0.37
SCPTu 106	$N_{kt(CAUC)}$	14.1	16.7	19.2	2.0	0.12
	$N_{\Delta u(CAUC)}$	7.5	10.9	12.4	2.0	0.18
SCPTu 101	$N_{kt(FVT)}$	17.9	22	25.4	6.4	0.12
	$N_{\Delta u(FVT)}$	12.6	16.3	19.1	4.4	0.13

Note: S.D. = standard deviation; C.O.V. = coefficient of variation

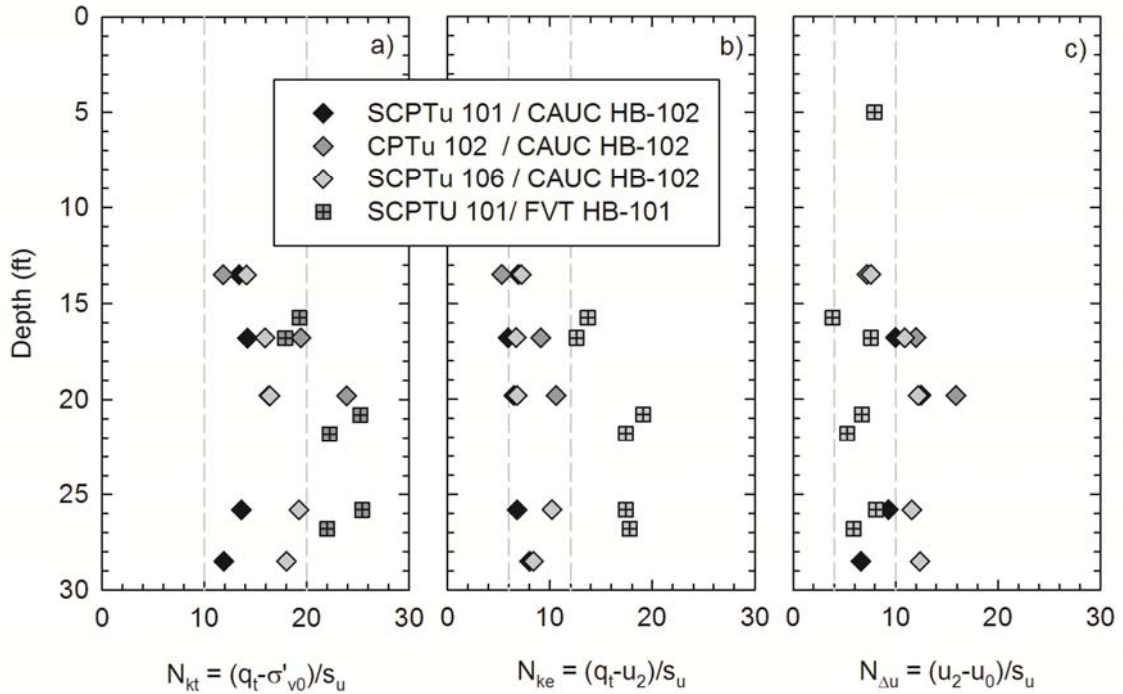


Figure 7.18: Subsurface profiles of  $N_{kt(CAUC \text{ and } FVT)}$ ,  $N_{ke(CAUC \text{ and } FVT)}$ , and  $N_{\Delta u(CAUC \text{ and } FVT)}$  correlated from (S)CPTu 101, 102, and 106 with  $s_u$  from triaxial CAUC testing and field vane shear testing (FVT) of Presumpscot clay at the I-395 Terminus site.

$N_{kt(CAUC)}$  correlated from SCPTu 106 (the closest sounding to HB-BREW-102) varied within a relatively narrow range from 14.1 to 19.2 over the entire profile, remaining within the suggested range of 10 to 20 from Lunne *et al.*, (1997).  $N_{kt(CAUC)}$  correlated from SCPTu 106 increased with increasing depth.  $N_{kt(CAUC)}$  correlated from the other two soundings illustrated more scatter and variability with depth.  $N_{\Delta u(CAUC)}$  correlated from SCPTu 106 also showed a decrease with depth until reaching approximately 20 feet, where OCR and  $s_u$  remained practically constant, and  $N_{\Delta u(CAUC)}$  matched this.  $N_{\Delta u(CAUC)}$  showed less scatter between the three soundings. Most  $N_{\Delta u(CAUC)}$  and all  $N_{\Delta u(FVT)}$  values plotted above the recommended range of 4 to 10 from Lunne *et al.*, (1997).

In general,  $N_{kt(CAUC)}$  is less than  $N_{kt(FVT)}$  throughout the profile. This is due to the fact that  $s_u$  from FVT is consistently less than  $s_u$  from CAUC, leading to differences in correlated  $N_{kt}$  values. The difference in measured  $s_u$  comes from differences in mode of shear between the two test methods, sample quality (there is no way of determining sample quality from the FVT), and other testing procedures which effect the  $s_u$  measurement. These are discussed further in Sections 3.2 and 3.4.4 for the FVT and CAUC methods, respectively. Similarly,  $N_{\Delta u(CAUC)}$  resulted in lower values than  $N_{\Delta u(FVT)}$  from the aforementioned factors.

There is variation in  $N_{kt(CAUC)}$  and  $N_{\Delta u(CAUC)}$  between the CPTu profiles. In the upper portion of the deposit, the variation is less whereas the softer, lower portion of the deposit causes more variation in the correlated cone factors. CPTu measurements in the soft clay are smaller compared to the stiffer clay, therefore even small changes in tip resistance or pore pressure measurements have large effects on the correlations.

Figure 7.19 presents  $s_u$  profile estimates using minimum, average, and maximum  $N_{kt(CAUC)}$  and  $N_{\Delta u(CAUC)}$  values from SCPTu 106. Inspection of Figure 7.19 shows that the  $N_{kt(CAUC)}$  average value of 16.7 follows the laboratory  $s_u$  closely throughout the entire profile and  $N_{\Delta u(CAUC)}$  predicts laboratory  $s_u$  more effectively in the softer portion of the deposit and does a poor job in the more overconsolidated portion. For  $N_{kt(CAUC)}$  average, the percent difference between CPTu estimated  $s_u$  and laboratory  $s_u$  ranged from -17% to 14% (188 psf and 83 psf, respectively). Percent difference between CPTu estimated  $s_u$  and laboratory  $s_u$  from  $N_{\Delta u(CAUC)}$  ranges from -37% to 12% (370 psf and 70 psf, respectively).

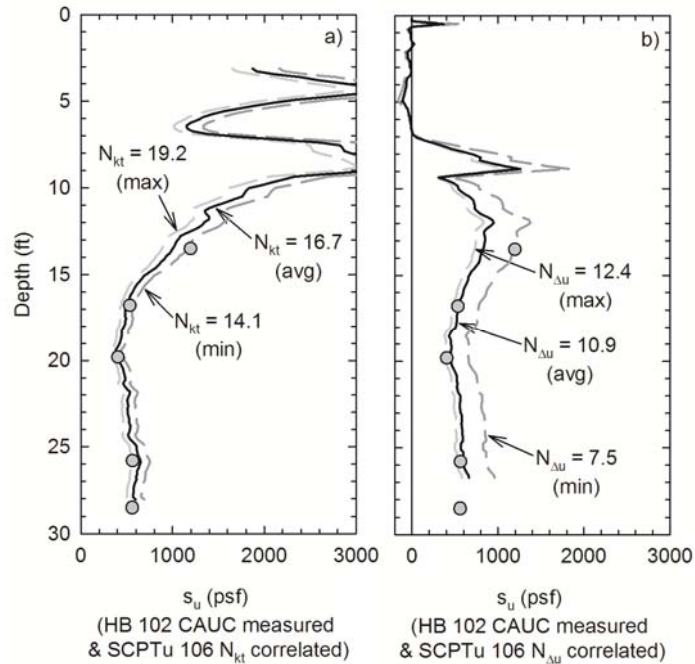


Figure 7.19: Subsurface profile of undrained shear strength ( $s_u$ ) with depth using the  $N_{kt(CAUC)}$  and  $N_{\Delta u(CAUC)}$  values from SCPTu 106 applied to measurements from SCPTu 106 and compared to the laboratory-determined  $s_u$  of Presumpscot clay samples from the I-395 Terminus site.

In summary, classification of Presumpscot clay at the I-395 Terminus site using CPTu correlations is best performed using a combination of Robertson  $F_r$  (1990) and Robertson (2009) for the shallow, more overconsolidated portion of the deposit (where  $OCR > 3.3$ ) and using Robertson  $B_q$  (1990) and Schneider *et al.*, (2008) for the deeper, more lightly consolidated clay. The stiff upper crust was identified as SBT 9 “very stiff fine grained” by the Robertson  $F_r$  (1990) and the softer clay was identified as SBT 3 “clays” in Robertson  $B_q$  (1990) and Schneider *et al.*, (2008). The transitional zone between the crust and the soft portion was not unanimously correctly identified by any of the charts, but in general classified as SBT 4 or 5 “silt mixtures” and “sand mixtures”.

For stress history correlations, highly overconsolidated clay at the I-395 Terminus site, the  $k$ -value was well below the recommended range of Lunne *et al.*, (1997) and under predicted OCR and  $\sigma'_p$  when applied to the rest of the deposit. In the lower portion of the deposit below the

highly overconsolidated layer, averaging the  $k$ -values in this region provided a  $k$ -value of 0.34, and when applied to SCPTu, gave reasonable predictions of  $\sigma'_p$  throughout the profile. Undrained shear strength at the site was best estimated throughout the entire profile using an average  $N_{kt(CAUC)}$  of 16.7 and was reasonably estimated using a  $N_{\Delta u(CAUC)}$  average of 10.9.  $s_u$  in the overconsolidated portion was not well predicted using the  $N_{\Delta u(CAUC)}$  average.



## 8 COMPREHENSIVE COMPARATIVE ANALYSIS

### 8.1 Chapter Overview

This chapter presents the analysis of the methods used to correlate cone penetration testing with pore pressure measurements (CPTu) results with classification, stress history ( $\sigma'_p$ ), and undrained shear strength ( $s_u$ ) as measured from laboratory testing of high quality samples of the Presumpscot clay for each of the four research sites. The methods were selected based on their prevalence in geotechnical practice and applicability to the Presumpscot clay based on suggestions from published literature. Detailed results of classification,  $\sigma'_p$ , and  $s_u$  estimated from CPTu measurements at each site are available in Chapters 4 through 7.

In this chapter, a brief description of the Presumpscot clay deposits at each site and resulting CPTu classifications and correlations are presented. It should be noted that all four research sites had existing superstructures and/or foundation elements existing at the site and hence the resulting stress history may be affected by this previous loading. At the end of the following site summaries, Figure 8.1 through Figure 8.4 illustrates the range of CPTu measurements encountered at each site and the  $\sigma'_p$  and  $s_u$  profiles obtained from laboratory testing on samples collected at each site for comparison. For simplicity, only one CPTu profile from each site is plotted (even though multiple CPTu soundings were performed at three of the sites) and analyzed throughout this chapter. The selected CPTu from each site was the sounding performed closest to the boring where high quality samples were collected for advanced laboratory testing and analysis. The variation in correlated properties and classification from the different CPTu soundings at each site is addressed in the site specific chapters.

#### 8.1.1 The Route 26/100 Falmouth Bridge Site

The Falmouth Bridge is located along Route 26/100 across the Presumpscot River in Falmouth, ME. Presumpscot clay at this site was approximately 63 feet thick. Natural water

content of the clay varies from 37% to 54%, Plastic Limit (PL) ranges from 19 to 29, Liquid Limit (LL) ranges from 29 to 54, and Liquidity Index (LI) ranges from 0.9 to 2.2. The sensitivity of the clay ranges from 9 to greater than 100, indicating a "quick" deposit. Overconsolidation ratio (OCR) of the clay begins at 3.4 near the top of the deposit, decreasing to 1.8 at approximately 25 feet below ground surface (the extent of groundwater fluctuation), where the stress history reaches nearly normally consolidated conditions.  $s_u$  from direct simple shear (DSS) testing ranges from 305 psf to 766 psf, generally increasing uniformly with depth. Based on the work of Karlsrud and Hernandez-Martinez (2013),  $s_u$  from DSS is in the order of 0.74 times the anisotropically consolidated undrained compression (CAUC) strength for high quality samples. Based on this, the equivalent triaxial compression  $s_u$  of the Presumpscot clay at the Route 26/100 Bridge is estimated to range from 411 psf to 969 psf. Throughout this chapter, the resulting DSS and CAUC  $s_u$  will be presented to allow for comparison to the other sites, which were characterized using CAUC  $s_u$ .

The Stress History and Normalized Engineering Parameter (SHANSEP) testing was not performed on the laboratory samples because of equipment limitations. However, a best-fit recompression line can be fit to the recompression triaxial CAUC data (as shown in Section 4.2.4), and the resulting  $s_u$ -OCR relationship for the Presumpscot clay based on DSS and the CAUC equivalent  $s_u$  is shown in Equation 8.1 and 8.2, respectively.

$$s_{uDSS(OC)} = 0.21 \cdot OCR^{0.50} \quad 8.1$$

$$s_{uCAUC-DSS(OC)} = 0.28 \cdot OCR^{0.51} \quad 8.2$$

### 8.1.2 Martin's Point Bridge Site

Martin's Point Bridge (MPB) spans from the southern tip of Falmouth Foreside along Route 1 to Martin's Point in Portland, Maine. The Presumpscot clay deposit at the site is located

in a tidally influenced location. The depth of the clay at the site is approximately 40 feet and is submerged below sea level. Natural water content ranges from 31% to 44%, PL ranges from 17 to 26, LL ranges from 24 to 47, and LI ranges from 0.66 to 1.72. Sensitivity ranges from 2.2 to 8.7 (with some higher outliers), indicating a deposit of moderate sensitivity. OCR decreases uniformly with depth from 6.8 near the top of the deposit to 3.1 at the bottom, thus the entire deposit is overconsolidated.  $s_u$  determined from CAUC testing on undisturbed samples ranges from 661 psf to 1,557 psf, with a general uniform increase with depth. The resulting SHANSEP  $s_u$ -OCR relationship based on the recompression analysis and the true SHANSEP analysis for the Presumpscot clay at the site is shown in Equation 8.3 and 8.4, respectively:

$$s_{uCAUC(OCR)} = 0.12 \cdot OCR^{1.12} \quad 8.3$$

$$s_{uCAUC(OCR)} = 0.28 \cdot OCR^{0.83} \quad 8.4$$

The resulting SHANSEP equation at this site provided a poor prediction of the  $s_u$  profile.

### 8.1.3 The Route 197 Richmond-Dresden Bridge Site

The Route 197 Bridge connects the Town of Richmond, ME and the Town of Dresden, ME over the Kennebec River along Route 197. The Presumpscot clay deposit at the site is approximately 23 feet thick at its deepest in the middle of the riverbed and submerged in freshwater conditions. Natural water content ranges from 27% to 42%, PL ranges from 17 to 22, LL ranges from 33 to 40, and LI ranges from 0.57 to 1.14. Sensitivity of the clay ranges from 8 to 45, indicating moderate to quick conditions. OCR decreases uniformly with depth from 5.8 at the top of the deposit to 2.2 at the bottom, thus the entire deposit is overconsolidated. It is hypothesized that part of the alluvium deposit has been scoured away, resulting in overconsolidation.  $s_u$  determined from CAUC testing on undisturbed samples ranges from 527 psf

to 877 psf, with a general uniform increase with depth. The resulting SHANSEP  $s_u$ -OCR relationship based on the recompression analysis and the true SHANSEP analysis for the Presumpscot clay at the site is shown in Equation 8.5 and 8.9, respectively:

$$s_{uCAUC(OC)} = 0.27 \cdot OCR^{0.67} \quad 8.5$$

$$s_{uCAUC(OC)} = 0.27 \cdot OCR^{0.77} \quad 8.6$$

The resulting SHANSEP equation at this site provided a good prediction of the  $s_u$  profile.

#### 8.1.4 I-395 Terminus Site in Brewer

The I-395 Terminus site in Brewer, ME (BR) is located adjacent to the US Route 1A on the ramp connector for I-395 West. The groundwater table at the site is at the ground surface. The Presumpscot clay deposit is approximately 28 feet thick, but is comprised heavily of silt particles (ranging from 52% to 75% by composition.) The site is located near the inland extent of the Presumpscot glacial marine deposition. Natural water content ranges from 23% to 40%, PL ranges from 19 to 22, LL ranges from 31 to 37, and LI ranges from 0.22 to 1.28. Sensitivity of the clay ranges from 1 to 4, indicating low sensitivity of the deposit. OCR in the overconsolidated crust ranges from 8.6 to 12.1, but decreases to 1.5 in the softer, bottom portion of the deposit.  $s_u$  determined from CAUC testing on undisturbed samples in the softer portion of the deposit ranges from 404 psf to 564 psf. The resulting SHANSEP  $s_u$ -OCR relationship based on the recompression analysis and the true SHANSEP analysis for the Presumpscot clay at the site is shown in Equation 8.7 and 8.8, respectively:

$$s_{uCAUC(OC)} = 0.30 \cdot OCR^{0.78} \quad 8.7$$

$$s_{uCAUC(OCR)} = 0.26 \cdot OCR^{0.70}$$

8.8

The resulting SHANSEP equation at this site provided a poor prediction of the  $s_u$  profile.

#### 8.1.5 Comparison of the Measured Soil Properties

This section summarizes the soil properties determined from the laboratory testing and the CPTu measurements at each site and draws conclusions from the comparison of this data. The purpose is to give the reader an understanding of ranges of values from the CPTu measurements for corresponding stress history and/or undrained shear strength profiles of Presumpscot clay. The Presumpscot clay deposits at each of the site will be compared and contrasted to highlight the difference in the soil properties via differences in geologic history and anthropomorphic effects.

Figure 8.1 presents  $\sigma'_p$ ,  $s_{us}$ , and sensitivity ( $S_t$ ) of the Presumpscot clay at each site. Figure 8.2 presents the  $s_u$  results at all four sites from both the laboratory testing and field vane shear testing (FVT). Figure 8.3 presents corrected tip resistance ( $q_t$ ), sleeve friction ( $f_s$ ), and pore pressure measurements ( $u_2$ ) collected from the CPTu sounding closest to the samples borings at each site. Figure 8.4 presents the three normalized CPTu measurements of tip resistance ( $Q_t$ ), sleeve friction ratio ( $F_r$ ), and normalized pore pressure ( $B_q$ ) for the same soundings at each site. Table 8.1 presents the SCPTu sounding and the boring at each site used for the correlations presented in this chapter. Note that modified Shelby tube sampling was performed at all four sites and Sherbrook block sampling was performed at the Route 26/100 Bridge site.

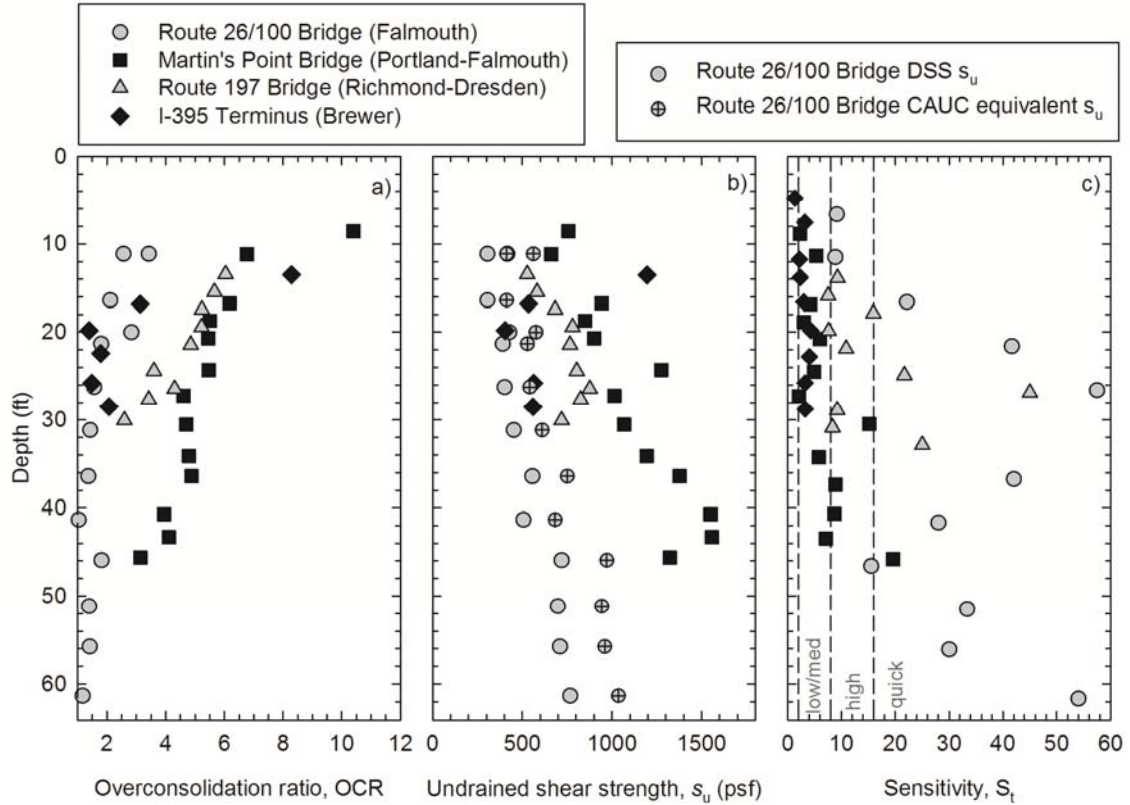


Figure 8.1: Laboratory test results of overconsolidation ratio (OCR), undrained shear strength ( $s_u$ ) from triaxial shear, and sensitivity ( $S_t$ ) of Presumpscot clay collected at the four research sites.

Table 8.1: Summary of the SCPTu sounding and the boring with sampling used at each for the correlations presented in this section

Site	SCPTu	Boring
<i>Route 26/100 Bridge</i>	SCPTu-P301	BB-FRR-BT303/BB304
<i>Martin's Point Bridge</i>	SCPTu-101	BB-FPPR-317
<i>Route 197 Bridge</i>	SCPTu-109	BB-RDKR-206
<i>I-395 Terminus Site</i>	SCPTu-106	HB-BREW-102

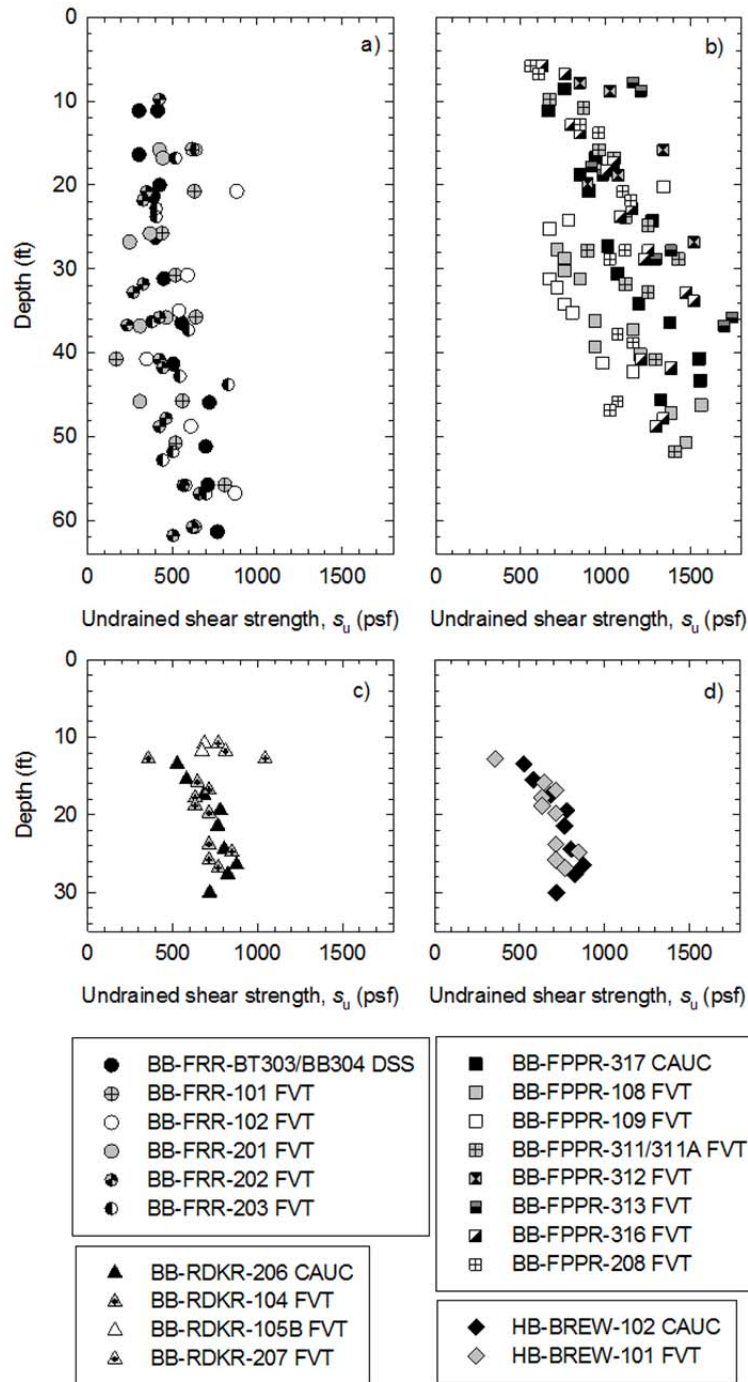


Figure 8.2: Laboratory test results of overconsolidation ratio undrained shear strength ( $s_u$ ) shown as the gray circles compared to field vane shear test results (FVT) at a) Route 26/100 Bridge b) Martin's Point Bridge c) Route 197 Bride and d) I-395 Terminus site.

The overconsolidation ratio (OCR) of the Presumpscot clay at the four research sites ranged from 12.1 to 1.0. At each site, the OCR values reached their highest magnitude at the top of the deposit and generally decreased with depth. Practically normally consolidation conditions (i.e. OCR=1) were reached at the lower portion of the deposits at the Route 26/100 Bridge and the I-395 Terminus site. Between these two sites, the low OCR soil in the bottom portion of each deposit has similar  $s_u$  values within these depths.  $s_u$  of the Presumpscot clay from these sites from approximately 15 feet to 30 feet depth remain with a narrow range of 400 psf to 600 psf, matched by similar OCR values of 1.0 to 2.1. However, the upper portion of the I-395 Terminus site is more desiccated and silty than the upper portion of the Route 26/100 Bridge deposit resulting in higher OCR and  $s_u$  values at the I-395 Terminus site within the shallow portion of the deposit. Normalized  $s_u$  values to in situ vertical effective stress for normally consolidated deposits generally range from 0.20 to 0.30, and within the shallow portion of the I-395 Terminus site,  $s_u/\sigma'_{v0}$  was as high as 1.68 whereas  $s_u/\sigma'_{v0}$  at the Route 26/100 Falmouth Bridge site reached a maximum value of 0.33.

At Route 197 Bridge and Martin's Point Bridge, OCR approached 2.2 and 3.1 at the bottom of the deposits, respectively. By definition, the Presumpscot clay at these depths has been stressed to 2.2 and 3.1 times their in situ state, respectively. From this, we can hypothesize geologic and anthropomorphic loading conditions which may have caused the observed increase in OCR. Anthropomorphic loading which would increase the stress levels (and hence the  $\sigma'_p$ ) throughout the entire clay deposits would be surface loading from bridge structures which have existed at each site for decades. This includes bridge abutments, piers, approach fill, or any other elements which will load the ground surface and dissipate with depth. At the Route 197 Bridge, the only bridge elements close enough to stress the Presumpscot clay deposit are the piers near the middle of the span, which are pile supported (Maine DOT, 2012). Since pile-supported elements transfer the load directly to the bedrock without loading the clay, the bridge piers likely



did not the cause increased OCR values at the site. Thus, the OCR likely derives from geologic deposition at the site which has since been scoured from the riverbed.

On the other hand, the Presumpscot clay deposit at Martin's Point Bridge may have been affected by anthropomorphic conditions. The north bridge approach (Falmouth side) includes an approximately 500 foot long earth embankment on the Falmouth shoreline (Golder Associates, 2011). According to the coordinates for the CPTu testing and the corresponding location plotted on Google Earth (2015), the distance between CPTu 101 and CPTu 104 from the edge of old earth embankment is 60 feet and 35 feet, respectively. Depending on the conditions at the bottom of the earth embankment (i.e. elevation of bottom of embankment, total unit weight of the fill used, lateral extent of fill slope below water elevation) the placed fill may have overconsolidated the Presumpscot clay deposit. Without more detailed information on the embankment, it is difficult to determine if (and how much) it effects the Presumpscot clay deposit, however one observation from the CPTu data reinforces this hypothesis. CPTu 103, which was performed further out away from the embankment resulted in lower  $q_t$  values compared to the other two soundings (Figure 5.16). Since  $q_t$  is directly related to the stiffness of the clay, it is intuitive that the Presumpscot clay at the location of CPTu 101 and CPTu 104 which has been (potentially) stiffened by the fill embankment would cause a higher tip resistance compared to the more "virgin" Presumpscot clay at the region of CPTu 103.

As expected,  $s_u$  of the Route 26/100 Bridge and the I-395 Terminus site is lower as compared to  $s_u$  of the other two deposits at similar depths. This is due directly to the degree of overconsolidation of the clay. A higher OCR results in stiffer clay which increases  $s_u$ . For comparison, the  $s_u$  determined from DSS testing at the Route 26/100 Bridge is plotted alongside the CAUC equivalent of those same samples using the conversion of  $s_{u(DSS)} = s_{u(CAUC)} * 0.74$ . Throughout this chapter, both  $s_u$  values from the Route 26/100 Bridge are used in the presentation of CPTu correlations. Conversely, OCR at the other two sites range from 2.6 to 6.7 at these same

depths which results in a larger range (and higher magnitude) of  $s_u$ .  $S_t$ , ratio of intact to disturbed  $s_u$  values, results show that the majority of samples at the Route 26/100 Bridge and the Route 197 Bridge classify as "high" or "quick" sensitivity, whereas samples at Martin's Point Bridge and the I-396 Terminus classify mostly as "low/medium" sensitivity.

Figure 8.5 illustrates graphically the relationship between measured soil properties and CPTu results. Intuitively, the tip resistance to an advancing cone will increase in stiffer clay (i.e. clay with higher  $s_u$ ) which is illustrated in Figure 8.5a.  $s_u$  in the figure is based on the x-axis on the top of the plot where the  $q_t$  is based on the x-axis at the bottom of the plot. The ratio of  $q_t$  to  $s_u$  in this plot is 18, is equivalent to an  $N_{kt}$  of 18. In Figure 8.5b, the OCR of undisturbed soil samples is compared to the  $Q_t$  of CPTu soundings. The ratio of  $Q_t$  to OCR in Figure 8.5b is 2.94, equivalent to a  $k$ -value of 0.34. The effectiveness of these correlations will be discussed subsequently. The purpose of Figure 8.5 is to illustrate that a relationship exists between measured soil properties in the laboratory and the CPTu measurements.

Figure 8.3 shows that a clear trend exists for the corrected tip resistance ( $q_t$ ) and pore pressure ( $u_2$ ) measurements. Route 26/100 Bridge and the I-395 Terminus site, which contain the normally consolidated "soft" zones of Presumpscot clay, exhibit lower  $q_t$  and  $u_2$  values of these measurements throughout the soft zone. This does not include the highly desiccated upper portion of the I-395 Terminus site, which provided very high tip resistance values and low/negative pore pressure measurements. The consistency of the lower measured  $q_t$  and  $u_2$  values for the two sites with "soft" Presumpscot clay as compared to the other two with stiffer clay signifies the ability of the CPTu to identify behavior of the clay deposit. Even without specific correlations to OCR or  $s_u$ , a geotechnical engineer can immediately identify at the least the relative in situ state of the clay. For instance, at Martin's Point Bridge, the (relative) high values of  $q_t$  (Figure 8.3a) and (relative) high values of  $f_s$  (Figure 8.3b) would suggest a deposit of stiff clay with a low sensitivity, which is exactly what is occurring at the site. Martin's Point Bridge exhibits the

highest measurements of  $q_t$  and  $f_s$  of all four sites, which is consistent with the highest OCR and  $s_u$  of all the Presumpscot clay deposits. At each of the four sites, as OCR and  $s_u$  decreases in the Presumpscot clay deposit, the  $q_t$  also decreases. Conversely, the measured  $u_2$  values do not consistently show the same trend ( $u_2$  always increases with depth, regardless of the OCR and  $s_u$ ). This behavior is expected in clay deposits. Furthermore, for Route 197 Bridge, an engineer would be able to observe the obvious sand seams located within the lower part of the deposit (seen as the localized peak in measurements throughout Figure 8.3 and Figure 8.4) and plan a testing schedule accordingly.

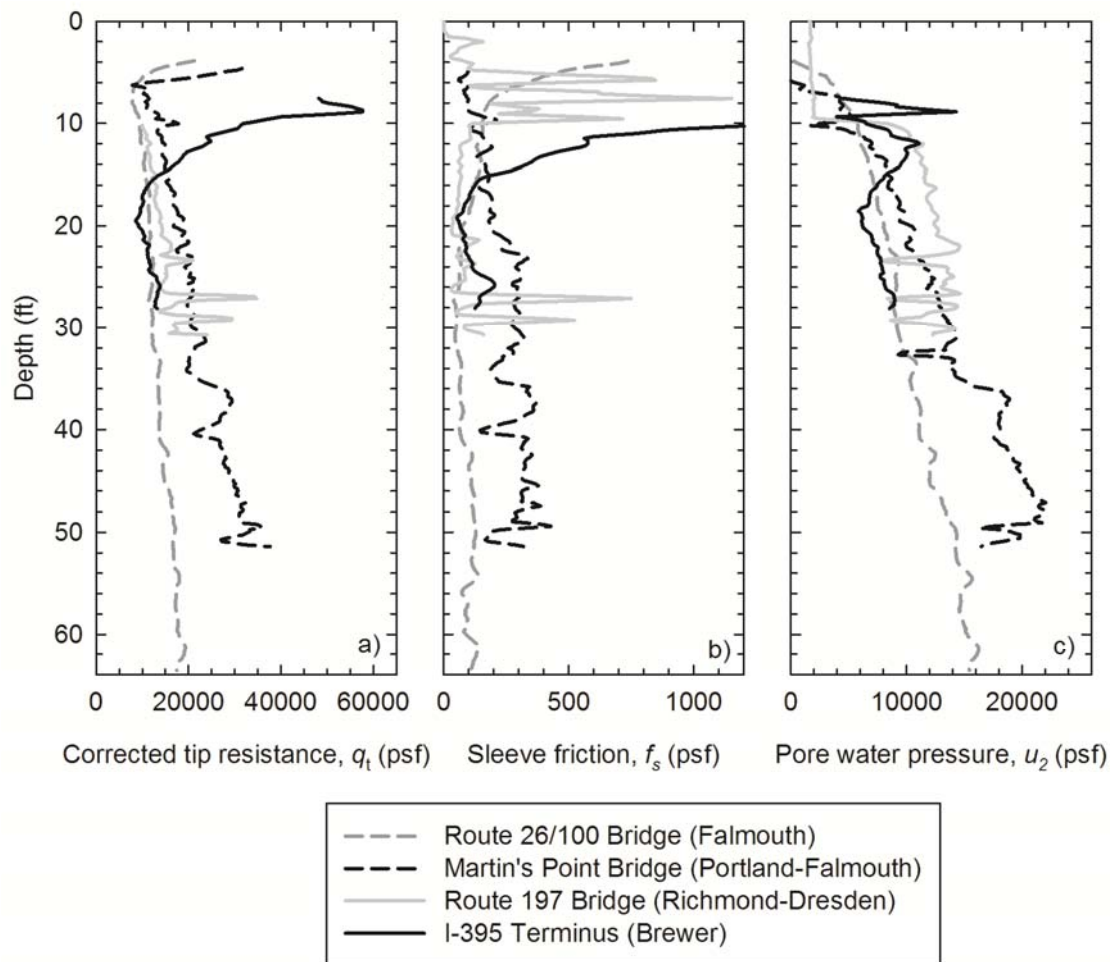


Figure 8.3: CPTu measurements of corrected a) tip resistance ( $q_t$ ), b) sleeve friction ( $f_s$ ), and c) pore water pressure ( $u_2$ ) collected in the Presumpscot clay deposits at the four research sites.

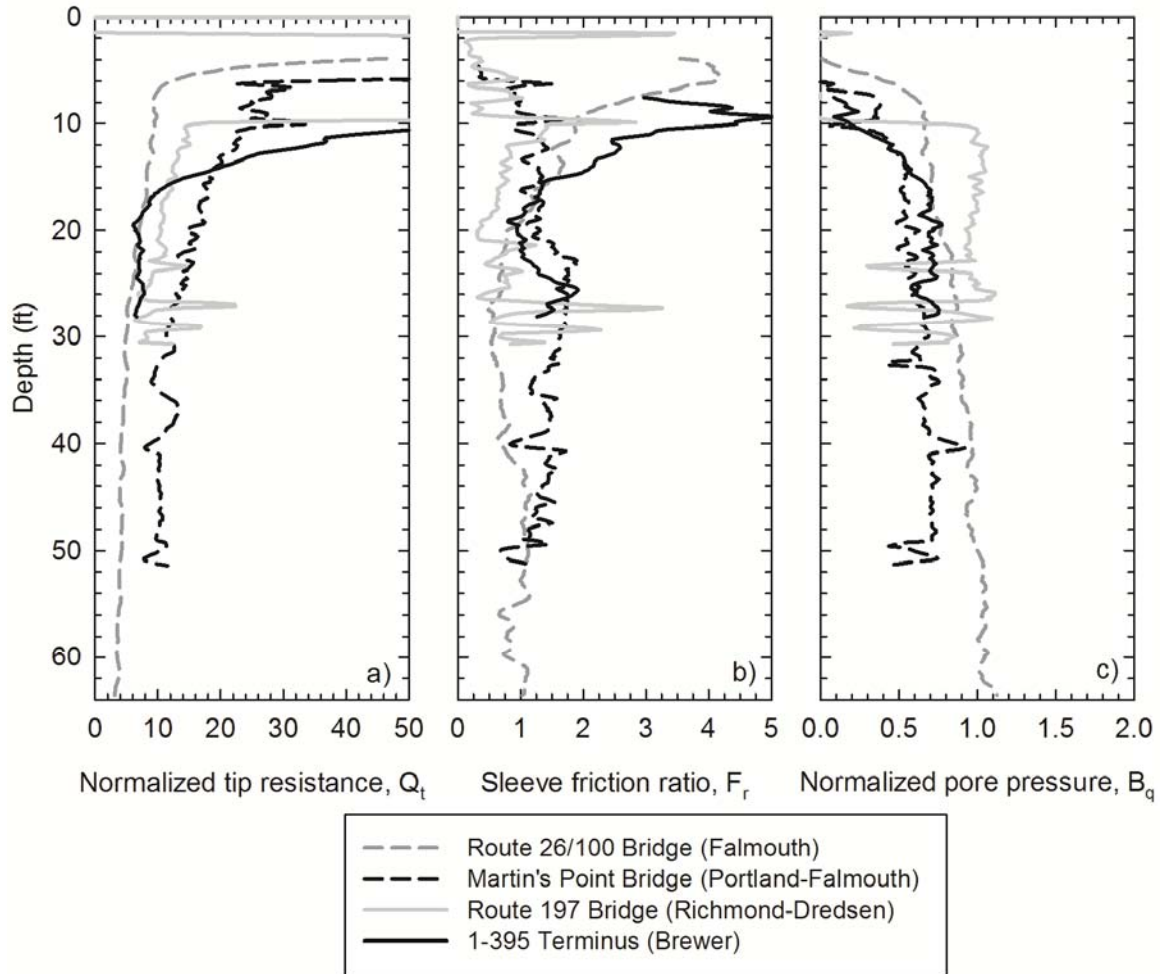


Figure 8.4: CPTu measurements of a) normalized tip resistance ( $Q_t$ ), b) sleeve friction ratio ( $F_r$ ), and c) normalized pore water pressure ( $B_q$ ) in the Presumpscot clay deposits at the four research sites.

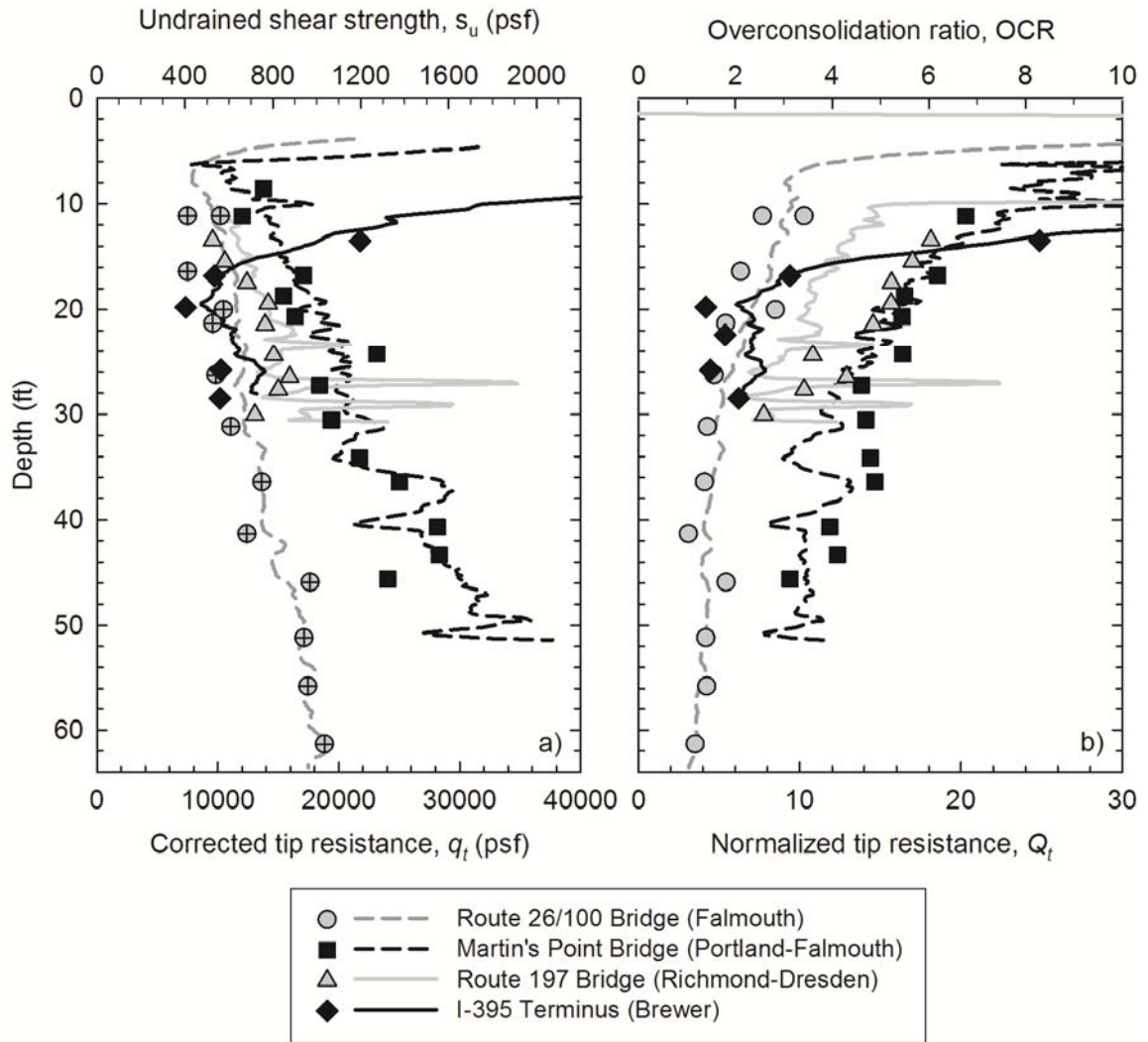


Figure 8.5: CPTu measurements compared to measured values of undrained shear strength and OCR of Presumpscot clay.

If the reader is curious for more details about each of the CPTu profiles shown in these figures and what it conveys about the deposit, each of the CPTu profiles are dissected in the site-specific chapters.

## 8.2 Benefits of Continuous Profiling

Many researchers and practitioners highlight the benefit of the continuous measurements of the CPTu technique, even the non-parameter data obtained from the test. For instance, CPTu

results can be used during a preliminary site investigation to determine depth and location and difference in resistance of various deposits, as well as the presence of silt and sand seams. With this knowledge, a precise sampling plan can be formulated (both location and depths of desired samples) even in real-time as the CPTu profiles appear on the data acquisition system's computer. A very simple, intuitive analysis can be conducted on the resulting profiles. Presumpscot clay will result in low tip resistance and sleeve friction values and high pore pressure values (greater than hydrostatic) than the typical granular material overlying and underlying the clay. In addition, silt and sand seams will be evident from sharp transitions in pore pressure and tip resistance and sleeve friction measurements with the clay layer. Figure 8.6 shows the CPTu measurement of corrected tip resistance at the Route 197 Bridge and a hypothetical 2 foot and 5 foot discrete sampling program. The purpose of the figure is to highlight the potential of important data which could be missed from discrete testing. For instance, a 5 foot field vane shear testing (FVT) depth program started from the top of the deposit would have completely missed both of the sand seams located at the bottom of the deposit.

Another benefit of CPTu testing in geotechnical investigations is the groundwater conditions collected from the test. Traditional drilling techniques usually identify the groundwater conditions by observing the sample moisture, using a water level meter in an open bore hole after equilibrium conditions are established, or installing a monitoring well. While most of these methods are usually adequate, it leaves room for error (particularly on the interpretation of soil sample moisture), or the potential for hole cave-in which does not provide the engineer with a water level. The CPTu test measures water pressure continuously. When the CPTu is advanced in free- draining soils, the hydrostatic water pressure can be back-calculated to solve for a depth

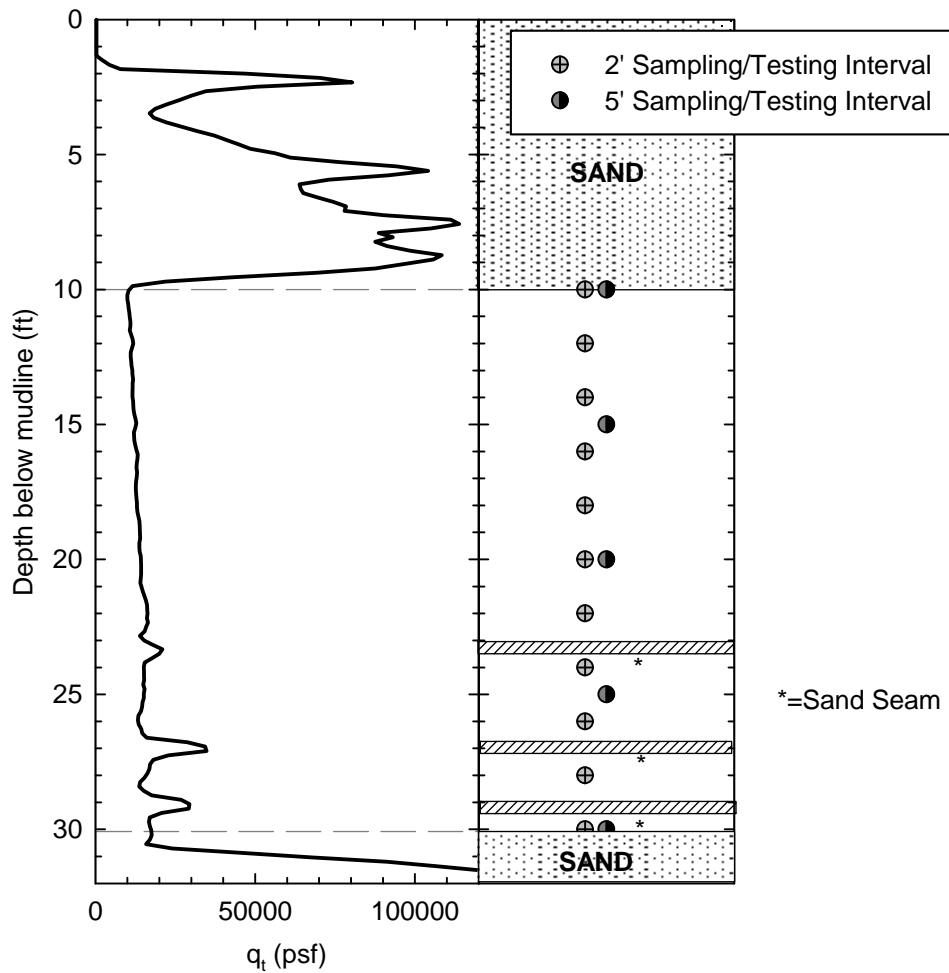


Figure 8.6: Schematic illustrating discrete sampling locations at 2 foot and 5 foot intervals within the subsurface of the Route 197 Bridge alongside the CPTu profile of corrected tip resistance.

of the groundwater table surface, provided  $u_2$  measurements are accurate. CPTu tests in clay soils result in excess water pressure from the undrained shear of the soil and do not provide accurate groundwater levels unless the penetrometer is left stagnant for long enough in the hole to allow complete pore pressure dissipation. However, the water pressure measurements in clay can provide useful data to the geotechnical engineer (beyond the engineer parameter correlations discussed in Section 8.5) if artesian pressures are occurring. At the I-395 Terminus site, artesian

water pressures were present in the Presumpscot clay layer and were identified by the CPTu sounding (Figure 7.11).

### 8.3 CPTu Classification Correlations

Classification of the Presumpscot clay was performed on Presumpscot clay using four empirical CPTu soil behavior charts (Figure 2.9). Samples of the clay were also collected at discrete depths and classified using the Unified Soil Classification System (USCS). The classification charts are based on behavioral characteristics of the soil and are empirically fit to Unified Soil Classification System (USCS, *ASTM D2435*) or other classification systems. Unlike USCS classification, which is based on disturbed samples, CPTu results as presented in the classification charts are affected by stress history, in-situ stresses, stiffness, macrofabric, and void ratio (Robertson, 1990). Equation 8.9 through 8.11 shows the equations used in the CPTu classification charts.

$$Q_t = (q_t - \sigma_{v0}) / \sigma'_{v0} = q_{net} / \sigma'_{v0} \quad 8.9$$

$$F_r = f_s / (q_t - \sigma_{v0}) = f_s / q_{net} \quad 8.10$$

$$B_q = (u_2 - u_0) / (q_t - \sigma_{v0}) = \Delta u / q_{net} \quad 8.11$$

where  $q_t$  = measured corrected tip resistance (psf),  $\sigma_{v0}$  = estimated in situ total vertical effective stress (psf),  $\sigma'_{v0}$  = estimated in situ vertical effective stress (psf),  $f_s$  = measured sleeve friction (psf),  $u_2$  = measured pore pressure (psf), and  $u_0$  = hydrostatic water pressure (psf)

Robertson (1990) ( $Q_t$ - $F_r$ ), Robertson (1990) ( $Q_t$ - $B_q$ ), Robertson (2009) ( $Q_t$ - $F_r$ ), and Schneider *et al.*, (2008) ( $Q_t$ - $B_q$ ) are the four CPTu classification charts which use normalized tip resistance ( $Q_t$ ) versus sleeve friction ratio ( $F_r$ ) or normalized pore pressure ( $B_q$ ). Robertson (2009) is a replica of Robertson (1990) with additional soil behavioral trends included in the chart so the classification of the soil will not differ between the two. Schneider *et al.*, (2008) uses  $Q_t$  and  $B_q$ .



Table 8.2 summarizes the effectiveness of the classification charts for classifying the Presumpscot clay at each of the four research sites as compared to the USCS classification. The criteria for "correct" classification are based on a match between the USCS classification and the classification predicted by the CPTu chart. In general, the soil behavior type Regions 3 and 4 (i.e. clays and silt mixtures) were considered acceptable for Robertson 1990 ( $F_r$ ), Robertson (1990) ( $B_q$ ), Robertson (2009). Schneider *et al.*, (2008) uses a different classification system, and for this the "clays" and "sensitive clays" regions were considered acceptable. Each percentage in Table 8.2 represents the fraction of Presumpscot clay samples classified in accordance with USCS which correlated with the soil behavior type on the CPTu classification charts. For instance, at the I-395 Terminus site, a total of 9 Presumpscot clay samples were collected and classified in the laboratory. CPTu data from the same depth of the undisturbed soil samples was plotted on the four classification charts (Figure 8.8), and USCS classification for 7 of the 9 tested samples matched with the plotted data on all of the classification charts, resulting in 78% effectiveness.

Table 8.2: Summary of SCPTu classification chart effectiveness for each Presumpscot clay site based on comparison to Unified Soil Classification System determined classification.

Site	CPTu Classification Chart			
	Percent effectiveness of:			
	Robertson (1990) $Q_t - F_r$	Robertson (1990) $Q_t - B_q$	Robertson (2009) $Q_t - F_r$	Schneider <i>et al.</i> , (2008) $Q_t - B_q$
Route 26/100 Bridge ( $n = 19$ )	100%	95%	100%	95%
Martin's Point Bridge ( $n = 13$ )	92%	100%	92%	100%
Route 197 Bridge ( $n = 9$ )	44%	89%	44%	89%
I-395 Terminus ( $n = 9$ )	78%	78%	78%	78%
	<b>84% (42/50)</b>	<b>92% (46/50)</b>	<b>84% (42/50)</b>	<b>92% (46/50)</b>

Classification of Presumpscot clay using the  $Q_r-B_q$  relationship Robertson (1990) and Schneider *et al.*, (2008) resulted in a cumulative 92% effectiveness (46 of the 50 samples) of all collected Presumpscot clay samples from the Shelby tube and Sherbrook block samples. There

doesn't appear to be a major difference for classification of the Presumpscot clay between the Robertson (1990) and Schneider *et al.*, (2008)  $B_q$ - $Q_t$  analyses effectiveness when comparing SBT to USCS classification. However, as discussed later in the chapter, the "sensitive clay" region of Schneider *et al.*, (2008) appears to be more effective in identifying Presumpscot clay deposits which are sensitive.  $Q_t$ - $B_q$  analyses was good for three out of the four sites and the  $Q_t$ - $F_r$  analyses was good for two out of the four sites but showed exceedingly poor performance for the Route 197 Bridge site (this will be discussed later in the section).

The distribution of classification data points on the charts can be a tool in identifying transitional zones to other materials, transitional zones within the Presumpscot deposit (e.g. between dry, crustal zones and soft, normally consolidated zones), and sand seams. An example of this stratification identified by the classification charts is shown in Figure 8.7. Figure 8.7 shows the soil profile at the Route 197 Bridge site, which can be split into three distinct layers: the overlying alluvial sand (light gray), the Presumpscot clay (black), and the underlying marine sand (dark gray). It is evident from inspection of Figure 8.7 that the sand layers above and below the Presumpscot clay exhibit different behavior during penetration of the CPTu through these layers. Tip resistance ( $q_t$ ) and sleeve friction ( $f_s$ ) measurements are higher, and variable, while pore pressure ( $u_2$ ) measurements are lower and hydrostatic (since the soil is free-draining). Conversely, the Presumpscot clay has low values of  $q_t$  and  $f_s$  while  $u_2$  increases dramatically compared to the sand layers. Stratification of the soil layers at the Route 197 Bridge site is relatively obvious from an initial inspection of the CPTu profiles; however, it is instructive to display the corresponding normalized measurements of these values (i.e.  $Q_t$ ,  $F_r$ , and  $B_q$ ) on the SBT charts to verify the stratification identified by the charts. As expected, data points collected in the sand layers resulted in higher  $Q_t$  and  $F_r$  values therefore plotting in the upper-left portion of Figure 8.7a and Figure 8.7c.

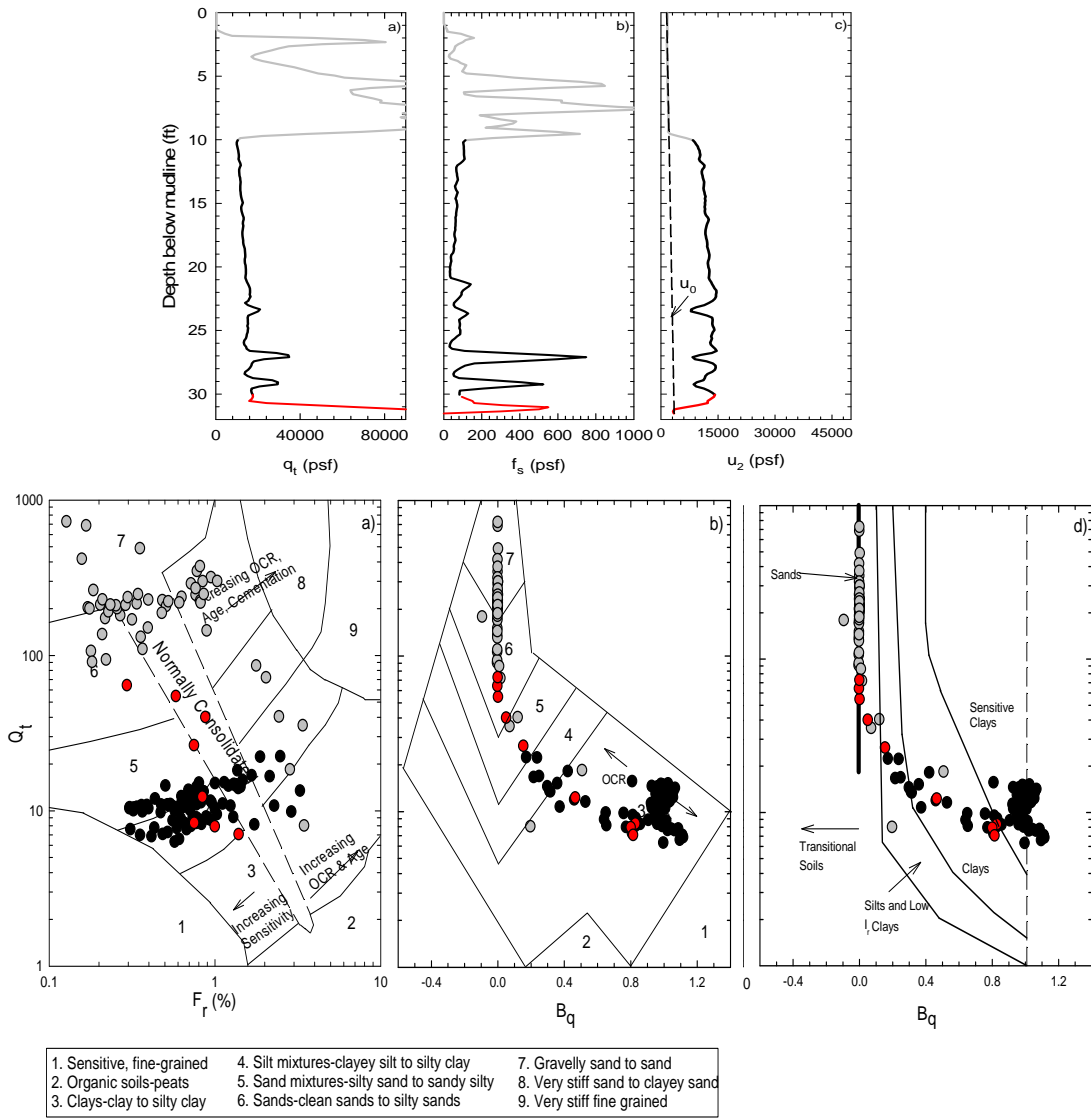


Figure 8.7: Comparison of CPTu profile collected at the Route 197 Bridge (modification of Figure 6.13, showing the soil layers by color) to the corresponding normalized measurement plotted on SBT classification charts.

A few of the data points from the sand plotted in the same cluster as the clay data and were scattered throughout the middle of the charts. This is a result of transitional soils as the deposit transitions from sand to clay or vice versa. In these soils, the CPTu results are a "hybrid" reading from both the sand (granular, drained soils) and the clay (cohesive, non-drained soils).

For Figure 8.7b, the data points collected in the sand layers plotted almost entirely on the  $B_q = 0$

line (i.e. no excess pore pressure during cone penetration), which is expected. Similar to the outlier data for the other two charts, the sand data which does not plot on the  $B_q = 0$  line is due to transitional soil. The SBT classification charts examined in this study properly delineated the stratification of the soil observed directly from the CPTu results.

The percent effectiveness values given in Table 8.2 compare USCS and SBT. Since the SBT classification is based solely on behavioral characteristics and not grain size and plasticity as is USCS classification, some differences are expected. The classification of the Presumpscot clay from the SBT charts may not be a mis-classification of the clay but rather a behavior to shear identified by the CPTu which the USCS classification method cannot indicate with grain size alone. Robertson (1990) states that the classification of soils via CPTu SBT charts cannot be expected to distinguish between grain sizes of material, but rather classify soils based on behavioral differences. Traditionally, cohesive soils are classified by the USCS in terms of the particle grain size of the soil and the resulting plasticity from Atterberg Limit testing (if the soil is cohesive, such as the Presumpscot clay). In almost all cases, the Presumpscot clay will classify as "CL" or "lean clay" in accordance with USCS, which is consistent with the results from the four research sites. Therefore, if the USCS classification provides no delineation of classification between Presumpscot clay which we know has varying properties on a site-specific, and even boring-specific, scale, classifying it as "CL" provides limited information. In the best case scenario, Atterberg Limit results can be loosely correlated to expected engineering properties (Terzaghi *et al.*, 1996). Therefore, the following classification analyses aim to provide guidance on the interpretation of SBT classification charts in Presumpscot clay in order to gain more insight into a comprehensive classification that directly provides information on the engineering properties of the soil.

Classification of Presumpscot clay using the  $F_r$ - $Q_t$  relationship (Robertson 1990; Robertson 2009) resulted in a cumulative 84% effectiveness (42 of the 50 samples) when compared to USCS classification. Both charts use the relationship between  $Q_t$  and  $F_r$  and contain identical classification regions, but Robertson (2009) includes predictions of soil properties such as OCR and sensitivity which go beyond classification. The purpose of analyzing the Robertson (2009) chart was to evaluate the accuracy of these predicted normalized soil property trends. A similar study in silty soft clay by Long (2008) experienced similar issues with difference in classification using the  $F_r$ - $Q_t$  relationship. This is thought to be potentially due to the sleeve friction measurement during CPTu testing being notoriously of low accuracy, as it is highly subject to rate of advance and calibration issues (Rogers 2006; NCHRP 2007).

The low effectiveness of the  $F_r$ - $Q_t$  relationship for the Route 197 Bridge SBT classification is likely a result of the high sensitivity of the clay in conjunction with a moderate OCR. Sandy soils have been found to have higher  $Q_t$  and lower  $F_r$  as compared to clay soils. Coincidentally, all of the "mis-classified" data points from the Route 197 Bridge plotted in Region 5 (sand mixtures), a region defined by comparably higher  $Q_t$  and lower  $F_r$  (Figure 8.8). Higher OCR will cause tip resistance (and hence  $Q_t$ ) to increase, while high sensitivity will cause sleeve friction (and hence  $F_r$ ) to decrease. The combination of these two behaviors imitates the behavior of a weak sand, which is exactly where the "mis-classified" data points plot (i.e., in the sand mixture region, but close to the border of silt mixtures).

Figure 8.8 presents the CPTu data from all four sites plotted on the SBT classification charts. Each symbol represents a USCS classification data point from a discrete undisturbed sample and the corresponding  $F_r$ - $Q_t$ - $B_q$  measurement from the SCPTu profile from the adjacent boring at the same depth. It should be noted that CH is "fat clay," CL is "lean clay," CL-ML is "silty clay," and ML is "silt" in accordance with USCS. Figure 8.8 reveals that a large majority of the collected Presumpscot clay samples classified as CL, which is expected. Other classifications included

three samples of CH at Route 26/100 Falmouth Bridge, one CL-ML (with sand) at Martin's Point Bridge, and three ML samples at Route 26/100 Falmouth Bridge. The difference between CL, CL-ML, and CH is due to the difference in Atterberg Limit results which is directly related to the mechanical behavior of the clay under different moisture contents (Mitchell and Soga, 2005). The threshold between CL and CH is a Liquid Limit (LL) of 50, and the three CH samples had LL values of 54, 52, and 51. The three ML samples had low enough Plasticity Index values (9, 11, 17) with respect to their LL values to classify as ML. Plotted data points which include the "with sand" descriptor indicate samples with greater than 15% of material by weight which was retained on the number 40 sieve (the "sand" grain size). Accordingly, since differences in the grain size composition and plasticity measurements of Presumpscot clay signify a difference in mechanical behavior of the soil, one may expect different CPTu measurements between the samples. For instance, it has been shown that clays with higher LL have correspondingly higher compressibility (Mitchell and Soga, 2005), so one may expect that the tip resistance of CH Presumpscot clay to be lower than CL soils. However, analysis of Figure 8.8 does not agree with some of the expected behavioral differences predicted from USCS such as this. Presumpscot clay samples which included sand grains or a higher percentage of silt would intuitively cause tip resistance and sleeve friction measurements to increase and pore pressure to decrease, representing CPTu data behavior that is typical of granular soils. However, none of these patterns were consistently observed from the CPTu results at any of the four sites. "CL with sand," "CL-ML with sand," and "ML" samples resulted in  $Q_t$  and  $F_r$  values which are comparable, and in some cases lower, than the corresponding values for CL samples. Based on the four research sites, the published SBT charts do not appear to have the ability to differentiate between Presumpscot clay samples which classify as ML versus CL or CL with sand versus just CL.

One observation that can be made from Figure 8.8 is the consistency of the data to plot within Region 3 "clay to silty clay" in the Robertson (1990) and "clay" or "sensitive clay" in the

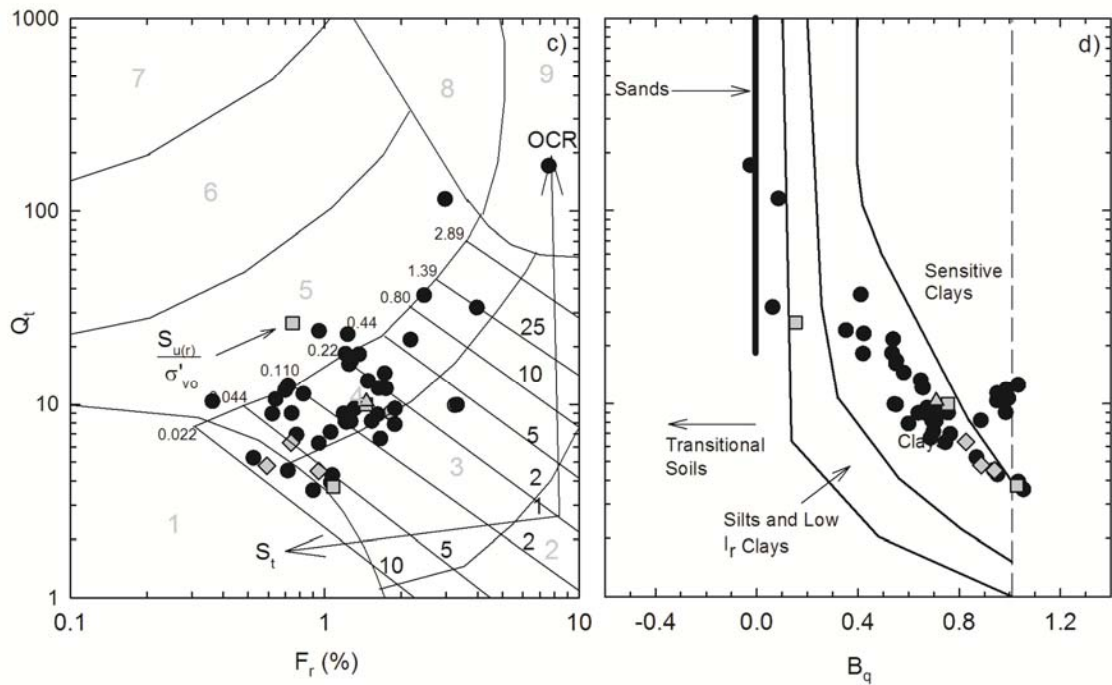
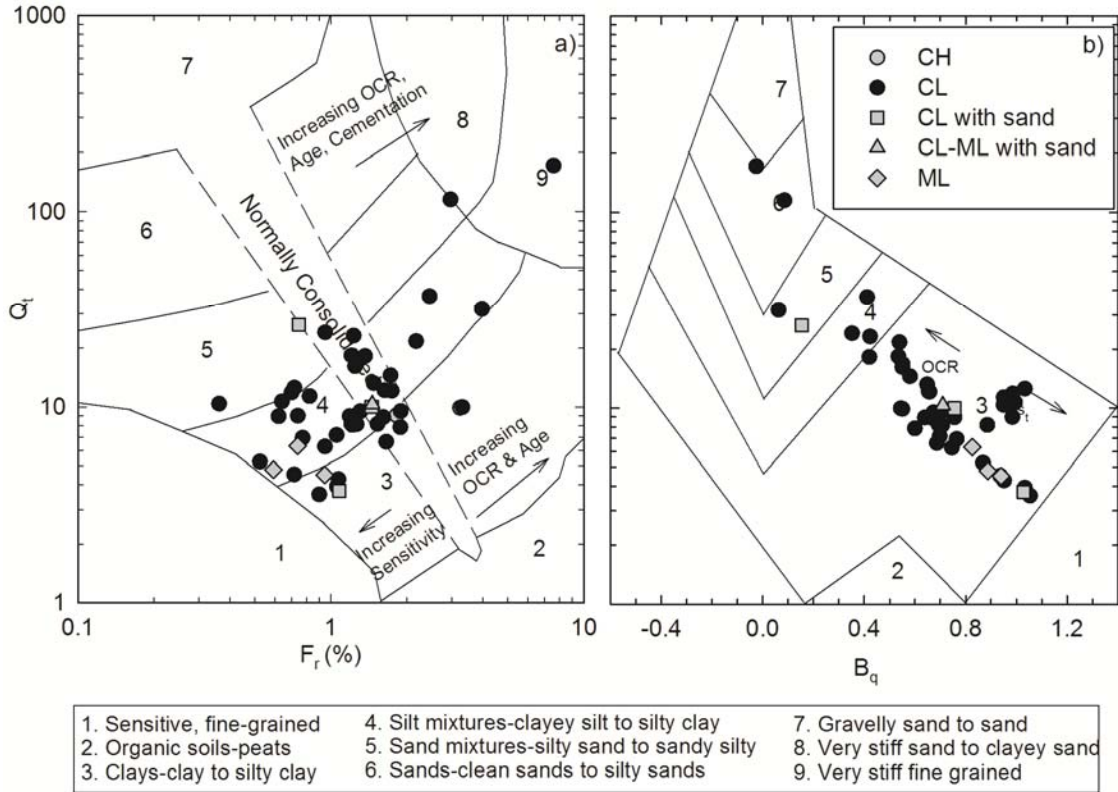


Figure 8.8: CPTu normalized data from all four Presumpscot clay research sites plotted with corresponding USCS classification of undisturbed soil samples. Note: CH = fat clay, CL = lean clay, CL-ML = silty clay, and ML = silt.

Schneider *et al.*, (2008) which are both  $B_q-Q_t$  analyses. Conversely, the CPTu data plots consistently within Region 4 "silt mixtures" using the Robertson (1990) and Robertson (2009), which are both  $F_r-Q_t$  analyses. To support this claim, data from the entire CPTu profile from Route 197 Bridge is plotted on two different Robertson (1990) charts in Figure 8.9, both the  $B_q-Q_t$  and the  $F_r-Q_t$  analyses. Whereas the data from Figure 8.8 corresponds to undisturbed soil samples, Figure 8.9 is the entire CPTu profile collected in the Presumpscot clay at the site (from approximately 10 feet to 30 feet below ground surface with data points collected every 2 inches) which we can reasonably assume classifies mostly as CL from the undisturbed soil samples at the site. The plotted data agrees with the conclusion that the same Presumpscot clay deposit will classify mostly as "silt mixtures" and "clays" when using the  $F_r-Q_t$  and the  $B_q-Q_t$  analyses, respectively. Robertson (1990) states that:

*"occasionally, soils will fall within different zones in each chart; in these cases judgment is required to correctly classify the soil behavior type. Often, the rate and manner in which the excess pore pressure dissipates during a pause in the cone penetration will significantly aid in the classification."*

Robertson (1990) provides examples from the literature of a hypothetical slightly overconsolidated clay which may be classified as "clay" on one of the charts and "silt mixture" on the other. This is similar to what is observed in the Presumpscot clay, and a dissipation test in the hypothetical clay showed a very slow decrease in the pore pressure measurements, indicating that "clay" is likely the more accurate classification.



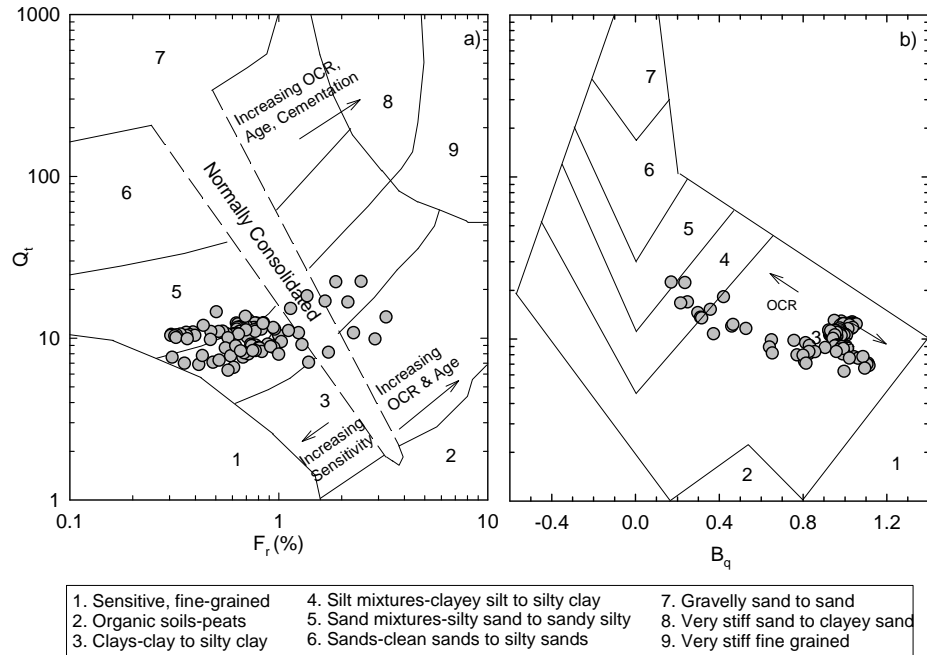


Figure 8.9: Comparison of Robertson (1990) a)  $Q_t$ - $F_r$  and b)  $Q_t$ - $B_q$  classification illustrating difference in predicted soil behavior type for CPTu data from the Route 197 Bridge site.

To determine which classification is more accurate for the Presumpscot clay between the "silt mixture" classification provided by  $F_r$ - $Q_t$  analysis and the "clays" classification provided by the  $B_q$ - $Q_t$  analysis, the results from the dissipation testing at the research sites is analyzed. Dissipation testing was not performed at Route 26/100 Bridge, but it was performed at the remaining sites. The results from the dissipation tests can be found in ConeTec (2011), ConeTec (2012), and ConeTec (2013). A dissipation tests is a pause in cone penetration to allow for the pore pressure dissipation over time to be measured. From this, an estimated hydrostatic groundwater level and the time it takes for the pore pressure to dissipate to 50% of the hydrostatic water level can be determined. This value,  $t_{50}$ , is a coefficient used in time rate of consolidation calculations of clay. The purpose of this analysis is to determine if the pore pressure behavior is more silt-like or clay-like. The author is not aware of a specific value of  $t_{50}$  which separates silt vs. clay, however Robertson (1990) discussed a  $t_{50}$  of 2 to 4 minutes as a threshold between silt and clay behavior. The  $t_{50}$  values determined from the dissipation tests in Presumpscot clay

ranged from 26.5 minutes (Martin's Point Bridge) to 37.6 minutes (Route 197 Bridge); clearly distinguishing the behavior as more "clay-like." Thus, the  $B_q$ - $Q_t$  analysis appears to more appropriately classify the Presumpscot clay.

Since the Presumpscot clay typically contains a high percentage of silt, the effect of silt content on classification was determined to see if there is a distinguishable difference in SBT classification based on silt content alone. Figure 8.10 illustrates CPTu classification data differentiated by silt content. Figure 8.10a and Figure 8.10b provides data from all four sites and Figure 8.10c and Figure 8.10d provide data from the Route 26/100 Bridge and Route 197 Bridge sites where sensitive deposits of Presumpscot clay are found. The purpose of isolating these two sites is to identify the influence of sensitivity on classification vs. silt content. For instance, a sample with higher silt content will likely result in lower measured pore pressure ( $B_q$ ) values while samples with high sensitivity will result in higher  $B_q$  values. By evaluating silt content on a basis of sensitivity, the effect of each on classification can be determined.

Analysis of Figure 8.10a and Figure 8.10b shows that silt content alone does have an effect on the  $F_r$ - $Q_t$  classification but does not appear to have an effect on the  $B_q$ - $Q_t$  classification. In general, samples with higher silt content resulted in higher  $F_r$  values (Figure 8.10a). On the other hand,  $B_q$  values did not decrease with increasing silt content. This  $B_q$  behavior is counterintuitive, since one would expect the pore pressure measurement to decrease as silt content, which is more permeable than clay, increases. A hypothesis for this behavior is that the influence of both sensitivity and overconsolidation ratio (OCR) of the Presumpscot clay dominates the pore pressure measurement (and subsequently the SBT classification) over silt content. Firstly, sensitive clay has been found to result in higher pore pressure measurements (Lunne *et al.*, 1997, Robertson 1990, Schneider *et al.*, 2008). Figure 8.10d shows sensitive deposits of Presumpscot clay, and in general,  $B_q$  does roughly decrease with increasing silt content. Pore pressure exerted during shear (i.e. cone penetration) is also strongly controlled by the amount of overconsolidation

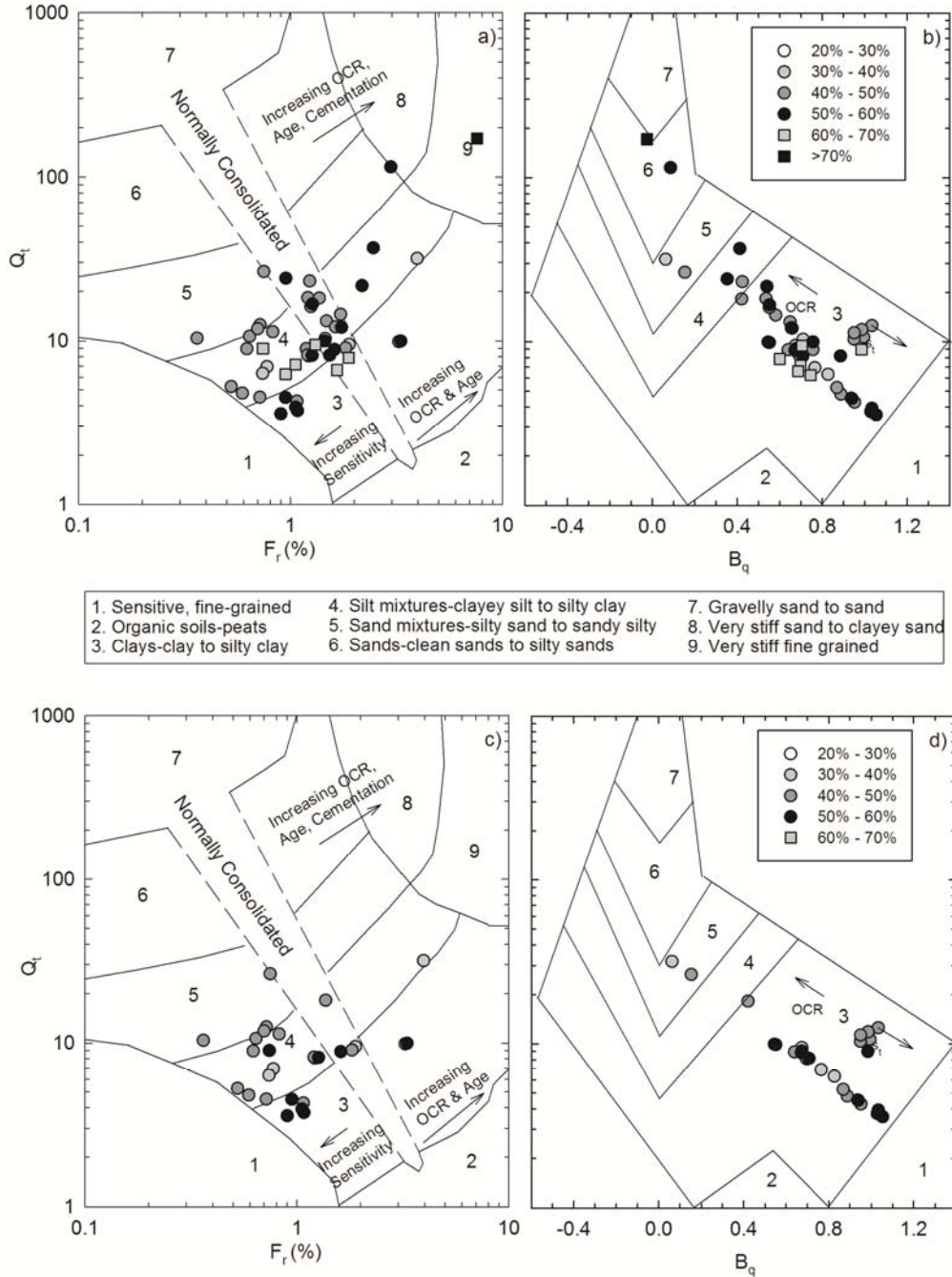


Figure 8.10: Comparison of CPTu data of Presumpscot clay from the four research sites plotted on SBT classification charts in accordance with silt content of the undisturbed soil samples. A and b show the data from all four sites and c and d show the results from only Route 26/100 Bridge and Route 197 sites (sensitive deposits).

of the clay, in which higher OCR results in lower  $B_q$ . This trend is also shown on the Robertson (1990) chart. Another observation of Figure 8.10a and Figure 8.10b is the tendency for data

points with higher silt content to move towards the "clay" and "sensitive clay" regions as opposed to the "sand mixtures" regions. It appears that clay content, regardless of the percent composition, dominates the Presumpscot clay classification on the SBT chart. Theoretically, the saturated clay will lubricate the silt particles and fill in the void spaces, encouraging clay-like (undrained) behavior as seen in the charts. Therefore, Presumpscot clay which has a higher percentage of silt but is normally consolidated may have a higher  $B_q$  value than other Presumpscot clay with a lower percentage of silt but a higher OCR. This hypothesis agrees with the analysis presented below related to the impact of OCR on classification (Figure 8.11). In conclusion, it appears that silt content alone lead to higher  $F_r$  values from CPTu SBT charts, but silt content needs to be considered with OCR and sensitivity when evaluating its effect on  $B_q$  measurements.

In addition to predicting soil classification, each of the four SBT charts also provide estimates of engineering properties based on the location of the plotted CPTu data points on the charts. These engineering properties include OCR, sensitivity, age, level of cementation, and normalized remolded shear strength. Of these properties, OCR, sensitivity, and remolded shear strength of the Presumpscot clay were measured in the laboratory on undisturbed samples. Hence, the effectiveness of the SBT charts to estimate these properties can be evaluated. Age and level of cementation of the Presumpscot clay were not measured in this study and is therefore omitted from the following analyses.

Figure 8.11 and Figure 8.12 compare the engineering properties of the Presumpscot clay measured in the laboratory to the predicted values/trends estimated in the Robertson (1990) and Robertson (2009)  $F_r$ - $Q_t$  plots and the Robertson (1990) and Schneider *et al.*, (2008)  $B_q$ - $Q_t$  plots (Figure 8.12). On each plot, the predicted trend being evaluated is bolded. The data plotted on the charts is from all four research sites.

Figure 8.11a and Figure 8.11c show CPTu data points from respective sample depths for each site plotted together with respect to the corresponding OCR values from laboratory testing. The predicted "Increasing OCR" trend from Figure 8.11a is upwards and to the right on the plot. In general, the data plot higher  $Q_t$  values as OCR increases. The upward direction of the predicted increasing OCR trend agrees well with the Presumpscot clay results. However, the rightward direction (i.e. increasing  $F_r$ ) does not appear to effectively delineate an increase in OCR for high OCR (i.e. OCR > 4 spans a broad  $F_r$  for a given  $Q_t$ ). Perhaps this observation led to the refinement of the OCR trends observed in Figure 8.11c, in which predicted OCR increases directly upwards, which is consistent with the plotted Presumpscot clay data. However, the predicted values of OCR at the right in the plot do not correlate well with the laboratory results. The *k-value* method discussed subsequently provided a better estimate of OCR values from CPTu results.

Furthermore, the "Normally consolidated" region in Figure 8.11a exhibited poor performance in predicting actual normally consolidated conditions of the Presumpscot clay. Only one of the 16 data points which plotted in this region had stress history conditions which could be considered approximately normally consolidated (i.e. OCR  $\leq$  1.5). Robertson (1990) does not discuss how the "normally consolidated" region was created other than stating that it "*represents approximately normally consolidated conditions.*" From inspection of the region, it extends from Region 7 (Gravelly sand) to Region 3 (clays), so it appears to be a very rough estimate of normally consolidated conditions for all types of granular and cohesive soil. This may explain why it does not apply well to the Presumpscot clay.

Figure 8.11b and Figure 8.11d plot the CPTu data from each site by the samples' sensitivity ( $S_t$ ) and normalized remolded shear strength ( $s_{u(r)}/\sigma'_{v0}$ ), respectively. Inspection of Figure 8.11b shows that the plot is generally effective in predicting an increase of  $S_t$  with a leftward trend in plotted data points (i.e. a decrease in  $F_r$ ). Conversely, Figure 8.11d does not

appear effective in plotting predicted values of  $s_{u(r)}/\sigma'_{v0}$ . In general, the plot over predicts  $s_{u(r)}/\sigma'_{v0}$ . However, the general trend of increasing magnitude of  $s_{u(r)}/\sigma'_{v0}$  did agree with upwards and to the right trend displayed in Figure 8.11b.

Figure 8.12 presents the predicted trends of OCR and  $S_t$  using Robertson (1990) and Schneider *et al.*, (2008)  $B_q$ - $Q_t$  plots. Robertson (1990)  $B_q$  predicts increases in OCR and  $S_t$  with direction of plotted data points on the chart while Schneider *et al.*, (2008) has a "sensitive clay" region. Analysis of Figure 8.12a and Figure 8.12b reveals that Robertson (1990)  $B_q$  is effective in estimating qualitative increases and decreases in both OCR and  $S_t$  in respect to location of the plotted data.

The behavior of clay during shear can be viewed theoretically to explain the location of the predicted trends for both OCR and  $S_t$ . From basic soil mechanics, soft to medium clays with higher OCR will have higher undrained shear strength and develop less positive excess pore pressure when sheared. This corresponds to a higher tip resistance and lower measured pore pressure during a CPTu (hence an upwards and leftwards trend on the SBT chart). Clays with higher  $S_t$  values are expected to exert higher excess positive pore pressure during shear, but in general, the undrained shear strength should be relatively unaffected (since sensitivity only affects the post-shear strength). This, in theory, would translate to a horizontal rightward direction on the SBT chart. However, Robertson (1990) shows a rightwards and downward trend, indicating a lower expected tip resistance for higher  $S_t$  clays. While Robertson (1990) does not elaborate on this predicted trend, it can be hypothesized that the zone of influence around an advancing cone may capture the post-sheared behavior of the clay behind the cone tip. Furthermore, since sensitive clays shear at a lower strain, the  $s_u$  of clays on the outskirts of the zone of influence may be completely sheared and, in effect, influence the tip resistance reading (refer to Figure 2.6).

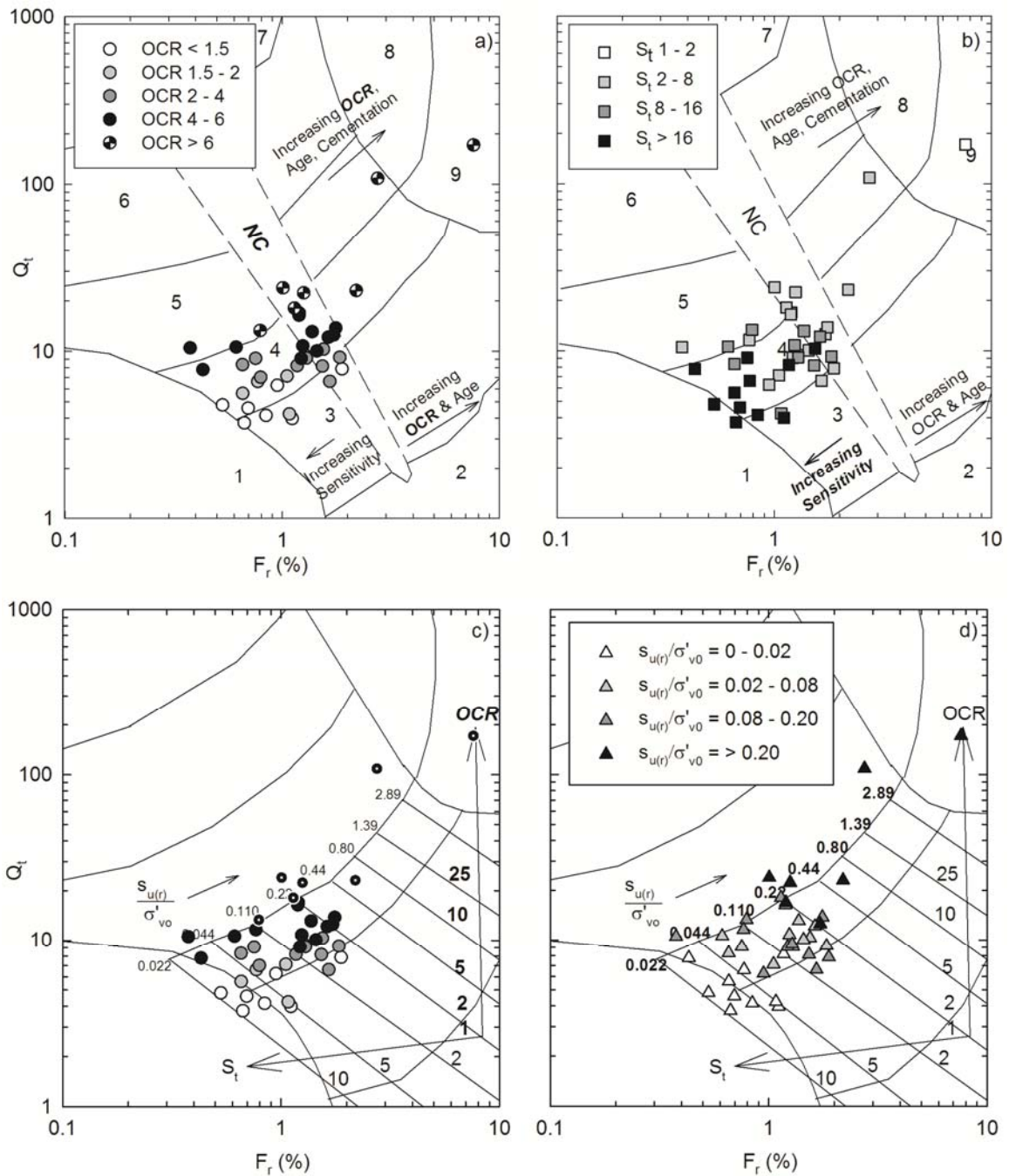


Figure 8.11: Evaluation of the predicted engineering properties from the Robertson (1990) and Robertson (2009) SBT classification charts of the Presumpscot clay. Values of OCR,  $S_t$ , and normalized remolded undrained shear strength ( $S_{u(r)}/\sigma'_{vo}$ ) were measured in the laboratory on high-quality samples.

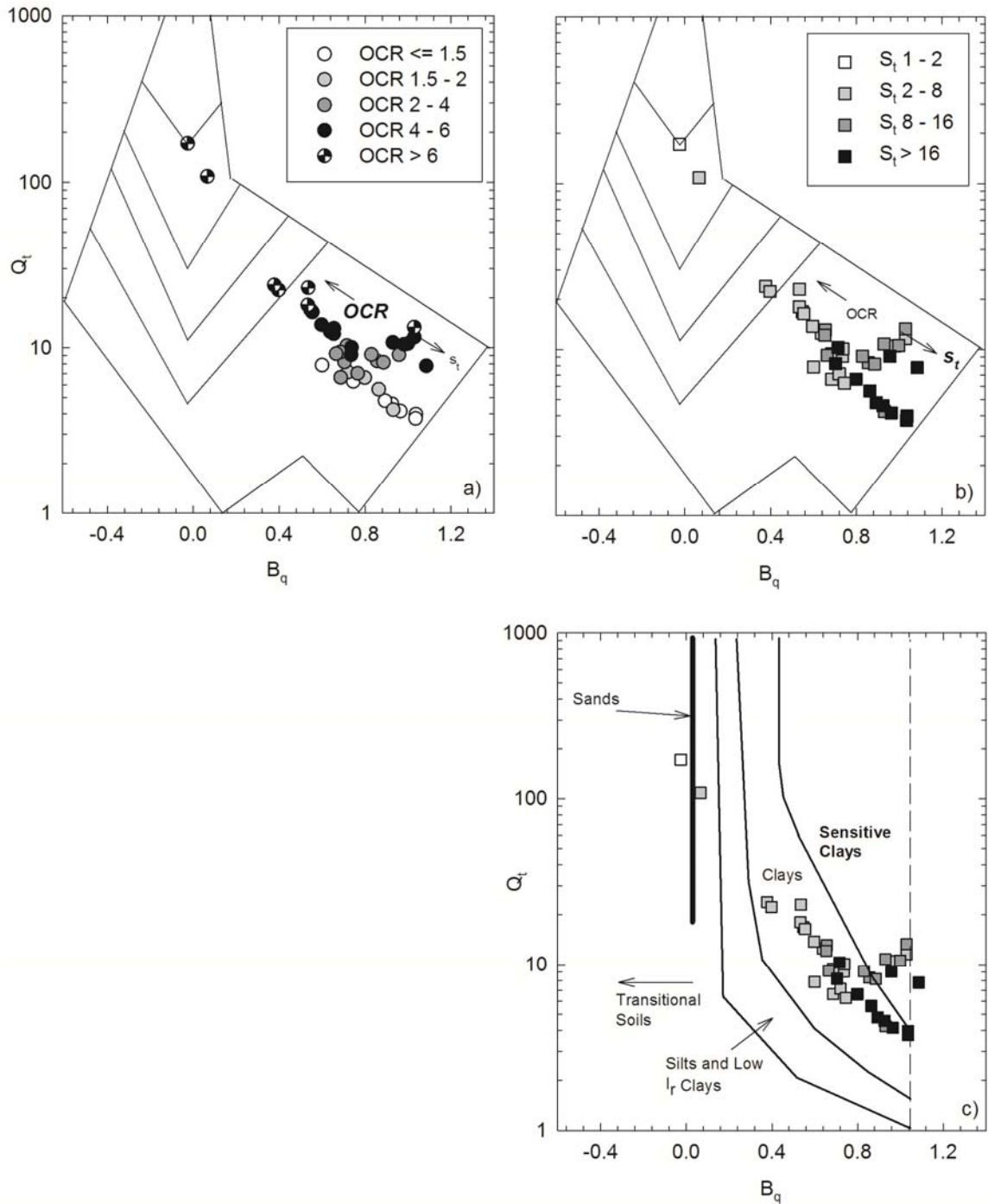


Figure 8.12 Evaluation of the predicted engineering properties from the Robertson (1990) and Schneider *et al.*, (2008) -  $B_q$  SBT classification charts of the Presumpscot clay. Values of OCR, and  $S_t$ , were measured in the laboratory on high-quality samples.



This downwards and rightward trend of increasing clay sensitivity matches the "sensitive clay" versus "clay" regions of the Schneider *et al.*, (2008)  $B_q$ - $Q_t$  plot. Review of the sensitive clay zone in Figure 8.12c versus the plotted sensitivity of the Presumpscot clay shows good agreement. Schneider *et al.*, (2008) states that "[the sensitive clay region] is not intended to exclude clay as sensitive, but rather highlight soils which may have highly collapsible structure." Results plotted on Figure 8.12c agree with this statement; where not all of the sensitive clay (i.e. clay with  $S_t > 8$ ) plotted in the region, all of the data which plotted in the region were sensitive.

In summary, the SBT classification charts provided 92% effectiveness for  $B_q$ - $Q_t$  analyses and 84% effectiveness for  $F_r$ - $Q_t$  analyses when compared to USCS classification. Subsurface layering (i.e. transitional zones, silt/sand seams) within the Presumpscot clay was identified well when plotting all data from a particular profile on the SBT charts (e.g. Figure 8.7). When comparing  $B_q$ - $Q_t$  and  $F_r$ - $Q_t$  SBT charts from Robertson (1990), Presumpscot clay plotted predominantly in Region 3 "clays" and Region 4 "silt mixtures" for the two charts, respectively. Analysis of the dissipation during the CPT showed more clay-like behavior (Region 3), so it appears that  $B_q$ - $Q_t$  charts are more effective in classifying the Presumpscot clay behaviorally. Silt content of the Presumpscot clay only appeared to affect the location that the CPTu data plotted on  $F_r$ - $Q_t$  charts, whereas OCR and sensitivity dominated  $B_q$ - $Q_t$  SBT charts over the silt content. Between the two types of  $B_q$ - $Q_t$  SBT (Robertson (1990) and Schneider *et al.*, (2008), the latter appears to be more appropriate for the determination of sensitivity. Classification between the two  $B_q$ - $Q_t$  charts did not differ between the sites in this study. The OCR and sensitivity trends on the  $B_q$ - $Q_t$  charts are good for relative estimates of trends, but values do not correlate with those given on the chart.

#### 8.4 Stress History

Stress history of clay refers to the preconsolidation pressure ( $\sigma'_p$ ) profile of the deposit and the corresponding ratio of  $\sigma'_p$  to the in situ vertical effective stress (i.e. OCR, or  $\sigma'_p/\sigma'_{v0}$ ).

Measurements of tip resistance ( $q_t$ ) have been found to relate directly to the  $\sigma'_p$ , and, if appropriate correlations are used in the processing of CPTu data, values of  $\sigma'_p$  and OCR can be directly obtained over the entire soil profile. This has a powerful implication for geotechnical investigations in Presumpscot clay if complete stress history profiles can be accurately determined for settlement, slope stability, and other geotechnical analyses. This section will provide a summary of the CPTu stress history results for the four Presumpscot clay research sites, including the variation in the calculated  $k$ -values at each deposit and between sites. Variation in  $k$ -values are expected, "*[CPTu estimated] OCR is influenced by sensitivity, preconsolidation mechanism, soil type, and local heterogeneity*" (Lunne *et al.*, 1997).

It has been observed from past studies, and corroborated with the results of this thesis, that CPTu stress history coefficients are unique to specific sites and even specific depths within a deposit. However, the differences between sites or over depths may be predictable based on other soil properties or CPTu measurements. Relationships between  $k$ -values (Equation 8.12) and OCR, Liquid Limit, and Plastic Limit have been proposed (Lunne *et al.*, 1997, Saye *et al.*, 2013). Relationships between the  $k$ -values and clay properties are investigated herein in effort to identify correlations so that future CPTu stress history interpretations can be performed more effectively in Presumpscot clay.

Undisturbed Sherbrook block samples and modified Shelby tube samples of Presumpscot clay collected at all four research sites were tested for consolidation properties using the constant rate of strain (CRS) test (Section 3.4.3). The strain energy method from Becker *et al.*, (1987) was used to determine the preconsolidation pressure ( $\sigma'_p$ ) from the resulting consolidation curves. CPTu soundings were conducted adjacent to the borings from which the samples were collected in order to correlate the CPTu measurements to the laboratory results of  $\sigma'_p$ . Overconsolidation ratio (OCR, or  $\sigma'_p/\sigma'_{v0}$ ) estimates were made using  $\sigma'_p$  and  $\sigma'_{v0}$  calculated from averaged unit

weight values obtained from the tested consolidation specimens and water table elevations observed in the CPTu and borings.

The *k-value* method was used to predict stress history of the Presumpscot clay at the four sites using the equations below

$$OCR = k * Q_t \quad 8.12$$

$$\sigma'_p = k * q_{net} \quad 8.13$$

where OCR = overconsolidation ratio ( $\sigma'_p/\sigma'_{v0}$ ), *k* = empirical constant,  $Q_t$  = normalized tip resistance (Equation 2.2),  $\sigma'_p$  = preconsolidation pressure (psf), and  $q_{net}$  = net tip resistance (psf, Equation 3.3). Note that the *k-value* for determining both  $\sigma'_p$  and OCR is the same coefficient, which has been found to generally range from 0.20 to 0.50 (Lunne *et al.*, 1997). Resulting *k-values* at the four Presumpscot clay research sites are summarized in Table 8.3.

Table 8.3: Stress history *k-values* back-calculated using discrete preconsolidation pressure measurements and depth corresponding CPTu results for Presumpscot clay.

Site		<i>CPTu k-value</i>				
		Minimum	Average	Maximum	COV	SD
Route 26/100 Bridge ( <i>Falmouth</i> )	<i>n</i> = 13	0.25	0.32	0.43	0.19	0.06
Martin's Point Bridge ( <i>Portland/Falmouth</i> )	<i>n</i> = 13	0.30	0.38	0.53	0.18	0.07
Route 197 Bridge ( <i>Richmond/Dresden</i> )	<i>n</i> = 9	0.31	0.45	0.55	0.16	0.07
I-395 Terminus Site ( <i>Brewer</i> )	<i>n</i> = 8	0.19	0.28	0.36	0.24	0.07

Note: *n* = number of tested consolidation samples, COV = coefficient of variation, SD = standard deviation

*k-values* calculated for Presumpscot clay from the four sites ranged from 0.19 to 0.55, with average values of 0.32 for Route 26/100 Bridge, 0.38 for Martin's Point Bridge, 0.45 for Route 197 Bridge, and 0.28 for I-395 Terminus Site. They agreed well with the published range of 0.20 to 0.50 from (Lunne *et al.*, 1997), with only one sample falling below the range and two samples falling above the range out of 42 total samples. Within the 0.20 to 0.50 range, however, the *k-values* appear to be scattered amongst the entire range. One general trend in the *k-value* results is the tendency for lower values in the more normally consolidated deposits (Route 26/100 Bridge and I-395 Terminus) and higher values for the more overconsolidated deposits (Martin's

Point Bridge and Route 197 Bridge). This is an observed relationship by Lunne *et al.*, (1997), which will be investigated in more depth later in the section.

Mayne (2014) presents a "unified approach" to the determination of  $\sigma'_p$  for clays. He suggests using a constant *k-value* of 0.33 to be a reasonable first order estimate of stress history for clay deposits. The *k-value* of 0.33 was developed using a hybrid cavity expansion theory and critical state soil mechanics, with an assumed drained friction angle of  $30^\circ$  and a rigidity index ( $G_0/s_u$ ) of 100, and the resulting correlation was verified with at least 27 different clay deposits throughout the world (Mayne 2014). This correlation was evaluated with respect to Presumpscot clay. Figure 8.13 presents  $\sigma'_p$  and OCR determined from laboratory data and predicted using a *k-value* of 0.33 (Mayne 2014). The figure illustrates that that  $k = 0.33$  provides a good approximation of stress history for Presumpscot clay.  $\sigma'_p(\text{estimated})/\sigma'_p(\text{measured})$  ranged from 0.60 to 1.76, where the  $k = 0.33$  correlation tends to overestimate  $\sigma'_p$  soils have low measured values of  $\sigma'_p$  (i.e.,  $\sigma'_p(\text{estimated})/\sigma'_p(\text{measured}) > 1.0$ ) and overestimate soils with greater measured values of  $\sigma'_p$  (i.e.,  $\sigma'_p(\text{estimated})/\sigma'_p(\text{measured}) < 1.0$ ). The use of  $k = 0.33$  correlation for lower OCR soils could likely overestimate  $\sigma'_p$  and possibly underpredict settlement, while for greater OCR soils, it could likely underestimate  $\sigma'_p$  and possibly overestimate settlement, depending on loading and a number of other factors. The comparison in Figure 8.14 confirms the observation of Lunne *et al.* (1997) that greater *OCR* corresponds with greater *k-values*.

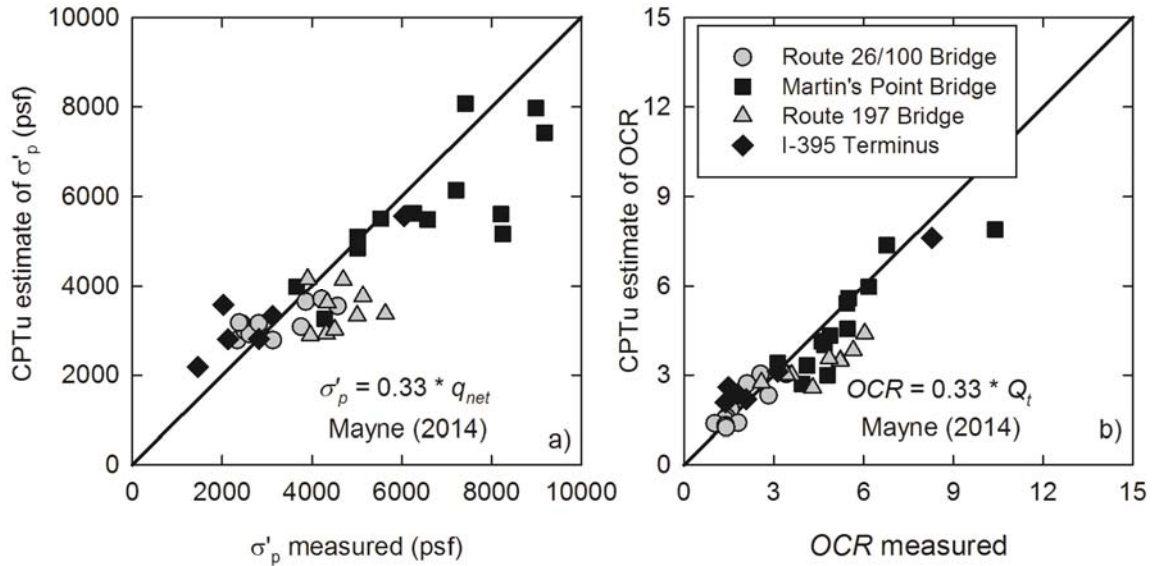


Figure 8.13: Overconsolidation ratio (OCR) and preconsolidation pressure estimated using a  $k$ -value of 0.33 as suggested by Mayne (2014).

Analysis of Figure 8.14 yields the tendency for Presumpscot clay samples from OCR of 4 to 6 to be consistently underestimated using the Mayne (2014) method (e.g. Route 197 Bridge and the Martin's Point Bridge). There are two possibilities to explain this deviation from the trend. Either Presumpscot clay with OCR from 4 to 6 tend to yield higher  $k$ -values or there is a specific clay property occurring at these two sites. When comparing the laboratory tests results of the undisturbed soil samples from the sites (e.g. content, grain sizes, activity, sensitivity, plasticity, and organic content), there doesn't appear to be a distinguishable property which separates the high OCR sites from the low OCR sites. This includes water. In fact, the Route 26/100 Bridge and the I-395 Terminus (the two sites which matched the trend) are the most dissimilar when it comes to plasticity and silt and clay content.

Figure 8.14 presents the  $k$ -values calculated at each site with corresponding values of OCR in order to evaluate the relationship proposed by Lunne *et al.* (1997) along with the 0.20 to 0.50 range of typical values. Figure 8.14 indicates a potential relationship of larger  $k$ -values being associated with greater OCR values when OCR ranges from 1.0 and 4.0. The three data points

that are contrary to the *k-value* - OCR trend from OCR 1 to 4 are from the deepest portion of the Presumpscot clay at the Route 26/100 Bridge in Falmouth. Figure 8.14 illustrates that the linear relationship assumed in the *k-value* method between  $Q_t$  and OCR (or  $q_{net}$  and  $\sigma'_p$ ) is an oversimplification. If the relationship was linear, the *k-value* in Figure 8.14 would remain perfectly horizontal for varying OCR, however, this is clearly not the case. It can be argued from Figure 8.14 that *k-value* for OCR 1 to 4 approximately increases whereas *k-value* beyond OCR of 4 stay relatively constant or slightly decrease. In effect, if this change in *k-value* with changing OCR were to be adopted into the *k-value* equations (Equation 8.12 and 8.13) the resulting relationship would not be linear.

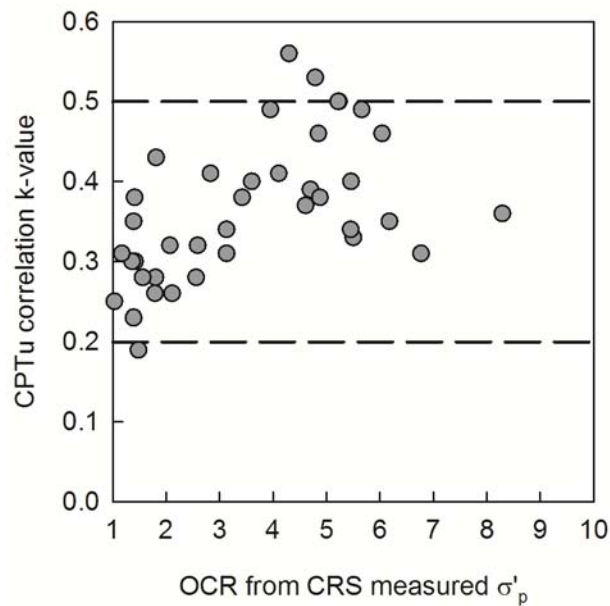


Figure 8.14: CPTu k-value versus OCR for the Presumpscot clay.

This behavior may be caused by multiple factors. Firstly, from Equation 8.13, *k-value* is defined as the ratio of  $\sigma'_p$  to  $q_{net}$ . As OCR increases from 1 to 4, the *k-value* increases, and the  $q_{net}$  measurement relative to the  $\sigma'_p$  decreases. Practically all strength and deformation properties of clays change as the OCR changes, so it is likely that the change in  $q_{net}$  relative to the  $\sigma'_p$  (i.e. *k-*

*value*) is due to complex changes in the stress state, stiffness, and void ratio of the clay which is being measured by the cone penetrometer. This may include the ratio of horizontal to vertical stress, a change in the "radius of influence" of the cone from increased stiffness, pore pressure measurements affecting the measured tip resistance. A similarly complex phenomenon may be occurring from OCR of 4 to 6 (or greater), in effect increasing the measurements on  $q_{net}$  relative to  $\sigma'_p$ . When using the traditional coefficient of lateral earth pressure ( $K_o$ , or ratio of horizontal effective stress to vertical effective stress) equation developed by Mayne and Kulhawy (1982), with an OCR of 4.0 and a drained friction angle of  $30^\circ$  to  $35^\circ$  (typical for clays with plasticity similar to the Presumpscot clay), the  $K_o$  ranges from 0.94 to 1.0, indicating that any further increase in OCR will cause the horizontal effective stress to be greater than the vertical effective stress, which may account for the more significant scatter in *k-value* beyond an OCR of 4.

However, it appears that the simplification of the *k-value* equation gives reasonable estimates of  $\sigma'_p$  for the research sites in this thesis. Figure 8.15 displays the  $\sigma'_p$  profiles at all of the research sites using the site-specific average *k-value* along with  $\pm 1$  standard deviation. For comparison,  $\sigma'_p$  determined from the laboratory consolidation testing is plotted with the profiles. At all of the sites, the  $\pm 1$  standard deviation values provided a reasonable expected range of  $\sigma'_p$  values whereas the average values provided good predictions of  $\sigma'_p$  for the entire profile. Stress history at each of the sites was unique and the CPTu was able to capture and reasonable predict the  $\sigma'_p$  profile at each of the sites. For instance, at the I-395 Terminus site, the top layer of Presumpscot clay is highly overconsolidated and the bottom is nearly normally consolidated, and the average *k-value* of 0.28 at the site was applied to the  $q_{net}$  profile, and the resulting profile followed this trend.

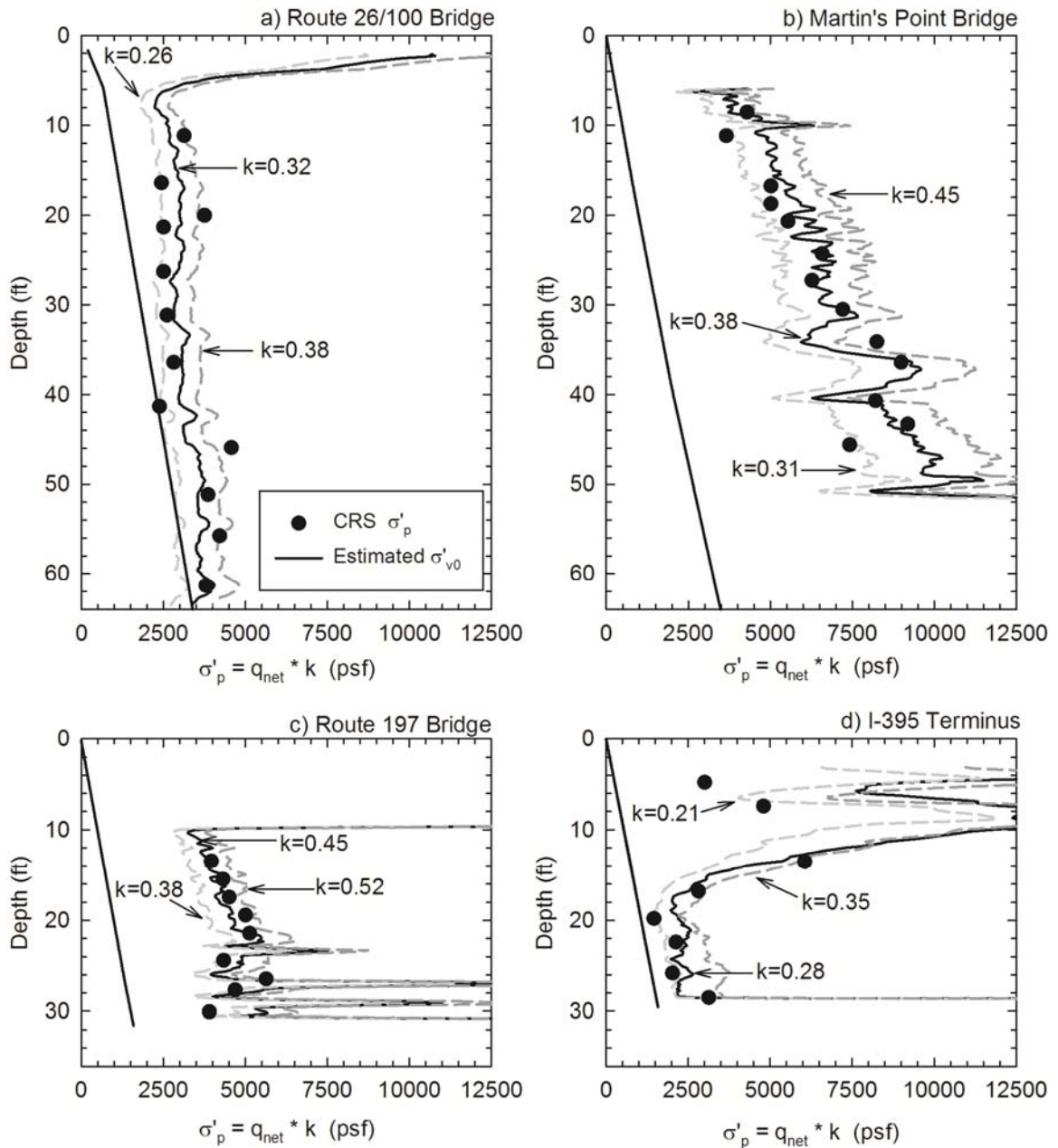


Figure 8.15: Estimates of  $\sigma'_p$  versus depth for a) Route 26/100 Bridge b) Martin's Point Bridge c) Route 197 Bridge and d) I-395 Terminus using average and  $\pm 1$  standard deviation for each site.

Correlations between clay properties and *k-values* for the Presumpscot clay were analyzed. These properties included OCR (Figure 8.14), undrained shear strength ( $s_u$ ), liquidity index (LI), water content, sensitivity, and silt and clay content. Aside from the relationship to



OCR, statistical analysis of these relationships provided linear  $R^2$  values of no greater than 0.20, even when the correlations were conducted on a site-specific basis. Exponential, power, and other trend line functions were also checked without success. The lack of relationship between  $k$ -value and measured Presumpscot clay properties is consistent with published literature. Lunne *et al.*, (1997), DeGroot and Ladd (2010), Been *et al.* (2010), Abu-Farsakh, (2007) all state that the  $k$ -value is a site specific value, and most also agree that there doesn't appear to be a correlation to any clay property beyond a generalized trend of larger  $k$ -values with higher OCR soils.

Figure 8.16 illustrates the analysis of measured parameter  $B_q$  with OCR at the four sites and the corresponding trend line. There is a general decreasing trend observed between  $B_q$  and OCR measured at three of the four sites, however at Route 197 Bridge, there is an increasing trend. This observation is analogous to the discussion in Section 8.3. At the Route 26/100 Bridge, Martin's Point Bridge, and I-395 Terminus, the pore pressure measured during the shearing of higher overconsolidated clays is less (from basic soil mechanics), and therefore a decreasing trend between  $B_q$  and OCR is displayed. However, increasing sensitivity of clay will also increase  $B_q$  measurements. The clay at Route 197 Bridge is overconsolidated and sensitive, so the influence of sensitivity on the  $B_q$  "overpowers" the influence from the rate of overconsolidation of the clay. At the Route 26/100 Bridge, the clay is practically normally consolidated and sensitive, hence a decreasing trend (since the effects are compounding instead of counteracting). Essentially, Figure 8.16 shows that the relationship between OCR and  $B_q$  is complex and site-specific, and does not provide a straightforward method in helping to select a  $k$ -value. While there is a decreasing power trend at the Route 26/100 Bridge, Martin's Point Bridge, and I-395 Terminus between the two parameters, there is an increasing power trend at the Route 197 Bridge.  $R^2$  values range from 0.51 to 0.78.

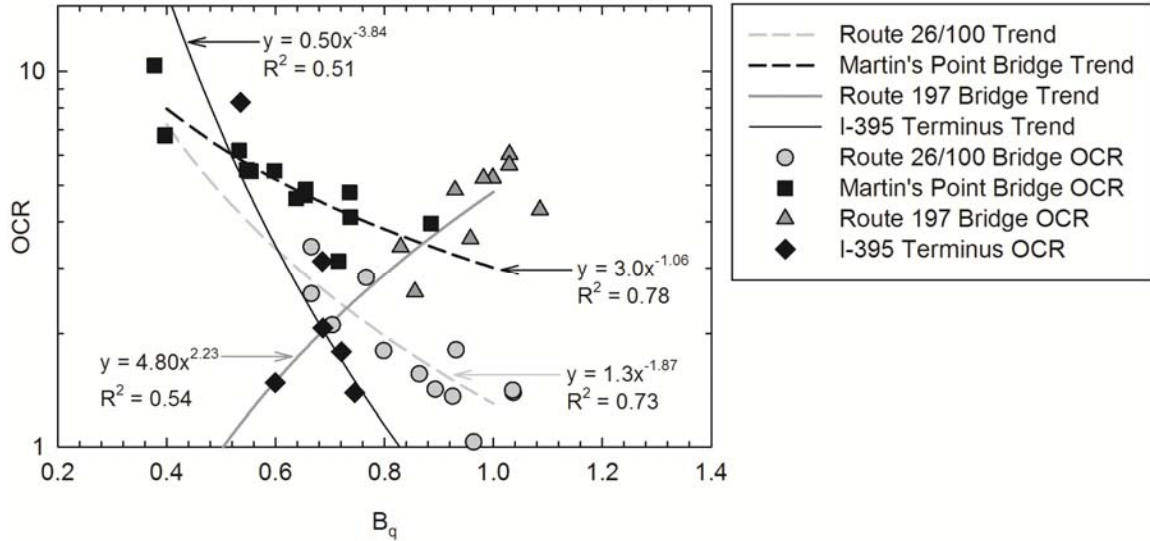


Figure 8.16: Analysis of OCR and  $B_q$  relationship for the Presumpscot clay research sites.

#### 8.4.1 Saye *et al.* (2013) Method

Saye *et al.* (2013) present a SHANSEP-based approach to determining *k-value* using either liquid limit (LL) and plasticity index (PI) of collected clay samples and this method was evaluated for the Presumpscot clay. Section 2.3.2 outlines the framework of the method and the resulting equations evaluated for the Presumpscot clay in this section. In the method,  $\sigma'_p$  and OCR are estimated using a *k-value* which is adjusted based on LL and PI of recovered samples. The following table compares the  $R^2$  values of the  $\sigma'_{p(calculated)}$  vs.  $\sigma'_{p(measured)}$  using the site-specific average *k-value* and the Saye *et al.*, (2013) method for LL and PI for each site, as well as the cumulative  $R^2$  values for all four sites combined.

Table 8.4: Summary of  $R^2$  values for  $\sigma'_p$  calculated versus  $\sigma'_p$  measured using different CPTu stress history methods.

SITE	<b><math>R^2</math> values for <math>\sigma'_p</math> calculated vs. <math>\sigma'_p</math> measured</b>		
	Site specific average $k$ -value	Saye <i>et al.</i> , (2013) using LL	Saye <i>et al.</i> , (2013) using PI
<b>Route 26/100 Bridge (Falmouth) <math>n = 13</math></b>	0.49	0.28	0.27
<b>Martin's Point Bridge (Portland/Falmouth) <math>n = 13</math></b>	0.62	0.45	0.50
<b>Route 197 Bridge (Richmond/Dresden) <math>n = 9</math></b>	0.00	0.13	0.16
<b>I-395 Expansion Site (Brewer) <math>n = 6</math></b>	0.86	0.92	0.92
<b>All sites combined (<math>n = 41</math>)</b>	0.82	0.71	0.68

where  $\sigma'_p$  = preconsolidation pressure,  $n$  = number of tested samples

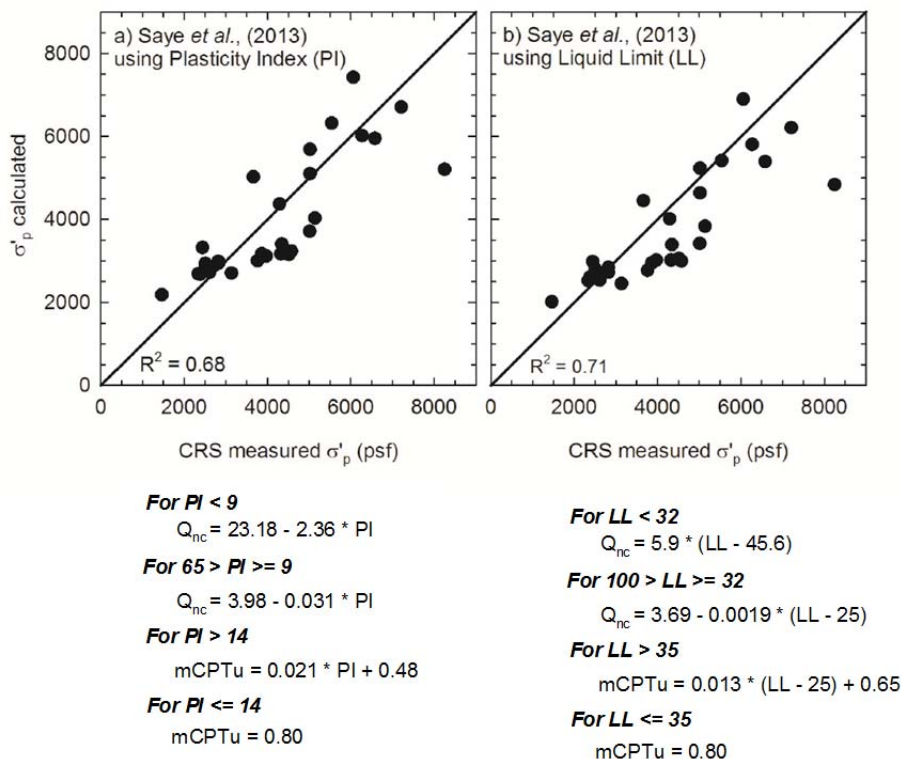


Figure 8.17: Analysis of the Saye *et al.*, (2013) method using Presumpscot clay data.

For the Route 26/100 Bridge and Martin's Point Bridge, the site-specific  $k$ -value for each site resulted in a better correlation to the  $\sigma'_p$  determined from laboratory testing as compared to either of the Saye *et al.*, 2013 methods. However, for the other two sites, the Saye *et al.*, 2013

method resulted in slightly higher  $R^2$  values. The latter two sites had less data points for comparison and a smaller spread of  $\sigma'_p$  values, and since the LL and PI at each of these sites does not vary greatly throughout the deposit (Table 6.1 and Table 7.1), it is likely fortuitous that the Saye *et al.*, (2013) resulted in higher  $R^2$  values. The reason the  $R^2$  values for the Route 197 Bridge are so low is because the  $\sigma'_p$  values at the site are relatively constant with depth, therefore a linear trend line applied to the  $\sigma'_{p(\text{calculated})}$  vs.  $\sigma'_{p(\text{measured})}$  plot is being fitted to a small concentration of data points, and hence a lower  $R^2$ .

The Saye *et al.* (2013) Atterberg Limits correlation was created using a variety of clay deposits all over the world which have variable and different plasticity (i.e. LL and PI) values, whereas the Presumpscot clay has much more consistent LL and PI values. The results from this analysis are presented in.  $\sigma'_p$  and OCR estimated using the *k-values* from the Saye *et al.* (2013) method correlated less than when using the Mayne (2014) recommendation of  $k = 0.33$ .

#### 8.4.2 Stress History Sensitivity Analysis

A sensitivity analysis was performed to predict settlement of a hypothetical load applied to the Presumpscot clay deposit at the I-395 Terminus site using  $\sigma'_p$  and OCR predicted from both the laboratory results and the CPTu results. The purpose of the analysis was to evaluate the effect of varying *k-values* on predicted settlement and how those predicted settlement magnitudes compare to the magnitudes predicted from the laboratory testing results of high quality specimens. The model was created by separating the Presumpscot clay deposit at the site (approximately 28 feet in thickness) into 8 sub-layers, each sub-layer represented by an undisturbed sample which was tested in the laboratory for index and consolidation properties. Total settlement of the deposit was obtained by summation of the settlement determined for each sub-layer. Settlement values were estimated using the traditional consolidation settlement calculation of clay (Equation 88.14).

$$S_c = C_r * \frac{H_0}{1 + e_0} * \log\left(\frac{\sigma'_p}{\sigma'_{v0}}\right) + C_c * \frac{H_0}{1 + e_0} * \log\left(\frac{\sigma'_{v0}}{\sigma'_p + \Delta\sigma'_{v0}}\right)$$

8.14

where  $C_r$  = recompression index,  $H_0$  = height of layer,  $e_0$  = initial void ratio,  $\sigma'_p$  = preconsolidation pressure,  $\sigma'_{v0}$  = in situ vertical effective stress,  $C_c$  = virgin compression index,  $\Delta\sigma_v$  = applied total stress.

In the settlement equation, the compression indices and void ratio values came from the laboratory tested samples, the in situ effective stress was estimated using a total unit weight of 113 pcf (average value of all of the samples) and a water table at the ground surface (which is consistent with the findings from the site investigation), and the height was the height of the individual sub-layer. Table 8.5 summarizes the values used for each of the sub layer in the analysis.

Table 8.5: Values used in CPTu settlement analysis, reference Table 7.4.

Layer	H <sub>0</sub> (ft)	e <sub>0</sub>	C <sub>r</sub>	C <sub>c</sub>	σ' <sub>v0</sub> (psf)	σ' <sub>p</sub> (psf)
1	2.6	0.69	0.10	0.22	243	3007
2	4.4	0.87	0.06	0.33	374	4804
3	4.8	0.93	0.06	0.29	683	6057
4	3.1	0.99	0.10	0.35	850	2819
5	2.8	1.21	0.06	0.35	1002	1462
6	1.9	1.05	0.08	0.34	1133	2130
7	3.1	0.95	0.06	0.30	1305	2026
8	2.8	0.79	0.07	0.21	1442	3133

Note: H<sub>0</sub> = layer height, e<sub>0</sub> = initial void ratio, C<sub>r</sub> = recompression index, C<sub>c</sub> = virgin compression index, σ'<sub>v0</sub> = in situ effective stress, σ'<sub>p</sub> = preconsolidation pressure

The remaining parameter,  $\sigma'_p$ , was the variable within the analysis. This value varied on the  $k$ -value chosen and resulted in different estimates of settlement. For the settlement estimated from laboratory testing, the  $\sigma'_p$  was taken from the resulting consolidation curve (shown in Table 8.5) and applied to the entire sub-layer. For the settlement estimated from the CPTu  $k$ -value

method, the minimum, maximum, and average  $k$ -values were applied to the entire deposit and the resulting  $\sigma'_p$  values were averaged within each sub-layer. Figure 7.17 illustrates the three  $\sigma'_p$  profiles at the site using the minimum, maximum, and average  $k$ -value at the site.

The applied load in the model was distributed to the entire deposit with a constant magnitude. This loading scheme (i.e. no reduction with depth) may be analogous to different heights of fill being placed at the site over a large area. Results from the settlement analysis indicate that the stress history modeled from the laboratory data and the CPTu  $k$ -value method using an average  $k$ -value from the site of 0.28 provide similar estimates of settlement for all loading scenarios, where difference in settlement range from 0.1 inches to 1.0 inches.

Table 8.6 presents the estimated magnitudes of settlement (in inches) from the model.

Results from the settlement analysis indicate that the stress history modeled from the laboratory data and the CPTu  $k$ -value method using an average  $k$ -value from the site of 0.28 provide similar estimates of settlement for all loading scenarios, where difference in settlement range from 0.1 inches to 1.0 inches.

Table 8.6: Magnitudes of predicted settlement of the Presumpscot clay at the I-395 Terminus site using stress history modeled from the laboratory testing and the  $k$ -value CPTu method.

Total Settlement of Presumpscot Clay layer (in inches)				
Stress History Model	Applied Stress ( $\Delta\sigma_v$ )			
	500 psf	1000 psf	1500 psf	2000 psf
Laboratory CRS $\sigma'_p$	3.0	5.7	8.3	10.7
CPTu $k$ -value = 0.19 (min)	11.4	16.1	20.1	23.8
CPTu $k$ -value = 0.28 (avg)	2.9	4.9	7.3	10.2
CPTu $k$ -value = 0.36 (max)	2.9	4.7	5.9	7.1

Depending on the application, 1.0 inch may be within acceptable limits of settlement estimates from "actual" settlement (assuming that the laboratory stress model is correct). When comparing the results of the CPTu  $k$ -value models, the maximum  $k$ -value (of 0.36) resulted in

similar magnitudes of settlement as the average *k-value* for the 500 psf and 1,000 psf loading conditions. As the applied stress increased, the difference in estimated settlement between the two methods increased. Settlement calculated from the CPTu *k-value* method using the minimum value of 0.19 overestimated for all loading conditions, reaching as high as 13 inches greater than the laboratory stress history model. Thus, using the minimum CPTu *k-value* at the site does not provide reasonable estimates of settlement for any loading conditions.

The similarity of predicted settlement between the laboratory data, average CPTu *k-value*, and maximum CPTu *k-value* for the 500 psf and 1,000 psf loading conditions is due to the overconsolidation of the clay at the site. When the sum of the applied stress to the clay does not surpass  $\sigma'_p$ , consolidation of each layer is due only to recompression only. The stress history profile of these three models indicated that the 500 psf and 1,000 psf loading conditions remained below the  $\sigma'_p$  for almost all of the sub-layers in the three models. However, the stress history from the minimum CPTu *k-value* of 0.19 estimated that the bottom 5 sub-layers exceeded  $\sigma'_p$  in both the 500 psf and 1,000 psf loading conditions, causing settlement estimates to increase dramatically. As the selected *k-value* increases, than predicted  $\sigma'_p$  become overestimated and resulting settlement magnitudes decrease, and conversely, as the selected *k-value* decreases, than predicted  $\sigma'_p$  become underestimated and resulting settlement magnitudes increase.

Review of the results from this analysis suggests that the degree of accuracy expected for settlement estimates from the selected CPTu *k-value* depends on the stress history of the Presumpscot clay deposit and the loading conditions. If the in situ OCR of the deposit is high and the  $\sigma'_p$  is not surpassed by the loading conditions, it appears that the average *k-value* and maximum *k-value* provide reasonable estimates of settlement. If the OCR of the deposit is low and the stress conditions will be greater than the  $\sigma'_p$ , than settlement magnitudes become more sensitive to the selection of the *k-value*. In essence, the average *k-value* appeared to provide

similar estimates to the laboratory data, whereas minimum and maximum values only match the laboratory data well for overconsolidated deposits. If CPTu measurements are available for a deposit and the engineer is attempting to determine settlement based on a selected *k-value*, it may be advantageous to create a sensitivity analysis for different *k-values* and determine if acceptable settlements are predicted from reasonable *k-values*. If small changes in *k-values* result in large changes in estimated settlement than the risk involved with using the *k-value* method may be too high.

#### 8.4.3 Summary

In summary, the *k-value* method appears to provide a reasonable estimate of  $\sigma'_p$  and OCR profiles in the Presumpscot clay. The most preferable method to determine an accurate *k-value* is to perform as many consolidation tests on high quality samples as possible and back-calculate the *k-value* based on the resulting  $\sigma'_p$  value(s). A *k-value* of 0.33 suggested by Mayne (2014) provides a practical, first order estimate of *k-value* that can be applied to CPTu results in Presumpscot. *k-value* averages at the four sites ranged from 0.28 to 0.45. *k-value* appears to increase from OCR values of 1 to 4, and subsequently maintain or slightly decrease from OCR 4 to 6, all the while remaining within the suggested ranges (from Lunne *et al.*, 1997) of 0.20 to 0.50. There was not enough data for samples with an OCR greater than 6 to come to a definite conclusion for *k-value* trends beyond this value.

The level of acceptability for using the *k-value* to perform geotechnical analysis such as settlement calculations is a site-specific task. If the *k-value* method is used at a Presumpscot clay site, that a high quality sample be obtained within the more normally consolidated portion of the deposit, and tested in the laboratory for  $\sigma'_p$ , from which a *k-value* can be back calculated (the more samples the better). This *k-value* (or values) should be compared to the ones determined in this study to ensure it remains within a reasonable range. Thereafter, a sensitivity analysis should



be formulated and the resulting change in settlement estimates (or whatever is being analyzed) be quantified by a changing  $k$ -value. From this, a decision can be made whether to proceed with the analysis using the determined  $k$  or to collect more samples to increase the confidence in the selected  $k$ -value.

## 8.5 Undrained Shear Strength

Undrained shear strength ( $s_u$ ) of the Presumpscot clay was measured at the four research sites using laboratory and *in situ* methods. Laboratory methods included direct simple shear (DSS) testing on Sherbrook block and modified Shelby tube samples collected from the Route 26/100 Bridge site and anisotropically consolidated undrained compression (CAUC) triaxial testing on the tube samples collected from the other three sites. Additionally, field vane shear testing (FVT) was performed at all four sites. A comparison between the  $s_u$  measured from the different testing methods is presented in Section 3.4.8. In summary,  $s_u$  from laboratory methods is preferred over the FVT because sample quality is measurable, boundary conditions are well controlled, and there is more consistency in results with the DSS and CAUC methods over the FVT. Accordingly, the CPTu correlations to  $s_u$  estimated from laboratory methods are separated from  $s_u$  determined from FVT.

This section summarizes the CPTu cone factors  $N_{kt}$  and  $N_{\Delta u}$  determined at each of the four Presumpscot clay deposit research sites. The resulting cone factors will be compared to measured soil properties (such as stress history or index properties) to evaluate potential correlations. As discussed in Section 2.3.3, these types of correlations have been developed for other clays, and the effectiveness of these correlations will be compared and assessed for their applicability to the Presumpscot clay. Equations 8.15 through 8.16 show the three CPTu cone factors.

$$N_{kt} = q_{net}/s_u \tag{8.15}$$

$$N_{\Delta u} = \Delta u / s_u$$

8.16

where  $q_{net}$  = net tip resistance (psf, Equation 3.3),  $s_u$  = undrained shear strength,  $q_t$  = corrected tip resistance (psf, Equation 3.2),  $u_2$  = measured pore pressure (psf),  $\Delta u$  = difference between measured pore pressure and hydrostatic pore pressure (psf,  $u_2 - u_0$ )

The three cone factors were back-calculated using  $s_u$  from the DSS, CAUC, or FVT results with the corresponding CPTu measurements at the same depth. This was performed at all four sites at all depths of  $s_u$  testing. Table 8.7 and Table 8.8 summarize the minimum, maximum, average, coefficient of variation, and standard deviation of the back-calculated  $N_{kt}$  and  $N_{\Delta u}$  cone factors separated by the reference  $s_u$ .  $N_{ke}$  is omitted from the analysis because it is found to provide unreliable results in the Presumpscot clay and is not recommended for use to determine  $s_u$  (discussed below). The results in the table are separated by the reference  $s_u$ . Throughout this chapter, the reference  $s_u$  is denoted as a subscript on the cone factor.

Table 8.7: Summary of Presumpscot clay CPTu cone factor  $N_{kt}$ .

Site	Reference $s_u$	$N_{kt}$				
		Minimum	Average	Maximum	S.D.	C.O.V.
Route 26/100 Bridge ( $n=13$ )	DSS	15.0	20.5	31.4	4.9	0.24
*Route 26/100 Bridge ( $n=13$ )	CAUC	12.3	16.8	25.7	4.0	0.20
Martin's Point Bridge ( $n=13$ )		11.0	15.9	18.6	2.6	0.16
Route 197 Bridge ( $n=9$ )		11.7	14.6	17.6	1.9	0.13
I-395 Terminus Site ( $n=5$ )		14.1	16.7	19.2	2.0	0.12
Route 26/100 Bridge ( $n=44$ )	FVT	10.8	22.2	54.6	7.7	0.14
Martin's Point Bridge ( $n=53$ )		8.6	15.6	41.0	5.4	0.32
Route 197 Bridge ( $n=15$ )		7.9	15.0	31.5	5.9	0.19
I-395 Terminus Site ( $n=6$ )		17.9	22.0	25.4	6.4	0.12

Note:  $s_u$  = undrained shear strength, DSS = direct simple shear, CAUC = anisotropically consolidated undrained compression (triaxial compression), FVT = field vane shear test,  $n$  = number of tested samples, SD = standard deviation, COV = coefficient of variation,

\*= $s_{u(CAUC)}$  determined from 1.35 \* DSS

Cone factor  $N_{kt(DSS)}$  ranged from 15.0 to 31.4 with an average value of 20.9 and  $N_{\Delta u(DSS)}$  ranged from 13.6 to 22.1 with an average of 17.4. This is in the upper range of values suggested by most literature for the  $N_{kt}$  cone factor, and in fact is higher than any suggested ranges of  $N_{\Delta u}$

that the author could find. Cone factors from the literature (Section 2.3.3) were developed mostly using a reference  $s_u$  of triaxial compression (TC, i.e., CAUC), so it is expected for the cone factors back-calculated from DSS testing to be higher since  $s_u$  from DSS testing is lower than  $s_u$  from CAUC. As discussed previously in this chapter,  $s_u$  determined from DSS can be converted into a CAUC strength using a conversion of  $s_{u(DSS)} = s_{u(CAUC)} * 0.74$ . In doing this,  $N_{kt(CAUC)}$  and  $N_{\Delta u(CAUC)}$  factors can be calculated for the Route 26/100 Bridge. The resulting  $N_{kt(CAUC)}$  ranged from 12.3 to 25.7 with an average of 16.8 and the  $N_{\Delta u(CAUC)}$  ranged from 11.1 to 18.1 with an average of 14.1.

Table 8.8: Summary of Presumpscot clay CPTu cone factor  $N_{\Delta u}$ .

Site	Reference	$N_{\Delta u}$				
	$s_u$	Minimum	Average	Maximum	S.D.	COV
Route 26/100 Bridge ( $n=13$ )	DSS	13.6	17.3	22.1	2.3	0.13
*Route 26/100 Bridge ( $n=13$ )	CAUC	11.1	14.1	18.1	1.9	0.11
Martin's Point Bridge ( $n=13$ )		5.0	9.7	13.3	2.1	0.22
Route 197 Bridge ( $n=9$ )		12.7	14.1	17.2	1.6	0.11
I-395 Terminus Site ( $n=5$ )		7.5	10.9	12.4	2.0	0.18
Route 26/100 Bridge ( $n=44$ )	FVT	8.4	19.9	52.8	7.7	0.14
Martin's Point Bridge ( $n=53$ )		0.4	8.6	18.0	4.1	0.41
Route 197 Bridge ( $n=15$ )		8.2	13.1	23.8	3.6	0.15
I-395 Terminus Site ( $n=6$ )		12.6	16.3	19.1	4.4	0.13

Note:  $s_u$  = undrained shear strength, DSS = direct simple shear, CAUC = anisotropically consolidated undrained compression (triaxial compression), FVT = field vane shear test,  $n$  = number of tested samples, SD = standard deviation, COV = coefficient of variation, \* =  $s_{u(CAUC)}$  determined from  $1.35 * s_{u(DSS)}$

Cone factor  $N_{kt(CAUC)}$  ranged from 11.0 to 19.2 with average values of 15.9 for Martin's Point Bridge, 14.6 for Route 197 Bridge, 16.7 for I-395 Expansion site, and 16.8 for Route 26/100 Bridge.  $N_{\Delta u(CAUC)}$  ranged from 5.0 to 17.2 with an average value of 9.7 for Martin's Point Bridge, 14.1 for Route 197 Bridge, 10.9 for I-395 Terminus site, and 14.1 for Route 26/100 Bridge.  $N_{kt}$  has been found to generally range from 10 to 20 with an average of 15 for clays

(Lunne *et al.*, 1997).  $N_{kt(CAUC)}$  for Presumpscot fits within this range at the upper end.  $N_{\Delta u(CAUC)}$  values from this study fall well above suggested ranges of values of 4 to 10 for similar clays. The average values for each of the four Presumpscot research sites were close to 10 or higher (with maximum values as high as 18.1).

Coefficient of variation (COV) for  $N_{kt(CAUC)}$  ranged from 0.12 to 0.20 and for  $N_{\Delta u(CAUC)}$  ranged from 0.11 to 0.22. Standard deviation for  $N_{kt(CAUC)}$  ranged from 1.9 to 4.9 and for  $N_{\Delta u(CAUC)}$  ranged from 1.6 to 2.3. Using the COV as an evaluation of effectiveness; both of the cone factors resulted in similar effectiveness (i.e. comparable ranges of COV). Thus, in general, neither one of the two factors appeared to be consistently more effective than the other in the Presumpscot clay. However, an interesting trend did appear between the COV, cone factor, and clay sensitivity of the Presumpscot clay.  $N_{\Delta u(DSS \text{ or } CAUC)}$  from the two sensitive clay sites (Route 26/100 Bridge and Route 197 Bridge) resulted in COVs which were less than or equal to the COVs for the  $N_{kt(DSS \text{ or } CAUC)}$  at the sites. Conversely, the  $N_{kt(DSS \text{ or } CAUC)}$  COV at the non-sensitive clay sites (Martin's Point Bridge and I-395 Terminus) was lower than the  $N_{\Delta u(DSS \text{ or } CAUC)}$  at those same sites. This suggests the possibility of superior performance of  $N_{kt}$  for non-sensitive deposits and  $N_{\Delta u}$  at sensitive deposits of Presumpscot clay.

The average  $N_{kt(CAUC)}$  at the four sites remained within a small range of values between 14.6 and 16.8. There did not appear to be a trend between specific sites and values of  $N_{kt(CAUC)}$ .  $N_{kt(FVT)}$  averages from the sites fell within a broader and higher range of values between 15.0 and 22.2. Higher  $N_{kt(FVT)}$  than  $N_{kt(CAUC)}$  values are expected because  $s_u(CAUC)$  is higher than  $s_u(FVT)$ .  $N_{\Delta u(CAUC)}$  ranged between 9.7 and 14.1 and  $N_{\Delta u(FVT)}$  ranged from 8.6 to 19.9.  $N_{\Delta u(CAUC)}$  at Route 26/100 Bridge and Route 197 Bridge resulted in identical values of 14.1 whereas the values at Martin's Point Bridge and I-395 Terminus site are 9.7 and 10.9, respectively. Route 26/100 Bridge and Route 197 Bridge both contain sensitive deposits of Presumpscot clay, and as

discussed later in the section, the similarity between the  $N_{\Delta u(CAUC)}$  values at each pair of sites suggests a potential correlation between sensitivity and  $N_{\Delta u(CAUC)}$ .

As expected, the  $N_{kt(FVT)}$  and  $N_{\Delta u(FVT)}$  had a wider range of values. The greater spread resulting from the FVT results is expected both because there were more FVT test results than DSS/CAUC test results at each site and  $s_u$  from FVT is almost always more variable than laboratory testing because of natural soil variability and operator/equipment dependence.  $N_{kt(FVT)}$  ranged from 7.9 to 54.6 with average values of 22.2 for Route 26/100 Bridge, 15.6 for Martin's Point Bridge, 15.0 for Route 197 Bridge, and 22.0 for I-395 Terminus.  $N_{\Delta u(FVT)}$  ranged from 0.4 to 52.8 with average values of 19.9 for Route 26/100 Bridge, 18.0 for Martin's Point Bridge, 23.8 for Route 197 Bridge, and 16.3 for I-395 Expansion terminus. Figure 8.18 illustrates  $N_{kt(FVT)}$  and  $N_{\Delta u(FVT)}$  compared to  $N_{kt(DSS \text{ or } CAUC)}$  and  $N_{\Delta u(DSS \text{ or } CAUC)}$  determined at each of the four research sites. It is also important to note that some of the variation in FVT correlation to the cone factors comes from the fact that the FVT were performed at various locations throughout the site, sometimes up to 200 feet away from the CPTu sounding, whereas all the laboratory results were from the same boring and correlated to a CPTu within 30 feet next to that boring. Also shown as the black dotted vertical lines on Figure 8.18 are "typical" ranges of  $N_{kt}$  and  $N_{\Delta u}$  found in similar studies of other clays to illustrate how the Presumpscot clay compares to these. While these published ranges are not limiting values (i.e. the absolute minimum and maximum values from all of the literature), they do encompass the majority of resulting values for  $N_{kt}$ .

Inspection of Figure 8.18 reveals the trend that both  $N_{kt}$  and  $N_{\Delta u}$  data to mostly plot within or above the published ranges of values. For  $N_{kt(CAUC \text{ or } DSS)}$ , all but six data points plotted within the range of 10 to 20, illustrating good agreement between the CPTu strength correlation in Presumpscot clay and other clay soils. The six points above the published range are all  $N_{kt(DSS)}$  values from Route 26/100 Bridge, and since DSS testing results in lower  $s_u$  estimates, higher

values of  $N_{kt}$  would be expected. The CAUC correlated  $s_u$  for those same data shifted four out of six of the resulting values into the range, leaving only two of the data points above 20. Only seven out of the 40  $N_{\Delta u(CAUC \text{ or } DSS)}$  values remained within the published range of 4 to 10, while the other 33 were above the range. The maximum value from the researched literature in other soft clays was 13.1 (Remai, 2013), and from the geotechnical design recommendations of Lunne *et al.*, (1997) was an  $N_{\Delta u(CAUC \text{ or } DSS)}$  value of 10. The *average* values from each of the Presumpscot clay sites ranged from 9.7 to 17.3.

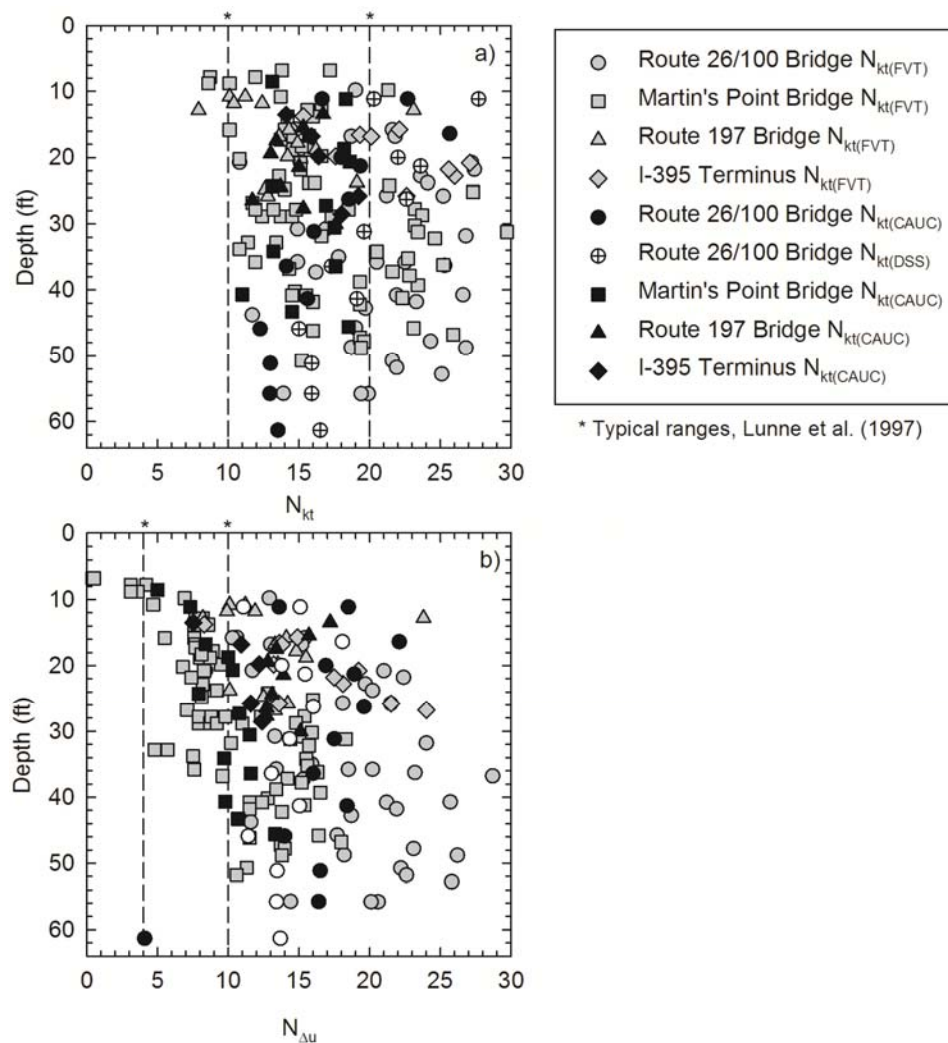


Figure 8.18:  $N_{kt}$  and  $N_{\Delta u}$  factors determined from laboratory testing and field vane shear testing (FVT) at all four Presumpscot clay research sites.

Clearly, there is a tendency for  $N_{\Delta u}$  values in Presumpscot clay to be higher than other clay soils. It is not immediately clear why the Presumpscot clay deviates from the  $N_{\Delta u}$  trend of most other clay soils, but the source stems from the increased ratio of pore pressure to undrained shear strength (i.e. Equation 8.16).

$N_{kt(FVT)}$  ranged from 7.9 to 54.6 and  $N_{\Delta u(FVT)}$  ranged from 8.4 to 52.8 with averages from each of the four sites summarized in Table 8.7 and Table 8.8. Overall, the  $N_{kt(FVT)}$  and  $N_{\Delta u(FVT)}$  factors varied more widely than the factors correlated to laboratory testing, which is expected. The FVT is a different mode of shear than CAUC, and relates more closely to DSS, however the rate is faster and the boundary conditions are less controllable. The accuracy of FVT results are highly dependent on the operator and typically result in a scatter of  $s_u$  values. Subsequently, the correlated  $N_{kt(FVT)}$  and  $N_{\Delta u(FVT)}$  factors showed this. One observation made from the data collected at the four sites indicated a better averaged  $N_{kt(FVT)}$  and  $N_{\Delta u(FVT)}$  factor with increased number of FVT tests.

#### 8.5.1 Correlations to $N_{kt}$ and $N_{\Delta u}$

Researchers have proposed relationships between clay properties and the CPTu cone factors  $N_{kt}$  and  $N_{\Delta u}$ . Plasticity index (PI), overconsolidation ratio (OCR), and  $s_u$  has been found to correlate with the cone factors in some studies, which included clay deposits in Norway, Canada, the North Sea, and Denmark using  $s_u$  from CAUC, DSS, triaxial extension, and FVT (Aas *et al.*, 1986, Karlsrud *et al.*, 1996, Lunne *et al.*, 1985, Rad and Lunne, 1988). Other studies have shown no correlation between these factors (La Rochelle *et al.*, 1988, Powell and Quarterman 1988, Hong *et al.*, 2010, Almeida *et al.*, 2010, and Wei *et al.*, 2013). In addition, a correlation between CPTu measurement of normalized pore pressure ( $B_q$ ) and  $N_{\Delta u}$  has been suggested. If these correlations do exist for the Presumpscot clay, they could provide an improved approach to the selection of the  $N_{kt}$  and  $N_{\Delta u}$  cone factor for specific sites. All of the aforementioned relationships

were evaluated for  $N_{kt(CAUC\ or\ DSS)}$  and  $N_{\Delta u(CAUC\ or\ DSS)}$  determined from the four research sites.  $N_{kt(FVT)}$  and  $N_{\Delta u(FVT)}$  were not correlated to other properties because clay properties at the FVT depths are not known since samples were not collected at the depths of the tests. Figure 8.19 presents cone factor  $N_{kt(CAUC\ or\ DSS)}$  versus PI, OCR,  $s_u$ , and  $B_q$ . Figure 8.20 presents  $N_{\Delta u(CAUC\ or\ DSS)}$  versus the same measurements.

Figure 8.19 and Figure 8.20 confirm the variability of the glacial Presumpscot clay and indicate no clear relationships between  $N_{kt}$  and  $N_{\Delta u}$  with the majority of comparison parameters (e.g.  $N_{kt}$  and OCR, PI, and  $B_q$  and  $N_{\Delta u}$  and OCR and PI). Figure 8.19 illustrates  $N_{kt}$  compared with measured values of OCR, PI,  $s_u$  and  $B_q$ . Three of the four presented correlations are inconclusive and do not suggest relationships between  $N_{kt}$  and OCR, PI, and  $B_q$ . However,  $N_{kt}$  and  $s_u$  appear to have a generally sharply decreasing trend from approximately 250 psf to approximately 400 psf, whereafter the  $N_{kt}$  stays relatively constant with increasing  $s_u$  in between values of 10 and 20. Correlations between the same four parameters and  $N_{\Delta u}$  are illustrated in Figure 8.20. Correlation of  $N_{\Delta u}$  to OCR and PI was not conclusive, but there was potential when analyzing  $s_u$  and  $B_q$ . In general, the  $s_u$  and  $N_{\Delta u}$  showed a relatively poor correlation, but may suggest a decreasing trend of  $N_{\Delta u}$  with increasing  $s_u$  from approximately 250 psf to approximately 800 psf, whereafter  $N_{\Delta u}$  stays relatively constant with increases in  $s_u$ . Literature expanding on this correlation was not located. However, there was a correlation observed between  $B_q$  and  $N_{\Delta u}$  which is supported by additional literature. The increasing  $N_{\Delta u}$  with increasing  $B_q$  relationship is discussed below.

There is some correlation between  $N_{\Delta u(CAUC\ or\ DSS)}$  and both  $s_u$  and  $B_q$ , where  $N_{\Delta u(CAUC)}$  is generally lower for higher  $s_u$  soils and greater for larger  $B_q$  values. The latter agrees with findings from similar studies in clay performed by Karlsrud *et al.* (1996) and Lunne *et al.* (1985). The observed trends from these three studies between  $N_{\Delta u}$  and  $B_q$  are presented in Figure 8.20c along with the plotted Presumpscot clay data. Both studies show a linearly increasing trend in  $N_{\Delta u}$  with



$B_q$ , which agrees well with the trend of CAUC Presumpscot clay data. However, the Presumpscot clay from all of the four research sites plots well above the general trend from these studies.

It is not immediately clear why the  $N_{\Delta u(CAUC \text{ or } DSS)}$  values are consistently much higher than comparable studies in other clays.  $N_{\Delta u}$  is equal to the difference in measured pore pressure and hydrostatic conditions ( $\Delta u$ ) divided by the  $s_u$  (Equation 8.16). Therefore, for  $N_{\Delta u}$  to be higher than other clays, either the measured pore pressure must be higher for other clay with similar  $s_u$  values or the  $s_u$  must be lower for similarly measured pore pressure values (or a combination of both).

To attempt to explain this phenomenon, the pore pressure as it relates to the  $s_u$  can be observed by the Skempton's "A" parameter (ratio of pore pressure to shearing stress) measured during the CAUC laboratory tests. If the A parameter is much higher in Presumpscot, one may conclude that this will likely translate to CPTu testing and may explain the higher  $N_{\Delta u(CAUC \text{ or } DSS)}$  values. However, this is not the case. Skempton's "A" parameter for insensitive clays may vary from 0.3 to 0.7, where "A" may vary from 1.5 to 2.5 for sensitive clay (Lambe and Whitman, 1967). A parameters of the Presumpscot clay at both sensitive and non-sensitive sites did not exceed 1.0 for any CAUC test, and aside from one CAUC test (at the I-395 Terminus), all values fell below the 0.7 upper-limit provided by Lambe and Whitman (1967). While Skempton's "A" values were not reported for the three similar CPTu studies shown in Figure 8.21c, one can conclude that they are probably comparable to Presumpscot clay values. One conclusion is that both the  $N_{kt}$  and  $N_{\Delta u}$  values are generally higher than similar studies, indicating that the  $s_u$  of the Presumpscot clay is high for CPTu measurements  $u_2$  and  $q_t$ . This is likely because of high silt content. But there is still clay acting as the dominant material around the silt and sand particles.

The resulting  $N_{\Delta u(CAUC)}-B_q$  range of the Presumpscot clay (shown as the gray dotted line in Figure 8.20) is bound by the following equations:

$$N_{\Delta u(CAUC)} = 1 + 11.3 * B_q \quad 8.17$$

$$N_{\Delta u(CAUC)} = 5 + 11.3 * B_q \quad 8.18$$

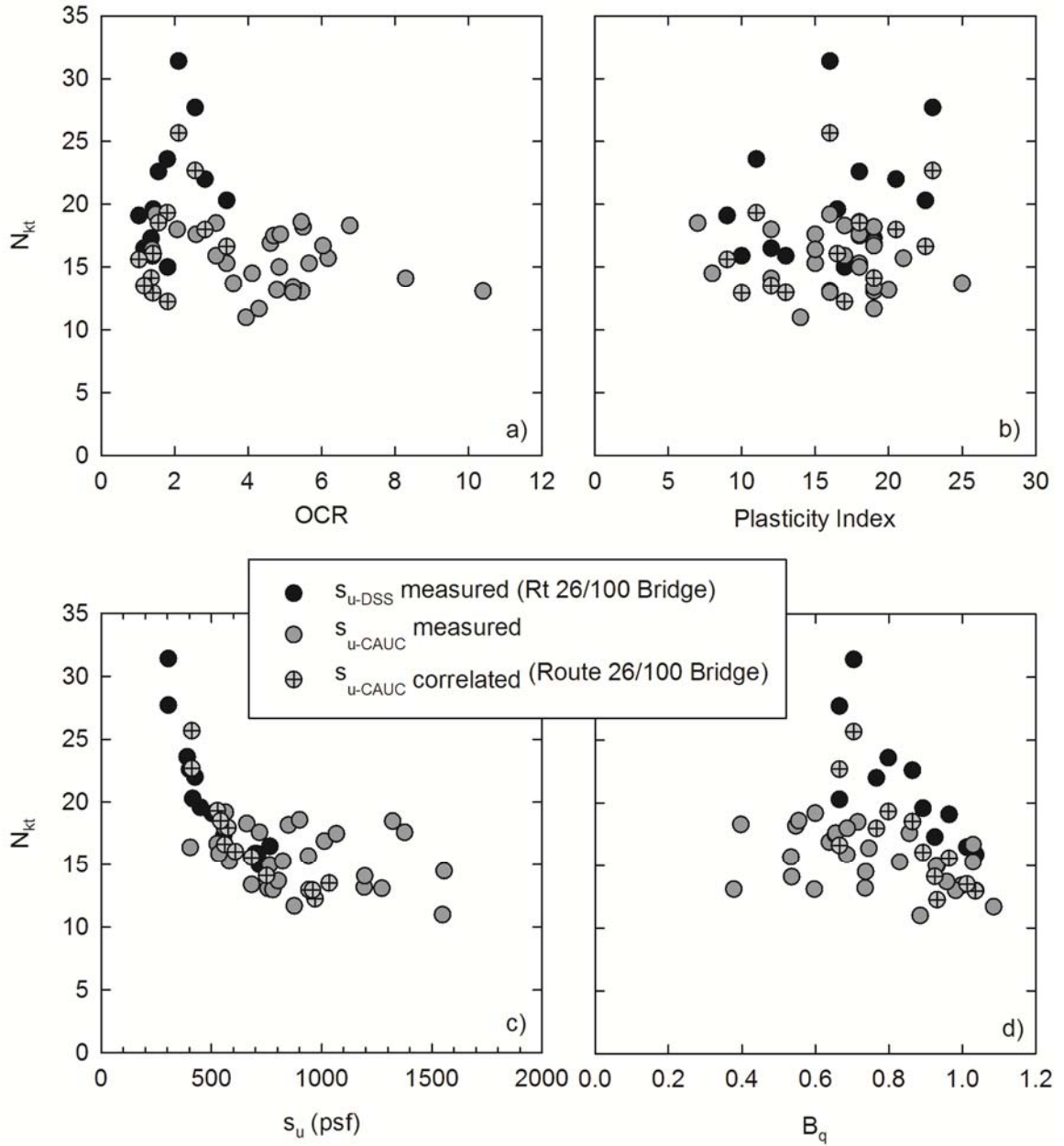


Figure 8.19: CPTu cone factor  $N_{kt(CAUC \text{ or } DSS)}$  for the Presumpscot clay correlated to a) overconsolidation ratio (OCR), b) Plasticity Index (PI), c) undrained shear strength ( $s_u$ ) and d) normalized pore pressure ( $B_q$ ).

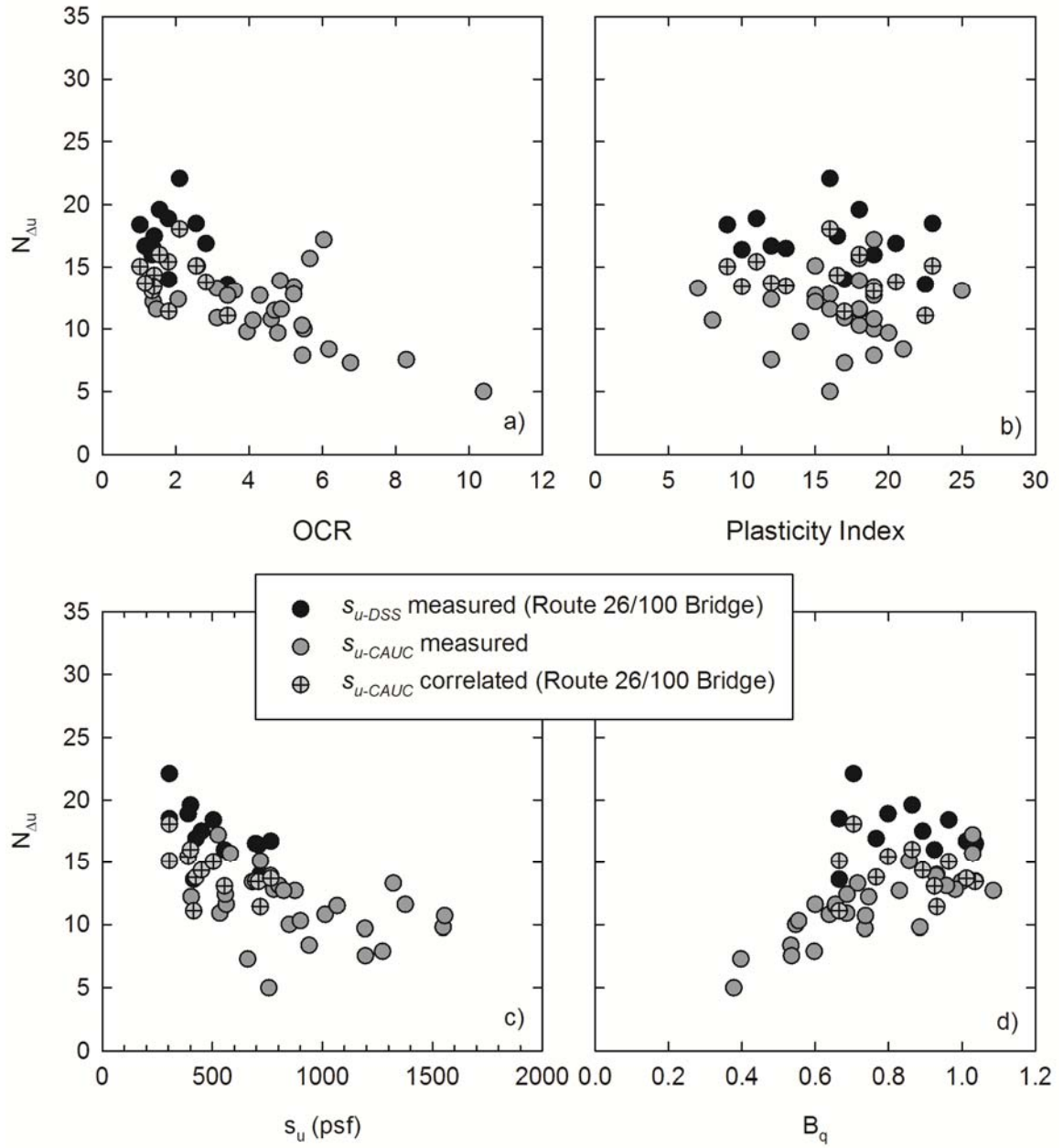


Figure 8.20: CPTu cone factor  $N_{\Delta u(CAUC \text{ or } DSS)}$  for the Presumpscot clay correlated to a) overconsolidation ratio (OCR), b) Plasticity Index (PI), c) undrained shear strength ( $s_u$ ) and d) normalized pore pressure ( $B_q$ ).

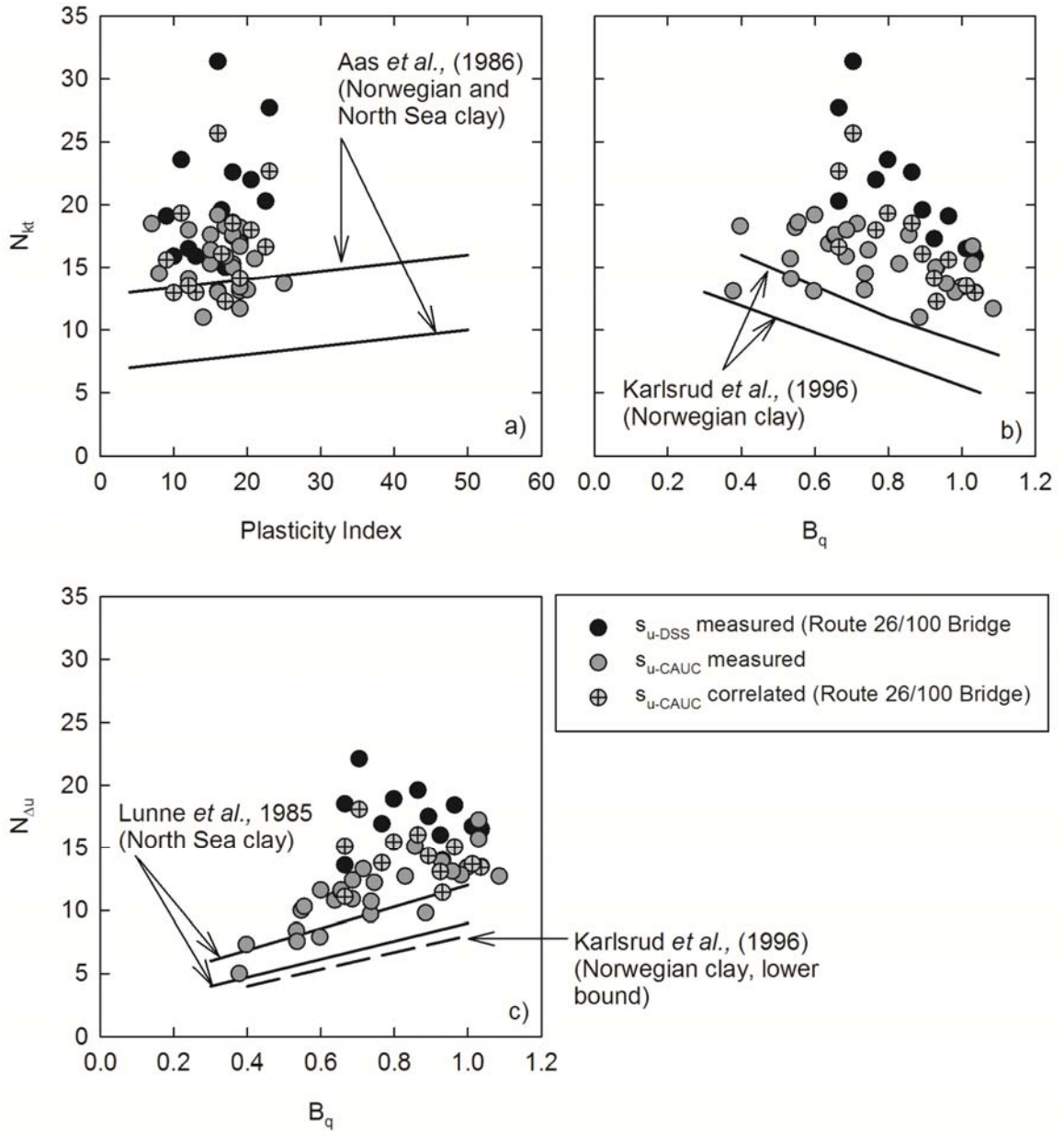


Figure 8.21: Presumpscot clay CPTu data compared to ranges from a) Aas *et al.*, (1986) b) Karlsrud *et al.*, (1996), and c) Lunne *et al.*, (1985) and Karlsrud (1996).

$N_{Au}$  values calculated at Route 26/100 Bridge and Route 197 Bridge (high sensitivity) are consistently higher than those calculated at Martin's Point Bridge and I-395 Terminus (low sensitivity). Figure 8.22 presents a relationship, updated from Karlsrud (2005), between

sensitivity,  $N_{\Delta u}$ , and OCR. The relationship resulted in the following equations for the Presumpscot clay for deposits with sensitivity less than 15 and greater than 15, respectively:

$$N_{\Delta u(CAUC)} = 17 - 3.7 * \ln(OCR) \quad 8.19$$

$$N_{\Delta u(CAUC)} = 19 - 4.0 * \ln(OCR) \quad 8.20$$

These equations are in the same format as the SHANSEP power equation. The first integer in the above equations represents the  $N_{\Delta u}$  value for normally consolidation conditions, equivalent to the normalized shear strength "S" SHANSEP parameter. The number multiplied by the natural log function represents the magnitude of the slope of the line, and is equivalent to the exponential "m" SHANSEP parameter.

#### 8.5.2 Been *et al.*, (2010) Method

Been *et al.* (2010) proposed a SHANSEP-based approach for determining  $N_{kt}$  and  $k$ -value (Section 2.3.3) directly from CPTu measurements. They do not propose that this method can be used to replace laboratory or field testing to obtain  $s_u$  or stress history (which they explicitly state is the most effective method and is universally supported in the literature), but they do suggest using the method when testing data is available and reasonable estimates of SHANSEP parameters are known. The method was developed by manipulating the SHANSEP equation (Equation 8.21; Ladd and Foott, 1974) to accommodate CPTu measurements.  $N_{kt}$  (Equation 8.15) and  $k$ -value (Equation 8.13) are substituted for  $s_u$  and OCR, respectively where SHANSEP  $S$  and  $m$  parameters remain, which are assumed to be constant for an entire deposit (Ladd and Foott, 1974). The resulting relationship between stress history and strength is shown as Equation 8.22:

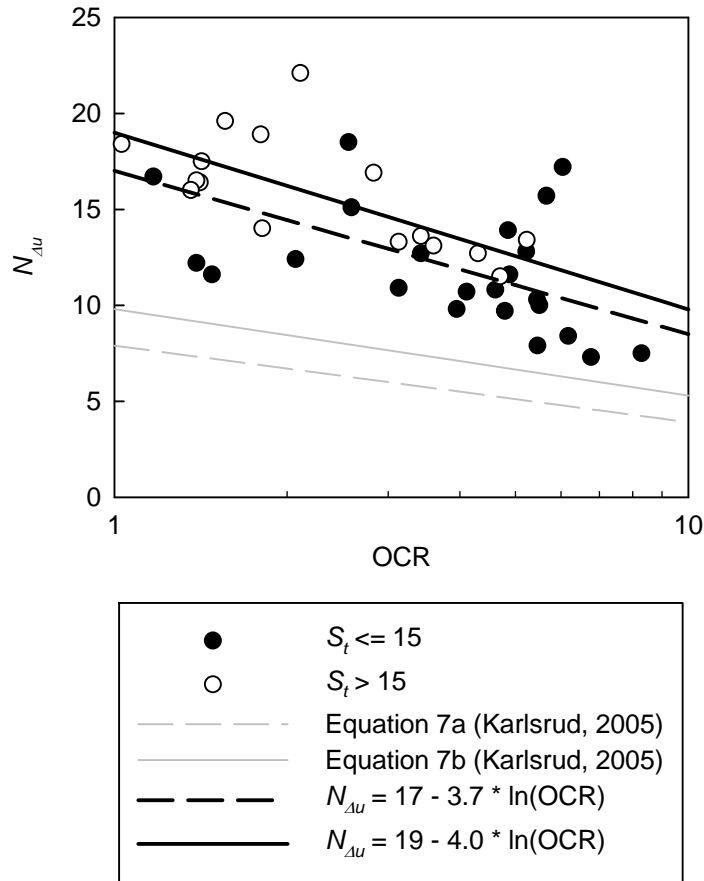


Figure 8.22: Undrained shear strength coefficient  $N_{\Delta u}$  vs. OCR, separating data points of high sensitivity and low sensitivity for Presumpscot clay.

$$(s_u/\sigma'_{v0})_{(OC)} = S * OCR^m \quad 8.21$$

$$N_{kt} * S * k^m = [(q_t - \sigma'_{v0})/(\sigma_{v0})]^{(1-m)} \quad 8.22$$

where  $s_u$  = undrained shear strength,  $\sigma'_{v0}$  = *in situ* vertical effective stress,  $\sigma_{v0}$  = *in situ* total stress, OC notates overconsolidated state,  $S = (s_u/\sigma'_{v0})$  for normally consolidated conditions, OCR = overconsolidation ratio,  $m$  = exponential coefficient found to range from approximately 0.5 to 1.0, and  $q_t$  = corrected tip resistance measured from the CPTu sounding. Table 2.2 summarizes some  $S$  and  $m$  parameters determined from studies in Presumpscot clay and Boston Blue clay.

The Been *et al.* (2010) method assumes that the left side of Equation 8.22 is constant for a deposit as a necessary simplifying assumption. The authors propose re-arranging Equation 8.22 to solve for  $N_{kt}$  using an assumed reasonable  $k$ -value and then identifying the trend of  $N_{kt}$  with depth. The authors suggest this be performed assuming multiple, and a range of,  $k$ -values to identify the corresponding range of  $N_{kt}$ . Thereafter, the authors suggest the same process to identify an appropriate  $k$ -value using multiple reasonable estimates of  $N_{kt}$ . At the end of the process, the result is an expected range of both the  $k$ -value and  $N_{kt}$ , which can provide guidance for the selection of each variable.

This method was evaluated for the Presumpscot clay at the Route 197 Bridge because it was the only site that was found to have proper characterization of  $s_u$  based on the true SHANSEP equation. Route 26/100 was not included because SHANSEP testing was not performed on the tested samples for that site, and the resulting SHANSEP analysis gave poor predictions of  $s_u$  (as compared to the CAUC laboratory results) at Martin's Point Bridge and the I-395 Terminus site. SHANSEP  $S$  and  $m$  parameters are specified in Equation 6.2 and the  $k$ -value and  $N_{kt}$  were available from the CPTu correlation to laboratory results, therefore all variables were known for Equation 8.22.  $N_{kt}$  and  $k$ -value were separately solved for using Equation 8.22 and compared to the measured strength values determined from recompression CAUC triaxial testing (Table 6.6). When  $N_{kt}$  was being solved for, the  $k$ -value assumed was the one solved for the tested sample at that depth. Similarly, when  $k$ -value is being solved for, the  $N_{kt}$  is known from the CAUC tested sample at that depth. Figure 8.23 presents the ratio of  $N_{kt}$  and  $k$ -values estimated from the Been *et al.* (2010) method to the actual value.

The Been *et al.* (2010) method underestimated both  $N_{kt}$  and  $k$ -value at the Route 197 Bridge compared to the values obtained directly from the laboratory testing. Underestimates of  $N_{kt}$  will lead to an over prediction of  $s_u$ , and underestimates of  $k$ -value will lead to under predictions of OCR. In the case of  $s_u$  predictions, the Been *et al.* (2010) errs on the "un-

conservative" side (i.e. falsely high values if  $s_u$ ), and for OCR predictions it errs on the "conservative" side (i.e. low values of OCR and subsequent over-predictions of settlement).

For the Been *et al.*, (2010) analysis shown above, the  $k$ -values and  $N_{kt}$  values were known at each depth directly from laboratory testing on samples. It is likely that if this method was used in the future in Presumpscot clay, that one value would be assumed for both of these parameters throughout the whole profile, which would further provided an analysis different than the in situ strength and stress history state. The results do not correspond well with the laboratory values ( $N_{kt}$  differed as much as 4.5 and  $k$ -values as much as 0.16), and it appears as though the Been *et al.*, (2010) analysis may not be suitable for the Presumpscot clay as SHANSEP analyses have been shown to produce different strength and stress history relationships than measured parameters from the sites.

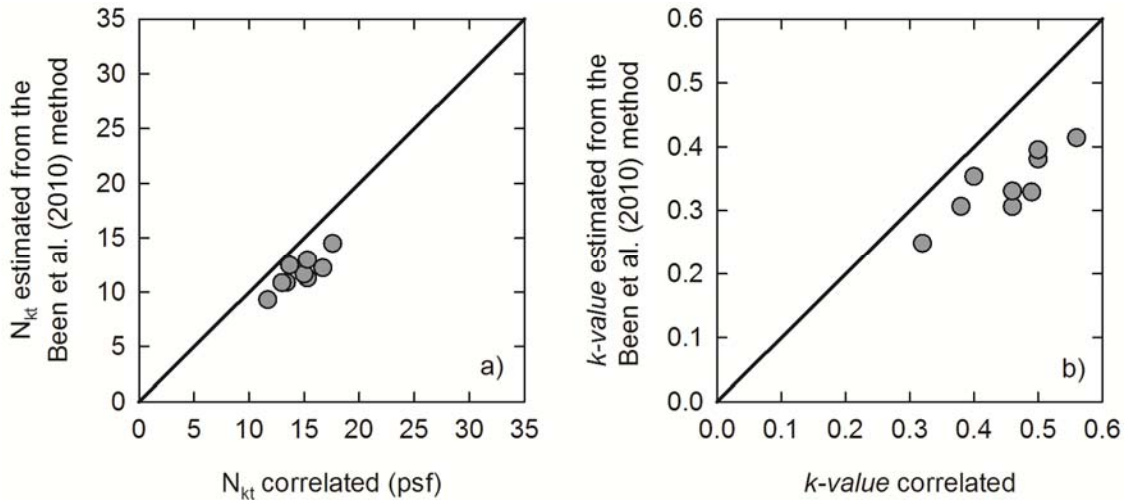


Figure 8.23:  $N_{kt}$  and  $k$ -value estimated from the Been *et al.*, (2010) method compared to actual values back-calculated from laboratory testing of Presumpscot clay



Table 8.9: Summary of k-values and  $N_{kt}$  values from Route 197 Bridge after the Been et al., (2010) method.

<b>Depth (ft)</b>	<i>Values assumed in analysis (from lab testing)</i>		<i>Resulting Been et al., (2010) values</i>		<i>Percent Difference</i>	
	$N_{kt}$	$k$	$N_{kt}$	$k$	$N_{kt}$	$k$
13.5	16.7	0.46	12.2	0.31	-31%	-40%
15.5	15.3	0.49	11.3	0.33	-30%	-39%
17.5	13.4	0.50	10.9	0.38	-21%	-27%
19.4	13.0	0.50	10.8	0.40	-18%	-23%
21.4	15.0	0.46	11.6	0.33	-25%	-33%
24.4	13.7	0.40	12.5	0.35	-9%	-12%
26.4	11.7	0.56	9.3	0.41	-23%	-30%
27.7	15.3	0.38	13.0	0.31	-16%	-21%
30.1	17.6	0.32	14.5	0.25	-19%	-25%

### 8.5.3 Undrained Shear Strength Sensitivity Analysis

From a geotechnical design standpoint, it is advantageous to determine the effect of a changing  $N_{kt}$  and  $N_{\Delta u}$  on the estimated  $s_u$  profile from CPTu results. If (hypothetically) selecting an  $N_{kt}$  of anywhere from 10 to 20 provides an adequate design  $s_u$  profile, than less time and effort has to be spend in identifying an appropriate  $N_{kt}$  value. On the other hand, if an  $N_{kt}$  of 14 provides a factor of safety of 1.3 for the stability of a hypothetical slope and an  $N_{kt}$  of 14.5 provides a factor of safety of 0.90 for that hypothetical slope, there is an obvious advantage to identifying the appropriate  $N_{kt}$  factor. Figure 8.24 and Figure 8.25 present the estimated  $s_u$  profiles at each of the four research sites using the site-specific average,  $\pm 1$  standard deviation. The resulting  $s_u$  profiles are compared to the laboratory-determined  $s_u$ .

The general shape of the  $s_u$  profile predicted from both  $N_{kt}$  and  $N_{\Delta u}$  at the four sites followed closely the trend of the laboratory data. In fact, some laboratory data were intersected by  $N_{kt}$  and  $N_{\Delta u}$  profiles (i.e. the average  $N_{kt}$  and  $N_{\Delta u}$  at that site was equal to  $N_{kt}$  and  $N_{\Delta u}$  at that depth). However, there is not complete correlation of  $s_{u(DSS)}$ . This may be because CPTu profiles are

influenced by multiple factors including disturbance or localized changes in geology between the CPTu location and the boring location. In general, selecting the average  $N_{kt}$  and  $N_{\Delta u}$  at each site and applying it to the entire profile resulted in CPTu derived  $s_u$  profile with both the same shape and magnitude as the  $s_u$  from the laboratory testing. Furthermore, the  $\pm 1$  standard deviation resulted in good lower and upper bound  $s_u$  profiles, respectively.

The average  $N_{kt}$  and  $N_{\Delta u}$  provides the most comparable  $s_u$  profile to the laboratory testing results. The task then becomes determining whether or not the difference in  $s_u$  between the CPTu and the laboratory testing (and assuming that the laboratory testing is the "correct" value) is acceptable. Figure 8.24 and Figure 8.25 illustrate the difference between  $s_u$  predicted using the  $N_{kt}$  and  $N_{\Delta u}$  average values varies in magnitude from 0 to close to an 800 psf difference. The tolerability for differences of this magnitude in the  $s_u$  is a site-specific problem, which is directly controlled by the type of geotechnical analysis being performed and its application. To illustrate an example of this, a sensitivity analysis was performed on the  $s_u$  of Presumpscot clay at the Route 26/100 Bridge using a slope stability model. The purpose of the sensitivity analysis was to quantify the effects of selecting  $s_u$  from different methods as applied to a slope stability analysis, particularly the difference in CPTu cone factors  $N_{kt}$  and  $N_{\Delta u}$ .  $s_u$  estimates were made using laboratory direct simple shear (DSS) testing results, assumed  $s_u$  profile from H&A (2009) using field vane shear testing (FVT) results, CPTu cone factor  $N_{kt}$  and CPTu cone factor  $N_{\Delta u}$ . The selected  $N_{kt}$  and  $N_{\Delta u}$  values varied in order to determine the effect of changing cone factors on slope stability.

The slope was modeled using geometry and soil profiles from "Geologic Profile A-A" (H&A 2009) of the Route 26/100 north bridge approach and using the Slide 6.0 software (RocScience, 2014). Friction angles of the fill, interbedded marine deposit, and marine sand soil layers were assumed to be  $34^\circ$ ,  $32^\circ$ , and  $32^\circ$  respectively. Total unit weights of the fill, interbedded marine

deposit, and marine sand soil layers were assumed to be 130, 125, and 120 pounds per cubic feet (pcf) respectively. These assumed parameters are within typical ranges of properties for these soils and have little effect of the resulting factors of safety of the slope.

The Presumpscot clay deposit was divided into twelve layers, each layer representing a "tributary" area from the undisturbed sampling depths from borings BB-FRR-BT303/BB304. A unit weight of 111 pcf (the average value of all DSS specimens) was used for the entire profile of Presumpscot clay for simplicity. The slope strength was modeled using a total stress analysis (friction angle of clay = 0), which is consistent with the controlling failure mode when using undrained shear strength. The water table elevation was assumed to be at elevation 18.3 feet, which was reported as the "normal water" elevation (H&A, 2009). The assumed undrained shear strength ( $s_u$ ) in each of the 12 layers is shown in Table 8.10.

Each of the 12 layers within the Presumpscot clay deposit in the model had a different  $s_u$  value. For the DSS strength model, the  $s_u$  determined from DSS testing (Table 4.7) was used in each layer. For the FVT model an assumed  $s_u$  profile was applied to each layer based on the FVT test results. For the CPTu cone factor model, the resulting  $s_u$  profiles from the assumed cone factors (Figure 4.15) were applied to each layer. The resulting factor of safety for each strength model is summarized in Table 8.11.

It should be noted that the slope geometry, soil properties, and general site conditions used in the model are hypothetical conditions used to create the sensitivity analysis based on the authors' interpretations. Hence, the resulting factors of safety do not represent actual site condition at the Route 26/100 Bridge and are intended for educational comparative purposes only.

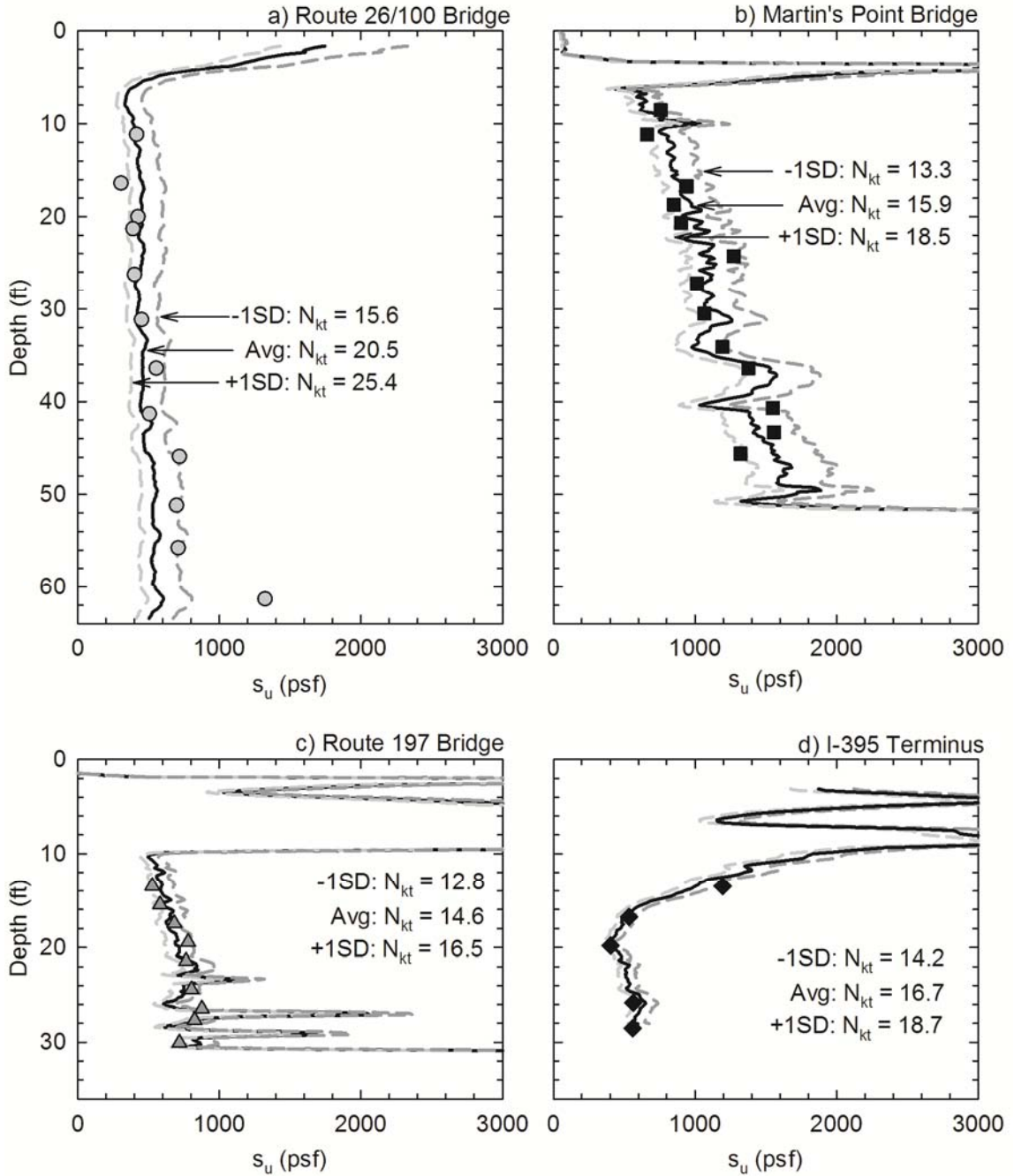


Figure 8.24: Profile of undrained shear strength ( $s_u$ ) using the site-specific CPTu  $N_{kt}$  values compared to the laboratory determine  $s_u$  for a) Route 26/100 Bridge, b) Martin's Point Bridge, c) Route 197 Bridge, and d) I-395 Terminus

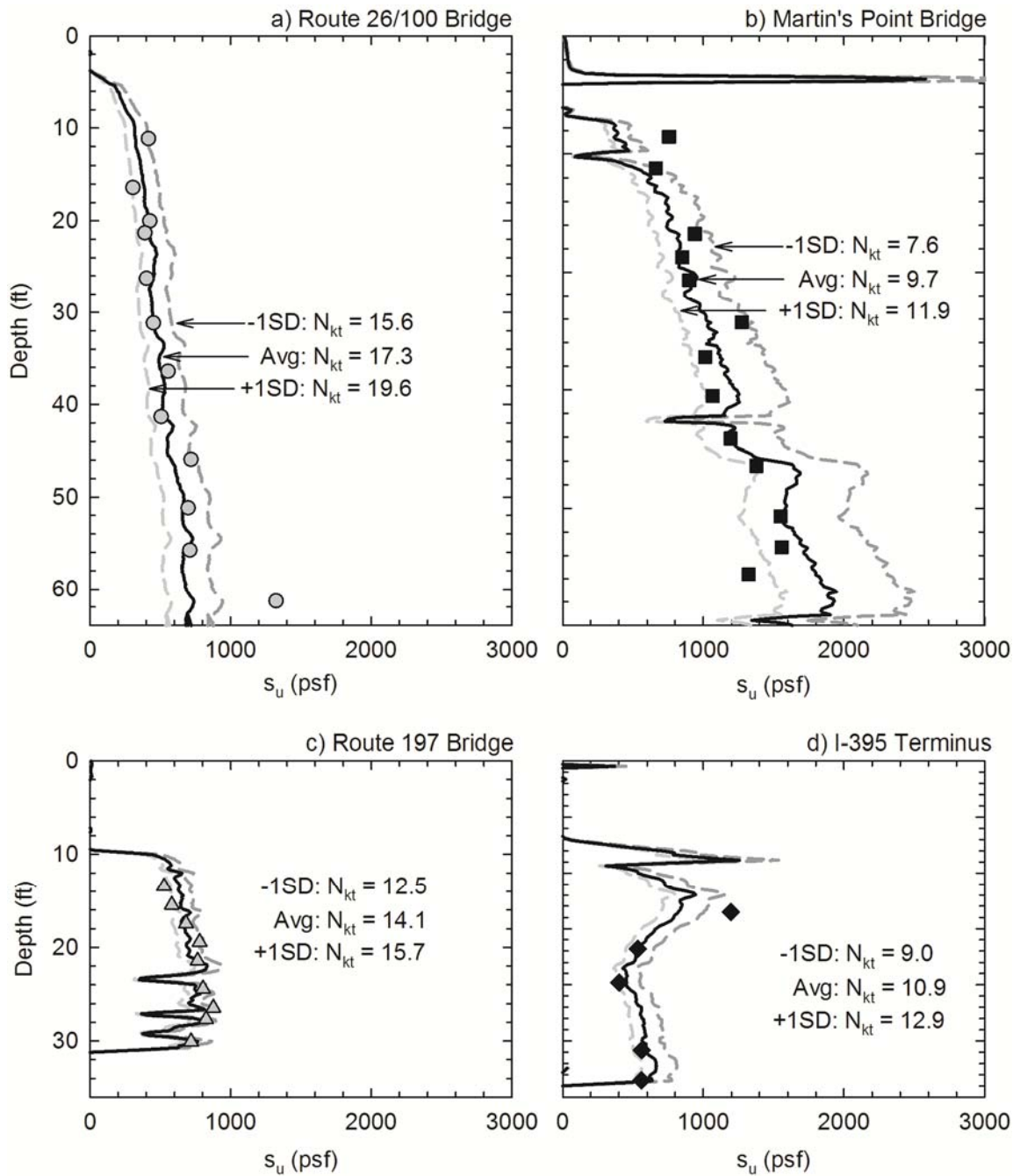


Figure 8.25: Profile of undrained shear strength ( $s_u$ ) using the site-specific CPTu  $N_{\Delta u}$  values compared to the laboratory determine  $s_u$  for a) Route 26/100 Bridge, b) Martin's Point Bridge, c) Route 197 Bridge, and d) I-395 Terminus.

Table 8.10: Undrained shear strength ( $s_u$ ) values for the 12 modeled Presumpscot layer in the sensitivity analysis.

Depth (ft)	Layer	Undrained shear strength at mid-depth (psf)								
		Avg.	$N_{kt}$			$N_{\Delta u}$			DSS	FVT
			Min.	Max.	Avg.	Min.	Max.			
0-13.95	Presumpscot 1	588	817	390	219	280	172	416	346	
13.95-18.35	Presumpscot 2	446	620	296	380	485	299	305	176	
18.35-20.65	Presumpscot 3	449	625	298	409	522	321	426	330	
20.65-23.75	Presumpscot 4	449	624	298	442	565	348	390	350	
23.75-28.7	Presumpscot 5	433	603	288	443	566	174	401	379	
28.7-33.8	Presumpscot 6	441	613	293	466	595	366	451	416	
33.8-38.85	Presumpscot 7	461	642	306	511	653	402	555	453	
38.85-43.75	Presumpscot 8	470	654	313	543	693	427	505	489	
43.75-49.65	Presumpscot 9	516	717	343	596	761	469	718	528	
49.65-53.8	Presumpscot 10	538	748	357	665	850	523	697	565	
53.8-58.7	Presumpscot 11	545	758	362	679	867	534	710	598	
58.7-68	Presumpscot 12	565	786	375	721	921	567	766	650	

Note: Depth 0 is the start of the Presumpscot clay layer, avg. = average, min. = minimum, max. = maximum, DSS = direct simple shear, FVT = field vane shear test

The resulting hypothetical factor of safety of the slope using the  $s_u$  from DSS and FVT test results are 1.00 and 0.81, respectively. The lower factor of safety of the FVT results from the generally lower predicted  $s_u$  from the test method as compared to the DSS. The hypothetical failure plane from the DSS model intersects the middle/top portion of the slope whereas the FVT model slope failure occurs at the bottom of the deposit. Lower predicted  $s_u$  at deeper portions of the deposit using the FVT is the source of this finding.

As expected, as the  $N_{kt}$  and  $N_{\Delta u}$  cone factors increased, the predicted  $s_u$  of the clay decreased, and the resulting factor of safety decreased. From the minimum  $N_{kt}$  of 17.7 to the maximum  $N_{kt}$  of 33.5, the factor of safety of the slope decreased from 1.17 to 0.54, a difference of more than two fold between the values. For most stability applications, this difference would be unacceptable. Similarly, the predicted factor of safety decreased from 1.11 using the  $s_u$  profile from the lowest  $N_{\Delta u}$  of 17.4 to a factor of safety of 0.61 with the highest  $N_{\Delta u}$  of 26.7. There was less than two fold

difference between the factors of safety using the maximum and minimum  $N_{\Delta u}$ ; however, the predicted factors of safety values are significantly different.

Table 8.11: Factors of safety of the Presumpscot clay slope model at the Route 26/100 Falmouth Bride modeled with different undrained shear strength methods

<b>Shear Strength Model</b>	<b>Factor of Safety</b>	<b>% Difference from DSS</b>
<i>DSS</i>	1.00	0%
<i>FVT</i>	0.81	-11%
$N_{kt} = 17.7$ ( <i>minimum</i> )	1.17	8%
$N_{kt} = 24.5$ ( <i>average</i> )	0.81	-10%
$N_{kt} = 33.5$ ( <i>maximum</i> )	0.54	-30%
$N_{\Delta u} = 17.4$ ( <i>minimum</i> )	1.11	5%
$N_{\Delta u} = 21.0$ ( <i>average</i> )	0.92	-4%
$N_{\Delta u} = 26.7$ ( <i>maximum</i> )	0.61	-24%

*Note: DSS = direct simple shear, FVT = field vane shear test*

One observation from the stability analyses results was the similarly predicted hypothetical failure plane orientation of the DSS  $s_u$  and the CPTu  $N_{\Delta u}$  averaged undrained shear strength correlation. In these models, the weakest part of the deposit was identified as the upper portion of the deposit (Figure 8.26 and Figure 8.27) and this is where failure was predicted in the hypothetical model. Conversely, FVT  $s_u$  and CPTu  $N_{kt}$  average value shear strength profiles resulted in a hypothetical failure plane which crossed the bottom of the clay deposit, indicating that the undrained shear strength at the deeper depths controlled the stability of the slope.

Review of Figure 4.15 supports the differences observed in the failure slope between  $s_u$  profiles estimated from  $N_{kt}$  and  $N_{\Delta u}$ . In the upper portion of the deposit, the  $N_{kt}$  and  $N_{\Delta u}$  (average values) predicted  $s_u$  similarly, but as depth increases, the CPTu predicted  $s_u$  using  $N_{\Delta u}$  average matches the increase in  $s_u$  estimated from DSS testing. This increase is expected, since clay

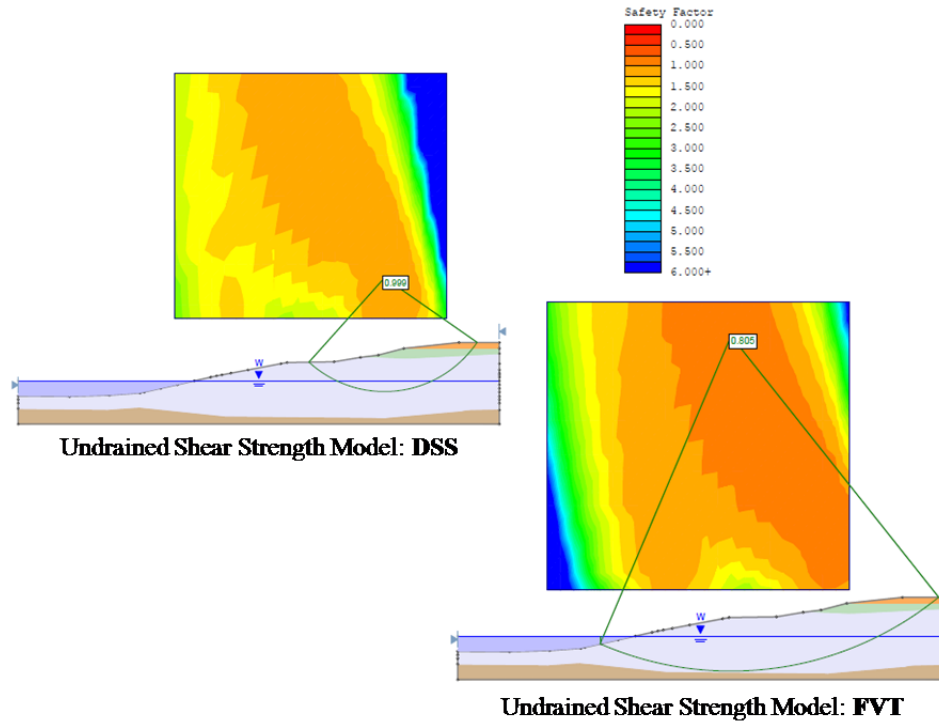


Figure 8.26: Slope stability results of Presumpscot clay at the Route 26/100 Famlouth Bridge site using direct simple shear (DSS) and field vane shear testing (FVT)  $s_u$  models.

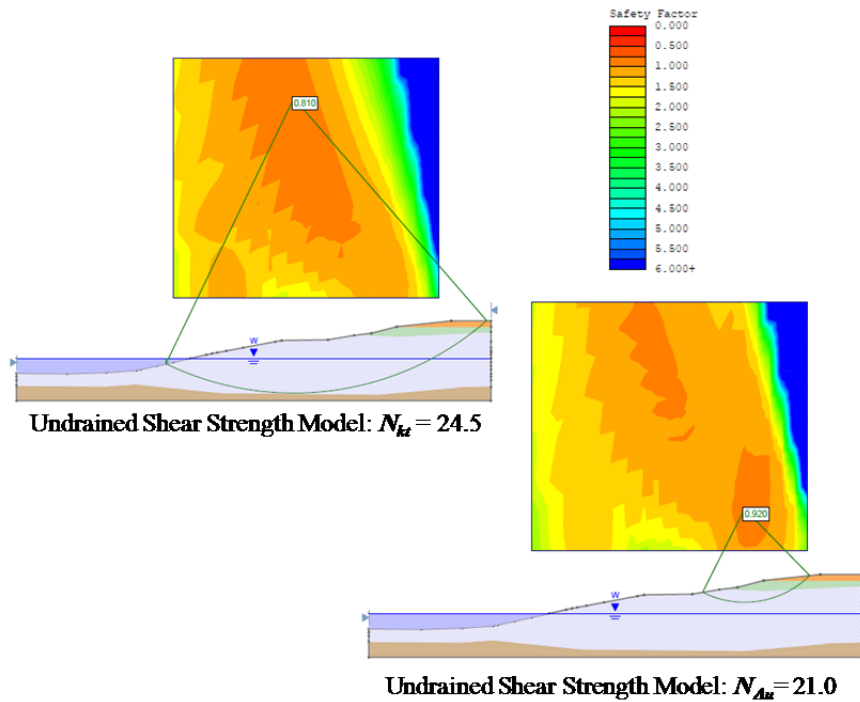


Figure 8.27: Slope stability results of Presumpscot clay at the Route 26/100 Famlouth Bridge site using CPTu cone factors  $N_{kt}$  and  $N_{\Delta u}$  undrained shear strength models



deposits which are relatively normally consolidated (such as the deposit at Route 26/100 Bridge) typically increase in  $s_u$  with increasing overburden pressure. However, CPTu predicted  $s_u$  using  $N_{kt}$  did not identify this increase with depth and remained relatively constant with depth. This explains the under-prediction of  $s_u$  near the bottom of the deposit, and hence the failure plane intersecting this location. The  $s_u$  profile estimated from FVT results had a similar effect.

In general, the CPTu predicted  $s_u$  using average  $N_{kt}$  and  $N_{\Delta u}$  provided lower but relatively similar factors of safety than the  $s_u$  using the DSS values. From the model, the average  $N_{\Delta u}$  gave only a 0.04% difference from the DSS factor of safety. Factor of safety using the FVT and average  $N_{kt}$  were identical. Minimum and maximum  $N_{kt}$  and  $N_{\Delta u}$  values resulted in a large variation in factors of safety of the hypothetical slope, ranging from as low as 0.54 to 1.17. This indicates the risk involved with using only one  $s_u$  data point to correlate to CPTu results and reinforces the importance of addition data points for improved average values.

#### 8.5.4 Shear Strength Summary

To summarize the CPTu shear strength section, the section began by presenting the  $N_{kt}$  and  $N_{\Delta u}$  values determined at each site and the corresponding maximum, minimum, coefficient of variation, and standard deviation. This included the results from both the laboratory testing and the FVT. The laboratory data showed less scatter than the FVT data. It was identified that the average  $N_{kt}$  and  $N_{\Delta u}$  values applied to each CPTu profile provided reasonable estimates of the  $s_u$  profile, but the level of acceptability is a site-specific issue. To illustrate this, a sensitivity analysis was performed using  $N_{kt}$  and  $N_{\Delta u}$  values (compared to laboratory and FVT) of the Route 26/100 Bridge applied to a slope stability analysis of Presumpscot clay. Preference between  $N_{kt}$  and  $N_{\Delta u}$  was not directly apparent, however, Presumpscot clay deposits with higher sensitivity provided smaller COV values for  $N_{\Delta u}$  and non-sensitive sites provided smaller COV values for  $N_{kt}$ . This may be fortuitous; however, and it should be explored further.

Since an extensive laboratory testing program such as the ones performed at the sites in this thesis are not typically available to geotechnical engineers, the second portion of the section presented potential methods for determining  $N_{kt}$  and  $N_{Au}$  values from additional measured properties. This included the use of the FVT, correlation to index properties, and a theoretical analysis from Been *et al.*, (2010) using a  $N_{kt}$ - $k$ -value-SHANSEP relationship. These resulting correlations were compared to similar studies in other clays to determine if other correlations could be utilized in the Presumpscot clay.

For CPTu interpretation in Presumpscot clay, the following process is recommended for collecting high quality information to develop CPTu correlations to  $s_u$ :

- Avoid using published correlations and ranges of  $N_{Au}$  values. In general, the values in the Presumpscot clay were higher than most recommended ranges. Published ranges show values to generally be between 4 and 10, whereas resulting  $N_{Au(CAUC)}$  values in this research ranged from 5.0 to 18.1, with average values from each of the four sites being larger than 10. Conversely, the  $N_{kt}$  values from the research fit it better with recommended ranges, which are generally from 10 to 20.  $N_{kt(CAUC)}$  site averages ranged from 14.6 to 16.8.
- Collect high quality undisturbed tube samples at routine intervals across the entire depth of the Presumpscot from a single boring located in a region of the site with typical conditions (as determined by prior CPTu testing). Measure  $s_u$  using CAUC triaxial shear and back-calculate both  $N_{kt}$  and  $N_{Au}$  values for use across the entire site with other CPTu profiles, including those with non-typical results. More than one sample should be collected and tested and the average  $N_{kt}$  and  $N_{Au}$  values respectively. If desired, the CPTu can be performed prior to the

borings in order to identify the Presumpscot layer thickness and any soft or unusual zones which should be included in the sampling procedures.

- Field vane tests (FVT) are a staple of investigations in the Presumpscot and should continue to be performed across the site, particularly in areas adjacent to the corresponding CPTu sounding (but at least 20 CPTu hole diameters away) and undisturbed sample boring, as well as in locations identified as having variability to obtain other direct measures of  $s_u$ . FVTs are less costly and provide real-time estimates of  $s_u$ , although as shown in this study they are more variable and may present both higher and lower  $s_u$  values than higher quality samples tested under controlled stress and strain conditions in the laboratory.  $s_u$  from FVTs can additionally be used to assess  $N_{kt}$  and  $N_{\Delta u}$  values for correlation to su strength from nearby CPTu profiles if design using FVT strength is desired.
- Utilize both the  $N_{kt}$  and  $N_{\Delta u}$  CPTu factors in  $s_u$  analyses. Both factors provided similar  $s_u$  profiles when the average values were used, so the use of both factors will provide redundancy.
- Been *et al.*, (2010) analysis did not provide reasonable predictions of  $N_{kt}$ . This is thought to be due to the inconsistency of  $s_u$  and OCR predicted of the Presumpscot clay using the SHANSEP relationship on which the Been *et al.*,(2010) method is based.
- Check the resulting  $N_{\Delta u}$  values with the following correlations which were determined specifically for the Presumpscot clay based on results from the four research sites:
  - $N_{\Delta u}$  vs.  $B_q$  (Equations 8.17 and 8.18)
  - $N_{\Delta u}$  vs. OCR and  $S_t$  (Equations 8.19 and 8.20)

- Correlations between  $N_{kt}$  and Plasticity Index (PI), OCR, and  $B_q$  found in the literature should not be used, as they have been shown in this study to be inconsistent for Presumpscot clay.

## 8.6 Seismic Characteristics

Seismic measurements were made during cone penetration testing (SCPTu) at the four research sites. Shear wave velocity ( $V_s$ ) was measured at discrete, 3.28 ft intervals and is shown for the four sites together in Figure 8.28. With values of total unit weight measured from intact CRS consolidation samples at the natural water content and  $s_u$  measured from laboratory shear strength testing (CAUC/DSS), small strain shear modulus ( $G_0$ ) and rigidity index ( $I_r$ ) were calculated for each depth where  $V_s$ ,  $\gamma_s$ , and  $s_u$  were measured.  $V_s$ ,  $G_0$ , and  $I_r$  are presented in Figure 8.28 to provide expected ranges of the values for the Presumpscot clay.

$V_s$  ranged from 364 ft/s to 1050 ft/s at all four of the research sites. The increases with depth are likely due to the increase in overburden stress.  $G_0$  ranged from 450 ksf to 3748 ksf and also increased with depth due to overburden stresses. A report by Long and Donohue (2008) studied 11 Norwegian clay sites using both surface waves and CPTu to obtain  $V_s$  values. The studied clay ranged from 17% to 60% clay, had OCR of 1.0 to 6.0, and sensitivities ranging from 2 to 1000. Values of  $V_s$  in the study ranged from 131 ft/s to 1,148 ft/s and  $G_0$  values ranged from 56 ksf to 5,140 ksf. In general, the ranges of both  $V_s$  and  $G_0$  for the Norwegian soils are similar to the Presumpscot clay. Long and Donohue (2008) also suggested that  $G_0$  and OCR and  $G_0$  and void ratio ( $e_0$ ) are related for clays, which is illustrated in Figure 8.28 for the Presumpscot clay. Neither of the relationships appeared to be applicable to the Presumpscot clay.

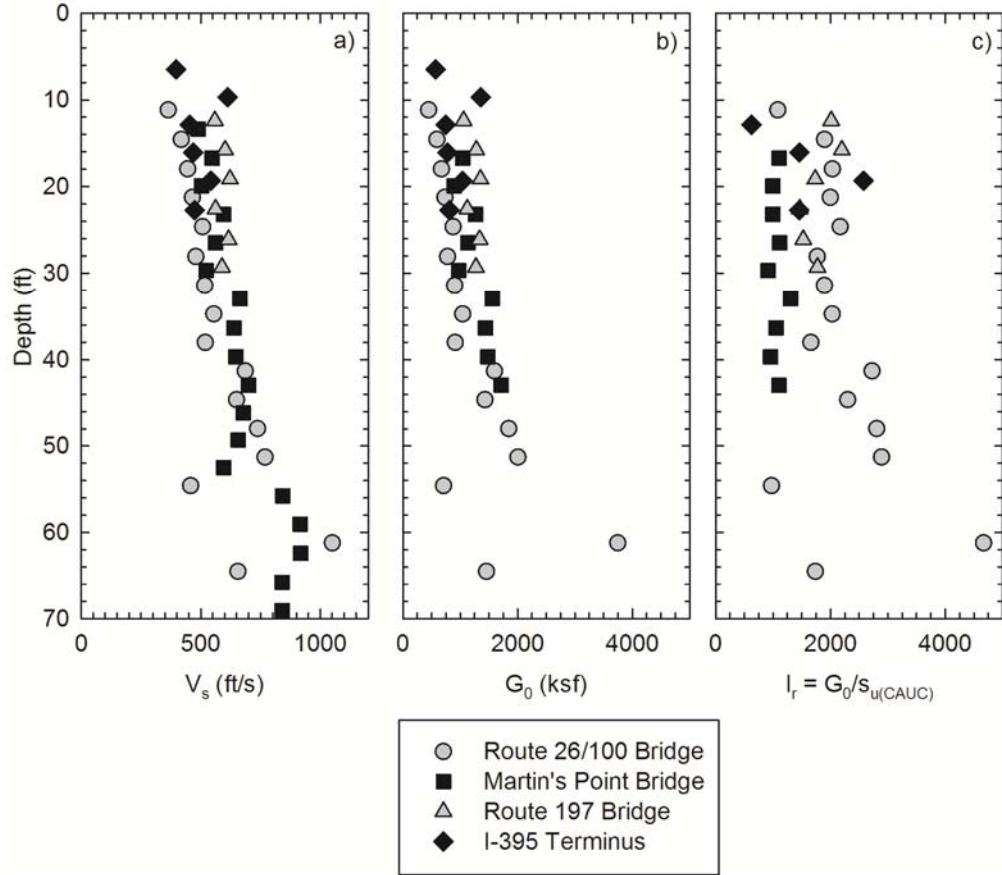


Figure 8.28 Measurements of a) Shear wave velocity ( $V_s$ ) b) Small strain shear modulus ( $G_0$ ) and c) Rigidity index ( $I_r$ ) in the Presumpscot clay.

Rigidity index ( $I_r$ ) is defined as the small strain shear modulus ( $G_0$ ) divided by the  $s_u$  and provides a relative measure of shear stiffness.  $I_r$  effects primarily the rate of consolidation of clays (Lunne *et al.*, 1997) and is used in shallow foundation design.  $I_r$  determined with  $s_u$  from CAUC triaxial testing ranged from approximately 650 to 4,670 and average of 1713.  $I_r$  exhibited no apparent trend with depth or other soil properties.

Measurements of  $G_0$  and  $I_r$ , when compared to other published data, and verify that the tested Presumpscot clay falls into the range of typical values for soft to medium glacially deposited clays. One advantage to measuring  $V_s$  in Presumpscot clay, which was not evaluated in this thesis, is the ability to use those measurements to provide a Seismic Site Classification in

accordance with ASTM 7-10. There is a threshold from  $V_s$  values above and below 600 ft/s (between Class D and Class E), and as seen in Figure 8.28, the  $V_s$  measurements can be close to this threshold. So even if they are not used to obtain engineering parameters, the  $V_s$  values can provide guidance on the selection of Seismic Site Classification.

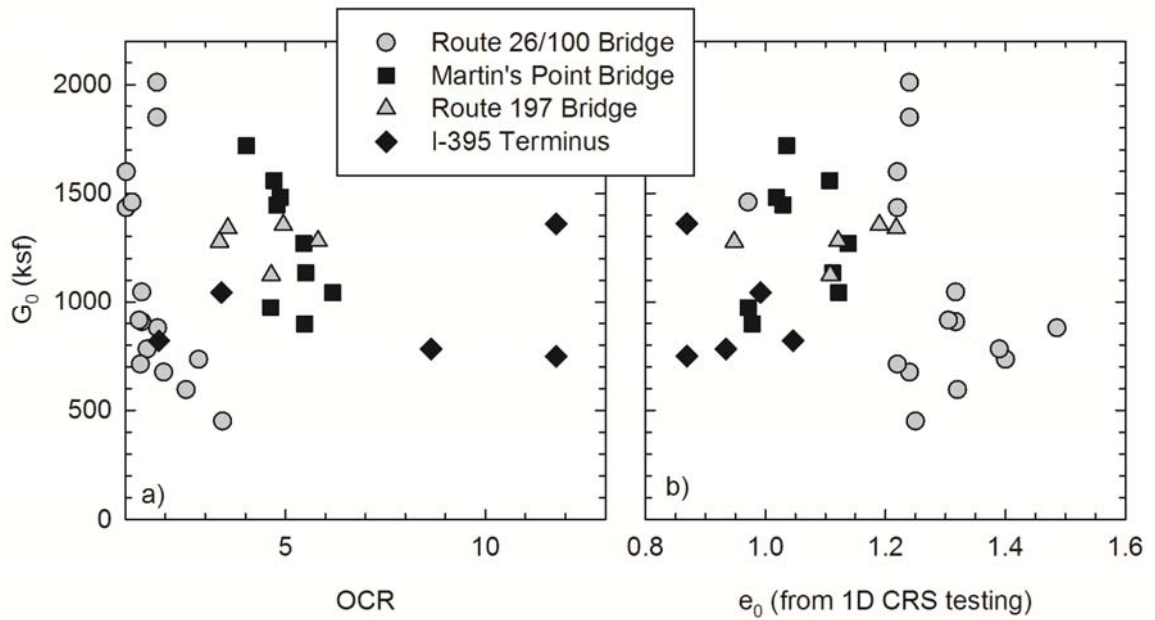


Figure 8.29: a)  $G_0$  vs. OCR and b)  $G_0$  vs. void ratio ( $e_0$ ) for the Presumpscot clay research sites.

## 9 CONCLUSIONS AND RECOMMENDATIONS

One of the greatest challenges that geotechnical engineers face in the State of Maine is the proper characterization of the soft, silty Presumpscot clay for settlement and stability analyses. Current practice involves measurement of soil properties at discrete locations within the subsurface, either from field vane shear testing (FVT) or laboratory testing of disturbed and undisturbed samples. Identification of properties at discrete locations required interpolation between collected data, which may lead to unidentified features in a portion of the subsurface. Additionally, the methods by which soil properties are measured rely heavily on driller and operator procedures that are variable and thus produce information of varying quality. The cone penetration test with pore pressure measurements (CPTu) offers quick and continuous measurements of soil response to penetration that, with the use of correlations to engineering properties, can assist in geotechnical design and "fill in the gaps" of discrete testing by providing estimates of complete profiles of properties critical to design in clays such as overconsolidation ratio (OCR) and undrained shear strength ( $s_u$ ). The CPTu is the most robust geotechnical tool for identifying subsurface layering, discrete low-strength and high-strength horizons (e.g. slip planes or silt/sand seams), and groundwater conditions (hydrostatic and artesian) (DeGroot and Ladd 2010, Rogers 2006).

This chapter presents conclusions and recommendations for the use of the cone penetration test (CPTu) for site characterization and determination of engineering properties of the Presumpscot clay in Maine. Existing CPTu interpretation methods were evaluated by comparing soil classification, preconsolidation pressure ( $\sigma'_p$ ), and undrained shear strength ( $s_u$ ) predicted from CPTu measurements to values obtained from laboratory testing on high quality undisturbed samples. Recommendations for future work are presented at the end of the chapter.

Geotechnical investigations were performed at four sites containing deposits of Presumpscot clay from coastal and inland river locations in Maine. The investigations included

field vane shear testing (FVT) and index and advanced laboratory testing of high quality, undisturbed Sherbrook block or Shelby tube samples collected from each site. Specimens from all undisturbed samples were tested for classification in accordance with the Unified Soil Classification System (ASTM D2487), stress history (e.g.,  $\sigma'_p$  and OCR) using constant rate of strain (CRS) consolidation testing, and undrained shear strength ( $s_u$ ) using triaxial compression and direct simple shear (DSS) testing. Cone penetration testing with pore pressure measurements (CPTu) was performed adjacent to borings where FVT and sampling was conducted during each investigation in order to correlate measured properties of the clay to the CPTu results.

### 9.1 Non-parametric CPTu Interpretations

Continuous measurements of tip resistance, sleeve friction, and pore pressure provided during CPTu profiling can be used to inform on the nature of Presumpscot clay deposits before the data is interpreted and correlated to engineering parameters. Granular and cohesive (i.e., clay and silt) soils yield different CPTu measurements (e.g. sands yield higher tip and sleeve friction, low to no excess pore water pressure), thus transitions between Presumpscot clay and underlying/overlying deposits is evident directly from the CPTu sounding. Groundwater conditions can also be identified during a CPTu. If penetration is occurring in a free-draining soil, the measured pore pressure can be extrapolated to a groundwater surface elevation. Additionally, if artesian pressures are present, they can be identified from the measured pore pressure CPTu profile. Furthermore, within the Presumpscot clay, overconsolidation ratio (OCR) has been found to relate directly to the normalized tip resistance ( $Q_t$ ). Therefore, the transition from the upper stiff and/or desiccated zone into the lower softer zone or any significant changes in overconsolidation will be evident from CPTu soundings. Additionally, if any zones, layer, or pockets within a Presumpscot clay deposit result in fluctuating CPTu measurements, this may indicate silt/sand seams or softer pockets of Presumpscot clay. The identification of "typical" conditions, as well as variations or discontinuous conditions through CPTu profile can be useful



for planning further investigations of the site using other in situ tests or sampling and laboratory testing programs to identify typical or problematic conditions at the site.

## 9.2 Classification of Soil Type

Classification charts based on the relationship between CPTu measurements of normalized tip resistance ( $Q_t$ ) and normalized pore pressure ( $B_q$ ) best classify the Presumpscot clay in this study. In particular, the Schneider *et al.* (2008) analysis performed best at classifying and highlighting the potential for sensitivity of the Presumpscot clays studied. Current geotechnical practice typically uses the Robertson (1990) normalized tip resistance ( $Q_t$ ) vs. sleeve friction ratio ( $F_r$ ), however, the findings from the study soil indicate that this analysis was less consistent compared to classification analyses based on normalized tip resistance ( $Q_t$ ) vs. normalized pore pressure ( $B_q$ ). If the Robertson (1990)  $Q_t$ - $F_r$  and  $Q_t$ - $B_q$  analyses are used for classification of the Presumpscot clay from CPTu measurements, the results from this study suggest that data can be expected to generally plot within Region 4 "clayey silt and silty clay" within the plot using  $Q_t$ - $F_r$  analysis and generally plot within Region 3 "clay to silty clay" within the plot using  $Q_t$ - $B_q$  analysis. These are both consistent with the Unified Soil Classification System characterization of the majority of the specimens tested as low plasticity clay, CL. When classifying clay soils based on  $F_r$ , the SBT charts are relying on a measurement which may range from 0 psf to approximately 500 psf (see Figure 8.3 for the sleeve friction measurements at the Presumpscot clay sites in this study), whereas pore pressure measurements can exceed 20,000 psf (or more, depending on the depth of the deposit and other characteristics, see Figure 8.3 for the pore pressure measurements at the Presumpscot clay sites in this study). Therefore, classification based on pore pressure as opposed to sleeve friction allows for a more specific classification based on precise measurements. It should be additionally noted that  $Q_t$ - $B_q$  SBT classification was found to be more reliable than  $Q_t$ - $F_r$  classification, which agrees with published literature (Long, 2008). Sleeve friction is generally a less reliable measurement than pore pressure due to the

following factors: pore pressure effects on the end of the sleeve; tolerance in dimensions between the cone and the sleeve; surface roughness of the sleeve; load cell design and calibration (Lunne *et al.*, 1997).

Because of the limited amount of sensitive clay soils encountered in this study, additional research should be conducted using more sensitive Presumpscot deposits before the "sensitive clay" regions of the Schneider *et al.*, (2008) and Robertson (1990)  $B_q$ - $Q_t$  classification analyses are used to confidently identify sensitivity of Presumpscot clay. Two of the four sites in this study contained sensitive clay (ranging from 9 to greater than 100), and both of these sites plotted consistently within the sensitive clay region of the Schneider *et al.* (2008)  $Q_t$ - $B_q$  analysis, but did not plot within the sensitive clay region of the Robertson (1990)  $Q_t$ - $B_q$  analysis. Moreover, some data points from a non-sensitive deposit of Presumpscot clay plotted within the sensitive clay region of the Schneider *et al.*, (2008) plot. Further studies should consist of performing CPTu in Presumpscot clay deposits with known high sensitivity and comparing their performance using both the Schneider *et al.*, (2008) and the Robertson (1990)  $Q_t$ - $B_q$  classification analyses to further assess the ability of the charts to differentiate between sensitive and non-sensitive deposits of Presumpscot clay.

### 9.3 CPTu Correlation to Stress History

The *k-value* method using normalized tip resistance,  $Q_t$ , and a constant,  $k$ , provided reasonable first-order estimates of  $\sigma'_p$  and OCR of the Presumpscot clay when compared with  $\sigma'_p$  measured during constant rate of strain (CRS) one-dimensional consolidation testing. *k-value* ranged from 0.19 to 0.55 across the profiles from the four sites, and agreed well with the typical range of values of 0.20 to 0.50 as suggested by Lunne *et al.* (1997). Analyses to identify potential relationships between changing *k-values* and measured index and engineering properties of the Presumpscot did not yield any clear relationships between the *k-value* and index properties or  $s_w$ , however, a potential relationship was established between *k-value* and OCR (i.e.,  $\sigma'_p/\sigma'_{v0}$ ), which

should be explored by additional research. Results from this study suggest that the *k-value* may increase in magnitude as OCR increases from 1.0 to 4.0 (where this is also an expected increase in  $K_0$  or lateral earth pressure at rest), and a weak trend of *k-value* decreasing or remaining constant with increased OCR for OCR values greater than 4.

The range in *k-values*, both from an individual site and between sites, from this study illustrates the importance of developing and using site-specific correlations for more than an initial investigation. A first order estimate of  $\sigma'_p$  and OCR using a *k-value* of 0.33 recommended by Mayne (2014) provides a reasonable estimate of stress history from CPTu results. In general, a *k-value* of 0.33 resulted in underestimates of  $\sigma'_p$  and OCR, which would cause overestimates of settlement magnitudes in the Presumpscot clay.

The resulting average *k-values* for the Route 26/100 Bridge site is 0.32, for Martin's Point Bridge is 0.38, for Route 197 Bridge is 0.45, and for the I-395 Terminus is 0.28. The resulting standard deviation in *k-values* was 0.06 for Route 26/100 Bridge and 0.07 for the remaining three sites. The average and standard deviation for data from all four sites is 0.36 and 0.10, respectively. A sensitivity analysis was performed for settlement of a hypothetical load at the I-395 Terminus site using both the measured laboratory stress history, and CPTu *k-values* representing the minimum, maximum, and average *k-values* determined from CPTu-stress history correlations for that site that were applied to the CPTu profile. The sensitivity analysis results illustrated that the settlement estimated from both the average and the maximum *k-values* compared well with the laboratory results for a broad range of additional total stresses, whereas the minimum *k-value* severely overestimated the settlement magnitudes.

It is recommended that a *k-value* of 0.33 be used for preliminary estimates OCR and  $\sigma'_p$ -profiles in Presumpscot clay. If the OCR and  $\sigma'_p$  values are used in geotechnical design/analyses, they should be verified by laboratory consolidation testing on high quality undisturbed samples.

Furthermore, a site-specific sensitivity analysis should be formulated to determine the effect of a changing  $k$ -value on resulting factors of safety in order to determine the need for sampling to narrow the site-specific  $k$ -value. The correlations presented by Saye *et al.*, (2013) using Liquid Limit (LL) and Plasticity Index (PI) did not provide an appropriate method for determining OCR and  $\sigma'_p$  profiles based on index test results in the Presumpscot clay because the LL and PI do not differ much from site to site.

#### 9.4 CPTu Correlation to Undrained Shear Strength

Undrained shear strength CPTu correlation factors  $N_{kt}$ ,  $N_{ke}$ , and  $N_{\Delta u}$  (Equations 8.15 through 8.16) were determined for the Presumpscot clay at the four research sites using reference undrained shear strength ( $s_u$ ) obtained from triaxial compression (TC) and direct simple shear (DSS) laboratory testing on high quality, undisturbed samples and field vane shear testing (FVT) performed *in situ*. Findings from this study suggest that  $N_{ke}$  provides an unreliable correlation.  $N_{ke}$  provided poor and inconsistent estimates of  $s_u$  of Presumpscot clay, since the difference between measured tip resistance and pore pressure (from which the cone factor is derived) is often very small, especially in sensitive clay deposits.

Study findings identify that typical values recommended from the geotechnical literature of  $N_{kt}$  and  $N_{\Delta u}$  overestimate  $s_u$  for Presumpscot clay, as CPTu- $s_u$  correlated factors  $N_{kt}$  and  $N_{\Delta u}$  from the four sites were within the upper range of, and above, of the range of typical values from similar studies in soft clay, particularly for  $N_{\Delta u}$ . The resulting average  $N_{kt(CAUC)}$  for the Route 26/100 Bridge site is 16.8, for Martin's Point Bridge is 15.9, for Route 197 Bridge is 14.6, and for the I-395 Terminus is 16.7. The resulting standard deviations are 4.0, 2.6, 1.9, and 2.0 for these data, respectively. The resulting average  $N_{\Delta u(CAUC)}$  for the Route 26/100 Bridge site is 14.1, for Martin's Point Bridge is 9.7, for Route 197 Bridge is 14.1, and for the I-395 Terminus is 10.9. The resulting standard deviations are 1.9, 2.1, 1.6, and 2.0 for these data, respectively. The

resulting average and standard deviation  $N_{kt(DSS)}$  are 20.5 and 4.9 and the resulting average and standard deviation  $N_{\Delta u(DSS)}$  are 17.3 and 2.3. Coefficients of variation (COV) for  $N_{kt}$  was lowest for non-sensitive site and COV for  $N_{\Delta u}$  was lowest for sensitive clay sites. The potential for this reliability correlation (i.e. higher effectiveness of  $N_{\Delta u}$  for sensitive deposits and  $N_{kt}$  for non-sensitive deposits) should be investigated further.

Reference  $s_u$  (TC vs. DSS vs. FVT) had a large influence on the resulting undrained shear strength cone factors. Cone factors developed using  $s_u$  measured from DSS testing for the Route 26/100 site (approximately 74% of the  $s_u$  value from TC, Ladd and DeGroot 2003) was compared to cone factors developed using the correlated estimated TC testing  $s_u$ . It was found that the average CPTu cone factors  $N_{kt}$  and  $N_{\Delta u}$  both increased in magnitude by greater than 5. CPTu cone factor  $N_{kt(CAUC)}$  from all four sites ranged from 11.0 to 25.7 and cone factor  $N_{\Delta u(CAUC)}$  ranged from 5.0 to 18.1. CPTu cone factor  $N_{kt(DSS)}$  ranged from 15.0 to 31.4 and cone factor  $N_{\Delta u(DSS)}$  ranged from 13.6 to 22.1. The higher  $N_{kt}$  and  $N_{\Delta u}$  from DSS testing as compared to CAUC testing derived from the  $s_u$  measured in the laboratory procedure. In CAUC testing, the deviator stress is directly vertical ( $0^\circ$ ), where the deviator stress for DSS testing is somewhere between  $30^\circ$  and  $60^\circ$  (DeGroot and Ladd, 2010), which results in a separate measurement of  $s_u$  and subsequently  $N_{kt}$  and  $N_{\Delta u}$ .

$N_{kt(FVT)}$  and  $N_{\Delta u(FVT)}$  provided relatively similar average values compared to the  $N_{kt(CAUC)}$  and  $N_{\Delta u(CAUC)}$  factors when enough FVT were performed, however the standard deviation and coefficient of variation was larger (indicating larger data scatter). Laboratory determined  $s_u$  (i.e. CAUC and DSS testing) is the most reliable reference shear strength because the sample quality of the tested specimens can be determined. In addition, the boundary conditions and testing procedures of laboratory tests can be well controlled, whereas the FVT can have some unexpected influences of testing error or unforeseen site conditions (such as a silt or sand seam

within the tested sample, which can easily be observed before testing is conducted on laboratory samples).

No correlations were found to exist between cone factor  $N_{kt}$  and clay properties such as Plasticity Index (PI), OCR, or  $s_u$  for the Presumpscot clay. However, findings from the study suggest that a potential relationship exists between OCR and  $N_{\Delta u}$  and a moderate to strong relationship exists between normalized pore pressure  $B_q$ , sensitivity ( $S_t$ ) and  $N_{\Delta u}$  (Figure 8.20, Equations 8.17 through 8.20)

A sensitivity analysis using a range of both  $N_{kt}$  and  $N_{\Delta u}$  was performed using a slope stability model to identify just how important choice of a CPTu cone factor to estimate the design undrained shear strength of a deposit of Presumpscot clay. The slope was modeled using geometry and soil profiles from "Geologic Profile A-A" (H&A 2009) of the Route 26/100 north bridge approach and using the computer program Slide 6.0 (RocScience, 2014). The undrained shear strength profile was modeled by dividing the Presumpscot clay into 12 layers represented by laboratory DSS  $s_u$ , FVT  $s_u$ , and the correlated CPTu  $s_u$  determined using the average, minimum and maximum  $N_{kt}$  and  $N_{\Delta u}$  cone factors. As expected, as the  $N_{kt}$  and  $N_{\Delta u}$  cone factors increased, the predicted  $s_u$  of the clay decreased, and the resulting factor of safety of the slope in the hypothetical analysis decreased. From the minimum  $N_{kt}$  of 17.7 to the maximum  $N_{kt}$  of 33.5 correlations for this site, the factor of safety of the slope decreased by 30%. For most stability applications, this difference would be unacceptable. Similarly, the predicted  $N_{\Delta u}$  factor of safety decreased by 20% when changing  $s_u$  from that determined using the lowest  $N_{\Delta u}$  value of 17.4 to the highest  $N_{\Delta u}$  value of 26.7. There was not as much of a difference in these two values as compared to the  $N_{kt}$ ; however, the predicted factors of safety values were still significantly different. For determining the appropriate  $N_{kt}$  and  $N_{\Delta u}$  cone factors at a Presumpscot clay deposit, the best method is to collect high quality undisturbed samples at multiple depths within a deposit,

determine laboratory values of  $s_u$  using CAUC testing methods from these samples, and back-calculate  $N_{kt}$  and  $N_{\Delta u}$  factors to apply to the profile for that specific deposit. Multiple  $s_u$  values should be determined since  $N_{kt}$  and  $N_{\Delta u}$  was found to vary with depth, and the resulting average values provided good correlations. Furthermore, it is ideal to corroborate the  $N_{kt}$  and  $N_{\Delta u}$  factors with FVT results from nearby borings. FVT should be performed as closely to the CPTu as possible (although not any closer than 20 CPTu hole diameters) and in accordance with applicable ASTM standards to achieve reliable results. The resulting  $N_{kt}$  and  $N_{\Delta u}$  average value from FVT should match reasonably well with the values obtained from laboratory testing. For a conservative analysis, the higher value can be used.

Another important observation from the stability analyses results was the similarly predicted failure plane orientation between the soil modeled using the DSS  $s_u$  results and the soil modeled using the CPTu  $s_u$  profile estimated using  $N_{\Delta u(DSS)}$ . In these models, the weakest part of the deposit was identified as the upper portion of the deposit (Figure 8.26 and Figure 8.27) and this is where the failure occurred. Conversely, the soil models based on FVT  $s_u$  and the CPTu  $s_u$  estimated using  $N_{kt(DSS)}$  resulted in a failure plane that crossed the bottom of the clay deposit, indicating from the results of these shear strength models that the undrained shear strength at the deeper depths controls the stability of the slope. For this particular site it appears that  $N_{\Delta u}$  is a more appropriate cone factor to use to represent laboratory  $s_u$  measurements.

For CPTu interpretation in Presumpscot clay, the following process is recommended for collecting high quality information to develop CPTu correlations to  $s_u$ :

- Avoid using published correlations and ranges of  $N_{\Delta u}$  values. In general, the values in the Presumpscot clay were higher than most recommended ranges. Published ranges show values to generally be between 4 and 10, whereas resulting  $N_{\Delta u(CAUC)}$  values in this research ranged from 5.0 to 18.1, with average

values from each of the four sites being larger than 10. Conversely, the  $N_{kt}$  values from the research fit in better with recommended ranges, which are generally from 10 to 20.  $N_{kt(CAUC)}$  site averages ranged from 14.6 to 16.8.

- Collect high quality undisturbed tube samples at routine intervals across the entire depth of the Presumpscot from a single boring located in a region of the site with typical conditions (as determined by prior CPTu testing). Measure  $s_u$  using CAUC triaxial shear and back-calculate both  $N_{kt}$  and  $N_{\Delta u}$  values for use across the entire site with other CPTu profiles, including those with non-typical results. More than one sample should be collected and tested and the average  $N_{kt}$  and  $N_{\Delta u}$  values respectively. If desired, the CPTu can be performed prior to the borings in order to identify the Presumpscot layer thickness and any soft or unusual zones which should be included in the sampling procedures.
- Field vane tests (FVT) are a staple of investigations in the Presumpscot and should continue to be performed across the site, particularly in areas adjacent to the corresponding CPTu sounding (but at least 20 hole diameters away) and undisturbed sample boring, as well as in locations identified as having variability to obtain other direct measures of  $s_u$ . FVTs are less costly and provide real-time estimates of  $s_u$ , although as shown in this study they are more variable and may present both higher and lower  $s_u$  values than higher quality samples tested under controlled stress and strain conditions in the laboratory.  $s_u$  from FVTs can additionally be used to assess  $N_{kt}$  and  $N_{\Delta u}$  values for correlation to  $s_u$  strength from nearby CPTu profiles if design using FVT strength is desired.
- Utilize both the  $N_{kt}$  and  $N_{\Delta u}$  CPTu factors in  $s_u$  analyses. Both factors provided similar  $s_u$  profiles when the average values were used, so the use of both factors will provide redundancy and corroborate  $s_u$  at the site.



- Check the resulting  $N_{\Delta u}$  values with the following correlations which were determined specifically for the Presumpscot clay based on results from the four research sites:
  - $N_{\Delta u}$  vs.  $B_q$  (Equations 8.17 and 8.18)
  - $N_{\Delta u}$  vs. OCR and  $S_r$  (Equations 8.19 and 8.20)
- Correlations between  $N_{kt}$  and Plasticity Index (PI), OCR, and  $B_q$  found in the literature should not be used, as they have been shown in this study to be inconsistent for Presumpscot.

## 9.5 Shear Stiffness

Shear wave velocity,  $V_s$ , ranged from 364 ft/s to 1050 ft/s and showed a general increase with depth for all four of the research sites. These values indicate that the Presumpscot deposits studied are soft to stiff clay. Small strain shear modulus,  $G_0$ , ranged from 450 ksf to 3748 ksf and showed a general increase with depth and overburden stresses at each of the four sites. These values of  $G_0$  indicate the soil is "young, uncemented clay" (Long and Donohue, 2008). The resulting  $G_0$  values did not appear to correlate with OCR or void ratio. It is important to note that while some correlations exist in the literature that can be used to estimate  $G_0$  from CPTu measurements of tip resistance and void ratio, however  $G_0$  is extremely site dependent and the recommendations of this study is that  $V_s$  measurements be made and  $G_0$  subsequently correlated with actual measurements of soil density determined from undisturbed tube samples. Note that the soil classifications from the  $V_s$  and  $G_0$  measurements were taken from Long and Donohue (2010). The combination of  $G_0$  and measured  $s_{u(CAUC)}$  yields the rigidity index,  $I_r$ . Values of  $I_r$  range from 650 to 4,670 between the four sites.

One advantage to measuring  $V_s$  in Presumpscot clay, which was not discussed in depth in this thesis, is the ability to use those measurements to provide a Seismic Site Classification in accordance with ASTM 7-10. There is a threshold from  $V_s$  values above and below 600 ft/s

(between Class D and Class E), and as seen in Figure 8.28, the  $V_s$  measurements can be close to this threshold. Therefore, if the seismic measurements are not used to obtain engineering parameters,  $V_s$  values can provide guidance on the selection of Seismic Site Classification.

## 9.6 Future Work

Correlations were made between the CPTu and engineering properties of the Presumpscot clay as outlined in Chapter 1 of this paper. Based on the findings from this study and the potential for increased reliability of the correlations, the following work is suggested for future research:

- 1) Conduct SCPTu testing at more sites to create a larger database for which correlations can be developed.
- 2) Determine if the "sensitive clay" region of the *Schneider et al.*, (2008) plot can consistently identify sensitive Presumpscot clay deposits using additional CPTu data from both sensitive and non-sensitive deposits of Presumpscot clay.
- 3) Investigate the relationship between the stress history correlation *k-value* and OCR. It appears that the two parameters may be correlated as suggested by similar research, but further research in the Presumpscot clay is needed before a definitive conclusion is made. Findings from this research indicate that *k-value* may increase with increasing OCR for  $OCR < 4$ .
- 4) Confirm that the cone factors  $N_{kt}$  and  $N_{Au}$  in the Presumpscot clay are consistently higher than most published averages. A preliminary correlation between sensitivity and cone factor emerged from the findings; however this finding may be fortuitous since there were only four sites studied.
- 5) Investigate the correlations between cone factor  $N_{Au}$  and OCR and  $B_q$ . Preliminary findings show a potential correlation to OCR and a strong correlation to  $B_q$ . If the correlations are further refined, the processes of selecting an appropriate  $N_{Au}$  will

become more effective. Confirm Equations 8.17 through 8.20 and provide appropriate ranges for Presumpscot clay  $N_{Au}$  values.

## REFERENCES

- Abu-Farsakh, M. (2007). Possible Evaluation of Overconsolidation Ratio of Clayey Soils from Peizocone Penetration Tests. *Geo-Denver 2007* .
- Andrews, D. (1986). "The Engineering Aspects of the Presumpscot Formation," Geologic and Geotechnical Characteristics of the Presumpscot Formation Maine's Glaciomarine "Clay" Symposium, Andrews, D.W., Thompson, W.D., Sandford, T.C., and Novak, I.D., Eds. Augusta, ME, 20 March 1987, 17 pp.
- American Society of Testing and Materials (ASTM). (2005). Soil and Rock (1): D420 - D5611. *Annual Book of Standards, Volume 04.08*. Philadelphia, Pennsylvania.
- American Society of Testing and Materials (ASTM). (2007). D5778. *Annual Book of Standards, Volume 04.08*. Philadelphia, Pennsylvania.
- Baxter, C.D.P., Bradshaw, A.S., Ochoa-Lavergne, M., and Hankour, R. (2002). "DSS Test Results Using Wire-Reinforced Membranes and Stacked Rings," *GeoFlorida 2010: Advances in Analysis, Modeling, and Design (ASCE GSP 199)*, Orlando, Florida, February 20-24, pp. 600-607.
- Becker, D. E., Crooks, J. H. A., Been, K., and Jeffries, M. G. (1987). "Work as a criterion for determining in situ and yield stresses in clays." *Canadian Geotech. J.*, 24(4), 549-564.
- Been, K., Quinonez, A., and Sancio, R. B. (2010). "Interpretation of the CPT in engineering practice." *2nd International Symposium on Cone Penetration Testing*, Huntington Beach, CA. 19 p.
- Belknap, D. F. (1987). "Presumpscot Formation Submerged on the Maine Inner Shelf," *Geologic and Geotechnical Characteristics of the Presumpscot Formation Maine's Glaciomarine "Clay" Symposium*, Andrews, D.W., Thompson, W.D., Sandford, T.C., and Novak, I.D., Eds. Augusta, ME, 20 March 1987, 18 pp.
- Borns Jr., H. W., Doner, L. A., C, C., Jacobson Jr., G. L., Kaplan, M. R., Kreutz, K. J., . . Weddle, T. K. (2004). *The Deglatiation of Maine, USA*. Orono: Elsevier B.V.
- Boylan, N., Long, M., Ward, D., Barwise, A., and Georgious, B. (2007). "Full flow penetrometer testing in Bothkennar Clay." *Proceedings of the 6<sup>th</sup> International Conference, Society of Underwater Technology, Offshore Site Investigations and Geotechnics (SUT-OSIG)*, London, September: pp. 177-186.

- Butcher, A.P., Campanella, R.G., Kaynia, A.M. and Massarsch, K.R. (2005). "Seismic cone downhole procedure to measure shear wave velocity." *Proceedings of the 10<sup>th</sup> International Conference, Society of International Society of Soil Mechanics and Geotechnical Engineering (ISSMGE), Baltic Regional Conference*, Riga, Latvia, 2005 pp. 5
- ConeTec. (2011). *ConeTec Field Report - Martin's Point Bridge*. West Berlin, NJ. Unpublished.
- ConeTec. (2012). *ConeTec Field Report – Route 197 Bridge Replacement Project*". West Berlin, NJ. Unpublished.
- ConeTec. (2013). *ConeTec Field Report – Brewer Wilson*. West Berlin, NJ. Unpublished.
- DeGroot, D. J. (2003). "Laboratory measurement and interpretation of soft clay mechanical behavior." *Soil Behavior and Soft Ground Construction; Geotech. Spec. Pub., No. 119*, J.T. Germaine, T.C. Sheahan, and R.V. Whitman, Eds., ASCE, Reston, VA., 167-200.
- DeGroot, D. J., & Ladd, C. C. (2010). Site Characterization of Cohesive Soil Deposits Using In Situ and Laboratory Testing. *American Society of Civil Engineers* , 565-607.
- Devin, S.C. (1990). *Flowslide potential of natural slopes in the Presumpscot Formation*, M.S. Thesis, University of Maine, Orono, ME.
- Devin, S. C., & Sandford, T. C. (1995, October 23-27). Landslides in Glaciomarine Clays of Coastal Maine. *Landslides under static and dynamic conditions: Analysis, Monitoring and Mitigation*, pp. 1-20.
- Geo-Equipment, G. (2014). *Instrumentation*. Retrieved from Gouda Geo-Equipment: <http://www.gouda-geo.com/products/instrumentation>
- Geonor (2010). Fall Cone Brochure:<http://www.geonor.com/PDF/Fall%20Cone%20Brochure.pdf>
- Golder Associates Inc. (2011a). *Preliminary Geotechnical Data Report – Martin's Point Bridge Replacement, Part 2*. Freeport, ME.
- Golder Associates Inc. (2011b). *Supplemental Geotechnical Data Report – Martin's Point Bridge Replacement*,. Freeport, ME.
- Golder Associates Inc. (2012). *Final Design Phase Geotechnical Data Report – Maine Kennebec Bridge, Richmond-Dresden, ME*. Maine DOT WIN 12674.00. Freeport, ME.
- Hansbo, S. (1957). "A New Approach to the Determination of the Shear Strength of Clay by the Fall-Cone Test." *Proc., Royal Swedish Geotechnical Institute*. 14, 1-49.

- Haley & Aldrich (2009). "Geotechnical Design Report: Replacement Bridge over Presumpscot and Maine Central Railroad, Maine DOT PIN 15094.00, Routes 26/100 – Falmouth, Maine."
- Holtz, R.D., Kovacs, W.D and Sheahan, T.C. (2011). *An Introduction to Geotechnical Engineering*, 2<sup>nd</sup> Ed. Pearson, Upper Saddle River, NJ.
- "I-395 Terminus" 44°46'18.36" N 68°43'14.60" W. *Google Earth*, October, 2013. April 2014.
- IGeoTest. (2014). *Instrumentation*. Retrieved from IGeoTest: [http://igeotest.com/es/geotecnia\\_terrestre/instrumentacion.asp](http://igeotest.com/es/geotecnia_terrestre/instrumentacion.asp)
- Karlsrud, K., Lunne, T., and Brattlieu, K. (1996). *Improved CPT Correlations Based on Block Samples*. Reykjavik: Nordisk Geoteknikermote.
- Karlsrud, K., Lunne, T., Kort, D.A. and Strandvik, S. (2005), "CPTU Correlations for Clays," *Proceedings of the 16<sup>th</sup> International Conference on Soil Mechanics and Geotechnical Engineering, Osaka*, September 2: pp. 693-702.
- Karlsrud, K., & Hernandez-Martinez, F. (2013). Strength and Deformation Properties of Norwegian Clays from Laboratory Tests on High-Quality Block Samples. *Canadian Geotechnical Journal* , 50, 1273-1293.
- Kelley, J., Belknap, D., Kelley, A., and Claesson, S. (2010). *A Model For Drowned Terrestrial Habitats with Associated Archeological Remains in the Northwestern Gulf of Maine, USA*. Elsevier.
- Kim, D.S. and Stokoe II, K.H. (1995). "Deformation Characteristics of Soils of Small to Medium Strains," *Proceedings of the 1<sup>st</sup> International Conference on Earthquake Geotechnical Engineering*, pp. 89-94.
- Ladd, C.C. (1991). "Stability evaluation during staged construction," *J. Geotech. Engng. Div.*, ASCE, 117(4), 540-615.
- Ladd, C.C. and DeGroot, D.J. (2003). "Recommended practice for soft ground site characterization: Arthur Casagrande Lecture," *12<sup>th</sup> Panamerican Conf. on Soil Mech. and Geotech. Engng.*, Cambridge, MA, 3-57.
- Ladd, C.C., Young, G.A., Kraemer, S.R., and Burke, D.M. (1999). "Engineering properties of Boston blue clay from special testing program." *Special Geotechnical Testing: Central Artery/Tunnel Project in Boston, Massachusetts*. ASCE GSP 91, 1-24.
- Ladd, C.C. and Foott, R. (1974). "New design procedure for stability of soft clays." *J. Geotech. Engng. Div.*, ASCE, 100(GT7), 763-786.

- Lambe, T., & Whitman, R. (1967). *Soil Mechanics*. Boston: John Wiley & Sons.
- Landon, M.M. (2007). *Development of a Non-Destructive Sample Quality Assessment Method for Soft Clays*. Ph.D. Dissertation, University of Massachusetts Amherst, Amherst, MA.
- Langlais, N.D. (2011). *Site Characterization using the Seismic Piezocone in Presumpscot Clay and Development of Piezocone Correlations to Engineering Parameters*, M.S. Thesis, University of Maine, Orono, ME.
- Lefebvre, G. and Poulin, C. (1979). "A new method of sampling in sensitive clay." *Canadian Geotech. J.*, 16(1), 226-233.
- Long, M. (2008). Design Parameters From In Situ Tests in Soft Ground. *Geotechnical and Geophysical Site Characterization – Proceeding of the 3<sup>rd</sup> International Conference of Site Characterization*, 89-115.
- Long, M., & Donohue, S. (2010). Characterization of Norwegian marine clays with Combined Shear Wave Velocity and Piezocone Cone Penetration Test (CPTU) Data. *Canadian Geotechnical Journal*, 47, 709-718.
- Lunne, T., Berre, T., Andersen, K.H., Strandvik, S. and Sjørnsen, M. (2006). "Effects of sample disturbance and consolidation procedures on measured shear strength of soft marine Norwegian clays." *Canadian Geotech. J.*, 43(7), 726-750.
- Lunne, T., Robertson, P.K., and Powell, J. (1997). *CPT and Piezocone Testing in Geotechnical Practice*, Blackie Academic & Professional, London, 312 pp.
- Maine DOT. (2010). *Martin's Point Bridge Preliminary Geotechnical Report*. Augusta, ME.
- Maine Department of Transportation. (2012). *Maine Kennebec Bridge Route 197 Over Kennebec River Richmond and Dresden, Maine*. MaineDOT Report Fed No. AC-BH-1267(400), May 11, 2012, pp. 216
- Maine Department of Transportation. (2013). *Martin's Point Bridge Replacement Project*. Retrieved from Maine.gov: <http://www.martinspointbridge.com>
- "Martin's Point Bridge." 43°41'34.65" N 70°14'40.97" W. *Google Earth*, March 18, 2012. October 2013.
- "Martin's Point Bridge." 43°41'34.65" N 70°14'40.97" W. *Google Earth*, September 27, 2014. March 2015.
- Mayne, P.W. and Kulhawy, F.H. (1982). "K<sub>0</sub>-OCR relationships in soil." *Geotech. Engng. Div. ASCE*, 108(GT6), 851-872.

- Mayne, P.W. (1991) "Determination of OCR in Clays by Piezocone Tests using Cavity Expansion and Critical State Concepts." *Soils and Foundations*, 31(2), pp. 65-76.
- Mayne, P. (2014). Interpretation of Geotechnical Parameters from Seismic Penetrometer Tests. *International Symposium on Cone Penetration Testing*, (p. 27). Las Vegas.
- Mitchell, J. K., & Soga, K. (2005). *Fundamentals of Soil Behavior*. Hoboken: John Wiley & Sons.
- Morgan, M. (1987). "Highway Embankments on the Presumpcot Formation," *Geologic and Geotechnical Characteristics of the Presumpcot Formation Maine's Glaciomarine "Clay"* Symposium, Andrews, D.W., Thompson, W.D., Sandford, T.C., and Novak, I.D., Eds. Augusta, ME, 20 March 1987, 18 pp.
- Nguyen, HQ., DeGroot, D.J. and Lunne, T. (2014). "Small Strain Shear Modulus of Marine Clays from CPT," *3<sup>rd</sup> International Symposium on Cone Penetration Testing* Symposium, Las Vegas, NV, 12-14 May 2014, pp. 601-610
- NCHRP (2007). "National Cooperative Highway Research Program (NCHRP) Synthesis 368: Cone Penetration Testing - A Synthesis of Highway Practice." Transportation Research Board, Washington D.C. <[http://onlinepubs.trb.org/onlinepubs/nchrp/nchrp\\_syn\\_368.pdf](http://onlinepubs.trb.org/onlinepubs/nchrp/nchrp_syn_368.pdf)> accessed 11/30/2011.
- Remai, Z. (2013). Correlation of undrained shear strength and CPT resistance. *Periodica Polytechnica*, 39-44.
- "Route 197 Bridge" 44°05'21.95" N 69°46'58.00" W. *Google Earth*, November 25, 2011. October 2013.
- "Route 197 Bridge" 44°05'21.95" N 69°46'58.00" W. *Google Earth*, September 18, 2013. April 2014.
- Robertson, P. (Director). (2012). *Webinar #1: Introduction to Cone Penetration Testing (CPT) by P.K. Robertson* [Motion Picture].
- Roberston, P. (2009). Interpretation of Cone Penetration Tests - A Unified Approach. *Canadian Geotechnical Journal*, 46(1) 1337-1355.
- Robertson, P. (1990). Soil Classification Using the Cone Penetration Test. *Canadian Geotechnical Journal*, 27(1) 151-158.
- Rogers, D. (2006, May 1). Subsurface Exploration Using the Standard Penetration Test and the Cone Penetration Test. *Environmental & Engineering Geoscience*, XII(2), pp. 161-179.



- Sandbækken, T., Berre, T., and Lacasse, S. (1985) "Oedometer testing at the Norwegian Geotechnical Institute." *Consolidation of Soils: Testing and Evaluation, ASTM STP 892*, 329-353.
- Sandford, T.C. and Amos, J. (1987). "Engineering Analysis of Gorham Landslide," *Geologic and Geotechnical Characteristics of the Presumpscot Formation Maine's Glaciomarine "Clay"* Symposium, Andrews, D.W., Thompson, W.D., Sandford, T.C., and Novak, I.D., Eds. Augusta, ME, 20 March 1987, 28 pp
- Saye, S. R., Lutenecker, A. J., Santos, J., & Kumm, B. P. (2013, July). Assessing Overconsolidation Ratios in Soil with Piezocone: Referencing Soil Index Properties. *Journal of Geotechnical and Geoenvironmental Engineering*, 139, 1075-1085.
- Schneider, J.A., Randolph, M., Mayne, P., and Ramsey, N. (2008). "Analysis of Factors Influencing Soil Classification Using Normalized Piezocone Tip Resistance and Pore Pressure Parameters. *Geotechnical and Geoenvironmental Engineering*, 134(11) 1569-1586.
- Schnitker, D.F. and Borns, H.W. (1987). "Depositional Environment and Composition of the Presumpscot Formation," *Geologic and Geotechnical Characteristics of the Presumpscot Formation Maine's Glaciomarine "Clay"* Symposium, Andrews, D.W., Thompson, W.D., Sandford, T.C., and Novak, I.D., Eds. Augusta, ME, 20 March 1987, 13 pp.
- Terzaghi, K., Peck, R. B., & Gholamreza. (1996). *Soil Mechanics in Engineering Practice*. New York: John Wiley & Sons.
- Thompson, W.B. (1987). "The Presumpscot Formation in Southern Maine," *Geologic and Geotechnical Characteristics of the Presumpscot Formation Maine's Glaciomarine "Clay"* Symposium, Andrews, D.W., Thompson, W.D., Sandford, T.C., and Novak, I.D., Eds. Augusta, ME, 20 March 1987, 22 pp.
- Vertek (A division of Applied Research Associates) (2014). *CPT Cones and Data Acquisition Systems*. Retrieved from VertekCPT.com: <http://www.vertekcpt.com/cpt-cones-and-data-acquisition-systems>.
- Weaver, J. (1987). "Case History: Embankment Failure at Fore River Test Section, Portland Maine," *Geologic and Geotechnical Characteristics of the Presumpscot Formation Maine's Glaciomarine "Clay"* Symposium, Andrews, D.W., Thompson, W.D., Sandford, T.C., and Novak, I.D., Eds. Augusta, ME, 20 March 1987, 15 pp.
- Wei, L., Pant, R., Tumay, M. (2010) A Case Study of Undrained Shear Strength Evaluation from In Situ Tests in Soft Louisiana Soil. *Soil Behavior and Geo-Micromechanics*. Shanghai, China, 3-5 June 2010, pp. 35-42.

## **BIOGRAPHY OF THE AUTHOR**

Mathew Allen Hardison was born in Lewiston, Maine on October 21, 1990. He attended Lisbon Elementary School, Durham Middle School, and Lisbon High School, and eventually the University of Maine, following eerily in the steps of Stephen King. However, Mathew did not find such a passion in writing horror novels, so he settled with geotechnical engineering.

While at the University of Maine, Mat participated in various organizations such as ASCE Concrete Canoe Team, Chi Epsilon, Sigma Nu Fraternity, the Tutor Program, and Graduate School Government. Throughout the first two summers of his undergraduate career, Mat was an Engineering Technician Intern for the construction management division of Summit Environmental Consultants performing site inspections of concrete and soils. During his third summer between junior and senior year, Mat was a Site-Civil intern for Woodard & Curran. With wide eyes for the "real engineering world" and the thought of a constant paycheck, Mat set his sights on the transition from undergraduate into the civil engineering profession and brushed the idea of graduate school under the rug. However, a mere month away from freedom, Melissa Landon approached Mat with an enticing offer for a M.S. pursuit with research involving a new investigation technique. Mat eventually accepted, graduated from the University of Maine in May of 2013 and dove directly into graduate school the following month.

While in graduate school, Mat developed a passion for geotechnical engineering, which is a relatively recently developed profession and is wide open for creative and inventive design. He will begin work for Summit Geoengineering Services as a geotechnical engineer starting in January of 2015. He is a candidate for Master of Science degree in Civil Engineering from the University of Maine in August 2015.